CHEMICAL ENGINEERING TRANSACTIONS, Volume 14, 2008
Edited by G. Marino, E. Bardone, A. Viglia
 ISBN 978-88-95608-02-0

Small Animal Imaging Facility: a metabolic and structural imaging center

R. Grassi[1], C. Cavaliere[1], M. Corona[2], S. Castaldo[2], D. Di Napoli[2], L. Corsi[2], B. Andria[2], M. A. Di Pasquale[3], S. Cozzolino[2], A. Rotondo[1]

[1] Radiology Section, Second University of Naples
[2] Center of Biotechnologies, [3] Radioprotection Section, Antonio Cardarelli Hospital

Key words: microMR, microCT, microUS, preclinical imaging, imaging facility set-up

Aim

The ever-increasing number of experiments carried on rodents (mostly rats and mice) couples with advances in small animal imaging systems such as microPET, optical, microCT, microMR, ultrasound and microSPECT. In this context a technical center set-up for small animals imaging is required.

Methods

We recently designed a facility targeted to provide the best support to a wide range of investigators involved in multidisciplinary researches. The metabolic and structural imaging center was born thanks to a collaboration among the Second University of Naples, the university of Naples "Federico II", and the "A. Cardarelli" Hospital of Naples. The Facility for Small Animal Imaging (SAIF) is dedicated to research studies on rodents. We critically examined both research and regulatory issues. Our facility will be able to satisfy a wide range of needs: training for researchers, study scheduling, data acquisition, archiving, image display, and analysis. The SAIF is equipped with an hybrid custom-made system microSPECT/Optical, a 7T microMR system, a microCT scanner, and microUS. The main applications are: toxicology screening, viral infections development, gene therapy, hepatic diseases, oncological imaging, functional and physiological imaging and others. The SAIF is staffed with: biologists, clinicians, biotechnologists, veterinarians, physicians, radiologists etc.
Furthermore it will house more than 5.000 animals, also providing a constant procedural support in surgery, imaging, and analysis.

Characteristics of equipment

Micro-CT (GE eXplore Locus)

The GE eXplore Locus scanner is an X-ray computed tomography system capable of performing imaging studies of specimen or small animals in vivo . The Locus system uses a X-ray detector with kV range of 35-80, and mA range of 0-500. The system has three isotropic resolution settings (27, 45 and 90μm) with a field of view (FOV) up to 80 mm in diameter. The Locus system uses a CCD with 10 micron square detector element and 100 mm x 50 mm active area. The scan time is of 5-60 min depending on the protocol used, with a sensitivity of milliMolar order.

Micro-CT (GE eXplore Locus)

Micro-MRI (7T Bruker)

The 7T 30-cm bore Bruker Biospec scanner is a dedicated imaging system equipped with several shielded gradients for in vivo applications (< 50 micron). The BioSpec system is also equipped for multinuclear and spectroscopy imaging (i.e. 1H, 31P, 15N, 13C, 19F). This instrument includes a breathing and heart gating/monitoring system to limiting negative effects on image quality. This feature is essential to study animals with an high breath and heart rate.

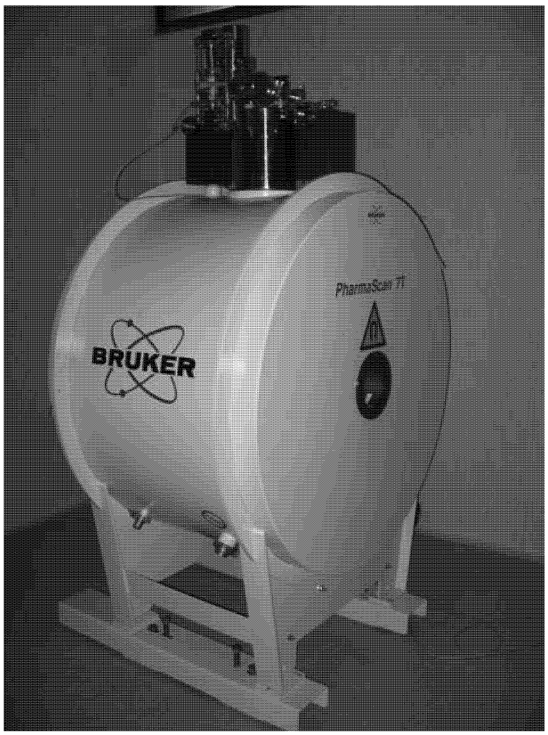

Micro-MRI (7 T Bruker)

Micro-PET (GE eXplore VISTA)

The GE eXplore VISTA microPET is a positron emission tomography scanner with a 3 cm (axial) x 6.7 cm (transverse) field of view. The system has an absolute sensitivity of 3% with a spatial resolution of ~1.2 mm in the center of the field, when using OS-EM for image reconstruction.

SPECT/FRI

MediSPECT/FRI is a sperimental, and small animal dedicated scanner for radiolabeled and fluorescence imaging, with a small field of view (2-56 mm), and a big spatial resolution (0.12 mm). Detector for Ionizing Radiations: hybrid detectors in Siliceous pixels (thick 0.3 mm), and in Cadmium Tellurium (thick 0.1 mm) linked to a reader chip MEDIPIX2; the detectors are matrices 256 x 256 with a gap of 55 □m, and a sensible area of 1.4 cm x 1.4 cm. Collimators: tungsten pinhole (diameter 0.3, 0.4, 1.0 mm) for Tc-99m, and I-125 tracers; Mask with opening coded for I-125.

Micro-US (VisualSonics Vevo 770)

The VisualSonics 770 High-Resolution Imaging System enables visualization, assessment, and measurement of anatomical structures and hemodynamic function in non-invasive imaging studies of small animals. B-mode (2D and 3D), power Doppler (2D and 3D), M-mode and pulsed-Doppler imaging mode are available for anatomical, cardiac and flow analysis, respectively. The high frequency at which the 770 operates (20-55MHz) allows for achieving spatial resolution down to 30 microns, the highest spatial resolution currently available in real time imaging.

MSI Center Flat

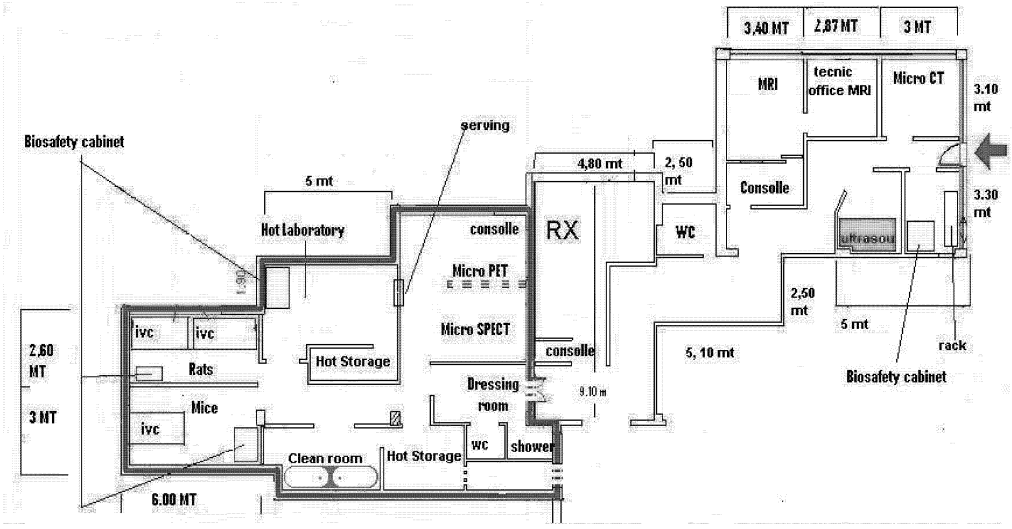

Biotechnology Center vivarium

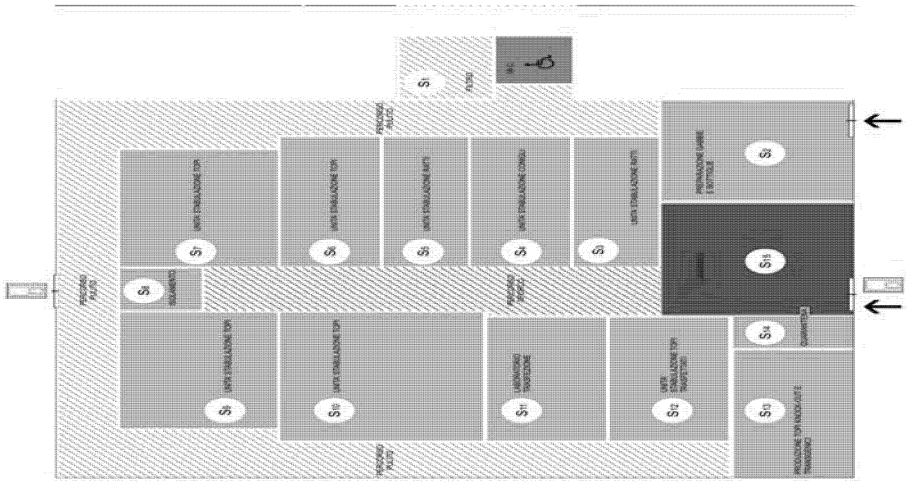

The vivarium is designated to hold mice, rats, and rabbits. It occupies an area of about 250 mq, including 8 housing units, two laboratories, as well as quarantine and isolation units able to hold about 5000 animals. Moreover a constant procedural support in surgery, imaging, and analysis is provided.
We have created as well a facility able to maximize our resources supporting the investigators as better as possible. At the same time we are focused to efficient network set-up between different specialists in order to obtain an adequate multidisciplinary approach .

Conclusions

We have created as well a facility able to maximize our resources supporting the investigators as better as possible. At the same time we are focused in efficient network between different specialists to obtain an adequate multidisciplinary approach.

The ever-increasing number of experiments carried on rodents (mostly rats and mice) couples with advances in small animal imaging systems such as microPET, optical, microCT, microMR, ultrasound and microSPECT. In this context a technical center set-up for small animals imaging is required.

We recently designed a facility targeted to provide the best support to a wide range of investigators involved in multidisciplinary researches. The metabolic and structural imaging center was born thanks to a collaboration among the Second University of Naples, the university of Naples “Federico II”, and the “A. Cardarelli” Hospital of Naples. The Facility for Small Animal Imaging (SAIF) is dedicated to research studies on rodents. We critically examined both research and regulatory issues. Our facility will be able to satisfy a wide range of needs: training for researchers, study scheduling, data acquisition, archiving, image display, and analysis. The SAIF is equipped with a hybrid custom-made system microSPECT/Optical, a 7T microMR system, a microCT

scanner, and microUS. The main applications are: toxicology screening, viral infections development, gene therapy, hepatic diseases studies, oncological, functional and physiological imaging and others. The SAIF is staffed with: biologists, clinicians, biotechnologists, veterinarians, physicians, radiologists, etc.

Bibliography

1. Stout DB. , Chatziioannou AF. , Lawson TP. , Silverman RW. , Gambhir SS. and Phelps ME. . (2005) Small Animal Imaging Center Design: The Facility at the UCLA Crump Institute for Molecular Imaging. Molecular Imaging and Biology 7(6): 393-402.
2. Contag CH, Bachmann MH (2002) Advances in in vivo bioluminescence imaging of gene expression. Annu Rev Biomed Eng 4:235–260.
3. Borah B, Gross GJ, Dufresne TE, Smith TS, Cockman MD, Chmielewski PA, Lundy MW, Hartke JR, Sod EX (2001) Three-dimensional microimaging (MRmicroI and microCT), finite element modelling and rapid prototyping provide unique insights into bone architecture in osteoporosis. Anat Rec 265: 101–110.
4. Turvey SE, Swart E, Denis MC, Mahmood U, Benoist C, Weissleder R, Mathis D. (2005) Noninvasive imaging of pancreatic inflammation and its reversal in type 1 diabetes. J. Clin. Invest. 115(9):2454-2461.
5. Cherry SR and Gambhir SS (2001) Use of positron emission tomography in animal research ILAR J 42: 219–32.
6. Sharma V and Piwnica-Worms D (2002) Molecular imaging of gene expression and protein function in vivo with PET and SPECT. J. Magn. Reson. Imaging 16: 336–51.
7. Stypmann J. (2007) Doppler ultrasound in mice. Echocardiography 24(1):97-112.

CHEMICAL ENGINEERING TRANSACTIONS, Volume 14, 2008
Edited by G. Marino, E. Bardone, A. Viglia
 ISBN 978-88-95608-02-0

The role of singularity points in the dynamics of a chemostat

CAMMAROTA Andrea acammarota@unisa.it
MICCIO Michele mmiccio@unisa.it
POLETTO Massimo mpoletto@unisa.it
Dipartimento di Ingegneria Chimica ed Alimentare, Università di Salerno
Via Ponte don Melillo - 84084 FISCIANO SA
Italy

In this work the dynamic behavior of a chemostat has been theoretically studied with the support of the singularity theory. The bioreactor is described by a simple two-dimensional, unstructured ODE model accounting for biomass and controlling substrate mass balances with variable yield coefficient. The main aim is an in-depth investigation on the dynamics of the bioreactor, in particular on the presence and the role of codimension one singularities. In comparison with the previous work of Ajbar (2001), a more extensive analysis has been performed and the role of all the involved parameters is evaluated. In particular, the effects of kinetic parameters and yield variability on the dynamics of the bioreactor are systematically investigated. Therefore, for this system, an exhaustive non-persistent bifurcation diagram is drawn; it allows exploiting the conditions that determine dynamic regimes in the bioreactor and, to some extent, their stability features.

1 Introduction.

The chemostat is a continuous bioreactor for microbial cultivation operating at a constant reaction volume and characterised by a constant inlet flow rate of constant composition (Bailey & Ollis, 1986). It is, probably, the simplest and the most widespread type of continuous bioreactor. Its dimensionless mass balance equations can be expressed in the following form:

$$\begin{cases} x'(t) = [\mu(s(t)) - dil - k_d]x(t) \\ s'(t) = dil(1 - s(t)) - \dfrac{\mu(s(t))}{y(s(t))}x(t) \end{cases} \tag{1.}$$

where x is the biomass concentration, s the limiting substrate concentration and *dil* the dilution rate. The adopted growth kinetics is the one proposed by Andrews (Bailey & Ollis, 1986) which models the effect of substrate inhibition on microbial reproduction:

$$\mu(s) = \frac{s}{k + s + k_I s^2} \tag{2.}$$

According to Smith & Waltman (1995), the model in eq. (1) with a constant yield is not capable of explaining any oscillatory behaviour in a chemostat, independently of the kinetic expression chosen to describe the microbial growth. In the work by Pilyugin &

Waltman (2003), it is stated that a necessary condition to ensure the existence of dynamical regimes is to assume that the yield is not constant but dependent on the substrate concentration. A common assumption in literature to model periodic behaviour of a chemostat is to suppose a linear dependence of the yield coefficient on the substrate concentration (Agrawal et al., 1982). Therefore, it is assumed that:

$$y(s) = 1 + y_1 s \tag{3.}$$

A coefficient k_d, which takes account of the maintenance rate (van Bodegom, 2005), has been introduced in eq. (1): as reported in that paper, this term is included in the interval (0.01 - 0.1) in several experimental observations. In this work, an in-depth investigation about the existence and nature of the dynamical regimes for this type of reactor is performed: in particular, the analysis performed by Ajbar (2001) has been extended detecting all the sets of codimension one singularity for steady and Hopf points and plotting them in a non-persistent bifurcation diagram in the parameter plane spanned by k and k_I. This procedure allows obtaining information about the occurrence of global bifurcations. Furthermore, the effect produced by y_1 on the occurrence of singularities is investigated.

2 Complete singularity diagram of a chemostat.

2.1 A list of the investigated singularity points

Before drawing the non-persistent bifurcation diagrams, a short explanation of the meaning of this instrument is appropriate: in a compact subset P of the parameter plane spanned by k and k_I, it is possible to plot some one-dimensional manifolds (e.g., curves) that determine the partition of P in some regions which show qualitatively similar solution diagrams of static and dynamical regimes as a function of the dilution rate. Unfortunately, this instrument is not problem-free. Golubitsky & Schaeffer (1985) reported a general theorem which states the topological equivalence for steady state solution diagrams belonging to the same region and also a weaker extension to the case of Hopf points, but no exhaustive conclusions can be drawn for periodic regimes or global bifurcations. However, despite this lack of generality about these complex behaviours, the singularity diagrams permit to obtain some interesting insights into them.

The static singularities, which occur in a chemostat with a kinetic law given by eq. (2) and a yield expression described by eq. (3), are:

1. Codimension one: transcritical (collision of two steady state branches with an exchange of respective stability properties).
2. Codimension two: pitchfork (a single stable (resp. unstable) steady state branch bifurcates into three steady state branches, two of them being stable (resp. unstable) and the third one unstable (resp. stable)).

The occurring dynamical singularities are:

1. Codimension one: Takens-Bodganov (TB) bifurcation (collision and annihilation of a Hopf and a homoclinic bifurcation on a saddle-node point), Hopf convergence or H_{01} singularity (collision of two

supercritical or two subcritical Hopf points), Bautin or H_{10} bifurcation (change from supercritical to subcritical type for a Hopf point or vice versa).

A third class of lines must be plotted in the singularity diagram: a limit to physically meaningful regimes on a solution diagram is that dil≥0; therefore, the loci of transcritical, saddle-node or Hopf points occurring when dil=0 are the ones that separate regions in which such bifurcations occur from the ones in which they have disappeared in the corresponding solution diagrams.

2.2 Singularity diagram for a chemostat with y_1=10 and k_d=0.05.

The above listed loci are computed by deriving the Lyapunov-Schmidt reduction for both static and Hopf points and then determining the analytical equations that satisfy the degeneracy conditions for each type of singularity (Golubitsky & Schaeffer, 1985).

In figure 1, the singularity diagram for the case y_1=10 and k_d=0.05 is reported; in figure 2, the solution diagrams corresponding to the regions defined in figure 1 are plotted. These latter have been obtained using the continuation software AUTO2000 (Doedel et al., 2006).

A general description of the system can be given by comparing the dynamics of the resulting 13 regions. Zone 13, characterised by high values of both k and k_I which determine a very small μ(s), shows only washout solutions: in fact, these conditions prevent the population from growing because the maintenance term is greater than the growth process. The lines that delimit this subset are the threshold of minimum functionality of the bioreactor and, if the physical parameters lie over them, then the choice of substrate is inadequate or there are some other limiting factors that prevent the culture from growing in such a chemostat. Even the regions close to this border line are characterised by low productivities and steady solutions with low dilution rates; in fact the maximum growth rate can also be limited to 1% of the theoretical maximum growth rate (see plot 11 in figure 2).

As reported by Ajbar (2001), the equation of the pitchfork singularity line is $k=k_I$. If $k>k_I$, dynamical phenomena are quite unlikely: in fact, periodic behaviours for $k>k_I$ occur only when the inhibition constant is very low (region 6). The black dashed line separates the regions in which the intersection of the nontrivial and the washout branch occurs from the ones in which they do not cross: in the latter case, the washout solution is always stable and the stable manifold of the intermediate unstable regime separates the basin of attraction of this point from the one corresponding to the nontrivial stationary point.

The behaviour of the system is much more interesting when $k<k_I$: under the pitchfork singularity line, a saddle-node bifurcation, essentially due to the presence of the maximum in the kinetic law, appears in the solution diagram. In this case the nonlinearities of the system have a stronger influence and this is proved by the appearance of dynamical solutions. In regions 3 and 8, periodic solutions originating from H_{01} singularity points are present. The two plots related to region 3 pinpoint a limit of the singularity approach: as can be observed, a single diagram is not sufficient to characterise the dynamical behaviour of this zone (i.e., it does not show all equivalent solution diagrams).

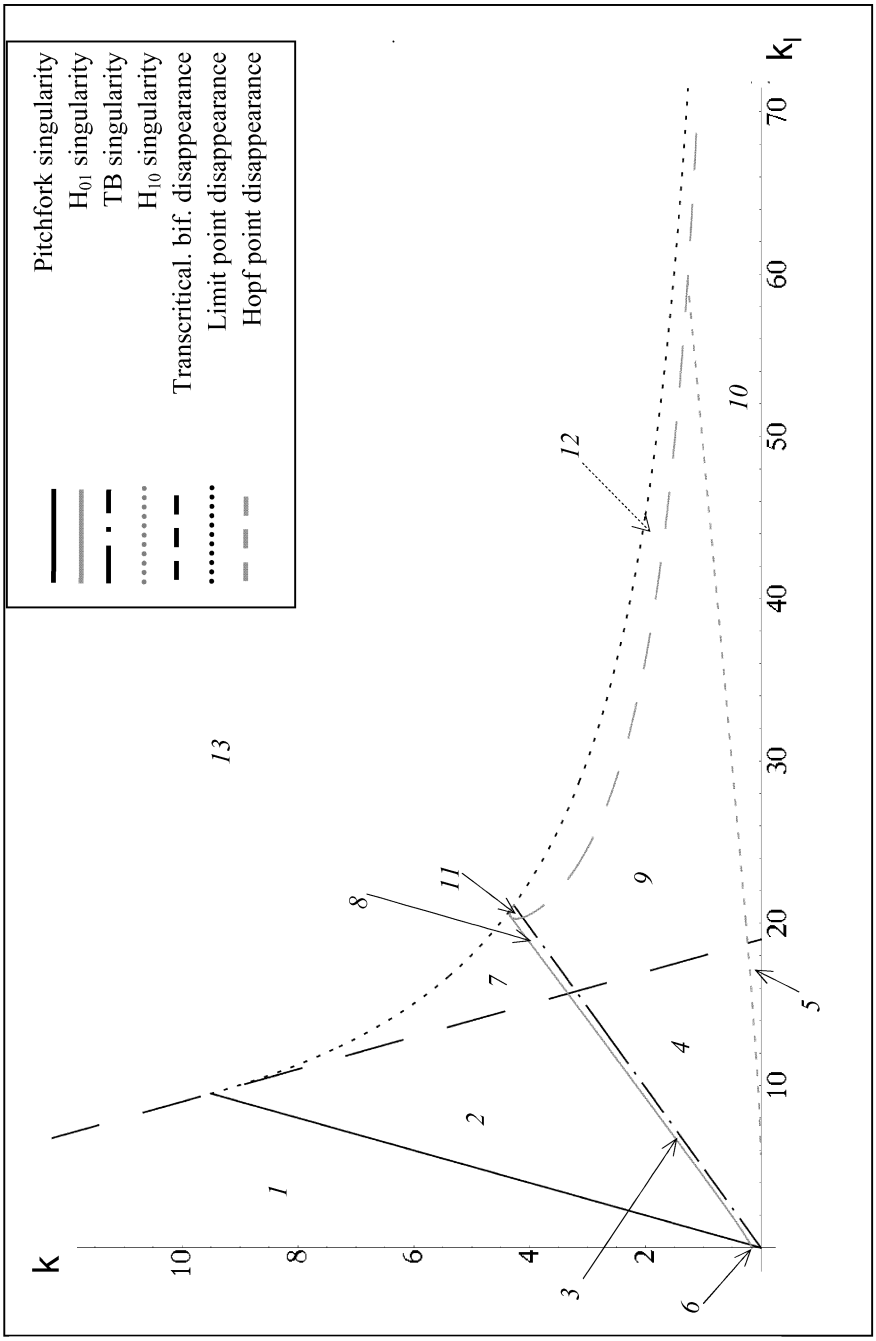

Figure 1: Singularity diagram for a chemostat with an Andrews growth kinetics and linear yield (y_1=10, k_d=0.05). Numbers are used to identify the regions in which the subset P of the 2D parameter subspace is partitioned.

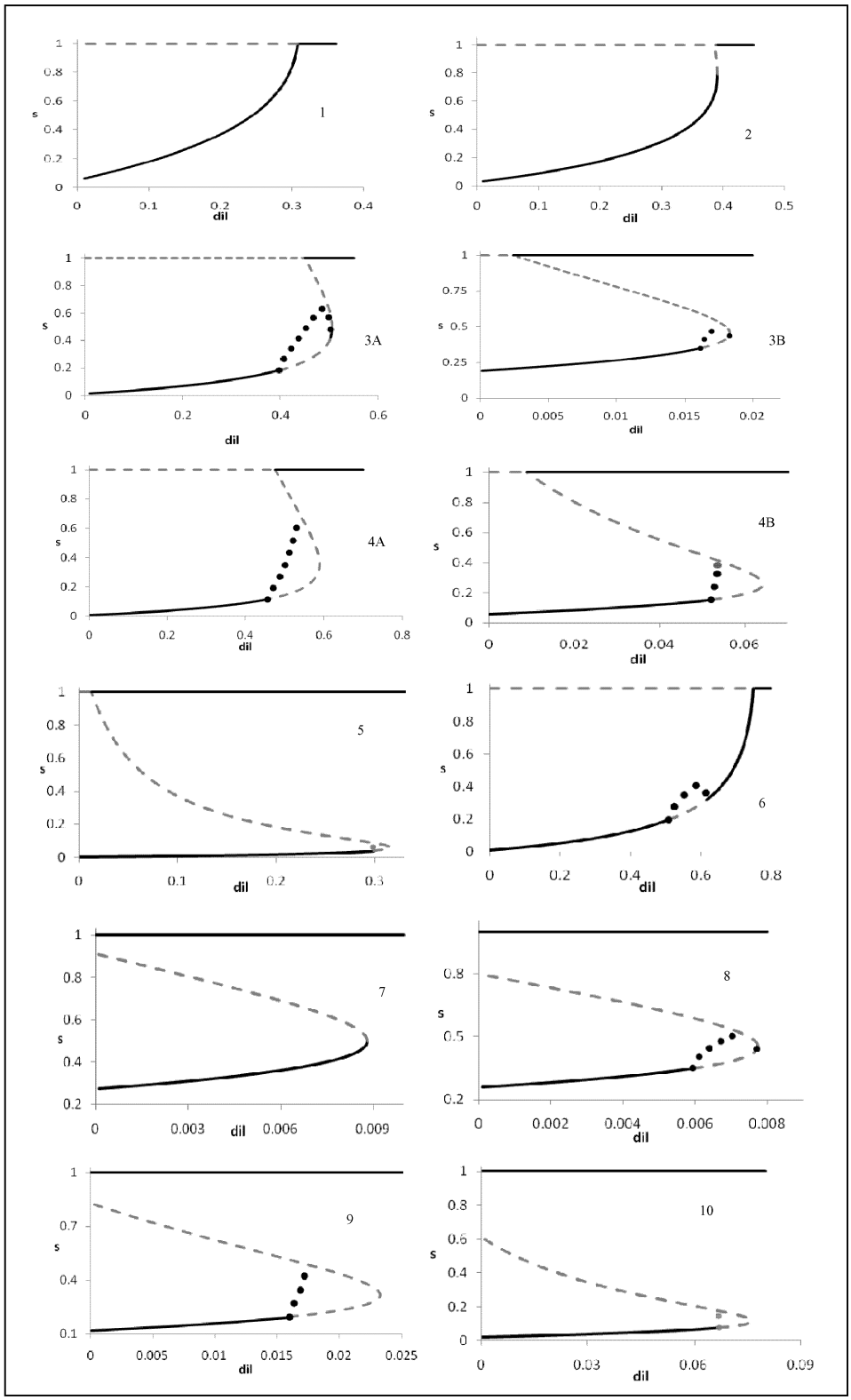
1
2
3A
3B
4A
4B
5
6
7
8
9
10
s
dil

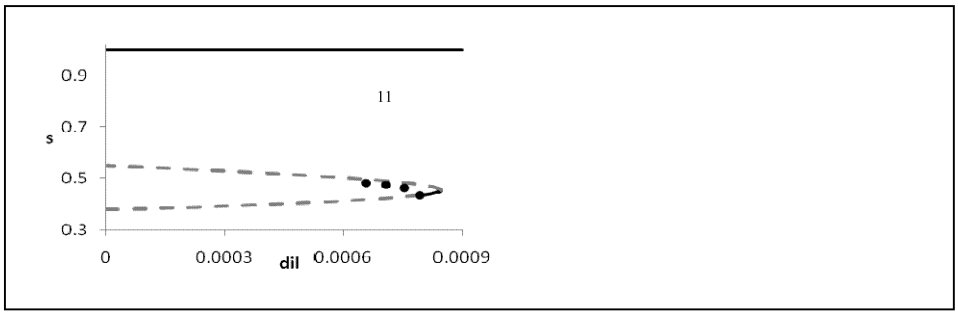

Figure 2 (on two pages): Solution diagrams for the regions defined in the previous figure 1.

In this case, the intersection of the stable periodic regime with the unstable steady state can cause the breakage of the periodic branch into two pieces terminating with a homoclinic bifurcation on the unstable steady branch: plot 3A shows the case in which a continuous periodic branch connects the two Hopf points, while plot 3B describes the case in which the global bifurcations appear: in the latter situation, the interval of dilution rates included between the ones in which homoclinic phenomena occur, is characterised by the absence of stable regimes except from the washout ones. Furthermore, region 8 has dynamical features similar to case 3B rather than 3A (with the only difference that the transcritical point does not appear in the solution diagram).
The dash-dot line indicates a TB singularity, that is, a collision between a Hopf point and the saddle-node (or limit) point. As defined before, a homoclinic bifurcation also converges in this point: this implies that, on the upper side of this line but close to it, the solution diagram must be similar to the one described in 3A of figure 2; in fact, this topology permits the collapse of the right Hopf point and the adjacent homoclinic bifurcation on the limit point when the dilution rate approaches the bifurcation value. In the lower part of the plot in figure 1, (that is, under the TB locus), only the left Hopf point and its correspondent homoclinic bifurcation survive as indicated by diagrams 4A, 4B and 9 in figure 2. Also in region 4 some global bifurcations occur and, hence, two non-equivalent solution diagrams are required to characterise it. In diagram 4A the periodic branch for the left Hopf is made up of only stable periodic orbits like the ones in region 3 while for high k_I and low k a fold bifurcation appears (starting from the homoclinic one) and some unstable limit orbits arise: in particular, the homoclinic bifurcation occurs between an unstable point and an unstable limit cycle for this subset of region 4 (see plot 4B). A similar phenomenon can be observed also in region 9.
The dotted gray line indicates the singularity locus in which the instability of the periodic orbits branch expands up to the Hopf point eliminating the stable ones: therefore both in region 5 and 10, the Hopf point is subcritical and no stable periodic orbits exist.
A final remark has to be made about the disappearance of Hopf points: the dashed gray line indicates the boundary for this type of singularity. In the part of parameter space

bordered by the H_{10} and the TB singularity, two Hopf points occur; in region 11 one of these points disappears while the second one vanishes when the right part of the curl line which encloses region 11 is crossed. As already said, under the TB singularity line a single Hopf point exists: this bifurcation point disappears when the dashed gray line is crossed: in this region all the steady points are unstable and the only stable regimes are periodic ones (as in region 12, for which the solution diagram is not reported here).

3 The effect of y_1 on the dynamics of the chemostat

A description about the effect of y_1 on the singularity diagram follows. In order to evaluate its influence, the singularity diagrams for different values of these parameters are drawn.

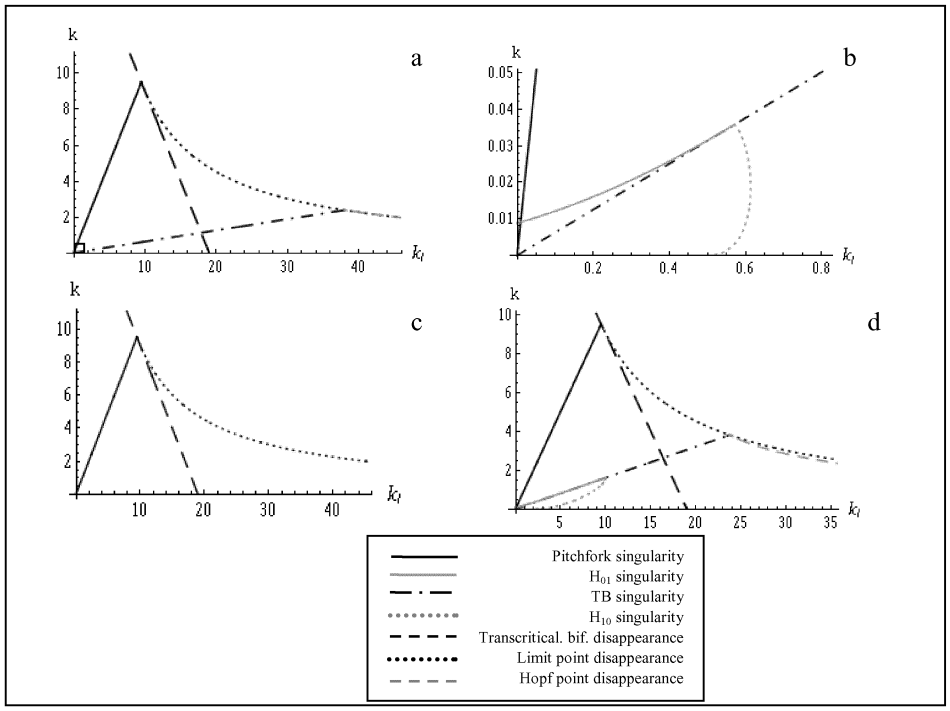

Figure 3: Singularity diagrams for k_d=0.05, (a) y_1=2, (b) magnification of the detail in the black square for case (a), (c) y_1=0.5, (d) y_1=5.

In agreement with the conclusions obtained by Ajbar (2001), only if $y_1>1$ is it possible to observe dynamical regimes. Therefore, if $y_1<1$, the only singularity lines that are present in the diagram are the pitchfork and the disappearance ones (therefore only static singularity lines, as can be observed in figure 3c).

In figure 3a and b, the singularity diagram for y_1=2 is reported. As can be seen, a first evident effect is the significant reduction of the region between the H_{01} and the TB singularity curves: differing from the previous case, the two lines cross each other

causing the interruption of the H_{01} curve in the intersection point that will be called S where also the H_{10} singularity curve converges; therefore the region with the presence of two Hopf points is much narrower than in the case y_1=10 and the S point is a singularity with a higher codimension than one as there is a convergence of two codimension one curves in it. Similarly to figure 1, the region included between TB and H_{10} line shows solution diagrams with a single periodic branch and the closer the parameter point to Bautin curve is, the smaller the portion of periodic stable solutions around the Hopf point is in the corresponding solution diagram (this behaviour is similar to the ones in figure 2 case 4B): in fact, stable limit cycles disappear if the parameters belong to the region behind both the TB and the H_{10} curves (like the one plotted in figure 2 case 5). An obvious consequence of this observation is that from a TB point located on the left of S, the Hopf point collapsing on it is supercritical while it is subcritical if the TB point is positioned on the right of S in figure 3a and b.
Therefore it is possible to conclude that stable periodic regimes (which can be effectively observed) are possible only for parameter points lying in the area enclosed by the vertical axis, the H_{01} and the H_{10} singularity lines. Comparing figures 1, 3a, 3c and 3d, it can be deduced that decreasing the y_1 value, the TB-H_{01}-H_{10} intersection singularity point moves progressively towards the origin up to vanishing for y_1=1; hence, lowering y_1 limits more and more the occurrence of stable periodic regimes (see, for example the case y_1=2 plotted in figure 3b in which the region with stable limit cycles is very small); on the contrary when the parameter increases, the TB-H_{01}-H_{10} intersection moves towards the disappearance loci until it vanishes. At this point, it generates the curl of the dashed gray curve, which encloses region 11 in figure 1 and indicates a different disappearance mechanism for the two Hopf points.

4 Conclusions

A final summary about the dynamics of the chemostat is that the effect due to the positive slope of the yield function with substrate concentration is the main cause of oscillating regimes; unstable periodic regimes are possible as well as subcritical Hopf points (that Ajbar, 2001, did not indicate) as the inhibitive action becomes stronger; instead, the occurrence of stable periodic regimes is more likely for rapidly growing yields and low inhibition constant.

5 References

Agrawal, P., Lee C., Lim, H. C., Ramkrishna, D., 1982, Chem. Eng. Sci. 37, 453
Ajbar, A., 2001., Chem. Eng. Sci. 56, 1991.
Bailey G.E., Ollis D.F, 1986 Biochemical Engineering Fondamentals. MacGraw Hill.
Doedel E.J. et al. 2006, Auto 2000. http://sorceforge.net/projects/auto2000.
Golubitsky M. & Schaeffer A., 1985,. Singularities and groups in bifurcation theory. Springer Verlag
Kuznetsov, Y.A., 2000, Elements of Applied Bifurcation Theory. Springer, New York.
Pilyugin S.S.- Waltman P., 2003, Mathematical Biosciences. 182, 151-166.
Smith M. & Waltman P., 1995, The theory of the chemostat. Cambridge Univ. Press.
Van Bodegom P., 2007,. Microbial ecology. 53, 513.

CHEMICAL ENGINEERING TRANSACTIONS, Volume 14, 2008
Edited by G. Marino, E. Bardone, A. Viglia
 ISBN 978-88-95608-02-0

Heterologous protein production by yeast in aerated fed-batch cultures: relevance of the host strain viability

Romano V.[1], Paciello L.[1], Parascandola P.[1], Palermo V.[2], Mazzoni C.[2], Falcone C.[2], de Alteriis E.[3]
[1]Dip.to Ingegneria Chimica e Alimentare, Università di Salerno, Via Ponte Don Melillo, 84084 Fisciano, Salerno, Italy; [2]Dip.to Biologia Cellulare e dello Sviluppo, Università "La Sapienza", Piazzale Aldo Moro 5, 00185 Roma, Italy; [3]Dip.to Biologia Strutturale e Funzionale, Università degli Studi di Napoli "Federico II", Via Cinthia 80100, Napoli, Italy

The auxotrofic *S. cerevisiae* BY4741, carrying the fusion *PIR4-IL1β*, and able to secrete the human interleukin-1β into the culture medium, has been employed in an aerated bioreactor working as a fed-batch. Notwithstanding proper formulation of the culture medium, the performance of the host strain BY4741 [Pir4-IL1β] in fed-batch was not satisfactory: biomass density was far from that expected, glucose and ethanol accumulated during the runs. To test if the oxidative stress was responsible for the observed behaviour, the mutant BY4741 Δyca1, deleted for the *YCA1* gene, coding for a caspase-like protein involved in yeast apoptosis, was transformed with the expression cassette containing the fusion *PIR4-IL1β*, and assayed in the same aerated fed-batch system. The different performances exhibited by both BY4741[Pir4-IL1β] and BY4741 Δyca1 [Pir4-IL1β], together with the study of death kinetics during operation runs, evidenced the relevance of strain viability in the operative conditions employed.

1. Introduction

Saccharomyces cerevisiae has been recognized as the most useful eukaryotic microorganism for heterologous protein production since 1978, when its genetic transformation was established (Hinnen et al., 1978).

S. cerevisiae is a glucose-sensitive yeast and displays aerobic alcoholic fermentation on glucose (Alexander and Jeffries, 1990). The regulation of glucose metabolism in yeast has a major implication in the production of heterologous proteins, since a complete oxidative metabolism of the carbon source should be maintained during the process to achieve high cell densities with high yields of recombinant product (Mendoza et al., 1994). In this concern, fed-batch technique, which permits substrate limitation, offers a tool for both metabolic control of sugar overflow metabolism and oxygen consumption rate, avoiding engineering limitations with respect to cooling and oxygen transfer (Enfors, 2001).

In the present paper, the auxotrofic *S. cerevisiae* BY4741, carrying the fusion *PIR4-IL1β,* has been employed as host strain to produce human interleukin-1β (IL-1β) in an aerated bioreactor working as a fed-batch. This strain already revealed capable to express and secrete interleukin-1β as a growth-linked product into the medium of shake-flask cultures (Romano F. et al., 2007).

To achieve high biomass yield and productivity, an exponentially increasing feed was initially applied to the bioreactor; then, the feed was switched to a constant value,

to get over the oxygen transfer rate limitation in the reactor. In the operative conditions employed, the behaviour of the recombinant strain was far from that expected.

Considering that fed-batch operations were carried out under vigorous and continuous aeration, it has been hypothesized that oxidative stress could play a significant role in determining the observed behaviour. To test this hypothesis, the mutant BY4741 Δyca1, deleted for the *YCA1* gene, coding for a caspase-like protein involved in yeast apoptosis (Madeo et al., 2002; Mazzoni et al., 2005) was transformed with the expression vector containing the fusion *PIR4-IL1β*, and assayed in the same aerated fed-batch system.

The performances exhibited by both the recombinant strains, BY4741 [Pir4-IL1β] and BY4741 Δyca1 [Pir4-IL1β], were compared and cell death kinetics during operation runs examined.

2. Materials and Methods

2.1 Strains

S. cerevisiae strain BY4741 *(MATα, ura3Δ0, leu2Δ0, met15Δ0, his 3Δ1)* (EUROSCARF collection, Heidelberg, Germany), transformed with a YEplac vector containing the gene fusion *PIR4-IL1β* (Romano F. et al., 2007), and indicated as BY4741 [Pir4-IL1β] was used in this work.

The same expression vector was employed to transform the deletion mutant *S. cerevisiae* BY4741 Δyca1 (*MATα, ura3Δ0, leu2Δ0, met15Δ0, his3Δ1, yor197w::kanMX4)* (Madeo et al., 2002). Yeast transformants were selected for rail prototrophy on SD medium (0,67% YNB, 2% glucose and required auxotrophy at the concentration of 10 μg ml^{-1}).

2.2 Fed-batch cultures

Fed-batch cultures were perfomed in a 2.5 l stirred Bioflo 110 (New Brunswick, Sc.). Cultivation started with a batch phase using 1 l of defined mineral (DM) medium, prepared according to Verduyn et al. (1992), containing 20 g glucose and supplemented with vitamins, trace elements and bactocasaminoacids (BectonDickinson & Co., Sparks, MD 21152 USA) (Romano F. et al., 2007). Oxygen was supplied by sparging the bioreactor with air at a flow of 1 vvm and the cascade system acted with the agitation speed, automatically increasing or decreasing until the DOT set-point (30% air saturation) was reached. The culture pH was maintained at 5.00 by automatic addition of 2 N KOH.

When glucose was completely depleted, the feeding was started with a solution containing 50% w/v glucose, other than vitamins, trace elements, iron sulphate and bactocasaminoacids (Romano F. et al., 2007).

The exponential profile of flow rate *F(t)* was obtained from the mass balance on limiting substrate (Enfors, 2001) and calculated according to:

$$F = F_0 \cdot \exp(\mu \cdot t) \qquad (1)$$

where F_0 was given by:

$$F_0 = \frac{\mu \cdot (X_0 \cdot V_0)}{S_R \cdot (Y_{X/S})} \qquad (2),$$

X_0 and V_0 were biomass density and volume at the start of feeding, respectively; S_R was the concentration of the growth limiting substrate in the reservoir; $Y_{x,s}$ was the respiratory biomass yield; and μ was the specific growth rate of the producer strain. The exponential feeding was built up to ensure a constant μ of 0,16 h^{-1}, below the maximum (μ_{max}= 0,39 h^{-1}), which was evaluated in a preliminary experiment carried out in Erlenmeyer flask containing DM medium (Romano et al., 2007).

After the exponentially increasing flow rate, feed was switched to a constant value. During fed-batch runs, aeration was accomplished as described above in the case of the batch phase, except for the air flow which was of 1.5 vvm and pH maintained by automatic addition of 10% v/v NH_4OH. Dow Corning 1510 (dil. 1:10) was used as antifoam. The bioreactor was inoculated with an adequate aliquot of a 24 h pre-culture, to give an initial $O.D._{590}$ of 0.2 in the bioreactor.

All the fed-batch cultures were carried out in triplicate.

2.3. Biomass determination

Biomass was determined by optical density measurements at 590 nm and dry weight determination. Unless otherwise stated, biomass is always referred as dry weight. In the latter case, culture samples were washed twice, resuspended with distilled water, and dried for 24 h at 105 °C . Parallel samples varied about 3-5%. The calibration curve relating $O.D_{590}$ values to biomass concentration provided a correlation factor of 2.45 $O.D_{590}$ per mg ml^{-1}.

Cell viability during fed-batch runs was determined by viable count on supplemented DM agar plates, incubated at 30 °C for 48 h.

2.4. Analyses

Samples were quickly withdrawn from fed-batch cultures, filtered on 0.45 μm GF/A filters (Millipore, Bedford, MA USA) and filtrates analysed to determine residual glucose, ethanol and interleukin-1β concentrations. Residual glucose in the medium was determined by GOD-Perid from R-Biopharm (Roche, Mannheim, Germany). Ethanol production was measured with the enzymatic kit (176290) from R-Biopharm (Roche, Mannheim, Germany). Interleukin-1β was determined by immuno-blot analysis in Bio-Dot® Microfiltration Apparatus (Bio-Rad, Hercules, CA, USA) and quantified by densitometric analysis (MultiAnalyst, Bio-Rad) using the human EuroClone IL-1β as a standard (Romano V. et al., 2007). All samples were analysed in triplicate and the values of standard deviation obtained varied between 3-5%.

3. Results

3.1 Growth of *S. cerevisiae* BY4741 [Pir4-IL1β] in aerated fed-batch culture

Saccharomyces cerevisiae BY4741 [Pir4-IL1β] was cultured in the aerated bioreactor, employing DM medium and glucose as carbon source. After a batch phase of 16 h, exponential feed was started and maintained for 21 h, then the feed was switched to a constant value for 9 h.

In Fig. 1a, total biomass of the producer strain and total amount of the fusion protein secreted into the medium during the fed-batch phase, are reported. The recombinant product accumulated along the entire time course of growth, with a yield ($Y_{p,x}$) of 387 ng mg^{-1}. After 20-22 h of feeding, no further increase in biomass and, consequently, in product, was observed.

Yeast metabolism was fully oxidative in the first 8-10 h of the exponential feeding, being residual glucose in the medium absent and ethanol concentration at the same level achieved at the end of the batch phase (Fig. 1b). Then, the behaviour of the recombinant yeast was no longer consistent with the feeding profile applied: accumulation of glucose in the medium and concomitant ethanol production were observed (Fig. 1b). Apparently, glucose up-take of yeast cells was impaired and/or the amount of viable cell in the bioreactor diminished. The resulting excess glucose determined the shift of yeast metabolism towards fermentation.

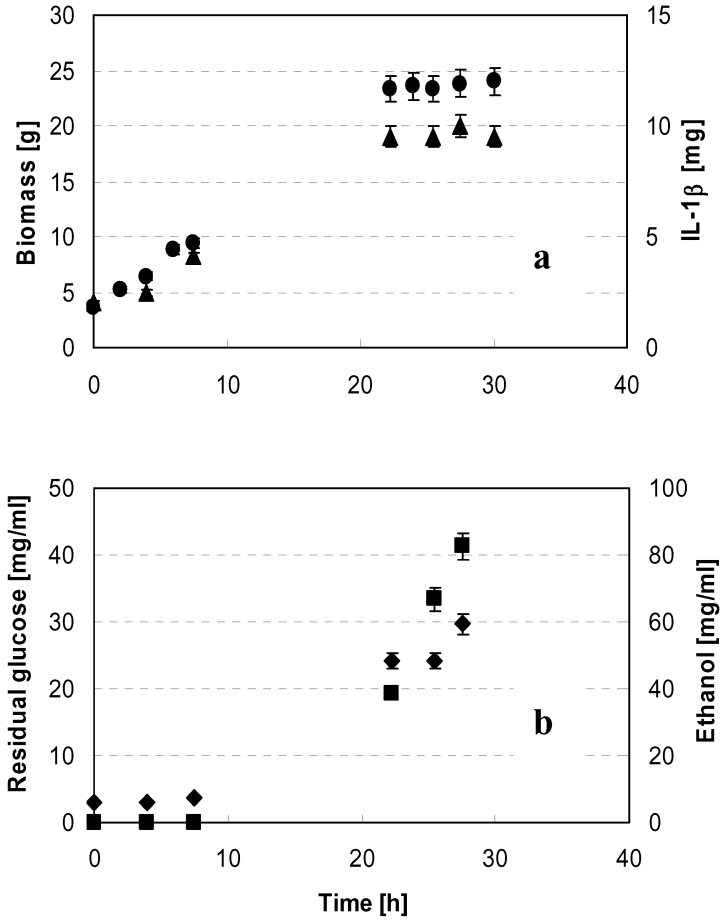

Fig. 1. Fed-batch run with BY4741 [Pir4-IL1β]: total biomass (●) and total amount of recombinant protein (▲) (**a**); residual glucose (■) and ethanol (♦) in the medium (**b**).

In the same operative conditions, a baker's yeast strain, isolated from a commercial sample, was able to display a fully respiratory metabolism along the entire fed-batch run (data not shown), achieving a final biomass concentration of 77 mg ml^{-1}, significantly higher than that obtained with BY4741 [Pir4-IL1β] (14,7 mg ml^{-1}, considering that the final volume of the broth-culture was 1.7 l) (Fig. 1a).

3.2. Comparison between BY4741 [Pir4-IL1β] and BY4741 Δyca1 [Pir4-IL1β] in aerated fed-batch cultures

Considering that fed-batch operations were carried out under continuous aeration, it was supposed that oxidative stress could affect strain viability and, consequently, explain the behaviour of the recombinant yeast. To test this hypothesis, the mutant BY4741 Δyca [Pir4-IL1β] was assayed in the same operative conditions previously employed for BY4741 [Pir4-IL1β].

Total biomass and residual glucose of BY4741 Δyca [Pir4-IL1β] monitored along the fed-batch run, are reported in Fig. 2, and compared to the corresponding data obtained with the original strain. Growth of the deletion mutant prolonged for further 10 hours with respect to that of BY4741 [Pir4-IL1β] (Fig. 2, top panel). As a consequence, total final biomass was 34 *vs*. 25 g of the original strain. Accordingly, a higher amount of recombinant protein was obtained, since the product yield ($Y_{p,x}$) remained the same (data not shown). Also in the case of the deletion mutant, glucose accumulated in the medium (Fig. 2, bottom panel), even though to a lesser extent.

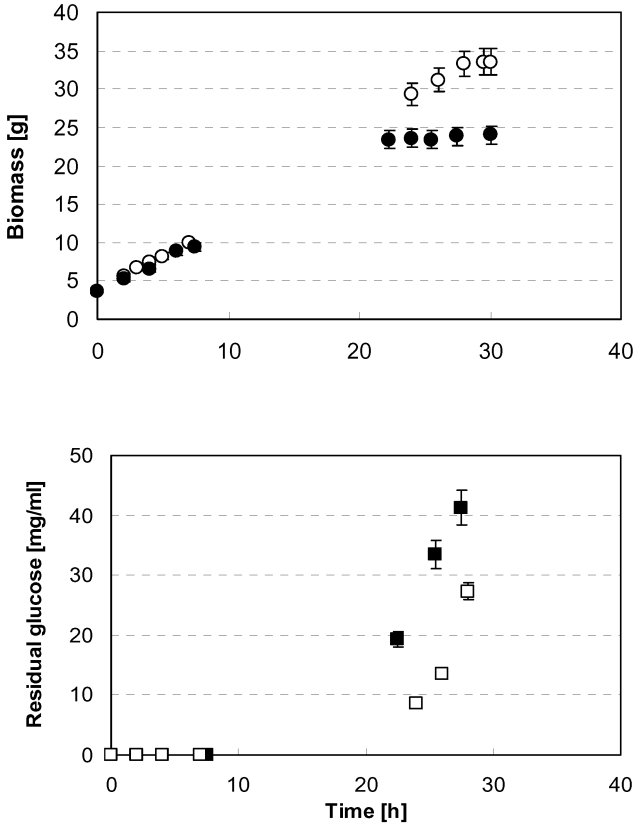

Fig. 2. Performance in fed-batch of the two recombinant strains: total biomass (●) and residual glucose (■) of BY4741 [Pir4-IL1β]; total biomass (○) and residual glucose (□) of BY4741 Δyca [Pir4-IL1β].

Cell viability of both BY4741 [Pir4-IL1β] and BY4741 Δyca [Pir4-IL1β] was monitored during the respective fed-batch runs by viable count of colony forming units (c.f.u.) and expressed as the ratio c.f.u./O.D.$_{590}$, where O.D.$_{590}$ corresponded to the total biomass (viable and dead cells) present in the bioreactor. Data obtained are reported in Fig. 3. Viability of both the strains diminished during the runs, though in the case of the deletion mutant the value of the specific death rate constant was lower than that of the original strain (0,011 *vs.* 0,026 h^{-1}, respectively). Apparently, the deletion in the *YCA1* gene increased host viability, in the operative conditions examined.

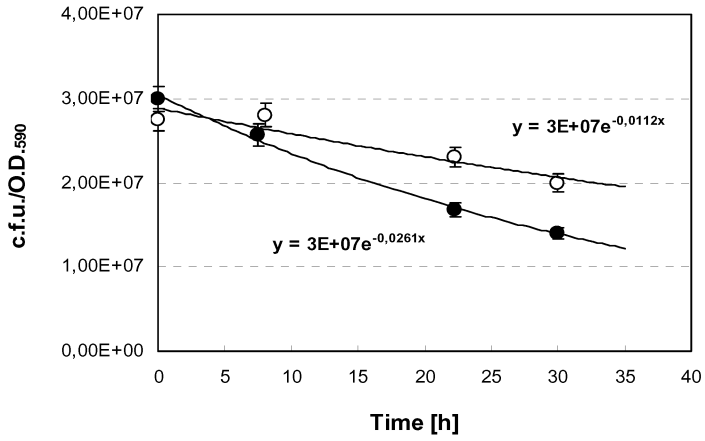

Fig. 3. Death kinetics of the two recombinant strains, BY4741 [Pir4-IL1β] (●) and BY4741 Δyca [Pir4-IL1β] (○) during fed-batch runs.

4. Discussion

In heterologous protein production by *S. cerevisiae* strains, auxotrophic host systems (*i.e.* strains with multiple auxotrophic mutations, such as *leu2*, *ura3*, *his3*, *trp1*, etc.), derived from industrial yeast strains, are widely used to ensure maintenance of expression vectors with selectable markers (Çakar et al., 1999). These systems are usually isogenic and haploid, differently from industrial strains which are usually diploid or polyploid and prototrophic.

Heterologous protein production with *S. cerevisiae* strains is mostly performed in bioreactors working in a fed-batch mode to avoid engineering limitations and exert metabolic control by sugar limitation. The latter promotes oxidative metabolism in the host with high biomass and product yields.

Notwithstanding proper formulation of the culture medium, the recombinant BY4741 [Pir4-IL1β], grown in fed-batch reactor, is able to sustain a fully oxidative metabolism only half-way through the exponential feeding, then the carbon source begins to accumulate and ethanol is produced until cell growth definitively stops. As a matter of fact, BY4741 cells precociously begin to die during the run, as shown by cell death kinetics.

This unexpected behaviour cannot be ascribed to the so-called "metabolic burden", consequent to the introduction of the foreign DNA (Görgens et al., 2001), since it is observed also in the case of the wild type BY4741 (data not shown).

Deletion of *YCA1* gene undoubtedly improves host viability. This supports the hypothesis that oxidative stress, arising during the continuous and vigorous aeration in the bioreactor, is highly probable and consistently leads to apoptotic scenarios. Apoptosis or programmed cell death (PCD) is now recognized to occur also in yeasts (Madeo et al., 1999).

Under oxidative stress, yeast cells would produce reactive oxygen species (ROS), which would induce *YCA1* gene to produce the protein caspase, involved in the regulated process of PCD (Madeo et al., 2002).

However, the performance of the deletion mutant as well, is far from that of an industrial strain. Apparently, other environmental stresses, deriving from process conditions (e.g. shear stress) are exerted on the yeast cells and result more severe for auxotrofic strains with respect to prototrophic ones and, mostly, haploid *versus* diploid. Indeed, *S. cerevisiae* BY4741, a haploid strain mutagenized to introduce many auxotrophies, could be intrinsically weaker than prototrophic yeasts.

The results obtained show that host viability is a relevant strain feature which has to be carefully evaluated in the set up of a bioprocess. However, taking into consideration that auxotrophic strains continue to be both useful tools acting on genes involved in the sensitivity to different stress and longevity, and convenient platforms in the field of heterologous protein production (Pronk, 2002), new metabolic and bioprocess strategies should be developed for a better their exploitation.

Acknowledgements

This work was partially supported by University of Naples "Federico II" (Research Departmental Funds, 2007) and of University of Salerno (funds ex 60%, 2006-07, Research project: "Heterologous protein production by engineered yeast cells and fed-batch modelling").

5. References

Alexander M.A., T.W. Jeffries, 1990, Respiratory efficiency and metabolite partitioning as regulatory phenomena in yeasts. Enzyme Microbiol. Technol.12, 2-19.

Çakar Z.P., U. Sauer, J.E. Bailey, 1999, Metabolic engineering of yeast: the perils of auxotrophic hosts. Biotechnol. Lett. 21: 611-616.

Enfors S.O., 2001, Baker's yeast. In: C. Ratledge and B. Kristiansen, Eds., Basic Biotechnology. Cambridge University Press, p. 377-389.

Görgens J.F., W. van Zyl, J.H. Knoetze, B. Hahn-Hägerdal, 2001, The metabolic burden of the *PGK1* and *ADH2* promoter systems for heterologous xylanase production by *Saccharomyces cerevisiae* in defined medium. Biotechnol. Bioeng. **73**: 238-245.

Hinnen A., J.B. Hicks, G.R. Fink, 1978, Transformation of yeast. Proc. Natl. Acad. Sci. USA. 75: 1929-1933.

Madeo F., E. Fröhlich, M. Ligr, M. Grey, S.J. Sigrist, D.H. Wolf , K.U. Fröhlich, 1999, Oxygen stress: a regulator of apoptosis in yeast. J. Cell Biol. 145: 757-767.

Madeo F., E. Herker, C. Maldener, S. Wissing, S. Lachelt, M. Herlan, M. Fehr, K. Lauber, S.J. Sigrist, S. Wesselborg, K.U. Frölich, 2002, A caspase-related protease regulates apoptosis in yeast. Mol. Cell 9: 911-917.

Mazzoni C., E. Herker, V. Palermo, H. Jungwirth, T. Eisenberg, F. Madeo, C. Falcone, 2005, Yeast caspase-1 links messenger RNA stability to apoptosis in yeast. EMBO Reports 6: 1076-1081.

Mendoza-Vega O., J. Sabatiè, S.W. Brown, 1994, Industrial production of heterologous proteins by fed-batch cultures of the yeast *Saccharomyces cerevisiae*. FEMS Microbiol. Rev. 15: 369-410.

Pronk J.T., 2002, Auxotrophic yeast strains in fundamental and applied reasearch. Appl. Envir. Microbiol. 68: 2095-2100.

Romano F., E. de Alteriis, I. Andrès, J. Zueco, M.M. Bianchi, L. Paciello, V. Romano, P. Parascandola, 2007, Use of the cell wall protein Pir4 as a fusion partner for the expression of heterologous proteins in *S. cerevisiae.* Proceedings IX Annual Congress FISV, Riva del Garda (TN), 26-29 September 2007.

Romano V., L. Paciello, F. Romano, E. de Alteriis, L. Brambilla, P. Parascandola, 2007, Interleukin-1β production by *Z. bailii* [pZ_3KlIL-1β] in aerated fed-batch reactor: importance of inoculum physiology and bioprocess modelling. Process Biochem., in press.

Verduyn C., E. Postma, W.A. Scheffers, J.P. Van Dijken, 1992, Effect of benzoic acid on metabolic fluxes in yeasts: a continuous-culture study on the regulation of respiration and alcoholic fermentation. Yeast 8: 501-517

CHEMICAL ENGINEERING TRANSACTIONS, Volume 14, 2008
Edited by G. Marino, E. Bardone, A. Viglia
 ISBN 978-88-95608-02-0

Ultrasound Extraction of Active Principles with Hypoglycaemic Activity from Medicinal Plants

Ani Alupului*, Vasile Lavric
University Politehnica of Bucharest, Chemical Engineering Department
RO-011061, Polizu 1-7, Bucharest, Romania
*alupului_ani@yahoo.com

Intensification is a secure and worthy method of improving either a rather lengthy (time consuming) or an energy intensive (far from normal conditions) process, searching for the increase of at least one of the major parameters governing it: the kinetic, through the partial transfer rates, the interfacial area or the driving force, seen as the distance from the actual state of the process and its equilibrium. Ultrasound assisted extraction acts primarily upon the kinetic of the extraction process, and secondarily upon the interfacial area, through the eventual disintegration of larger particles. Compared with maceration, infusion or decoction, it improves the process decreasing both operating time and temperature while increasing the extraction yield. This intensive technique, biochemically safe unless overexposure, was used to obtain active principles with hypoglycaemic activity (sweet diterpenic steviol glycosides) from a medicinal plant with high economical potential: *Stevia rebaudiana* leaves. Distilled water or a mixture of water and ethanol in several ratios were employed as solvent. The active principles were quantified by HPLC. An Artificial Neural Network was used to model the ultrasound assisted extraction, due to its ability to cope with complex processes and superior generalization capacity.

Keywords: Ultrasound assisted extraction, HPLC, Medicinal plants, Stevioside, *Stevia rebaudiana Bert.*, Artificial Neural Network.

1. Introduction

Stevia rebaudiana, native from Paraguay, is used as herbal sweetener for over 1500 years. Extracts of *Stevia rebaudiana* are part in weight-loss programs because of its ability to reduce the cravings for sweet and fatty foods, to treat the diseases diabetes, hypoglycaemia, candidasis, high blood pressure, skin abrasions and inhibiting growth and reproduction of bacteria-like plaque (Gregersen *et al.*, 2004). *Stevia*'s greatest appears to be a natural alternative to artificial sweeteners (such as aspartame or sodium saccharin). The sweetness in Stevia rebaudiana is mainly attributed to two glycoside compounds: stevioside (3-10% of dry leaf weight) and rebaudioside A (1-3%) which can be up to 250 times sweeter than sucrose (Duke, 2006). The glycosides of *Stevia rebaudiana* leaves have been extracted using classical techniques: maceration, infusion or decoction, either requiring long processing time and low efficiency (maceration), or the facing thermal degradation (infusion and decoction) (Vinatoru, 2001).

In order to increase the productivity, several intensification techniques like ultrasonic waves, supercritical fluids or microwaves were associated with extraction of plant's compounds to improve the yield and quality of extracted products. From these, ultrasound assisted extraction seems to be economically most promising (inexpensive, simple and efficient), being employed to extract active compounds such saponins, steroids and triterpenoids from *Chresta spp.* about three times faster than with the traditional extraction methods (Schinor *et al.*, 2004). The main benefits of use of ultrasound in solid-liquid extraction include the increase of the extraction yield and faster kinetics (Kiel, 2007).

The purpose of the present experiment is to study the some parameters of extraction: dry leaves particle size, solvents nature, sample weight to solvent ratio (w/v), temperature, stirring and output power of the ultrasound and to determine the optimum domain in a reliable ultrasound assisted extraction protocol. High-performance liquid chromatography (HPLC) is used to separate and quantify the stevioside due to its high reproducibility, good linear range, ease of automation and ability to analyze the number of constituents in botanicals and herbal samples (Dacome *et al.*, 2005).

2. Materials and Methods

2.1 Reagents and plant material

Stevioside (S3572, assay ≥98% (HPLC), form: solid , colour: white, free soluble in water and ethanol, solubility H2O: >20 mg/mL, storage temp: 2-8°C, chemical name: 4α-13-[(2-O-β-D-Glucopyranosyl-β-D-glucopyranosyl)oxy]kaur-16-en-18-oic acid β-D-glucopyranosyl ester, chemical formula: C38H60O18 – see Figure 1, molecular weight: 804.87) used as the standard chemical was obtained from Sigma Chemicals.

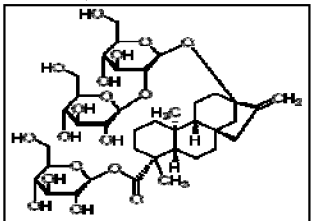

Figure 1 Stevioside – Structural formula

Chromatographic grade – double distilled water, HPLC grade acetonitrile, aqueous ethanol and distilled water was used as extraction solvents and mobile phase.

Dry leaves of *Stevia rebaudiana* were purchased from the Paraguay Medicine Market. They were stored in dark bags to protect them from humidity and light and, before each bunch of experiments, they were cut into pieces of the appropriate equivalent diameter.

2.1 Experimental setup

Two ultrasonic bath (Model T420 Elma and Model T460 Elma), both working at 35 kHz frequency and an output power of 70 W and 170 W respectively were employed. For stirring and heating a TK-22 Magnetic stirrer with heating was used. For chromatographic measurements, a HPLC system Agilent Technologies 1200 series model with UV-VIS detector was used. After the extraction process for all the methods, the filtrate was separated from the residual plant material by vacuum pump filtration.

2.2 Classic extraction

Maceration was used as reference for comparisons with the ultrasound assisted and hot extraction methods. Maceration was performed with 10 g of *Stevia rebaudiana* dry leaves with three particle sizes (0.315 mm, 2 mm and 6.3 mm) and different solvents:

distilled water and water/ethanol mixtures (55% and 70%) with different sample weight to solvent volume ratio (w/v): 1/10, 1/8, 1/5. The mixture was left at room temperature for 24 h in closed Erlenmeyer flasks, small volumes for analysis being probed at 5, 20, 45, 120, 240 minutes and at the end of the process. The hot extraction (infusion and decoction) was performed with 10 g of *Stevia rebaudiana* dry leaves having 0.315 mm equivalent diameter, at a sample weight to water volume ratio of 1/5 (w/v) and temperatures of 40 ^{0}C and 90 ^{0}C into Erlenmeyer flasks. For infusion (40 ^{0}C), samples were taken at 5, 10, 20, 25 and 35 minutes while for decoction (90 ^{0}C), samples were taken at 1, 2, 3, 5 and 8 minutes. Both maceration and hot extraction were performed with and without stirring.

2.3 Ultrasound assisted extraction

Samples of 10 g of dry leaves from *Stevia rebaudiana* with four particles sizes (0.315 mm, 2 mm, 6.3 mm and crushed dry leaves) were mixed with different solvents: distilled water and water/ethanol mixtures (55% and 70%) with different sample weight to solvent volume ratios: 1/10, 1/8, 1/5 (w/v) then placed into the ultrasound assisted extractors at room temperature. The ultrasonic baths were filled with liquid water into which glasses with samples were placed and sonicated for 1, 3, 5, 10, 15, 20, 25, 35, 40, 50 and 60 minutes at 70 W and 170 W respectively output power.

2.4 Dry residue analysis. Extractive values

According to the Romanian Pharmacopoeia (10th edition) approximately 2 g (2 ml) of extract was placed into a flat-bottomed glass dish (36 mm diameter and 28 mm height) covered to prevent evaporation of solvent before weighting. After weighting, the extract was dried in oven at 103 ^{0}C for 3 h. The content of extractive substances in the plant material was calculated from the mass of dry extract and the initial mass of plant subject to experiment. The concentration of extractive substances in the liquid extract was calculated from the mass of dry extract and the volume of liquid extract. The extractive value of the soluble compounds from the extract was calculated as a mass percentage of dry residue (g/100 g extract).

2.5 Determination of steviol glycosides percentages using HPLC

Standard solution (2.2 mg/5 mL) of stevioside was prepared in the mobile phase consisting of mix HPLC grade acetonitrile and bi-distilled water (80:20, v/v). Standard series in the concentration range of 100-1000 µg/mL were obtained from the stock solution. The mobile phase was used as solvent for all HPLC studies. The HPLC analysis conditions were performed by isocratic elution with a flow rate of 0.4 mL/min. All solvents were filtered through a 0.22 µm Millipore filter. Volumes of 5 µL extracts prepared from each sample were directly injected into HPLC then the peak areas at the characteristic wavelength of the steviol glycosides were measured. The UV-VIS detector was set to 210 nm and peak areas were integrated automatically using Agilent software. Separation was carried out using a Supelcosil LC-NH2 or equivalent (length: 15 - 30 cm; inner diameter: 3.9 - 4.6 mm) and flow rate was set to 0.4 mL/min for an isocratic elution at 40 ^{0}C as column temperature. The instrument was calibrated pumping mobile phase through it until a drift-free baseline is obtained. The Agilent software recorded the chromatograms of the sample standard solution.

All the computations concerning the quantitative analysis were performed with external standardization of the measured peak areas. The results were obtained as the mean value of three separate injections. Using the measured peak areas of stevioside from the sample solution and of the standard solution, the percentage of the extracted stevioside was computed as: % stevioside = [Ws/W] x [Aa/As] x 100, where Ws is the mass of stevioside in the standard solution (mg), W is the mass of sample (mg), As and Aa are the peak area of stevioside from standard and sample solutions. The measurements of stevioside from samples of *Stevia rebaudiana* were done according to stevioside standard. At flow rate of 0.4 mL/min the retention time was 1.076 min for stevioside as shown in Figure 2.

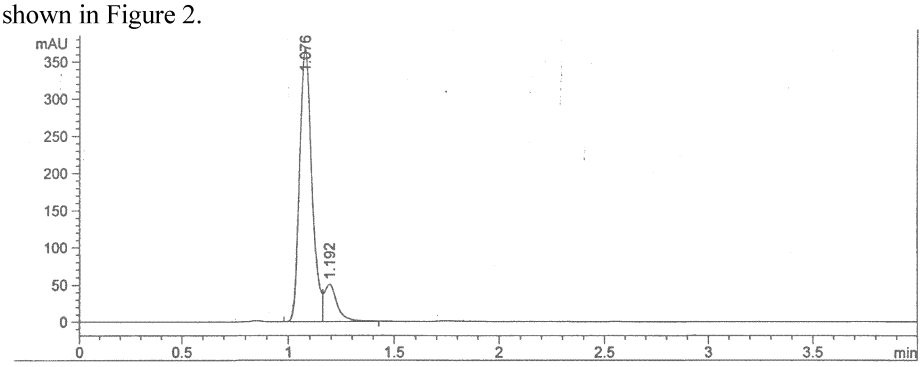

Figure 2. Chromatogram of 2.2 mg/mL standard (Stevioside)

3. Results and Discussions

The HPLC method was applied to quantify the stevioside in the leaves of *Stevia rebaudiana*, the results of different extraction protocols being presented in Tables 1 and 2, and Figures 3 and 4.

3.1 Results obtained for classic extraction

Table 1. Maceration extraction – dry residual and extracted stevioside obtained after 24 hours

	a. Sample weight to solvent volume ratio			*b.* Equivalent diameter dry leaves, mm			*c.* Solvent nature and proportions		
	1/10	1/8	1/5	0.315	2.0	6.3	water	ethanol 55%	ethanol 70%
g d.r. /100 g extract	3.39	4.16	7.07	7.07	3.30	3.17	7.07	4.04	3.28
g stevioside / 100 g extract	0.99	1.05	2.24	2.24	0.97	0.77	2.24	0.98	0.77

a. Influence of the sample weight to solvent volume ratio upon the maceration extraction yields (0.315 mm equivalent diameter dry leaves, distilled water)
b. Influence of the particles size dry leaves on the maceration extraction yields (1/5 sample weight to solvent volume ratio, distilled water)
c. Influence of the solvent nature on the maceration extraction yields (0.315 mm equivalent diameter dry leaves, 1/5 sample weight to solvent volume ratio)

Although not unexpected, the results from Table 1 show a remarkable dependency of extraction upon the granularity of the solid phase and the type of the liquid phase, but

quite normal with respect to the sample weight to solvent volume ratio. As the volume used for extraction increases, the concentration of the extracted species decreases, while their mass could either be the same, or increase too. In the latter case, to whom belongs the actual experiment (data not shown), the extracted species reached the thermodynamic saturation for the lowest volume of the liquid phase used. According to experimental data (Table 2), the dimension of particles plays a key role in extraction of soluble components from *Stevia rebaudiana*, a sharp decrease appearing when passing from sub-millimetre to millimetre range, proving that diffusion inside solid phase is the limiting step. Ethanol seems to inhibit sharply extraction of stevioside from *Stevia rebaudiana*, due, probably, to its higher molecule and lower propensity of having hydrogen bonds with stevioside molecules. From now on, the water will be the extractive agent and the leaves granularity will be 0.315 mm, unless otherwise stated.

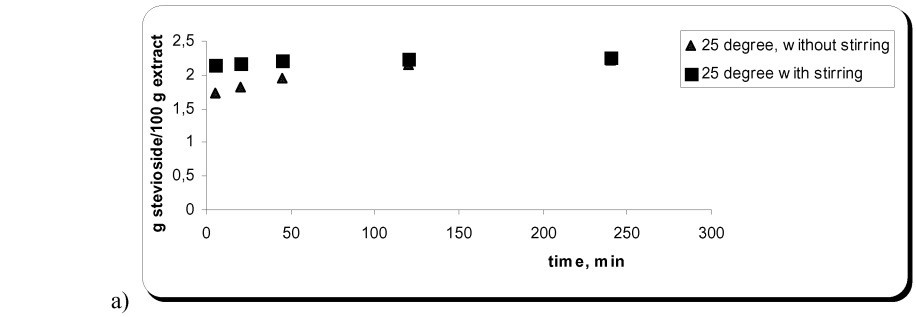

a)

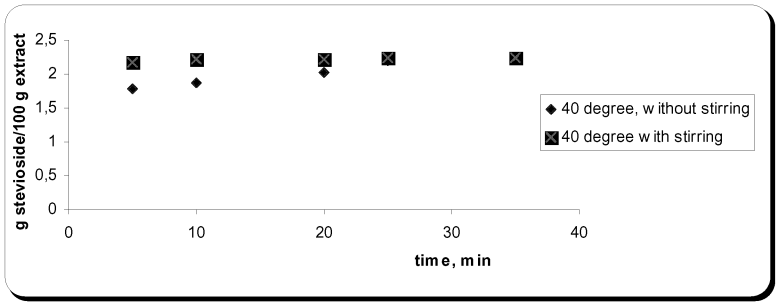

b)

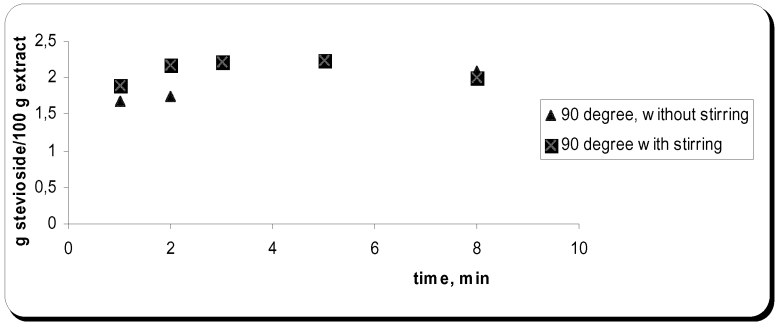

c)

Figure 3. The results for classic extraction; the influence of temperature and stirring upon the extraction yield in time a) 25ºC, b) 40 ºC, c) 90 ºC

When a supplemental kinetic energy is introduced from outside into the liquid phase

through heating, what modifies is the process rate, not the thermodynamic equilibrium, as can be observed from Figure 3, a)-c). If stirring is superimposed (increasing even more the kinetic energy of the liquid phase dissipating mechanical energy), the extraction process becomes even faster, although for the highest temperature its contribution decreases significantly (see, for comparison, the vertical distance between points at the beginning of the process in Figure 3, a-c). The thermal degradation of the valuable compound starts manifesting, as an important downside of increasing the temperature of extraction (Figure 3, c).

3.2 Ultrasound assisted extraction experiments

Table 2. Ultrasound assisted extraction results obtained after 20 min of sonication

	a). Equivalent diameter of dry leaves, mm				*b).* Solvent nature		
	0.315	2.0	6.3	crushed leaves	water	ethanol 55%	ethanol 70%
g d.r./100 g extract	7.08	7.02	7.0	6.97	7.08	7.05	7.03
g stevioside / 100 g extract	2.26	2.25	2.22	2.20	2.26	2.25	2.23

a). Influence of the equivalent diameter of dry leaves upon the ultrasound assisted extraction yields (1/5 sample weight to solvent volume ratio, distilled water)
b). Influence of the solvent nature upon the ultrasound assisted extraction yields (0.315 mm equivalent diameter of dry leaves, 1/5 sample weight to solvent volume ratio)

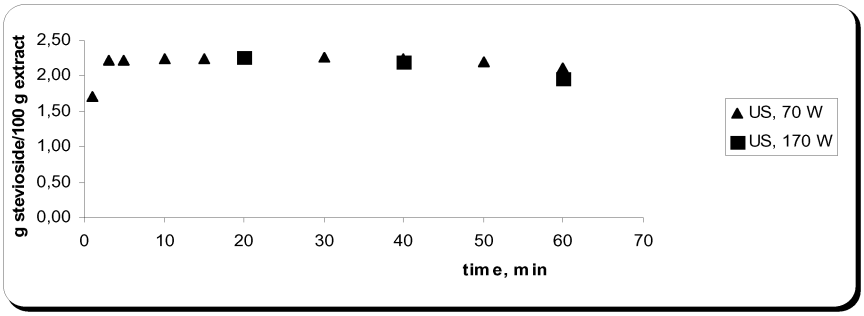

Figure 4. Ultrasound - assisted extraction results. Influence of the output ultrasound power on the extraction yield on time (70 W and 170 W, respectively).

When using ultrasound waves as intensification technique, the extraction rate increases dramatically, the stevioside concentration attaining its maximum value for less than five minutes (see Figure 4 for details). At the same time, neither the granularity of the solid, nor the type of the liquid seem not to count anymore in the economy of the extraction process, as pointed out by the data from Table 2. Even when crushed leaves are used, not only the dry residual is almost the same, but also the stevioside concentration. Also, the presence of ethanol becomes unimportant, the yield in stevioside having the same value as for pure water. This is the effect of the sharp increase of the local turbulences, which increase the mass transfer through diffusion inside the solid and also faster mixing of the liquid, thus maintaining the highest possible driving force. Increasing the

power of the ultrasonic field has no beneficial effect, proving that an optimum ratio of power and liquid, solid or both volumes should exist. The main drawback is the danger of overexposure, when the valuable species ends up being destroyed (see Figure 4, the decrease in the concentration of stevioside for long times), although this could be a threat only for labile species.

3.3. Comparative discussions

The experimental results show that stevioside content of *Stevia rebaudiana* dry leaves is higher than reported in literature. The highest stevioside content was removed from the solid phase by ultrasound assisted extraction, about 10.26 % of dry leaf weight. Compared to maceration, ultrasound assisted extraction increased the productivity more than two hundred times, decreasing the time of completion. With respect to hot extraction, whose performance is by far better than maceration, ultrasound assisted extraction has the main advantage of working at ambient temperatures, thus avoiding the thermal overexposure. Contrary to ultrasound overexposure, the thermal one has a very narrow time window, largely increasing the probability of happening thus needing a rather tight control (see Figure 3, c, where there are only three minutes between optimum and thermal degradation, in Figure 4 this interval is over fifty minutes). Like hot extraction, ultrasound assisted intensification needs special equipment to be functional, which means higher investments, and electricity to produce the ultrasonic waves, which means higher operating costs than maceration. So, a soundly economic analysis should be done, in order to choose the best extraction procedure.

4. Artificial Neural Network modelling

Taking into account the complexity of the ultrasound assisted extraction, given not only by the multitude of the implied parameters, but also from the complex interactions between the mass transfer and the local velocity field heavily affected by the ultrasonic waves, the Artificial Neural Network concept was considered for modelling. An ANN is composed of elements (artificial neurones, organised in layers as the topological structure of the brain, but far less complicate) that perform in a manner similar to the most elementary functions of the biological neurone. The ANN mimics a number of the brain's characteristics: learn from experience, generalise from previous examples and abstract essential characteristics from input containing scattered data, as any self-organizing system. Learning means to present, repeatedly, to an ANN a set of couples of input/output vectors, and to force it to optimize some metric like a sum of squared distances real per desired output. A synthetic neuron (except those of the input layer) processes the sum of the weighted signals received from its dendrites according to its threshold function and outputs the answer through its axon to the following neurons. The threshold function could be of any type of the generalized logistic curve. Matching the ANN output to the real world passes through the attached neuron weights, which modify until the learning criterion is fulfilled. Generalization means the capacity to give a correct answer to a question outside the learning set and relies on ANN capacity of finding out the hidden rules that govern the process, even if, at this time, it can not be mathematically expressed. Anyway, the time consuming step is the learning phase.

The feed-forward ANN used to model the ultrasound assisted extraction has the simplest structure with a single neuron in the hidden layer, three neurons in the input layer (equivalent diameter of dry leaves, sample weight to solvent volume ratio and

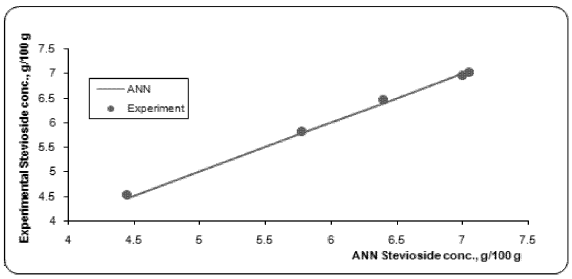

Figure 5. The parity plot of ANN vs. Experimental concentrations of stevioside

output power) and five neurons in the output layer, for the time profile (up to ten minutes) of the stevioside concentrations. This way the ANN has the minimum possible number of weights which should be computed during the learning phase, for which the back-propagation algorithm was chosen. The lack of abundant data prevent us from making a thorough analysis of the best ANN topology, with the present data verifying only the capacity of the given ANN to satisfactorily model the ultrasound assisted extraction. A parity plot of the experimental vs. the learnt profiles is given in Figure 5, proving their good fit.

5. Conclusions

In this study, a HPLC method was developed and applied to quantify the stevioside content of the *Stevia rebaudiana*. Compared with classical extraction methods like maceration and hot extraction, the ultrasound assisted extraction proved to be a simpler but more effective procedure to obtain active compounds from medicinal plants; it works at lower temperatures, avoiding thermal degradation and higher rates, a very important asset for industry. ANN seems to be a good choice for modelling this process.

Acknowledgments

The authors would like to thank ing. Anton Perescu of National Institute of Research and Development for Biological Sciences and Prof. Dr. Ioan Burzo of University of Agronomical Sciences and Veterinary Medicine of Bucharest for their kind support.

6. References

1. Dacome, A.S., da Silva, C.C., da Costa, C.E.M., Fontana, J.D., Adelmann, J., da Costa, S.C., 2005, *Sweet diterpenic glycosides balance of a new cultivar of Stevia rebaudiana (Bert.) Bertoni: Isolation and quantitative distribution by chromatographic, spectroscopic, and electrophoretic methods*, Process Biochemistry, 40, 3587.
2. Duke, J.A., 2006, *Handbook of phytochemical constituents of Gras herbs and other economic plants*, FL. CRC Press, Boca Raton.
3. Keil, F.J., 2007, *Modeling of Process Intensification*, WILEY-VCH Verlag GmbH & Co. KGaA, Weinheim.
4. Schinor, E.C., Salvador, M.J., Turatti, I.C.C., 2004, *Comparison of classical and ultrasound-assisted extractions of steroids and triterpenoids from three Chresta spp.,* Ultrasonics Sonochemistry, 11, 415.
5. Gregersen, S., Jeppesen, P.B., Holst, J. J., Hermansen, K., 2004, *Antihyperglycemic effects of stevioside in type 2 diabetic subjects*, Metabolism 53, 73.
6. Vinatoru, M., 2001, *An overview of the ultrasonically assisted extraction of bioactive principles from herbs*, Ultrasonics Sonochemistry, 8(3), 303.

CHEMICAL ENGINEERING TRANSACTIONS, Volume 14, 2008
Edited by G. Marino, E. Bardone, A. Viglia
 ISBN 978-88-95608-02-0

Experimental and simulation analysis of membrane adsorbers used for the primary capture step in antibody manufacturing

Cristiana Boi, Simone Dimartino, Giulio C. Sarti
Dipartimento di Ingegneria Chimica, Mineraria e delle Tecnologie Ambientali
Università di Bologna
via Terracini 34, 40131 Bologna (Italy)

Membrane chromatography is a novel protein purification technique developed to overcome the major limitations due to packed beads, such as long process time, mass transport controlled by diffusion and high pressure drops.
In this work, the adsorption of human IgG onto new Protein A affinity membranes has been studied in detail. To this aim, several chromatographic cycles have been measured at different experimental conditions. A mathematical model for protein purification with affinity membrane adsorbers has been developed and validated with experimental data.

1. Introduction

Protein A chromatography has become the preferred choice for the capture step of antibody manufacturing. However, its high costs and the growth of antibody applications has driven the search for alternative technologies (Low et al. 2007). Membrane affinity chromatography is one of the processes that are receiving increasing attention as a possible alternative to bead-based chromatography, even if its industrial application is still far afield due to the low binding capacity of affinity membranes with respect to chromatography beads (Thommes and Etzel 2007).
In this work, a new affinity membrane endowed with a very interesting binding capacity for human IgG is studied in view of its use in the capturing step of a monoclonal antibody production process. The membranes have been extensively tested with pure polyclonal IgG solutions and with a cell culture supernatant containing IgG_1. The effects of flow rate and IgG concentration in the feed on the separation performance have been studied in detail, considering binding capacity, selectivity and process yield.
A model simulation of the complete affinity cycle has been developed and the experimental results have been compared with the simulated behaviour for different values of feed concentrations and feed flow rates.

2. Experimental

2.1 Materials and methods

A new Protein A membrane (Sartorius Stedim Biotech, GmbH), with nominal pore size of 0.45 μm, an average thickness of 200 μm and a void fraction of 55%, has been used for chromatographic separation of IgG. Pure polyclonal IgG, Gammanorm

(Octapharma, Sweden) and a cell culture supernatant containing IgG_1 (ExcellGene, Switzerland) were used as feed solutions.
The measure of IgG concentration of pure solutions was determined by UV readings at 280 nm (Shimadzu UV-1601). For complex solutions IgG concentration was determined by HPLC using a protein A affinity cartridge (PA ID, Applied Biosystems, Monza, MI, Italy) mounted on a liquid chromatography system (Alliance 2695 equipped with a dual wavelength UV detector 2487, Waters Milano, Italy). The purity of the eluted fractions was analyzed with size exclusion HPLC using a SEC column (Proteema 300, PSS, Mainz, Germany).

2.2 Dynamic experiments
Complete chromatographic cycles, adsorption, washing and elution have been performed using an Akta Purifier chromatographic system (GE Healthcare, Italy). A membrane column was prepared by cutting membrane discs of 2.5 cm diameter and inserting several membrane layers in a membrane holder; experiments have been carried out using layered stacks of 5 and 10 membranes.
Phosphate buffered saline, PBS, pH 7.4 was used as equilibration and washing buffer, 0.1 M glycine pH 3.5 as elution buffer and a solution of 1 M NaCl and 50 mM NaOH was used for regeneration. In experiments with pure IgG solutions, regeneration was performed every 5^{th} cycle while in experiments with the cell culture supernatant it was carried out after every cycle. The effects of different operating conditions, in particular flow rate and IgG feed concentration, on membrane performance have been thoroughly investigated.

2.3 Results
The membranes have been initially characterized in batch experiments with pure IgG solutions in order to obtain kinetic and equilibrium thermodynamic parameters. In particular, the Langmuir dissociation constant and the maximum static binding capacity have been obtained in previous work, as reported by Boi et al. 2007a, and are around 0.0934 mg/ml and 12.75 mg/ml, respectively.
Dynamic experiments with pure IgG solutions have been performed at different values of the feed concentration in the range of 0.15÷2.0 mg/ml and at flow rates ranging from 1 ml/min to 10 ml/min. The effect of concentration has been investigated in experiments performed at a constant flow rate in all process stages. As the concentration increases the breakthrough curve is sharper, indicating a better membrane utilization, and the onset of breakthrough is anticipated as can be observed in Fig. 1. Conversely, the effect of flow rate at a constant feed concentration is quite modest on the dynamic binding capacity.

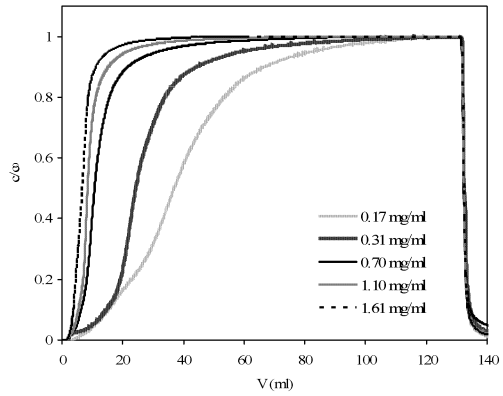

Fig. 1. Dimensionless adsorption and washing profiles at 10 ml/min for different values of IgG concentration in the feed.

Elution profiles for the same value of IgG concentration in the feed are shown in Fig. 2. As observed in previous works (Briefs and Kula, 1992, Dimartino et al. 2007) elution peaks are higher and narrower at low values of the feed flow rate and became shorter and broader as the flow rate increases.

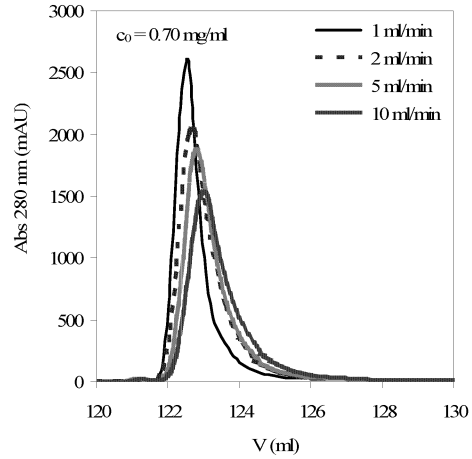

Fig. 2. Effect of flow rate on elution performance for experiments performed with 0.70 mg/ml of IgG in the feed and a layered stack of 10 membranes.

Due to the low titer in IgG, around 0.1 mg/ml, the cell culture supernatant was used as received. Experiments were performed at different flow rates and a typical absorbance profile is shown in Fig. 3. Fractions have been collected every millilitre and analyzed with both Protein A and SEC HPLC analysis. The results indicate that the elution peak is formed by pure IgG and that the membranes are endowed with very good selectivity.

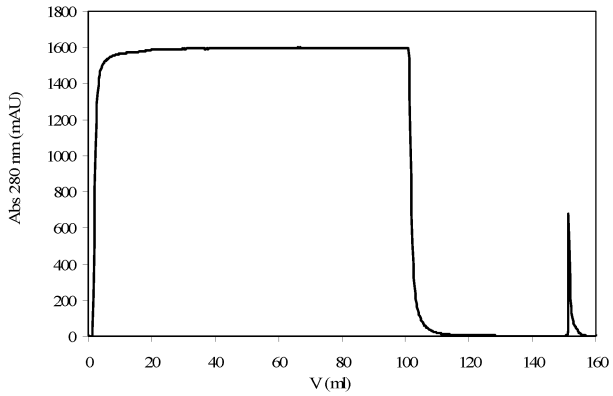

Fig. 3. Absorbance profile for experiments performed with the cell culture supernatant at 5 ml/min constant flow rate using a stack of 5 membranes.

3. Mathematical model

3.1 Theoretical basis and model solution

The model is based on the adsorption of a single protein on affinity membranes and is able to describe all process stages, namely adsorption, washing and elution. The mathematical description considers the effects of system non idealities, generally called system dispersion, due to mixing, channelling, dead-volumes, that are particularly important in bench scale membrane chromatography (Sarfert and Etzel 1997).

The mathematical formalism adopted consists in a mass balance over the membrane column coupled with a kinetic equation that describes the interactions between the protein and the ligand immobilized on the membrane matrix. Description of the adsorption and washing stages is based on the model developed by Suen and Etzel 1992, while the elution step is described with a first order kinetic equation.

The model equations, together with the relevant initial and boundary conditions, have been implemented in Aspen Custom Modeler© simulation environment and solved using the finite difference method. In industrial applications, especially for antibody capture, chromatographic columns are operated up to 10% breakthrough. Since the onset of breakthrough is the most important part of the curve, fitting of the adsorption stage has been carried out up to 50% breakthrough.

The model has been validated using experimental data obtained for the adsorption of pure polyclonal IgG on affinity membranes under different operating conditions (Dimartino et al. 2007, Boi et al. 2007a).

3.2 Simulation results

The adsorption and washing profiles calculated with the model considered have been compared with experimental results obtaining a rather satisfactory agreement with the data, as it can be noted from Fig. 4.

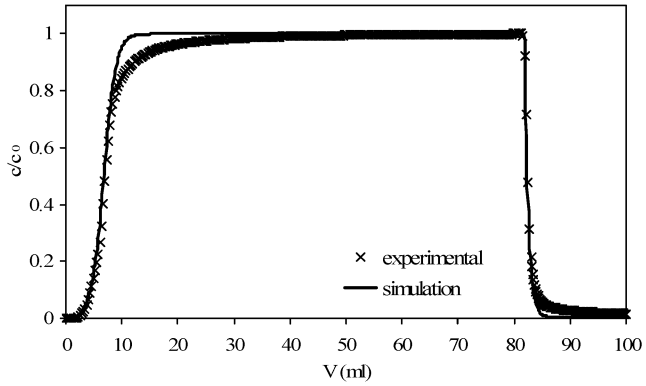

Fig. 4. Comparison between experimental data and model results for experiments performed with pure IgG solution at 1.48 mg/ml in the feed and constant flow rate of 10 ml/min using a layered stack of 10 membranes.

The model is able to describe well all process stages, as it can be observed in Fig. 5 in which the IgG profile, obtained by Protein A analysis, has been compared with the simulation results, for the experiments with the cell culture supernatant.

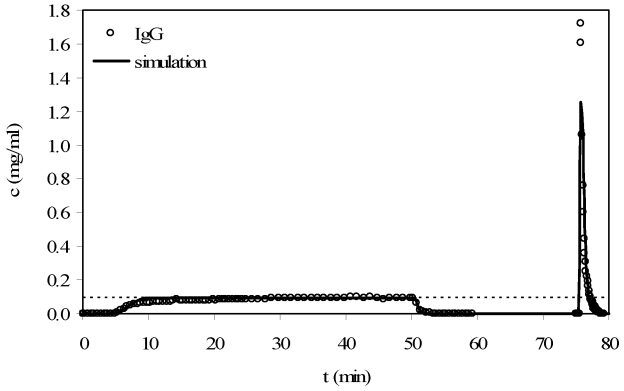

Fig. 5. Comparison between experimental results and simulations for IgG purification from the cell culture supernatant at a flow rate of 2 ml/min using a layered stack of 5 membranes.

4. Conclusions

A new protein A affinity membrane has been experimentally characterized to determine its potential application in an IgG capture step of an antibody manufacturing process. The results obtained indicate that this new membrane is endowed with a high binding capacity and very good selectivity for IgG, thus they can be used to overcome the throughput limitation and other well known drawbacks of traditional bead-based chromatographic columns.

A mathematical model that describes membrane affinity chromatography has been developed and validated considering the system under investigation (protein A affinity membrane-human IgG). This model satisfactorily describes all the process stages and is an useful tool for process design and for the simulation of a capturing step based on membrane adsorbers.

Acknowledgement

This work has been performed as part of the "Advanced Interactive Materials by Design" (AIMs) project, supported by the Sixth Research Framework Programme of the European Union (NMP3-CT-2004-500160).

5. References

Boi C., S. Dimartino and G.C. Sarti, 2007a, Advances in membrane affinity chromatography for the recovery of antibodies, submitted to Biotechnology Progress

Boi C. and G.C. Sarti, 2007b, Development and characterization of affinity membranes for immunoglobulin purification, Separation Science and Technology, 42, 2987.

Briefs, K.G. and M.R. Kula, 1992, Fast protein chromatography on analytical and preparative scale using modified microporous membranes, Chem. Eng. Sci. 47, 141.

Dimartino S., C. Boi and G. C. Sarti, 2007, Dynamic characterization of affinity membranes for monoclonal antibodies purification. AIChE Annual Meeting Conference Proceedings, Eds. The American Institute of Chemical Engineers, New York, 306c.

Low, D., R. O'Leary and N.S. Pujar, 2007, Future of Antibody purification. J. Chromatogr. B 848, 48.

Sarfert F.T. and M.R. Etzel., 1997, Mass transfer limitations in protein separations using ion-exchange membranes, J. Chromatogr. A, 764, 3.

Suen S.Y.and. M.R. Etzel, 1992, A mathematical analysis of affinity membrane bioseparations, Chem. Eng. Sci. 47, 1355.

Thommes, J. and M. Etzel, 2007, Alternatives to Chromatographic Separations. Biotechnol. Prog., 23, 42.

CHEMICAL ENGINEERING TRANSACTIONS, Volume 14, 2008
Edited by G. Marino, E. Bardone, A. Viglia
 ISBN 978-88-95608-02-0

Assessment of the Kinetics of Phenol Bioconversion by *Pseudomonas sp. OX1*

G. Olivieri[1], M.E. Russo[1], A. Di Donato[2], A. Marzocchella[1], P. Salatino[1]
Università degli Studi di Napoli 'Federico II'
[1] Dipartimento di Ingegneria Chimica - P.le V. Tecchio, 80 – 80125 Napoli, Italy
[2] Dipartimento di Biologia Strutturale e Funzionale
Complesso Universitario di Monte S. Angelo - Via Cinthia - 80126 Napoli, Italy

The present contribution reports on the characterization of the kinetics of phenol conversion by *Pseudomonas. sp. OX1* in a continuously-operated, stirred reactor. The investigation has been carried out in a 2 L reactor, mechanically stirred. The phenol containing solution is delivered at dilution rates (D) varying from 0.025 to 0.5 h^{-1}. The phenol conversion process has been characterized in terms of time resolved measurements the concentration in the liquid phase of phenol, cells, 2-hydroxymuconic semialdehyde, the oxygen uptake rate, the total organic carbon and the total nitrogen. Data were processed to assess the kinetic models - and related parameters – of phenol conversion and cell growth under a wide range of operating conditions, from quasi-batch up to values close to the wash-out conditions. The bacterial maintenance was also assessed for growth on phenol. Kinetic parameters and phenol-to-biomass fractional yield coefficient were significantly different from those estimated during batch cultures. The maximum phenol degradation rate was of about 0.5 g/(L h).

1. Introduction

Phenolic compounds and their derivatives are present in significant amounts in raw wastewaters from different industrial sources. Their concentration must be strictly limited because of the deleterious effect of these molecules on a variety of biochemical functions. Several bacterial strains are able to use aromatic hydrocarbons as a primary source of carbon and energy (Whited and Gibson, 1991). The wide range of aromatic substrates that can be metabolized by these microrganisms constitutes a powerful tool for the bioremediation of environmentally harmful compounds.

Pseudomonas sp. OX1 was isolated from the activated sludge of a wastewater treatment plant, and its ability to mineralize several aromatic hydrocarbons (Baggi et al., 1987) might be relevant for bioremediation strategies. This bacterium grows using as unique carbon and energy sources a large variety of aromatic molecules including phenol, cresols and dimethylphenols, and also non-hydroxylated molecules, even at high concentration (Baggi et al., 1987; Bertoni et al., 1996; Viggiani et al., 2006). Lodato et al. (2007) have showed that this microrganism may convert azo-dyes under anaerobic conditions. In particular, cells may convert any amount of dye if a balanced cycle of anaerobic-aerobic process is carried out. It is likely that metabolites accumulated during the aerobic phase, associated to growth/maintenance of *Pseudomonas sp.* OX1, are

responsible for dye conversion during the subsequent anaerobic phase.

It should be taken into account that phenol degradation by *Pseudomonas* strains is generally limited both by substrate inhibition and by low specific conversion rates (Yang and Humphrey, 1975; Onysko et al., 2002). These issues have stimulated efforts toward adoption of reactor configurations that are specifically suitable for the potential of *P. species* and provide process intensification. In particular, the immobilization of the microrganisms on solid carriers combined with the use of three-phase (gas/liquid/solid) fluidised bed reactors may be adopted for process intensification (Heijnen et al., 1990; Bryers, 2000; Russo, 2008). In any case, design and optimized operations of the bioreactor with free or immobilized cells need a kinetic characterization of the process under operating conditions close to the industrial applications.

A research program is active at the Chemical Engineering and at the Functional and Structural Biology Departments of the University of Naples Federico II aiming at the development of biotechnologies for bioremediation of water effluents with free and immobilized microbial cells. The present contribution is focused on the kinetic characterization of the phenol conversion process by free *Pseudomonas sp.* OX1 in a continuously operated well stirred reactor. The phenol conversion process has been characterized in terms of time resolved measurement of the concentration in the liquid phase of phenol (Ph), cell (X), 2-hydroxymuconic acid semialdehyde (HMAS), oxygen uptake rate (OUR), total organic carbon (TOC) and total nitrogen (TN).

2. Materials and method

2.1 Microrganisms and culture media

Pseudomonas specie OX1 was a gift of Dr. Paola Barbieri (Functional and Structural Biology Department, Università dell'Insubria, Varese, Italy). Stock cultures were maintained, through periodic subculture every week, at 4°C on agar-M9 plates containing 20 mM glucose (Sigma-Aldrich) as carbon and energy sources as reported in Viggiani et al. (2006).

The composition of the liquid medium (pH=6.9) adopted in pre-cultures and cultures is reported by Viggiani et al. (2006). Phenol was used as carbon source.

2.2 Apparatus

Figure 1 reports a sketch of the experimental apparatus. Continuous cultures were carried out in a 2 L bench-scale mechanically stirred bioreactor (Biobundle - Applikon) equipped with two 35 mm "Rushton Turbine" stirred on the axel. The temperature of the reactor was controlled by external circulating water in the glass jacket. Oxygen supply to the culture has been ensured by sparging air at the bottom of the reactor and by proper setting of the mixing rate. Dissolved oxygen was determined by a "Clark-type" probe (Mettler-Toledo, INPRO 6050). Air flow was sterilized by means of 0.22 μm filters (Millex FG - Millipore). A water-cooler at the gas outlet acts as humidity trap to minimize water loss by air stripping. Liquid was continuously fed and withdrawn

to/from the reactor by means of a peristaltic pump (Gilson Miniplus 3). Sampling was carried out by means of a submerged pipe equipped with a silicone septum at the top.

The liquid reservoir was a 50 L stainless steel tank equipped with six ports located at the top.

Sterilization of the bioreactor and ancillary apparatus was carried out *in situ* by means of 3 bar saturated steam provided by a steam generator (PG AUTO 9 – Lelit). Sterilization conditions were: 100°C for 40 min.

2.3 Operating Conditions and Procedure

All tests were carried out at 30°C and no pH control was adopted.

Pre-cultures were grown in previously autoclaved 250 mL shake bottles filled with 100 mL of M9 medium and phenol (2 mM). Bottles were incubated for 15 h on a rotary shaker at 125 rpm and 30°C.

The reactor with 1L medium (phenol 190 mg/L) and any ancillary apparatus were steam sterilized for 40 min. Air flow rate and agitation were set at 200 nL/h (3.3 vvm) and 500 rpm, respectively. 100 mL of preculture in late exponential growth phase was inoculated into the reactor and growth was carried out under batch-wise conditions for 1 day. Then the phenol bearing stream was fed continuously at the set flow rate. Drained liquid flow rate was measured by time resolving the weight of the liquid collected at the outlet. Sampling were carried out from bioreactor and reservoir typically at a time interval of about 1h. The phenol conversion process has been characterized in terms of time resolved measurements of pH, X, Ph, HMAS, OUR, TOC and TN in the liquid phase. Typically, runs lasted between 7 and 20 days before the reactor was stopped,

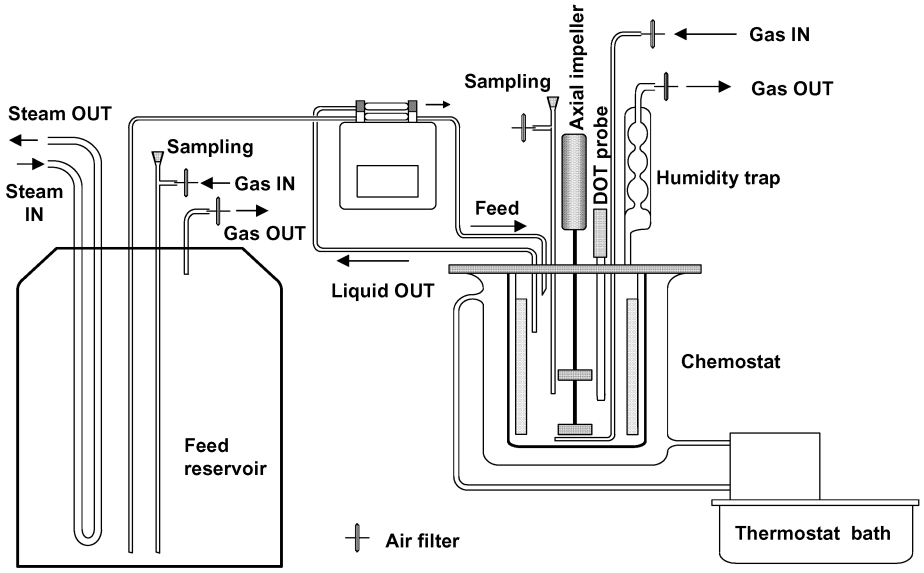

Figure 1 – Experimental apparatus.

cleaned, sterilized and a new run started.

2.4 Analysis

Analysis of culture samples was carried out after centrifugation at 11,000 rpm for 10 min. The solid phase was characterized for biomass concentration. The cell density was measured as optical density at 600 nm (Cary 50 -Varian). Calibration tests indicated that the optical density is proportional to *P. specie* dry mass and under the operating conditions tested it resulted 1.5 OD_{600}=1 g_{DM}/L. Elemental analysis of dry biomass was carried out by a C/H/N 600 LECO analyser. Liquid phase of the sampled cultures was characterised in terms of concentration of soluble components. pH was measured by a pHmeter (Hanna Instruments). Phenol and HMAS concentration were measured by UV-VIS absorption at 271 and 380 nm respectively (ε_{271}=1.65 $mM^{-1}cm^{-1}$, ε_{380}=29 $\mu M^{-1}cm^{-1}$). TOC and TN were measured by means of a TOC/TN analyzer (V_{CSH} – Shimadzu). OUR was measured by means of a respirometric assay according to the APHA Standard Methods (1992) in a 10 mL bottle equipped with a DOT probe.

3. Kinetics and Stoichiometry Model

The growth stoichiometry of an aerobic microbial culture can be described by means of a non-structured model:

$$\frac{1}{Y_{X/TOC}}TOC+\frac{1}{Y_{X/O2}}O_2+\frac{1}{Y_{X/TN}}TN+...\rightarrow X+.... \quad (1)$$

where $Y_{X/TOC}$, $Y_{X/O2}$, $Y_{X/TN}$ are the fractional yield coefficient of biomass with respect to TOC, O_2 and TN. Similar fractional yields can be defined referring to the elemental biomass composition ($Y^{C}_{X/TOC}$, $Y^{O}_{X/O2}$ and $Y^{N}_{X/TN}$). The fate of each substrate may be distinguished in two paths: the consumption of substrate for growth and for maintenance. In agreement with the model proposed by Pirt (1965) and with reference to a generic substrate S it results:

$$\frac{1}{Y_{X/S}}=\frac{1}{Y^{*}_{X/S}}+\frac{m_S}{\mu} \quad (2)$$

where $Y^{*}_{X/S}$ is the theoretical maximum fractional yield and m_S the maintenance coefficient.

The material balance referred to cell, phenol and oxygen and extended to the reaction volume under steady state conditions are:

$$\mu=D \quad (3a)$$

$$\frac{\mu}{Y^{*}_{X/Ph}}X^{OUT}+m_{Ph}X^{OUT}=D\left(Ph^{IN}-Ph^{OUT}\right) \quad (3b)$$

$$OUR = K_L a_L \left(O_2^{eq} - O_2^{OUT} \right) \tag{3c}$$

The model eq.s 3 relies on the following assumptions: i) the maintenance contribute to the phenol consumption (see eq. 2) was taken into account; ii) convective flow of oxygen in the liquid streams was neglected; iii) the contribute of gas convective flow to the phenol balance was neglected (Viggiani et al., 2006).

The growth kinetics of free *P. sp. OX1* in batch culture by adopting phenol as carbon source was characterized by Viggiani et al. (2006). In particular, the kinetics was described by the Haldane model:

$$\mu = \mu^M \frac{Ph}{K_{Ph} + Ph + \frac{Ph^2}{K_I}} \tag{4}$$

Viggiani et al. (2006) reported values of $\mu^M = 0.71\ h^{-1}$, K_{Ph}=0.31 g/L, K_I=0.13 g/L. The kinetics was such that the maximum of μ=0.17 h^{-1} is at Ph=0.2 g/L. Moreover, the fractional yield coefficient $Y_{X/Ph}$ resulted 0.82 for Ph<400 mg/L and decreased to zero for Ph approaching 600 mg/L.

4. Results and Discussions

The reactor system has been characterized for what concerning the residence time distribution of the liquid phase and the gas-liquid mass transport phenomena under operating conditions of interest for the present investigations (Chianese, 2007). In particular, the reactor behaves as a CSTR even over a time scale one order smaller than that characteristic of the conversion process, 6 h (inverse of the expected maximum value of μ=0.17 h^{-1}).

Figure 2 shows relevant data of a representative run carried out in the bioreactor. The reactor was operated under batch conditions for one day, then the phenol bearing stream (Ph^0 = 450 mg/L) was fed to the reactor at volumetric flow rate Q=55 mL/h (D=0.055 h^{-1}). The process was characterized in terms of soluble species concentration and of OUR until steady state conditions were established, and then the liquid volumetric flow rate was stepwise increased. The vertical dashed lines mark the times at which the dilution rate was changed. The pH was about 6.9 throughout the run, without any pH control. The concentration of HMAS (data not reported) was characterized by a sharp increase after one day of continuous operation up to value of about 16 μM and a decay to negligible values within two days. Data measured during the run reported in Fig. 2 were worked out according to the model described in section 3 (eq.s 1, 2 and 3) and value of the results are reported in Fig. 3 as a function of D (run 1).

Data of phenol-to-biomass fractional yield coefficient ($Y_{X/Ph}$) and phenol in the reactor are reported in Figure 3 as a function of the dilution rate and parametric in the phenol

concentration in the fed stream, ranging between 0.44 and 1.0 g/L. It is noteworthy that data did not depend on the run and on the culture age (the time measured since the reactor inoculation). Therefore, the possible effects of wall growth of cells may be ruled out.

The agreement of the $Y_{X/Ph}$ vs D data with the Pirt model (eq. 2) appears satisfactory. Data regression yields: the theoretical maximum fractional yield $Y^*_{X/Ph}$ =1.31 g_{DM}/g and the phenol maintenance coefficient m_{Ph}=0.0034 $g/(g_{DM} \cdot h)$.

Figure 3 shows that the phenol conversion was about complete for D smaller than 0.45 h^{-1} and that wash-out conditions establish at D between 0.45 and 0.6 h^{-1}. Moreover, it should be mentioned that the culture age of the test at D=0.6 h^{-1} was of about one week. These observations further support the negligible role of the cell wall growth on the performance of the reactor.

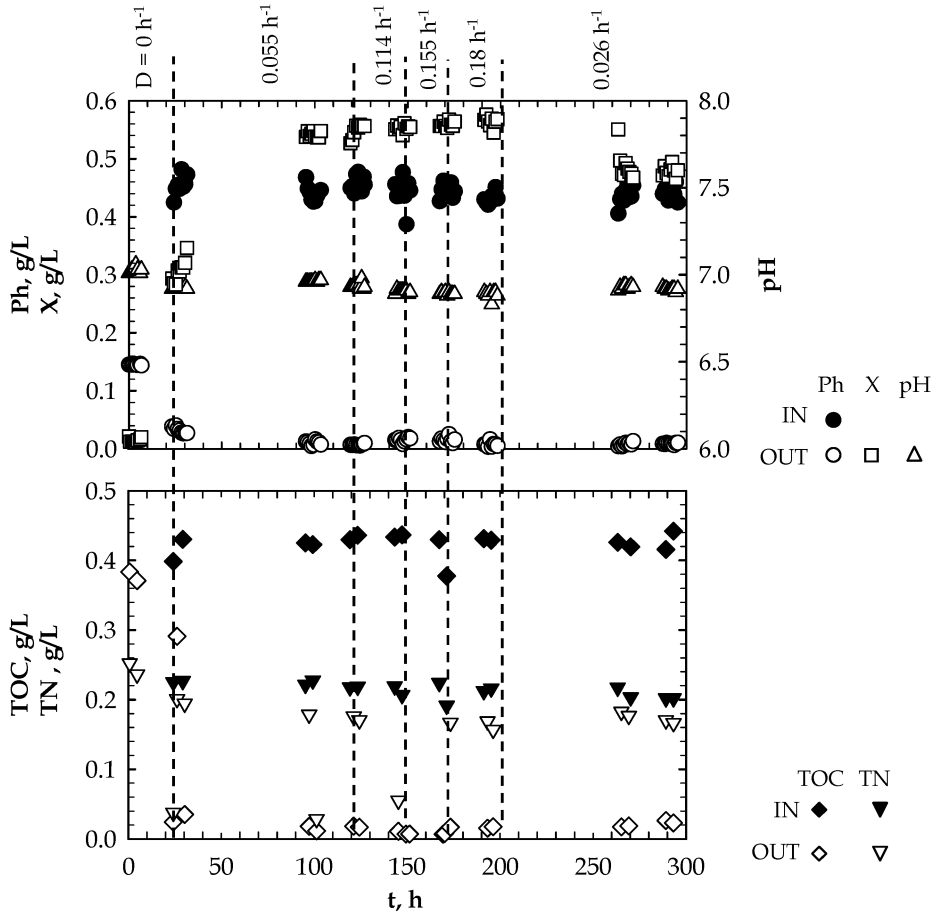

Figure 2 – Relevant data measured during a continuous culture of Pseudomonas sp. OX1. Medium: M9 added of phenol (carbon source).

The performance of the bioreactor in terms of amount of phenol degraded for unit of time and volume was estimated by working out data of liquid flow rate and phenol conversion measured during the tests. It results that the maximum throughput of the bioreactor was about 0.50 g_{Ph}/(L h) at a phenol concentration in the feed stream of about 1.0 g/L. The performance resulted quite high when compared with data available in literature (Allsop et al., 1992; Feitkenhauer et al., 2003).

The comparison of the kinetic parameters and fractional yield coefficient, $Y_{X/S}$, estimated in the present work with those estimated in batch culture experiments (Viggiani et al., 2006) is now in order Under continuous culture conditions the maximum growth rate results about 3 times that estimated by means of batch cultures (0.6 h^{-1} vs 0.17 h^{-1}). The $Y_{X/S}$ in continuous culture conditions is 1.5 times that estimated in batch culture conditions. The difference between the two sets of data suggests that the growth behaviour of *P. sp. OX1* strongly depends on the culture modality, similarly to previous investigation carried out with other bacteria (Strobel, 1995; Feitkenhauer et al., 2003). The higher value of $Y_{X/S}$ measured in continuous culture should indicate that phenol was degraded very efficiently by *P. sp. OX1*. Partial accumulation of metabolites in the liquid phase during the first transient period points out that the pathways to complete the phenol conversion may be kinetically disadvantaged with respect to the initial phenol degradation pathway. The observed behaviour may be due to the time-scale of the metabolic mechanism and in particular to the comparison of the cell relaxation time with the time scales of the reactor (Bailey and Ollis, 1986). In batch conditions the environment of cell growth changes continuously with the time (nutrient depletion, biomass increase etc.). In a continuous culture growth conditions remain stable in the time. Therefore, it is evident that for some bacteria the batch cultures may not be considered representative of quasi-steady states and non structured models can not be adopted.

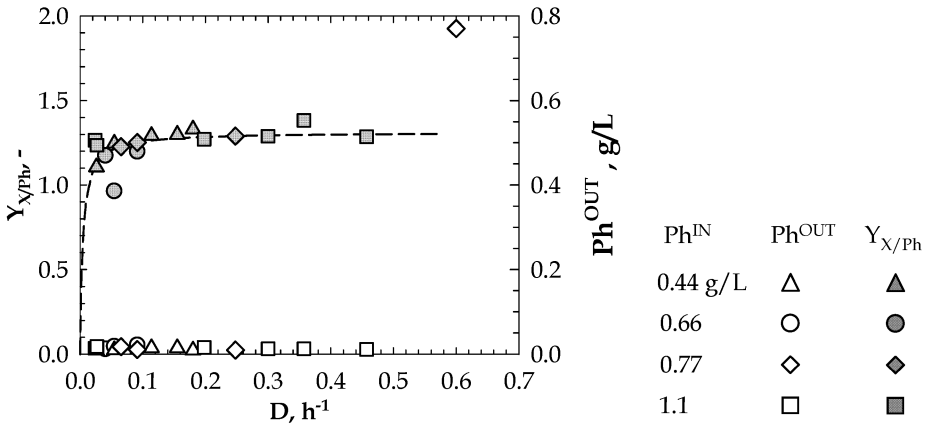

Figure 3 - Phenol to biomass fractional yield and phenol concentration in the reactor as a function of the dilution rate.

Acknowledgements

This work was supported by grants from the Ministero dell'Università e della Ricerca Scientifica (Progetti di Rilevante Interesse Nazionale, PRIN). The authors gratefully acknowledge the support of Miss Valeria Chianese.

Nomenclature

D	Dilution rate	Ph	Phenol concentration
HMAS	2-hydroxymuconic acid semialdehyde	TN	Total nitrogen carbon
		TOC	Total organic carbon
K_La_L	Mass transfer coefficient	X	Biomass concentration
m	maintenance coefficient	Y	Fractional yield coefficient
O_2	Oxygen concentration		
OUR	Oxygen uptake rate	μ	Biomass specific growth rate

References

Allsop P.J., Y. Chisti, M. Moo-Young, G.R. Sullivan, 1993, Biotechnol. Bioeng., 41, 572

APHA Standard Methods for the Examination of Water and Wastewater, 1992, APHA, Washington DC USA.

Baggi G, P. Barbieri, E. Galli, S. Tollari, 1987, Appl. Environ. Microbiol. 53, 2129.

Bailey J.E. and D.F. Ollis, 1986, Biochemical Engineering Fundamentals. New York. Ed. McGraw-Hill.

Bertoni G., F. Bolognese, E. Galli, P. Barbieri, 1996, Appl. Environ. Microbiol. 62, 3704.

Bryers J.D., **BIOFILMS II**, Wiley-Liss, 2000

Chianese V., 2007. Graduation Thesis in Molecular and Industrial Biotechnology, University of Napoli Federico II

Feitkenhauer, H., S. Schnicke, R. Muller, H. Markl, 2003, J. of Biotechnology 103, 129

Heijnen J.J., A. Mulder, R. Weltevrede, P.H. Hols and H.L.J.M. van Leeuwen, 1990, Chem. Eng. Technol. 13, 202

Lodato A., F. Alfieri, G. Olivieri, A. Di Donato, A. Marzocchella, P. Salatino, 2007, Enz. and Microbial Technology, 41, 646

Onysko K.A., C.W. Robinson, H.M. Budman HM, 2002, Can J. Chem. Eng. 80,239.

Pirt S. J., 1965, Proc. Roy. Soc. (London), Ser. B 163(991), 224.

Russo M.E., 2008, PhD Thesis in Biotechnology Science "Intensification of Bioconversion Processes: Design and Development of Reactors with High Biocatalyst Loading", University of Napoli Federico II

Strobel H.J., 1995, Current Microb., 31, 210

Viggiani A., G. Olivieri, L. Siani, A. Di Donato, A. Marzocchella, P. Salatino, P. Barbieri and E. Galli. 2006, J. Biotechnol. 123, 464.

Whited G.M., D.T. Gibson, 1991,. J. Bacteriol. 173, 3010.

Yang R.D., A.E. Humphrey, 1975, Biotech. Bioeng. 17, 1211.

CHEMICAL ENGINEERING TRANSACTIONS, Volume 14, 2008
Edited by G. Marino, E. Bardone, A. Viglia
 ISBN 978-88-95608-02-0

Novel expression systems for recombinant protein production at low temperatures

Maria Giuliani[1], Ermenegilda Parrilli[1,2], Maria Luisa Tutino[1,2], Giovanni Sannia[1] and Gennaro Marino[1,2]
[1]Department of Organic Chemistry and Biochemistry, University of Naples "Federico II" Complesso Universitario M.S. Angelo via Cinthia 4, 80126, Napoli Italia
[2]Faculty of Biotechnological sciences, University of Naples "Federico II"

One of the main limitations experienced while producing proteins in conventional bacterial mesophilic systems is the need to operate at their optimal growth temperature (usually 37 °C) for the production process. Since temperature has a general negative impact on protein folding due to the strong temperature dependence of hydrophobic interactions that mainly drive the aggregation reaction, the production of recombinant proteins at low temperatures represents an exciting model to improve the quality of the products. Recombinant protein production in psychrophilic bacteria, i.e. at temperature as low as 4°C, may minimise undesired hydrophobic interactions during protein folding, desirably resulting in enhancing the yield of soluble and correctly folded products. In this context, a few cold adapted species are under early but intense exploration as cold cell factories, among them, *Pseudoalteromonas haloplanktis* being a representative example. The efficiency of cold-adapted expression systems was tested by fully soluble and biologically competent production of several thermal-labile and aggregation-prone products in *Ph*TAC125 such as the mature human nerve growth factor and a yeast α-glucosidase Furthermore, with respect to *E. coli*, *Ph*TAC125 is extremely efficient in secreting proteins in the culture medium. By the use of a psychrophilic α-amylase as secretion carrier for the extra-cellular targeting of recombinant proteins an efficient gene-expression system was set up. Observed efficiency of the cold-adapted system (secretion yield was always above 80%) placed it amongst the best heterologous secretion systems in Gram-negative bacteria reported so far.

1. Introduction

The number of candidate proteins to be used as biopharmaceuticals or in industrial processes is rapidly increasing in recent years (Pavolu *et al.*, 2005). However, efficient expression of genes in homologous/heterologous expression systems and rapid purification steps are actually major bottlenecks. In fact, although many recombinant proteins have been successfully produced by common prokaryotic (*Escherichia coli*) and eukaryotic (yeasts and CHO cells) hosts, these conventional systems have often proved to be unproductive due to the special properties of the protein to be produced. Indeed, beside the obvious impossibility of achieving a large scale production of thermally labile proteins at the normal *E. coli* growth temperature, degradation of the product by the host proteases and the incorrect folding of the nascent polypeptides, resulting in the protein aggregation and accumulation as insoluble inclusion bodies, are sometimes observed (Speed *et al.*, 1996). To overcome the above mentioned limits of *E. coli* as host for recombinant protein production, a rational experimental approach has

consisted in lowering the cultivation temperature (Baneyx, 1999), since this change has a pleiotropic consequence on the folding process. Inclusion bodies formation is a process mainly driven by hydrophobic interactions which are directly dependent on temperature (Kiefhaber *et al*., 1991). There are many examples in literature describing the effectiveness of enhancing solubility of a number of difficult proteins by this approach (Vasina and Baneyx, 1997). The growth of *E. coli* below 37 ºC has been often explored to minimise aggregation but without consistent, protein-irrespective results. The major drawback in *E. coli* cultivation at sub-optimal temperatures is, however, the decrease in biomass production which reduces the global process productivity. Therefore, the use of psychophilic bacteria as alternative expression hosts is the compelling choice towards the exploitation of industrial processes at temperatures as low as 0°C.

2. The psychophilic host: *Pseudoalteromonas haloplanktis* TAC125

P. haloplanktis TAC125 is a Gram-negative bacterium isolated from an Antarctic coastal seawater sample collected in the vicinity of the French Antarctic station Dumont D'Urville, Terre Adélie. It can be classified as a Eurypsychrophile (i.e. a bacterium growing in a wide range of low temperatures; Atlas and Bartha, 1993) and was the first Antarctic Gram-negative bacterium of which the genome was fully sequenced and carefully annotated (Médigue *et al*., 2005). Genomic and metabolic features of this bacterium, accounting for its remarkable versatility and fast growth compared with other bacteria from aqueous environments, were discovered by combining genome sequencing and further *in silico* and *in vivo* analyses. *P. haloplanktis* TAC125 is able to duplicate in a wide range of temperatures (0-30°C), with an apparent optimal growth temperature a t 20°C, where the observed duplication time in rich medium is 31 minutes (Tutino *et al.,* 1999). However, the bacterium still duplicates at fast speed even at lower temperatures (at 4°C, one cell division is completed in about 100 min; unpublished results from this laboratory) and, when provided with sufficient nutrients and aeration, it grows to very high density (up to A_{600}=20) under laboratory settings, even at 0°C. This growth performance makes it one of the faster growing psychrophiles so far characterised. Fast growth rates, combined with the ability of *P. haloplanktis* TAC125 to reach very high cell densities even under laboratory growth conditions and to be easily transformed by intergeneric conjugation (Duilio *et al*., 2004a), made this bacterium an attractive host for the development of an efficient gene expression system at low temperatures.

3. Genetic tools for recombinant protein production at low temperatures

3.1 The psychrophilic expression vector

A few other reported examples of recombinant protein production in psychrophiles made use of molecular signals (such as the origin of replication and the transcriptional promoter) derived from mesophiles. A different philosophy inspired the construction of our gene-expression systems, which derived from the proper assembly of true phychrophilic molecular signals into a modified *E. coli* cloning vector. By combining

mesophilic and psychorophilic genetic signals a collection of psychophilic gene-expression vectors was set up to produce recombinant proteins in *P. haloplanktis* TAC125. The mesophilic signals consist of the pUC18-derived origin of replication (OriC) and a selection marker gene (a β-lactamase encoding gene), allowing the plasmid to replicate either in *E. coli* or in the phychrophilic host. Another crucial mesophilic signal is represented by the OriT sequence, the conjugational DNA transfer origin from the broad host range plasmid pJB3 (Blatny *at al*., 1997). Structural and functional studies led to the isolation of the psychrophilic origin of replication (OriR) from the *P. haloplanktis* TAC125 endogenous plasmid pMtBL (Tutino *et al*., 2001).

3.2 Phsychrophilic promoters

3.2.1 Constitutive expression

The structural/functional characterisation of *P. haloplanktis* TAC125 promoters was carried out by random cloning of genomic DNA fragments and identification of promoter sequences by evaluating their capability to express a promoter-less reporter gene (Duilio *et al*., 2004). By this promoter-trap strategy, a collection of constitutive psychrophilic promoters showing different strengths at different temperatures was identified. The implementation of the above described psychrophilic promoters in the pMtBL-derived shuttle vectors resulted in the set up of cold-adapted gene-expression systems, characterised by the constitutive production of the recombinant protein.

3.2.2 Regulated expression

Sometimes efficient production can only be achieved by fine tuning the recombinant gene expression. This goal can be reached by using regulated promoters and efficient induction strategies. Recently, by using a differential proteomic approach, we isolated and characterised a two-component system. This regulatory system is responsible for the transcriptional regulation of the gene coding for an outer protein porine, and it is strongly induced by the presence of L-malate in the medium (Papa *et al*., 2006). The regulative region of the porine gene was used for the construction of an inducible cold expression vector, where the recombinant protein expression is under L-malate control.

3.3 Molecular signals for protein addressing

3.3.1 Periplasmic secretion

Although the production of recombinant protein in the host cytoplasm is the preferred strategy many processes due to higher production yields, this approach cannot be pursued when the wanted product requires the correct formation of disulphide bonds to attain its catalytic competent conformation. Indeed as for all Gram-negative bacteria, *P. haloplanktis* TAC125 cytoplasm is a reducing environment and the formation of disulphide bridges is confined in the periplasmic space. From the genome analysis, we know that *P. haloplanktis* TAC125 contains all the canonical periplasmic export machineries (Medigue *et al*., 2005). Therefore, gene fragments encoding two signal peptides from psychrophilic secreted proteins following different translocation mechanisms have been cloned in the psychrophilic expression vectors, under the control of different promoters in order to allow the signal peptides N-terminal fusion for periplasmic addressing of recombinant proteins.

3.3.2 Extra-cellular secretion

In order to combine the effects of low temperatures on the recombinant product solubility with the advantages linked to extra-cellular protein targeting, a gene expression system for the production and extra-cellular secretion of recombinant proteins in psychrophilic bacteria was set up. The novel system makes use of the psychrophilic α-amylase from *P. haloplanktis* TAB23 (Feller *et al*., 1992) as a secretion carrier. This exo-protein is produced and secreted as a larger precursor with a long C-terminal propeptide that is not mandatory for the α-amylase secretion when it is produced by recombinant cold-adapted bacteria the propeptide (Tutino *et al*., 2002; Cusano *et al.,* 2006a). Starting from the latter observation, the secretion of chimeric proteins obtained by the replacement of α-amylase C-terminal propeptide with a passenger protein was studied (Cusano *et al.,* 2006b). The novel genetic system allows the easy in-frame cloning of any gene downstream of the mature psychrophilic α-amylase encoding region (Figure 1). The spacer between the carrier and passenger proteins contains the motif -Ala-Ser-Ser-Thr- recognised and cleaved by a *P. haloplanktis* TAC125 secreted protease that allows the separation of the protein of interest from the secretion carrier when it reaches the extra-cellular medium.

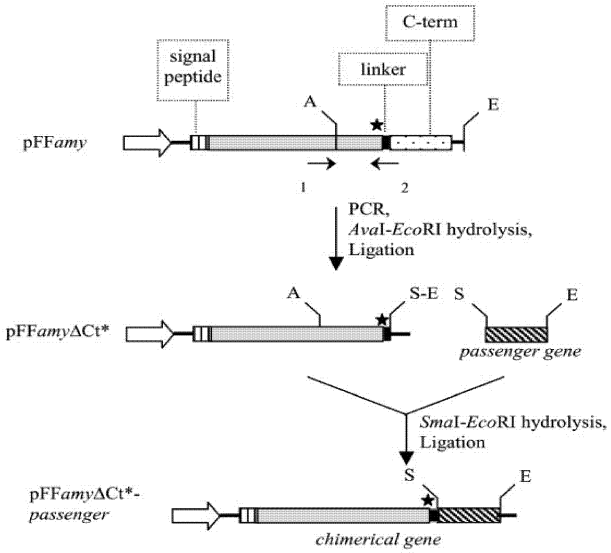

Figure 1 The genetic system for recombinant protein secretion in *P. haloplanktis* TAC125 extra-cellular medium. *White arrow*, *P. haloplanktis* TAC125 *aspC* promoter; signal peptide, sequence encoding *P. haloplanktis* TAB23 α-amylase signal peptide; C-term, α-amylase C-terminal propeptide encoding sequence; linker, α-amylase linker encoding sequence; A, *AvaI*; E, *EcoRI*; S, *SmaI* restriction endonuclease sites; *black arrows,* PCR primers. The *black star* indicates the *P. haloplanktis* TAC125 exo-protease cleavege site.

4. Recombinant protein production in *P. haloplanktis* TAC125

4.1 Cytoplasmic production: *P. haloplanktis* TAE79 β-galactosidase and *Saccharomyces cerevisiae* α-glucosidase

Two "difficult" proteins were produced to test performances of the cold expression system inducible by L-malate (Papa *et al*., 2007). These proteins (the psychrophilic β-galactosidase from *P. haloplanktis* TAE79 and the *S. cerevisiae* α-glucosidase) were chosen because they can hardly be expressed in mesophilic hosts even at sub-optimal temperature conditions. When the β-galactosidase was produced in *E. coli* cells at 18°C, 20mg of catalytically active enzyme was produced per litre of culture. Analogously, recombinant yeast α-glucosidase produced in *E. coli* aggregates in an insoluble form and the active soluble amount of protein was less than 1% of the total production (Le Thanh and Hoffmann, 2005). Both recombinant psychrophilic β-galactosidase and yeast α-glucosidase were produced in *P. haloplanktis* TAC125 (Figure 2A and B) as soluble and catalytically active enzymes at 15°C. Structural and kinetic analysis of the recombinant proteins showed that both enzymes were nearly identical to their native counterparts. Experimental conditions for optimal protein production in the cold expression system were also defined. Under optimal expression conditions, recombinant β-galactosidase is produced with high yields (620-720 mgL^{-1}), indicating that the inducible system can be very effective in the expression of psychrophilic proteins that are usually poorly produced in mesophilic hosts. A significantly lower production yield is observed for yeast a-glucosidase (27 mgL^{-1}) possibly due to the different codon usage between the eukaryotic and bacterial organisms. Nevertheless, the cold expression system yielded a satisfactory amount of this protein in a soluble and active form.

4.2 Periplasmic production: *h-β-NGF*

Another example of "difficult" protein is the mature form of the human nerve growth factor (h-NGF), a neurotrophin which found promising applications as a therapy agent in several neurological disorders such as Alzheimer's disease (Lad *et al*., 2003). Therapeutical applications require the expression and purification of a large amount of functional protein. However, the recombinant production of this protein exhibits several problems in the conventional host *E. coli,* due to its tendency to form insoluble aggregates either when produced as prepro-protein or as mature form (Dicou *et al*., 1989; Rattenholl *et al.*, 2001). Vigentini *et al*., (2006) reported the expression of the mature form of human NGF gene in *P. haloplanktis* TAC125 and investigated the production and the cellular localisation of the recombinant protein. The protein constitutively produced at 4°C was soluble and efficiently translocated in the host periplasmic space (Figure 2C). A gel exclusion chromatography also indicated that the protein was largely in a dimeric form, the quaternary structure required for its biological activity (Harmer *et al.*, 2003).

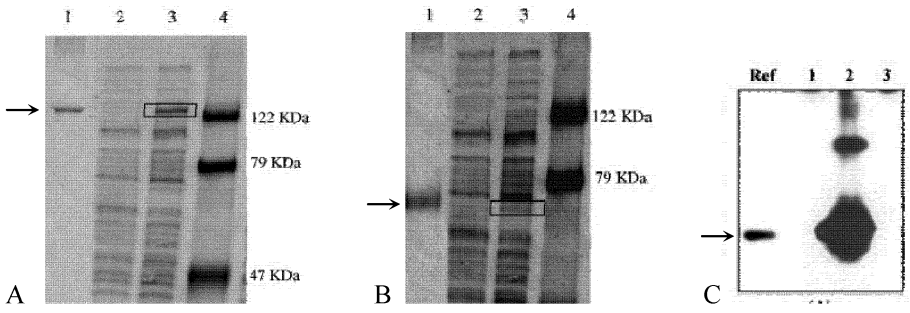

Figure 2 Recombinant protein production in *P. haloplanktis* TAC125. **A** Recombinant production of the thermally labile β-galactosidase from *Ph*TAE79 in *Ph*TAC125 cells. 7,5% SDS PAGE gel electrophoresis of protein extracts from *Ph*TAC125 cells harboring p(PSHAb0363) and grown in minimal medium at 15°C in the absence (lane2) and in the presence (lane3) of L-malate, in comparision with β-galactosidase from *Ph*TAE79 used as control (lane1). The recombinant protein is indicated by an *open box.* **B** Recombinant production of the mesophilic α-glucosidase from *Saccaromyces cerevisiae* in *Ph*TAC125 cells. 7,5% SDS PAGE gel electrophoresis of protein extracts from *Ph*TAC125 cells harboring pUCRPGLUCP1 and grown in minimal medium at 15°C in the absence (lane2) and in the presence (lane3) of L-malate, in comparision with commercial α-glucosidase from yeast used as control (lane1). The recombinant protein is indicated by an *open box.* **C** rh-NGF production and cellular localisation in recombinant PhTAC125. Western blotting analysis of periplasmic (lane2) and cytoplasmic (lane3) fractions of 4°C grown PhTAC125-pPM13*psDngf* recombinant cells. Polyclonal anti-h-NGF antibodies were used for immunodetection. As positive control, 50ng of rm-NGF proteins was loaded in lane1.

4.3 Extra-cellular secretion of several heterologous proteins

One strategy to improve the protein production process in to target the protein to the outer compartment of the host cell. This strategy avoids inclusion body formation and the majority of the proteolytic proteins in the cytoplasm and achieves a primary purification reducing the costs of downstream processes. Cusano *et al.*, (2006b) described the setting up and utilisation of a cold gene expression system in *P. haloplanktis* TAC125 implemented for the specific secretion of recombinant proteins in the extra-cellular medium by the use of the psychrophilic α-amylase as a secretion carrier. Three chimerical proteins, obtained by fusing intra-cellular proteins to the psychrophilic exo-enzyme, were produced in *P. haloplanktis* TAC125 and their secretion kinetic was evaluated. The results demonstrated that the cold adapted secretion system is extremely efficient since all tested chimeras were correctly localised in the extra-cellular medium with a secretion yield always above 80% (Table1). Furthermore, reported activity data indicated that the system also allows the correct disulphide bond formation of chimera components (Cusano *et al.,* 2006b).

Table 1

Secretion yield of chimerical proteins in recombinant *P. haloplanktis* TAC125 cells

vector	α-amylase (UI/ml)		α-amylase	alkaline phosphatase	**secretion yield**[a]
	p	em	em(%)	em(%)	
pFF*amyΔ*Ct-*dsbA*	0.12 ± 0.01	3.58 ± 0.03	97	4	**93**
pFF*amyΔ*Ct-*trpC*	0.07 ± 0.02	3.65 ± 0.03	98	5	**93**
pFF*amyΔ*Ct-*blaM*	1.23 ± 0.03	6.21 ± 0.03	83	1	**82**

Data are average results of three independent experiments. The volume of periplasmic fraction was made the same as corresponding extra-cellular medium to allow a comparison. UI, international units; p, periplasmic extract; em, extra-cellular medium fraction; em(%), percentage of the activity in extra-cellular medium fraction of the total activity (periplasmic plus extra-cellular medium fractions). [a] The difference between the em (%) of amylase activity and em (%) of alkaline phosphatase activity.

5. Conclusions

Over the last decade the number of set ups of reliable genetic systems for recombinant gene expression in cold adapted hosts was significantly enhanced. Our results demonstrated that the production of recombinant proteins in psychrophilic bacteria is not only a mature and reliable technology but it is also a successful strategy to overcome the product solubility problems often occurring in conventional systems such as in *E. coli*. In this context, *P. haloplanktis* TAC125 and the gene expression systems set up have a valuable biotechnological potential as non-conventional systems for the production of "difficult" proteins.

References

Atlas R.M., Bartha R., 1993, Microbial ecology: fundamentals and applications, 3rd ed. Benjamin/Cummings, Redwood City California

Baneyx F., 1999, Curr. Opin. Biotechnol., 10:411-21

Blatny J.M., Brautaset T., Winther-Larsen H.C., Haugan K., Valla S., 1997 Appl. Environ. Microbiol., 63:370-9

Cusano A.M., Parrilli E., Duilio A., Sannia G., Marino G., Tutino M.L., 2006a FEMS Microbiol. Lett., 258-67-71

Cusano A.M., Parrilli E., Marino G., Tutino M.L., 2006b, Microb. Cell. Factory, 5:40-7

Dicou E., Houlgatte R., Lee j., von Wilcken-Bergmann B., 1989, J. Neurosci. Res., 22:13-19

Duilio A., Madonna S., Tutino M.L., Pirozzi M., Sannia G., Marino G., 2004, Extremophiles 8:125-132

Feller G., Lonhienne T., Deroanne C., Libioulle C., van Beeumen J., Gerday C., 1992, J. Biol. Chem., 267: 5217-21

Feller G., D'Amico S., Benotmane A.M., Joly F., van Beeumen J., Gerday C., 1998, J. Biol. Chem., 273: 12109-15

Harmer N.J., Chirgadze D., Hyun Kim K., Pellegrini L., Blundell T.L., 2003, Biophys. Chem., 100:545-53

Kiefhaber T., Rudolph R., Kohler H.H., Buchner J., 1991, Biotechnology (NY), 9:825-829.

Lad S.P., Neet K.E., Mufson E.J., 2003, Curr. Drug Targets CNS Neurol. Disord. 2:315-34

Le Thanh H., Hoffmann F., 2005, Biotechnol. Prog., 21:1053-61

Médigue C., Krin E., Pascal G., Barbe V., Bernsel A., Bertin P.N., Cheung F., Cruveiller S., D'Amico S., Duilio A., Fang G., Feller G., Ho C., Mangenot S., Marino G., Nilsson J., Parrilli E., Rocha E.P.C., Rouy Z., Sekowska A., Tutino M.L., Vallenet D., von Heijne G., Danchin A., 2005, Genome Research 15:1325-35

Papa R., Glagla S., Danchin A., Schweder T., Marino G., Duilio A., 2006, Extremphiles 10:483-91

Papa R., Rippa V., Sannia G., Marino G., Duilio A., 2007, J. Biotechnol. 127-199-210

Pavolu A. K. and Belsey M., 2005 Eur. J. Pharm. and Biopharm. 59(3):389-396

Rattenholl A., Ruoppolo M., Flagiello a., Monti M., Vinci F., Marino G., Lilie H., Schwarz E., Rudolph R., 2001, J. Mol. Biol., 305:523-33

Speed M.A., Wang D.I., King J., 1996, Nat. Biotechnol., 14:1283-7

Tutino M.L., Duilio A., Fontanella B., Moretti M.A., Sannia G., Marino G., 1999, Cold-adapted organisms: ecology, physiology, enzymology and molecular biology. Spriger, Berlin, pp335-48

Tutino M.L., Duilio A., Parrilli E., Remaut E., Sannia G., Marino G., 2001, Extremophiles, 5:257-64

Tutino M.L., Parrilli E., Giaquinto L., Duilio A., Sannia G., Feller G., Marino G., 2002, J. Bacteriol., 184:5814-7

Vasina J.A., Baneyx F., 1997, Prot. Express. Purif., 9:211-8

Vigentini I., Merico A., Tutino M.L., Compagno C., Marino G., 2006, J. Biotechnol., 127:141-50

CHEMICAL ENGINEERING TRANSACTIONS, Volume 14, 2008
Edited by G. Marino, E. Bardone, A. Viglia
 ISBN 978-88-95608-02-0

Protoplast Fusion Technology and Its Biotechnological Applications.

Nitin Verma*,M.C.Bansal,Vivek Kumar
Department of Paper Technology,Indian Institute of Technology,Roorkee,Saharanpur Campus,Saharanpur,247001,India.
*Corresponding author:nitiniit2004@rediffmail.com

Protoplasts are the cells of which cell walls are removed and cytoplasmic membrane is the outermost layer in such cells.Protoplast can be obtained by specific lytic enzymes to remove cell wall.Protoplast fusion is a physical phenomenon,during fusion two or more protoplasts come in contact and adhere with one another either spontaneously or in presence of fusion inducing agents. By protoplast fusion it is possible to transfer some useful genes such as diesese resistance,nitrogen fixation ,rapid growth rate ,more product formation rate,protein quality,frost hardiness,drought resistance,herbicide resistance ,heat and cold resistance from one species to another. Protoplast fusion an important tools in strain improvement for bringing genetic recombinations and developing hybrid strains in filamentous fungi. Protoplast fusion has been used to combine genes from different organisms to create strains with desired properties.These are the powerful techniques for engineering of microbial strains for desirable industrial properties. Protoplast fusion would continued to be an existing area of research in modern biotechnology.This technique in the future will be one of the most frequently used research tools for tissue culturists, molecular biologists, biochemical engineers and biotechnologists..This review describes the protoplast fusion technology and its biotechnological applications.

Introduction:

The protoplast includes the plasmalemma and everything contained within ie.the entire cell without its inherent cellulosic cell wall.In protoplast technology ,Two genetically different protoplast isolated from the somatic cells and are experimentally fused to obtain parasexual hybrid protoplasts.The hybrid protoplast contained heteroplasoic cytoplasm and two fused parent nuclei.Fusion of protoplast is relatively a new versatile technique to induce or promote genetic recombination in a variety of prokaryotic and eukaryotic cells(Bhojwani S.S. et al 1977).Protoplast fusion may be used to produce interspecific or even intergeneric hybrids.Protoplast fusion becomes an important tool of gene manipulation because it breakdown the barriers to genetic exchange imposed by conventional mating systems.Protoplast fusion technique has a great potential for genetic analysis and for strain improvement.It is particularly useful for industrially useful microorganisms(Murlidhar R.V and Panda T. 2000).

Enzymes used for breaking of cell walls:

For protoplast fusion it is important that the cell wall of plant and microorganisms is degraded .So various enzymes used for this process.cellulase and pectinase or macerozyme acting on plant cell wall.Bacterial cell wall are degraded by the action of lysozyme.Fungal wall degraded by Novozyme -234 which includes glucanase and chitinase. *Streptomyces* cell wall degraded by action of lysozyme and achromopeptidase (Narayanswamy S 1994)(Jogdand S.N 2001).

Methods of protoplast fusion:

Protoplast fusion can be broadly classified into two categories:

Spontaneous fusion: Protoplast during isolation often fuse spontaneously and this phenomenon is called spontaneous fiusion .During the enzyme treatment,protoplast from adjoining cells fuse through their plasmodesmata to form multinucleate protoplasts.

Induced fusion:Fusion of freely isolated protoplasts from different sources with the help of fusion inducing chemicals agent s is known as induced fusion.Normally isolated protoplast do not fuse with each other because the surface of isolated protoplast carries negative charges (-10mV to -30mV) around the outside of the plasma membrane. And thus their is a strong tendency in the protoplast to repel each other due to their same charges .So this type of fusion needs a fusion inducing chemicals which actually reduce the electronegativity of the isolated protoplast and allow them to fuse with each others(Narayanswamy S 1994).

The isolated protoplast can be induced to fuse by three ways;

Mechanical fusion:In this process the isolated protoplast are brought into intimate physical contact mechanically under microscope using micromanipulator or perfusion micropipette.

Chemofusion:Several chemicals has been used to induce protoplast fusionsuch as sodium nitrate ,polyethylene glycol,Calcium ions(Ca^{++}). Chemical fusogens cause the isolated protoplast to adhere each other and leads to tight agglutination followed by fusion of protoplast (Pasha C.R et al 2007) (Jogdand S.N.2001).In order to convert cellulosic materials to ethanol by single step process , Srinivasan R and Panda T(1997) carried out chemofusion between protoplasts of *Trichoderma reesei* QM9414 and *Saccharomyces cerrevesei* NCIM 3288 .Observed successful fusion suggest that endoglucanase is the key enzyme in the success of fusion.Iwata M et al(1986) were obtained Tetracycline resistant (Tet^r),erythromycin resistant (Ery^r) fusants of *Lactobacillus fermentatum* 604 carrying a 10 megadalton Tet^r plasmid and *L.fermentatum* 605 carrying a 38 megadalton Ery^r plasmid by means of polyethylene glycol induced protoplast fusion.

Chemofusion is a non specific,inexpensive,can cause massive fusion product,can be cytotoxic and non selecetive and having less fusion frequency.

Electrofusion: Recently ,mild electric stimulation is being used to fuse protoplast .In this two glass capilliary microelectrode are placed in contact with the protoplast .An electric field of low strength ($10Kvm^{-1}$) gives rise to dielectrophoretic dipole generation within the protoplast suspensionThis leads to pearl chain arrangement of protoplasts. Subsequent application of high strength of electric fields (100 kvm^{-1}) for some microseconds results in

electric breakdown of membrane and subsequent fusion(Ushishima S.T et al 1991) (Jogdand S.N.2001).Groth DI(1987) et al carried out electofusion of *Penicillium* protoplasts,after diaelectrophoresis and foun viable fusion products.Dimitrov AP and Christov AM(1992) reported electrically induced protoplast fusion using pulse electric field for diaelectrophoresis and suggest the possibility of electrically indused protoplast fusion at cation concentration that prevents fusion when sine – wave fields are applied.Gaint protoplast of *Pleurotus cornucopiae* were fused using the glass microelectrode fusion technique.To induce fusion Ca^{++} was necessary .Polyethylene glycol 400 (PEG) promoted fusion but also increased the adhesion of protoplasts(Magae Y et al 1986).In order to regulate electrofusion Urano N et al(1998) studied electrofusion procedures for yeast breeding and reported that cell membrane fusion behaviour of respiration deficient yeasts(P^-) was remarkably different from the normal yeasts(P^+).Induction of cell membrane fusion in P^+ protoplast appeared under the pulse conditions (height 2.5-5.5 $kVcm^{-1}$and duration 25-430μs) and the time interval of morphological change from the long to short state was 3–11 s. On the other hand, induction of cell membrane fusion in P^- protoplasts appeared under the higher pulse condition (height: 4.0–7.0 kV cm^{-1} and duration: 20–500 μs). The time interval of the morphological change from the long to short state was 110–170 s in cell membrane fusants of P^- protoplasts. The ξ-potential of P^+ protoplasts was −10 to−30 mV and that of the P^- protoplasts was −25–−60 mV. The surface charge of the P^- protoplasts was more negative than that of P^+ protoplasts; therefore, regulation of electrofusion among various kinds of yeast strains was possible by changing the surface charge of the protoplasts using mitochondrial mutations.

Electrofusion is easy to control having fusion frequency upto 100%.gives reproducibility.less cytotoxic.But equipment is sophisticated and expensive.

Mechanism of protoplast fusion:

The mechanism of protoplast fusion is not fully known .Several explanations have been put forward to understand the mechanism of protoplast fusion.Some are explained here:When the protoplasts are brought into close proximity ,this is followed an induction phase thereby changes induced in electrostatic potential of the membrane results in fusion .After the fusion,The membranes stabilizes and the surface potential returns to their former state.Other literature showed when the protoplasts are closely adhered ,the external fusogens cause disturbance in the intramembranous proteins and glycoproteines.This increases membrane fluidity and creates a region where lipid molecule intermix,allowing coalescence of adjacent membranes.The negative charge carried by protoplast is mainly due to intramembranous phosphate groups .The addition of Ca^{++} ions causes reduction in the zeta potential of plasma membrane and under this situation protoplasts are fused(Peberdy J.F 1980).The high molecular weight polymer (1000-6000) of PEG acts as a molecular bridges connecting the protoplasts. calcium ions linked the negatively charged PEG and membrane surface .On elution of the PEG ,the surface potential are disturbed ,leading to intramembrane contact and subsequent fusion, Besides this ,the strong affinity of PEG for water may cause local dehydration of the membrane and increase fluidity,thus inducing fusion.Protoplast fusion

takes place when the molecular distance between the protoplasts is 10A or less .This indicates that protoplast fusion is highly a traumatic events.(Jogdand S.N,2001)(Narayanswamy S 1994)

Protoplast fusion in fungi:

Production and regeneration of protoplasts is a useful technique for fungal transformations.Commercial preparation of enzymes which contain mixture of products to digest fungal cellwall used .Novozyme 234 includes (glucanase and chitinase) enzyme mixture is added to rapidly growing fungal tissue suspensed in an osmotic buffer (e.g.0.6 mol^{-1},KCl,1.2 mol^{-1},Sorbitol or 1.2 $mol^{-1}MgSO_4$).The protoplasts and DNA are mixed in presence of 15%(w/V)PEG 6000 and pH buffer (TRIS HCl).10 mml^{-1}.PEG causes clump formation in protoplasts. At 37^0C ,grow mycelium on cellophone placed on agar overnight.Incubte with enzyme at 30^0C for 1.5 hours in empty petridish having KCl,than filter protoplasts,wash protoplast in KCl (Centrifuge and resuspended the pellets).Protoplast fusion frequency in fungi is 0.2 -2%(Srinivas R.T and Panda T 1997)(Jogdand S.N 2001)

Protoplast technology for *Streptomyces* species:

Streptomyces spp also do not have natural means of mating .For obtaining protoplasts from *Streptomyces* lysozyme is used which breakes glycan portion of peptidoglycan wall.Cultures from spore suspension (2 days in shaker at 30^0C) harvest by centrifugation ,Resuspended in 0.03 mol^{-1} sucrose, washed and reharvest,Than resuspended in lysozyme solution in protoplasting medium(30 min – 2 hr at 30^0C) (Kohlar J and Darland G et al 1988) (Tehrani J.L et al 1992).

Protoplast fusion in bacteria:

In bacteria protoplast can be obtained and fusion can be carried out with low frequency in some gram positive organisms.For gram negative bacteria it is possible to obtain protoplast but regeneration is difficult. The procedure is highly efficient and yields upto 80% transformants (Iwata M. et al 1986) (Jogdand S.N.2001).

Biotechnological applications of protoplast fusion:

Protoplasts contained all the intracellular organelles of cells and form a vital link in transfer of micromolecules between cyto organelles,currently most of the laboratories engaging in fungal genetics are using gene manipulation procedures based on protoplasts.Therefore to further improve the genetic properties of these strains using protoplast fusion are attempt to develop methods for preparation and regeneration of protoplasts.The process involves protoplast mutagenesis,transformation and protoplast fusion (Evans D.A.1983). The direct bioconversion of cellulosic materials to ethanol by the intergeneric fusants between *T.reesei* and *Saccharomyces cerevesie* appears to be are of the best technique for an alternative approaches for ethanol production Also this process is helpful in the production of a complete set of cellulases by the protoplast fusion of *T.reesei* and *A.niger* (one produced more amount of endo and exoglucanase and other produced more β- glucosidase(Ahmed M

and Berkley EI 2006).Prabhavarthy V.R. et al (2006) reported that the isolated protoplast from *Trichodermma reesei* strain PTr2 showed high CMCase activity with 80% of fusants and more than two fold increment in enzyme activities with two fusants SFTr2 and SFTr3 as compared to the parental strain PTr2.Nazari R et al(2005) carried out intraspecific protoplast fusion with polyethylene glycol 1000 in *Streptomyces griseoflavus* to increase the production of desferrioxamine B chelator that absorbs additional iron from the blood of thalasemia patients.A haploid glucoamylase producing strains of *Saccharomyces diastatiacus* lacking the pof gene and thus unable to produce phenolic off flavour in beer was constructed by classical genetic techniques.Protoplast fusion was perfomed between this strain and a brewing polyploidy *Saccharomyces uvarum* strain .Some clones derived from fusion products can produce low carbohydrate beer of acceptable flavor(Janderova B et al 1990).Rygielska J.K (2004) obtained interspecific fusants of starch fermenting yeasts *Schwanniomyces occidentalis* ATCC 48086 and yeasts *Saccharomyces diaastiacus* ATCC 13007 and *Saccharomyces cerevisiae*.The fusants showed the tolerance to cyclohexamide(0.001%) in case of *Schwanniomyces occidentalis* ATCC 48086 and the ability of *Saccharomyces yeasts* to grow at 40^0C. and also improved the ability to synthesize amylolytic enzymes to improve the biochemical ability of yeasts .Amylase hyper producing ,catabolite repression resistant recombinant strains were produced by intraspecific protoplast fusion of thermophillic fungus *Thermomyces lanuginosus* strains (Rubinder K et al 2000) (Zhao K et al(2004) studied on the preparation and regeneration of protoplast from Taxol producing fungus *Nodulisporium sylviforme* ,found that the combination of 4 enzymes (lywallzyme,snailase,lysozyme and cellulase) obtained higher the preparation frequency of protoplast than that of any of them used alone. Zhang ZB et al(2007) carried out protoplast fusion between the *Helminthosporium gramineum* sub sp,*Echinchloae* (HGE)strain ,HMI and *Curvularia lunata* (CL) to breed new strains with improved spore productivity and form fusant strains had increased production of the Phytotoxin ophiobolin A,compared with HMI.Liu WH etal(1996) carried out protoplast fusion between the protoplast of an inducible cholesterol oxidase producing bacterium *Arthrobacter simplex* USA 18 and a constitutive cholesterol oxidase producer strain US 3011 in the presence of 20-40% polyethylene glycol 6000 and the resultant fusants showed the cholesterol oxidase activity in a cholesterol containing medium with 20-60% higher than that of parental strains.Brume MD et al (1992) carried out protoplast fusion of morphologically and biochemically different *Claviceps purpurea* strains producing ergotoxins without introducing selective auxotrophic markers .Fused strains showed about ten fold higher alkaloid production than parental strains.Javedekar VS et al (1995)construct a highly flocculent yeast with a killer character by protoplast fusion .Resultant yeasts also being resistant to the fungicide at a concentration of 100 µg/ml.Pasha et al (2007) reported that protoplast fusion followed by sequential mutations gave a stable and good performing fusant with maximum utilization of reducing sugars in the media.They fused the protoplasts of thermotolerant *Saccharomyces cerevisiae* and mesophilic,xylose-utilizing *Candida shehatae* by electrofusion,and the selected best fusant was mutated sequentially.The mutant fusant CP11 was found to be stable and used for lignocellulosic fermentation and gave an ethanol

yield of 0.459 g g^{-1} productivity of 0.67 g/l/h and fermentation efficiency of 90%.Electrically induced protoplast fusion employed for hybrid construction in ergosterol producing yeast strains.Some fusion products proved to be hybrid with respect to ergosterol content and to remain stable over several generations(Avram D et al 1992).Yari S et al (2002) studied the effects of protoplast fusion on δ- endotoxins production in *Bacillus thuringiensis* spp (H14) found that *Bacillus thuringiensis* fusants have 1.48 time more δ-endotoxins than wild type.According to US Patent 7241588 Fusants of *Penicillium chrysogenum* and *Cephalosporium acremonium* produced a novel lactam antibiotic .Kohlar J and Darland G(1988) investigated the protoplast fusion in *Streptomyces avermitillis* which involved in avermectin biosynthesis.resulting fusants showed improved properties in respect to ,rifampicin resistance and maintaing the ability to carry out the metylation of C-5 hydroxyl of the avermectin molecules.Arti Das and Anuradha Ghosh (1989) carried out protoplast fusion between two strains of *Aspergillus niger* 8-2 a fast growing strain and poor producer of glucoamylase and *Aspergillus niger* 8-7 ,a slow rowing strain and good producer of enzyme and the resulting fusant produced 68% more glucoamylase than parental strains.Bakthiari M.R.et al(2007) carried out protoplast fusion between different strains of *Tolypocladium inflatum* .One of the recombinants produced cyclosporine 2.8 times more than parental strain.

References :

Ahmed M,El Barkly,2006,Gene Transfer between Different *Trichoderma* Species and *Aspergillus niger* through intergeneric protoplast fusion to convert ground rice straw to citric acid and cellulase ,Appl Biochem Biotechnol;135:117-132.

Avram D,I.Petcu,M.Radu,F.Dan and R.Stan,1992,Electrically induced protoplast fusion for ergosterol producing yeast strain improvement .J Basic Microbiol,32,369-372.

Bhojwani S.S,J.B.Powar and E.L.Cocking,1977,Isolation,culture and division of protoplast,Plant Sci Lett,8,85-89.

Brume MD,V.G.Parker,M.Alacemi and H.Socici,1992,Strain improvement of *Claviceps purpurea* by protoplast fusion without introducing auxotrophic markers.Appl Microbiol Biotechnol ,38.

Dimitrova AP and A.M.Christov,1992,Electrically induced protoplast fusion using pulse electric fields for dieelectrophoresis.Plant Physiol,100,2008-2012.

Evans DA,1983,Agricultural application of protoplast fusion .Nature Biotechnology,1, 253-261.

Gokhale DV,U.S.Puntambekar and D.N.Deobagkar,1993,Protoplast fusion :A tool for intergeneric transfer in bacteria.Biotechnol Adv,11,199-217

Groth D I,H.E.Jacobs,W.Kunkel and H.Berg,1987,Electrofusion of *Penicillium* protoplast after dielectrophoresis.J Basic Microbiol,27,341-344.

Iwata M,M.Mada and H.Ishiwa,1986,Protoplast fusion of *Lactobacillus fermentum*.Appl Environ Microbiol,52,392-393.

Janderova B,F.Cvrckova and O.Bendova,1990,Construction of the dextrin-degrading pof brewing yeast by protoplast fusion ,J Basic Microbiol,30,issue 7,499-505.

Javadekar VS,H.Sivavaman and D.V.Gokhle,1995,Industrial yeast improvement :Construction of a highly flocculant yeast with a killer character by protoplast fusion.J Ind.Microbiol ;15: 94-102.

Jogdand S.N. 2001.Protoplast Technology,Gene Biotechnology,Himalaya Publishing house 3rd ed 171-186.

Kohler J and G.Darland,1988,Protoplast fusion in *Streptomyces avermitillis*.J Ind Microbiol Biotechnol .

Liu WH,L.W. Chow and C.K.Lo,1996,Strain improvement of *Arthrobactor simplex* by protoplast fusion.J Ind Microbiol Biotechnol,16,257-260

Magae Y,Y.Kashwagi,M.Senda and T.Sasaki,1986,Electrofusion of gaint protoplast of *Pleurotus cornucopiae* .Appl Microbiol Biotechnol,24,509-511.

Murlidhar RV and TPanda,2000,.Fungal protoplast fusion : A revisit.Bioprocess Biosyst Engg ,22,429-431.

Narayanswamy S,1994,Plant cells and tissue cultures.Plant Protoplast:Isolation,Culture and Fusion ,391-469.TATA MCGraw Hill Publishing Company ,New Delhi,India.

Nazari R.,A.Akbarzadeh,D.Norouzian,B.Farahmand,J.Vaez,A.Sadegi,F.Hormozi,K.M.Rad and B.Zarbaksh,2005,Applying intraspecific protoplast fusion in *Streptomyces griesoflavus* to increase the production of Desferrioxamines B.Curr Sci ,88,11,1815-1820

Pasha C,R.C.Kuhad and C.VRao,2007,Strain improvement of thermotolerant *Saccharomyces cerevessie* VS3 strain for better utilization of lignocellulosic substrates.J Appl Microbiol ,103,1480-1489.

Prabavarthy VR,mathiavanan N,Sagadevan E ,Murugesan K,Lalithakumari D 2006,Intrastrain protoplast fusion enhances carboxymethylcellulase activity in *Trichodermma reesei*.Enzyme Microbial Technol;38:719-723.

Rubinder K,B.S.Chadha,S.Singh and H.S.Saini,2000,Amylase hyperproducing haploid recombinant strains of *Thermomyces lanuginosus* obtained by intraspecific protoplast fusion.Can J Microbiol ,46,669-673.

Rygielska JK,2004,Obtaining hybrids of distialliary yeasts characterized by the ability of fermenting starch.Elec J Pol Agri Univ;Series Biotechnol.

Srinivas R and T.Panda,1997,Localization of carboxymethyl cellulase in the intergeneric fusants of *Trichodermma reesei* QM 9414 and *Saccharomyces cerevisee* NCIM 3288.Bioprocess Biosystems Engg ,18,71-73.

Urano N,S.R.Higha and H.Hirai,1998,Effect of mitochondria on electrofusion of yeast protoplast. Enzyme Microbiol Technol.1998 ,23,107-112

Ushijima S,T.Nakadai and K.Uchida,1991,Interspesfic electrofusion of protoplasts between *Aspergillus oryzae* and *Aspoergillus sojae.*Agri Biol Chem,55,129-136.

YariS,D.N.Inanlou,F.Yari,M.Salech,B.Farahound andA.Akbarzadeh,2002,Effects of protoplast fusion on δ-endotoxin production in *Bacillus thuringiensis* spp CH 141.Iran Biomed J,6,25-29.

Zhang ZB,N.R.Burgos,J.P.Zhang and L.O.YU,2007,Biological control agent for rice weeds from protoplast fusion between *Curvularia lunata* and *Helminthosporium gramineum.*Weed Sci ,55,599-605.

Zhao, K,D,.Zhou ,W.Ping and J.Ge,2004, Study on the preparation and regeneration of protoplast from Taxol-Producing fungus *Nodulisporium sylviforms*.Nat Sci,2,52-59.

Method for producing novel lectan antibiotic from protoplast fusion strain.United states Patent 7241588.

.

CHEMICAL ENGINEERING TRANSACTIONS, Volume 14, 2008
Edited by G. Marino, E. Bardone, A. Viglia
 ISBN 978-88-95608-02-0

Unstructured models for batch cultures of *lactobacillus helveticus*

Abdallah Bouguettoucha[1, 2] Béatrice Balannec[2], Saci Nacef[1], and Abdeltif Amrane[2]
[1]Département de Génie des Procédés, Faculté des Sciences de l'Ingénieur, Université Ferhat Abbas, 19000 Sétif, Algeria
e. mail : abd_Bouguettoucha@yahoo.fr, Nacef_S @yahoo.fr
[2]Equipe Chimie et Ingénierie des Procédés - Université de Rennes 1 / ENSCR
UMR CNRS 6226 "Sciences Chimiques de Rennes"
ENSCR, Campus de Beaulieu, avenue du Général Leclerc, 35700 Rennes, France.
e. mail : Abdeltif. Amrane @univ-rennes1.fr, Beatrice.Balannec@univ-rennes1.fr

In the recent year's one can observe a growing interest in lactic acid production, which plays an important role in various applications in food, pharmaceutical and textiles industries More recently, lactic acid fermentation has received much attention because of an increasing demand for new bioengineering materials such as biodegradable polymers and the recent rise in the cost of petroleum, which is usually used as feed stock for production of lactic acid in conventional chemical processes. For a better understanding of the fermentation process and its optimization, a model is of a great help. Owing to the complexity of structured models, unstructured models can be preferred and have proven to accurately describe lactic acid fermentation in a wide range of experimental conditions and media. The aim of this work was to develop an unstructured model based on the experimental results of lactic acid fermentation using *Lactobacillus helveticus* growing on whey permeate supplementation. The first model was developed for cultures without pH control; an additional term to account for the undissociated lactic acid (and pH) inhibition was introduced in the Luedeking-Piret model. The model was found to match both experimental growth and production data. During cultures at pH controlled at 5.9, a corrective term was introduced in the Luedeking-Piret model to account for cessation of production due to carbon substrate limitation. This model matched experimental data accurately. To avoid the use of two expressions for production rate depending on the culture conditions, the above expressions were merged, leading to a unique expression taking into account both effects, a nutritional limitation effect and an inhibitory effect. Results obtained show that the generalized model gave a satisfactory description of experimental data in various culture conditions, since it was validated during cultures at pH control and in absence of pH control, as well as for different nitrogen supplementation of culture media.

1. Introduction

A great interest was reserved for lactic acid production in these last years by several authors. This product plays an important role in various applications mainly in the food industry, but also in the production of pharmaceuticals, cosmetics and textiles industries (Rojan and al., 2007). The continuous increase in its demand has received recently

much attention due to its increasing applications in the preparation of new bioengineering materials such as biodegradable polymers like polylactic acid (PLA), and the more recent rise in the cost of petroleum, which is usually used as feed stock for production of lactic acid in the conventional chemical processes. Lactic acid found also many other applications, such as medical sutures, green solvents (Dutta and Henry, 2006; Wee and al.2006). The industrial production of lactic acid can be carried out by two alternative technologies: chemical synthesis from fossil fuels and biotechnological processes. Nowadays, the fermentative production of lactic acid is the world's leading technology (about 90% of world production).

To increase the efficiency of the lactic acid fermentation processes, various cell culture methods have been investigated (Nandasana and Kumar 2007, Lin and Wang 2007). However, batch fermentation remains the most commonly used approach in industrial lactic acid production. Mathematical models may be useful for understanding the fermentation process and its optimization (modelling experimental data and studying the effects of experimental conditions on cultures kinetics) (Gadgil and Venkatesh, 1997; Amrane and Prigent, 1994a and 1999a). Lactic acid kinetics can be modelled par both structured or unstructured models; structured models have been reported to accurately describe lactic acid fermentation, but are complicated for many normal use (J. Nielsen 1991; Gadgil and Venkatesh, 1997). Unstructured models can be therefore preferred and have proven to accurately describe lactic acid fermentation in a wide range of experimental conditions and media. Some unstructured models were developed in the laboratory based on the partial linking between growth and lactic acid production (Luedeking and Piret, 1959). Additional terms were introduced in the Luedeking and Piret expression, to account for cessation of lactic acid production when carbon became limiting, namely to describe experiments carried out at a constant (and optimal) pH, 5.9 (Amrane and Prigent, 1994a and 1994b; Amrane 2001), or to account for the inhibitory effect of the undissociated lactic acid (and pH), occurring during cultures without pH control, which is the case during seed cultures (Amrane and Couriol 2002). The aim of this work is to develop new models, based on theses previously proposed models.

2. Materials and Methods

2.1. Microorganism

Lactobacillus helveticus strain *milano* used throughout this work was kindly supplied by Dr A. Fur (Even Ltd, Ploudaniel, France). Stock cultures were maintained on 10 % ($w.v^{-1}$) skim milk and deep-frozen at -16°C. As required, these cultures were thawed and reactivated by two transfers in 10 % ($w\ v^{-1}$) skim milk (42°C, 24h).

2.2. Media

Whey permeate powder (SIAB, Chateaubourg, France) was used as a carbon source; the powder was reconstituted at 57 g L^{-1}, corresponding to a lactose concentration of 48 g L^{-1}. Before use, and after clarification, the solution was pumped through two heat exchangers at 80 and 16 °C respectively (mean residence time: 20 seconds). The solution was left to decant overnight at 4 °C, and the supernatant was then supplemented with a 5 g L^{-1} of yeast extract or the following *RM* supplementation (g L^{-1}): yeast extract (*YE*), 20; trypsic and pancreatic casein peptones, 5 each (all from Biokar, Pantin, France).

2.3. Culture conditions

Batch culture was carried out in a 2 L fermentor (SET 2M; SGI, Toulouse, France), magnetically stirred (300 rpm), at 42°C and without pH control. Seed culture was carried out in a 0.25 L laboratory-designed glass fermentor. Both fermentors were equipped with an aseptic recirculation loop (Watson-Marlow 501 U peristaltic pump; Volumax, Montlouis, France) incorporating a laboratory-made turbidimeter. As the turbidity was continuously recorded, the total biomass could be calculated on-line after dry weight calibration; the observed standard deviation was ±0.2 g L^{-1}.
Bacteria were precultivated by inoculating sterile culture medium with 0.8 % (v/v) of the second skim milk transfer. Then, 1.6 L of pasteurised culture medium was inoculated with 0.2 L seed culture (11% v/v), and the reaction proceeded.

At the end of both preculture and culture, the final biomass and lactic acid concentrations were determined as previously described (Amrane and Prigent, 1994a).

3. Results

3.1 Model without pH control (inhibition model)

During lactic acid fermentation, the accumulated lactic acid decreases the pH value. The acidic pH inhibits fermentation (Luedeking and Piret, 1959, Amrane and Prigent, 1994b). To overcome this inhibition, the pH is maintained during culture at its optimal value for lactic acid production (Hanson and Tsao 1972, Venkatesh et al 1993), at which the final free lactic acid concentration (approximately 0.3 g/l) is below the inhibitory threshold (Gätje and Gottschalk 1991). Since the positive effects of precultivating without pH control was shown (Amrane and Prigent 1996, Amrane and Prigent 1998), the above models are not convenient for seed culture. Indeed, they do not take into account the inhibition observed in absence of pH control. Several models involving lactic acid inhibition can be found in the available literature, which consider non-competitive product inhibition (Dutta et al. 1996, Ohara et al. 1992), or other types of inhibition (Pinelli et al. 1997, Biazar et al. 2003) by the total lactic acid produced. It is now recognised that the main inhibitory species is the undissociated form of the lactic acid. From this, the Luedeking-Piret model (1959) was modified by introducing an additional term to account for the undissociated lactic acid inhibition (Balannec et al. 2007):

$$\frac{dp}{dt} = A * \frac{dx}{dt} + B * x * \left(1 - \frac{[HL]}{[HL]_{inh}} \right) \quad (1)$$

Where $[HL]$ and $[HL]_{inh}$ were the undissociated lactic acid concentration and its inhibitory concentration.
The Verlhust model which proved to satisfactory describe growth kinetic (Moraine and Rogovin 1996, Pandey 2000) was used in this work:

$$\frac{dx}{dt} = \mu_{max} * \left(1 - \frac{x}{x_{max}} \right) * x \quad (2)$$

Integration of equation (2) gave:

$$x = x_0 * x_{max} * \frac{e^{\mu_{max} * t}}{x_{max} - x_0 + x_0 * e^{\mu_{max} * t}} \quad (3)$$

Where x_0 and x_{max} were the initial and maximal values of the biomass concentration and μ_{max} was the maximal specific growth rate.

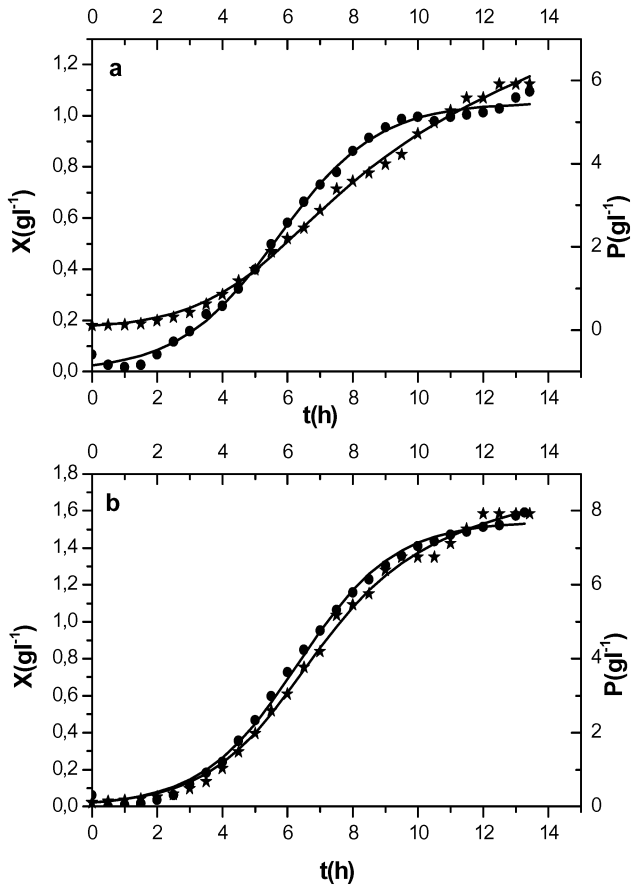

Figure 1. Growth (•) and lactic acid production (*) kinetics during batch cultures of L. helveticus *growing without pH control on whey supplemented with 10 g* L^{-1} *yeast extract (a) and the RM supplementation (b); calculated data (—) by means of the growth model (Eq.3) and the product inhibition model(Eq.1).*

The model was found to match both experimental growth and production data, and was validated in various culture conditions, namely for a large range of nitrogen supplementations of whey permeate (Balannec et al 2007).

3.2 Model at pH controlled at 5.9 (substrate limitation model)

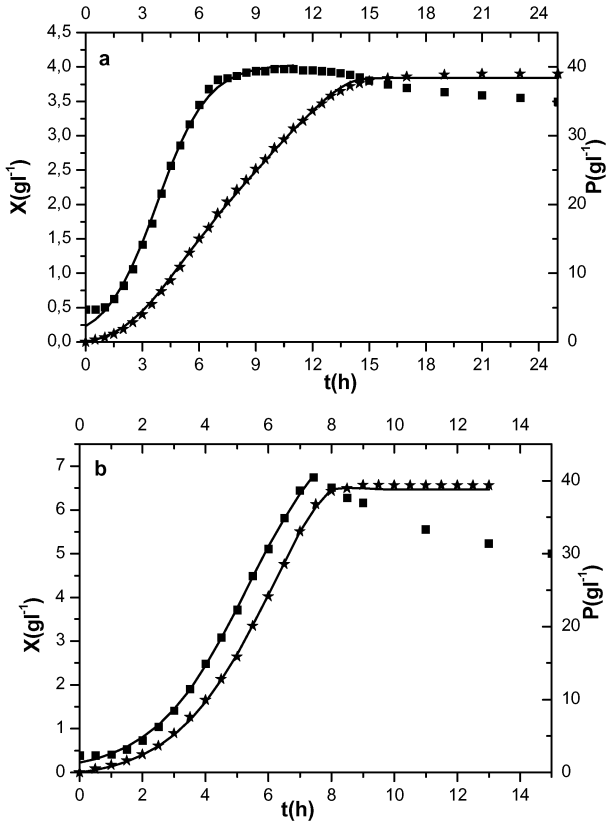

Figure 2. Growth (•) and lactic acid production (*) kinetics during batch cultures of L. helveticus *growing at pH controlled at 5.9 on whey supplemented with 10 g* L^{-1} *yeast extract (a) and the RM supplementation (b); calculated data (—) by mean of the growth model (Eq.1)and the substrate limitation model for production (Eq.4).*

As previously shown lactic acid production ceased at the beginning of cell death irrespective of the considered nitrogen supplementation, namely when carbon became limiting, since bacteria are unable to use the carbon content of autolysed cell (Amrane 2001). Cessation of production was therefore concomitant to cessation of lactose consumption. The corrective term s_{res} was thus replaced by an expression taking into account the carbon substrate limitation.

$$\frac{dp}{dt} = A * \frac{dx}{dt} + B * x * \left(1 - \frac{s_{Lim}}{s}\right) \qquad (4)$$

Where s and s_{lim} were the lactose concentration at time t and the end of batch (the limiting carbon concentration), respectively. This model was successfully tested for a large range of nitrogen supplementation (Bouguettoucha et al.2007); the model accounted for the whole production kinetics.

3.3 Generalized model

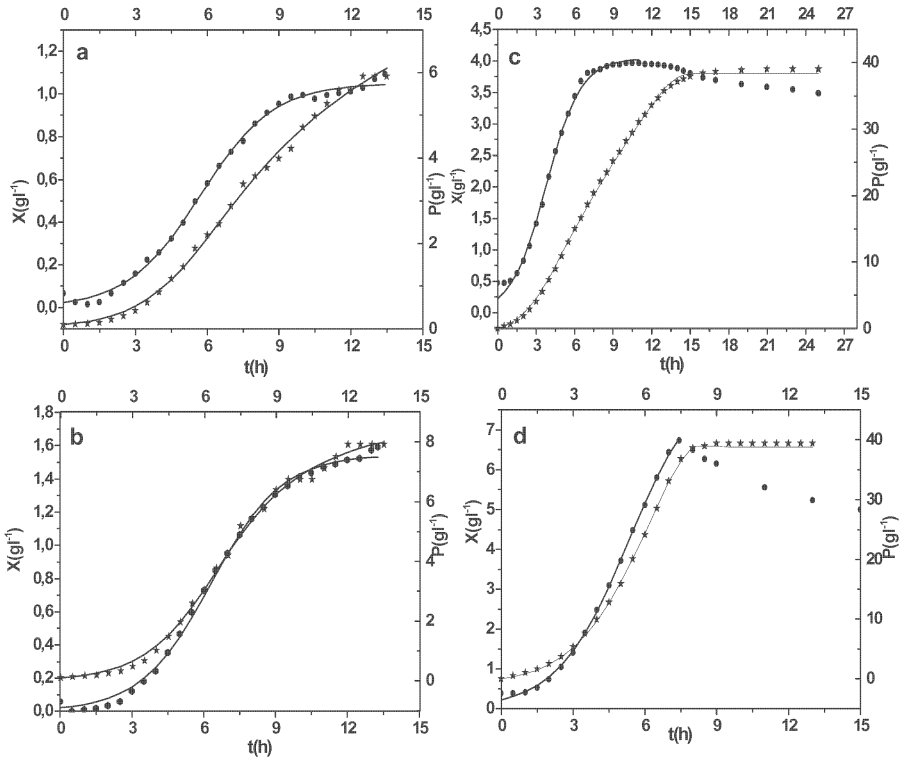

Figure 3. Growth (•) and lactic acid production (*) kinetics during batch cultures of L. helveticus *growing without pH control (a, b) and at pH controlled at 5.9 (c, d) on whey supplemented with 10 g L^{-1} yeast extract (a, c) and the RM supplementation (b, d); calculated data (—) by means of the growth model (Eq.1) and the generalized model for production (Eq.5).*

To avoid the use of two expressions to describe production rate (involving nutritional limitations, Eq.1 or an inhibitory pH effect, Eq.4), depending on culture conditions, the above expressions were merged, leading to an unique expression taking into account both effects, a nutritional limitation effect and an inhibitory effect:

$$\frac{dp}{dt} = A * \frac{dx}{dt} + B * x * \left(1 - \frac{s_{lim}}{s}\right) * \left(1 - \frac{[HL]}{[HL]_{inh}}\right) \qquad (5)$$

To describe the growth rate, the Verlhust model (eq.3) was considered. The generalized model gave a satisfactory description of experimental data in various culture conditions, since it was validated during cultures at *pH* controlled (Fig. 3a et b) and in absence of *pH* control (Fig. 3c et d), as well as for different nitrogen supplementation of culture media (Bouguettoucha et al. 2007).

4. Conclusion

The inhibition model was found to match both experimental growth and production data recorded without pH control, namely in the case of an inhibitory effect of the undissociated lactic acid (and the pH); the model was validated in various culture conditions, namely for a large range of nitrogen supplementation of whey permeate. The substrate limitation model was successfully tested for a large range of nitrogen supplementation; the model matched whole production kinetics recorded during cultures at pH controlled, namely in the case of nutritional limitations. Satisfactory results were also obtained by considering the generalized model, which matched experimental data in various culture conditions, since it was validated during cultures at pH controlled and in absence of pH control, as well as for different nitrogen supplementation of culture media.

5. References

Amrane A, and Y. Prigent, 1994a, Lactic acid production from lactose in batch culture: analysis of the data with the help of a mathematical model; relevance for nitrogen source and preculture assessment. Appl Microbiol Biotechnol 40:644-649.

Amrane A, and Y. Prigent, 1994b, Mathematical model for lactic acid production from lactose in batch culture: model development and simulation. J Chem Tech Biotechnol 60:241–246.

Amrane A, and Y. Prigent, 1996, A novel concept of bioreactor: specialized function two-stage continuous reactor, and its application to lactose conversion into lactic acid, J. Biotechnol. 45: 195-203

Amrane A and Y. Prigent, 1998, Identification and experimental validation of a criterion allowing prediction of cellular activity for preculture of lactic acid bacteria, J. Ferment. Bioeng. 85: 328-333.

Amrane A. and Y. Prigent, 1999a, Analysis of growth and production coupling for batch cultures of *Lactobacillus helveticus* with the help of an unstructured model. Process Biochem 34:1-10.

Amrane A. and Y. Prigent, 1999b, Differentiation of pH and free lactic acid effects on the various growth and production phases of *Lactobacillus helveticus*. J Chem Technol Biotechnol 74:33-40.

Amrane A., 2001, Batch cultures of supplemented whey permeate using *Lactobacillus helveticus*: unstructured model for biomass formation, substrate consumption and lactic acid production. Enzyme Microb. Technol. 28: 827-834.

Amrane A and Couriol C., 2002, unstructured model for seed culture without pH control of *Lactobacillus helveticus* growing on supplemented whey permeate. J. Chem Technol Biotechnol. 77:1-845 ().

Biazar J. M. Tango E. Babolian and R.Islam, 2003, Solution of the kinetic modelling of lactic acid fermentation using Adomian decomposition method, Appl. Math. Comput. 144: 433-439.

Balannec B., A. Bouguettoucha and A. Amrane, 2007, Unstructured model for batch cultures without pH control of *Lactobacillus helveticus* – Inhibitory effect of the undissociated lactic acid. Biochem Eng J 35:289-294.

Bouguettoucha A, B. Balannec, S. Nacef, and A. Amrane, 2007, A generalised unstructured model for batch cultures of *Lactobacillus helveticus.* Enzyme Microb Technol 41:377-382.

Dutta R. and M. Henry, 2006, Lactic acid: recent advances in products, processes and technologies – a review. J Chem Technol Biotechnol 81:1119-1129.

Gadgil C.J. and K.V.Venkatesh, 1997, Structured model for batch culture growth of *Lactobacillus bulgaricus*. J Chem Tech Biotechnol 68:89-93.

Gätje G and G. Gottschalk, 1991, Limitation of growth and lactic acid production in batch and continuous cultures of *Lactobacillus helveticus*, Appl. Microbiol. Biotechnol. 34: 446-449.

Hanson T.P., and G.T., Tsao, 1972, Kinetic studies of the lactic acid fermentation in batch and continuous cultures, Biotechnol. Bioeng. 14: 233-252.

Lin H. T. and F. S. Wang, 2007, Optimal design of an integrated fermentation process for lactic acid production, AIChE. Journal, 53, (2): 449-459

Luedeking R. and E.L. Piret, 1959, A kinetic study of the lactic acid fermentation. Batch process at controlled pH. J Biochem Microbiol Technol Eng 1:393–412.

Moraine R.A. and P. Rogovin, 1996, Kinetics of polysaccharide B-1459 fermentation, Biotechnol. Bioeng. 8: 511-524.

Nandasana A. D. and S. Kumar, 2007, Kinetic modelling of lactic acid production from molasses using *Enterococus fecalis* RKY1, Biochemical Eng. J. DOI 10 1016/j.bej.2007.07.014.

Nielsen J., K., Nikolajsen and J. Villadsen, 1991, Structured modelling of a microbial system: I. A theoretical study of lactic acid fermentation, Biotechnol. Bioeng. 38 1-10

Pinelli D., R.A., González-vara, Y.D., Matteuzzi and F., Magelli, 1997, Assessment of kinetic models for the production of L- and D- lactic acid isomers by *Lactobacillus casei* DMS 20011 and *Lactobacillus coryniformis* DMS 20004 in continuous fermentation, J. Ferment. Bioeng. 83: 209-212.

Pandey A., C.R. Soccol and D. Mitchell, 2000, New developments in solid state fermentation: I -bioprocesses and products, Process Biochem. 35: 1153-1169.

Rojan P.J, K.M. Nampoothiri and A. Pandey, 2007, Fermentative production of Lactic acid from biomass: an overview on process development and future perspectives. Appl Microbiol Biotechnol 74:524-534.

Venkatesh K.V., M.R. Okos, and P.C. Wankat, 1993, Kinetic model of growth and lactic acid production from lactose by *Lactobacillus bulgaricus*, Process Biochem. 28: 231-241.

Wee Y.J., J.N. Kim and H.W. Ryu, 2006, Biotechnological production of lactic acid and its recent applications, Food Technol. Biotechnol. 44 (2) 163–172.

CHEMICAL ENGINEERING TRANSACTIONS, Volume 14, 2008
Edited by G. Marino, E. Bardone, A. Viglia
 ISBN 978-88-95608-02-0

Use of a mathematical model to investigate the influence of nitrogen consumption on pH during fermentation

Akin H., Brandam C., Meyer X-M.and Strehaiano P.
Laboratoire de Génie Chimique - UMR CNRS/UPS/INPT 5503
BP 1301, 5 rue Paulin Talabot - 31106 Toulouse cedex 1, FRANCE
E-mail : Cedric.Brandam@ensiacet.fr

This work deals with the use of a mathematical model to investigate the influence of the nitrogenous source on the pH during alcoholic fermentation in winemaking. If the influence of the assimilation of ammoniac by yeasts on pH is well developed in the literature, the results are more dubious concerning the assimilation of the amino acids. In order to discriminate various assumptions, a model of pH calculation developed by Akin et al. (2007) was used. So, fermentations in media with different nitrogenous source were carried out. The application of the model to fermentation medium whose nitrogen source was made up only of ammoniac gave very satisfactory results and confirms the assumption found in the literature that the assimilation of one mole of ammonia releases one mole of proton in the medium. The use of the model made it possible to invalidate two assumptions concerning the impact of the assimilation of the amino acids on the pH. The most probable assumption is that the assimilation of the molecules of amino acids charged positively led to the emission of protons in the extra cellular medium.

1. Introduction

Nitrogen compounds are important for the growth and the metabolism of yeast. It is quantitatively the second nutriment of the yeast, after the carbon element. During the alcoholic fermentation, in winemaking, nitrogen of grape must is assimilated by yeast cells for their growth. However, nitrogen is present under variable and complex forms: ammonium ions, amino acids, peptides and proteins. It is known that only ammonium ions and some amino acids are able to be metabolised by yeasts. The kinetic of the fermentation and aroma production are particularly influenced by the quantity and the nature of amino acids. So, the effect of nitrogen as precursors has been studied for long time (Cantarelli, 1957; Ough, 1964). More recently, the problem of yeast nitrogenous nutrition became a major research subject in oenology.

Various studies (Sigler and al., 1981; Kotyk, 1989) reported a pH decrease during alcoholic fermentation by *Saccharomyces cerevisiae* on medium where ammonium ions were the only nitrogenous source. The assimilation of ammonium ions by the yeast would be linked to the excretion of protons in the extra cellular medium. According to Won J.I and al. (1993) when one mole of ammonium is used, one mole of protons is excreted: $NH4^{+} \rightarrow NH3\,(\text{in cell}) + H^{+}$

So, the decrease of pH would be directly proportional to the ammonium ions assimilated by yeasts.

Contrary to ammonium, the mechanisms of assimilation of amino acids by yeast seem more complex. Several authors (Grenson and al., 1970; Salmon, 1989) studied the type of exchange taking place between the intra cellular and extra cellular medium but no clear conclusion can be drawn from these works. The impact of the assimilation of amino acids by yeasts on the evolution of the pH is not clearly identified.
In previous studies (Akin et al., 2007), we proposed a mathematical model to calculate the pH of a grape must during the fermentation. This model has been validated on synthetic medium and natural grape musts. In this work, we propose to use this model to test different assumptions drawn on the assimilation of ammonium ions and amino acids.
Two fermentations with different nitrogenous source were performed.

2. Materials and methods

2.1. Micro organism

Saccharomyces cerevisiae QA-23 commercialised by Lallemand inc. was used as it is a classical yeast strain for white winemaking.

2.2. Fermentation media and operating conditions

Fermentation were carried out on synthetic media whose composition was close to grape must: glucose (200 $g.L^{-1}$), malic acid (6 $g.L^{-1}$), citric acid (6 $g.L^{-1}$), KH_2PO_4 (0.75 $g.L^{-1}$), K_2SO_4 (0.5 $g.L^{-1}$), $MgSO_4$, 7 H_2O (0.25 $g.L^{-1}$), $CaCl_2$, $2H_2O$ (0.16 $g.L^{-1}$), NaCl (0.2 $g.L^{-1}$), a mixture of oligo elements, vitamins and anaerobia factors. The nitrogen source differed with experiments: ammonium ions for an equivalent of 420 mg $N.L^{-1}$ for the medium MS_NH4 and a mixture of amino acids for an equivalent of 305 mg $N.L^{-1}$ for the medium MS_AA. The pH of media was adjusted to 3.3 before autoclaving with NaOH solution (8N).

2.3. Compounds and pH measurement

The determination of cell concentration was done using an electronic analyser Beckman Coulter, model M3 according to the Coulter method “Electrical Sensing Zone”. pH was measured on line with a precision of 0.05 unit of pH. Concentrations of ammonium, malic and lactic acids were measured by enzymatic kits (MicroDom). Citric, acetic and succinic acid, ethanol and glycerol were measured by HPLC method. Individual amino acid concentrations were determined by Biochrom 30 method.

2.4. pH calculation model

pH calculation model used in this study was developed by Akin et al. (2007). This model was based on thermodynamic equilibrium of electrolytic compounds in solution. The molality of hydrogen ions and thus the pH are determined by solving a non linear algebraic equations system consisted of mass balances, chemical equilibrium equations and electroneutrality principle.

3. Results and discussions

3.1. Fermentation of the MS_NH4 medium

The fermentation on the MS_NH4 medium was performed during 110h. Ammonium ions is the only nitrogen source. The evolution of the main compounds concentration is plotted on figure 1.

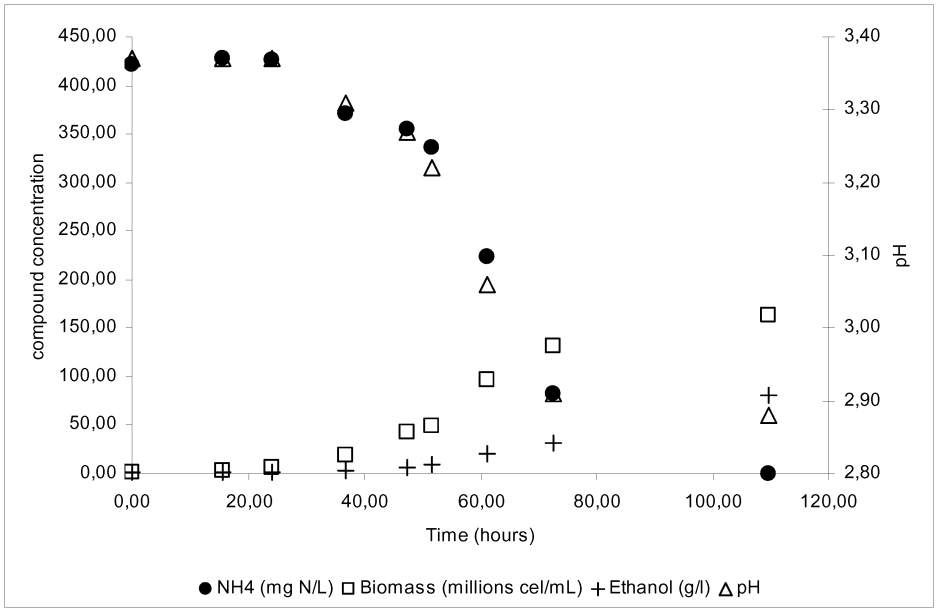

Figure 1. Evolution *of biomass, ethanol, ammonium and pH during fermentation carried out on the MS_NH4 medium*

During the first fermentation period (0 to 40 hours), the metabolic activity was slow: a slow consumption of ammonium ions (about 30 mgN.L^{-1}), a low production of biomass (3.10^6 cells.mL^{-1}) and ethanol (4 g.L^{-1}). A little decrease of pH was observed, from 3.37 to 3.31. During the second period, between 40 and 110 hours, the metabolic activity increased. At the end of the fermentation, ethanol concentration was about 82 g.L^{-1}, biomass attained almost 160.10^6 cells.mL^{-1} and ammonium was entirely consumed. The decrease of pH was also emphasized since its final value was 2.90.

The measurement of organic acid concentrations indicates that very small quantities were produced: 0.16 g.L^{-1} of succinic acid, 0.18 g.L^{-1} for acetic acid. Citric and malic acids remained constant to 6 g.L^{-1} during the whole fermentation.

3.2. pH Simulations

The pH calculated with the model (3.37) at the very beginning of the fermentation when the medium composition is perfectly known is in agreement with the experimental value. Some compounds contents were considered as constant during fermentation like for instance mineral cations. The others (ethanol, sugar, organic acids and ammonium) were considered to be variable and have been measured at different times for which pH values can be calculated by the model.

The model expresses the hypothesis formulated by Castrillo J.I et al. (1995) and Won J.I et al. (1993): when ammonium ions which are on the cation form (NH_4^+) at the pH of the must are consumed by yeasts, one mole of proton is released to ensure the electoneutraly principle.

Results are shown in figure 2. They show a very good agreement between calculated and experimental pH values since the maximal deviation is less than the precision of the measure.

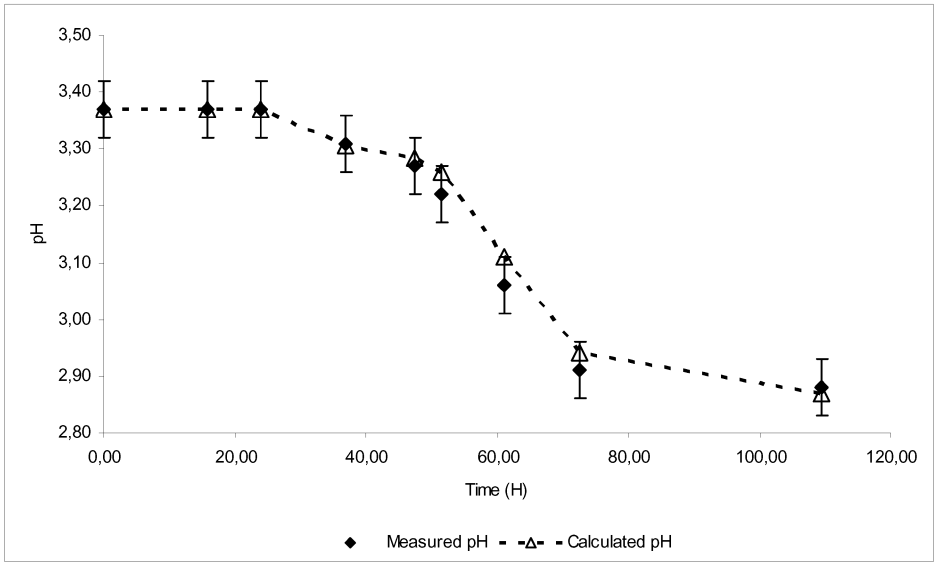

Figure 2. *Comparison of experimental and simulated pH values in MS_NH4 medium (initial pH=3.37; T=20°C)*

3.3. Fermentation of the medium MS_AA

In MS_AA medium, amino acids brought 305 mg of nitrogen by liter which could be assimilated by yeast. The fermentation has also been carried out and the evolutions of the major compounds concentrations are plotted on figure 3.

As for the fermentation on MS_NH4 medium, we can distinguish two periods. During the first period (0 to 20 hours), only 2 $g.L^{-1}$ of ethanol are produced, biomass attained only 3.10^6 $cells.mL^{-1}$ and few amino acids were consumed (about 40 $mgN.L^{-1}$). pH kept constant to its initial value of 3.23. During the second period (20 to 110 hours), ethanol production increased to reach 94 $g.L^{-1}$ at the end of the experiment. Concentration of biomass rose to 200 millions cells per millilitre and amino acids were totally consumed. The measurement of organic acid concentrations revealed that only 0.3 $g.L^{-1}$ of succinic acid and 0.3 $g.L^{-1}$ of acetic acid were produced. Malic and citric acids remained constant to their initial concentration of 6 $g.L^{-1}$.

The pH value decreased from 3.23 to 3.13 after 50 hours of the fermentation which corresponds to the assimilation of amino acids. After this time, pH increased regularly to reach 3.25 at the end of the experiment. We have already shown (Akin et al., 2007) that the ethanol effect on the organic acids dissociation is responsible for this rise.

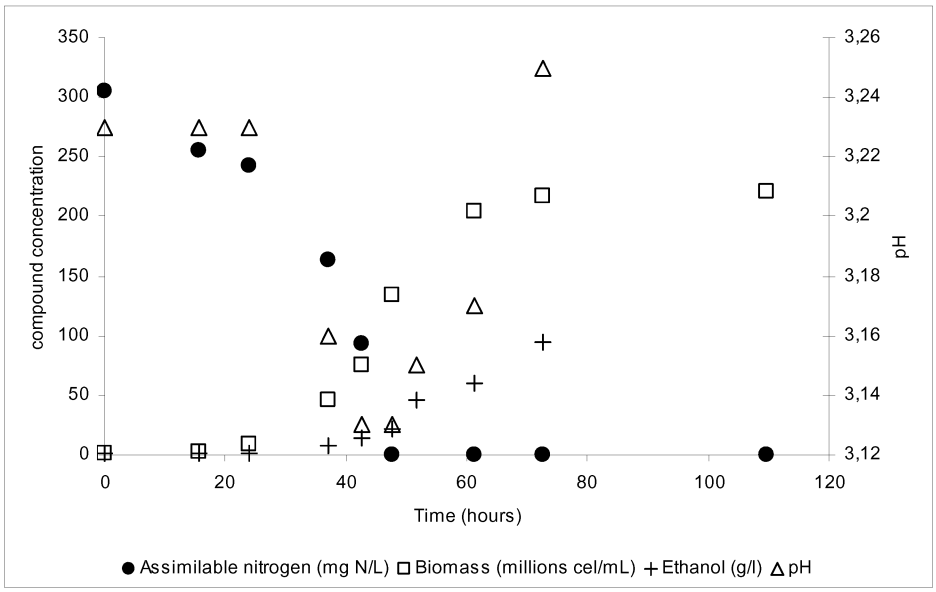

Figure 3. Evolution *of biomass, ethanol, total amino acids and pH during fermentation carried out on MS_AA medium (initial pH=3.23; T=20°C)*

3.4. pH simulations

As for MS_NH4 medium, the initial pH of MS_AA medium was perfectly predicted by the model. The knowledge of the medium composition allowed calculating an initial pH of 3.23. The complexity of the phenomena linked to the assimilation of amino acids by yeasts was underlined in the literature. The type of exchange which takes place when amino acids pass through cell membrane are not yet known with accuracy and certainty. To integrate the amino acids consumption in the model, three hypotheses were tested:

- Hypothesis 1: assimilation of amino acid does not influence the pH
- Hypothesis 2: consumption of one mole of amino acid causes the excretion of one mole of H^+ like for the ammonium consumption
- Hypothesis 3: consumption 1 mole of amino acid charged positively only causes excretion of 1 mole of protons to respect electroneutrality principle.

Under these hypotheses, the pH evolution was simulated and compared to experimental data.

According to hypothesis 1, the decrease of pH observed between 0 and 50 h during the fermentation of medium MS_AA would not be caused by amino acids consumption. However, any other phenomenon could explain it since organic acids production was very low. So, the pH decrease seems to be necessarily linked to amino acids consumption and so hypothesis 1 is rejected.

pH were calculated under the hypothesis 2 (figure not showed). Minimum pH calculated was 3.03, that is lower than the experimental one (3.13). Thus, the assimilation of amino acids induces a decrease of pH but only some of them seems to cause the excretion of protons.

To test the third hypothesis, it is necessary to evaluate amino acids proportion according to their electronic charge. Each amino acid has a equilibrium constant (pK_1) for their

acid function (COOH) and an equilibrium constant (pK_2) for their amine (NH_2) function. Some of them also have a third equilibrium constant (pK_3) linked to their radical. With these values of pK, it is possible to determinate the proportion of each form of amino acids: cationic, anionic or neutral as a function of pH. For the initial pH of 3.23, table 1 gives the proportion of each amino acids of the must.

Table 1. Quantity of nitrogen brought by each amino acid

Amino acids	Aspartic acid	Thréonine	Sérine	Glutamic acid	Glutamine	Proline	Cystéine
% cation (2+)	0,00	0,00	0,00	0,00	0,00	0,00	0,00
% cation (1+)	5,54	20,08	8,36	7,69	8,01	4,99	0,00
% neutral	76,52	79,92	91,64	84,27	91,99	95,01	0,00
% anion	17,94	0,00	0,00	8,05	0,00	0,00	0,00
%anion (2-)	0,00	0,00	0,00	0,00	0,00	0,00	0,00

Amino acids	Cystine	Méthionine	Isoleucine	Leucine	Tyrosine	Phénylalanine	Lysine
% cation (2+)	0,00	0,00	0,00	0,00	0,00	0,00	0,00
% cation (1+)	0,00	7,36	10,95	11,18	8,54	8,54	91,82
% neutral	0,00	92,64	89,05	88,82	91,46	91,46	0,00
% anion	0,00	0,00	0,00	0,00	0,00	0,00	0,00
%anion (2-)	0,00	0,00	0,00	0,00	0,00	0,00	8,18

Amino acids	Glycine	Alanine	Valine	Histidine	Tryptrophan	Arginine
% cation (2+)	0,00	0,00	0,00	0,00	0,00	0,00
% cation (1+)	11,65	11,41	12,63	3,74	14,52	91,99
% neutral	88,35	88,59	87,37	96,10	85,48	0,00
% anion	0,00	0,00	0,00	0,16	0,00	0,00
%anion (2-)	0,00	0,00	0,00	0,00	0,00	8,01

With these calculations and with the measure of individual concentration of amino acid, we were able to determine the total concentration of amino acids on cationic, anionic and neutral form during the fermentation (table 2).

In our medium, with amino acids repartition, there are 70% amino acids globally in neutral form, 27 % have 1 positive charge, 1,3 % have 2 positives charges and 1,3 % have only 1 negative charge.

In the model, to respect electroneutrality principle, each amino acid assimilated under the cationic form involves a proton excretion whereas each amino acid on anionic form involves neutralisation of one proton in the medium and amino acids on neutral form have no effect on proton concentration.

With these assumptions, simulation of pH values of the medium MS_AA was realised. Results are shown on figure 4. We noticed a good adequacy between the calculated and experimental pH. The maximal deviation was 0.04 point of pH that is less than the precision of the measure.

***Table 2**. Amino acids proportions according to their charge during fermentation*

Time (hours)	Alpha amino nitrogen (mg N/L)	Positive amino acids (mg N/L) A+	Positive amino acids (mg N/L) A2+	Neutral amino acids (mg N/L) A±	Negative amino acids (mg N/L) A-	Negative amino acids (mg N/L) A2-
0	305,0	83,2	5,0	213,2	3,6	0,0
15,7	256,0	69,7	4,2	179,1	3,0	0,0
24	243,0	66,1	4,0	170,0	2,9	0,0
36,937	163,0	49,1	3,1	108,9	1,9	0,0
42,63	93,0	33,1	2,2	56,9	0,7	0,0
47,53	0,0	0,0	0,0	0,0	0,0	0,0
61,16	0,0	0,0	0,0	0,0	0,0	0,0
72,55	0,0	0,0	0,0	0,0	0,0	0,0
109,54	0,0	0,0	0,0	0,0	0,0	0,0

The simulation results were globally in agreement with the experimental data when hypothesis 3 was formulated. So, the global charge of amino acids would determine the pH evolution. However, additional experiments with different proportion of each amino acid are necessary to validate this hypothesis.

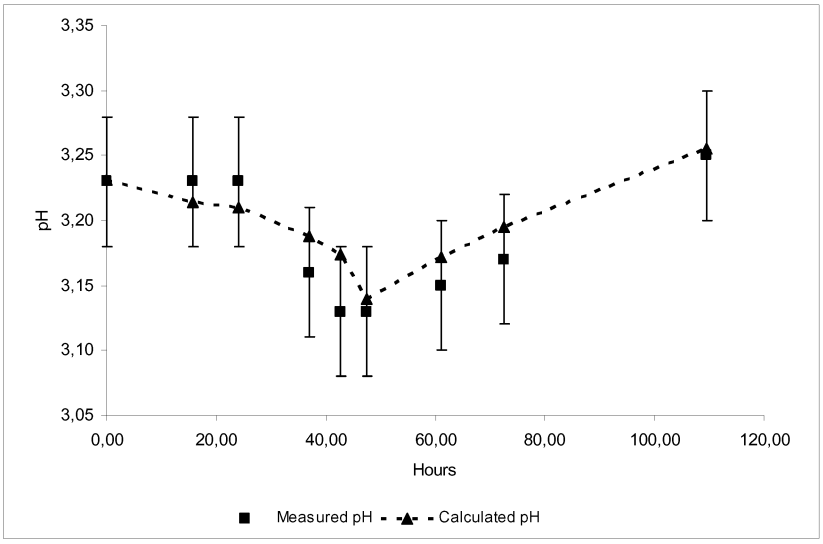

***Figure 4.** Comparison of experimental and calculated pH in MS_AA medium (Initial pH=3.23; T=20°C)*

4. Conclusion

At the end of this study, it can be stated with certainty that the acidification of the medium during alcoholic fermentation is linked to the assimilation of the nitrogen source. On a medium where nitrogen was only brought by ammonium (420 mg $N.L^{-1}$),

the pH decreases down to 0.47 pH unit. With amino acids as nitrogen source (305 mg $N.L^{-1}$) the decrease of the pH was lower, only 0.1 unit of pH.
The model of pH allowed us to suggest that only the cationic form of amino acids was responsible for the pH decrease.
This assumption must be validated with additional fermentations realised on synthetic medium as well as on natural grape musts.

5. References

Akin H., C.Brandam, X-M. Meyer and P. Strehaiano, 2007, A model for pH determination during alcoholic fermentation of a grape must by Saccharomyces cerevisiae, Chem. Eng. Process, doi:10.1016/j.cep.2007.11.014

Cantarelli, C., 1957, On the activation of alcoholic fermentation in winemaking, part II Am . J . Enol . Vitic . 8:167-175

Castrillo J.I., DE Miguel I., Ugalde U.O. (1995) Proton production and consumption pathways in yeats metabolism. A chemostat culture analysis Yeast 11, 1353-1365.

Grenson M., Hou C., Crabeel M. (1970) Multiplicity of amino acid permeases in Saccharomyces cerevisiae. IV. Evidence for general amino acid permease. Journal of Bateriology 103(3), 770-777

Kotyk A., 1989, Proton extrusion in yeast. In Fleischer S. and Fleischer B. (Eds) Method in enzymology, vol 174 (Biomembranes, part U). Academic Press, New York, 592-603

Ough, L. D., 1964, In Methods in Carbohydrate Chemistry (Whistler, R., ed), Vol. IV, pp.91-98.

Salmon J.M., 1998, Relations levure- milieu, *In* : OEnologie - fondements scientifiques et technologiques, pp. 415-444, ed. FLANZY C., Technique et Documentation, Lavoisier, Paris, France.

Sigler K., Knotkova A. and Kotyk A. (1981) Factor governing sbstrate induced generation and extrusion of proton in yeast. Biochim. Biophys. Acta, 643, 572-582

Won J.I., Y.L Yang., B.G Kim and C.Y Choi., 1993, Adaptative control of specific growth rate based on proton production in anaerobic fed-batch culture. Biotechnolgy letters 15 (5), 511-516.

CHEMICAL ENGINEERING TRANSACTIONS, Volume 14, 2008
Edited by G. Marino, E. Bardone, A. Viglia
 ISBN 978-88-95608-02-0

Mathematical Modelling Aspects of *Trichoderma reesei* System :A Review

Nitin Verma*,M.C.Bansal.,Vivek Kumar
Department of Paper Technology,Indian Institute of Technology,Roorkee,Saharanpur Campus,Saharanpur,247001,India.
*Corresponding author:nitiniit2004@rediffmail.com

Modelling the growth and product formation characteristics of various microorganisms is a very challenging task.There are many different approaches to modeling the microbial kinetics .Simplistic unstructured model do not offer much in terms of elucidating the exact nature of these processes.However more structured model often involve introducing process variables that can not be estimated reliably.Several studies dealing with modeling the growth and morphology of complex microorganisms such as filamentous fungi have been published in recent years.Complete quantitative description of its behaviour would lead to large sets of mathematical expressions describing the time evolution of a large number of variables.Futheremore ,these equations would contain a large number of parameters which would be difficult to obtain experimentally.Optimization of the productivity of biochemical processes by the optimal control approach is in general a difficult task.Accomplishement of such a task depends on the complexicity of model describing the biochemical process. The value of mathematical models to organize data, to consider interactions in complex systems in a rational way ,to correct the conventional wisdom and to understand essential qualitative features of biological system has been clearly documented in prior research.Impact of this research in biotechnology discovery has so for been limited ,but this will change in the future if we are adept in recognizing emerging opportunities and in integrating new concepts and tools into our research. In this review paper we are discussed the various model describing fungal growth system and also emphasized on *Trichodermma* system .

Introduction:

By definition ,biochemical engineers are concerned with biochemical system,often with systems employing growing cells.Even the simplest living cells is a system of such for bidding complexity that any mathematical description of it is an extremely modest approximation.The use of mathematics to provide a rigrous ,systematic and quantitative linkage between molecular and microscopic phenomenon on one hand and macroscopic process performance on the other hand(Baily J.E.1998).The study of filamentous fungi can be difficult through experimental means alone due to the complex city of their natural growth habitats and the microscopic scale of growth (eg Tip vesicle translocation and hyphal tip extension,mycelial growth)Mathematical modeling provides a complimentary ,powerful and efficient method of investigation.The aim of mathematical modeling is not to

form an extremely complex system of equation in an attempt to mirror reality instead the aim to reduce a complex (biological) system into a simple (mathematical system)that can be analyzed in for more details and from which key properties can be identified .Thus the aim of mathematical modeling is not about what to include ,but instead what can be omitted (Boswell G.P2003)(Melatiadis J et al 2001).Models can be categorized into probability or kinetic models (measuring growth rate or generation time) according to the mathematical approaches used.In case of filamentous fungi ,estimation of growth rate is more complicated owing to the formation of surface colonies and also of hyphae throughout the carbon source,a cell count is not appropriate.Empericals models simply describes the conditions underwhich a experiment was performed,that is the effect on microbial growth of the physical and chemical components of the carbon source.Such models are usually polynomials.(Gibson M.A and Hocking D.A. 1997)(Bail S and Klis F.M1999). Mathematical modeling of microbial growth has been used to estimate parameters (specific growth rate and lag time) required to study growth under different physical and chemical conditions.Mathematical models can be either empirical or mechanistic .Mechanistic models are preferred because they are derived to represent the biochemical processes controlling microbial growth.However,if the mechanism governing the process is unknown,mathematical fractions have to be used empirically.(Lopez S etal 2004)(Anseley M et al 1990).In this paper we are much emphasized various model on fungal growth system in generalized way and also on *Trichoderma* growth system

The various models describing fungal growth system:

Although a large body of work on the mathematical modeling of fungi is now established,many vital queries still remain unanswered and relevant and important problems un addressed. Predictive modeling of filamentous fungus growth has not received the same level of attention as that of bacterial growth.This may well be because of the inherent complexities associated with the quantification of fungal growth.Measurment of hyphal extension rates usually reported as radial growth rate ,is probably the simplest and most direct measures but it does not necessarily represents the true nature of fungal growth .Fungal hyphae can penetrate the physical 3-dimensions matrix of carbon souces.There are various models of fungal growth system have been studied.few are explained here.

Model of fungal mycelial growth:In general ,attempts at the mathematical modeling of fungal growth have either focused on mycelial level ,using quanitities such as biomass yield or have focusssed on growth on hyphal level such as hyphal tip growth ,branching.In the former spatial proportions are generally ignored ,while the latter temporal effects are often neglected The fungal mycelium is modeled as a distribution consisting of three components : active hyphae(Corresponding to those hyphae involved in the translocation of internal metabolites), Inactive hyphae(Denoting those hyphae not involved in translocation or growth.eg hyphal tips) An important distinction is made nutrients located within the fungus(internal) and those free in the outside environments(external).Intarnally located materials is used for metabolism and biosynthesis eg in the extension of hyphal tips

(creating new hyphae)branching (creating new hyphal tips)maintain and the uptake of external nutrient resources.This model is based on the physiology and growth characteristics of fungus(Boswell G.P.etal 2003)
In terms of the five variables (active hyphae,inactive hyphae,hyphal tips,internal substrate and internal substrate)The model has the following structure:
Change in active hyphae in a given area = New hyphae (laid down by moving tips)+reactivation of inactive hyphae-inactivation of active hyphae.
Change in inactive hyphae in a given area= Inactivation of active hyphae- reactivation of inactive hyphae-degradation of inactive hyphae.
Changes in hyphal tips in given area= Tip movement out of /into area+ branching from active hyphae-anaostomosis of tips into hyphae.
Changes in the internal substrate in the given area= Translocation (active and passive mechanisms)+ uptake into the fungus from external sources –maintanence cost of hyphae-growth costs of hyphal tips-active translocation costs
Change in external substrate in the given area= Diffusion of external substrare out of /into area –uptake by fungus.
The interactions between the components listed above satisfy the following system equations which are obtained from standerd conservation laws:

$\delta m/\delta t = f_m(m,m',p,s_i,s_e)$ = new hyphae- inactive hyphae

$\delta m'/\delta t = f_{m'}(m,m',p,s_i,s_e)$ = Inactivated hyphae – degradation

$\delta p/\delta t = -\delta/\delta_x J_p(m,m',p,s_i,s_e)+fp\ (m,m',p,s_i,s_e)$ =(tip migration)+(branching – anastomosis)

$\delta si/\delta t$ =[$-\delta/\delta x\ Ji^{pas}(m,m',p,s_i,s_e)+j_i^{act}(m,m',p,s_i,s_e)]+fi(m,m',p,s_i,s_e)$ = [translocation(passive andactive)]+[(uptakegrowthtrans.costs)]

$\delta s_e/\delta t = -\ \delta/\delta x\ J_e(m,m',p,s_i,s_e) + fe\ (m,m',p,s_i,s_e)$ = diffusion + (- uptake)

Where J and f denotes the flux (migration) and reaction (creation /loss) terms respectively,for each quantity.m(x,t)the active hyphal density at time t where x denotes spatial position;m'(x,t),the inactive hyphal density;p(x,t),the tip density;$s_i(x,t)$,the internal substrate concentration;and $s_e(x,t)$,the external substrate concentration. (Boswell G.P et al 2002) (Boswell G.P et al 2003)
Model of Fungal spore germination:Bizukojk M and Ledkowitz(2006) reported spore germination kinetics, according to this spores may be divided into 3 phases:Spore swelling germ tube emergence and germ tube elongation takes place in the first phase,The spores begins to swell increasing its dormant diameter significantly until a germ tube emerges in the second phase.In the third phase the elongation of germ tube is observed and its growth is usually exponential.

Kinetic model for the process of spore germination:The biomass content in the presented system is indirectly estimated as mean hyphal area because for the early stages of growth of any filamentous fungus.

$dA/dt = k_{sw} A$.This equation is valid if $t<t_e$,where t_e is the time when the tubes start to emerge.For t> te the following system of ordinary differential equation to be proposed.

$dcs/dt = - Y_{SA} ks.K_{I,INT}.K_{IA}.A/.K_{I,INT} + c_{INT}. K_{IA} + A$

$dc_N/dt = -Y_{NA} k_N K_{I,INT}.K_{IA}.A/.K_{I,INT} + c_{INT}. K_{IA} + A.$

$dc_{INT}/dt = - k_{INT}.c_{INT}/c_{INT} + K_{INT} - \mu_{INT}$

$dA/dt = \mu A$

Where μ is the specific growth rate of biomass expressed as the sum of the growth due to each substrate:

$\mu = ks.K_{I,INT}.K_{IA}.A/.K_{I,INT} + c_{INT}. K_{IA} + A + k_N K_{I,INT}.K_{IA}.A/.K_{I,INT} + c_{INT}. K_{IA} + A + k_{INT}.c_{INT}/c_{INT} + K_{INT}.$

WhereA,mean protected area of hyphae; c_{INT},Concentration of internal storage compounds;c_N,concentration of nitrogen source;c_S,concentration of carbon source;C,Circularity index;k_{INT},Internal storage compound uptake constant rate;k_N,N-source uptake constant rate,k_S,C-source uptake constant rate,k_{SW},spore swelling constant rate;$K_{I,A}$,Inhibition constant due to dimension of hyphae;$K_{I,INT}$,inhibition constant due to internal storage compound;K_{INT},saturation constant;L,mean hyphal length;te,spore swelling time,Y_{NA},yield of N source to hyphae;Y_{SA},yield of C source to hyphae, μ,specific growth rate of biomass.

Model of fungal hyphal tip growth: Tindemas S.H et al (2006) have been investigated the fungal tip growth and proposed vesicle supply centre(VSC) and diffuse vesicle supply centre model. According to VSC model vesicles mediated cell growth are created in the golgi bodies and first transported to the Spitzenkorper which act as an organizing center .From their the vesicles are released to ultimately fuse with the plasma membrane .The mathematical abstraction of the Spitzenkorper is a point like object called the vesicle supply center.These vesicles released randomly in all directions and move in a straight lines from the VSC to cell envelop.Once a vesicles hits the plasma membrane ,it fuses with the membranes and externalizes its contents causing a local expansion of the cell envelop .The model assumes the amount of wall material delivered to the cell envelop to be the same for any solid angle,as seen from the VSC.To this end the simplest explanation for an isotropic motion of the vesicles through the cytoplasm and instantaneous exocytosis at the cell wall.Diffusion allows for a finite vesicle exocytosis rate to be incorporated into the model in

a natural way,through the boundry conditions.The effective diffusion constant of the vesicles can be estimated from the Einstein relation $D=k_B T/6\mu\eta a$ assuming the vesicle size a to be roughly 50 nm and the viscosity η equals to that of water yields a diffusion constant of about $4\mu m^2/s$ taking into account the fact that cytoplasm is more viscous than water then D~ 1 $\mu m^2/s$.This implies that vesicles will take only a few secods to travel the VSC to the cell wall,making diffusion a viable method of vesicle delivery within the hyphal tip.

Models of *Trichoderma* growth system:

The *Trichodermma* system (like any other biological system)is of a complex nature.Complete quantitative description of its behaviour would leads to large sets of mathematical expressions describing the time evolution of a large number of variables.Furthermore ,these equations would contains a large number of parameters which would be difficult to obtain experimentally.The models describing biomass and product formation are listed as follows:

Biomass related models:

Modified Monod model: $dx_1/dt = \mu\ x_1\ (1 - 1/1\text{-}a\ (x_1\text{-}x_f)$, Where $a = So/K_s\ (x_f\text{-}x_o)$

Polynomial model: $dx_1/dt = \mu\ x_1[1 - (x_1/x_f)^q$

Humphery's model: $dx_1/dt = \mu\ x_1 - \delta\ x_1$Where $\mu = \mu_m\ .S/Ks+s$ and $\delta = \delta_m\ (1\text{-}S/K'_s + s)$

The generalized logistic model: $dx_1/dt = -\ x_1\ [1 - X_1/K_1]\{a_1 + 2a_2\ t + 3a_3\ t^2\}$

Whereas the enzyme production model are as follows:

The enzyme decay model: $dx_2/dt = b_1\ x_1 - b_2x_2$

Polynomial model: $dx_2/dt = b_1\ x_1 - (b_2x_2)^{b3}$

The generalized logistic model: $dx_2/dt = -\ X_2(1\text{-}X_2/K_2)\ \{a_4 + 2a_5t + 3a_6t^2\}$

Where a_1,a_2,a_3 are the coefficients of the polynomial in the generalized logistic growth model;a_4,a_5,a_6 are the coefficients of the polynomial in the generalized logistic product model;b_1 is the enzyme synthesis rate constant;b_2 is the enzyme decay rate constant;b_3 is the power coefficient in the polynomial model for enzyme synthesis;K_1 is the limiting cell mass concentration in biomass logistic model;K_s is the saturation constant,K'_s is the saturation death rate constant;q is the power coefficient in polynomial model;S is the substrate concentration;t is the fermentation time;x_0 is the intial biomass concentration;x_1 is the biomass concentration at time t;x_2 is the enzyme activity at time t;x_f is the final biomass concentration;δ is the specific death rate; μ is the specific growth rate.

Modified Monod model and Polynomial model for biomass are the simplified versions of the monod equation and do not require substrate concentration for determination.However they could not account for the death phase of the system.The model suggested by

Humpery's on the other hand assumes the growth rate to be the net effect of actual growth and death and depended on the concentration of limiting substrate present (Rakshit S.K and Sahai V 1991).

Thouldur A et al (1999) described structured and unstructured growth kinetic models

Unstructured kinetic model:.The simplest kinetic model assumes that sugars are converted into mycelial cell biomass ,which produce enzymes.

$dL/dt = - \mu_L \ X/Y_L$, $dZ/dt = - \mu_Z \ X/Y_Z$

$dX/dt = \mu_L X + \mu_Z \ X - k_d X$, $dP/dt = r_P.X$

Where L,Z,X and P are the lactose ,xylose ,cell mass and protein concentration respectively.The specific growth rates on lactose and xylose are μ_L and μ_Z respectively.Y_L and Y_Z are the corresponding cellmass yield.k_d is an endogenous growth terms ,r_P is the specific protein production rate.When both lactose and xylose present in the medium ,xylose is preferentially taken up.The following forms are postulated for the specific growth rate and protein production:

$\mu_L = (\mu_{maxL} .L/K_{S,L}+L)(K_{I,L}/K_{I,L}+Z), \mu_{L=\mu maxz} .Z/K_{S,z}+Z,$

$r_P = \alpha \mu_L+\beta \qquad t \geq 24h, rP = 0 \qquad t < 24h$

Structured Kinetic model:The structured kinetic model incorporates a limited amount of structure in the cell mass component.Cell mass divided into three categories – Primary mycelia,Secondary mycelia,Spores than the equations

$dL/dt = - \mu_L \ X_P/Y_L$, $dZ/dt = - \mu_Z \ X_P/Y_Z$, $dX_P/dt = (\mu_L + \mu_Z - k_1 - k_{d1})$, $dX_s/dt = k_1 X_P-(k_2+k_{d2})X_s$, $dX_0 = k_2 X_s$ Than

$dX/dt = dX_P/dt + dX_s/dt + dX_0 = (\mu_L + \mu_Z) X_P - k_{d1} X_P - k_{d2} X_s$

$dP/dt = r_P X_s$,

Where L,Z,X and P are the lactose ,xylose,cell mass and protein concentration,respectievely and X_P, X_s and X_0 are the cell mass contribution from primary mycelia,secondary mycelia and spores.The specific growth rates on lactose and xylose are μ_L and μ_Z respectively;Y_L and Y_Z are the corresponding cell mass yields.k_1 and k_2 are the constant rate terms for the conversion of primary mycelia to secondary mycelia and for the conversion of secondary mycelia to spores,respectively.k_{d1} and k_{d2} are endogenous death term and r_P is the specific protein production rate(Thouldar A Wet al 1999).

Velkovaska et al (1997) pointed out the concept of primary and secondary mycelium of *T.reesei* growth in terms of product formation.Cellulase (as a product) production by

Trichodermma can be defined as a Gaden III Type process.During this process two phase are noticeable.Primary and Secondary.In the primary phase ,biomass accumulation and normal metabolic activities reach their maximum then in secondary,later phase ,product accumulation and formation rate reach their maximum values.Microscopic observation shows that our young cells of *Trichoderma reesei* in the initial period of growth (the first several days) are not very active for production of cellulase enzyme.After the fast initial formation of primary mycelium ,microscopic analysis showed that mycelium structure starts to changeafter approximetaly 2-3 days and the eventual appearance of chlamydospores which is an important organs of asexual survivals and usually appears as a result of substrate exhaustation.Substrate exhaustation triggers a physiological transformations(appearance of secondary mycelium) in the cells to survive in medium with cellulose as the only substrate.More concentrated microsomes are found into young growing tips of secondary mycelia,these newer microsomes have a higher capacity to carry out protein synthesisand responsible for product formation.

The *Trichoderma* system is very complex .For development of model equations existance of structured biomass as primary and secondary mycelium are taken into account.

$dX_p/dt = \mu_m S X_p/K_s + S - k_1.X_p$ For primary mycelium

$dX_s/dt + k_1 X_p - k_d X_s$ For secondary mycelium

$dX/dt = \mu_m S X_p/K_s + S - k_d X_s$ For total biomass concentration

X in the medium is the sum of both mycelia types. The other constants are described earlier.

References :

Aynsley M.,A.C.Wood and A.R.Wright,1990,A mathematical model for the growth of mycelial fungi in submerged culture.Biotechnol Bioeng ,35,820-830.

Bail S and F.M.Klis,1999,Mechanistic and mathematical inactivation studies of food spoilage fungi.Fun Gen Biol,27,199-208.

Baily JE.,1998,Mathematical modeling and analysis in biochemical engineering : Past accomplishment and future oppurtunites.Biotechnol.Bioengg,14,8-20.

Bizukojk M and S.A.Ledakomicz,2006,Kinetic model for predict biomass content for *Aspergillus niger* germinating spores in the submerged culture.Process Biochem ,41,1063-171.

Boswell GP,H.Jacobs,F.A.Davidson,G.M.Gadd and K.Ritz,2002,Funnctional consequences of nutrient translocation in mycelial fungi,J .Theor Biol,217,459-477.

Boswell GP.,H.Jacobs ,G.M.Gadd,K.Ritz and F.A.Davidson,2003,A mathematical approach to studying fungal mycelia,Mycologist ,17,165-171.

Dahtigry P.,S.Marin ,M.Beyer and N.Morgan,2007,Mould germination :Data treatment and modeling .Int J food Microbiol,114,17-24.

Gibson AM and A.D.Hocking,1997,Advances in the predictive modeling of fungal growth in food .Trends Food Sci Technol,8,353-358.

Lopez S.,M.Prieto MS.Dijkstra and J.France,2004,Statistical evaluation of mathematical models for microbial growth.Int J food Microbiol,96,289-300.

MeletiadisJ.,J.F.G.MMeis,J.W.Mounton,andE.U.Palul.2001,Analysis of growth characteristics of filamentous fungi in different nutrient media .J Clin Microbiol,39,478-484.

Rakshit SK. and V.Sahai,1991,Optimal control strategy for the ethanol production of cellulase enzyme using the new mutant *Trichoderma reese*i E-12.Bioprocess Engg ,6,101-107.

Thouldar A,W.F.Ramirez and J.D.McMillan,1999,Mathematical modeling and optimization of cellulase proteins production using *Trichiodermma reesei* RL-P37,Biotechnol Bioengg ,66,1-15.

Tindermans SH.,N.Kern and B.M.Mulder,2006,The diffusive vesicle supply centre model for tip growth in fungal hyphae.J Theor Biol,238,937-948

Velkovska S.,M.R.Morten and D.F.Ollis,1997,Kinetic model for batch cellulase production by *Trichodermma reesei* RUT C30 ,J Biotechnol,54,83-94.

CHEMICAL ENGINEERING TRANSACTIONS, Volume 14, 2008
Edited by G. Marino, E. Bardone, A. Viglia
 ISBN 978-88-95608-02-0

Non-local phenomena under heat and mass transfer in the high rate processes

A.S. Muratov, A.M. Brener, O.S. Balabekov
State University of South Kazakhstan, Kazakh-Turkish International University
Take-Khan av.5, Shimkent, Kazakhstan

The paper deals with the theoretical description of intensive regimes of heat and mass transfer which are typical for high rate transport phenomena in chemical reactors. The operation cycle in case of high-intensity fast processes is short and the entire process can be performed under transient conditions. Problems of modeling high-intensity processes involve construction of equations with retarded and divergent arguments, which takes account of the actual mechanism of transfer phenomena in the medium. In our paper non-local equations of the heat and mass transfer in technological processes are developed. The conditions of validity of the obtained equations and their solutions are discussed. The generalization of relaxation transfer cores applied to multicomponent systems is developed. It is established that the time dependence of the cross transfer cores is non-monotonous and has a maximum. This is a specific phenomenon caused by the effect of thermal diffusion or the Soret effect. The new methodology of calculating the intensity of heat and mass transfer processes accompanied by cross effects has been carried out.

1. Mathematical model

Consideration of the relaxation time and long-range interaction of structural components of a medium is a great practical and theoretical problem (Rudyak, 1987, p. 270) that is very relevant in cases of high-intensity fast processes. In this connection, the control of high-intensity process is limited and it is important to calculate correctly and select the best values of determining parameters. The time nonlocality of transfer processes under high-intensity conditions can be described by the model of relaxation cores of transfer [6]. Relaxation cores of transfer are the cores of integral transforms that, in the statistical theory of dissipation processes, relate fluxes with thermodynamic forces [1, 6]. Noteworthy are the wide possibilities of modeling by relaxation cores of transfer under a minimum of phenomenological approaches, which makes the method good for a study of the effect of the spatial-time nonlocality on the heat- and mass-transfer phenomena. The total structure of the component mass fluxes and heat flux in an *n*-component system according to this method has the following form according to (Jou, Casas-Vazquez and Criado-Sancho, 2001, p. 225):

$$J(R,t) = J(R,t_0) + \sum_{k=1}^{n+1} \iint dt_1 dR' N_{ik}(R,R',t,t_1) F_k(R',t), \tag{1}$$

where J are the substances fluxes; N_{ik} are the relaxation transfer cores; F_k are the thermodynamic forces; t is a time; R is a space vector.

Limiting one self to the time nonlocality in the multicomponent system, one can write expressions for the *n* linearly independent mass fluxes (Kim, Brener, 1996, p. 260).

$$J_i = -\sum_{k=1}^{n} \int_0^t dt_1 N_{ik}(R, t-t_1) \nabla\left(\frac{\nu_k(R,t_1)}{T}\right) - \int_0^t dt_1 N_{ih}(R, t-t_1) \frac{\nabla T}{T^2}, \quad (2)$$

$$J_h = -\sum_{k=1}^{n} \int_0^t dt_2 N_{hk}(R, t-t_2) \nabla\left(\frac{\nu_k(R,t_1)}{T}\right) - \int_0^t dt_2 N_{hh}(R, t-t_2) \frac{\nabla T}{T^2}, \quad (3)$$

where ν_k are the chemical potentials; T is the temperature.

To obtained a compact description and simplify transformations, let us assume $\nu_{n+1} = -1$. Then, in expressions (2), (3), one can replace the subscript *h* by *n* + 1 and write a unified form for the mass fluxes and heat flux in the multicomponent system (Brener, Muratov, Tashimov, 2004, p. 326):

$$J_i = -\sum_{k=1}^{n+1} \int_0^t dt_1 N_{ik}(R, t-t_1) \nabla\left(\frac{\nu_k(R,t_1)}{T}\right). \quad (4)$$

To analyze the total structure of the transfer equations, we use the special model equation, derived in (Brener, 2006, p. 566):

$$\frac{\partial I_{ik}}{\partial t} = \eta_{ik} \nabla\left(\frac{\nu_k}{T}\right) - \frac{I_{ik}}{\tau_{ik}}, \quad (5)$$

where τ_{ik} are the relaxation times and

$$I_{ik} = \int_0^t dt_1 N_{ik}(R, t-t_1) \nabla\left(\frac{\nu_k(R,t_1)}{T}\right). \quad (6)$$

Using (10), as a result of the repeated differentiation up to derivatives of the (*n*+ 1)-th order, the following relationships are obtained:

$$\frac{\partial^p J_i}{\partial t^p} = \sum_{j=0}^{p-1} (-1)^{j+1} \frac{\partial^{p-1-j}}{\partial t^{p-1-j}} \left(\sum_{k=1}^{n+1} \frac{\eta_{ik} \nabla(\nu_k / T)}{\tau_{ik}^j} \right) + (-1)^{p+1} \sum_{k=1}^{n+1} \frac{I_{ik}}{\tau_{ik}^p}. \quad (7)$$

Subsequent transformations are based on the conservation laws:

$$\frac{\partial \nu_i}{\partial t} + \nabla \cdot J_i = 0 . \tag{8}$$

Acting on expression (7) by the nabla operator and using (8), one can obtain, as a result, the differential equation of the (n + 2)-th order for the potential of each of the components of the system:

$$L\left(\frac{\partial^{n+2}(\nu_i)}{\partial t^{n+2}}, \frac{\partial^{n+1}(\nu_i)}{\partial t^{n+1}}, ..., \frac{\partial \nu_1}{\partial t}; \nu_i, .., \nu_n \right) = 0 . \tag{9}$$

The generalization of model approach (Kim, Brener, 1996, p. 261) to calculating relaxation cores for multiple components can be presented as

$$\frac{\partial N_i}{\partial t} = -N_i \tau_{ii}^{-1} + \sum_{\substack{k=1 \\ k \neq i}}^{n} N_k \tau_{ik}^{-1} . \tag{10}$$

Here, for filling to the Onsager principle, it is assumed that $\tau_{ik} = \tau_{ki}$.

The matrix of set (10) is symmetrical; therefore, all its eigenvalues are real. In this connection, by analogy with the result (Brener, 2006, p. 570), solution of (10) can be represented as the sum of the forward and cross components of the cores of transfer:

$$N_i = \sum_{k=1}^{n} N_{ik} , \tag{11}$$

where all items are real exponents and *Nik* = *Nki*. Hence, a relationship of the form of (9) again occurs.

The nonlinear generalization of flow equations (1) can be represented in a nonlocal quadratic form with tensor cores (Brener, 2006, p. 571):

$$\begin{aligned} J_i = &-\sum_{k=1}^{n+1} \int_0^t dt_1 N_{ik}^{(1)}(R, t - t_1) \cdot \nabla \left(\frac{\nu_k(R, t_1)}{T} \right) - \\ &- \sum_{k=1}^{n+1} \sum_{p=1}^{n+1} \int_0^t \int_0^t dt_1 dt_2 N_{ikp}^{(2)}(R; t - t_1; t - t_2) : \nabla \left(\frac{\nu_k(R, t_1)}{T} \right) \nabla \left(\frac{\nu_p(R, t_2)}{T} \right) . \end{aligned} \tag{12}$$

In the weakly nonlinear approximation, one can assume

$$\left\| N_{ikp}^{(2)} \right\| = \varepsilon \left\| N_{ik}^{(1)} \right\| \left\| N_{ip}^{(1)} \right\|, \tag{13}$$

where ε is the series expansion parameter. As the parameter, one can use the ratio of the two Knudsen numbers that are calculated by two specific spatial scales for the elastic and inelastic molecular collisions, respectively.

The simple non-linear generalization of the model (10) considering the cross effects in a two-component system looks as follows

$$\begin{cases} \dfrac{\partial N_m}{\partial t} = -N_m \left(1 - \varepsilon_m N_m\right) \tau_m^{-1} + N_h \left(1 - \varepsilon_h N_h\right) \tau_\times^{-1}, \\ \dfrac{\partial N_h}{\partial t} = N_m \left(1 - \varepsilon_m N_m\right) \tau_\times^{-1} - N_h \left(1 - \varepsilon_h N_h\right) \tau_h^{-1} \end{cases} \tag{14}$$

2. Model results

The solution of submitted model for a two-component system can be written in the form

$$N_m = N_{mm} + N_{mh}, \tag{15}$$

$$N_h = N_{hh} + N_{hm}, \tag{16}$$

where

$$N_{mm} = \frac{\eta_m}{\lambda_2 - \lambda_1} \left[\left(\lambda_2 + \frac{1}{\tau_m} \right) \exp\left(\lambda_1 s\right) - \left(\lambda_1 + \frac{1}{\tau_m} \right) \exp\left(\lambda_2 s\right) \right], \tag{17}$$

$$N_{hh} = \frac{\eta_h}{\lambda_2 - \lambda_1} \left[\left(\lambda_2 + \frac{1}{\tau_h} \right) \exp\left(\lambda_1 s\right) - \left(\lambda_1 + \frac{1}{\tau_h} \right) \exp\left(\lambda_2 s\right) \right], \tag{18}$$

$$N_{mh} = N_{hm} = \frac{\eta_\times}{\tau_\times \left(\lambda_2 - \lambda_1\right)} \left[\exp\left(\lambda_1 s\right) - \exp\left(\lambda_2 s\right) \right] \tag{19}$$

In the approximation of system quasi non-equilibrium, from the condition of attenuation of distortions, it is follows that both characteristic quantities $\lambda_{1;2}$ should be negative. From this, one can obtain the inequality for direct and cross relaxation times:

$$\tau_\times > \sqrt{\tau_m \tau_h}\ . \tag{20}$$

Let us introduce the dimensionless parameters that characterize the correlations of relaxation times of the forward and cross distortions:

$$\alpha_1 = \frac{\tau_m}{\tau_h};\quad \alpha_2 = \frac{\tau_m}{\tau_\times};\quad z = \alpha_2 \sqrt{\alpha_1} \tag{21}$$

Figure 1 depicts the typical curves for the time history of relaxation transfer cores under the different quantities of the parameters obtained by numerical experiment.

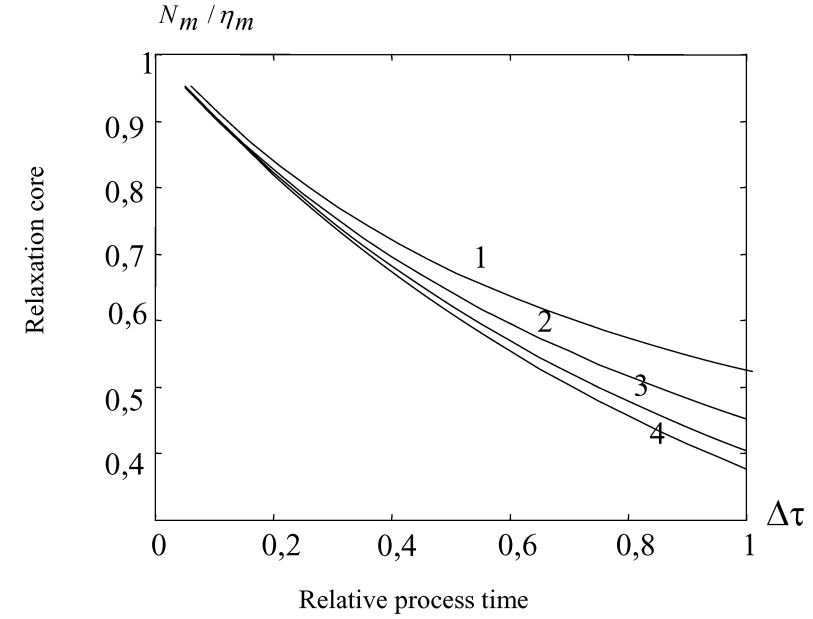

A)

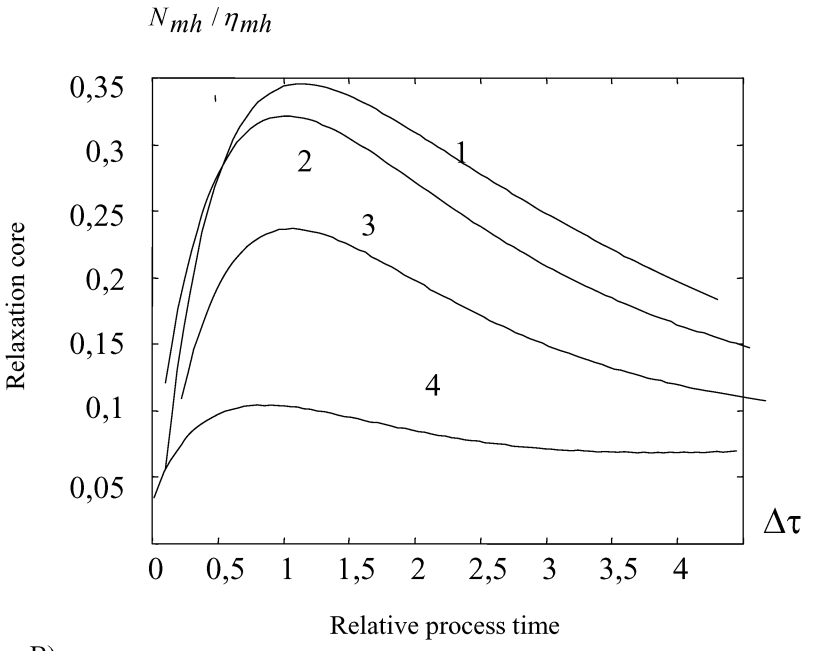

B)

Figure 1. (A) - Characteristic time dependences of the direct diffusion relaxation core of transfer at α_1 = 1.4 and (B) - the development of cross relaxation distortion at α_1 = 0.6; z = (1) 0.2, (2) 0.4, (3) 0.6, (4) 0.8.

The time dependence of the cross core of transfer has a maximum (Fig. 1 - B). This is a specific phenomenon caused by the effect of thermal diffusion or the Soret effect. The maximum of the time dependence of the cross core of transfer determines the period of increase in the initial distortions of the temperature and concentration fields that is due to influence of thermodynamic cross effects. From this, one can obtain the formula for the specific period of increase in distortions:

$$\Delta t\uparrow = \frac{\ln(\lambda_2/\lambda_1)}{\lambda_1 - \lambda_2}. \tag{22}$$

3. Practical recomendations

In a compact form the calculations order for one-dimension tubular through-reactor with allowing for the non-local phenomena can be described as follows.
The simplified system of heat and mass transfer reads:

$$\tau_1 \frac{\partial^2 \nu}{\partial t^2} = (-1 + \tau_1 \mathrm{N}_1)\frac{\partial \nu}{\partial t} + D\Delta\nu\,, \tag{23}$$

$$\tau_2 \frac{\partial^2 T}{\partial t^2} = (-1 + \tau_2 \mathrm{N}_2)\frac{\partial T}{\partial t} + a\Delta T\,, \tag{24}$$

Let us introduce the extended variables using scales of the relaxations times order: $t;\quad \theta = \frac{t}{\tau};\quad x$. Thus solutions of (23), (24) look as follows

$$\nu = \nu_0 + \tau_1\nu_1\,,\ T = T_0 + \tau_2 T_1\,. \tag{25}$$

The zero and first approximations are determined from the equations

$$\frac{\partial^2 \nu_0}{\partial \theta^2} = -\frac{\partial \nu_0}{\partial \theta},\ \frac{\partial^2 T_0}{\partial \theta^2} = -\frac{\partial T_0}{\partial \theta};\tag{26}$$

$$\frac{\partial^2 \nu_1}{\partial \theta^2} = \frac{\partial \nu_1}{\partial \theta} + N_1\frac{\partial \nu_0}{\partial \theta} + \frac{\partial^2 \nu_0}{\partial x^2},\ \frac{\partial^2 T_1}{\partial \theta^2} = \frac{\partial T_1}{\partial \theta} + N_1\frac{\partial T_0}{\partial \theta} + \frac{\partial^2 T_0}{\partial x^2}. \tag{27}$$

From these equations it follows the characteristic solutions.
Zero-order:

$$\nu_0 = \nu_0(x)\big|_{t=0} + C_\nu \exp(-\theta);\ T_0 = T_0(x)\big|_{t=0} + C_T \exp(-\theta). \tag{28}$$

First order:

$$\nu_1 = (C_\nu + A_\nu\theta)\exp(-\theta);\ T_1 = (C_T + A_T\theta)\exp(-\theta). \tag{29}$$

The effective mass diffusivity is calculated with amendment to non-local phenomena:

$$D_{ef} = \chi D_{ef}(0). \tag{30}$$

According to this approach the engineering methodology for calculating chemical reactors with accounting of non-local phenomena and cross effects was carried out. Figures 2 and 3 depict some results of the above investigations.

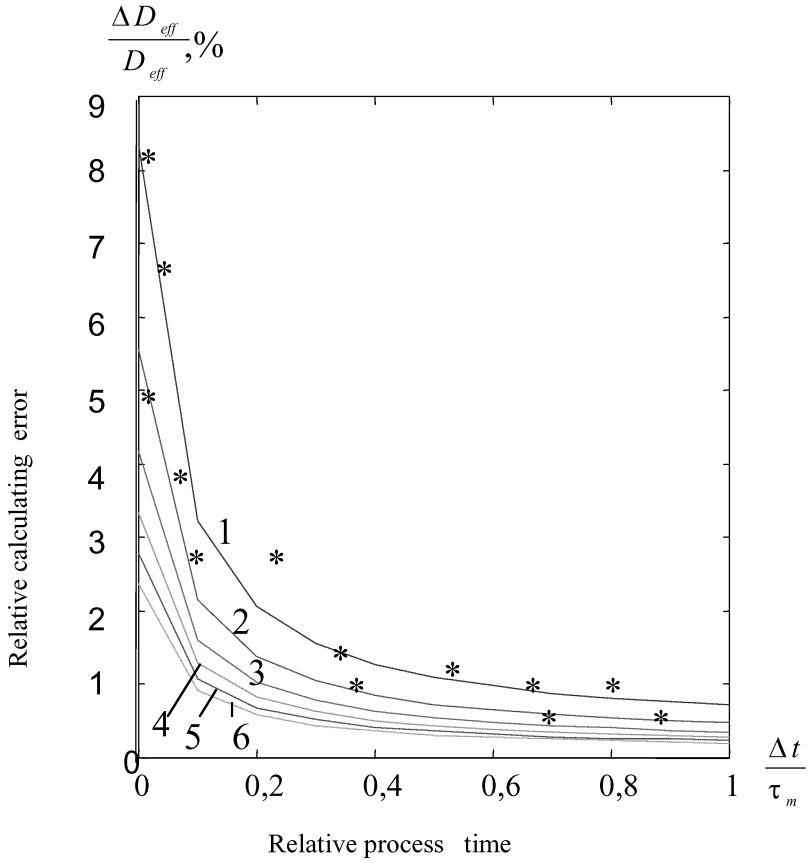

$1-\alpha_1 = 0{,}4;\ 2-\alpha_1 = 0{,}6;\ 3-\alpha_1 = 0{,}8;\ 4-\alpha_1 = 1{,}0;\ 5-\alpha_1 = 1{,}2;\ 6-\alpha_1 = 1{,}4$

Figure 2. The relative deviation of the effective mass diffusivity from the nominal under calculating with accounting to non-local phenomena

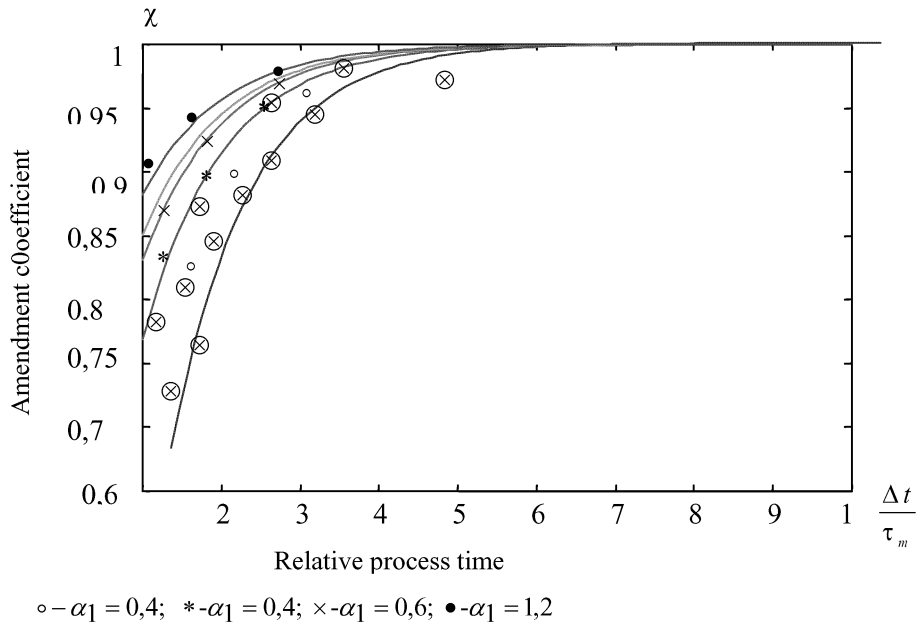

Figure 3. Amendment coefficients under calculating effective diffusivities for high rate processes.

The nonlinearity and the high order of the obtained equations are unusual and complicate their practical use. Yet their capability to describe the various effects caused by the nonlinearity of the medium and cross effects is rather wide and can justify subsequent investigations. That work is likely to be of importance to practice in process engineering including biotechnology processes. It seems that methods for describing transport phenomena in complex systems such as biological or biotechnological systems may be interesting for specialists in biotechnology.

4. References

Rudyak, V.J. Statistic theory of the dissipative processes in gas and liquids, 1987, Nauka, Novosibirsk (in Russian)

Jou, D., Casas-Vazquez, J., and Criado-Sancho, M., Thermodynamics of Fluids under Flow, 2001, Berlin: Springer.

Kim, L.A., Brener, A.M. Time non-locality of the heat and mass transfer equations in the high rate technological processes. Theor. Foundations of Chem. Engineering, 1996, 30, No3.

Brener, A.M., Muratov, A.S., and Tashimov, L., Non-Linear Model of Time Dependent Relaxation Cores for the Systems with Cross Transfer Effects, Proc. VIII Int.Conf. on Advanced Computational Methods in Heat Transfer, 2004, Lisbon, Portugal.

Brener, A.M. Nonlocal Equations of the Heat and Mass Transfer in Technological Processes. Theor. Foundations of Chem. Engineering, 2006, Vol. 40, No. 6.

CHEMICAL ENGINEERING TRANSACTIONS, Volume 14, 2008
Edited by G. Marino, E. Bardone, A. Viglia
 ISBN 978-88-95608-02-0

Improvements in PHA Production, Control and Applications

Berezina Nathalie, Talon Olivier and Paternostre Laurent
NATISS R&D Centre, rue des Foudriers 1, 7822 Ghislenghien, Belgium
berezina.n@natiss.be; talon.o@natiss.be; paternostre.l@natiss.be

The productivity and copolymerisation control of PHBV were improved *via* specific feeding (sodium glutamate 10 g/L and sequential addition of valeric acid). The active monitoring of PHA content in cells was made possible through TGA analysis based on the large degradation temperature difference between PHAs and the rest of the cells. Finally a kinetic model for the depolymerisation of PHA was proposed and discussed.

1. Introduction

Industrial biotechnology is a well known tool for production of fine and specialty chemicals, mostly for pharmaceutical and cosmetic industries. Polymers are a new emerging domain for expansion of Industrial Biotechnology. Such polymers may be considered as well as material (Sudesh et al. 2000) as natural concentrates of chiral products (Seebach et al. 1987).
One of the most promising such obtained class of polymers is the poly(hydroxyalkanoates) (PHA) one. PHA are a huge family of bacterial polymers, they present interesting performances and chirality properties, but they suffer from too expensive and tricky production.
That is why a lot has to be done for improvements in PHA's production, analysis (control) and synthons application.

2. PHA production

In order to optimise the production of PHB and PHBV by *C. necator*, we made 2 experimental designs. We worked with experimental designs types 2^{k-p}, with k=3 and p=1. This allowed us to evaluate 6 factors in 8 experiments (Berezina et al. 2007).

First we wanted to enhance *C. necator* biomass. Indeed, as the PHA production depends on nutrient control, most of the authors (Potter et al. 2004, Mantzaris et al. 2002) use to allow the bacteria to grow under limited nutrient conditions: minimum mineral media with only carbon supply used for the PHA production (typically glucose, fructose, sodium gluconate etc.). On the other hand, it is known (Steinbüchel et al. 2003) that the PHA production is made in two steps: *C. necator* growth followed by PHA accumulation.

Different substrates were reported to be biomass enhancers such as citric acid (Wang et al. 1997), sodium glutamate (Elbahloul et al. 2005, Barclay et al. 2001, Sauer et al.

2004, Wang et al. 2001, Wang et al. 2000, Sonavane et al. 2003), aminolevulinic acid (Hungerer et al. 1995) or aspartate (Sonavane et al. 2003). The most efficient biomass enhancer seems to be sodium glutamate whereas citric acid is also supposed to influence valerate content of final PHBV (Akyiama et al. 1992, Steinbüchel et al. 2003); finally glucose concentration can also play a key role as well in biomass growth as in PHA production.

Thus in the first experimental design (Table 1) we evaluated: citric acid supply (0 or 2 g/L), sodium glutamate supply (10 g/L or 20 g/L) and glucose concentration during the accumulation step (10 g/L or 30 g/L).

Table 1 : Factor's effects of both experimental designs

Factors	DW	PHA	PHA/g_{DW}	PHA/$g_{glucose}$
Citric acid (2 g/L)	-3	6	-4	-1
Glutamate (10 g/L)	15	25	15	8
[G] 30 g/L at 48h	15	4	13	4
[G] 30 g/L at t_0	4	-3	0.4	0.9
P(O_2) (30 %)	0.2	-1	-0.8	0.5
Valeric acid (4x5g/L)	-0.2	1	0.8	-0.5

During the second experimental design we evaluated: glucose concentration at t_0 (10 g/L or 30 g/L), P(O_2) (3% or 30%) and valeric acid supply manner (4x5g/L or 1x20 g/L).

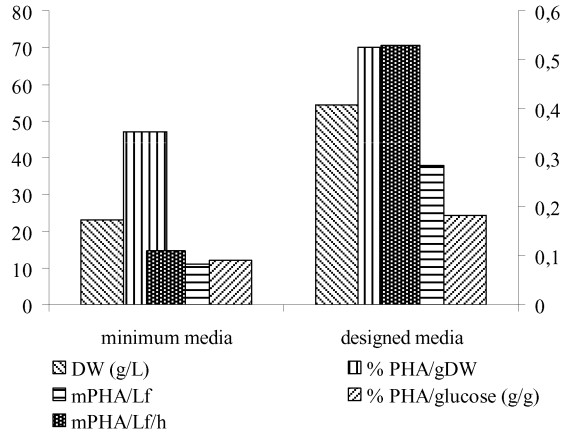

Figure 1 : Majors variables evolution before (minimum media) and after (designed media) the 2 experimental designs

The citric acid supply, $P(O_2)$ variation and valeric acid supply manner resulted in no benefice on DW, PHA content, PHA production, PHA/glucose yield or the whole system productivity (Table 1), whereas an important beneficial effect of glucose concentration at 30 g/L (either at the beginning of the fermentation or during the accumulation step) and of glutamate supply at 10 g/L (at 20 g/L results were less interesting due to the extra ammonium supply present in glutamate) was observed (Table 1).

After the completion of control fermentations, which consisted in the combination of best factors, we obtained the following improvements (Figure 1): Dry Weight enhancement on 250%, PHA content on 30%, Volumetric production on 400%, PHA/glucose yield on 200% and Productivity on 500%.

Table 2 : PHBV analysis

Valeric acid supply[1]	HV (mol %)		DSC		SEC	
	GC	NMR	T_g	T_m	$\overline{M_n}$	Ip
4 times	7	9	3	168[2]	120000	1.9
1 time	4	5	0	171[3]	220000	1.4

1. final valeric acid amount is the same in both cases
2. bimodal pick
3. monomodal pick

The manner of valeric acid supply has poor influence on growth, but deeply influences as well the valerate content as the polymer structure (Table 2). Valerate content grows from 4% (unique addition) to 8% (multiple additions). The results are even more interesting when comparing other analysis: SEC clearly indicates 2 different types of polymers and DSC suggests a block system for multiple additions and a statistic system for single addition.

These results are consistent with Srienc's group suggestions (Kelley et al. 2001, Mantzaris et al. 2001, Pederson et al. 2006): switching of carbon source results in increasing of valerate content and block copolymer structure.

3. PHA analysis

The parameters usually followed in a fermentation process, such as optical density, dry weight or glucose concentration do not give any direct information about the yield of PHBV production.

The control of the bacterial production of poly(hydroxyl alkanotes) (PHA) is usually (Sudesh et al. 2000, Steinbüchel et al. 2003) done by an extraction method. A large sample (ca 10 mL) is withdrawn from the fermentation reactor. The sample is then centrifuged before to undergo a freeze-drying step. The lyophilizate is then immersed in chloroform for the extraction of the PHA from the cells, and filtered. After precipitation of the filtrate and drying of the PHA such obtained, one can at last, after several days, have an idea of the yield of the process at the time the sampling was made. It is obvious that, for a more or less one week long fermentation process, this method is unsuitable for a reactive monitoring, not to mention the large use of solvents.

We improved and developed the method previously reported by Hahn et al. (1995) (Talon et al. 2007). TGA performed on pure PHBV and on PHBV still enclosed in bacteria showed that a significant gap exists between the thermal degradation temperatures of the PHA and of the cells. It appears indeed that the PHA is fully degraded at 210-220 °C, whereas the weight loss due to the degradation of the cells only begins at about 250-260 °C (Figure 2).

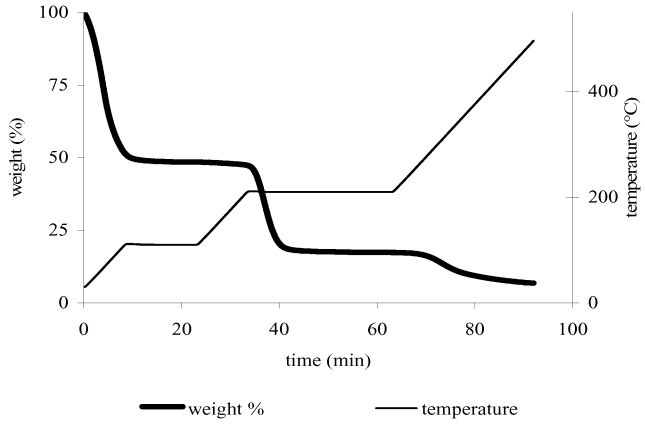

Figure 2 : time course evolution of temperature program and weight (%) evolution

When used to follow two fermentations done in identical conditions, the results of the thermogravimetric method show (Figure 3) that both the fermentation process and the method of assay are reproducible.

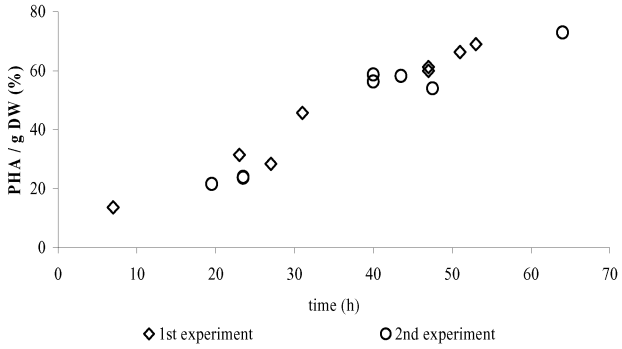

Figure 3 : Reproducibility of TGA analysis between 2 similar experiments

In order to confirm the validity of the method, a fermentation experiment was followed according to the two methods (extraction and TGA methods). The results are shown in Figure 4, where it can be seen that the results provided by the two methods are quite comparable. Moreover, it seems that the thermogravimetric method would give more exact results, since they are a little higher than those obtained with a single extraction step, and it is well known that the yield of only one extraction is not quantitative.

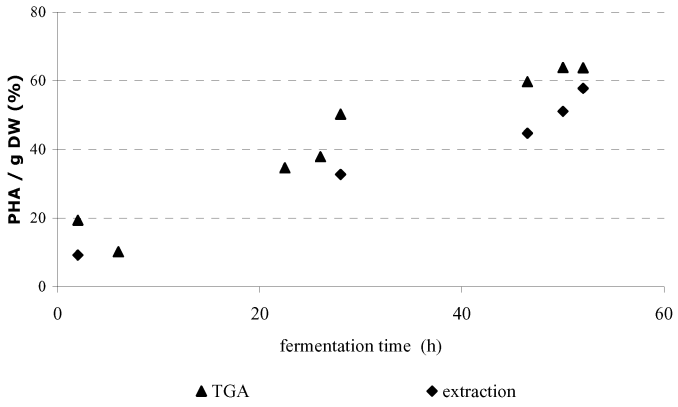

Figure 4 : Comparison between 2 methods of PHA content's measurement

4. PHA Applications

Across different applications of PHA one can be interested by using their chiral monomers, i.e. β-hydroxyacids. Indeed, PHA are perfectly chiral polymers, as well their monomers are, and β-hydroxyacids are very useful products. β-hydroxyacids can be used by themselves (mostly in cosmetic industry) and as chiral synthons for a range of

products such as lactones, β-lactams, dioxanones, (Seebach et al. 1987) or even proven antibiotics as tienamycin (Chiba et al. 1985) or elaiophylin (Seebach et al. 1986, Evans et al. 1997).

The depolymerisation of PHA has been of interest for a long time. Pioneering work on the PHB depolymerisation was performed by Merrick et al. (1964) and consisted on enzymatic depolymerisation of non purified polymer. Pyrolysis approach developed by Morikawa et al. (1980) produced mostly crotonic acid. More recent results (Lee et al. 2000, Lee et al. 1999) concerned the alcoolysis approach, finally Ren et al. (2005) worked on *in situ* depolymerisation of PHA_{MCL} (medium chain length PHA).

Herzog et al. (2006) proposed a kinetic model for polyester depolymerisation by lipases, but no kinetic model is yet available for the PHA depolymerisation, to our knowledge.

We wanted to make a simple kinetic model for the depolymerisation of the non purified PHA, i.e. still contained inside the cells. This means that we have to treat 2 reactions: the transfer across the cells' membranes and the depolymerisation of the free PHA.

$$PHA_c \xrightarrow{k_1} PHA_f \xrightarrow{k_2} \beta\text{-hydroxybutyric acid} \quad (1)$$

PHA_c represents PHA inside of bacterial cells
PHA_f represents free PHA in the reaction media

On first approximation we can assume that the percentage of depolymerisation will essentially depend on PHA transfer across cell membrane. The second reaction is supposed to be much faster than the PHA transfer (ester hydrolysis in aqueous basic media), $k_2 >> k_1$. In that case the only important parameter to be measured will be the PHA content in cells and we can express the depolymerisation process as following:

$$\%\ \text{depolymerisation} = \frac{PHAi}{PHA\ (t)} \quad (2)$$

PHAi being initial content of PHA in cells
PHA (t) being the content of PHA in cells at instant t

In order to check this kinetic model, we made an experiment with 10 molar NaOH. We compared results obtained by HPLC analysis of produced β-hydroxybutyric acid with remained PHA content in cells measured by previously described TGA method (Figure 5). We can observe quiet a correct correlation between the theoretic model and the experimental data.

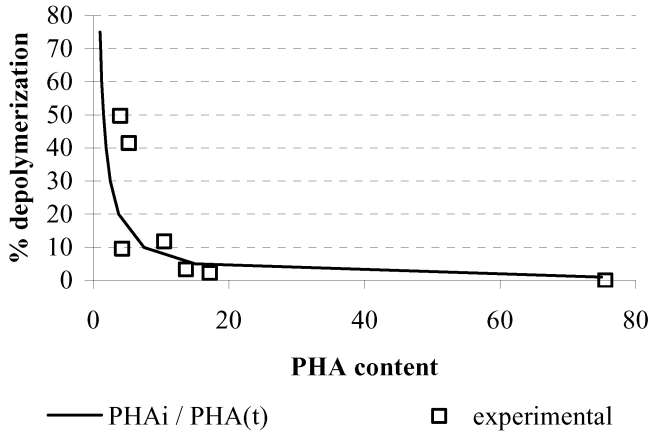

Figure 5 : Comparison of the kinetic model with the experimental depolymerisation

However, we may assume that that weaker the base the wronger the hypothesis that the depolymerisation step can be neglected in regard of the diffusion step. Therefore, even if this kinetic model is satisfactory at the first stage it should be précised for being more universal for this system.

5. Conclusion

In this work we applied the experimental design system to investigate 6 different factors for PHA production. We succeeded to identify the most important benefit factors which allowed us to enhance the whole system PHB productivity for 5 times. We also succeeded to control the PHBV structure (block or statistical) by valeric acid supply manner.

Further developed thermogravimetric analysis enables a rapid control of the evolution of a fermentation process, and therefore can offer the opportunity of being reactive enough to adapt the process parameters when something seems to go wrong. This method of assay provides good and reproducible results, and it is solvent free and hugely time-saving.

Finally, we turned our interest to the PHA's depolymerisation and established a satisfactory kinetic model for the combination of membrane transfer and depolymerisation reactions.

6. References

Akiyama, M., Taima, Y. and Doi, Y., 1992, Appl. Microbiol. Biotech., 37, 698.

Barclay, S.S., Woodley J.M., Lilly M.D., Spargo P.L. and Pettman A.J., 2001, Biotech. Lett., 23, 385.

Berezina N., Colin T., Bensaid A., Paternostre L, in European Bioperspectives Proceedings, Cologne, 2007

Chiba, T. and Nakai, T., 1985, Chemistry Letters, 651.

Elbahloul Y., Krehenbrink M., Reichelt R., Steinbüchel A., 2005, Appl. Environ. Microbiol., 71-2, 858

Evans D.A., Fitch D.M., 1997, J. Org. Chem., 62, 454

Hahn S.K.; Y.K. Chang, Biotech. Tech., 1995, 9, 873.

Herzog, K., Muller, R. J. and Deckwer, W. D., 2006, Polym. Degrad. Stability, 91, 2486-2498.

Hungerer C., Troup B., Romling U., Jahn D., 1995, J. Bacteriol., 177-6, 1435

Kelley, A. S., Mantzaris, N. V., Daoutidis, P. and Srienc, F., 2004, Nano Lett., 1, 481.

Lee, S., Lee, Y. and Wang, F., 1999, Biotech. Bioeng., 65, 363.

Lee, Y., Park, S. H., Lim, I. T., Han, K. and Lee, S., 2000, Enz. Microbiol. Tech., 27, 33.

Mantzaris, N. V., Kelley, A. S., Srienc, F. and Daoutidis, P., 2001, AIChE Journal, 47, 727.

Mantzaris, N. V., A. S. Kelley, et al., 2002, Chem. Eng. Sci., 57, 4643.

Merrick, J. M. and Doudoroff, M. ,1964, J. Bacteriol., 88, 60-71.

Pederson, E. N., McChalicher, C. W. J. and Srienc, F., 2006, Biomacromolecules, 7, 1904.

Pötter M., Muller H., Reinecke F., Wieczorek R., Fricke F., Bowien B., Friedrich B., Steinbüchel A., Microbiology, 2004, 150 2301.

Ren, Q., Grubelnik, A., Hoerler, M., Ruth, K., Hartmann, R., Felber, H. and Zinn, M., 2005, Biomacromolecules, 6, 2290.

Sauer K., Cullen M.C., Rickard A.H., Zeef L.A.H., Davies D.G., Gilbert P., 2004, J. Bacteriol., 186-21, 7312

Seebach, D., Chow, H. F., Jackson, R. F. W., Sutter, M. A., Thaisrivongs, S. and Zimmermann, J., 1986, Liebigs Ann. Chem., 1281.

Seebach, D., Imwinkelried, R. and Stucky, G., 1987, Helv. Chim. Acta, 70, 448.

Sonawane, A., Kloppner, U., Derst, C. and Rohm, K. H., 2003, Arch. Microbiol, 179, 151.

Steinbüchel, A. and Lutke-Eversloh, T., 2003, Biochem. Eng. J., 16, 81.

Sudesh K., Abe H., Doi Y., 2000, Prog. Polym. Sci., 25, 1503

Talon. O, Berezina N., Lewillon P., Allert F., Dombrun E., Paternostre L., in Bioplastics 2007 proceedings, Montreal

Wang, S. J. and Loh, K. C., 2000, Biotech. Bioeng., 68, 437.

Wang F., Lee S.Y., 1997, Appl. Environ. Microbiol., 63-9, 3703.

Wang, S. J. and Loh, K. C., 2001, Biodegradation, 12, 189.

CHEMICAL ENGINEERING TRANSACTIONS, Volume 14, 2008
Edited by G. Marino, E. Bardone, A. Viglia
 ISBN 978-88-95608-02-0

Interlocking of primary and secondary metabolism in antibiotic-producing actinomycetes

E. Stegmann[1], B. Hadatsch[1], C. Kittel[1], O. Puk[1], R. Menges[1], R. Süßmuth[2], W. Wohlleben[1]

[1]*Institute of Microbiology, Mikrobiologie/Biotechnologie, Eberhard-Karls-Universität Tübingen, Auf der Morgenstelle 28, 72076 Tübingen, Germany*
Email: evi.stegmann@biotech.uni-tuebingen.de
[2]*Institute of Chemistry, Technische Universität Berlin, Strasse des 17. Juni 124, 10623 Berlin, Germany*

Glycopeptides such as vancomycin are the drugs of last resort for the treatment of severe infections caused by antibiotic resistant gram-positive bacteria. As a model strain for analysing and manipulating glycopeptide biosynthesis we have chosen *Amycolatopsis balhimycina* which synthesizes the vancomycin-type glycopeptide balhimycin.
The 66-kb gene cluster encoding the biosynthesis of balhimycin was identified and sequenced. The biosynthetic pathway was elucidated and functions were assigned to all genes of the cluster.
Five out of seven amino acids of the heptapeptide backbone are – directly or indirectly – derived from the shikimate pathway: two molecules β-hydroxytyrosine (β-Ht) and hydroxyphenylglycine (Hpg) and one molecule dihydroxyphenylglycine (Dpg). In addition to the genes encoding the biosynthetic enzymes typical for secondary metabolism, the balhimycin gene cluster includes two genes (*pdh, dahp*) which encode key enzymes of the shikimate pathway. Since a second copy of each of these two genes is found in the genome outside of the balhimycin cluster, we assume that the "pathway-specific" enzymes are responsible for an optimized provision of tyrosine, a precursor of the non-proteinogenic amino acids β-Ht, Hpg and Dpg.
In the efficient excretion of balhimycin an ABC-transporter is involved whose inactivation led to an intracellular accumulation of balhimycin.
Bbr, a StrR-type regulator, is involved in the transcriptional control of the biosynthetic genes. Furthermore a two component regulator system (VanRS) was identified which may encode an overriding control system responding to the presence of glycopeptide.
In order to improve the yield of balhimycin, gene inactivation and overexpression studies were performed. The manipulation of the transcriptional regulation as well as targeted intervention in the primary metabolism should result in an increased balhimycin production.

Primary and secondary metabolism

Primary metabolites are elementary puzzle pieces for all microorganisms: They are end products of catabolism, set up to form primary intermediates such as amino acids, nucleotides, vitamins, carbohydrates, and fatty acids. These biosynthetic intermediates are subsequently assembled into the complex and essential metabolites that give structure and biological function to the organism.

Secondary metabolites are produced only by small groups of organism and are not required for growth. They are structurally diverse, generally produced in mixtures with other members of the same chemical family, and formed at low specific growth rates.
Important classes of secondary metabolites are the antibiotics. The metabolic pathways of the primary metabolism often supply the precursors of the antibiotics. There is an early common part which then branches to the synthesis of a primary metabolite on the one hand and to a secondary metabolite on the other.
In some cases, primary end product feedback inhibits the common part of the pathway and thus impairs production of secondary metabolites and accumulation of the precursors. The amount of precursors and cofactors required for synthesis of antibiotics is usually sufficiently low to be easily accommodated by the central carbon metabolism of the cell. In cases that the precursors for antibiotic synthesis are cellular building blocks such as amino acids, carbon is drained from the anabolic routes rather than the central carbon metabolism. To obtain high yield strains it is not only important to increase expression of the biosynthesis genes, but also the activity of the anabolic pathway. The situation is generally more complex when there is a requirement for specific precursors that are synthesized by enzymes encoded by genes in the biosynthesis gene cluster (Gunnarsson et al., 2004).

Glycopeptide biosynthesis

Synthesis of specific precursors plays an important role in the biosynthesis of glycopeptide antibiotics. Glycopeptides such as vancomycin are the drugs against antibiotic resistant gram-positive bacteria. The best analyzed strain for glycopeptide biosynthesis is *Amycolatopsis balhimycina*, the producer of the vancomycin-type glycopeptide balhimycin (Nadkarni et al., 1994) (Figure 1).

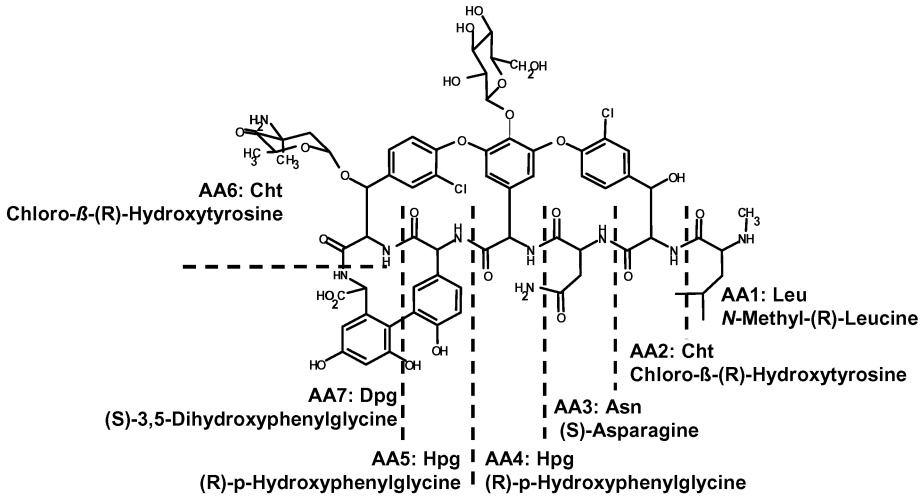

Figure 1: Structure of the glycopeptide balhimycin produced by *A. balhimycina*.

Using a “Reverse Genetics” approach the 66-kb gene cluster (Pelzer et al., 1999) encoding the biosynthesis of balhimycin has been identified. By a combination of genetics, biochemistry and analytical organic chemistry the biosynthetic pathway has been elucidated and the function of nearly all genes of the cluster has been proven.

The biosynthesis starts with the pathway-specific supply of the non-proteinogenic amino acids β-hydroxytyrosine (β-Ht), hydroxyphenylglycine (Hpg) and dihydroxyphenylglycine (Dpg) which form together with (N-methyl) leucine and asparagine the heptapeptide backbone of balhimycin. β-Ht and Hpg are derived from the shikimate branch of amino acid biosynthesis including unusual modification reactions (Hubbard et al., 2000; Puk et al., 2002, Puk et al. 2004).

Hpg is derived from the aromatic ring of tyrosine and the α-carbon of tyrosine is the carboxylic acid carbon of 4-Hpg. In the balhimycin biosynthetic gene cluster three *orfs* (*pgat*, *hmaS* and *hmo*) are located which show high similarity to the genes that participate in the biosynthesis of Hpg from prephenate in the chloroeremomycin producer *Amycolatopsis orientalis* (Hubbard et al. 2000). Therefore, an analogous biosynthetic pathway was postulated for the Hpg-biosynthesis in *A. balhimycina*.

The three genes which are required for the biosynthesis of β-Ht are also localized in the balhimycin biosynthetic gene cluster: the perhydrolase, Bhp, the nonribosomal peptide synthetase module, BpsD and the monooxygenase, OxyD. Inactivation of all these three genes resulted in null mutant strains of *A. balhimycina*. Supplementation of these mutant strains with β-Ht restored balhimycin production thus confirming the involvement of Bhp, BpsD and OxyD in β-Ht-biosynthesis. The proposed model suggested tyrosine being loaded onto BpsD with subsequent β-hydroxylation of BpsD-bound tyrosine catalysed by OxyD (Puk et al., 2004). The last step is the hydrolysis of β-Ht from the BpsD complex due to the action of the hydralase Bhp in order to deliver the free amino acid.

The nonproteinogenic amino acid Dpg is synthesized via a polyketide synthase mechanism (PKSIII) similar to that known from plant chalcon/stilben synthases (Pfeifer et al., 2001). Four genes forming an operon (*dpgABCD*) are required to provide Dpg. Inactivation of DpgA, the predicted polyketide synthase resulted in the loss of balhimycin production. Restoration was achieved by supplementation with 3,5-dihydroxyphenylacetic acid, which is both, a possible product of the PKS and a likely precursor of Dpg. Enzyme assays with the protein expressed in *Streptomyces lividans* showed that DpgA uses only malonyl-CoA as substrate (Pfeifer et al., 2001). The heterologous co-expression of all *dpg* genes in *S. lividans* led to the accumulation of 3,5-dihydroxyphenylglyoxylic acid. The final step in the pathway of Dpg is the transamination. Inactivation of the predicted transaminase gene (*pgat*) resulted in a null mutant strain and in accumulation of 3,5-dihydroxyphenylglyoxylic acid. Restoration of balhimycin production in this mutant was only possible by simultaneous supplementation with (S)-3,5-dihydroxyphenylglycine and (S)-4-hydroxaphenylglycine, indicating that the transaminase is essential for the formation of both amino acids (Pfeifer et al. 2001). Similar to Hpg, the formation of Dpg requires tyrosine as amino donor which thus interconnects Dpg biosynthesis with the shikimate pathway.

Subsequently, the amino acids are linked by non-ribosomal peptide synthetases (Recktenwald et al., 2002). The aromatic side chains are interconnected by P450 monooxygenases (Süßmuth et al., 1999; Zerbe et al., 2002; Stegmann et al., 2006); a series of reactions which occur in a strict order (Bischoff et al., 2001a; 2001b) and lead to the first antibiotically active intermediate. The NADH/FAD-dependent halogenase BhaA catalyzes the chlorination of the two β-Hts (Puk et al. 2002). The substrates of the oxygenases as well as of the halogenase are not free biosynthetic precursors, but rather intermediates which are bound to the NRPS (Bischoff et al., 2005). The resulting cross-linked heptapeptide is then finally modified by methylation and glycosylation.

The final step in the secondary metabolite biosynthesis is the excretion of the products, often mediated by specific transporters. A gene (*tba*) encoding a putative ABC-transporter is part of the cluster. To prove its involvement in balhimycin excretion *tba* was inactivated by gene replacement which did not interfere with growth and did not affect balhimycin

resistance. However, in the supernatant of the *tba* mutant less balhimycin was detected compared to the wild type; and the intracellular balhimycin concentration was 10 times higher in the *tba* mutant than in the wild type.
The biosynthesis is regulated by a StrR-type regulator, which was shown to bind in front of different operons of the balhimycin gene cluster (Shawky et al. 2007). This probably ensures coordinated expression of the biosynthetic genes at the end of the exponential growth phase as shown by RT-PCR. However, it is not known, which signal controls the expression of the *bbr* gene.
In addition to the mentioned structural and regulatory genes the cluster also contains putative resistance genes with similarity to *vanY* (encoding a putative D,D carboxypeptidase) and *vanR* and *vanS* (putative two component regulatory system sensing cell wall antibiotics) (Shawky et al., 2007).

Interconnection of primary and secondary metabolism in balhimycin biosynthesis

The supply of precursors or cofactors from primary metabolism might be a limiting factor for secondary metabolite production, in order to maximize product yields. Thus it is necessary to redirect primary metabolic fluxes in a manner that supports high secondary metabolite productivities (Thykaer and Nielsen, 2003). Current knowledge of the biochemistry of primary metabolism pathways in actinomycetes is limited but considered to be important for further rational improvement of strains overproducing aromatic amino acids and derived compounds (Hodgson, 2000). The non-proteinogenic amino acids β-Ht and Hpg of the heptapeptide backbone are directly derived from the aromatic amino acid tyrosine. In addition, tyrosine is the amino donor in the Dpg biosynthesis indicating a key role of the shikimate pathway in precursor supply. As a consequence, the supply of tyrosine may be rate controlling during high-yield glycopeptide production.
The aromatic amino acid L-tyrosine is derived from chorismate, the end product of the shikimate pathway. The key enzymes of the shikimate pathway are responsible for the following steps: DAHP synthase, the first enzyme of the shikimate pathway, condenses the pentose phosphate pathway intermediate D-erythrose 4-phosphate and the glycolytic pathway intermediate phosphoenolpyruvate to DAHP. The chorismate mutase (Cm) catalyses the transformation of chorismate to prephenate. L-tyrosine biosynthesis further proceeds by conversion of prephenate into 4-hydroxy-phenylpyruvate (via prephenate dehydrogenase, Pdh). 4-hydroxy-phenylpyruvate is subsequently transaminated (via aromatic amino acid aminotransferase) to yield L-tyrosine (Michal, 1999). Aromatic amino acid biosynthesis in bacteria is strictly regulated via feedback control mechanisms. Antibiotic biosynthesis may require specific metabolic adaptations, e.g. expression of isoenzymes that serve to avoid feedback regulation by aromatic amino acids.
The balhimycin biosynthetic gene cluster encodes two genes *pdh* and *dahp* which show high similarity to corresponding genes of the primary metabolism. Interestingly, *pdh* is also conserved within the glycopeptide biosynthesis gene clusters of chloroeremomycin (*cep*), dalbavancin (*dbv*), complestatin (*sta*) and teicoplanin (*tcp*), whereas *dahp* exists only in the *cep* cluster; a divergent Dahp synthase is encoded by the *tcp* cluster, but is counted among the unique functions (Donadio et al., 2005).
From the preliminary data of the *A. balhimycina* genome sequencing project it is known that a second copy of the *dahp* and *pdh* genes is located elsewhere in the genome. Therefore, for Dahp and Pdh in the balhimycin biosynthetic gene cluster “pathway specific” functions can be postulated. This assumption is further supported by regulatory studies where it has been demonstrated that these two genes are, like the structural biosynthetic genes, under the control of Bbr, the StrR like regulator of the

balhimycin gene cluster. Analysis on possible operon structures within the balhimycin biosynthesis gene cluster reveals a co-transcription of several genes (Pfeifer et al., 2001; Puk et al., 2004, Shawky et al., 2005). For example it can be suggested that *bbr* and *pdh* comprise an operon as well as the genes expand from *dvaA* to *dahp*. Since gel retardation assays revealed that Bbr binds specifically to the upstream regions of the regulator gene *bbr*, and *dvaA,* involved in the dehydrovancosamine synthesis, *pdh* and *dahp* are Bbr regulated genes. Further, in RT-PCR experiments the expression of *bbr* was analyzed in correlation to growth and antibiotic production together with the expression pattern of some biosynthetic genes. The expression of *bbr* occurs simultaneously with that of the studied biosynthetic genes starting at least 8h before the onset of antibiotic production confirming the results of the gel retardation experiments. These results indicate that components of the primary metabolism are important for a higher antibiotic production (Figure 2). Since Pdh is the first enzyme of the tyrosine branch efficient flux towards hydroxyphenylpyruvate is an essential precondition. Whilst much attention has been paid to the pathways and regulation of the balhimycin biosynthesis, less is known of the pathways and the regulation of primary metabolism. With the imminent completion of the total genome sequence of *A. balhimycina*, understanding of the primary metabolism pathways and their interconnection to the secondary metabolism will be gained. This knowledge will be used for rational improvement of aromatic amino acids and balhimycin production in *A. balhimycina*.

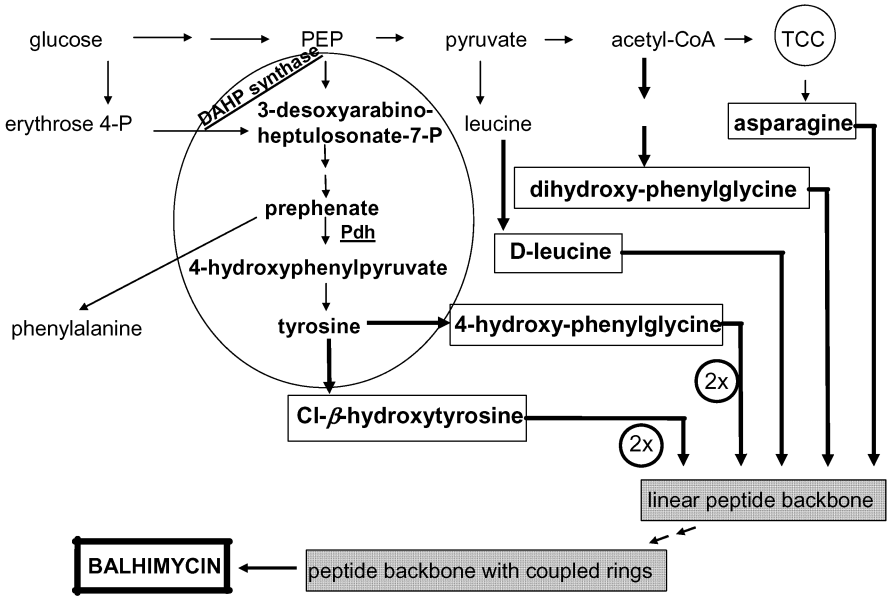

Figure 2: Interconnection of primary and secondary metabolism in balhimycin biosynthesis.

Highlighted by the circle is the tyrosine biosynthesis. Underlined are the enzymes DAHP synthase, 3-desoxyarabino-heptulosonate-7-phosphate synthase, and pdh, prephenate dehydrogenase. The thick arrows indicate the connection to balhimycin biosynthesis. Proteinogenic (leucine and asparagines) and non proteinogenic amino acids (dihydroxy-phenylglycine, 4-hydroxy-phenylglycine and Cl-β-hydroxytyrosine) are shown in white boxes , balhimycin intermediates in grey boxes. P, phosphate; PEP, phosphoenyl pyruvate; TCC, Tri-carbon cycle;

Literatur

Bischoff, D., S. Pelzer, B. Bister, G.J Nicholson, S. Stockert, M Schirle,. W.Wohlleben, G. Jung and R.D. Süßmuth, 2001a, The biosynthesis of vancomycin-type glycopeptide antibiotics – the order of cyclization steps, Angew. Chem. Int. Ed. 40, 4688-4691.

Bischoff, D., S. Pelzer, A. Höltzel, G. Nicholson, S. Stockert, W. Wohlleben, G. Jung and Süßmuth, R., 2001b, The biosynthesis of vancomycin-type glycopeptide antibiotics – new insights into the cyclization steps, Angew. Chem., Int Ed. 40, 1693-1696.

Bischoff, D., B. Bister, M. Bertazzo, V. Pfeifer, E. Stegmann, G.J. Nicholson, S. Keller, S. Pelzer, W. Wohlleben and R.D. Süßmuth, 2005, The biosynthesis of vancomycin-type glycopeptide antibiotics--a model for oxidative side-chain cross-linking by oxygenases coupled to the action of peptide synthetases, Chembiochem. 6, 267-72.

Donadio, S., M. Sosio, E. Stegmann, T. Weber and W. Wohlleben, 2005, Comparative analysis and insights into the evolution of gene clusters for glycopeptide antibiotic biosynthesis, Mol Genet Genomics. 274, 40-50.

Gunnarsson N., A. Eliasson and J.Nielsen, 2004, Control of fluxes towards antibiotics and the role of primary metabolism in production of antibiotics, Adv Biochem Engin/Biotechnol. 88, 137-178. DOI 10.1007/b99260 Springer-Verlag Berlin Heidelberg.

Hodgson, D.A., 2000 Primary metabolism and its control in streptomycetes: a most unusual group of bacteria, Adv Microb Physiol. 42, 47-238. Review.

Hubbard, B.K., M.G. Thomas and C.T. Walsh, 2000, Biosynthesis of p-hydroxyphenylglycine, a non-proteinogenic amino acid constituent of peptide antibiotics, Chem. Biol. 7, 931-942.

Michal, G., 1999, Biochemical pathways. Spektrum Akad. Verl., Heidelberg, Berlin.

Nadkarni, S.R., M.V. Patel, S. Chaterjee, E.K.S. Vijayakumar, K.R. Desikan, J. Blumbach, and B.N. Ganguli, 1994, Balhimycin, a new glycopeptide antibiotic produced by *Amycolatopsis sp*. Y-86,21022, J. Antibiot. 47, 334-341.

Pelzer, S., R. Süßmuth, D. Heckmann, J. Recktenwald, P. Huber, G. Jung and W. Wohlleben, 1999, Identification and analysis of the balhimycin biosynthetic gene cluster and its use for manipulating glycopeptide biosynthesis in the producing organism *Amycolatopsis mediterranei* DSM5908, Antimicrob. Agents Chemother. 43, 1565-1573.

Pfeifer, V., G.J. Nicholson, J. Ries, J. Recktenwald, A.B. Schefer, R.M. Shawky, J. Schröder, W. Wohlleben, and S. Pelzer, 2001, A polyketide synthase in glycopeptide biosynthesis: the biosynthesis of the non-proteinogenic amino acid (S)-3,5-dihydroxyphenylglycine, J. Biol. Chem. 276, 38370-38377.

Puk, O., P. Huber, D. Bischoff, J. Recktenwald, G. Jung, R.D. Süßmuth, K.-H. Van Pee, W. Wohlleben and S. Pelzer, 2002, Glycopeptide biosynthesis in *Amycolatopsis mediterranei*: Function of a halogenase and a haloperoxidase/perhydrolase, Chem. Biol. 9, 225-235.

Puk, O., D. Bischoff, C. Kittel, S. Pelzer, S. Weist, E. Stegmann, R.D. Süßmuth, and W. Wohlleben, 2004, Biosynthesis of chloro-beta-hydroxytyrosine, a nonproteinogenic amino acid of the peptidic backbone of glycopeptide antibiotics, J Bacteriol. 186, 6093-6100.

Recktenwald, J., R. Shawky, O. Puk, F. Pfennig, U. Keller, W. Wohlleben and S. Pelzer, 2002, Nonribosomal biosynthesis of vancomycin-type antibiotics: a heptapeptide backbone and eight peptide synthetase modules. Microbiology 148, 1105-1118.

Shawky, R.M., E. Stegmann, A. Wietzorrek, O. Puk, E. Takano, W. Wohlleben, 2007, The border sequence of the balhimycin biosynthesis gene cluster and characterization of Bbr, a StrR-like pathway-specific regulator, J Mol Microbiol Biotechnol. 13, 76-88.

Stegmann E, S. Pelzer, D. Bischoff, O. Puk, S. Stockert, D. Butz, K. Zerbe, J. Robinson, R.D. Süssmuth and W. Wohlleben, 2006, Genetic analysis of the balhimycin (vancomycin-type) oxygenase genes, J Biotechnol., 124, 640-653.

Süßmuth, R., S. Pelzer, G. Nicholson, T. Walk, W. Wohlleben and G. Jung, 1999, New advances in the biosynthesis of glycopeptide antibiotics of the vancomycin type from *Amycolatopsis mediterranei*, Angew. Chem. 111, 2096-2099.

Thykaer, J., and J. Nielsen, 2003, Metabolic engineering of beta-lactam production, Metab Eng 5, 56−69.

Zerbe, K., O. Pylypenko, F. Vitali, W. Zhang, S. Rousett, M. Heck, J.W. Vrijbloed, D. Bischoff, B. Bister, R.D. Süßmuth, S. Pelzer, W. Wohlleben, J.A. Robinson and I. Schlichting, 2002, Crystal Structure of OxyB, a Cytochrome P450 Implicated in Oxidative Coupling Reaction During Vancomycin Biosynthesis, J. Biol. Chem. 277, 47476-47485.

CHEMICAL ENGINEERING TRANSACTIONS, Volume 14, 2008
Edited by G. Marino, E. Bardone, A. Viglia
 ISBN 978-88-95608-02-0

A New Formula (Bg Z1) For More Efficient Delivery Of *B. Thuringensis Var. Israelensis* Endotoxins Against Mosquito's Larvae

S. Dell'Aversana (*), L. Tranchino (*), V. G. Di Grazia (*), G. Mele (*), G. Lacertosa (**), A. Petrozza (**), F. Cellini (**)
(*) Bio & Geo S.r.l., Caserta
(**) Metapontum Agrobios S.r.l., Metaponto (MT)

The evaluation of the effects by which physical, chemical and biological agents (temperature, moisture, pH extremes, sunlight, proteolytic enzymes, bacteria, etc.) affect stability of the active substance of a biological insecticide, as the present one based on *B. thuringiensis israelensis* against mosquito's larvae, is a prerequisite to identify the appropriate mix of ingredients (antioxidants, radical scavengers, UV protectants, etc.) required to protect the active substance during field application. Furthermore it is necessary to study how to avoid not homogeneous application, or settling of the product in aquatic environment, that can leave large sensible areas not covered by the active substance and spoil the overall insecticidal effect displayed by the product. The final objective is to develop a formulate with appropriate characteristics and persistence time for large scale field applications. Actually a new product with these characteristics (named BG z1) has been developed by Bio & Geo S.r.l. by fermenting a *B. thuringiensis israelensis* H14 strain, recovering and drying the parasporal crystals and than formulating these crystals as emulsifiable liquid concentrate, with the addition of protective ingredients and surfactants to enable easy mixing with water for an application as a spray on large areas to fully exploit the insecticidal properties displayed even at ppm concentration.

1. Introduction

The insect control, especially those harmful to agriculture and public health, involves traditionally the use of chemicals that often can display negative drawbacks being toxics, not only to the target insects, but also to beneficial ones, as well as to animals and men. In addition, insects often develop resistance against these chemicals, after many successive applications, and this effect can have dramatic consequence in terms of increasing treatment doses and frequencies required, multiple pesticides, etc. and, at the end, in terms of heavy damage of environment.
So the alternative of biological insecticides, offered by modern biotechnologies, has been welcome and it is developing very much, well beyond expectations, particularly for the treatment of urban areas and/or for insects that can give rise to public health problems. This is the case of Dipteral insects (mosquitoes, etc.) that are able to transmit heavy dangerous illness such as Yellow Fever and Dengue (see particularly Aedes aegypti, etc.). The active substances, widely employed for the application against diptera larvae, are protein endotoxins produced by *Bacillus thuringiensis var israelensis* (Bti) as crystal parasporal inclusions. These proteins degrade quickly in nature and so

they are not harmful to environment. But these advantageous elements produces the main inherent biopesticide disadvantages: the short persistence time in field conditions due to degradation effects by chemical, biological, physical and natural agents (temperature, moisture, pH, sunlight, bacteria, etc.). The present work is focused on these effects with the final objective to develop a new formulate with appropriate characteristics and persistence time.

2. Materials and Methods

2.1 Microbial strain

A strain of *Bacillus thuringiensis var. israelensis* (Bti) was isolated from soil samples and named z1. Microbiological characteristics and protein profiles of Bti z1 were identical to the reference strain, ATCC 35646 *Bacillus thuringiensis var. israelensis* serovar H14 (FIGURE 2).

2.2 Technical powder and formulate production

The production of experimental products has been developed by Bio & Geo S.r.l. in its laboratory and plants in Caserta (FIGURE 1), by fermenting the Bti z1 strain described above, recovering and drying the parasporal crystals (Technical Powder: TP) and than formulating these crystals as emulsifiable liquid concentrate (Formulate: FO), with the addition of protective ingredients and surfactants to enable easy mixing with water for an application as a spray on large areas.

FIGURE 1 Bio & Geo Plant facility in Caserta

2.3 Gel electrophoresis of active proteins

The protein profiles of the products obtained from Bti z1 fermentation has been obtained by standard SDS-PAGE gel electrophoresis (Lee et al. 2001): resuspending the spore-crystal mixture in the buffer (60mM Tris-HCl-(pH 6.8), 25% glycerol, 2% SDS, 5% 2-mercaptoethanol, 0.1% bromophenol blue), boiling it for 10 min, and subjecting it to SDS-10% polyacrylamide gel electrophoresis. SDS-PAGE was performed on a 10% separating gel with a 3% stacking gel. The gel was stained with 0.1% Coomassie brilliant blue (Sigma Co., USA).

To be noticed the two bands (130 kDa and 70 kDa, indicated by the arrows) characterizing the pesticidal crystal proteins of such Bti strains:

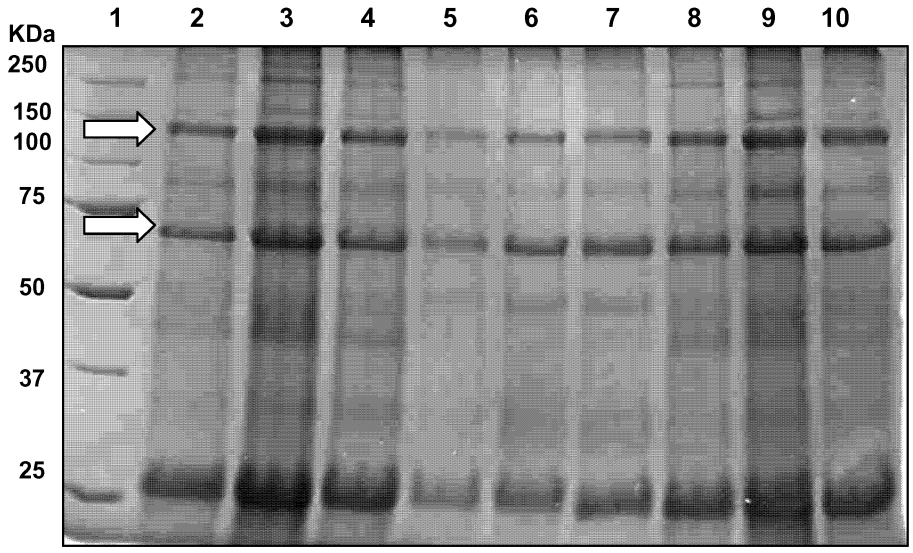

FIGURE 2 Gel electrophoresis of Bti active proteins in the technical powder obtained from z1 strain fermentation (at different charges: lanes 2 (20 mg/ml); 3 (40 mg/ml) and 4 (30 mg/ml)), from ATCC strain fermentation (lanes 8 (20 mg/ml); 9 (40 mg/ml) and 10 (30 mg/ml)) and in the formulate BGz1 (lanes 5 (100 mg/ml); 6 (200 mg/ml) and 7 (300 mg/ml)).

2.4 Bioassay

Efficacy of a technical powder or a formulation is generally determined by measurement against a standard formulation and expressed in terms of International Toxic Units (ITU/mg) (de Barjac 1983). Potency is calculated by:

LC50 of the standard

---------- x potency of the standard = Potency of the sample (ITU/mg)

LC50 of the sample

Where LC50 is the lethal concentration of that substance that produced a 50% mortality frequency in standard conditions.

2.5 Large scale field tests

The tests have been carried out in two drainage canals in Metaponto plain (Basilicata Region - South of Italy). The test product was sprayed on the infested area and samples of water were collected before and after the treatment to measure the variation of concentration of mosquito diptera larvae (microscopic observation) versus time. Multiple samples are taken at each time to get statistically sound results (average and % Abbott test values are shown at the point 3). The results were compared with untreated controls on the same infested drainage canals

FIGURE 3 Large scale field test site

3. Results and Discussion

3.1 Laboratory Tests

Preliminary laboratory tests have been carried out to evaluate direct intrinsic activity and stability properties of the active substance as function of basic parameters, such as dosage, temperature, pH, etc. These studies make the basis to understand the actual performance of the bio-insecticides, such as the formulate BG z1, although indirect effects and interaction of environmental factors determine the final overall efficacy. These indirect effects have been studied in the second part of the work (3.2 Large scale field tests).

DOSAGE AND CONCENTRATION

The larvicidal activity of technical powder and of the formulate BGz1 measured in the laboratory is shown in figure 4 in terms of average mortality frequency of Culex pipiens larvae as function of the concentration of the tested substance supplied. Actually the activity appears to be very high: it is enough a very low concentration (fraction of ppm) for causing a lethal effect. Typical lethal concentrations LC50 (for 50% mortality) are 0.08 mg/l for technical powder (activity about 3,000 ITU/mg) and 0.32 mg/l for the formulate (activity about 750 ITU/mg). The ratio of these two activities correspond to the “dilution ratio” of the active substance during the formulation process (addition of 3

parts of ingredients to 1 part of technical powder). The actual ratio of activity displayed in field conditions by TP and FO is obviously totally different and makes the reason for the required formulation process.

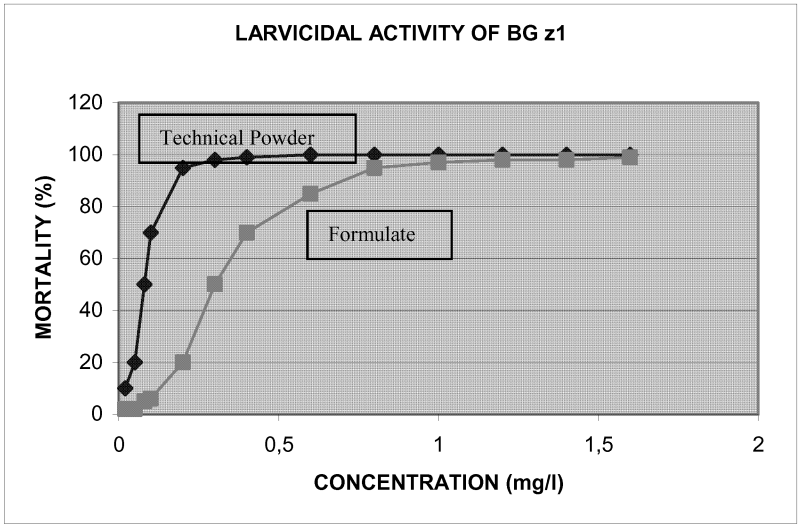

FIGURE 4 Larvicidal activity of technical powder and BGz1 formulate

TEMPERATURE

In general terms temperature is a very significant factor in the decomposition – deactivation processes of the active substance. In the present case it was possible to demonstrate that the active substance, being a protein crystal, is quite stable at ambient temperature, both as technical dry powder and as a formulate, at least during the storage phase of the product (less than 10% decay of the activity for year). The situation becomes much more intriguing during the application phase when temperature effects combine with other degradation effects and, even more important, with activity and feeding behaviour of the insects. For example the reduced activity of Bt observed at low temperature has been described as indirect consequence of the reduced activity and amount of feeding by target larvae, rather than by any other direct effect (Walker 1995).

pH EXTREMES

In general terms pH of the product can affect its stability and activity in many ways, but in the present case it was possible to demonstrate a quite good stability of the formulate, both during the storage phase of the product and during the application, unless very low (less than 4) or high (more than 8) pH environment is present. Actually alkaline components can break down the active proteins fairly quickly (pH higher than 10); for this reason buffering chemicals could be included in pesticide formulations if pH extreme environment is expected in the area of application. But the normal pathway for converting microbial protoxins to the biologically active toxins, after ingestion by susceptible insect larvae, should not be obstructed by formulation ingredients.

PHOTODECOMPOSITION

Natural sunlight, especially the ultraviolet (UV) portion of the spectrum (UV-B, UV-A), has been demonstrated to be responsible for inactivation of microbial insecticides

(Behle et al., 1997) and the specific damage to Bt insecticidal proteins appeared to be related to the damage of the tryptophan residues of the Bt protoxin by solar radiation in the 300-380 nm range (Pusztai et al. , 1991). A recent publication (Wan et al., 2007) suggests the utilization of melanin as photoprotective ingredient in bioinsecticide applications. These aspects have been taken into account in BGz1 formulation that has been designed to protect Bt protein crystals from UV damage, as indicated by laboratory experiments, that demonstrated no inactivation effect, at least in the lab. experimental conditions.

SETTLING CHARACTERISTICS

Bio-insecticides are normally applied directly to water for the control of mosquitos and blackflies. Rapid sedimentation of protein crystals, and the consequent removal of active substance from the surface where larvae normally feed, is than an important limitation on the efficacy of such applications. The present formula BG z1, being based on the addition of lipid and surfactants, have been designed to prolong residence time of Bt protein crystals at the surface of water, as indicated by laboratory experiments that demonstrated stable, homogeneous emulsion formed by mixing BG z1 with water.

3.2 Large Scale Field Tests

Final large scale field tests have been carried out to evaluate direct, indirect and overall actual performance of the formulate BG z1 in the presence of environmental factors.

Two main tests have been carried out in two drainage canal trials in Metaponto plain. The test product was compared with an untreated control, spraying BGz1 formulate on two mosquito diptera larvae infested drainage canals.

In general terms, the activity displayed by BGz1 product can be judged very high in both trials (almost complete disinfestations in very short time (1- 4 hours) even at low dosage (1 kg/ha), but a quite large difference is observed in the two trials: the first one being much more successful, with higher efficacy values.

	TEST 1			TEST 2		
	BGz1 treated area	CONTROL area	Efficacy	BGz1 treated area	CONTROL area	Efficacy
	Average (n/l)	Average (n/l)	(% test Abbott)	Average (n/l)	Average (n/l)	(% test Abbott)
Time = 0	54	54		47	47	
1 h	11	76	85.5%	18.5	36.0	48.6%
4 h	3	86	96.5%	10.7	23.5	54.5%
24 h	2	91	97.8%	10.5	23.3	54.8%

It is quite interesting to notice that these differences are not due to basic parameters (product, dosage, etc. are the same) but to a number of indirect factors playing a role in the test 2: such as the larger amount of vegetation present, the lower temperature, the physiological state of the larvae at the time of treatment (October 2007).

The effect of low temperature and of the declining activity of the larvae has already discussed above (Walker 1995). The effect of the amount of vegetation present is

understandable too, in terms of larger area to be covered and of presence of vegetation exudates; in any case this effect has been noticed by other researchers too (unsuccessful control of Culex peus in a primary oxidation pond with a dense cover of water hyacinth and reduced effectiveness of Bti against Odagmia ornate in the presence of dense vegetation: Mata et al. 1986).

4. Conclusions

The present investigation stressed the need to protecting the active substance of biological insecticides during the application phase (Bt formulations frequently have half-lives of up to 10 days, while unformulated Bt may have a half-life of only a few hours: Dent, 1993). For this reason a new formula (BG z1) for more efficient delivery of Bti endotoxins against mosquito's larvae has been developed. Samples of this new product have been prepared by Bio&Geo and tested at large scale field level, in collaboration with Metapontum Agrobios. Very positive results have been obtained in terms of stability, activity, persistence in field conditions and environmental protection. Registration of this new product is in progress by Italian Authorities.

5. References

Barjac, H. de (1983), "Bioassay procedure for samples of Bacillus thuringiensis israelensis using IPS-82 standard", World Health Organization WHO/VBC/84.892

Behle R. W. , Mcguire M. R., Shasha B. S., (1997), "Effects of sunlight and simulated rain on residual activity of Bacillus thuringiensis formulations", Journal of economic entomology, vol. 90, n 6, pp. 1560-1566

Dent D.R., (1993), "The use of B. thuringiensis as an insecticide" in Jones D.G. ed. "Exploitation of Microrganisms", London Chapman & Hall, pp 19-44

Lee I. H., Y.H. Je, J.H. Chang, J.Y. Roh, H.W. Oh, S.G. Lee,S.C. Shin, K.S. Boo (2001), "Isolation and Characterization of a Bacillus thuringiensis ssp. kurstaki Strain Toxic to Spodoptera exigua and Culex pipiens", Current Microbiology, vol 43, 284-287

Mata, V., Weiser, J., Olejnicek, J., Tonner, M. & Kluzak, Z. (1986) "Possibilities of application of preparations based on Bacillus thuringiensis in the biological control of black fly larvae. Dipterologica Bohemoslovaca IV. Sbornik referatu z VIII. Celostatniho Dipterologickeho Seminare, 135-138.

Putzai M., Fast P., Gringorten L., Kaplan H., Lessard T., Carey P. R., (1991), "The mechanism of sunlight-mediated inactivation of B. thuringiensis crystals" Biochem. J. vol 273, pp 43-47

Walker, E. D. (1995), "Effect of low temperature on feeding rate of Aedes stimulans larvae and efficacy of Bacillus thuringiensis var. israelensis (H-14)" Journal of the American Mosquito Control Association 11, 107-110.

Wan X., H.M. Liu, Y. Liao, Y. Su, J. Geng, M.Y. Yang, X.D. Chen, P. Shen (2007) "Isolation of a novel strain of Aeromonas media producing high levels of DOPA-melanin and assessment of the photoprotective role of the melanin in bioinsecticide applications", Journal of Applied Microbiology, vol.103, n 6, pp 2533-2541

CHEMICAL ENGINEERING TRANSACTIONS, Volume 14, 2008
Edited by G. Marino, E. Bardone, A. Viglia
 ISBN 978-88-95608-02-0

Saccharothrix algeriensis, a new antibiotic producer: investigations on its secondary metabolism

Strub C[1], Brandam C[1], Meyer X[1] and Lebrihi A[1]
[1] *Laboratoire de Génie Chimique, UMR-CNRS 5503,*
BP 1301, 5 rue Paulin Talabot, 31106 Toulouse cedex 1

The constant growth of the antibiotic world market leads to study rare actinomycete. Therefore, the bacterium *Saccharothrix algeriensis* which products new antibiotics of dithiolopyrrolone class is studied in liquid culture.
The aim of this work is to better apprehend the mechanisms which govern the bacterial growth as well as the dithiolopyrrolones synthesis and to capitalize this knowledge in a general reactional scheme of the metabolism.
The growth of *Saccharothrix algeriensis* was performed in a batch reactor, on a semi-synthetic medium. The growth, the thiolutine (the main dithiolopyrrolone) and the carbon dioxide production and the substrates consumption were monitored. The influence of the substrate concentration on growth and on the production of dithiolopyrrolones was evaluated. It seems that diauxic growth occurs on amino acids then on glucose. The thiolutine synthesis would be induced by carbon substrates exhaustion and by ammonium ions deficiency. Glucose seems to exert a catabolite repression on the secondary metabolic activities of the cell.

1. Introduction

The production of new bio active molecules is now a major concern to answer to the fact of the proliferation of microbial pathogen strains resistant to the molecules currently available (Butler et al. 1996; Critchley et al. 2007; Linares et al. 2007). Thus researches tend to exploit the biodiversity in order to find new bio active molecules with microbial origin (Boudjella et al, 2005). In this context, the bacterium *Saccharothrix algeriensis*, belonging to actinomycetes family and producing new antibiotics of dithiolopyrrolone class, has been isolated in Saharan soils in Algeria (Zitouni et al. 2004). Dithiolopyrrolone antibiotics have others interesting properties: antifungi, insecticide and anticancer activities (Webster and Chen, 2000; Minamiguchi et al. 2001, Webster et al. 2002, Xu 1998).
Sa algeriensis is able to produce at least five dithiolopyrrolone antibiotics: thiolutine, senecyol-pyrrothine (SEP), tigloyl-pyrrothine (TIP), isobutyryl-pyrrothine (ISP) and butanoyl-pyrrothine (BUP) as shown in figure 1. *Sa algeriensis* is the only known microorganism able to produce TIP and SEP (Lamari et al. 2002; Bouras et al. 2006). Recent works showed that the nature of the radical ® depends on the culture medium composition. Each association "organic acid-heterocycles" leads to different molecules with different properties, which makes it an interesting model to study (Bouras et al. 2006; Bouras et al. 2007). But few data exist on the macroscopic behaviour of the bacterium in a semi-synthetic medium.

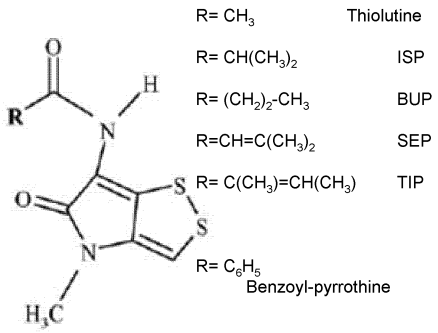

Fig.1 *Dithiolopyrrolonne antibiotic structures*

The aim of this work is to study the development of *Sa algeriensis* in different conditions to capitalize knowledge on its metabolism and at term to control qualitatively and quantitatively dithiolopyrrolone production. The development of *Sa algeriensis* was followed on semi-synthetic medium where majority of the substrates was identified. The cultures have been carried out in batch reactor with probes for monitoring and controlling physical and chemical environment of the bacterium. In parallel substrates and products concentrations have been followed by offline measurements.

2. Materials and Methods

2.1 Flasks and reactors cultures conditions

Sa algeriensis NRRL B-24137 was used in this study. Spores were maintained in 25% glycerol at -20°C. Spores were obtained from solid culture of *Sa algeriensis* on conservation medium.

For the precultures, a volume of 100 mL of semi synthetic medium was inoculated by 3.5 mL of spores suspension and incubated on a rotary shaker (New Brunswick Scientific Co., NJ, USA) at 250 rotation per minute (rpm) and 30°C for 52 h.

Reactors were inoculated with 100 mL of preculture. Cultures were performed in a NBS fermentor containing 2 L of medium. Culture lasted for at least one week. pH was maintained at 7± 0.035 by automatic addition of NaOH solution (1 $mol.L^{-1}$) and HCl solution (1 $mol.L^{-1}$). Aeration rate of one vessel volume per minute (vvm) was employed. The agitation rate was controlled to keep the dissolved oxygen level above 30% of the saturation with a starting rate of 150 rpm. The pH and dissolved oxygen level were monitored using Ingold specific electrodes. Temperature was regulated at 30°C. O_2 and CO_2 content in the exhaust gas were determined by a gas analysor (Servomex 4100, paramagnetic transductor for O_2 and infrared transductor for CO_2).

2.2 Culture media compositions

Conservation media: International Streptomyces project 2 (ISP2)

The ISP2 medium had the following composition (per liter of distilled water): 10 g malt extract, yeast extract 4 g, glucose 4 g and agarose 18 g.

Growth and production medium

The semi-synthetic medium used as growth and production medium contained (per litter of distilled water): glucose 15 g, yeast extract 2 g, NaCl 2 g, $(NH_4)_2SO_4$ 2 g, KH_2PO_4 0.5 g, K_2HPO_4 1g, $MgSO_4.7H_2O$ 0.2g, $CaCl_2.2H_2O$ 1 g, and MOPS 2 g, Uracil 20 mmol.

2.3 Analytical procedures

For the estimation of dry cell weight (DCW), 3 mL samples of homogenized culture broth were centrifuged at 16000 g for 10 min in preweighed Eppendorf tubes. Pellet was washed twice with distilled water. Supernatant was kept for other analysis. Eppendorf tubes containing pellets were dried at 105°C for 48 h, and weighted after being cooled for 30 min in a dessicator (Bouras et al., 2006). The measurement relative error is 5 %.

The analysis of dithiolopyrrolone antibiotics was carried out by non polar chromatography (HPLC, Bio-Tek Instruments (Bouras et al., 2007)) The measurement relative error is 10 %. Supernatant coming from DCW determination was filtered at 0.2 µm and used to measure metabolites.

A biochemical analyzer with enzymes fixed on membrane has been used (YSI2700 select) to quantify glucose. Amperometric quantification after the enzymatic oxidation allows determining glucose concentration in the culture broth. The amperometer answer is linear for a concentration in glucose between 0 and 25 $g.L^{-1}$. The measurement relative error is 3 %.

Ammonium ions and α-amino nitrogen have been quantified using specific enzymatically methods (Diagnostics Ammonia kit from Boehringer-Mannheim, using glutamate deshydrogenase and Microdom kit using glutamate oxydase respectively) and an automatic multiparametric analyser (Mascott Lisabio). The signal answer is linear for concentrations in α-amino nitrogen and ammonium ion between 0 and 500 $mg.L^{-1}$. The measurement relative error is 5 %.

3. Results

3.1 Growth on semi-synthetic medium

Figures 2 and 3 present the evolution of glucose, α-amino nitrogen, biomass, ammonium ion and thiolutine during a batch culture of *Sa algeriensis* on semi-synthetic medium. Four periods can be distinguished. The first period (1) is a growth phase of the microorganism. It is accompanied by a diminution of α-amino nitrogen concentration (figure 2); it is to say amino acids consumption, and an increase in the ammonium ions concentration. It could be explained by the deamination of the consumed amino acids from yeast extract (figure 3). There is no apparent glucose consumption, by against the amino acids are quickly consumed by the bacterium. The second period (2) is characterized by a brake in the growth. During this period, the rest of the amino acids and the glucose are consumed. The ammonium ions concentration is stable. The third period is a growth phase on glucose and ammonium ions longer than the first one on amino acids (3). The ammonium ions could be used as nitrogen source. The last period (4) is characterized by a decrease of biomass concentration that seems to coincide with ammonium ions exhaustion. It is probably caused by cell lysis.

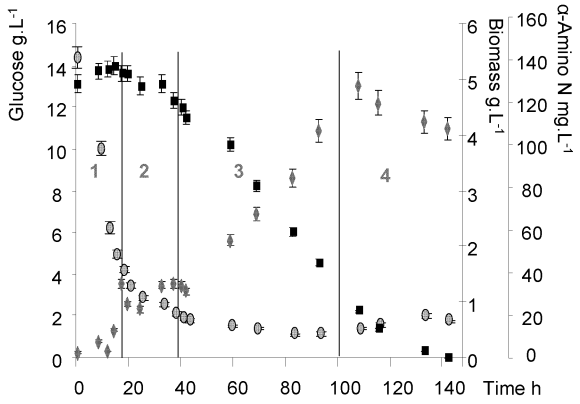

Fig.2 *Sa. algeriensis batch culture on semi-synthetic medium in batch reactor, 30°C, pH 7.00 ± 0.035 upH, 0.5 vvm and 250 rpm.* ○ *α-amino N (mg.L^{-1}),* ■ *glucose (g.L^{-1}) consumption and* ◈ *biomass production (g.L^{-1}).*

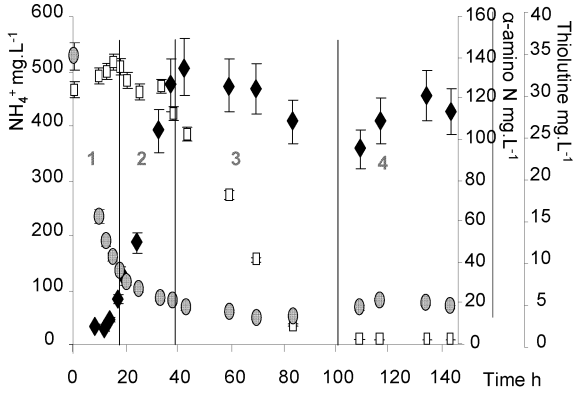

Fig.3 *Thiolutine production* ♦ *(mg.L^{-1}),* α*-amino N* ○ *(mg.L^{-1}), and ammonium ions* □ *(mg.L^{-1}) in Sa algeriensis batch culture on semi-synthetic medium, 30°C, pH 7.00 ± 0.035 upH, 0.5 vvm and 250 rpm.*

Sa algerinsis growth seems to be diauxic (Narang and Pilyugin 2006) on semi-synthetic medium. Indeed, in the first time, the amino acids are used for biomass production (period 1), and then when they are almost exhausted, after an adaptation period (period 2), the bacterium uses glucose and ammonium ions for its development (period 3). The fact that other actinomycetes have a diauxic growth confirms our comments (Novotna et al. 2003).

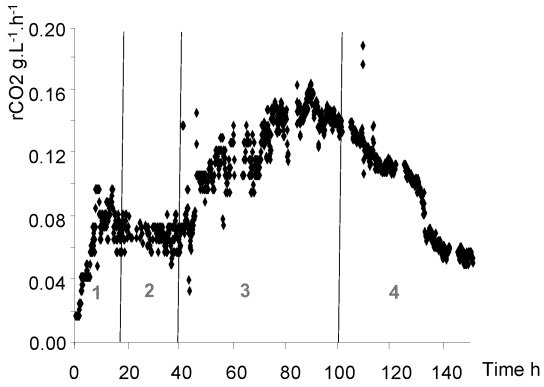

Fig.4: *Sa. algeriensis batch culture on semi-synthetic medium in batch reactor, 30°C, pH 7.00 ± 0.035 upH, 0.5 vvm and 250 rpm. ♦ Carbon dioxide consumption speed (r_{CO2} in $g.L^{-1}.h^{-1}$).*

Figure 4 shows the CO_2 production speed evolution during the same culture.
It appears that the evolution phases of CO_2 production speed is perfectly calked on the phases of the biomass development (Figure 2). The period 1 is accompanied by an increase of the CO_2 production speed. It does not change during the period 2 because of this adaptation phase. The next period (3) is characterized by an increase of the CO_2 production speed. The last period of cells lysis (4) is accompanied by a decline in this production speed. From a practical point of view, the on-line study of the carbon dioxide production by gas analysis allows observing the important metabolic events, like biomass development or changes of consumed substrate. As a result, the on-line CO_2 measures can be used as a mean of monitoring the culture in absence of off-line measures.

3.2 Secondary metabolism induction

The thiolutine production in parallel to the α-amino nitrogen and ammonium ions consumptions is presented in figure 3. The thiolutine concentration starts to increase at the end of the period 1 when most of the amino acids are exhausted from the culture broth. In the period 3, the thiolutine concentration decreases. The thiolutine would be degraded or transformed into other dithiolopyrrolones derivatives by the microorganism. There is a second phase of thiolutine production following ammonium ion depletion during the period 4. Carbon and nitrogen limitations induce a slowdown in growth or metabolic activity of the microorganism which would cause the thiolutine synthesis in the culture broth (Wilson and Bushell 1995; Melzoch et al. 1997). However, the fact that a microorganism produces sequentially its secondary metabolites is rarely described in literature (Bushell and Fryday 1983).

3.3 Glucose catabolite repression

Figure 5a presents the thiolutine production as a function of the time at three glucose concentrations (3, 5.5 and 8 $g.L^{-1}$). Figure 5b presents biomass production at three different times of culture for these same glucose concentrations. The three concentrations allow the thiolutine production. On the other side, it is important to notice that they have no impact on biomass production. However, production depends on the initial glucose concentration. Culture containing 8 $g.L^{-1}$ glucose reaches the lower production (14.8 $mg.L^{-1}$ in 30 h) while the one containing the least of glucose allows the best production of thiolutine (3.28$mg.L^{-1}$ in 30 h). The more initial glucose concentration in the culture medium the less production of thiolutine in the first 30 h of culture is.

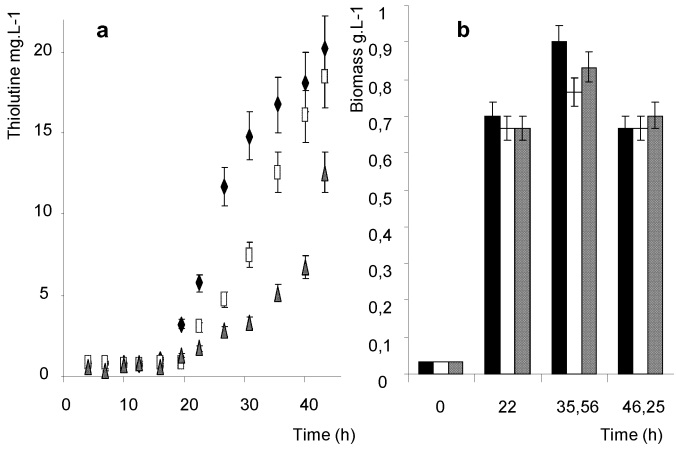

Fig.5 *a) Thiolutine production ($mg.L^{-1}$) versus different glucose concentrations. ♦: 3 $g.L^{-1}$; □ :5.5 $g.L^{-1}$ and ▲ :8 $g.L^{-1}$. b) Biomass production ($g.L^{-1}$) versus different glucose concentrations black: 3 $g.L^{-1}$; white :5.5 $g.L^{-1}$ and grey :8 $g.L^{-1}$. Sa. algeriensis batch culture on semi-synthetic medium in batch reactor, 30°C, pH 7.00* ± 0.035 upH, 0.5 vvm and 250 rpm

Moreover, the observation of figure 5b shows that whatever the time of culture, biomass produced is nearly the same in the three conditions. It seems that the glucose has a repressive effect on the secondary metabolism. Then it does not affect the growth of the bacterium. This regulation exists in other actinomycetes (Demain 1998; Hodgson 2000) but not on theirs biosynthetic activities.

4. Conclusion

Sa algeriensis is able to grow from several substrates sequentially consumed. On the other hand, from a practical point of view, the CO_2 consumption speed measure allows an easily monitoring of the various culture phases. The secondary metabolism of this actinomycete seems to be inducted by exhaustion of different carbon and nitrogen substrates which are in the culture broth. Thiolutine production occurs when the substrate which is currently metabolised became limiting. As the several changes of substrate during the batch culture, the production phenomenon can occur several times during a batch culture.

The establishment of a general reaction scheme should allow validating the hypotheses the diauxic growth of the microorganism. It will be tested on other experimental conditions. A mathematical model representing the growth of the bacterium can be developed. At term, it will allow the control of the produced derivate, and certainly the production of dithiolopyrrolone class new members

5. References

Bouras N. (2005) Régulation de la production d'antibiotiques dithiolopyrrolones chez *Saccharothrix algeriensis* NRRL B-24137, PhD Thesis, Institut National Polytechnique de Toulouse, France.

Bouras N., F. Mathieu, N. Sabaou and A. Lebrihi, (2006) Effect of amino acids containing sulfur on dithiolopyrrolone antibiotic productions by *Saccharothrix algeriensis* NRRL B-24137, J. Appl. Microbiol., 100(2),390.

Bouras N., F. Mathieu, N. Sabaou and A. Lebrihi (2007) Influence on dithiolopyrrolone antibiotic production by organic acids in *Saccharothrix algeriensis* NRRL B-24137. Process Biochemistry, 42(6),925.

Butler J.C., J. Hofmann, M.S. Cetron, J.A. Elliott, R.R. Facklam and R.F. Breiman , 1996, The continued emergence of drug-resistant *Streptococcus pneumoniae* in the United States: an update from the Centers for Disease Control and Prevention's Pneumococcal Sentinel Surveillance System, J. Infect. Dis., 174(5),986.

Boudjella H., K. Bouti, A. Zitouni, F. Mathieu, A. Lebrihi and N. Sabaou, 2005, Taxonomy and chemical characterization of antibiotics of Streptosporangium Sg 10 isolated from a Saharan soil, Microbiol. Research, 161(4),288.

Bushell M.E. and A. Fryday (1983) The application of materials balancing to the characterization of sequential secondary metabolite formation in *Streptomyces cattleya* NRRL 8057, J. Gen. Microbiol., 129(6),1733.

Critchley I.A., S.D. Brown, M.M. Traczewski, G.S. Tillotson and N. Janjic, 2007, National and regional assessment of antimicrobial resistance among community-acquired respiratory tract pathogens identified in a 2005-2006 U.S. Faropenem surveillance study, Antimicrob. Agents Chemother, 51(12),4382.

Demain A.L. (1998) Induction of microbial secondary metabolism. Internatl. Microbiol.,1, 259.

Hogdson D.A. (2000) Primary metabolism and its control in Streptomyces, *Adv.* Microbio. Physiol., 42,47.

Lamari L., A. Zitouni, H. Boudjella, B. Badji, N. Sabaou, A. Lebrihi, G. Lefebvre, E. Seguin and F. Tillequin, 2002, New dithiolopyrrolones antibiotics from

Saccharothrix sp. SA 233 : I. Taxonomy, fermentation, isolation and biological activities, J. Antibiot. (Tokyo), 55,696.

Linares L., C. Cervera, F. Cofán, M.J. Ricart, N. Esforzado, V. Torregrosa, F. Oppenheimer, J.M. Campistol, F. Marco and A. Moreno, 2007, Epidemiology and outcomes of multiple antibiotic-resistant bacterial infection in renal transplantation, Transplant. Proc., 39(7),2222.

Melzoch K., M.J. Teixeira de Mattos and O.M. Neijssel (1997) Production of actinorhodin by *Streptomyces coelicolor* A3(2) grown in chemostat culture, Biotechnol Bioeng 54(6),557.

Minamiguchi K., H. Kumagai, T. Maduda, M. Kawada, M. Ishizuka and T. Takeuchi, 2001, Thiolutine, an inhibitor of huvec adhesion to vitronectin, reduces paxillin in huvecs and suppresses tumor cell-inducted angiogenis, Int. J. Cancer, 93, 307.

Narang A. and S.S. Pilyugin (2006) Bacterial gene regulation in diauxic and non-diauxic growth, J. Theor. Biol. 244(2),326.

Novotna J., J. Vohradsky, P. Berndt, H. Gramajo, H. Langen, X.M. Li, W. Minas, L. Orsaria, D. Roeder and C.J. Thompson (2003) Proteomic studies of diauxic lag in the differentiating prokaryote *Streptomyces coelicolor* reveal a regulatory network of stress-induced proteins and central metabolic enzymes, *Mol. Microbiol.,* 48(5),1289.

Xu C.,1998, The stability and cytotoxic properties of xenorxides and xenorhabins, secondary metabolites of the entomopathogenic nematode symbiont, Xenorhabdus bovienii (Enterobacteriaceae), Thesis submeted in partial fulfillement of the requirements for the degree of Master of science.

Webster J.M., J. Li and G. Chen, 2000, Anticancer property of dithiolopyrrolones, US patent n° 6020360.

Webster J.M., G. Chen, K. Hu and J. Li, 2002, Bacterial metabolites, In: Entomopathogenic Nematology, R Gaugler R. (ed.). CAB International. 99.

Wilson C.G. and M.E. Bushell (1995) The induction of antibiotic synthesis in *Saccharopolyspora erythraea* ad *Streptomyces hygroscopicus* by growth rate decrease is accompanied by a down-regulation of protein synthesis rate, FEMS microbiol. lett., 129(1),89.

Zitouni A., L. Lamari, H. Boudjella, B. Badji, N. Sabaou, A. Gaouar, F. Mathieu, A. Lebrihi and D.P.Labeda, 2004, *Saccharothrix algeriensis sp. nov.,* isolated from Saharan soil. Int. J. Sys.t Evol. Microbio.,54,1377.

CHEMICAL ENGINEERING TRANSACTIONS, Volume 14, 2008
Edited by G. Marino, E. Bardone, A. Viglia
 ISBN 978-88-95608-02-0

Effect Of Inulin Suplementation Of Milk To Prepare Fermented Biomilks

Ricardo Pinheiro de Souza OLIVEIRA[1], Patrizia PEREGO[2], Attilio CONVERTI[2], Maricê Nogueira de OLIVEIRA[1]

[1]Departamento de Tecnologia Bioquímico-Farmacêutica, Faculdade de Ciências Farmacêuticas, Universidade de São Paulo. Av. Prof. Lineu Prestes, 580. 05508-000 - São Paulo, SP – Brasil.

[2]Dipartimento di Ingegneria Chimica e di Processo, Università degli Studi di Genova, Via Opera Pia 15, I-16145 Genova, Italy

Actually, functional fermented milks have to exhibit multiple benefits for the health, associated to good organoleptic characteristics. These are strengthened by the addition of probiotics as well as certain soluble fibers, among which inulin. The aim of this work was the evaluation of the effect of inulin supplementation of milk basis on the production of probiotic fiber-enriched fermented milks. To this purpose, we investigated the kinetics of acidification of inulin supplementation of milk (0, 1, 2 and 4 g/100 g) throughout the fermentation, the probiotic survival, the post-acidification and the firmness of fermented fiber-enriched milks, stored at 4°C either for 24 h or after 7 days since their preparation. This work shows that the biomilk preparation is influenced either by the supplemented amount of inulin or by the co-culture composition. According to the selected co-culture, inulin addition to the milk influenced the kinetic parameters of acidification, the concentration of probiotics, the post-acidification and the firmness of fermented fiber-enriched milk.

1. Introduction

Nowadays, consumers are demanding for foods with increasingly properties, such as pleasant flavor, low-calorie value or low fat content, and benefic health effects. Within this context, food industry has been trying to offer products with improve flavor and appearance. In addition, functional dairy products offer requirements, benefits to health that are strengthened by the addition of probiotics as well as by certain types of soluble fibers known as prebiotic.

Prebiotics are non-digestible food components that beneficially act on the host because they selectively stimulate either the proliferation or the activity of bacterial populations that are desirable in the colon. Moreover, prebiotics may inhibit pathogen multiplication, ensuring additional benefits to host's health. Such components mostly

act on the large intestine, even though they can also impact the microorganisms inside the small one (Roberfroid 2000; Mattila-Sandholm et al. 2002).

Lactic-acid bacteria (LAB) isolated from humans' and animals' gastrointestinal tract is known as probiotics. These organisms, when used in large amounts in the preparation of foods and dairy products, should survive the passage through the upper digestive tract. Besides, probiotic microorganisms should be able to adhere to intestinal cells, providing beneficial effects in the intestinal tract (Gilliland 1989). When such organisms are largely consumed, they help in the intestinal balance (Ferreira 2003). In order to produce the desired benefits, probiotics bacteria should be present in the products in viable counts during their whole shelf-life.

To this purpose, we investigated throughout the fermentation by *Streptococcus thermophilus* in co-culture with *Lactobacillus delbrueckii* subsp. *bulgaricus*, *Lactobacillus acidophilus, Lactobacillus rhamnosus and Bifidobacterium animalis* subsp. *Lactis* the kinetics of acidification of inulin supplementation of milk (1, 2 and 4 g. 100 g^{-1}), the probiotic survival, the post-acidification and the firmness of fermented fiber-enriched milks, stored at 4°C either for 24 h or after 7 days since their preparation.

2. Material and Methods

2.1 Experimental Procedure

Five strains of pure commercial *starter* freeze-dried cultures (Danisco, Sassenage, France) were used: *Streptococcus thermophilus* TA040 (St) and *Lactobacillus delbrueckii* subsp. *bulgaricus* LB340 (Lb) (yogurt microorganisms) and *Lactobacillus acidophilus* LAC4 (La), *Lactobacillus rhamnosus* LBA (Lr), and *Bifidobacterium animalis* subsp. *lactis* BL 04 (Bl) (probiotics microorganisms). Pre-cultures were prepared in which bacteria average counts in the different pre-cultures ranged from 6.1 to 6.5 LogCFU.mL^{-1}.

Milk prepared adding 13 g of skim powder milk (Molico, Nestlé, Araçatuba, Brazil) in 100 g of distilled water (M) was supplemented with inulin (Beneo TM, ORAFTI Active Food Ingredients, Oreye, Belgium), specifically 1 (SM1), 2 (SM2) and 4 (SM4) $g.100g^{-1}$, and them thermally treated at 90°C for 5 min in water bath (550 THE, Fisatom, São Paulo, Brazil). The heat treated milk was collected into 1.0 L sterile flasks, cooled in ice bath, distributed into 250 mL sterile Shott flasks inside laminar flow chamber, and stored at 4°C for 24 h, before using.

After inoculation, flask samples were transferred on water bath equipment assembled to a CINAC (*Cynetique d´acidification*, Ysebaert, Frépillon, France) system and, batch fermentations were performed at 42°C up to pH 4.5 corresponding to the final fermentation time. Fermentations were carried out in duplicate and monitored using the CINAC system which allows to continuously measure and record of pH as well as to evaluate acidification rates throughout the run (Spinnler and Corrieu, 1989). From the collected data, the acidification rates (dpH/dt) were calculated as the time variation of pH and expressed as 10^{-3} pH units . min^{-1} (V_{max}). At the end of the incubation period, the following kinetic parameters were also calculated: (i) t_{max} (h): time in which the

maximum (V_{max}) acidification rates were reached and (ii) $t_{pH4.5}$(h): time to reach pH 4.5. Not supplemented milk (M) was used as control.

2.2 Milk Chemical Composition and Firmness Analyses

Physico-chemical analyses (fat, gross protein, lactose and total solids) were carried out in inulin-supplemented milk according to Schmidt-Hebbel (1956), A.O.A.C (1995) and INSTITUTO ADOLFO LUTZ (1985) methods, in triplicate. The results were expressed in g.100 g^{-1}. Fermented milk post-acidification was determined by pH measurement using a pHmeter model Q-400M1 (Quimis, São Paulo, Brazil). Acidity, expressed in percentage of lactic acid, was evaluated by titration using a 0.11N NaOH solution according to AOAC (1995) methodology No. 907.124. Fermented milk firmness was measured at 8ºC using a TA-XT2 Texture Analyzer (Stable Micro Systems Ltd., Godalming, United Kingdom). The operation conditions were: probe type acrylic P/25P (2.5 cm diameter), 10 mm penetration, and 10 mm s^{-1} speed). Firmness was expressed as the maximum penetration, in N.

2.3 Counts of Probiotic Bacteria

Bacterial enumerations were carried out either after 24h or after seven days since storage of fermented milks at 4ºC. One mL of sample was diluted with 9 mL of 1% sterile peptonated water. Afterwards, serial dilutions were done and bacteria were counted applying the in-depth platelet technique. All media were obtained from Merck (Darmstadt, Germany). St colonies were enumerated in M17 agar by aerobic incubation at 37 ºC for 48 h. Lb enumeration was carried out in MRS Agar medium with pH adjustment at 5.4 by acetic acid addition, and aerobic incubation at 37 ºC for 48 h. La and Lr were enumerated in the same medium with pH adjustment at 5.4 by acetic acid addition, and anaerobic incubation at 37 ºC for 72 h. Bl was enumerated as La and Lr without any pH adjustment (IDF 1996, 1997, 2003).

2.4 Statistical Analyses

Results were submitted to analyses of variance (ANOVA) using the Statistica Software 6.0. Mean values were compared using the Tukey test at $P<0.05$.

3. Results and Discussion

3.1 Milk Chemical composition

Fat, protein and solid contents ranged respectively from 0.03 to 0.06 g·100 g^{-1}, 4.00 to 4.10 g·100 g^{-1}, and 13.20 to 15.63 g·100 g^{-1}. No statistically significant difference was observed in fat and protein contents whereas those of total solids values were

statistically different. Lactose content ranged from 4.43 to 4.63 g·100 g^{-1}, with significant statistical differences when 4 g·100 g^{-1} of inulin was added.

3.2 Kinetics of Acidification

The fermentation times ($t_{pH4.5}$) ranged between 5.2 to 11.2 h. There was a statistically significant variation in this parameter, which was shorter in milks that received inulin as supplement mostly at 4 g.100 g^{-1}concentrations, whereas St-Lr cultures was strongly affected at such inulin level. However, for St-Lb (SM1), St-Lr (SM1 and SM2), and St-Bl (SM1) co-cultures, the fermentation times were close to those obtained at the other concentrations (Figure 1).

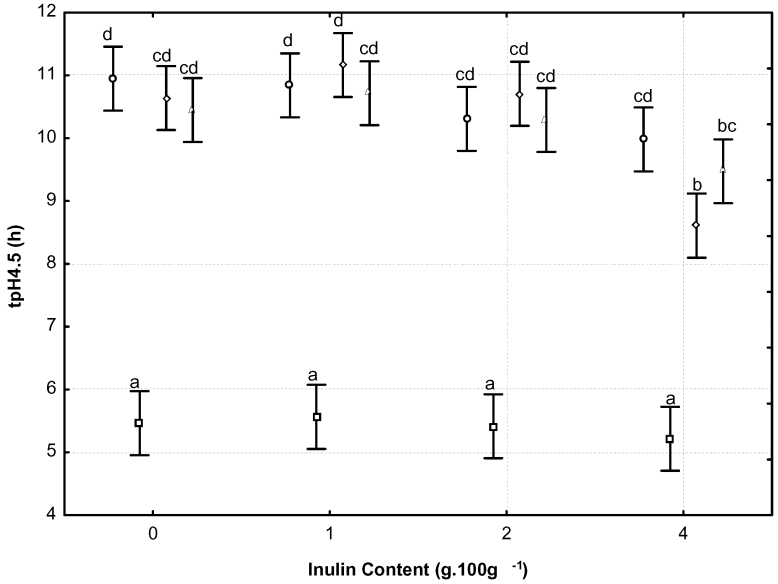

Fig. 1. *Effect of inulin addition to milk on the duration of fermentation ($tpH_{4.5}$) by Lactobacillus bulgaricus, Lactobacillus acidophilus, Lactobacillus rhamnosus, and Bifidobacterium lactis in co-culture with Streptococcus thermophilus. (o) St-La;(□) St-Lb; (◊) St-Lr; (Δ) St-Bl.*

Inulin influenced significantly the acidification kinetics of the milk for probiotics cultures. Maximum acidification rates (V_{max}) increased with inulin contents. Milk supplementation with 4 g.100 g^{-1} of inulin reduced the fermentation time of *S. thermophilus* and *L. rhamnosus* co-culture.

3.3 Post-Acidification and Acidity

pH values ranged from 4.32 (St-La/M) to 4.48 (St-Lr/M) after one day of fermentation (D1), and from 4.15 (St-La/SM4) and 4.37 (St-La/M) after seven days (D7). On

average, there was a 0.14 upH decrease after seven-day storage at 4°C. Using the St-Lb and St-La co-cultures, the post-acidification was stronger when using 4 g.100 g^{-1} of inulin, while there was a higher post-acidification of milk supplemented with 1 g.100 g^{-1} of inulin using St-Lr and St-Bl co-cultures. After one day of fermentation, the acidity ranged from 0.81 (St-Bl/M) to 1.03 g.100g^{-1} of lactic acid (St-La/SM2). Using the St-Lb co-culture the amount of lactic increased with inulin concentration in the formulation, but only the highest inulin concentration (4 g.100 g^{-1}) exhibited a statistically significant difference. Using the St-La co-culture the addition of 2 g.100 g^{-1} of inulin yielded the highest production of lactic acid compared to all tested co-cultures. Concerning St-Lr co-culture the highest production of lactic acid (0.94 g.100 g^{-1}) was obtained using 1 g.100 g^{-1} of inulin. The lowest values of lactic acid were found using the St-Bl co-culture, and they ranged from 0.81 g.100 g^{-1} of lactic acid in Ml to 0.86 g.100 g^{-1} in SM1, with a statistically significant difference between them. After seven days of fermentation (D7), lactic acid production was always higher than after one day (D1), ranging from 0.90 g.100 g^{-1} (St-Lr/M) to 1.20 g.100 g^{-1} of lactic acid (St-La/SM2). Taken as an average, the increase in lactic acid production was 0.13 g.100 g^{-1}. The addition of inulin supported higher post-acidification for all investigated co-cultures.

3.4 Probiotic Bacteria Counts

The counts for *S. thermophilus* after 1 day of fermentation ranged from 8.67 (St-Bl) to 9.45 Log CFU.mL^{-1} (St-Lr) in SM1, without no statistically significant difference between the cultures. After 7 days of fermentation, counts ranged from 8.18 (St-Bl) to 9.42 Log CFU.mL^{-1} (St-Lr) in the same medium, with statistically significant differences. In average, the addition of 4g100 g^{-1} of inulin resulted in 0.40 log CFU.mL^{-1} decrease for La and 0.69 Log CFU.mL^{-1} for Lr.

After one day of fermentation, probiotic counts ranged from 7.37 (St-Lr/ M) to 9.13 Log CFU.mL^{-1} (St-Bl/SM4). There was a statistically higher growth of St-Lb in milks supplemented with inulin. Compared to the control the growth of La in milk supplemented with inulin was slightly higher, with a statistically significant difference. However, no appreciable variation between counts of Lr in milk supplemented or not with 1 g.100 g^{-1} of inulin was observed, whereas it became appreciable when 2 and 4 g.100 g^{-1} of inulin was added. Indeed, inulin showed a statistically significant *in vitro* bifidogenic effect, with higher counts in milks supplemented with inulin. After 7 days of fermentation he viability of *L. acidophilus* and *B. lactis*, probiotic bacteria, decreased by ~0.04 and ~0.15 Log CFU.mL^{-1}, respectively. However, counts remained stable for *L. rhamnosus* and *L. bulgaricus* cultures. Milk supplemented with inulin had a significant influence on the survival of these probiotic bacteria.

Probiotic counts were higher than 7.37 Log CFU.mL^{-1}. The inulin showed an *in vitro* bifidogenic effect, stimulating the growth of *B. lactis*; this effect was more pronounced using *B. lactis* than the other probiotic cultures. Counts remained almost stable after seven days of storage at 4°C.

3.5 Firmness

After one day of fermentation (D1), firmness ranged from 0.28 (St-Lb/M) to 0.47 N (St-Lr/SM4). At seven days (D7) it increased, on average, when compared to D1 by ~0.06 N, varying from 0.33 (St-Lb/M) to 0.54 N (St-Lr/SM4). Such results demonstrate that the supplementation of milk with inulin resulted in stronger firmness for all products and agree with those reported by MARTIN et al. (1999) and OLIVEIRA et al. (2001).

Acknowledgement

The authors thank the FAPESP (Research Foundation of the State of São Paulo), DANISCO and ORAFTI Active Food Ingredients for furnishing the cultures and the inulin, respectively.

4. References

AOAC. ASSOCIATION OF OFFICIAL ANALYTICAL CHEMISTS. **Official Methods of Analysis** 16.ed. Washington, 1995. 1141p.

FERREIRA, C L L (2003). Grupo de bactérias láticas: caracterização e aplicação tecnológica de bactérias probióticas. In *Prebióticos e Probióticos: Atualização e Prospecção*, pp. 7-33. Ferreira, C.L.L. ed., Viçosa - MG: UFV.

GILLILAND, S E (1989). Acidophilus milk products: a review of potential benefits to consumers. *Journal of Dairy Science* **72** 2483-2494.

IDF (1996) *Preparation of Samples and Dilutions for Microbiological Examination*, Standard No. 122C, International Dairy Federation, Brussels, Belgium.

IDF (1997) *Dairy Starter Cultures of Lactic Acid Bacteria (LAB) – Standard of Identity*, Standard No. 149A, International Dairy Federation, Brussels, Belgium.

IDF (2003) *Yoghurt / Enumeration of Characteristic Microorganisms – Colony Count Technique at 37°C*, Standard No. 117, International Dairy Federation, Brussels, Belgium.

INSTITUTO ADOLFO LUTZ. (1985) Normas Analíticas do Instituto Adolfo Lutz: Métodos químicos e físicos para análise de alimentos. 3.ed. São Paulo: Imprensa Oficial do Estado de São Paulo, v.1, 533p.

MARTIN, N C, SKOKANOVA, J, LATRILLE, E, BÉAL, C and CORRIEU, G (1999) Influence of fermentation and storage conditions on the sensory properties of plain low fat stirred yoghurts. *Journal of Sensory Studies* **47** 151-164.

MATTILA-SANDHOLM, T, MYLLÄRINEN, P, CRITTENDEN, R, MOGENSEN, G, FONDÉN, R and SAARELA, M (2002). Technological challenges for future probiotic foods. *International Dairy Journal* **12** 173-182.

OLIVEIRA, M N, SODINI, I, REMEUF, F and CORRIEU, G (2001). Effect of milk supplementation and culture composition on acidification, textural properties and microbiological stability of fermented milks containing probiotic bacteria. *International Dairy Journal* **11** 935-942.

ROBERFROID, MB (2000) Defining functional foods. In: Gibson,G.R.; Willians, C.M. *Functional foods-concept to product.* Boca Raton: CRC, 2000. Chapter.1, p.9-27.

SCHMIDT-HEBBEL, H (1956) *Quimica y tecnologia de los alimentos*. Santiago: Editorial Salesiana, 313p.

SPINNLER, H E and CORRIEU, G (1989). Automatic method to quantify starter activity based on pH measurement. *Journal of Dairy Research* **56** 755-764.

CHEMICAL ENGINEERING TRANSACTIONS, Volume 14, 2008
Edited by G. Marino, E. Bardone, A. Viglia
 ISBN 978-88-95608-02-0

Bioconversion of ferulic acid obtained from wheat bran into vanillin

Luigi Sciubba[1], Diana Di Gioia[1], Leonardo Setti[2], Maurizio Ruzzi[3], Fabio Fava[1]
[1] DICASM, Engineering faculty, University of Bologna, Italy
[2] Department of Industrial Chemistry and Materials, University of Bologna, Italy
[3] Dipartimento di Agrobiologia e Agrochimica, Università della Tuscia, Viterbo, Italia

In this work the possibility of producing vanillin through microbial bioconversion from ferulic acid obtained from the enzymatic hydrolysis of wheat bran has been explored. The biocatalyst employed was *Escherichia coli* JM109/pBB1, a recombinant strain containing the genes from *Pseudomonas fluorescens* BF13 for the transformation of ferulic acid into vanillin. The substrate of the bioconversion, performed with resting cells of *E.coli* JM109/pBB1 grown on LB rich medium, was the crude hydrolizate obtained from wheat bran or a buffer containing ferulic acid recovered from the crude matrix with different methods, as adsorption on ion exchange resins, liquid-liquid extraction and solid phase extraction; these operations allowed the selective recovery of ferulic acid from carbohydrates present in the hydrolizates, thus obtaining an aqueous phase rich in reducing sugars. The removal of reducing sugars allowed to obtain higher bioconversion yields. The results of this work showed that vanillin can be obtained at interesting yields from ferulic acid extracted from wheat bran.

1.Introduction

Vanillin (4-hydroxy-3-methoxy-benzaldheyde) is one of the most common flavouring compounds in the food industry and its production reaches about 12000 tons per year. It is usually obtained from *Vanilla* pods, through a long and expensive process (the price of natural vanilla is about 2000-4000 $/kg), or through chemical synthesis, leading to a cheaper product (15$/kg) but of lower quality [Walton *et al.*, 2003]. Biotechnological production of vanillin from selected substrates (such as ferulic acid) could be an interesting alternative, as it is cheap and permits the labelling of the product as natural according to the US and European legislation [EC directive 88/388, 1988]. Ferulic acid is a phenolic compound present in large amount in the cell wall polysaccharides, such as wheat bran, which is an agricultural by-product obtained in huge quantity in Italy (1.6milion tons) and currently used only for animal feeds. Ferulic acid is linked to the cell wall through ester bonds and can be released breaking these bonds through enzymatic hydrolysis [Di Gioia *et al*., 2007]; then it can be converted into vanillin using as the biocatalyst a recombinant strain, *Escherichia coli* JM109/pBB1, containing the genes from *Pseudomonas fluorescens* BF13 for the transformation of ferulic acid into vanillin [Barghini *et al.*, 2007]. In this way a waste matrix such as wheat bran could be valorized, being a source of ferulic acid, to be transformed into a fine chemical product as vanillin.

2.Materials and methods

2.1 Micorganisms, buffers and media

Escherichia coli JM109/pBB1 was used in this study; this strains contains a plasmide derivative carrying a catabolic cassette for the conversion of ferulic acid into vanillin [Barghini *et al.*, 2007]. Rich medium LB was prepared according to Sambrook et al. Saline buffer (pH7) had the following composition(g/L): Na_2HPO_4 6,0; KH_2PO_4 3,0; NH_4Cl 1,0; NaCl 0,5.

2.2 Wheat bran hydrolizates production

Wheat bran was suspended in distilled water in the ratio 1:7 (7 liters of water per kg of wheat bran), then the suspension was subjected to thermal treatment (121°C for 20 min in an autoclave). Then the enzyme preparation, Fungamyl Super AX® (1%w/w) + Celluclast BG®(1%w/w), was added and this mixture was incubated at 30°C for 20h.

The hydrolizate was filtered on a paper, centrifuged at 6000rpm for 10 minutes, sterilized through a 0,20 μm porosity filter and stored at -20°C. The hydrolizate had a concentration of 200mg/L of ferulic acid, 50g/L of total sugars (30g/L of reducing sugars), pH=5,8 [Di Gioia *et al*., 2007].

2.3 Bioconversion experiments performed with resting cells of *Escherichia coli* JM109/pBB

A 1L-flask containing 100mL of rich medium LB+ampicillin (50μg/mL) was inoculated with 2%v/v with an over-night *E.coli* JM109/pBB1 culture, for the growth phase. The flask was incubated at 37°C and 150rpm until the culture reached an A_{600} of 1,5, usually after 3,5h of incubation. Then the cells were harvested by centrifugation (6000rpm, 10 minutes), washed with saline buffer pH7, resuspended in the bioconversion buffer (the crude hydrolizate or a buffer containing purified ferulic acid) at the concentration of 4mg wet biomass/mL, in a 100mL flask containing 20 mL of this solution and incubated at 30°C. Each hour 1-mL samples were taken out, acidified with 25ml of TCA 2M centrifuged at 12000rpm for 10 minutes and analyzed through HPLC-DAD reverse phase system.

2.4 Wheat bran hydrolizate purification

2.4.a Adsorption on ion exchange resins Amberlite IRA® 95

Ferulic acid was recovered by adding ion exchange resin Amberlite IRA® 95 (6%w/v, 50rpm, 4h) to the crude hydrolizate, then the hydrolizate was removed and the resin was washed with ethanol additioned with 4%HCl for 1h at room temperature. The alcoholic ferulic acid rich extract thus obtained was neutralized by using NaOH 2N and concentrated through evaporation in rotavapor; the solution was diluted in saline buffer in order to obtain a concentration of ferulic acid of 100mg/L. This operation allowed a ferulic acid recovery of 80% and a removal of 90% of reducing sugars.

2.4 b Liquid-liquid extraction with ethyl acetate

5mL of ethyl acetate were added to an equal volume of crude hydrolizate (pH=5,8), shaked and centrifuged for 5 minutes at 3000rpm, then the organic phase was taken out and put in a 50mL bottle; then 5mL of ethyl acetate were again added to the aqueous phase, centrifuged, then the two phase were collected and HPLC analyzed.

The organic phase was evaporated through rotavapor, the concentrated ferulic acid was resuspended in saline buffer in order to obtain a concentration of 100mg/L. The

recovery of ferulic acid was about 80% , while the reducing sugars removal was near to 95%.

2.4c Solid phase extraction with ISOLUTE ENV+®columns

The columns (20mL volume, 1g of packing) were first washed with 9mL of methanol 9mL of distilled water, then the crude hydrolizate was introduced. The columns were washed with 20mL of distilled water and the adsorbed ferulic acid was eluted twice with 12mL of absolute ethanol. The organic phase was evaporated through rotavapor, the concentrated ferulic acid was resuspended in saline buffer in order to obtain a concentration of 100mg/L. Ferulic acid recovery was about 95% and the reducing sugars removal was 95%. The aqueous phase (30g/L of reducing sugars) was sterilized through filtration, in case diluted in distilled water or additioned with yeast extract, and dispensed into sterile flasks.

3.Results

The first experiment was performed with resting cells of *E.coli* JM109/pBB1 grown on LB rich medium using the crude hydrolizate as the bioconversion matrix; it was employed undiluted (200mg/L of ferulic acid, 30g/L of reducing sugars), diluted 3:1 (150mg/L of ferulic acid, 22g/L of reducing sugars)and diluted 1:1 in saline buffer (100mg/L of ferulic acid, 15g/L of reducing sugars). Ferulic acid was quickly transformed into vanillin (Fig.1), but the product was converted, since the second hour of bioconversion, into vanillyl alcohol. Therefore the molar yields obtained in this set of experiments reached a maximum of 50% in the 3:1 diluted buffer and of 37% utilizing the 1:1 diluted matrix.

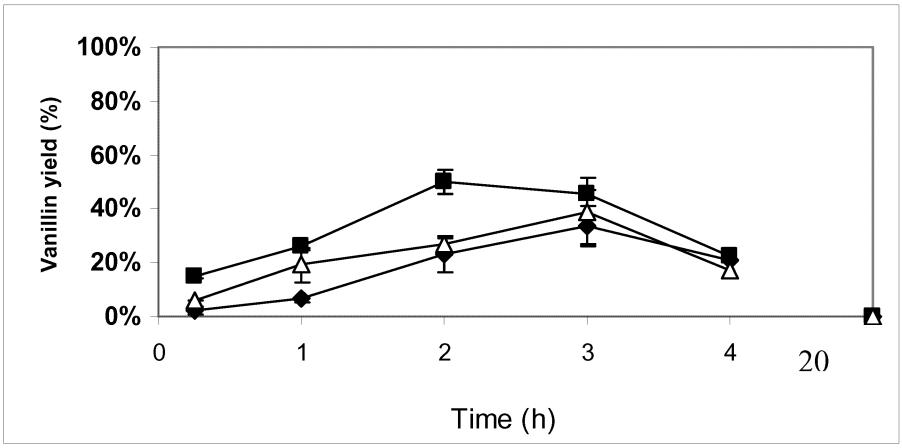

Fig.1: Vanillin molar yields obtained using the undiluted hydrolizate(◆), the hydrolizate diluted 3:1(■), and diluted 1:1 (△)

The following experiment was performed by adding 100mg/L of food grade ferulic acid both to the undiluted hydrolizate (300mg/L of ferulic acid, 30g/L of reducing sugars)

and to the 1:1 diluted hydrolizate (200mg/L of ferulic acid, 15g/L of reducing sugars) in order to explore the effects of higher concentration of substrate, with the same carbohydrate concentration, on the bioconversion process. Also in these experiments, the yields were not high and reached a maximum of 50% in the diluted hydrolizate (data not shown), suggesting that the low bioconversion yield could be due to the high reducing sugars concentration rather than the high ferulic acid initial concentration.
Therefore in the next experiments differents methods for the separation of ferulic acid from the carbohydrates of the crude hydrolizate were employed, i.e. a)adsorption on ion exchange resins, b)liquid-liquid extraction with ethyl-acetate (LLE), c)solid phase extraction (SPE).
In the first experiment of this set, the use of ion exchange resins Amberlite IRA® 95 allowed a recovery of ferulic acid of 80% and a removal of reducing sugars of 90%, obtaining a purified hydrolizate, which was diluted in order to obtain 50,100 and 200mg/L of ferulic acid, corresponding to 0,25 0,5 and 1,0 g/L of reducing sugars respectively. The bioconversion made on this matrix with resting cells of *E.coli* JM109/pBB1 showed a rapid conversion of ferulic acid into vanillin obtaining a molar yield of about 70% (Fig.2), suggesting that the elimination of sugars had a positive effect on the bioconversion process.

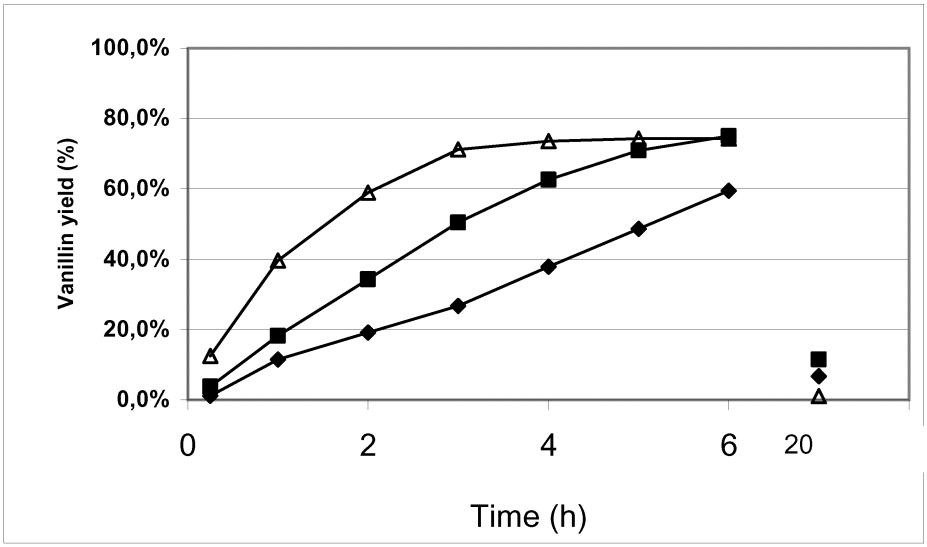

Fig.2: Vanillin molar yields obtained from 50mg/L(△), 100mg/L(■), and 200mg/L (◆) of ferulic acid recovered employing ion exchange resins Amberlite IRA® 95.

The second recovery method for ferulic acid from the hydrolizates was liquid-liquid extraction with ethyl-acetate; in this way the 78% of the ferulic acid was recovered and the 95% of sugars was removed. Ferulic acid was resuspended in saline buffer in order to obtain 100mg/L of ferulic acid (reducing sugars concentration in this matrix was 0,5g/L). The molar yields of the bioconversion performed on this purified

solution were very high and reached a maximum of about 80% (Fig.3) after 4 hours of bioconversion.
The third recovery method, solid phase extraction on ISOLUTE ENV+® columns, allowed a recovery of 95% of ferulic acid and a removal of 95% of reducing sugars. The bioconversion performed on solution (100mg/L of ferulic acid, corresponding to 0,5g/L of reducing sugars) had a maximum molar yield of 75% (Fig.3).
Therefore the results of the latter experiments confirmed the positive effect of the removal of sugars on the bioconversion yields.

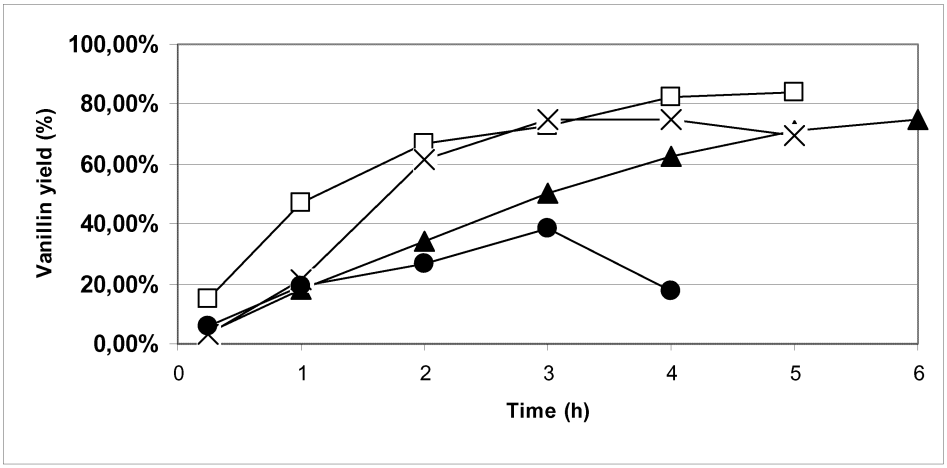

Fig.3: Vanillin molar yields reached using 100mg/L of ferulic acid obtained from the crude hydrolizate diluted 1:1(●), from adsorption on ion exchange resins(▲), liquid-liquid extraction with ethyl-acetate(□), solid phase extraction(X).

Conclusions

In this work the possibility of employing wheat bran as a source of ferulic acid for the bioconversion into vanillin has been explored.
The enzymatic hydrolysis of wheat bran allowed to obtain about 200mg/L of ferulic acid in a hydrolizate containing also 30 g/L of reducing sugars; however, the bioconversion yields obtained using the crude hydrolizate as the bioconversion matrix were not very high and reached a maximum of 50%, after 2hours of bioconversion diluting the hydrolizate in distilled water in the ratio 3:1.
Among the three different ferulic acid recovery methods employed in this study, i.e. adsorption on ion exchange resins Amberlite IRA® 95, liquid-liquid extraction with ethyl-acetate, solid phase extraction with ISOLUTE ENV+® columns, the most efficient was solid phase extraction, as ferulic acid recovery was 95%.
Maximum bioconversion yields were obtained, with resting cells of *Escherichia coli* JM109/pBB1, with ferulic acid recovered through liquid-liquid extraction with ethyl-acetate, and were about 80% starting from 100 mg/L of ferulic acid after 4 hours of bioconversion.

Therefore the results of this work showed that vanillin can be obtained at interesting yields from ferulic acid extracted from wheat bran, an agricultural by-product produced in large amounts in Italy.

References

[1] Walton N.J., Mayer M.J., Narbad A., 2003, Phytochemistry, 63:505-515
[2] EC directive 88/388 OJL 184 July, 15, 1988
[3] Di Gioia D. Sciubba L., Setti L., Luziatelli F., Ruzzi M., Zanichelli D., Fava F. 2007, Enzyme Microbial Technology, 41: 498-505
[4] Barghini P., Di Gioia D., Fava F., Ruzzi M., 2007, Microbial Cell Factories 6:13

CHEMICAL ENGINEERING TRANSACTIONS, Volume 14, 2008
Edited by G. Marino, E. Bardone, A. Viglia
 ISBN 978-88-95608-02-0

Shelf stability of lutein from marigold (*Tagetes erecta* L.) flowers in vegetable oils

Roberto Lavecchia and Antonio Zuorro
Department of Chemical Engineering, "Sapienza" University
Via Eudossiana, 18 – 00184 Roma (Italy)

The stability of lutein in sunflower and rice bran oils was investigated in the temperature range 25–40 °C. Experiments were made using a standardized plant extract at 5% by weight of lutein derived from the flowers of *Tagetes erecta* L. Samples of the pigment in oil were incubated at each temperature for up to 10 days and the time course of degradation was monitored. A kinetic analysis of the data showed that thermal degradation follows first-order kinetics, with apparent activation energies of 60.9 kJ mol^{-1} (in sunflower oil) and 44.9 kJ mol^{-1} (in rice bran oil). From the estimated kinetic parameters, the carotenoid half-life at 4 and 20 °C were determined. The results obtained indicate that lutein is more stable in sunflower oil. The observed differences in stability could be a reflection of the different fatty acid composition of the two oils and the presence of endogenous antioxidants.

1. Introduction

Lutein is a carotenoid pigment found in high concentrations in cruciferous and green leafy vegetables (Landrum et al., 2002). It is also present in significant amounts in maize, alfalfa and the petals of marigold (*Tagetes erecta* L.), from which it is extracted for commercial use. Chemically, lutein (3R,3'R-β,ε-carotene-3,3'-diol) is a dihydroxy derivative of α-carotene with hydroxyl groups located on the 3 and 3' carbons (Figure 1). Of the many carotenoids circulating in human plasma, only lutein and its structural isomer zeaxanthin are accumulated throughout the tissues of the eye (Bone et al., 1997). In the macular region of the retina they can reach concentrations as high as 1 pmol per square millimeter of tissue. Increasing evidence from epidemiological and experimental studies suggests that these macular carotenoids might have a role in maintaining or improving vision and, more importantly, in preventing onset or progression of age-related macular degeneration (Snodderly, 1995). The mechanism by which they exert their beneficial effects needs to be further elucidated but is probably twofold (Kirschfeld, 1982; Palozza and Krinsky, 1992). First, these carotenoids absorb light in the blue range, which is thought to be very harmful to the retina, thereby reducing the associated photo-oxidative damage. A second potential function involves their antioxidant properties, *i.e.*, the ability to quench free radicals and other reactive oxygen species, whose concentrations are particularly high in the retinal tissue.
As diet is the only source of lutein and zeaxanthin, enhancement of their intake by dietary supplementation or by fortification of foods is being actively considered as a means to increase their levels of in the organism.

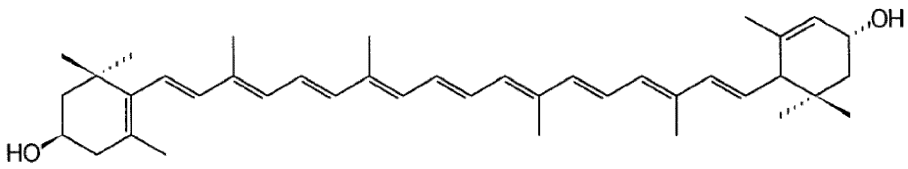

Figure 1 – Molecular structure of lutein.

In the past few years we have successfully included lutein, alone or in combination with other carotenoids, in yogurts and other food products. However, to ensure product quality and food safety an accurate prediction of shelf-life is also required. In this paper we present the results of an experimental study on the stability of lutein in sunflower and rice bran oils. Analysis of degradation rate data indicated that lutein is more stable in sunflower than in rice bran oil. The kinetic parameters estimated from these data allowed prediction of shelf-life for the two systems under different storage conditions.

2. Experimental

2.1 Materials

A standardized dry powder extract from the flowers of *Tagetes erecta* L. (at 5% by weight of lutein) was obtained from SCIDOOR HI–TECH BIOLOGY CO. (Shaanxi, China).

Sunflower and rice bran oils were purchased from a local market and stored at room temperature in the dark.

2.2 Methods

Solutions of different lutein concentrations were prepared by dissolving, under stirring, appropriate amounts of the powdered extract in the vegetable oils. Samples of the products were incubated at the desired temperature (25 or 40 °C) in a refrigerated incubator (FTC 90E, Velp Scientifica, Italy) for up to 10 days. At selected times, aliquots were withdrawn and analysed for lutein content. Lutein concentrations were determined by spectrophotometric measurement at 452 nm, where the absorption spectrum of the pigment displays a sharp peak. A double-beam UV–VIS spectrophotometer (Perkin–Elmer Lambda 25) and quartz cells of 1-cm path length were used.

3. Results and Discussion

Typical results showing the time variation of absorbance at 452 nm are presented in Figure 2. The observed absorbance changes were largely irreversible and were attributed to thermal degradation of lutein.

Degradation rates were calculated from the slope of the absorbance–time plots. At each

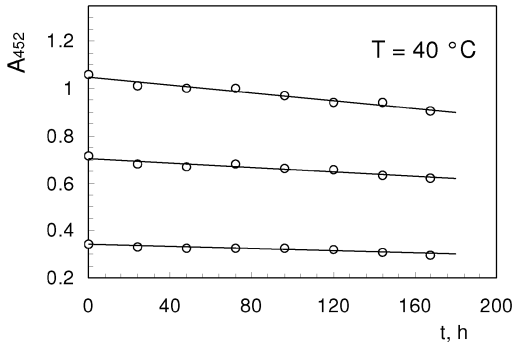

Figure 2 – Time changes of absorbance at 452 nm for lutein in sunflower oil at different initial carotenoid concentrations.

temperature and in each vegetable oil they were found to be linearly related to the undegraded lutein concentration (Figure 3). Accordingly, the kinetic data were interpreted by a first-order rate expression:

$$r = k(T)\, c \tag{1}$$

where r is the degradation rate, k is the first-order rate constant and c is the lutein concentration. To describe the temperature dependence of k we assumed the Arrhenius equation:

$$k(T) = k_0 \exp\left(-\frac{E_a}{RT}\right) \tag{2}$$

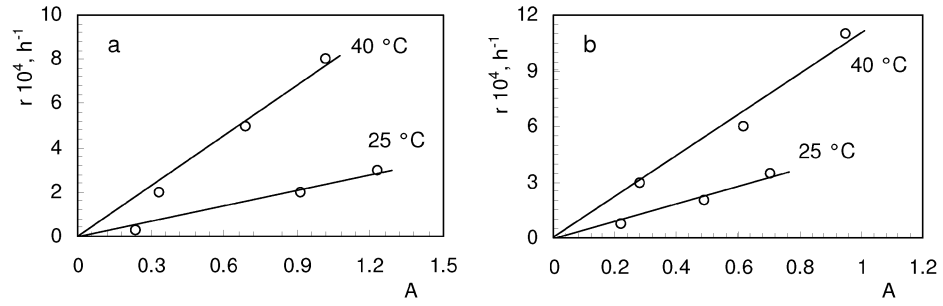

Figure 3 – Kinetic plots showing the dependence of degradation rate (r) on absorbance at 452 nm in: (a) sunflower oil and (b) rice bran oil.

where E_a is the apparent activation energy for degradation. Rate constants and activation energies were determined by least squares regression, leading to the results summarized in Table 1.

In both oils, as expected, lutein degradation increased with temperature. Values of the first-order rate constant were higher in rice bran oil than in sunflower oil, suggesting that lutein was more stable in the latter. According to the apparent activation energies, stability in sunflower oil (E_a = 60.9 kJ/mol) is more sensitive to temperature than in rice bran oil (E_a = 44.9 kJ/mol). These results cannot be directly compared with literature values due to the lack of kinetic studies on the degradation of this carotenoid. Apparent activation energies, however, are close to the value of 59.6 kJ/mol found for lycopene degradation in sunflower oil (Lavecchia and Zuorro, 2006). An activation energy of 61 kJ/mol is also reported by Lee and Chen (2002) for the degradation of a thin vacuum-deposited film of lycopene. Recently Koca et al. (2007) investigated the kinetics of colour changes in dehydrated blanched and unblanched carrots during storage. The authors found a first-order kinetics for thermal degradation of β-carotene, with activation energies of 66.1 kJ/mol and 38.9 kJ/mol, respectively, for blanched and unblanched samples. In contrast, higher values (between 82.8 and 109.6 kJ/mol) were obtained for the oxidative degradation of carotenoids, including lutein, in safflower oil (Henry et al., 1998). This study, however, was conducted at considerably higher temperatures (75–95 °C) and it cannot be excluded that, under these conditions, degradation might follow different pathways.

To quantify the storage stability of lutein-based products we determined their apparent half-life, *i.e.*, the time required for half of the initial amount of the pigment to disappear. For first-order kinetics, half-life depends only on temperature and can be calculated as:

$$\tau = \frac{ln\,2}{k(T)} \tag{3}$$

Half-lives in sunflower oil were equal to 101.2 days, at 25 °C, and 31.4 days at 40 °C. In rice bran oil the corresponding values were 62.3 and 26.3 days, respectively.

Figure 4 shows the effect of temperature on the half-life of lutein in the two vegetable oils. As is evident, the stability curve in sunflower oil is constantly over that in rice bran oil. Differences, however, decrease with temperature and tend to disappear above 45–50 °C.

Table 1 – Kinetic parameters for lutein degradation in the two vegetable oils.

Vegetable oil	*T (°C)*	*$k \cdot 10^4$ (h^{-1})*	*E_a (kJ mol^{-1})*
Sunflower	25	2.33 ± 0.48	60.9 ± 3.2
	40	7.56 ± 0.66	
Rice bran	25	4.61 ± 0.32	44.9 ± 2.7
	40	11.10 ± 0.74	

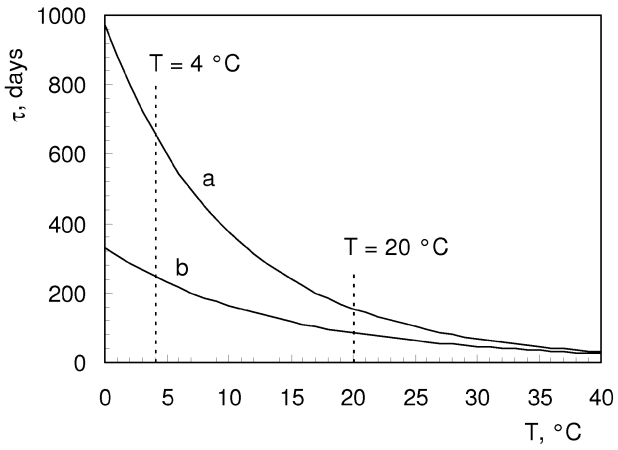

Figure 4 – Effect of temperature on the half-life of lutein (τ) in: (a) sunflower oil and (b) rice bran oil.

The reason for the observed differences in stability is to be found in the different properties of the two oils. As is illustrated by the values in Table 2, they differ both in fatty acid composition and in the type and level of antioxidant compounds.
It is generally accepted that the higher the degree of unsaturation of a vegetable oil, the faster is oxidative deterioration (Chan, 1987; Porter et al., 1995). Oxidation leads to the formation of highly reactive species, such as alkyl and peroxyl radicals, which can, in turn, increase the degradation of easily oxidizable compounds, as is lutein in our case. On the basis of these considerations, lutein should be more stable in rice bran oil, due to its lowest degree of unsaturation. Stability, however, is also affected by the presence of endogenous antioxidants, such as tocopherols and tocotrienols. Studies performed in non-polar environments have shown that tocopherols can protect β-carotene from oxidative damage (Mortensen and Skibsted, 1997a; Krinsky and Yeum, 2003). Similar results were obtained for lycopene (Mortensen and Skibsted, 1997b).

Table 2 – Fatty acid composition and antioxidant content of sunflower and rice bran oils (SFA: saturated fatty acids; MUFA: mono-unsaturated fatty acids; PUFA: poly-unsaturated fatty acids). Source: Codex Alimentarius Commission, 2001.

Vegetable oil	*SFA (wt %)*	*MUFA (wt %)*	*PUFA (wt %)*	*Tocopherols (mg/100 g)*	*Tocotrienols (mg/100 g)*
Sunflower	12	21	67	40.3–102.0	–
Rice bran	20	45	35	25.6–64.8	24.4–104.1

The underlying hypothesis is that tocopherols can regenerate the biologically active carotenoid molecules by an electron transfer mechanism (Mortensen et al., 2001). As regards the levels of endogenous antioxidants in the two oils, we note from the values given in Table 2 that sunflower oil contains more tocopherols than does rice bran oil, even if the latter has some additional amount of tocotrienols.

We can, therefore, hypothesize that at lower temperatures lutein degrades slowly in sunflower oil because of the higher content of tocopherols. As the temperature is increased, the protection offered by tocopherols may be overcome by the formation of reactive species caused by lipid peroxidation. Due to these opposing effects, differences in stability in the two vegetable oils tend to vanish, making it almost independent of oil type at temperatures higher than 45–50 °C.

In conclusion, it may be interesting to estimate lutein stability at two significant storage temperatures: 4 and 20 °C. By the use of eqn. (3) and the kinetic parameters obtained previously, at 4 °C we determined 659 and 247 days, respectively, in sunflower and rice brain oil. The corresponding values at 20 °C were 155 and 85 days, respectively.

4. Conclusions

Estimation of kinetic parameters of degradation and evaluation of shelf-life is essential for quality assurance of functional foods. The kinetic study outlined in this paper has shown that the stability of lutein in vegetable oils depends on temperature and oil type. Lutein is more stable in sunflower oil, but the values of half-lives are sufficiently high even in rice bran oil. This clearly supports the possibility of utilizing the commercially available lutein preparations to fortify vegetable oils or oily foods.

5. References

Bone R.A., J.T. Landrum and L.M. Friedes, 1997, Exp. Eye Res. 64, 211.

Chan H.W.S., 1987, Autoxidation of Unsaturated Lipids. Academic Press, London.

Codex Alimentarius Commission, 2001, Report of the 17th Session of the Codex Committee on Fats and Oils, London.

Henry L.K., G.L. Catignani and S.J. Schwartz, 1998, J. Am. Oil Chem. Soc. 75, 823.

Kirschfeld K., 1982, Proc. R. Soc. Lond. B 216, 71.

Koca N., H.S. Burdurlu and F. Karedeniz, 2007, J. Food Eng. 78, 449.

Krinsky N.I. and K.J. Yeum, 2003, Biochem. Biophys. Res. Commun. 305, 704.

Landrum J.T., R.A. Bone and C. Herrero, 2002, Astaxanthin, β-cryptoxanthin, lutein and zeaxanthin, in: Phytochemicals in Nutrition and Health, CRC Press, Boca Raton.

Lavecchia R. and A. Zuorro, 2006, Chem. Technol. AIJ 1, 80.

Lee M.T. and B.H. Chen, 2002, Food Chem. 78, 425.

Mortensen A. and L.H. Skibsted, 1997a, FEBS Lett. 417, 261.

Mortensen A. and L.H. Skibsted, 1997b, Free Radic. Res. 27, 229.

Mortensen A., L.H. Skibsted and T.G.Truscott, 2001, Arch. Biochem Biophys. 13, 385.

Palozza P. and N.I. Krinsky, 1992, Methods Enzymol. 213, 203.

Porter N.A., S.E. Caldwell and K.A. Mill, 1995, Lipids 30, 277.

Snodderly D.M., 1995, Am. J. Clin. Nutr. 62, 1448.

CHEMICAL ENGINEERING TRANSACTIONS, Volume 14, 2008
Edited by G. Marino, E. Bardone, A. Viglia
 ISBN 978-88-95608-02-0

Effect of the carbon and nitrogen sources on biosurfactant production by *Pseudomonas fluorescens* – Biosurfactant characterization

A.Yataghene[1], M. Abouseoud[2], R. Maachi[1], A. Amrane[3]
[1]Laboratoire Génie de la Réaction, Université Houari Boumediene, Institut de Chimie Industrielle, Alger, Algeria. E-mail: a.yataghene@yahoo.fr
[2]Centre Universitaire Yahia Fares de Médéa, Département Génie des Procédés Pharmaceutiques, Institut des Sciences de l'Ingénieur, Ain Dahab, Médéa, 26000, Algeria.
E-mail: Mahmoud103@hotmail.com
[3]UMR CNRS 6226 – Equipe CIP (Université de Rennes 1 – ENSCR)
ENSCR, 35700, Rennes, France. E-mail: abdeltif.amrane@univ-rennes1.fr

The production of biosurfactant by cells of *Pseudomonas fluorescens* Migula 1895, using the following Carbon (glucose, olive oil and hexadecane) and Nitrogen (urea, NH_4NO_3, KNO_3 and NH_4Cl) sources were examined in this work.
Olive oil and NH_4NO_3 as carbon and nitrogen sources were found to give the optimal yield of biosurfactant production (9 g L^{-1}) for an optimal C/N ratio of 10/1, and led to a decrease of the surface tension of the culture medium from an initial value of 69 mN m^{-1} to 30.5 mN m^{-1} at the end of culture. The critical micellar concentration was found to be 290 mg L^{-1}. Interfacial tension value was low with vegetable oil (2.5 mN m^{-1} with Sunflower oil) and high in case of aromatic oil (17.5 mN m^{-1} with toluene). The stability of the emulsion produced against sunflower oil was very stable during several days; leading to an emulsification index E24 of 80%. Wettability is also a useful parameter to characterize biosurfactants. The decrease of the contact angle reflects an improvement in the degree of wetting.

1. Introduction

Due to the features of high surface activity and biodegradability, biosurfactants produced by a variety of microorganismes have been studied extensively in recent years (Van Hamme et al 2006). Biosurfactants are amphiphilic compounds and are mainly classified into four categories based on the hydrophilic part: glycolipid type, fatty acid type, lipopeptide type and polymer type. Biosurfactants production is an important area of research, owing to the large number of potential applications, especially as substitutes for synthetic surfactants in oil and other industries (Banat et al 2000; Mulligan 2005).They can be used as emulsifiers, de-emulsifiers, wetting agents, foaming agents, functional food ingredients and detergents (Kosaric 1992). The major factors restricting the commercial viability of biosurfactants are the low yield and high production cost (Mukherjee et al 2006; Fiechter 1992). *Pseudomonas* are the best-known bacteria capable of utilizing hydrocarbons as carbon and energy sources and producing biosurfactants to enhance the uptake of such immiscible hydrophobic compounds (Al-Tahhan et al 2000; Rahman et al 2002). However, the available literature shows a lack of studies dealing with biosurfactant production by considering the use of carbon sources other than hydrocarbons.

2. Materials and Methods

2.1. Microorganisms

Pseudomonas fluorescens Migula 1895 [Al] (DSMZ; Braunschweig GERMANY) strain was used in this work.

2.2. Culture medium and fermentation condition

The *P. fluorescens* strain was pre-cultured at 30°C and 250 rpm agitation for 18h in a 250 ml Erlenmeyer flask containing 50 ml of sterilized culture medium (20 min at 120°C). The culture medium contained 1 ml of a solution (MS) of the following mineral salts (g l^{-1}): K_2HPO_4 2.7, KH_2PO_4 1.4, Mg $SO_4.7H_2O$ 0.6, $FeSO_4.7H_2O$ 0.01, NaCl 0.05 and $CaCl_2$ 0.02; 1g of the considered nitrogen source; and 2 % of the considered carbon source. The pH of the medium was adjusted to 6.8 with HCl or NaOH. Three carbon sources (Hexadecane, Glucose and Olive Oil) and four nitrogen sources (Urea, NH_4Cl, KNO_3 and NH_4NO_3) were considered.

2.3. Growth conditions

Erlenmeyer flasks containing 50 ml of sterile culture medium were inoculated with 2%(v/v) of *P. fluorescens* cells pre-culture and incubated at 30°C and 250 rpm agitation speed for 5 days.

2.4. Analytical techniques

During culture, samples were taken twice a day and the following parameters were controlled: medium acidity (pH), biomass yield (g dry matter l^{-1}), the emulsifying activity and the surface tension of the supernatant, after cells separation by centrifugation at 8000 rpm for 20 min. A decrease of the surface tension of the culture medium and an increase of the emulsifying activity allowed to characterize biosurfactant production.

Surface tension and interface tension

Surface tension and interface tension were determined by means of a K6 tensiometer (Krüss, Germany).

Determination of the emulsifying activity

To estimate the emulsifying activity, two equal volumes of supernatant and Hexadecane (2ml each) were added in a test tube and mixed at high speed for 2mn.The emulsion stability was determined after 24h. The emulsification index, E_{24} (%) was the ratio of the height of the emulsion layer by the total height of the mixture (Iqbal et al 1995).

Biomass concentration measurement

The biomass was deduced from dry cellular weight measurement. Cells were separated from culture broth by centrifugation for 20 min at 8000 rpm; they were washed twice with distilled water, dried at 105°C and weighed.

Biosurfactant Production

After centrifugation of the culture broth (20 min at 8000 rpm), the supernatant was treated with 3 volumes of acetone at 4°C. The precipitate was collected by centrifugation for 10 mn at 4000 rpm and dried under air flow.

Critical micellar concentration (CMC)

The Critical micellar concentration (CMC) corresponded to the concentration of an amphiphilic component needed to initiate the formation of micelles in the solution. The CMC is an important parameter, since no further effect is expected in the surface

activity above this concentration (Ligia 2006). The CMC was determined by measuring the surface tensions of dilutions of cell-free broth in distilled water up to a constant value of surface tension. Measurements of the surface tension of distilled water and of the mineral medium were used as controls. It was carried out by means a K6 tensiometer (Krüss, Germany).

Interfacial tension (IFT) and Foaming activity of biosurfactant

The IFT between biosurfactant solution (2 mg ml^{-1}) and different hydrocarbons (toluene, hexadecane), as well as sunflower oil was measured. For foaming activity measurement, the biosurfactant solution (1 mg ml^{-1}) was agitated manually during 1mn until foam became stable.

Biosurfactant stability

Influences of salt (0, 10, 20, 30, 40 % NaCl), pH (1.5, 6, 11 and 12) and temperature (20, 40, 60, 80 and 105°C) were examined.

Wettability Measurements

The sessile drop method was used to characterize the wettability of a layer of biosurfactant (BS) on polystyrene (PS) surface. The angles were measured using a goniometer. The energetic parameters of the BS surface free energy (γ_s) and its dispersive and no dispersive (polar) terms $(\gamma_s^d, \gamma_s^{nd})$ were calculated from the respective contact angles of water and diiomethane and the energetic parameters of water (liquid free energy, γ_l = 72.8 mJ m^{-2}, γ_l^d = 21.8 mJ m^{-2} and γ_l^{nd} = 51 mJ m^{-2}) and diiodomethane (γ_l = 50.8 mJ m^{-2}, γ_l^d = 50.8 mJ m^{-2} and γ_l^{nd} = 0 m J m^{-2}).

Fourier transforms infrared spectroscopy (FTIR)

The infrared adsorption bands identify specific molecular components and structures. For characterization, dried BS were ground with KBr and pressed to obtain pellets. Infrared absorption spectra were recorded on a FT-IR / Diffuse reflexion spectrometer, in the 4000-600 cm^{-1} range. KBr pellet was used as the background reference.

3. Results and Discussion

3.1. Optimal conditions for biosurfactant production

The carbon source is a major parameter in the production of biosurfactants (BS). The carbon sources generally used can be divided into three categories: carbohydrates, hydrocarbons and vegetable oils. In this study, the production of BS by *Pseudomonas fluorescens* was examined in the presence of glucose, hexadecane and olive oil. The following nitrogen sources were tested, NH_4Cl, KNO_3, NH_4OH and urea. In all cases, the surface tension (ST) decreased after 72 h cultivation; and this decreased was more pronounced in the case of the following couples of nitrogen and carbon sources, NH_4NO_3 and oil olive or urea and glucose (Table1). The higher value of E_{24} was recorded during *P. fluorescens* growth on urea and glucose based medium, while NH_4NO_3 and glucose based medium led to the higher biomass concentration (0.91 gL^{-1}).

Table 1. Surface tension ST and emulsification index E_{24} for the various culture media tested

	NH_4Cl		KNO_3		NH_4NO_3		Urea	
	ST	E_{24}	ST	E_{24}	ST	E_{24}	ST	E_{24}
Glucose	50	0	45	10	48	5	45	55
Oil olive	50	5	42	5	40	7	48	8
Hexadecane	52	15	43	5	50	2	50	8

Medium acidification was recorded during growth on glucose (Table 2), most likely due to the fermentative production of organic acid. However, this assumption has to be subsequently confirmed. Contrarily, no effect on pH of the use of olive oil or hexadecane was observed (Table 2). Whereas, the initial pH of culture media was 6.80.

Table.2. pH for different culture media

	glucose	olive oil	hexadecane
	pH	pH	pH
NH_4Cl	4.48	7.5	7.43
KNO_3	3.7	7.3	7.2
NH_4NO_3	3.5	6.3	7.3
Urea	7.9	7.51	7.6

The following carbon on nitrogen ratio 10, 20, 30, 50 were then considered for glucose + urea and olive oil + NH_4NO_3 based media. ST and E_{24} varied weakly in the range of concentrations tested, with optimal values of 28.5 mN m^{-1} and 40% during growth on olive oil and NH_4NO_3, when the lowest C/N ratio was considered (10). The minimum ST value (28.5 mN m^{-1}) was recorded at 110h. Surface tension decrease and emulsification index increase characterize biosurfactant production. After acetone precipitation and drying of the biosurfactant contained in the supernatant, between 6 and 9 g l^{-1} of biosurfactant were produced after 6 days of culture.

The emulsification index of the produced biosurfactant, determined at 24h (E_{24}), was found to be the highest when sunflower oil was considered (80%).

The critical micellar concentration (CMC) of the biosurfactant produced by *P. fluorescens* was 290 mg L^{-1} and occurred for a surface tension of 37 mN m^{-1}, as it can be deduced from Fig.1.

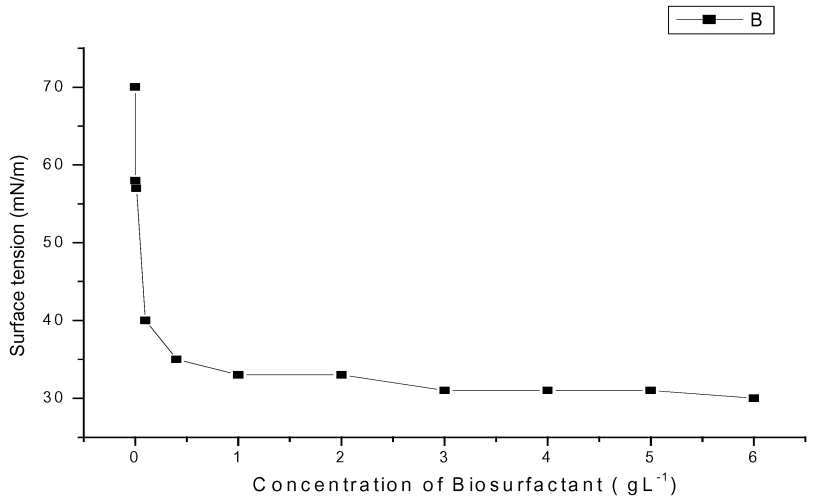

Fig.1.Determination of the critical micellar concentration (CMC) of the biosurfactant produced by *P. fluorescens*.

Table 3. Interfacial tension (IFT) of toluene, hexadecane and sunflower oil.

	Toluene	Hexadecane	Sunflower
Interfacial tension (mN m^{-1})	17.5	12	2.5

As expected, interfacial tension of the biosurfactant produced was low with vegetable oil and high with aromatic compound.

During growth on sunflower oil, a nearly constant value of the emulsification index was recorded for several days (E_{24} = 80%).
After manual agitation of the biosurfactant solution (1 mg l^{-1}) for 1 min, foam stability was shown for at least 1h.

3.2. Stability of the biosurfactant

In Fig.2a, the augmentation of the pH decreased the surface tension. In the range 20 to 60°C (Fig.2b) and 10 to 30 % NaCl (Fig.2c), the surface tension (ST) remained nearly constant.

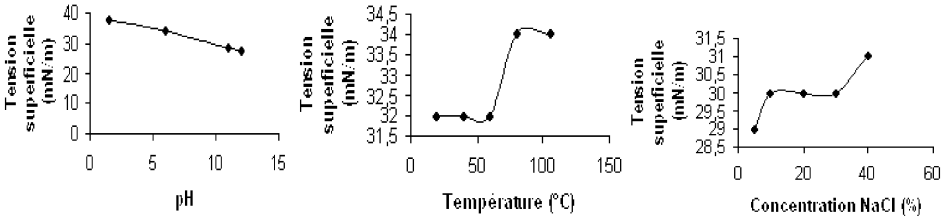

(a) (b) (c)

Fig.2.Effect of pH (a), temperature (b) and salinity (c) on the biosurfactant produced during *P. fluorescens* growth.

3.3. Fourier transforms infrared spectroscopy

Characteristic bands were found in the IR spectrum of biosurfactant, in the range 3000-2700 cm^{-1}, which are characteristics of several C-H stretching bands of CH_2 and CH_3 groups. The deformation vibrations at 1479 and 1413 cm^{-1} also confirmed the presence of alkyl groups. Carbonyl stretching band was found at 1732 cm^{-1} which is characteristic of ester compounds. The ester carbonyl group was also proved from the band at 1250 cm^{-1}, which corresponded to C-O deformation vibration.

3.4. Wettability and Surface Energy

The polystyrene (PS) surface with a biosurfactant layer was used for contact angle measurements of water and diiodomethane. The decrease of the contact angle reflects an improvement in the degree of wetting (Audic et al 2000). Indeed, contact angle measurements can be used to approch the wetting degree.

The surface energy γ_s was the sum of its dispersive and non dispersive components, $\gamma_s^d, \gamma_s^{nd}$:

$$\gamma_s = \gamma_s^d + \gamma_s^{nd} \quad (1)$$

The effects of the dispersive and non dispersive forces corresponded to long-range Lifschitz – van der Waals interactions and to short-range polar interactions, respectively (Poncin-Epaillard 1997); although the non dispersive energy could be expressed by a donor and an acceptor part (Hollander et al 1994). In our analysis, we considered the following model for the γ_s^d and γ_s^{nd} terms of the dispersive energy γ_s :

$$\gamma_l(1+\cos\theta) = 2\sqrt{\gamma_l^d \quad \gamma_s^d} + 2\sqrt{\gamma_l^{nd} \quad \gamma_s^{nd}} \quad (2)$$

Contact angles (degrees) were measured at 25° on PS surface with and without a layer of biosurfactant. Water and diiodomethane were employed to calculate γ_s^d, γ_s^{nd} and γ_s. The contact angles obtained for PS with BS were: θ_{water} = 43° and $\theta_{diiodomethane}$ = 58°. The obtained values are given in Table 4.

Table 4. Surface free energy (γ_s^d , γ_s^{nd} , γ_s) of polystyrene surface with a layer of biosurfactant.

γ_s (mJ m^{-2})	γ_s^{nd} (mJ m^{-2})	γ_s^d (mJ m^{-2})
57.2	27.5	29.7

The water contact angle decreased from 57° without biosurfactant to 43° in presence of biosurfactant. The surface free-energy was positive; the dispersive and non dispersive components were of the same order of magnitude. The decrease of the contact angle in presence of biosurfactant characterized a change of surface wettability.

4. References

Al-Tahhan R.A., T.R. Sandrin, A.A. Bodour and R.M. Maier, 2000, Rhamnolipid-induced removal of lipopolysaccharide from Pseudonomas aeruginosa : effect on cell surface properties and interaction with hydrophobic substrates. Appl. Environ. Microbiol. 66, 3262.

Audic J.-L., F. Poncin-Epaillard, D. Reyx and J.-C. Brosse, 2000, J. Appl. Polymer. Sci. 72, 1384.

Banat I.M., R.S. Makkar and S.S. Cameotra, 2000, Potential commercial applications of microbial surfactants. Appl. Microbiol. Biotechnol. 53, 498.

Beal R. and W.B. Betts, 2000, Role of rhamnolipid biosurfactant in the uptake and mineralization of hexadecane in *Pseudomonas aeruginosa*. J. Appl. Microbiol. 89, 158.

Desai J.D. and I.M. Banat,1997, Microbial production of surfactants and their commercial potential. Microbiol. Mol. Biol. Rev. 61, 47.

Fiechter A., 1992, Biosurfactants: moving towards industrial application. Trends Biotechnol. 10, 208.

Hollander A., J. Behnisch and H.J. Zimmermann, 1994, Chimical Analysis of Polymer Surfaces on a Molecular Scale. Polym. Sci. Part A: Polym. Chem. 32, 699.

Iqbal S., Z.M. Khalid and K.A. Malik, 1995, Enhanced biodegradation and emulsification of crude oil and hyperproduction of biosurfactants by a gamma ray-induced mutant of *Pseudomonas aeroginosa*. Lett. Appl. Microbiol. 21, 176.

Kosaric N., 1992, Biosurfactant in industry. Pure Appl. Chem. 64, 1731.

Mukherjee S, P . Das and R. Sen, 2006, Towards commercial production of microbial surfactants. Trends Biotechnol. 24, 509.

Mulligan C.N., 2005, Environmental applications for biosurfactants. Environ. Pollut. 133, 183.

Nitschke M. and G.M. Pastore, 2006, Production and properties of a surfactant obtained from *Bacillus subtilis* grown on cassava wastewater. Bioresource Technol. 97, 336.

Poncin-Epaillard F. and S. Vallon S, 1997, Illustration of surface crosslinking of different polymers treated in argonplasma. Macromol. Chem. Phys. 198, 2439.

Rahman K.S.M., T.J. Rahman, S. McClean, R. Marchant and I.M. Banat, 2002, Rhamnolipid biosurfactant production by strains of *Pseudomonas aeruginosa* using low-cost raw materials. Biotechnol. Prog. 18, 1277.

Rodrigues L.R., J.A.Teixeira and C. Henry, 2006, Isolation and partial characterization of a biosurfactant produced by *Streptococcus thermophilus* A. Colloides Surf. B: Biointerfaces 53, 105.

Van Hamme J.D., A. Singh and O.P. Ward, 2006, Physiological aspects. Part 1 in a series of papers devoted to surfactants in microbiology and biotechnology. Biotechnol. Adv. 24, 604.

CHEMICAL ENGINEERING TRANSACTIONS, Volume 14, 2008
Edited by G. Marino, E. Bardone, A. Viglia
 ISBN 978-88-95608-02-0

Fructooligosaccharides production from sucrose by *Aspergillus sp.* N74 immobilized in calcium alginate

Sánchez O.[a], Guío F.[b], García D.[b], Algecira N. [b], Silva E.[c], Caicedo L.[b]
[a] Department of Chemical Engineerting–Product and Process Design Group
Universidad de los Andes, Carrera 1E No. 19 A 40, Bogotá, Colombia
osanchez@uniandes.edu.co
[b]Department of Chemical Engineering–Chemical and Biochemical Process Group
Universidad Nacional de Colombia, Cra 30 Calle 45, Bogotá, Colombia
faguiov@unal.edu.co, dcgarciag@unal.edu.co,naalgecirae@unal.edu.co,
lamesac@unal.edu.co
[b]Department of Chemical Pharmaceutics,Universidad Nacional de Colombia,
Cra 30 Calle 45, Bogotá, Colombia
esilvag@unal.edu.co

Batch fructooligosaccharides (FOS) production by fructosyltransferase from *Aspergillus sp.* N74 immobilized in calcium alginate was studied. The used biomass for immobilization was obtained in 250 ml shake flask from the culture of 10^6 *Aspergillus sp.* N74 spores in 100 mL medium during 48 h. After biomass immobilization, the sucrose bioconversion was carried out with a mean dry weight biomass:reaction volume ratio of 0.4:100. pH, temperature and initial sucrose concentration effect on FOS production was evaluated, obtaining the higher transfructosylating activity and hydrolytic activity relation (3.78 to 5.62) at pH 5.0, 55ºC and 55-80% initial sucrose concentration for 5 h; at these conditions were obtained the greatest FOS productions (~ 50 % $^{w}/_{w}$ in sucrose basis). The results suggest that the fructosyltransferase from the native strain *Aspergillus sp.* N74 could be an appropriated enzyme for the commercial production of FOS.

1. Introduction

Fructooligosaccharides (FOS) are oligosaccharides of fructose containing a single glucose moiety, they are produced by the action of fructosyl transferasa (FTase, E.C. 2.4.1.9) from many plants and microorganisms. The FOS formed contains fructosyl units bounded at the β-2,1 position of sucrose, they are mainly composed by 1-kestose, nystose and 1-β-fructofuranosyl nystose (Sangeetha *et al.*, 2005b; Kaplan and Hutkins 2000; Yun, 1996; Hidaka *et al.*, 1988). FOS with low polymeric grade display better therapeutic properties than those with a high polymeric degree. They are about 0.4 and 0.6 times as sweet as sucrose and have been used in the pharmaceutical industry as a functional sweetener (Sangeetha *et al.*, 2005b; Biedrzycka and Bielecka, 2004; Heyer and Wendenduerg, 2001; Yun, 1996; Kühbauch, 1972). FOS present properties such as low caloric values, noncariogenic properties, decrease levels of phospholipids, triglycerides and cholesterol, help gut absorption of calcium and magnesium, are useful for diabetic products and are used as prebiotics to stimulate the bifidobacteria growth in

the human colon (Sangeetha *et al.*, 2005b; Biedrzycka and Bielecka, 2004; Roberfroid and Delzenne, 1998; Yun, 1996; Crittenden and Playne, 1996; Yamashita *et al.,* 1984).

FOS are industrially produced from sucrose by microbial enzymes with transfructosylating activity. Most of these enzymes have been found in fungi such as *Aspergillus*, *Aureobasidum, Arthrobacter* and *Fusarium*. Nevertheless, commercial FOS may contain glucose, fructose and sucrose in more than 500 g per kg of total FOS dry weight (Sangeetha *et al.*, 2005a-b; Yun, 1996).

FOS production with immobilized *Aspegillus japonicus* entrapped in calcium alginate (Cruz *et al.*, 1998) and gluten (Chien *et al.*, 2001) have been made. With the different immobilization techniques the possibility of continuous process for FOS production is being considered, using other microorganisms like *Aureobasidium pullulans, Aspergillus japonicus* (Sheu *et al.*, 2002) and *Penicillium citrium* (Park *et al.*, 2005), achieving positive results with respect to enzyme activity and a reaction time near to FOS production with free microorganisms (Kim *et al.,* 1996).

Thus, the searches of new potent transfructosylating–enzyme producers with their best reaction conditions are desirable in order to scale-up the process. In this study was evaluated the batch-FOS production from sucrose by immobilized cells of *Aspergillus sp* N74 in calcium alginate.

2. Materials and methods

2.1 Chemicals

Sodium alginate used for immobilization procedure was purchased to Sigma (USA). The sucrose was food–grade, while other chemicals were analytical grade.

2.2 Microorganism and spore production

The fungus *Aspergillus sp.* N74 was isolated from a sugar cane crop in La Peña (Colombia). In a previous study (Sánchez, 2006), this strain showed a high transfructosylating activity and the best sugar-bioconversion was at pH 5.5, 60ºC and initial sugar concentrations higher than 55% (w/v). The strain was cultivated on malt extract agar (MEA) plates at 30±1ºC for 7 days. To prepare spore suspensions, spores were scraped down from the MEA plates with a sterilized tensoactive solution (15% w/v glycerol, 0.1% w/v Tween 80 and acetate buffer 0.1M (pH 6.0) q.s.f. 100 mL) and diluted to a concentration of about 1×107 spores mL-1 with sterilized water. The spore suspensions were kept at –20±1ºC and subcultured once a month.

2.3 Biomass Production

For the different assays the biomass production was made in 250 ml shaker flasks with 100 mL of culture medium (11% sucrose, 0.84% K_2HPO_4, 0.102% $MgSO_4 \cdot 7H_2O$, 0.088% KCl, 0.007% $FeSO_4 \cdot 7H_2O$, 0.085% $NaNO_3 \cdot 4H_2O$, 2.0% yeast extract, 0.136% $CaCO_3$, adjust to pH 5.5±0.1 with HNO3) inoculated with 1000 µL of $1x10^7$ spores ml^{-1} shaken at 30±1ºC and 250 r.p.m. for 48h (New Brunswick C76). The obtained biomass,

it was filtered and washed twice with phosphate buffer 50 mM (pH 5.5) before immobilization.

2.4 Mycelia immobilization

For the immobilization procedure, mycelia of the strain *Aspergillus sp.* N74 was homogenized with 50 mL 2% (w/v) of sodium alginate. The gel produced was pump by a peristaltic pump (Cole-Parmer-77200). The drops from this falling into a 0.2 M $CaCl_2$ under constant and weak agitation, changed into calcium alginate beads. The beads were kept at 4ºC for 24 h before use.

2.5 Enzymatic Reaction

The enzymatic reaction was carried out at temperature range 45-60 ºC, pH range 5.0-6.0 and 30-80% ($^{w}/_{v}$) initial sucrose concentration at 150 r.p.m. for 5 h. During the reaction time supernatant samples were taken for sugar analysis. The reaction was stopped by heating each sample in boiling water for 10 min.

At the end of the reaction, the biomass concentration was determinated after washing the pellets with 7% (w/v) sodium citrate. The obtained biomass was washed with 50 mM phosphate buffer (pH 5.5) and dried for 48 h at 105°C (Dorta *et al.*, 2006; Cruz *et al.*, 1998).

The transfructosylating activity and the hydrolytic activity were determined by measuring both the glucose (G) and fructose (F) present in the reaction mixture. One unit of transfructosylating activity was defined as the amount of enzyme required to transfer 1 µmole of fructose min−1. One unit of hydrolytic activity was defined as the amount of enzyme required to release 1 µmole of free fructose min^{-1}.

The enzymatic productivity was calculated as the transfructosylating (U_{tE}) or hydrolytic (U_{hE}) activity per reaction volume, while the specific activity was calculated as the transfructosylating (U_{tS}) or hydrolytic (U_{hS}) activity per dried weighted biomass (Fernández et al., 2004; Hidaka et al., 1988; Nguyen et al., 1999). Transfructosylating (U_t) and hydrolytic (U_h) activities were calculated at a time interval by Eq. 1 and 2, respectively.

$$U_t = \frac{\left\{ \mu\text{mol Glucose}\big|_{t_i} - \mu\text{mol Glucose}\big|_{t_0} \right\} - \left\{ \mu\text{mol Fructose}\big|_{t_i} - \mu\text{mol Fructose}\big|_{t_0} \right\}}{(t_i - t_0)} \quad (1)$$

$$U_h = \frac{\mu\text{mol Fructose}\big|_{ti} \quad \mu\text{mol Fructose}\big|_{t0}}{(t_i - t_0)} \quad (2)$$

Specific activity and volumetric productivity of the enzyme were evaluated through Eq. 3-4 and Eq. 5-6, respectively.

$$U_{tS} = \frac{U_t}{mg \text{ dried biomass}} \quad (3)$$

$$U_{hS} = \frac{U_h}{mg \text{ dried biomass}} \quad (4)$$

$$U_{tE} = \frac{U_t}{\text{Reaction volume}} \quad (5)$$

$$U_{hE} = \frac{U_h}{\text{Reaction volume}} \quad (6)$$

2.6 Analysis of sugars

The analysis of sugars was performed by high performance liquid chromatography (HPLC). The HPLC equipment consisted of a pump Waters 515 with an on line degasser, a refractive index (RI) detector Waters 410 and injection valve with a 20 μL loop.

A Sugar-Pak^{TM} (Waters) column was used for sucrose, glucose and fructose identification and quantification. The chromatographic conditions were: column temperature, 84 ºC; mobile phase, water at flow rate of 0.4 cm^3 min^{-1} and RI detector temperature, 40 ºC (Sánchez, 2006).

3. Results and discussions

Sucrose was rapidly converted into FOS and glucose. The results showed that increasing the initial sucrose concentration is increased the FOS production. Likewise results are reported by Hidaka *et al.* (1988), who observed the higher synthesis of FOS in concentrated sucrose solutions, although they tested sucrose concentrations up to 50%. Park and Almeida (1991), verified a considerable increase in FOS production and a decrease in the content of free fructose in the middle of the reaction when the sucrose concentration was increased from 30% to 60%, which was explained by the competition among water and substrates used as acceptors in the reactions catalyzed by the β-fructosyltransferase. Fernández *et al.,* (2004), Beker *et al.,* (2002), Yun *et al.,* (1990), Hidaka *et al.,* (1988), have reported the same performance.

The initial sucrose concentration and pH increased favored the transfructosylating activity and transfrutosylating volumetric productivity. The maximum specific transfructosylating activity and consequently volumetric productivity was obtained at pH 6.0 and 60ºC, (Fig. 1-2) but at this condition was obtained the highest hydrolytic activity and volumetric productivity. The remnant sucrose was no higher than 15% at the end of 5h but no significant differences in the activities were found between the first hour and the end of the reaction (5h). Likewise Hayashi *et al.,* (1992) and Cruz *et al.,* (1998), obtained the same perform for the enzyme produced by *Aspergillus japonicus*. This probably could be by the higher product intraparticle transportation time that favors the hydrolytic activity of the enzyme.

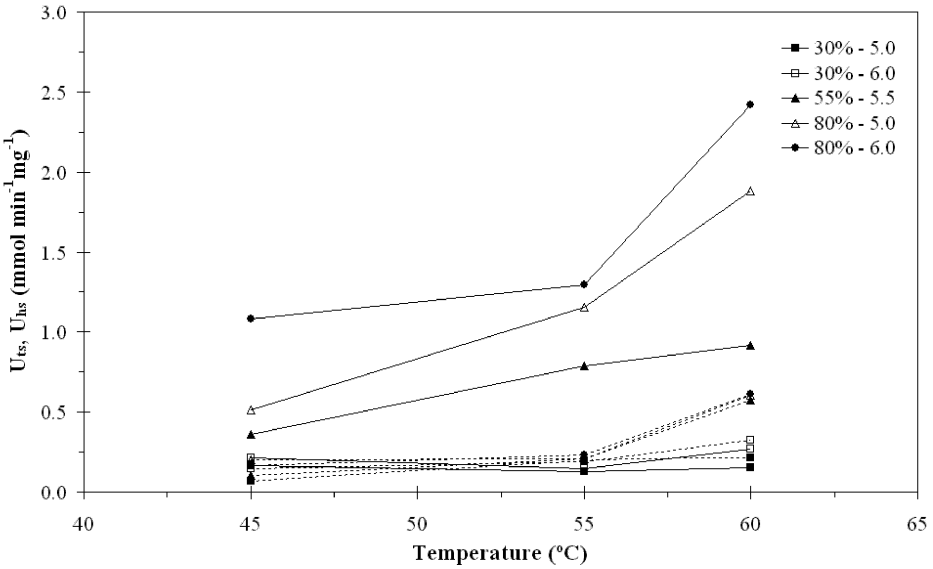

Figure 1. *pH, temperature and initial sucrose concentration effect on the specific transfructosylating (—) and hydrolytic (---) activity of the FTase produced by the immobilized mycelium of Aspergillus sp. N74 in calcium alginate.*

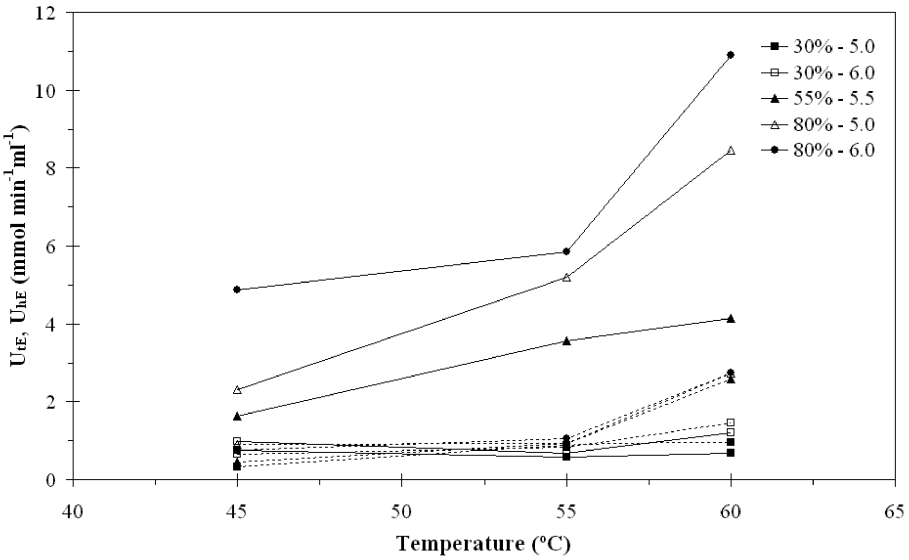

Figure 2. *pH, temperature and initial sucrose concentration effect on the volumetric transfructosylating (—) and hydrolytic (---) productivity of the FTase produced by the immobilized mycelium of Aspergillus sp. N74 in calcium alginate.*

Cruz *et al.,* (1998) have reported a transfructosylating activity and hydrolytic activity ratio from 1.94 to 8.91 for *Aspergillus japonicus* immobilized in calcium alginate at 60ºC, 60% initial sucrose concentration, pH 5.0. In this study, were obtained the better ratios (from 3.78 to 5.62) at pH 5.0, 55ºC and 55-80 % initial sucrose concentration. The result displayed an ezyme activity loss at 60°C due to the diminution on the U_t:U_h ratio (Table 1).

Table 1. U_t:U_h ratio for tested conditions

Initial sucrose (%) and pH	U_t:U_h ratio Temperature (°C)		
	45	55	60
30 %, pH 5.0	2.36	0.64	0.71
30 %, pH 6.0	1.47	0.79	0.83
55 %, pH 5,5	3.58	3.78	1.59
80 %, pH 5,0	2.53	5.62	3.10
80 %, pH 6,0	5.49	5.52	3.97

The best conditions for FOS production by the immobilized *Aspergillus sp.* N74 cells were like for the free cells reported by Sánchez (2006). At pH 5.0 and 60ºC with initial sucrose concentrations higher than 55%$^{w}/_{v}$, the FOS production was about a 50%$^{w}/_{w}$.

Several authors who have worked with immobilized cells (like *Penicillium citrinum* KCCM11663, *Aspergillus japonicus* and *Aureobasidium pullulans*) or immobilized enzyme (purified or commercial like Pectinex Ultra SP-L) have reported optimal values of pH, temperature and initial sucrose concentration, 5.0-6.0, 50-60ºC and 50-80%, respectively (Park *et al.,* 2005; Tanriseven and Aslan, 2005; Chien *et al.,* 2001; Yun *et al.,* 1990).

The enzymatic activity and productivity are influenced by the cell entrapping in calcium alginate. Compared the obtained enzyme activity and productivity for the free (Sánchez, 2006) and immobilized cells, there was a decrease of the calculated values U_{tS}, U_{hS}, U_{tE} and U_{hE} for all essay conditions with the immobilized microorganism. The loss of enzymatic activity could be due to the enzyme leakage from the permeabilized cells, which were entrapped in the alginate beads and chemical interactions between the polymeric matrix and the cells, which affected the enzyme production (Chien *et al* 2001).

Additionally, comparing FOS concentrations gotten in both cases, an increase in reaction time is observed to get a similar FOS production using free cells. This delay in the reaction time was probably due to the mass transfer limitation in the immobilized particles where contribution of diffusion resistance in the alginate matrix to the enzymatic reaction was evident. This behaviour is very similar to the results reported by Chien *et al.* (2001) and Yun *et al.* (1990), who carried out the FOS production using immobilized cells of *A. japonicus* in gluten and *Aureobasidium pullulans* entrapped in calcium alginate beads, respectively.

4. Conclusions

The *Aspergillus sp.* N74 immobilized in calcium alginate present a favorable performance for the fructooligosaccharides production. The specific transfructosylating activity showed a dependence on the reaction pH, temperature and initial sucrose concentration. The highest transfructosylating activity was found at 60ºC, pH 5.0 and a initial sucrose concentration higher than 55%$^{w}/_{v}$ with a Ut/Uh from 3.78 to 5.62.

The immobilization of the native strain *Aspergillus sp.* N74 could be an appropriated alternative for the study of scaled-up process of commercial FOS.

5. References

Beker, M., J. Laukevics, D. Upite, E. Kaminska, A. Vignats, U. Viesturs, L. Pankova and A. Danilevics, 2002, *Process Biochem.*, 38:701-706

Biedrzycka, E. and M. Bielecka, 2004, *Trends Food Sci. Technol.*, 15:170-175

Casas López, J.L., J.A. Sánchez Pérez, J.M. Fernández Sevilla, E.M. Rodríguez Porcel and Y. Chisti, 2005, *J. Biotechnol.*, 116:61–77

Chien, C.S., W.C. Lee and T.J. Lin, 2001, *Enzyme Microb. Technol.*, 29:252- 257

Crittenden, R.G. and M.J. Payne, 1996, *Trends in Food Science and Technology*, 7: 353-362

Cruz, R., V.D. Cruz, M.Z. Belini, J.G. Belote and C.R. Vieira, 1998, *Bioresour. Technol.*, 65:139-143

Dorta, C., Cruz, R., Oliva-Neto, P. and Camargo, D. J., 2006, J. Ind. *Microbiol. Biotechnol.* 33:1003–1009

Fernández, R.C., B. Guilarte, A. Juárez and J. Martinez, 2004, *J. Chem. Technol. Biotechnol.*, 79:268-272

Hayashi, S., K.M. Takasaki, H. Ueno and K. Imada, 1992. *World J. Microbiol. Biotechnol.*, 8:155-159

Heyer, A.G. and R. Wendenduerg, 2001, *Appl. Environ. Microbiol.*, 67:363-370

Hidaka, H., M. Hirayama and N. Sumi, 1988, *Agric. Biol. Chem.* 52:1181-1187

Kaplan, H. and R.W. Hutkins, 2000, *Appl. Environ. Microbiol.* 66:2682-2684

Kim, M.H., M.J. In, H.J. Cha and Y.J. Yoo, 1996, *J. Ferment. Bioeng.*, 82(5):458 – 463.

Kühbauch, W., 1972, Changes of the contents in glucose, fructose, sucrose and fructosans, as well as in the degree of polymerization of fructosan's molecules, in small leaves and stems of Orchard Grass during their growth. *Landwirtsch. Forsch.* 26, 2:173-181 (in German)

L'Hocine, L., Z. Wang, B. Jiang and S. Xu, 2000, *J. Biotechnol.*, 81:73-84.

Madlova, A., M. Antosova, M. Barathova, M. Polakovic, V. Stefuca and V. Bales, 1999, *Chem. Pap.*, 53(6) 366-369

Nguyen, Q.D., F. Mattes, A. Hoschke, J. Rezessy-Szabó and M.K. Bhat, 1999, *Biotechnol. Lett.*, 21:183-186

Park, M.Ch., J.S. Lim, J.Ch. Kim, S.W. Park, S.W. Kim, 2005, *Biotechnol. Lett.*, 27:127-130

Paul, G.C. and C.R.Thomas, 1998, *Adv. Biochem. Eng.*, 60:1-59

Roberfroid, M.B. and N.M. Delzenne, 1998, *Annu. Rev. Nutr.,* 18:117-143

Sánchez, O.F., 2006, Study of fructosyltransferase production by an Aspergilllus sp. native strain from sucrose in a bench-scale membrane reactor. M.Sc. Chemical Engineering Thesis, Universidad Nacional de Colombia, Sede Bogotá. (in Spanish).

Sangeetha, P.T., M.N. Ramesh and S.G. Prapulla, 2005a, *Process Biochem.*, 40:1085-1088

Sangeetha, P.T., M.N. Ramesh and S.G. Prapulla, 2005b, *J. Food Process. Eng.*, 68:57-64

Sheu, D., K.J. Duan, Ch.Y. Cheng, J.L. Bi and J.Y. Chen, 2002, *Biotechnol. Prog.*, 18:1282-1286

Tanriseven, A. and Y. Aslan, 2005, *Enzyme Microb. Technol.*, 36:550-554

van Balken, J.A.M., Th.J.G.M van Dooren, W.J.J. van den Tweel, J. Kamphuis and E.M. Meijer, 1991, *Appl. Microbiol. Biotechnol.*, 35:216-221

Yamashita, K., K. Kawai and M. Itakura, 1984, *Nutr. Res.*, 4:961-966

Yun J.W., K.H. Jung, J.W. Oh and J.H. Lee, 1990, *Appl. Biochem. Biotechnol.*, 24/25:299-308

Yun, J. W., 1996, *Enzyme Microb. Technol.*, 19:107-117

CHEMICAL ENGINEERING TRANSACTIONS, Volume 14, 2008
Edited by G. Marino, E. Bardone, A. Viglia
 ISBN 978-88-95608-02-0

Comparative Batch Growth Studies of Pure *Lactobacillus* Strains and Their Co-culture in Synthetic Medium with Different Neutralizing Agents

Manoj K. Ghosh[1], U.K. Ghosh[2]
Department of Paper Technology, Indian Institute of Technology Roorkee,
Saharanpur Campus, Saharanpur-247001, India
E-mail: [1]mkengg2004@rediffmail.com, [2]ghoshuk_iitr@yahoo.com

Lactobacillus strains have immense potential of being utilized as multifunctional microorganism used in various chemical, biochemical, food, pharmaceutical and dairy industries. Lactic acid (2-hydroxy propanoic acid) synthesized by different *Lactobacillus* strains serves as feed stock for various industries. To suppress the inhibitory effects of free lactic acid on microbial growth and synthesis, during fermentative production of lactic acid, the free lactic acid has to be converted to lactate form by employing neutralizers such as NaOH, $CaCO_3$, etc. In the earlier investigations, inhibitory effects of calcium carbonate towards growth and production and the specific role of calcium ions in phage infection of *Lactobacillus* have been reported. Therefore, in the present studies treatment of *Lactobacillus* with NaOH has been compared with that of $CaCO_3$ which is commonly used neutralizer in lactic acid fermentation. In present experimental investigation, studies on anaerobic batch fermentation with *Lactobacillus delbrueckii* (NCIM 2025), *L. pentosus* (NCIM 2912) and their co-culture have been carried out using glucose based synthetic media at 37°C, 180 rpm, initial pH 6.5 with pH maintained at 5.6 using either NaOH or $CaCO_3$ as neutralizer every 12 h. The first set of experiments with NaOH as neutralizer showed highest cell dry weight for *L. delbrueckii, L. pentosus* and their co-culture as 6.69, 11.51 and 23.95 g/l in 24, 24 and 36 h, respectively, while lowest pH values were 4.70, 4.55 and 4.50 attained in 48, 36 and 48 h, respectively. However, in the second set of experiments with $CaCO_3$ as neutralizer, the highest cell dry weights for *L. delbrueckii, L. pentosus* and their co-culture were observed as 9.09, 12.89 and 16.08 g/l, respectively in 48 h, while lowest pH values were 4.80, 4.70 and 4.88 attained in 48, 48 and 12 h, respectively.

1. Introduction

Lactobacilli are potent producers of wide range of antagonistic primary and secondary metabolites such as, organic acids, diacetyl (flavouring agent), bacteriocins (nisin) and antibiotics (Ross et al. 2002). Todorov et al.(2007) reported that *Lactobacilli* are also in demand for probiotic properties, as they play an important role in stabilizing the intestinal microflora by checking the colonization of pathogenic microorganisms. *Lactobacillus sp*. synthesize lactic acid (2- hydroxy propanoic acid) as their major product, that finds application in food, pharmaceutical and cosmetic industries and has various other industrial applications such as feedstock in preparation of different

chemicals (acrylic acid, propylene glycol, acetaldehyde and 2,3 pentandione), in adhesive formulation, as detergent builders, as terminating agents in phenol formaldehyde resins. Esters of lactic acid (stearoyl-2-lactylate, glyceryl lactopalmitate and glyceryl lactostearate etc.) are used as emulsifying agents in baking foods (Narayanan et al.2004a). It also serves as raw material for the production of poly lactic acid (PLA) which is a ecofriendly biodegradable polymer (Calabia et al. 2006). Adsul et al. (2007) reported that approximately 90% of world wide lactic acid production is through microbial fermentation and the rest is through hydrolysis of lactonitrile. Lactic acid production through chemical synthesis provides racemic DL lactic acid while microbial fermentation gives steriospecific L(+), D(-) or DL lactic acids based on specific microbial strains used (Altaf et al. 2006). The separation of particular form of lactic acid isomer from the racemic mixture is difficult and involves costly chromatographic techniques, hence production of lactic acid by microbial fermentation serves as a better option (Narayanan et al.2004b). Presser et al. (1997) reported that organic acids such as lactic acid are inhibitory towards bacterial growth as they can chelate essential growth elements like iron , while its undissociated form is lipophilic that could enter the bacterial cell and cause greater inhibition than externally active strong mineral acid. It has been reported by Mirdamadi et al.(2002) that without pH control of the fermentation broth, yield of lactic acid decreases by 30 – 50%, hence neutralizing agents such as sodium hydroxide, calcium carbonate and ammonium hydroxide are usually added, for higher yield of lactic acid. Inhibitory effect of $CaCO_3$ has also been observed on growth and production of *Lactobacillus* strains and pellet formation in *Rhizopus oryzae*. Sodium and calcium ions play biologically significant roles in prokaryotic and eukaryotic cells. It is reported by Sherman et al.(2006) that calcium is present in lower concentration than the sodium ions in the cells, and the cells keep calcium ions at low level as at higher concentrations calcium ions can bind to proteins and alter their enzymatic properties.

Thus with an objective to determine the effect of neutralizing agents like NaOH and $CaCO_3$ on biomass growth (cell dry weight) and pH drop(acid formation) , the present study included batch experiments with *Lactobacilli* pure culture and co-culture in glucose based synthetic media at 180rpm, 37^0C, initial pH6.5 and with pH maintained at 5.60. The study also evaluates the compatibility of co-culture with the neutralizing agent applied in terms of biomass growth and acid formation with respect to the *Lactobacillus* pure cultures.

2. Background Information

A living cell has to perform work in order to maintain difference in the composition of its internal medium with respect to the external one. When the work is carried out for the movement of solutes across the cell membranes, active transport of solutes across the cell membranes takes place against their electrochemical potential gradient. But diffusion of solutes (if polar) through membranes takes place down the electrochemical potential gradient, aided by the carrier proteins that overcome the activation energy required by that solute to enter through the lipid portion of the membrane (Jennings, 1995). During the fermentative production of lactic acid the enhancement of lactic acid concentration is reflected in the decline of pH in the fermentation broth. The

undissociated form of lactic acid is a strong growth inhibitor which diffuses across the cell membrane. Various theories have been proposed (Pieterse et al., 2005) about inhibitory effects of lactic acid on bacterial growth such as (i) Cytosol acidification due to acid influx, (ii) Dissipation of membrane potential and (iii) Accumulation of anions intracellularly. Intracellular accumulation of lactate anions from the diffusion of lactic acid in media can cause loss in water activity and end product inhibition, that can impede the regeneration of NAD^+ for the *Lactobacilli* under the anaerobic conditions when their cells could not regenerate NAD^+ through NADH oxidase. Thus it is suitable for *Lactobacilli* to maintain a proton gradient across the cell membrane, possessing a higher intracellular pH, than that of extra cellular medium. The influx of undissociated form of lactic acid (present in fermentation broth) in the bacterial cells causes the acidification of cytoplasm and dissipation of proton gradient. The cell in response effects extrusion of protons to maintain the proton gradient through energy dependent transport process. Hence the extra expenditure of energy on the internal pH maintenance causes growth inhibition and the growth may stop when the pH gradient collapses due to scarcity of catabolic energy meant for preventing the influx of undissociated acid in the cell (Bigelis et al., 1994). Effects of neutralizers such as NaOH, $CaCO_3$ and NH_4OH and their lactate salts on biomass growth and lactic acid production have been reported by (Hongo et al., 1986) Thus suitable neutralizing agents for pH control in fermentation broth during lactic acid production becomes necessary for conversion of undissociated lactic acid to their corresponding lactate salts.

3. Materials and Methods

The chemicals used in the present studies were of S. d. Fine, Qualigen and Merck make. Pure cultures of lactic acid bacteria, *Lactobacillus delbrueckii* NCIM 2025 and *L.pentosus* NCIM 2912 obtained from National Chemical Laboratory, Pune, India, were stored in MRS agar slants and subcultured monthly as directed. For carrying out the experiments on glucose based media, the above mentioned pure strains of *Lactobacilli* and their co-culture were precultured in MRS medium at 30°C and 150 rpm for 9 hours. The co-culture of *Lactobacilli* was prepared by using equal portions of inoculum dose from the two pure strains in the MRS media at 30°C and 150 rpm for 9 hours. Composition of one litre MRS medium was: 10g proteose peptone, 5g yeast extract, 10g beef extract, 20g dextrose, 1g tween 80, 2g ammonium citrate, 5g sodium acetate, 0.1g $MgSO_4.7H_2O$, 0.05g $MnSO_4$, 2g K_2HPO_4. One litre of glucose based synthetic media consists of : 60g glucose, 1.5g yeast extract, 0.1g sodium acetate, 0.05g KH_2PO_4, 0.05g K_2HPO_4, 0.02g $MgSO_4$, 0.003g $MnSO_4$, 0.003 $FeSO_4$. Two sets of fermentation experiments were carried out taking both the *Lactobacillus* pure cultures and the co-culture at 37°C, 180 rpm, 1.55 g/l (cell dry weight) inoculum with pH maintained at 5.60 at every 12 h with either 2% NaOH or 2% $CaCO_3$ as neutralizing agent. Initial pH was kept at 6.5 for each experiment. Biomass (cell dry weight) during fermentation in synthetic media was determined at every 12 h interval. The fermentation broth was centrifuged at 8000 rpm for 10 minutes to separate the cells from broth, leaving the supernatant. The precipitated cells were washed with 0.85% NaCl (to remove any remaining substrate) and were dried in preweighed

microporous papers at 70°C till attainment of constant weight. The pH values of fermentation broths due to acid production were recorded at every 12 h interval with the help of a digital pH meter.

4. Results and Discussions

The results of the batch experiments on glucose based synthetic media treated with NaOH or $CaCO_3$ as neutralizers have been provided in Table-1 and 2. For the first set of experiments using NaOH as neutralizer on glucose based synthetic production media (initial pH 6.5) with *Lactobacillus sp.* pure cultures and co-culture Fig.1 and Table 1 indicate that highest biomass (cell dry weight) production exists with co-culture. The co-culture has shown a higher pH drop (hence higher acid formation) with respect *Lactobacillus* pure cultures through the course of fermentation. From Fig. 1 and Table 1 it is also evidenced that during 24 to 60 h period for pure cultures and 24 to 48 h duration for co-culture, there is gradual increase of biomass (cell dry weight) every time accompanied by sharp pH drops from pH 5.6 indicating higher acid production which is probably because the cells were in a physiological state that favours more towards acid production than the biomass growth. This duration also includes the stationary phase of the batch curve. It is observed from Fig. 1 that, the stationary phase for the co-culture occurs later than the pure culture strains as the cells of the co-culture were actively engaged both in growth and acid synthesis. The co-culture had longer log phase, which can serve as significant basis for its use in industrial fermentation. The higher pH drops effected by pure strains and co-culture every 12 h as mentioned in Table 1, can be attributed to the beneficial effects of periodic make up of pH up to 5.6 every 12 h with NaOH as neutralizer to minimize

Table 1: Biomass growth and pH drop effected by *Lactobacillus sp.* pure strains and their co-culture with NaOH as neutralizer.

Time (h)	*L. delbrueckii*		*L. pentosus*		Co-culture	
	Biomass, g/l	pH	Biomass, g/l	pH	Biomass, g/l	pH
0	1.55	6.50	1.55	6.50	1.55	6.50
1.25	1.56	6.35	1.60	6.30	1.95	6.26
12	4.88	5.20	9.69	5.50	20.60	5.28
24	6.69	4.80	11.51	5.30	22.06	4.68
36	6.68	4.79	11.40	4.55	23.95	4.60
48	6.16	4.70	10.44	4.64	23.90	4.50
60	5.08	4.76	9.69	4.85	18.23	4.68
72	4.88	4.95	8.95	4.88	15.12	4.78
84	4.82	5.12	8.10	5.25	14.10	4.96
96	3.51	5.09	7.27	5.44	13.50	5.08
108	1.56	4.98	3.92	5.40	12.07	4.93

product inhibition in acid synthesis. In 84 h to 108 h duration the pH drop effected by *L.delbrueckii* is higher than the *L. pentosus* possibly due to higher temperature adaptability of *L. delbrueckii* (37 to 42 °C).

Table 2 : Biomass growth and pH drop effected by *Lactobacillus sp.* pure strains and their co-culture with $CaCO_3$ as neutralizer.

Time, h	*L. delbrueckii*		*L. pentosus*		Co-culture	
	Biomass, g/l	pH	Biomass, g/l	pH	Biomass, g/l	pH
0	1.55	6.50	1.55	6.50	1.55	6.50
1.25	1.56	6.42	1.60	6.46	1.98	6.40
12	4.20	5.60	4.64	5.44	11.52	4.88
24	7.25	5.28	5.06	5.20	12.36	5.34
36	8.95	5.16	12.61	4.88	15.75	5.14
48	9.09	4.80	12.89	4.70	16.08	5.38
60	5.36	4.89	10.01	5.22	10.04	5.42
72	4.13	5.30	8.51	5.18	8.82	5.40
84	3.64	5.27	7.55	5.10	7.25	5.43
96	3.12	5.23	7.10	5.06	6.34	5.47
108	3.05	5.14	4.89	4.71	5.46	5.48

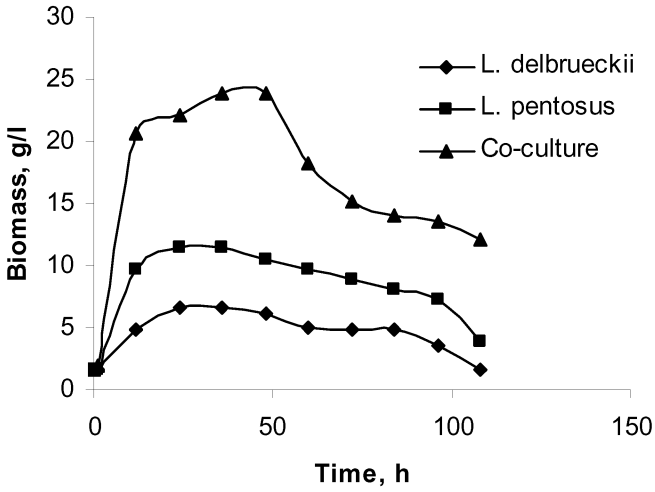

Figure 1: Variation in biomass growth with progress of fermentation in synthetic production medium with NaOH as neutralizer.

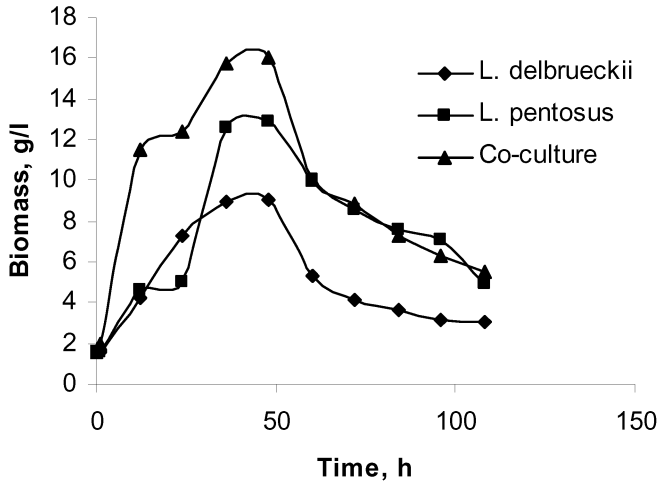

Figure 2: Variation in biomass growth with progress of fermentation in synthetic production medium with $CaCO_3$ as neutralizer.

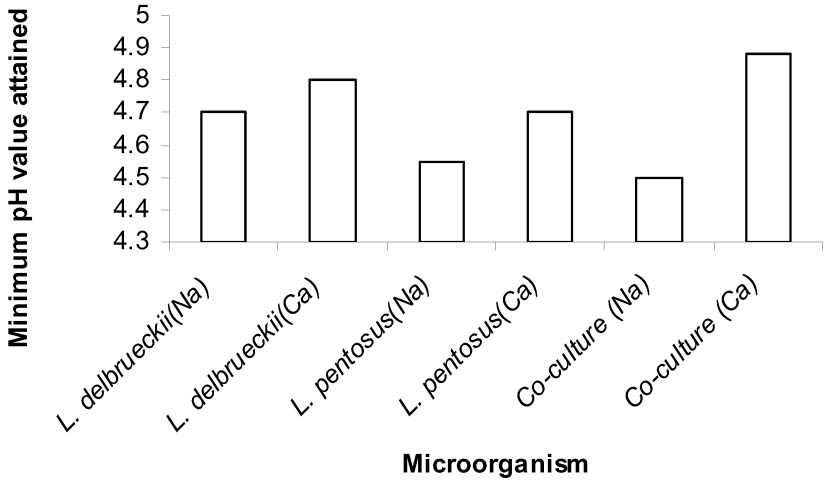

Figure 3: Minimum pH attained by Lactobacillus pure cultures and their co-culture in synthetic production medium with NaOH or $CaCO_3$ as neutralizer.

It is observed from Table 1 and Fig. 1 that the co-culture bears superiority over the *Lactobacillus* pure strains in synthetic production media with NaOH, because it exhibits advantageous traits such as, (i) higher biomass concentration (indicating

higher growth rate) at the end of log phase, which is accompanied with lowest pH drop value (hence higher acid synthesis), (ii) has longer log phase than the pure strains, with more biomass and higher pH drop values and (iii) better acid tolerance, as it produces high biomass even at low pH value in NaOH containing fermentation broth. In the first set of batch experiments with *L. delbrueckii, L. pentosus* and co-culture the pH drop in synthetic production medium with NaOH treatment, increased with increasing biomass formation in the log phase while the pH drop decreases with decrease in biomass concentration from stationary phase onwards till end of fermentation, which indicates reduction in acid production.

In the second set of batch experiments with $CaCO_3$ as neutralizer it can be observed from Table 2 and Fig. 2 that there is over all increase in biomass growth of pure *Lactobacillus* cultures as compared to those attained in the batch experiments with NaOH as neutralizer. Above observation can be due to the fact that calcium ions take part in cell division in some *Lactobacillus* species, as also reported earlier (Kojinin et al., 1970). However, the fall in pH values (hence acid formation) is lesser with $CaCO_3$ as compared to that in case of NaOH is evidenced from Fig. 3. Huang et al. (2004), reported a similar observation regarding fall in lactic acid yield above 1% $CaCO_3$ treatment of media in case of *Rhizopos oryzae* and *R. arrhizus*. Wantanabe et al. (1972) reported the roll of calcium ions in phage infection of *Lactobacillus sp*. cells, which may also be a possible reason for lower acid production with $CaCO_3$ treatment. It is observed from Table 2 that *Lactobacillus* pure cultures effect a higher fall in pH value as compared to the co-culture in presence of $CaCO_3$. The above observations show that (i) In presence of $CaCO_3$ the *Lactobacillus* cells attain a physiological state where the biomass growth is encouraged more than the acid formation. (ii) The co-culture showed lesser compatibility with $CaCO_3$ treatment in terms of acid production as compared to its performance in NaOH treated synthetic media. It is evident from the pH drop values of *L. delbrueckii* and *L. pentosus* given in Table 1 and Table 2, that NaOH treatment proves better for *L. delbrueckii*. Although *L. pentosus* attained the least pH value of 4.55 with NaOH treatment but it performs better in terms of pH drop (acid formation) in the latter stages (84 - 108 h) of fermentation in case of $CaCO_3$ treatment. Thus a higher acid synthesis activity was achieved for a longer duration by *L. pentosus* during fermentation in case of $CaCO_3$ treatment.

5. Conclusion

The results of the experiments with NaOH showed that the co-culture produces more acid than the pure strains of *Lactobacillus,* whereas in case of $CaCO_3$ treatment acid production was higher with pure strains. With NaOH as neutralizer lower pH values were evidenced in case of co-culture for a longer period of time (24 - 108 h). The lower values of biomass and acid production, in the second set of experiments suggest that $CaCO_3$ has inhibitory effect on the performance of co-culture.

6. References

Adsul M.G., A.J.Varma and D.V. Gokhale, 2007, Lactic acid production from waste sugarcane bagasse derived cellulose, Green Chemistry 9, 58.

Altaf,M., B.J. Naveena and G. Reddy, 2007, Use of inexpensive nitrogen sources and starch for L(+) lactic acid production in anaerobic submerged fermentation, Bioresource Technology 98, 498.

Bigelis, R., and S.P. Tsai, Microorganisms for organic acid production, Food biotechnology: Micro organisms, Y.H. Hui ed., 1994, Wiley- IEEE.

Calabia, B.P. and Y.Tokiwa, 2007, Production of D-lactic acid from sugarcane molasses, sugarcane juice and sugarbeet juice by *Lactobacillus delbrueckii,* Biotechnology Letters 29, 1329.

Hongo, M.,Y.Nomura and M.Iwah, 1986, Novel method of lactic acid production by electrodialysis fermentation, Applied and Environmental Microbiology 52, 316.

Huang, L.P., B. Jin, P. Lant and J. Zhou, 2004, Simultaneous saccharification and fermentation of potato starch waste water to lactic acid by *Rhizopus oryzae* and *Rhizopus arrhizus*, Biochemical Engineering Journal 23, 269.

Jennings, D.H., 1995, Primary active transport, The physiology of fungal nutrition, Cambridge University Press, Cambridge.

Kojinin, M., S. Suda, S. Hotta, K. Hamada and A. Sunganuma, 1970, Necessity of calcium ion for cell division in *Lactobacillus bifidus*, Journal of Bacteriology 104, (2), 1010.

Mirdamadi, S.,H. Sadeghi, N. Sharafi, M. Fallahpour,F.A. Mohseni and M.R. Bakhtiari, 2002, Comparison of lactic acid produced by fungal and bacterial strains, Iranian Biomedical Journal 6, (2&3), 72.

Narayanan, N., P.K. Roychoudhury and A. Srivastava, 2004a, L(+) Lactic acid fermentation and its product polymerization, Electronic Journal of Biotechnology 17, (2), 4.

Narayanan, N., P.K. Roychoudhury and A. Srivastava, 2004b, Isolation of adh mutant of *Lactobacillus rhamnosus* for the production L (+) Lactic acid, Electronic Journal of Biotechnology 17, (1), 2.

Pieterse,B., R.J. Leer, F.H.J. Shuren, and M.J. Vanderwerf, 2005, Unravelling the multiple effects of lactic acid stress on *Lactobacillus plantarum* by transcription profiling, Microbiology 151, 3881.

Pressor, K.A., D.A. Ratkowsky and T. Ross, 1997, Modelling the growth rate of *Escherichia coli* as a function of pH and lactic acid concentration, Applied and Environmental Microbiology 63, (6), 2357.

Ross,P.R., S. Morgan and C.Hill, 2002, Preservation and fermentation: Past, present and future, International Journal of Food Microbiology 79, (1-2), 3.

Sherman, A.S., Y.X. Li and J.E. Keizer, 2006, Whole cell models, Computational Cell Biology, Springer, Delhi (First Indian Reprint).

Todorov, S.D., M. Botes, S.T. Danova and L.M.T. Dicks, 2007, Probiotic properties of *Lactobacillus lactis ssp.lactis* HV219 isolated from human vaginal secretions, Journal of Applied Microbiology 103, 629.

Wantanabe ,K. and S. Taksue, 1972, The requirement of calcium in infection with *Lactobacillus* phage, Journal of General Virology 17, 19.

CHEMICAL ENGINEERING TRANSACTIONS, Volume 14, 2008
Edited by G. Marino, E. Bardone, A. Viglia
 ISBN 978-88-95608-02-0

Biofuels: Dream Or Reality - Enthalpic, Exergetic And Socioeconomical Analysis

Luciano Zanderighi Department of Physical Chemistry and Electrochemistry – University of Milano – Via Golgi 19 20137 Milano

Some aspects of bio fuel production, as a renewable source of energy, are analysed in terms of EROI (Energy Retuned On energy Input). Actually EROI can be evaluated in terms either of enthalpy (first thermodynamic axiom) or of exergy balance (second thermodynamic axiom). The two approaches are analysed and discussed. Bio fuel production competes with food production; moreover a large extension of land must be dedicated to bio fuel production. These and other factors influence the socio-economical conditions and the development of the countries overall the world.
Are bio fuels the right way to the solution of the energy for the world development?

Introduction

Many philosophers and thinkers of the ancient time had a dream: to build-up a device or an engine that could self produce work without any external contribution, which is a "perpetuum mobile". The investigation of such a marvellous engine was alive until 1775 (actually some patents on that subject are claimed also today) when the Académie Royale des Sciences de Paris decided not to publish any memory on whatever argument, design or project, dealing with "perpetuum mobile". This decision was the end line of a long discussion among the scientists, which started with Leonardo da Vinci (1452-1519), Cardano (1501-1576), Stevin (1548-1620), Huygens (1629-1695), and many other scientists, and stated for good the impossibility to produce work from nothing.
The modern version of the "perpetuum mobile" is the dream of the "renewable energy", an inexhaustible source of available energy.
Actually the world has a natural and inexhaustible source of energy in the sunlight that arrives continuously on the earth surface, and distributes in various forms, such as heat, wind, evaporation of water, photosynthesis, etc., some of which may be accumulated and utilized.
Unfortunately solar energy has certain characteristics that do not allow its easy use, such as for instance:

a) high dispersion on the earth surface (mean value 1000 w/m^2);
b) wide spectra of light frequencies (visible radiation is about 41% of all solar radiation with a wavelength in the range 400 e 700nm).
c) the sunlight arrives continuously but it is not continuously available.

For these reasons solar energy must be concentrated and stored. One natural and spontaneous way to store solar radiation is the photosynthesis process that transforms radiation energy into chemical energy.

It is well known that many forms of energy exit, and, according to the first axiom of thermodynamics, all these energies are equivalent and generally treated in terms of enthalpy. Actually not all energies have either the same characteristics nor the same capability to produce useful work. This capability can be assumed as a parameter to measure the quality of the energies.
In thermodynamics the useful work is measured in terms of exergy. According to Gaggioli [1] exergy is defined as the maximum amount of work that can be done by a subsystem as it approaches thermodynamic equilibrium with its surroundings by a sequence of reversible processes. In other words exergy is the amount of energy (enthalpy) that can be transformed in useful work, the other part is called anergy (useless energy).[2,3]
While enthalpy and the sum of exergy and anergy are subject to a conservation law, exergy exempts from it.
All processes dealing with concentration or storage of solar energy, including agriculture production, are analysed in terms of material and energy in- and out-flows, and the efficiency in storing energy is measured in terms of EROI: (Energy Returned)/(Energy Input). However, in many of these balances, the humane work, the energy for plant maintenance and the depreciation of the energy used for the machinery productions and for the plant buildings, are not considered, mainly since it is difficult to evaluate the weight of these energies in the total balance.
Moreover EROI may be evaluated either in terms of enthalpy or in terms of exergy: in the first case it is based on the classical concept of the energy conservation in a process flow sheet, and the difference between in and out enthalpy is a measure of the gain in energy (i.e. solar energy stored); in the second case the energy flows are weighted according to their capability to produce useful work: actually the aim is not to make an energy balance but rather to evaluate the amount of the obtained useful energy with respect to the one used.

Agronomical aspects of bio fuel

As a preliminary information the carbon dioxide reaction rate in photosynthesis process is 800 kg/km^2*h, under optimal irradiation conditions and a fertile land. This means that, by considering a mean irradiation of 8 h/day the theoretical maximum productivity is 48 t/ha*year of dry biomass. Actually the productivity is about half of the theoretical value, since it depends on many factors such as soil fertility, water availability, solar radiation, etc.
Nevertheless reference values of soil productivity are important for making some evaluation of the different agriculture production for bio fuel productions.
In table 1 some data of agricultural crop for biodiesel production are reported.
The process of oil transformation into biodiesel is a simple trans-esterification reaction since, in the presence of basic catalysts, methanol substitutes glycerine in the aliphatic ester.
The yield of the process is about one (w/w), that is one ton of biodiesel is produced from one ton of oil. Researches are studying new plants (Sandbox tree, Sea mango, Jatropha, etc) or genetically modified known plants (molecular assisted breeding), in order to increase the yield in oil (t/ha).

Table 1: Mean values of crop yield (t/ha) in Italy. (1tep=6,841 barrels)

CROP PRODUCTION	BEAN/SEED t/ha	OIL t/ha
RAPESEED	2,5 - 2,6	1,1 - 1,2
SUNFLOWER	2,6 - 3,0	1,3 -1,5
SOY	3,0- 3,5	0,6- 0,7

In India [4] a plant known as *Jatropha curcas*, that can be grown in wastelands, has attracted the interest of farmers, researchers and institutional investors since more than 1800 (l/ha) of oil can be produced.
Bio ethanol can be produced with a fermentation process of a sugar solution. The process is well known, but it is still under study with the aim of reducing the exergy duty.
Recently however, researches have started investigating the possibility to find an innovative process of ethanol production from cellulose competitive or even better, than from sugar.[5]

Table 2: Yield (l of bio ethanol/t of crop) of Bio ethanol from various crops.

BIOMASS	ETHANOL YIELD (l/t of crop)
SUGAR CANE	70
SORGHUM	85
BEET	100
CASSAVA	180
MAIS	360
WHEAT	340
RICE	430

EROI: E(n,x)ergy Returned / E(n,x)ergy Input

While the EROI evaluation in terms of energy (enthalpy) can be performed simply on the bases of a quantified flow sheet of the process, its evaluation in terms of exergy must consider the time and the place where the plant operates, and the final aim of the plant.

The subject of this presentation is the bio fuel production, so the analysis will be limited to this topic. The aim of bio fuel production is to get a fuel useful for feeding engine and vehicles as alternative to fuel of mineral origin.
The exergy returned can be easily evaluated from the process flow sheet. For the evaluation of the exergy input, all production steps from the land until the industrial plant must be considered.
While exergy input in terms of electric energy, gasoil, chemicals, fertilizers, that is all contributions related to material balance, are easily evaluated, on the contrary it is difficult to evaluate it for other inputs, not related to material balance, such as, for instance, human work, machinery, buildings and supporting structure depreciation. The contribution of all this factors to the exergy input can be defined only when time and space are well defined. For instance the contribution, as exergy input, of the human work evaluated today is different from the one evaluated ten years ago, since the life style of a worker has changed, that is the amount of exergy a man utilize for living; moreover exergy of the labour of a worker in a developed country weights higher than that of one in a developing countries, and this is in turn higher than that of a worker in an underdeveloped countries.
For the evaluation of the exergetic value of labour the following relation has been proposed [6,7]:

$$Ex_W = n\frac{Ex_{in}}{n_{tot}}$$

where n is the flux of work hours into the sector on analysis, n_{tot} is the total amount of work-hours per year and Ex_{in} the exergy influx to the society per year.
For what concern other contributions imputable to material goods, such as for instance machinery, buildings and supporting structure, the exergy evaluation for their construction can be performed as usual. Therefore on the bases of their depreciation, their contribution to the total exergy input can be evaluated.
A short cut method for the evaluation of the exergy of all investments can be evaluated on the basis of the monetary investment, according to the relation:

$$Ex_C = C\frac{Ex_{in}}{C_{ref}}$$

C in the capital depreciation, or the monetary flux, and (Ex/ C_{ref}) is the monetary measurement of the exergy [8]. The evaluation of this term has a certain degree of arbitrariness.
In table 3 EROI analysis for bio ethanol production in Italy, in term of enthalpy and exergy, are compared [9]. While EROI evaluated in terms of enthalpy seems to be favourable for solar energy accumulation in bio ethanol, the exergetic analysis indicates that, at least in Italy, the production of bio ethanol is only a conversion process of various subsidiary energies into ethanol.
For what concerns the production of ethanol from corn, according to US Department of Agriculture [10] the energy balance of ethanol is 1.34:1. This means that ethanol yields 34% more energy than it occurs to produce it, including growing the corn, harvesting it, transporting it and distilling it into ethanol. Other authors reported similar results

[11,12]. In a recent detailed study [13] the energy balance for corn grain ethanol is about 1,25:1, but the 25% gain is attributable to the energy credit for coproducts (as animal feed). Without this contribution the balance of ethanol itself is near zero. Other author state that the energy balance is negative [14,15].
Also the ethanol production from cellulose (all the production plants operating with the old Scholler process were closed in 1950 as no more economic) have had a revamping

Table 3 - EROI of different agricultural production in the Italian system.

BIOETANOL PRODUCTION: ENTHALPIC BALANCE (GJ/Ha)

AGRICULTURAL PRODUCTION	AGRICULT. EXERGY IN	INDUSTRIAL EXERGY IN	TOTAL EXERGY IN	TOTAL EXERGY OUT	EROI	DISTILLED ETANOL (l/Ha)
MAIS	34 ± 2	27 ± 0,5	76 ± 3	210 ± 8	2,76	3100
WHEAT	29 ± 2	27 ± 0,5	56 ± 2	130 ± 6	2,3	2050
BARLEY	22 ± 2	27 ± 0,5	49 ± 2	130 ± 6	2,6	2050
SUGARBEET	47 ± 3	73 ± 2	120 ± 6	180 ± 10	1,5	4500

BIOETANOL PRODUCTION: EXERGETIC BALANCE (GJ/Ha)

AGRICULTURAL PRODUCTION	AGRIC. EXERGY IN	INDUSTRIAL EXERGY IN	TOTAL EXERGY IN	EXERGY OUT	EROI	DISTILLED ETANOL (l/Ha)
MAIS	28 ± 2	13 ± 0,2	41 ± 3	52 ± 1	1,3	3100
WHEAT	22 ± 2	8 ± 0,2	30 ± 2	31 ± 1	1	2050
BARLEY	15 ± 2	8 ± 0,2	23 ± 2	31 ± 1	1,3	2050
SUGARBEET	28 ± 3	12 ± 0,2	50 ± 2	48 ± 4	0,96	4500

[16,17]; an excess of 60,000 Btu per gallon has been claimed [17]. Actually the exergy balance is similar to ethanol from corn, the only advantage derive from exergy saved in agriculture production if cellulose is obtained from forest and non fm plantations.

For what concerns the biodiesel production, the data are rather contradictory. While Pimentel and Patzek [18] assert a negative balance for all bio fuel production, according to a 1998 study of NREL[19] biodiesel production yields 3.2 units of fuel product energy for every unit of fossil energy consumed. This results agree with that reported in a detailed analysis [20] of bio diesel production in terms of exergy flow analysis (ExFA) based on mass and exergy flow diagram, without considering labour, machinery and building depreciation. ExFa analysis indicates that the efficiency of the industrial process is 98,54% ; actually this analysis is similar to the enthalpic analysis and gives

no additional information. I have made the calculation again, with a short-cut procedure, considering immobilized exergy, labour, etc. the obtained mean yield is in the range 1,7-2,1. This result is still optimistic in comparison with that reported in [13], where a detailed energy balance on soybean biodiesel, considering practically all factors (facility energy use, facility labourer energy use, facilities construction, transportation, household energy use, machinery production, fertilizers and pesticides, fossil fuel use, seeds) provides about 93% more energy than required in its production.
In conclusion it is possible to say that while for starch methanol there is not net gain in the exergy balance, for biodiesel the balance may be positive, it depends from when and where.

Socio-economical considerations

The world oil consumption is about 8,36 barrel/day that is 4,46 10^9 t/a. By assuming a land productivity of 1t /ha of bio-oil (sunflower or canola oil) and an optimistic value of EROI equal to 2 , the land surface to get a net added value (NAV) of 4,46 10^9 t/a resulted to be 8,92 10^9 ha. Actually the world productive land is 8,56 10^9 ha. This means that all available land is not sufficient to supply the actual oil needs. Moreover if one considers that all arable lands, now used for food production, amount to 2,8 10^8 ha the net production of bio-oil is limited to 1,4 10^8 t, that is about 3,1 % of total oil consumption, but this amount is alternative to food production.
In Italy the arable land amount to 13 10^6 ha and it would be possible to produce 6,5 10^6 t/a of bio-oil. Since the oil consumption in Italy is about 88 10^6 t/a , if one decide to abandon the food production for fuel production, that is to import foods instead of oil, the total annual production may support the oil consumption for 51 days.
On the bases of these figures it is clear that bio fuel production from renewable energy is not only a dream but, even worse, it is an unsound idea.
To the reported technical analysis one has to add some sociological considerations. The world is evolving quickly, the undeveloped people are rising up, their way of life is improving, and their needs of food are increasing both in quantity and in quality. According to a FAO report the mean world consumptions of cereals is 80% of that of developed countries, proteins about 70% and fats 50%. These data indicate that in the future more land must be devoted to food production, otherwise there will be a dramatic increase of food prices.[21]
Strictly bounded to evolution of underdeveloped country is the phenomenon of migration towards cities, that is how to prevent farm workers abandon their land.
It is my opinion that from an economic point of views the bio ethanol production was not a real business for Brazil, since instead of importing oil it imported energy in others forms like chemicals, farm machinery etc. Nevertheless the bio ethanol project had the great merit to promote an agricultural activity that allowed to keep people in the countryside. To day Brazil has a very strong economy, mainly based on agriculture. Brazil agriculture export amounts to about 27.000 million $ (4,5% of total world export).
In India the National Planning Commission has integrated the Ministries of Petroleum, Rural Development, Poverty Alleviation and the Environmental Ministry and others industrial groups and National Agencies in a project to cultivate 13,4 10^6 ha of land plus 4 10^6 of wastelands with Jatropha.[4] The aim is to produce 13 Million t of bio-diesel by 2013, that is about 20% of the consumption of mineral diesel by car. The demonstration project ($300 million) consists of 2 phases, each with 200.000 ha planted

in 8 states of 2 x 25.000 ha "compact area" each. The first results indicate that it is possible to produce 1,82 t/ha of Jatropha oil. Each state will have one esterification plant, which is meant to be economical from 80.000 t of bio-diesel onward, expected to come from 50 to 70000 ha each. Expected outputs from 400,000 ha are meant to be 0.5 Million t of bio-diesel, compost from the press cake, and massive generation of employment (16 Mio days/year) for the poor . Looking deep into the program, two great targets seem to stimulate all people involved: to improve degraded land resources, and to give an income to poor families, so that they don't leave the countryside.
These targets are in line with the social results of bio ethanol in Brazil.
There are other problems which need to be solved when such a large amount of land is dedicated for energy production: the use of water and of pesticides.
In all bio energy productions these two aspects have been underestimated.[22,23]
While bio fuel production may have some social justification in developing country, all technical, economical, social and ecological analysis indicate that the bio fuel choice is a losing strategy. Only economical grants from states to the local industries or farmers justify bio fuel production.

I would like to point out to another topic related to renewable energy. A true renewable transformation must be founded on a cycle that restores the starting conditions. This means that, in the balance, exergy consumption in restoring the environment (soil and water) polluted by the agrochemicals, or depleted by industrial plantation must be considered. In the case of corn ethanol the minimum cumulative exergy consumption is 7 times than the maximum shaft work of a car engine burning ethanol! [14]

Probably biomasses are not the right way for fuel production, new ways must be found and this is the main goal for researches.

References

1) Gaggioli, R.A. "Thermodynamics: Second Law Analisys" ACS Symposium n°122 American Chemical Society 1988, Washington D.C.
2) Göran Wall "Exergy : An Useful Concept" Insitute of Thoretica Physics-Report n° 77-42. University of Technology Chalmers and University of Götteborg.
3) Göran Wall " Perspective on the energy future using exergy" Statoil-NTNU(Norwegian University of Science and Technology) Global Watch Seminar- Trondheim- August 29-2003.
4) Centre for Jatropha Promotion & Bio diesel "Biodiesel in India 2004-2008"
5) Graf, A. ,T. Koehler "An evaluation of the potential for ethanol production in Oregon using cellulose-based feedstocks" Oregon Cellulose-Ethanol Study June 2000
6) Sciubba, E. "Beyond thermoeconomics? The concept of Extended Exergy Accounting and its application to the analysis and design of thermal system" Exergy Int. J. **1**(2):68-84(2000).
7) Nakićenović, N., Gilli P.V. and Kurz R. (1996) Regional and global exergy and energy efficiencies. *Energy* **21** (3), 223 – 237.
8) Reistad, G.M. "Available energy conversion and utilization in the United States" ASME J.Eng. Power **97**,29-34(1975)
9) Soave G., L. Zanderighi "Enthalpic and Exergetic Analysis of Bio-Ethanol as Energy Vector" Chemie Ingenieur Technik **73**(6) 589(2001).

10) Wang, M. , H. Shapouri, J. Duffield,USDA: “The Energy Balance of Ethanol: An Update.” National Agricultural Statistics Service, USDA. Aug 2002.
11) Kim, S., B. E. Dale “Allocation Procedure in Ethanol Production System from Corn Grain” International Journal Life Cycle Assessments, 2002 OnlineFirst: May 7th, 2002
12) Wang, M. , C. Saricks, D. Santini **“**Effects of Fuel Ethanol Use on Fuel-Cycle Energy and Greenhouse Gas Emissions” Argonne National Laboratory (1999)
13) Hill, J. , E. Nelson, D. Tilman, S. Polasky D. Tiffany “Environmental, economic, and energetic costs and benefits of biodiesel and ethanol biofuels” Proc. of the National Academy of Science **103**(30), 11206-11210 (2006)
14) Patzek, T,W., “ Thermodynamics of the Corn-Ethanol Biofuel Cycle” Critical Reviews in Plant Science **23**(6)519-567(2004).
15) Pimentel, D. “Ethanol Fuels: Energy Balance, Economics, and Environmental Impacts Are Negative” **12**(2)127-134(2003).
16) Morton, J., “BIOENERGY: A future for the Australian forest industry”, FOREST, 2001 - fwprdc.org.au
17) DiPardo, J. “Outlook for Biomass Ethanol Production and Demand”, Washington, DC: Energy Information Administration, 2004 - eia.doe.gov
18) Pimentel, D. , T.W. Patzek “Ethanol Production Using Corn, Switchgrass, and Wood; Biodiesel Production Using Soybean and Sunflower” Natural Resources Research **14**(1) 65-76(2005)
19) Sheehan, J.,V. Camobreco, J. Duffield, M. Graboski, H. Shapouri “An Overview of Biodiesel and Petroleum Diesel Life Cycles” NREL/TP-580-24772, National Renewable Energy Laboratori, May 1998
20) Talens L., G.Villalba, X.Gabarrell:”Exergy analysis applied to biodiesel production” Resources, Conservation and Recycling **51**(207)397-407(2007).
21) Kingsbury, K. “ After the oil crisis a food crisis?” TIME Friday, Nov, 16,2007.
22) Ortega, E., F.Günter, S.Hinton “THE ECO-UNIT: an ecomimetic settlement as a basis for sustainable development. Experience in Sweden and Brasil” Biannual International Workshop – Advances in Energy Studies- “Perspective on Energy Future” 12-16 September Porto Venere Italy,2006.
23) Coatanéa, E., M.Kuuva, P.E.Makkonnen, T.Saarelainen, M.O.Castillón-Solana “Analysis of the Concept of Sustainability: definition of conditions for using exergy as uniform environmental metric” Proceeding of 13° CIRP International Conference on Life Cycle Engineering- Leuven 31May-2 June 2007.

CHEMICAL ENGINEERING TRANSACTIONS, Volume 14, 2008
Edited by G. Marino, E. Bardone, A. Viglia
 ISBN 978-88-95608-02-0

Continuous production of biodiesel using a microtube reactor

Guoqing Guan, Katsuki Kusakabe*, Kimiko Moriyama, Nozomi Sakurai
Department of Living Environmental Science, Fukuoka Women's University,
1-1-1 Kasumigaoka, Higashi-ku, Fukuoka 813-8529, Japan
kusakabe@fwu.ac.jp

Transesterification of sunflower oil to biodiesel was carried out in a microtube reactor with either a T-type mixer or a micromixer. The effects of molar ratio of methanol to sunflower oil, flow rate, reaction temperature, and microtube size on the oil conversion were investigated. The oil conversions obtained in the microtube reactors were higher than those obtained in the lab-scale batch reactor. The oil conversions were obviously improved when a T-type mixer was replaced by a micromixer. Sunflower oil was completely converted to biodiesel even if the residence time was as short as 112 s at a reaction temperature of 60ºC for a microtube reactor (1 mm i.d. and 160 mm in length) with a micromixer.

1. Introduction

Biodiesel fuel (BDF) is a promising environmental-friendly fuel compared to petroleum diesel fuel (Al-Zuhair, 2007, Huber et al., 2006, Lotero et al., 2005), and generally produced by transesterification of vegetable oils or animal fats with methanol in the presence of an alkaline catalyst. However, the reaction rate is mainly controlled by diffusion between oil and methanol phases due to the low solubility of oil in the methanol phase. Therefore, a stirred batch reactor is commercially used to produce small amounts of BDF. In recent years, microreactor systems designed for small-scale continuous production have been widely studied (Hessel et al. 2005). In the microreactor system, mass and heat transfer could be greatly intensified due to its small

space with a large surface area-to-volume ratio. As a result, molecular diffusion through the interface could become less significant resistance to the two-phase reaction. In the present study, microreaction systems composed of microtube reactors and microfluidic mixers were used for the continuous production of BDF. Transesterification of sunflower oil to BDF with methanol and KOH catalyst was carried out in the microtube reactor. The effects of molar ratio of methanol to sunflower oil, flow rate, reaction temperature, microtube size on the oil conversion were investigated. The oil conversions in the microtube reactor with a micromixer were compared to those with a conventional T-type mixer.

2. Experimental

Sunflower oil for cooking use was purchased from a market, and dehydrate methanol, potassium hydroxide and acetic acid were obtained from Wako Pure Chemical Ind. Ltd., Japan. All chemicals were not purified before use. Stainless-steel microtube reactors (inner diameter = 0.4, 0.6 and 0.8 mm) were used to facilitate contact between oil and methanol phases. Transparent teflon FEP tubes (inner diameter = 0.8 and 1 mm) were also used for the production of BDF and the observation of fluid motion. A stainless-steel micromixer, provided by Okayama Prefecture Industrial Promotion Foundation, was a split and recombine type mixer.

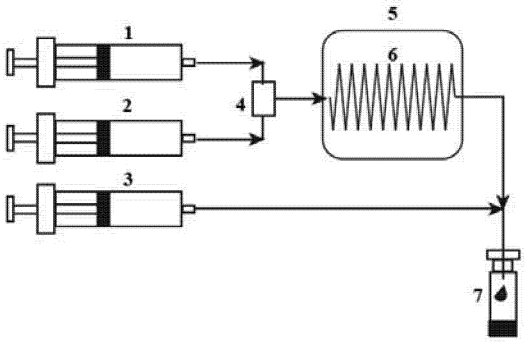

Fig.1 *Microreaction system for biodiesel production*
1. Vegetable oil; 2. Methanol/KOH; 3. Acetic acid;
4. T-type mixer or micromixer; 5. Thermostat oil bath;
6. Microtube; 7. Collection bottle.

A scheme for the experimental setup is shown in **Fig.1**. KOH was dissolved in methanol to adjust its concentration based on the oil weight to 1 wt%. Syringe pumps were used

for the feed of the liquids. The molar ratios of methanol to sunflower oil were adjusted by changing the liquid flow rates, and were 4.6, 11.3, and 23.9. Sunflower oil and methanol containing KOH were mixed at the T-type mixer or the micromixer. The mixture was then flowed into the heated microtube. The product was collected at the outlet of the microtube after the termination of reaction by addition of acetic acid. For comparison, a lab-scale batch experiment was performed using a 50 mL flask at 60ºC. Sunflower oil and methanol containing KOH were introduced into the flask simultaneously, and stirred at 600 rpm. The samples were recovered from the reaction mixture after the prescribed reaction time and immediately quenched by addition of acetic acid. The reaction was performed at 20, 40 and 60ºC.

The collected product was then centrifuged at 6000 rpm for 20 min. The upper BDF layer was rinsed with deionized water for several times to remove the residual inorganic components. 0.2 ml of the rinsed sample was diluted in 2 ml of hexane for analysis. Concentrations of the unreacted oil remaining in the products were analyzed by a high-performance liquid chromatography (HPLC, TOSOH, Japan) equipped with a silica-gel column (Shimpack CLC-SIL, Shimadzu, Japan) and a refractive index detector using a mobile phase of n-hexane/2-propanol=99.5/0.5 (v/v). Column temperature was kept at 40 ºC.

3. Results and discussion

3.1 Comparison of the microtube reactor with the batch reactor

Segmented flow was observed in the transparent teflon FEP tube at the outlet of T-type mixer. **Fig.2** shows the comparison of the oil conversion between the batch reactor and the microtube reactor (0.8 mm i.d.) with T-type mixer. In the case of microtube reactor, the

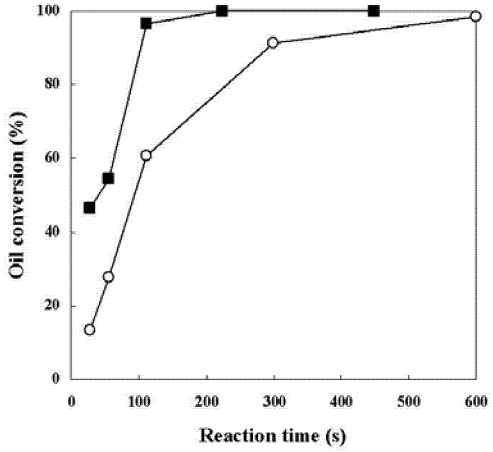

Fig.2 *Comparison of oil conversions when using microtube reactor and batch reactor. Molar ratio of methanol to oil = 4.6, reaction temperature = 60^{O}C*

reaction time was controlled by the length of microtube and the flow rate. The oil conversion was found to reach 100% after a reaction time of approximately 600 s for the batch reactor. For comparison, a reaction was carried out under the same conditions except for the reactor type. The 100% conversion was achieved for the reaction time of 240 s for the microtube reactor. The enhancement of the apparent reaction rate in the microtube reactor was caused by the mass transfer and temperature effects. Microtube provides high contact surface area between the immiscible two phases due to the formation of fine segments in the tube. Therefore the mass transfer rate can be enhanced through segmentation by providing a large specific interfacial area and phase internal flow (Malsch et al., 2008). In addition to the mass transfer effect, temperature in the reaction liquids rose quickly in the microtube compared to the batch reactor because of the small reaction volume.

3.2. Effects of microtube size and methanol/oil molar ratio

Transesterifications of sunflower oil were carried out at 60°C in the microtube reactors with different tube sizes and lengths. To fix the total flow rate and the value of the residence time to 28 s, microtube lengths were varied to 1000 mm for 0.4 mm i.d. tube, 640 mm for 0.6 mm i.d. tube, 360 mm for 0.8 mm i.d. tube and 160 mm for 1.0 mm i.d. tube. When the size of microtube was decreased, the flow rate in the microtube became high and therefore the oil conversion was increased due to small molecular diffusion distance as shown in **Fig.3**. Simultaneously, the behaviors of segmented flow were thought to be changed by the size of microtube and might be affected to the mass transfer. Detail observation of flow behaviors in microtube was need in the future work. Also we have to consider the pressure drop in the small microtube reactor.

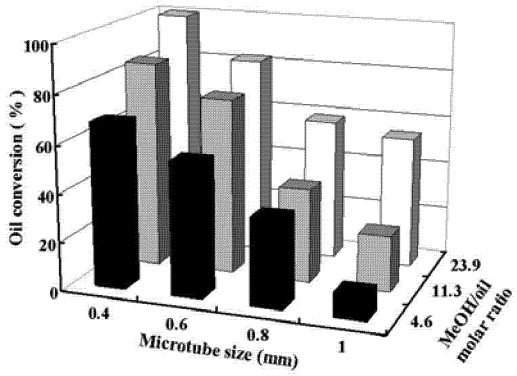

Fig.3 *Effects of microtube sizes and methanol/ oil molar ratios on oil conversions. Reaction temperature=60ºC; residence time=28s.*

The oil conversion increased with increase in the molar ratio of methanol to the oil as shown in Fig.3. This result is consistent with the results obtained in stirred batch reactors (Lotero et al., 2005). It is well recognized that transesterification of triglyceride with methanol is a reversible reaction. The excess mount of methanol shifted the equilibrium to the product side and thus increased the oil conversion. In the microtube reactor, segmented flow pattern was usually formed, and the molar ratio of methanol to the oil was adjusted by changing the flow rates of methanol and oil individually. From the observation of flow state, the length of segments, especially oil segments, was reduced by increasing the methanol flow rate. The change in flow behavior also affected the mass transfer rate.

3.3. Biodiesel production in microtube reactor with micromixer

A conventional T-type mixer is utilized to form a stable segmented flow in a microtube. Meanwhile, a dispersed flow of fine methanol droplets was observed at the outlet of the micromixer used in this experiment. The flow was then transferred from a dispersed flow to a segmented flow along the microtube. Large surface area obtained in the dispersed flow could enhance the reaction rate at the initial stage of transesterification.

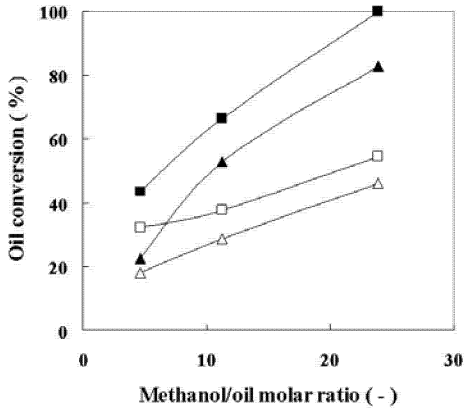

Fig.4 *Reaction enhancement by mixing effect. Residence time in microtube reactor (1 mm i.d. and 160 mm in length): ▲△; 56s; ■□;112s. Closed symbols: micromixer, Open symbols: T-type mixer. Reaction temperature=60 ºC.*

Fig.4 shows the comparison of the oil conversion between microtube reactors (inner diameter = 1 mm, 160 mm in length) with the T-type mixer and the micromixer. The oil conversions were high when the micromixer instead of the T-type mixer was used. The oil conversion was greatly improved at high molar ratio of methanol to oil in the

microtube reactor with the micromixer. Sunflower oil was completely converted to biodiesel when the residence time was as short as 112 s at a reaction temperature of 60℃ for a microtube reactor with a micromixer. Stamenkovic et al. (2007) investigated the transesterification of sunflower oil with methanol and KOH in a stirred batch reactor. Droplet size was approximately constant at the initial stage of the reaction and then rapidly reduced. The surface active compounds such as monoglycerides and diglycerides could inhibit the drop coalescence and favor formation of stable emulsion of small drops. Therefore the reaction system established in the microtube reactor with the micromixer would maintain the dispersed flow state for a while. In the previous paper (Guan et al., 2007), homogeneous production of BDF from corn oil was carried out by the addition of dimethyl ether as a cosolvent. The corn oil conversion of 100% was attained at room temperature by

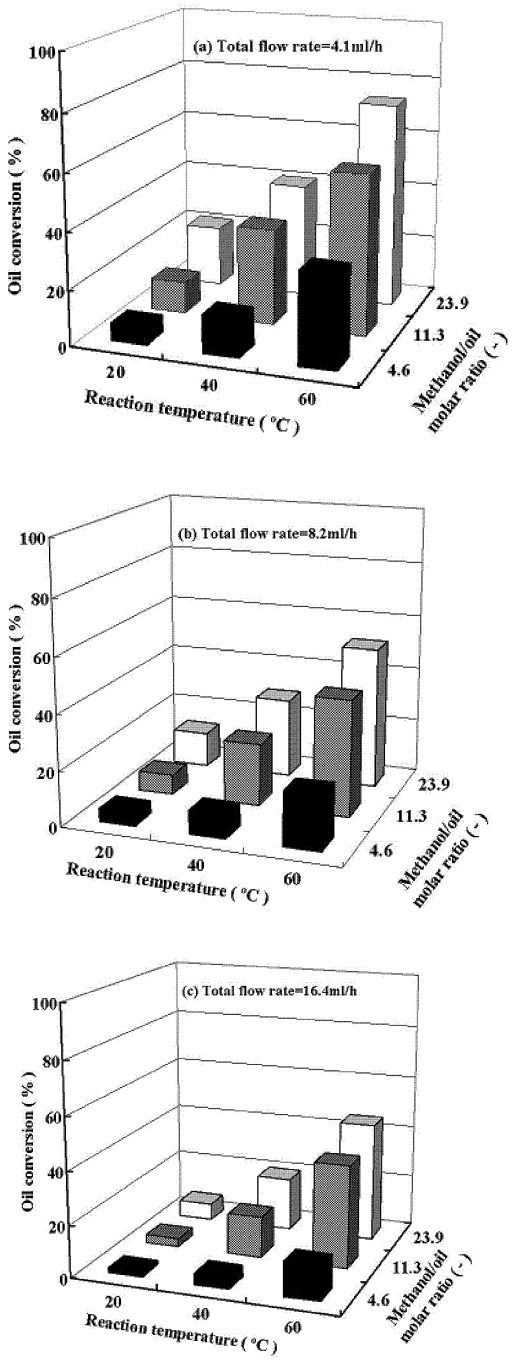

Fig.5 *Direct production of BDF in the micromixer. Total flow rate: (a); 4.1 mL/h, (b); 8.2 mL/h, (c); 16.4 mL/h.*

vigorously shaking within 20 s.

3.4. Biodiesel production in micromixer

Direct production of BDF in the micromixer was carried out at 20, 40 and 60°C. The product was collected at the outlet of the micromixer. As shown in **Fig.5**, the oil conversion at the reaction temperature of 20°C was less than 20%. Data of the oil conversion in the microtube with the micromixer in Fig.4 was obtained from the combination of the micromixer at room temperature and the microtube at 60°C. As a result, main reaction was performed in the microtube at 60°C in the case of Fig.4. .

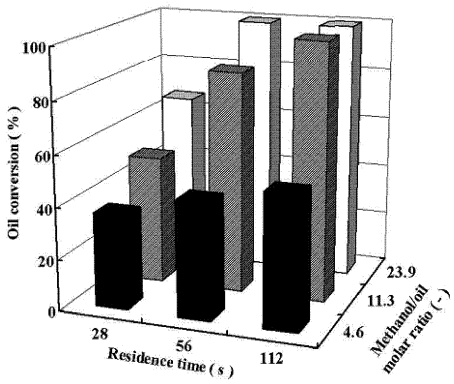

Fig.6 *Theoil conversion obtained when micromixer and microtube were heated at 60°C*

The oil conversion was rapidly increased with increase in the reaction temperature. The oil conversion at 60°C could attain 73.5% when the total flow rate was 4.2ml/h with a methanol/oil molar ratio of 23.9. If the problems with the pressure drop and the clogging in the complicated microchannel structure in the micromixer were discharged, the complete oil conversion would be realized only in a modified micromixer.

As shown in Fig.4, sunflower oil was completely converted to BDF for 112 s in the methanol molar ratio of 23.9 by using the microtube heated at 60°C and the micromixer at room temperature. When the micromixer and the micotube were heated at 60°C, the residence time and the methanol molar ratio to reach the 100% conversion became half as shown in **Fig.6**.

4. Conclusion

Continuous production of BDF by transesterification of sunflower oil was carried out in a microreaction system composed of a microtube with a T-type mixer or a micromixer. Comparing with the lab-scale batch reactor, microtube reactor showed better mass and heat transfer properties and obtained high conversion of sunflower oil. The oil conversion was obviously improved when a T-type mixer at the inlet of the microtube was replaced by a micromixer. It was found that 100% sunflower oil was converted to BDF even if the residence time was as short as 112 s at a reaction temperature of 60℃ for a microtube (1 mm i.d. and 160 mm in length) reactor with a micromixer. The oil conversion was increased with the decrease in microtube size.

5. References

Al-Zuhair S., 2007, Biofuels Bioproducts Biorefining, **1**, 57.

Guan, G., K. Kusakabe, N. Sakurai, K. Moriyama, 2007, Chem. Lett., 36, 1408.

Hessel V., H. Löwe, A. Müller, G. Kolb, 2005, Chemical Micro Process Engineering – Processing, Applications, and Plants, Wiley-VCH, Weinheim, Germany

Huber G., W., S. Iborra, A. Corma, 2006, Chem. Rev., **106**, 4044.

Lotero E, Y. Liu, D. E. Lopez, K. Suwannakarn, D. A. Bruce, J. G. Goodwin Jr., 2005, Ind. Eng. Chem. Res., **44**, 5353.

Malsch, D., M. Kielpinski, R. Merthan, J. Albert, G. Mayer, J.M. Köhler, H. Süβe, M. Stahl, T. Henkel, 2008, Chem. Eng. J., **135S**, S166.

Stamenkovic O.S., M.L. Lazic, Z.B. Todorovic, V.B. Veljkovic, D.U. Skala, 2007, Bioresouce Technol. ,98, 2688.

CHEMICAL ENGINEERING TRANSACTIONS, Volume 14, 2008
Edited by G. Marino, E. Bardone, A. Viglia
 ISBN 978-88-95608-02-0

Continuous Bioethanol and Biogas Production from Food Processing Waste

Zanette M.*, Torresendi M.*, Bolzonella D.°, Fatone F.*, Cecchi F.*
* Dipartimento Scientifico e Tecnologico, Università di Verona, Strada Le Grazie, 15. I-37134 Verona, Italia. Tel and fax +39 045 8027965; E-mail: franco.cecchi@univr.it
° Dipartimento di Scienze, Tecnologie e Mercati della Vite e del Vino, Università di Verona, via della Pieve 70, San Floriano (Verona).

1. Intoduction

The necessity to reduce CO_2 emissions and oil consumption has been determining a new interest in bio-energy and bio-fuels in recent years (Farrell et al., 2006). The most promising of these fuels is bio-ethanol, which can be used with a clean combustion, has a high octane number (103), is chemically stable, no toxic and biodegradable. Further, it can be used for vehicles transport as a mixture with oil or pure; in fact, as mixture does not require specific changes on the engine, while when used pure only small changes are requested. Finally, the CO_2 emission produced by the bio-ethanol combustion is "environmental friendly", because deriving by renewable energy sources. However, the actual production of bio-ethanol based on corn starch is not long sustainable because of ethical, environmental and economical constrains and a second generation of bio-ethanol from ligno-cellulosic materials is growing (Galbe and Zacchi, 2007), the so called LC-ethanol. Another important option for the production of bio-ethanol is the use of bio-waste rich in sugars or starchy materials (Mahro and Timm, 2007). The main advantages of this option are related to the reduced demand for pre-treatments and hydrolytic steps and the abundance of C6 sugars. These materials are produced in large amount in Europe and can be considered an important feedstock for biofuels production: the generation of food-processing waste has been estimated in 222 millions tonnes per year, vegetable and fruit being at 140 million of tonnes/year (Waldron, 2007).
In this study we considered the bio-ethanol production through the fermentation of waste from the pastry and confectionery industry, which are particularly rich in fermentable sugars. Important aspects of the study were the used of continuous reactors (without and with biomass recycling) and the use of the yeast *Saccharomyces cerevisiae* EC1118 without sterilisation of the treated material.
Further, in order to enhance the use of the raw material also the anaerobic digestion for methane production was implemented in the process according to the scheme reported in figure 1.

2. Materials and methods

The raw waste treated in the experimentation showed COD concentrations of some 600 g/L with large abundance (up to 90%) of glucose, sucrose and fructose. This was diluted (10:1) to reduce mixing problems. Bio-ethanol fermentation was carried out in a continuous anaerobic stirred reactor (15 litres volume), without sterilisation, working at 35°C. At the beginning of the work the reactor was inoculated with *Saccharomyces cerevisiae* (strain EC1118). The following parameters were monitored: biogas

production, ethanol, sucrose, glucose, fructose, glycerol, lactic acid, the volatile fatty acids (from C2 to C7) and biomass (on selective and no-selective Petri plates).
The first part of the study was devoted to the study of the system working as a continuous stirred tank reactor (CSTR) at different dilution rates (0.1; 0.2; 0.3; 0.5; 0.67; 0.75 and 1.33 d^{-1}) while in the second part, according to the results previously gained, the dilution was fixed at 0.5 d^{-1} and the biomass recycle was operated. Proved solid retention times were 2, 5, 10 and 15 days. After a steady state was reached, it was maintained for at least 4 HRTs and the mass balances were calculated. The biogas generated from the downstream of the fermentation process was estimated via BMP tests (Angelidaki et al., 2007). The BMP tests were run for the best reactor conditions: CSTR with biomass recycling at 0.5 d^{-1} and with SRT of 10 days. The distillation bottom samples were obtained from distillation of the liquid phase coming from the fermentation on a glass distillation column (lab-scale).

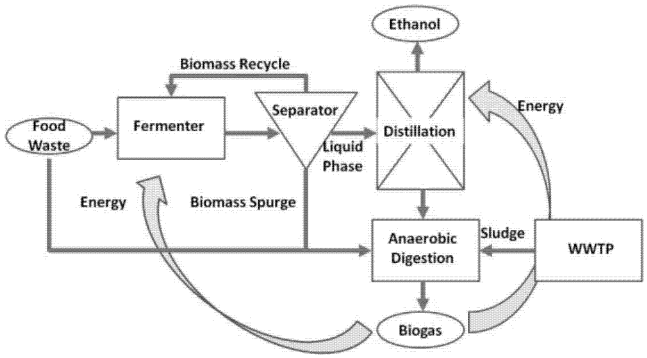

Figure 1-Scheme of the Plant for the production of bio-ethanol and biogas from food waste

3. Results and Discussion

3.1 Continuous fermentation trials at different dilution rates without recycling

The continuous fermentation tests were carried out operating at dilution rates in the range 0.1; 0.2; 0.3; 0.5; 0.67; 0.75 and 1.33 d^{-1} and feeding the reactor with a solution at some 60 g/L as COD. From the mass balance on carbon (fig. 2) one can note how at low dilution rates (0.1-0.2 d^{-1}) the system completely used the influent substrate (carbon was the limiting compound for growth); then, 45% of influent carbon was converted into ethanol and a high fraction of sugars was converted into undesired by-products (VFA, lactic acid, glycerol etc...). About 15% of the influent carbon underwent to by-products transformation. In this condition, carbon was the limiting element as shown by the biomass concentration at dilution rates of some 0.1 d^{-1}.
In a ideal CSTR the dilution rate and the kinetic constants are linked by the formula

$D = \mu - k_d$

where, D is the dilution rate, k_d the decay constant and μ the growth rate, all with units, d^{-1}.

In this system, when at D = 0.1 d^{-1} the two parameters showed similar magnitude and decay became an important factor because of the substrate scarcity.

On the other hand, when the dilution rate increased (greater then 0.3 d^{-1}) part of the sugars was not used and the fraction of carbon converted into ethanol progressively reduced while by-products disappeared. During all the periods analysed the fraction of carbon converted into glycerol was below 3%.

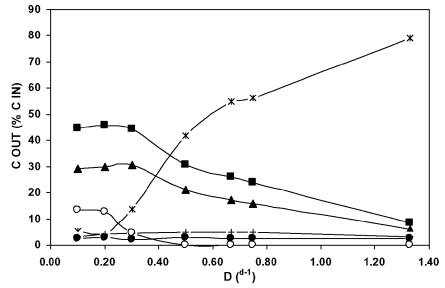

Fig. 2 Carbon mass balance for the single CSTR system

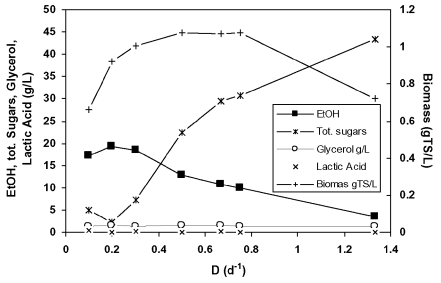

Fig. 3 The main parameters of the single CSTR system

When the dilution rate increased over 1 d^{-1} the biomass concentration decreased again since the value of D was similar to the maximal growth rate (D ≈ μ_{max}) as the system achieved the condition of wash-out. This fact was well explained by the ratio between the ethanol produced and the biomass produced (g/g): figure 4 shows that this ratio reached a pick at 25 g/g for dilution rates of some (0.6-0.8 d^{-1}) and values of some 20 g/g for dilution rate of some 0.5 d^{-1} while it reached values of some 5 g/g at dilution rates of 1.33 d^{-1}. In addiction, the maximum ethanol/utilized sugars ratio and the maximum specific productivity were obtained for a dilution rate of some 0.8 d^{-1}; however, in that condition, the sugars used where only 50% of the influent. So, in order to optimize the process yields, it was decided to operate with a dilution rate of 0.5 d^{-1} and biomass recycling.

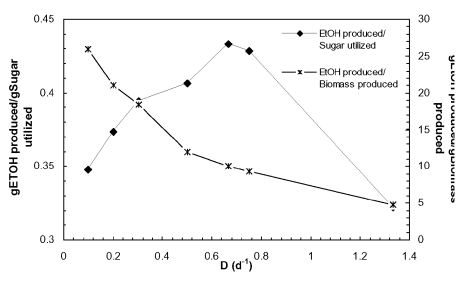

Fig. 4 EtOH produced/Sugars utilized and EtOH produced/Biomass produced for a single CSTR reactor

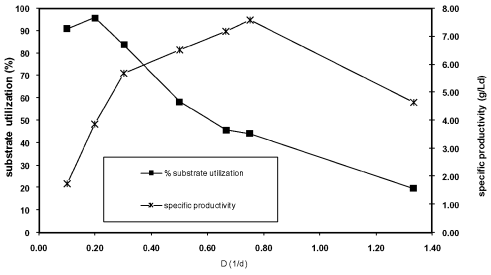

Fig. 5 Substrate utilization and Specific productivity for a single CSTR reactor

3.2 Continuous fermentation trials at different dilution rates with recycling

In the second part of the study the system was operated as a CSTR with biomass recycling at a dilution rate of 0.5 d^{-1}. The solid retention time (SRT) was varied between 2 and 15 days. Figure 6 shows the plot of the main parameters (sugars, ethanol and biogas) for different SRT: the ethanol concentration in the reactor increased with the solid retention time from 2 to 10 days and then remained constant at some 25 g/L when increasing the SRT from 10 to 15 days. On the other hand, the biogas production increased linearly with the SRT, passing from 10 to 40 L/day.

The mass balance for carbon is shown in figure 7: it turns out evident how, increasing the SRT, that is, increasing the biomass concentration in the reactor, the fraction of carbon converted to ethanol increased from 20 to 50%, the biogas increased from 10 to 40% while the effluent sugars disappeared, passing from 20 to less than 5%. By-products remained constant along the experimentation representing some 5% of the influent carbon.

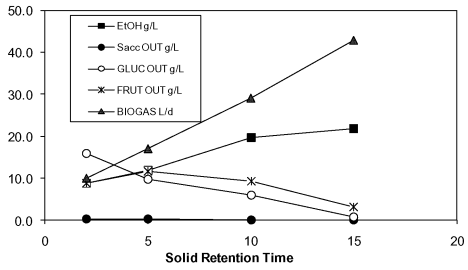

Fig 6 The main parameters for the system working like a reactor with biomass recirculation at constant dilution rate (0.5 d^{-1}) and a different SRT

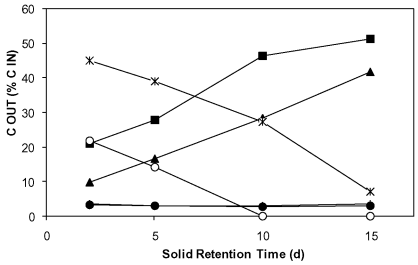

Fig.7 Carbon mass balance for the system working like a reactor with biomass recirculation at constant dilution rate (0.5 d^{-1}) and a different SRT

With specific reference to the ethanol/utilized sugars ratio (figure 8), this showed a trend similar to the ethanol concentration, presenting a maximum for solid retention times of some 10-15 days when the substrate utilisation was some 90% (figure 9). In those conditions the yield reached values of some 0.5 g/g, a value similar to that reported by Tao et al. (2005) who found in a recent research that it was possible to obtain some 0.488 g ethanol/g glucose operating under no-sterile conditions.

As for the specific productivity for ethanol (see figure 9), this increased from 4 to 10 g/L·d) for a SRT of some 10-15 days. Also this value was in good agreement with literature data where reported productivities are in the range 5 – 20 g/L·d with CSTR with biomass recycling and ethanol concentrations in the reactor are between 20 and 70 g/L (Sanchez and Cardona, 2008).

The concentration of active yeast biomass was monitored along the experimentation by means of microbiological control. In particular, that was evaluated via selective and no-

selective Petri plates: the concentration of active biomass remained constant at some $2.5x10^8$ CFU/mL despite the variation in dilution rates and solid retention times.

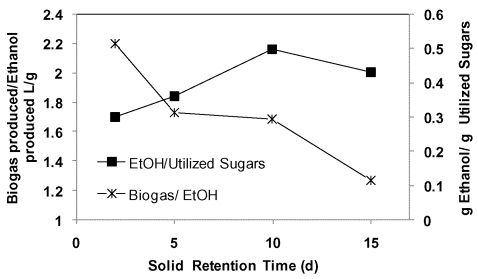

Fig. 8 EtOH produced/Sugars utilized and EtOH produced/Biomass produced for the system working like a reactor with biomass recirculation at constant dilution rate (0.5d-1) and a different SRT

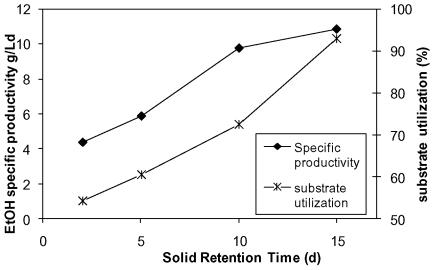

Fig. 9 Substrate utilization and Specific productivity for the system working like a reactor with biomass recirculation at constant dilution rate (0.5d-1) and a different SRT

3.3 BMP tests

In order to gain the maximal energy revenue from the treated waste, both the biomass spurge and the residual fraction after distillation were tested for biogas production.

The BMP tests, conducted under mesophilic and thermophilic conditions, showed the very high digestibility of the treated material. The biomass spurge of the fermentation and the distillation bottom stream reached values of 0.43-0.47 L biogas/g VS(biomass spurge) (Fig. 10) and 405mL biogas/gCOD (fig. 11) respectively distillation bottom stream. The maximum biogas production was reached in just few hours (less then 3 days) as the substrate is soluble and readily biodegradable.

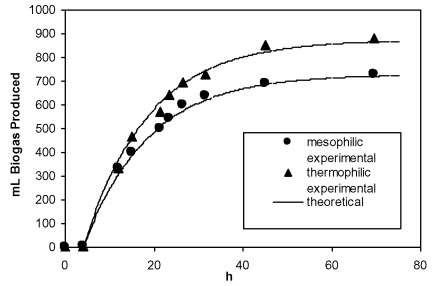

Fig. 10 BMP tests conduced on distillation bottom stream in mesophilic and thermophilic condition

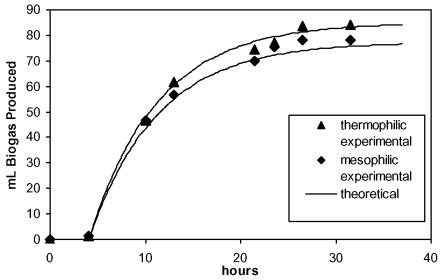

Fig 11 BMP tests conduced on biomass spurge in mesophilic and thermophilic condition

4. Conclusions

The following remarks can be derived from the study:

- food processing waste can be easily fermented in continuous anaerobic reactors working in mesophilic conditions without sterilisation. The process was able to show good yields (up to some 0.5 gEtOH/gused sugar) but with low substrate conversion when operating with dilution rates of some 0.5 d^{-1};
- to improve these results a biomass recycle was introduced. In this situation the system was able to convert up to 90% of the sugars with ethanol specific productivity of some 10 g/L·d when operating with a dilution rate of some 0.5 d^{-1} and a solid retention time of 10 days.
- Batch tests for biogas production carried out both in mesophilic and thermophilic conditions showed the possibility to produce some 0.4-0.5 m^3 of methane per kg of volatile matter fed. This biogas can be then conveniently converted to thermal and electric energy to improve the energy balance of the system.

5. References

Angelidaki I., Alves M., Bolzonella D., Borzacconi L., Campos L., Guwy A., Jenícek P., Kalyuzhnui S., Van Lier J. (2007). Anaerobic Biodegradation, Activity and Inhibition (ABAI). Institute of Environment & Resources. DTU, Lingby 2007. ISBN 978-87-91855-44-3.

Farrell A.E., Plevin R.J., Turner B.T. (2006). Ethanol can contribute to energy and environmental goals. Science, 311(5760), 506-508.

Galbe M., Zacchi G. (2007). Pretreatment of lignocellulosic materials for efficient bioethanol production. *Biofuels*, 108, 41-65

Mahro B., Timm M. (2007). Potential of biowaste from the food industry as a biomass resource. *Engineering in Life Sciences*, 7(5), 457-468

Sanchez O., Cardona C.A. (2008). Trends in biotechnological production of fuel ethanol from different feedstocks. *Bioresource Technology*, in press

Tao, F., Miao, J.Y., Shi, G.Y., Zhang, K.C. (2005). *Process Biochemistry*, 40(1), 183-187

Waldron K.(2007), Handbook of waste management and co-product recovery in food processing. Woodhead-CRC PRESS, Cambridge, UK, pp 662

CHEMICAL ENGINEERING TRANSACTIONS, Volume 14, 2008
Edited by G. Marino, E. Bardone, A. Viglia
 ISBN 978-88-95608-02-0

Fungal Biomass-Based Production of Lipids for Biodiesel Synthesis

D'Urso, A., Bubbico, R., Scarsella, M., Bravi, M.*
Dipartimento Ingegneria Chimica Materiali Ambiente; Sapienza – Università di Roma
via Eudossiana 18; I-00184 Rome (Italy)
*marco.bravi@uniroma1.it

Lipids for biodiesel fuel production are ordinarily being extracted from terrestrial plants, while alternative, fast-growing, lower cost sources are being sought in microbial sources. Microbial lipids can be extracted from many sources, but economical and technical issues mostly negate the possibility to use them in low oil cost destinations. The present paper revises the problems connected with low-cost microbial lipid production and investigates the use of fungi in the production of lipids by growing them on waste materials.

1. Introduction

Biodiesel fuels, short-chain esters of fatty acids, are generally obtained by transesterification of triacylglycerides (TAGs) derived from vegetable oils or animal fats. The most recent trend in biodiesel production deals with using specialised oil-rich crops (such as rapeseed) and devoting an increasing amount of land to their cultivation; this strategy, along with not being quantitatively significant, is postulated to create a competition for the cultivable land area with basic crops of our diet and economy and cause cost fluctuations of these latter. A minimally intrusive biofuel production policy should turn to waste materials as potential lipid sources.

Many microorganisms accumulate cytosolic lipid bodies, including microalgae, protozoans, fungi and prokariotes (Murphy et al., 2005). In the present work, the potential use of microbial biomass grown on agro-food waste is first surveyed to highlight potential contributions to the production of lipids for conversion into biodiesel. The second purpose of this work is presenting the results of a semi-model investigation of the production of fatty acids to be converted into biodiesel fuel by means of moulds. In particular, in this work, *Trichoderma viride* is being considered.

Trichoderma spp. are able to store lipids (Serrano-Carreon et al., 1992); *T. viride*, in particular, tolerates biorecalcitrant compounds and strongly acidic environments, thus envisaging interesting feeding scenarios based on environmentally critical wastewaters.

This investigation was performed by characterising the behavior of the fungus in a synthetic liquid growth medium containg glucose or lactose and on a fed-batch bioreactor where a culture of *T. viride* was grown on olive oil mill wastewater (OOWM), chosen because of its large production in South-European countries and its highly pollutant character.

2. Lipids from microorganisms

Microorganisms capable of accumulating lipids to more than 20% of their dry weight, and therefrom termed *oleaginous* (Ratledge and Wynn, 2002) can be used to extract *microbial* lipids, investigated and exploited as alternative sources of oils and fats for human consumption and, increasingly, for renewable energy production. Basic and applied research has covered fungal microorganisms, prokaryotes and microalgae.

Microbial lipids are not easy to produce economically. If fungi are cultured on glucose or sucrose derived from agricultural crops, the cost of turning one agricultural commodity into another at the relevant yield factor ($Y_{oil/sugar}$ ~0.2) and their respective costs ($cost_{sugar}$:$cost_{oil}$ ~1:4; Wynn and Ratledge, 2006) rule their production process out. Making microbial lipid production profitable requires either that price of the produced oil exceed that of commodity supplies and/or that a free carbon source is available. Currently, while the former opportunity is behind some running processes, all of them are being actively investigated.

Free carbon is available from two sources: inorganic, such as CO_2 from the atmosphere, or from combustion emissions, and organic, such as waste materials, in aggregated (waste solids) or dissolved state (wastewaters). High-value oily materials rich in nutritionally significant polyunsaturated fatty acids (PUFAs) are generally investigated for nutraceutical uses, thus requiring GRAS (Generally Recognised As Safe) practices: a suitable pick of microorganisms, raw materials, equipment and procedures and (mostly) ruling out waste materials. On the other hand, strict standards are (mostly) not required for such low value end-products as biofuels, which can benefit from free inorganic carbon from the atmosphere and free organic carbon from many by-products of the agro-food industry; on the other hand, however, the very same richness in PUFAs which makes microbial lipids nutritionally interesting raises concerns about the oxidative stability of the biodiesel fuel produced therefrom (Falk and Meyer-Pittroff, 2004).

Inorganic carbon sources provide photolithoautotrophic organisms with reducing equivalents at the same time they supply them carbon, energy being provided by (sun)light, thus leading to a net subtraction of CO_2; conversely, organic carbon sources provide chemoorganoheterotrophic organisms supplying energy, reducing equivalents and carbon at a time, thus leading to a net release of CO_2. Sometimes, the two metabolic behaviours coexist (mixotrophic metabolism), generally yielding an overall improved growth rate of the microbial biomass.

Lipid accumulation in the cells of microorganisms is a stress-induced response to the shortage of some nutrient other than the carbon source—usually nitrogen. Following starvation in a key nutrient, the cells enter a phase in which the excess carbon in the growth medium is converted into storage lipidic materials.

A typical profile for the accumulation of lipid in an oleaginous microorganism is shown in Figure 1. This shows that lipid accumulation in a microbial cell only begins when nitrogen is exhausted from the medium.

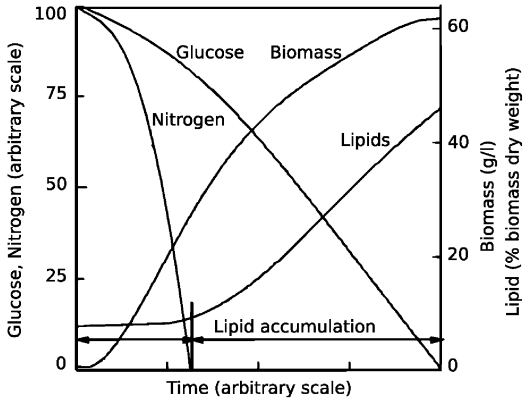

Figure 1: Schematic illustration of the time profile of lipid accumulation in an oleaginous microorganism (Wynn and Ratledge, 2006).

In heterotrophic cultures, the growth medium has to be formulated with a high C:N ratio to ensure that nitrogen is exhausted while other nutrients, including carbon, remain in excess. Usually a 40 to 50:1 carbon-to-nitrogen ratio (C:N) is used, although the optimal value needs to be determined for each individual organism. In order to maximise the cell biomass concentration and reduce the volume of treated suspension for the separation of the developed biomass, the nitrogen and carbon sources concentration may need to be increased while keeping their proportion; this enables a balanced growth phase to continue until the maximum biomass density that the fermentor can sustain is reached before the lipid accumulation phase begins.

Restoring the availability of the missing nutrient reverts the lipid accumulation mechanism, so that cellular materials are assembled again.

Similarly, photoautotrophic cultures of microalgae tend to accumulate lipids in nitrogen-limited media (Guschina et al., 2006).

A number of microalgae can supplement photoautotrophic metabolism with heterotrophic metabolism, thus exhibiting mixotrophy. True facultative mixotrophic microalgae (i.e., able to grow in either photoautotrophic and heterotrophic conditions), such as *Chlorella* spp., *Haematococcus pluvialis*, *Scenedesmus acutus* and *spirulina platensis* can be effectively grown on glucose and acetate. Mixotrophically grown *Chlorella* or *Haematococcus* grow faster than either pure photoautotrophically or heterotrophically grown biomass belonging to the same genera (Lee, 2001), exhibiting interaction coefficients between the photoautotrophic and heterotrophic metabolism (Ogbonna et al., 2002) lower than unity.

In true facultative mixotrophs, heterotrophic growth has been demonstrated by Miao and Wu (2006) to yield an increased lipid accumulation compared to photoautotrophic growth.

Most “free” carbon sources suitable for heterotrophic or mixotrophic cultures do not possess the required C:N ratio and/or are not concentrated enough to produce a high-

density culture. Exceptions exist, but may not be immediately ready for culture use—such as lignocellulosic residues, which need to be preliminarily hydrolysed to deliver their readily metabolisable sugars content.

Table 1 contains a small excerpt of microbial lipid sources from the open literature falling in all of the classes named above, and providing an introduction for the presented experimental results.

3. Lipids from *Trichoderma* spp.

3.1 Rationale for an Investigation

The rationale behind the idea of using fungi to store lipids lies in their general ability of growing on wood and other lignocellulosic materials thanks to a pool of intra- and extracellular phenyl-, glucan- and xylan-degrading or modifying enzymes (Hammel, 1997): *T. viride* (phylum Ascomycota), in particular, is a cellulase high producer (Domingues et al., 2000) which is able to grow in strongly acidic media (Brown and Halsted, 1975) and thus survives in acid wastewaters. The authors of this paper also highlighted the ability of *T. viride* to grow on phenolics-rich wastewaters in model growth media containing concentrated gallic acid in short- (D'Urso et al., 2007a) and long-duration experimental runs (2008a), olive oil mill, distillery and cork processing wastewaters in short duration runs (2007b) and olive oil mill wastewaters in long-duration runs (2008b).

Olive oil production delivers large amounts of wastes in liquid, dilute or concentrated suspension and solid state. Liquid and dilute suspensions (OOMWs) are expecially hard to dispose of, due to their high organic load (biochemical and chemical oxygen demand up to 100 and 220 g l^{-1}), their content of polyphenols, tannins and suspended solids and to their acidity (Annesini & Gironi 1991). While polyphenolic compounds exhibit a limited toxicity and biodegradability, tannins and simple phenolic compounds are highly toxic but biodegradable (Hamdi, Garcia & Ellouz, 1992). OOMW features a C:N ratio in the order of 10:1—20:1. Two-phase continuous centrifugation process feature increased processing capacity and extraction yield, and decreased water consumption and wastewater production (Alba, Hidalgo, Martínez, Ruiz, Moyano & Borja, 1995) exhibit a C:N ratio of 45±10:1.

High COD wastewaters are an interesting kind of carbon source, fitting nicely the need of low-cost microbial lipids production. In principle, these wastewaters can be used to feed any kind of biomass which is able to efficiently metabolise the sugars contained therein; in practice, they can end up hosting competing microorganisms unless the microbial process is run axenically, which would offset the economic benefits of a free carbon source. In this respect biorecalcitrant, low pH, high COD and high C:N ratio wastewaters are indeed a “special” kind of “free” carbon source, in that they would represent a unique selective environment for microorganisms (mostly) permitting a low-axenicity process conduite or, in the worst case, only requiring a mild pasteurisation before inoculation of the target microorganism.

Table 1. Some oleaginous microorganisms and their main lipids-production related performance (b.: batch...; Ref. key indicates first author-year, T.w. : *this work*).

Species	Substrate	Growth rate (h^{-1})	Biomass ($g_B\ l^{-1}$)	Lipid conc. ($g_L\ g_B^{-1}$)	Lipid prod. ($g\ l\ h^{-1}$)	Lipid type	$Y_{L/S}$	Lipid Unsat.	Ref.
			Fungi						
Candida curvata	glucose		13.5		0.16		0.29		W06
Candida curvata	lactose		18		0.22		0.31		W06
Candida curvata	xylose		15		0.27		0.37		W06
Apiotrichium curvatum	whey		20		0.38		0.36		W06
Trichoderma viride	glucose	0.012	2.2	0.162 (b.)					(T.w.)
Trichoderma viride	glucose	0.009 (b.)		0.35 (b.)		TAG	0.055	1.17 (b.)	(SC92)
Trichoderma viride	lactose	0.012	2.0	0.128 (b.)					(T.w.)
Trichoderma viride	sucrose					TAG			(SC92)
Trichoderma viride	xylose					TAG			(SC92)
Trichoderma viride	OOWM	0.012	20.0	0.074 (b.)					(T.w.)
Rhodotorula toruloides		0.13 (f.b.)	151 (f.b.)	0.48 (f.b.)		TAG	0.26	0.84 (f.b.)	L07
		0.135 (b.)	18.6 (b.)	0.68 (b.)		TAG	0.23		
Rhodotorula glutinis				0.72		TAG		0.67	
Mortierella isabellina	glucose		10.9	0.35		TAG	0.11	0.85	P07
Mortierella isabellina	lactose		9.5	0.37		TAG	0.14	0.83	P07
Cunninghamella echinulata	glucose		9.2	0.35		TAG	0.11	0.90	P07
Cunninghamella echinulata	lactose		0.6	0.05		TAG	0.01		P07
Mortierella alpina (DSM, W.-A. proc's)		0.516	26.4		40.5	TAG			
Yarrowia lipolytica				0.36	0.08	TAG	0.25	1.42	
Yarrowia lipolytica	Ind'l glycerol	0.21 (b.)	8.1 (c.)	0.43	0.12	TAG	0.43	0.93	
			Algae						
Chlorella vulgaris (true mixotroph)	CO_2 (Photoaut.)	0.110				TAG			O81
Chlorella vulgaris (true mixotroph)	glucose (Het.)	0.98				TAG			O81
Chlorella vulgaris (true mixotroph)	CO_2 + glc (Mix.)	0.198				TAG			O81
Chlorella protothecoides	CO_2 (Photoaut.)	0.015		0.15		TAG			X06
Chlorella protothecoides	CPH (Het.)	0.015	3.9	0.55		TAG			X06
Botryococcus braunii	CO_2 (Photoaut.)	0.014		0.27—0.86		HC			D05

3.2 Materials and Methods

The *T. viride* strain, originally from Centraalbureau voor Schimmelculters (CBS) of Baarn (Holland), was obtained from Prof. Lo Curto (University of Messina, Italy), conserved as a pure culture on glucose agar medium and carefully propagated therefrom in the growth medium.

3.3 Analytical Methods

The lipid analysis was carried out following Riuz et al. (2007) using two extractive solutions (S1 and S2) of dicloromethane and methanol 1:2 and 2:1 volume fractions. The biomass was first orbitally shacked; then, after centrifugation, the suspension was added to 50 ml of S1 and agitated for 2 hours at 150 rpm at 25 ºC. The liquid fraction was recovered by filtration and stored while the solid fraction was extracted in the same way with 50 ml of S2 and the liquid recovered, again, by filtration. The two extracts were mixed and the solvents were rotoevaporated, leaving the lipidic phase behind, which was dried for 24h in a drying oven. Standard solid content analyses (TSS) for wastewater treatment systems were also performed according to APAT and IRSA-CNR (2004). From the two, the lipid concentration was calculated.

3.4 Experimental Runs, Results and Discussion

The suitability of using wastewaters as a growth medium for oil-storing microorganisms was evaluated on *T. viride* and three different media, constituted by a pool of nutrients and microelements (adopted after Domingues et al., 2000) and one substrate. Two model substrates (glucose and lactose) and olive oil mill wastewater were used.

The OOWM tests were carried out with treatment in mind, e.g. targeting COD reduction. The biomass was inoculated in raw OOWM (featuring a C:N ratio which was estimated to be ~10:1 and grown for one week. Then, 100 ml of concentrated biomass suspension were used to make the lipid extraction.

Model systems nutrients and microelements were supplemented with glucose and lactose so as to obtain a C:N ratio equal to 60. The growth medium was inoculated with 100µL of biomass and grew under agitation for 7 days at 150 rpm and 25ºC with periodic biomass growth monitoring. Subsequently, the general lipid determination procedure was applied.

The results of the three runs are 7.4% (lipids on biomass dry weight), 16.2% and 12.8% respectively for the OOMW, glucose and lactose runs.

Serrano-Carreon et al. (1992) lipid accumulation tests on *T. viride* on C:N = 60 media using glucose and ammonium sulphate (matching our choice) as substrate and nitrogen source, respectively, attained ~13% lipid fraction after 7 days and 32% after 11 days. Clearly, lipid accumulation is accelerating after the first week of colture. Our culture was stopped after 7 days to match the time allowed for the OOWM treatment. The slightly lower lipid accumulation might be due to oxygen limitation. Lactose, appearently, leads to a lower lipid accumulation. The hydrolysis of the disaccharide may explain this delay; a comparable difference in lipid accumulation on glucose vs sucrose-fed cultures was indeed observed by the above Authors, and might require that the culture time be extended to reach comparable performance.

The OOWM culture exhibites a much worse lipid accumulation performance, and the question can be raised as to whether olive by-product treatment may be a suitable

opportunity to store lipids. The main reason is surely due to an unfavourable overall-C:N ratio; the second may be due to the carbon substrate distribution across several compounds, some of which are quickly metabolised, while others require some degradation before they can be metabolised, as observed before for disaccharides.
An answer to this question can be given if OOWM is combined (or replaced) by olive pomace, in that *T. viride* rapidly excrete a large amount of cellulase which, in the same time frame of lipid accumulation (some days), is able to degrade cellulose and might conceivably increase lipid accumulation.

4. References

Alvarez, H., Steinbüchel, A. Triacylglycerols in prokaryotic microorganisms. Applied *Microbiology and Biotechnology* 60 (4) 367—376 (2002).

Brown, D.E. and D.J. Halsted, 1975, The effect of Acid pH on the Growth of *Trichoderma viride*, *Biotech. and Bioeng.*, 17, 1199-1210.

Brown, D. E., Hasan, M., Lepe-Casillas, M. and Thornton, A. J. Effect of temperature and pH on lipid accumulation by *Trichoderma reesei*. *Applied Microbiology and Biotechnology*, 34 (3), 335—339 (1990).

Cohen, Z., Ratledge, C. (eds) Single Cell Oils . AOCS Press (2005).

Dayananda, C., Sarada, R., Bhattacharya, S., Ravishankar, G. A. Effect of media and culture conditions on growth and hydrocarbon production by *Botryococcus braunii* . Process Biochemistry 40 (9) 3125—3131 (2005).

Domingues, F.C., J.A. Queiroz, J.M.S. Cabral and L.P. Fonseca, 2000, The influence of culture conditions on mycelial structure and cellulase production by *Trichoderma reesei* Rut C-30, *Enzyme Microb. Technol.*, 26, 394–401

D'Urso, A., Galimberti, M., Bravi, M., Fungal Biomass-Based Processing of Phenolics-Rich Wastewaters. Proc. 8th Intl. Conf. on Chem. and Proc. Engng., Ischia, June 24—27 (2007a).

D'Urso, A., Russo, M., Bravi, M., Phenolic fraction removal by *Trichoderma viride*: an application on olive oil mill, distillery and cork processing wastewaters. Proceedings of Food and Agricultural Products: Processing and Innovations CIGR-III, Naples, (2007b).

D'Urso, A., Gapes, D., Bravi, M., Fungal biomass activity on synthetic wastewater containing glucose, acetic acid and gallic acid. *This conference* (2008a).

D'Urso, A., Gapes, D., Bravi, M., Bioremediation of Olive Oil Mill Wastewaters by Fungal (*T. viride*, strain 8/90) Sequencing batch reactor. *This conference* (2008b).

Falk, O., Meyer-Pittroff, R. The effect of fatty acid composition on biodiesel oxidative stability. European Journal of Lipid Science and Technology 106 (12) 837—843 (2004).

Guschina, I. A., Harwood, J. L. Lipids and lipid metabolism in eukaryotic algae. Progress in Lipid Research , 45 (2) 160—186 (2006).

Hammel, K. E., 1997, Fungal degradation of lignin. In: Driven by Nature: Plant Litter Quality and Decomposition. Eds. Cadisch and Giller. CAB International, Wallingford.

Hopwood, D. and de Vos, R. 20% by 2020: the way forward. *Refocus*, 8 (2), 22-25 (2007).

Lee, Y. K. Microalgal mass culture systems and methods: Their limitation and Potential J. Appl. Phycol. 13 (4) 307—315 (2001).

Li, Y. H., Liu, B., Zhao, Z. B., Bai, F. W. Optimization of Culture Conditions for Lipid Production by Rhodosporidium toruloides. *Chinese Journal of Biotechnology* 22 (4) 650—656 (2006).

Li, Y., Zhao, Z., Bai, F. High-density cultivation of oleaginous yeast *Rhodosporidium toruloides* Y4 in fed-batch culture . *Enzyme and Microbial Technology* 41 (3) 312—317 (2007).

Miao, X., Wu, Q. Biodiesel production from heterotrophic microalgal oil . Bioresource Technology 97 (6) 841—846 (2006).

Murphy, D. J. The biogenesis and functions of lipid bodies in animals, plants and microorganisms. *Progress in Lipid Research* 40 (5) 325—438 (2001).

Ogbonna, J. C., Ichige, E., Tanaka, H. Interactions between photoautotrophic and heterotrophic metabolism in photoheterotrophic cultures of *Euglena gracilis* . Applied Microbiology and Biotechnology 58 (4) 532—538 (2002).

Papanikolaou, S., Aggelis, G. Lipid production by *Yarrowia lipolytica* growing on industrial glycerol in a single-stage continuous culture. *Bioresource Technology* 82 1 43—49 (2002).

Papanikolaou, S., Galiotou-Panayotou, M., Fakas, S., Komaitis, M., Aggelis, G. Lipid production by oleaginous Mucorales cultivated on renewable carbon sources . European Journal of Lipid Science and Technology 109 (11) 1060—1070 (2007).

Ratledge, C., Wynn, J. P. The biochemistry and molecular biology of lipid accumulation in oleaginous microorganisms. *Adv. Appl. Microbiol.* 51 , 1—51 (2002).

Ratledge, C., Fatty acid biosynthesis in microorganisms being used for Single Cell Oil production, *Biochimie*, 86 (11) 807—815 (2004).

Ruiz, N., Dubois, N., Wielgosz-Collin, G., du Pont, T. R., Berge, J.-.P, Pouchus, Y. F., Barnathan., G.. Lipid content and fatty acid composition of a marine-derived *Trichoderma longibrachiatum* strain cultured by agar surface and submerged fermentations. Process Biochemistry 42, 676—680 (2007).

Serrano-Carreon, L., Hathout, Y., Bensoussan, M. and Belin, J.-M. Lipid accumulation in *Trichoderma* species. *FEMS Microbiology Letters*, 93 (2), 181—187 (1992).

Suutari, M. Effect of growth temperature on lipid fatty acids of four fungi (Aspergillus niger, Neurospora crassa, Penicillium chrysogenum, and Trichoderma reesei). *Archivers of Microbiology*, 164 (3), 212—216 (1995).

Tomati, T., Various authors . Stato dell'Arte sul problema dell'utilizzazione dei reflui oleari . Ministero della Ricerca Scientifica e Tecnologica della Repubblica Italiana , Programma Nazionale di Ricerca "Reflui del Sistema Agricolo-Industriale", Sottoprogetto reflui oleari (2000).

Woodbine, M. Microbial fat: Microorganisms as potential fat producers. *Prog. Ind. Microbiol.* 1, 179—245 (1959).

Wynn, J. P., Ratledge, C. , Microbial Production of Oils and Fats , in: Shetty, K., Paliyath, G., Pometto, A., Levin, R. (Eds.) Food Biotechnology , CRC Press,443—472 (2006).

CHEMICAL ENGINEERING TRANSACTIONS, Volume 14, 2008
Edited by G. Marino, E. Bardone, A. Viglia
 ISBN 978-88-95608-02-0

Production Of Hydrogen By Wastewater Sludge Using Anaerobic Fermentation In A Pilot Scale Reactor

B. La Licata*[@], A. Scaletta*, F. Sagnelli*, T. Tommasi[a] , P. Zitella* and B. Ruggeri [a]

*BioEnergy Lab, ENVIRONMENT PARK S.p.A. Via Livorno 60, 10144 Turin
[a]Dept. of Material Science and Chemical Engineering Polytechnic of Turin, Corso Duca degli Abruzzi, 24, 10129 Turin

[@] Corresponding author: barbara.lalicata@envipark.com
Keywords: Bio-hydrogen production, sewage sludge, pilot scale reactor, kinetics

The aim of this study is to investigate the production of bio-hydrogen, via dark anaerobic fermentation in a pilot scale reactor under batch conditions, using a mixed microflora. As inoculum, anaerobic digested sludge, collected from municipal wastewater treatment plant, was used after being pre-treated with HCl 1N for 24h (pH 3) in order to inhibit the methanogenic bioactivity. As a source of carbon, sucrose at high concentrations (100 g/l) dissolved in a medium containing salts and micronutrients was employed. During fermentation temperature was maintained at room conditions (20°C), pH ranged from 7.2 to 5.2, due to the formation of Volatile Fatty Acids (VFA_s), that showed a butyrate-type fermentation. The reactor produced approximately 70 l of gas containing hydrogen (46%) and carbon dioxide (54%) with a global yield of 0.32 mol H_2/mol sucrose, whereas no H_2S or CH_4 was detected, suggesting that acid pretreatment plays an important role in the elimination of methanogenic bacteria.
Formation of VFA_s, sucrose concentration and biomass concentration in terms of CFU/ml of *Clostridium spp*. were reported at different times. The investigation of these parameters led to a kinetic study for the description of the dark anaerobic fermentation process, in order to obtain data for future experiments for the production of bio-hydrogen with a continuous stirred tank reactor (CSTR).

1. Introduction

Hydrogen is a clean and sustainable vector of energy, that can be produced with different technologies. One way to produce hydrogen is via dark anaerobic fermentation from carbohydrates following the acetate-butyrate pathways. The microrganisms mainly involved in the production of bio-H_2 belong to the Clostridial species as reported by Kim et al., 2006. *Clostridium spp*. are anaerobic, Gram positive and spore-forming bacteria, able to resist to shocks like heat treatment or acid-basic treatment. Moreover *Clostridium spp*. can achieve the highest H_2 yield per mole of glucose in dark anaerobic fermentation (1.61÷2.36 mol H_2/mol glucose) (Taguchi et al., 1995). Many researchers used pure culture of *Clostridium spp.* to enhance bio-hydrogen production (Chen et al., 2005; Liu et al., 2006) but with a cost of the process much higher if compared to other productive technologies.

In order to make bio-H_2 production more cost effective, mixed microflora, such as activated or digested sludge should be used at mesophilic temperatures (Lin et al., 2004; Zhang et al., 2006). During anaerobic digestion methanogenic or sulphate-reducing bacteria, normally present in anaerobic sludge, consume hydrogen produced by acidogenic bacteria. For the inhibition of methanogenic bioactivity many pre-treatments were proposed, for example acidification, basification, freezing and thawing or thermal shock (Mu et al., 2006; Mohan et al., 2007; Ting et al., 2007). In this work acid pre-treatment was performed for anaerobic digested sludge, demonstrating that is an effective method to avoid methanogenesis during fermentation.
This study also investigates how key parameters, like VFA_s and biomass, evolve during anaerobic fermentation in mesophilic conditions. A kinetic model of fermentation was developed for future work on CSTR reactors.

2. Materials And Methods

2.1 Reactor design

Dark anaerobic fermentation was carried out in a batch reactor of 35 l. The pressure inside the reactor can be set by regulating a relief valve; as soon as the pressure inside exceeds the backpressure, gas passes through the valve and is collected in another vessel of 2,5 l connected to a compressor which pressurizes the gas, ready then to be stored in gas sampling bags SKC, 232 series.
The reactor is also equipped with a mixer with a maximum speed of 30 rpm, and with a pH and temperature control system to study the influence of these parameters on the fermentative process. To create anaerobic conditions, the system is provided with a gas inlet at the bottom of the reactor, where inert gas, i.e. nitrogen, can be injected continuously.

2.2 Experimental procedure

An anaerobic digested sludge derived from the municipal wastewater treatment plant of Turin (S.M.A.T. Torino) was used as inoculum. In order to inhibit the methanogenic bioactivity the sludge was first treated for 24h with HCl 1N to obtain pH = 3. In fact, as reported by Chen et al. (2002) and Mu et al. (2006) no methane production could be observed after pre-treating the sludge at values of pH in a range of 3÷4 for 24h.
After this period of time the reactor was then fed with a medium containing inorganic salts, micronutrients and sucrose. Experimentation was carried out with a ratio between sludge and sucrose medium of 1:10 (v/v); in order to obtain a volume of 25 l inside the reactor, 2,5 l and 22,5 l of sludge and medium respectively were introduced in the reactor.
As a source of carbon, sucrose, at a concentration of 100 g/l, was dissolved in a medium consisting of (all in mg/l): $NaHCO_3$ 2679, NH_4Cl 5358, KH_2PO_4 536, K_2HPO_4 536, $CaCl_2$ 1072, $NiSO_4 \cdot 6H_2O$ 116, $MgSO_4 \cdot 7H_2O$ 686, $FeCl_3$ 43, $Na_2B_2O_7 \cdot 10H_2O$ 15, $Na_2MoO_4 \cdot 2H_2O$ 30, $ZnCl_2$ 49, $CoCl_2 \cdot 6H_2O$ 45, $CuCl_2 \cdot H_2O$ 21, $MnCl_2 \cdot 4H_2O$ 64, yeast extract 107 (Fang et al., 2006). The theoretical specific ratio C/N was fixed at 30 in order to guarantee a good nutritional supply to microrganisms.
Anaerobic conditions were created insufflating nitrogen inside the reactor, till no oxygen could be detected. Pressure inside the reactor was set at values of 20÷30 mbar,r,

while temperature remained at room conditions at about 20°C. To avoid biomass stratification the stirrer was set at the maximum speed of 30 rpm. During the process no pH and temperature regulation occurred.
The gas produced was constantly measured with a volumetric gascounter (Sacofgas S1ATG4), as well as pH, ORP and temperature which were logged through a data acquisition system. Gas composition was continuously evaluated online with a gas cromatograph (Varian, CP 4900), for the determination of hydrogen, carbon dioxide, methane, nitrogen, oxygen and hydrogen sulphide content.

2.3 Chemical and biological analysis

During fermentation different samples were taken at the following times: 0, 24, 46, 64, 72 and 91 h. Sucrose content of these samples was determined with an enzymatic kit (R-Biopharm, AG). Clostridial Plate Count was also performed according to Galli et al., 2003 and Laird et al., 2004, while the total ATP content was measured by light emission using the enzyme luciferase (Promega) and a luminometer (Junior LB9509, Berthold Technologies). After filtration of the samples on 45µ Whatman filter papers (40 grades) in a vacuum system (IRSA-CNR, 2006), VFA_s (Acetate, Butyrate, Propionate, Iso-butyrate) and Ethanol were determined using a gas cromatograph (EPA, 3810 and EPA 8260C).

3. Results

3.1 Gas production

Dark anaerobic fermentation took place in approximately 5 days producing a total gas amount of 66.9 l. Thanks to the acid pre-treatment no methane and hydrogen sulphide production was observed. Only hydrogen, carbon dioxide and nitrogen were detected, with small amounts of humidity. Table 1 shows gas production and composition during the process. The presence of nitrogen in the gas is related to the preliminary sparging of inert gas to create anaerobic conditions. In effect nitrogen content decreased during production, while hydrogen and carbon dioxide rose, due to the biological activity of *Clostridium spp*. In Fig. 1a total gas, hydrogen and carbon dioxide cumulative volumes, and the ratio between hydrogen and carbon dioxide from the beginning till the end of the experiment are reported. pH, without being regulated, constantly decreased from 7.2 to 5.2, as well as ORP reduced from -250 mV to -440 mV at t = 72h, slightly raising at the end of fermentation; Fig. 1b reports the trend of these two parameters.

Table 1. Total gas production and percentage composition

Runtime (h)	V (l)	H_2	CO_2	N_2
0	0.0	0.0	0.0	100.0
40.4	3.3	0.0	0.0	100.0
49.7	5.4	1.5	7.4	91.1
63.88	17.9	16.6	44.3	39.1
72.57	38.2	35.2	54.4	10.4
91.63	65.4	44.1	51.7	4.2
100.62	65.7	42.1	51.0	6.9

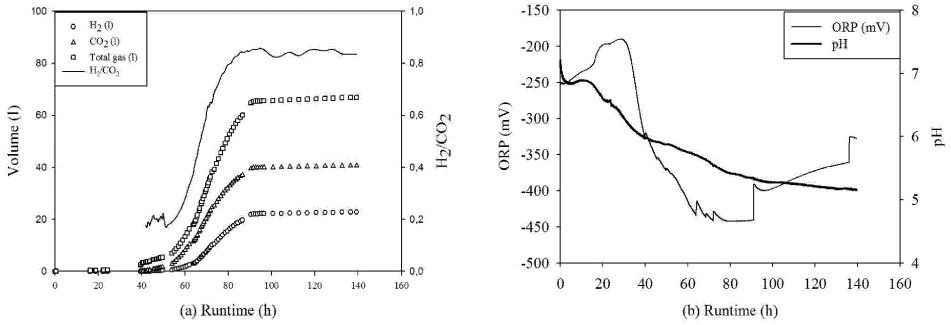

Fig. 1 – (a) Hydrogen, carbon dioxide , total gas production and hydrogen on carbon dioxide ratio; (b) pH and ORP

3.2 Chemical and biological analysis

Total sucrose decreased during fermentation from the starting concentration of 90 g/l till 51 g/l (Fig. 2a). In Fig. 2b the trend of bioluminescence proportional to the ATP level and the trend of biomass growth in terms of CFU/ml of *Clostridium spp.* are reported. The graph suggests that the maximum activity, in terms of viable colony count and chemiluminescence, was reached at t = 64h at the initial phase of hydrogen production.

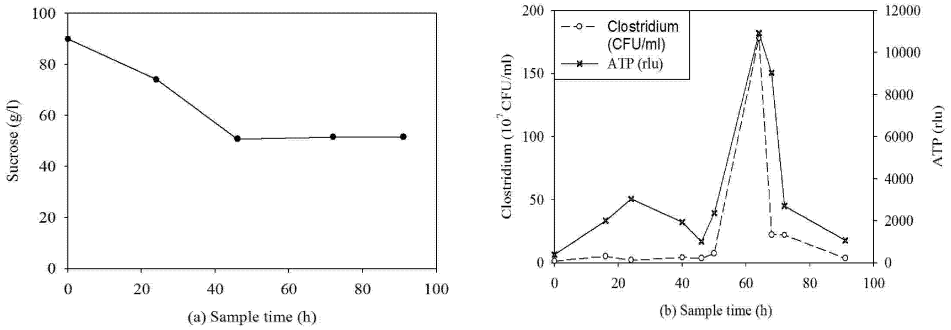

Fig. 2 – (a) Sucrose concentration; (b) Clostridial and ATP analysis

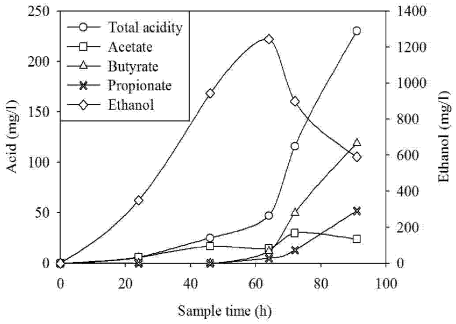

Fig. 3 –Volatile Fatty Acids (VFA_s)

Finally, Fig. 3 reports the volatile fatty acids (VFA_s) and ethanol produced along fermentation. The maximum concentrations of acetate, butyrate and propionate are 30, 120 and 52 mg/l respectively, while the total acidity reached its maximum at the end of fermentation at 230 mg/l. Besides the maximum concentration of ethanol was 1244 mg/l, observed at t = 64h at the initial phase of hydrogen production (Fig. 1a).

3.3 Kinetics study

On the basis of results reported in figures 1a and 2a two regression curves for hydrogen production and sucrose consumption were built. For both diagrams a modified Gompertz equation suitable for the description of the microbial growth in a batch culture was used. The hydrogen production was described with the modified model presented by Lay et al., 1999

$$H = H_{\max} \times \exp\left\{-\exp\left[\frac{R_{\max,H_2} \times e}{H_{\max}}(\lambda - t) + 1\right]\right\} \quad (1)$$

where H represents the cumulative volume of hydrogen produced (l) at the time t, $R_{max,H2}$ is the maximum value of hydrogen production rate (l/h) whereas λ is time of lag phase (h). By differentiating eq. (1) hydrogen production rate r_{H2} was calculated as

$$r_{H_2} = R_{\max,H_2} \times \exp\left\{-\exp\left[\frac{R_{\max,H_2} \times e}{H_{\max}}(\lambda - t) + 1\right] + \left[\frac{R_{\max,H_2} \times e}{H_{\max}}(\lambda - t) + 1\right] + 1\right\} \quad (2)$$

On the other side sucrose consumption could be represented by the modified Gompertz model proposed by Fan et al., 2004

$$S_0 - S = S_{\max} \times \exp\left\{-\exp\left[\frac{R_{\max,S} \times e}{S_{\max}}(\lambda - t) + 1\right]\right\} \quad (3)$$

where S_0 is the initial concentration of sucrose at t = 0h (90 g/l), S is the actual concentration inside the reactor and S_{max} is the maximum sucrose consumption. By differentiating the eq. (3), the rate of substrate consumption r_S is given by

$$r_S = R_{\max,S} \times \exp\left\{-\exp\left[\frac{R_{\max,S} \times e}{S_{\max}}(\lambda - t) + 1\right] + \left[\frac{R_{\max,S} \times e}{S_{\max}}(\lambda - t) + 1\right] + 1\right\} \quad (4)$$

All parameters in the equations were estimated by minimizing the sum square of errors between experimental data and model prediction. Equations 1 and 3 are reported in figure 4a and 4b.

The trend of hydrogen production rate is traced as a function of time as shown in Fig. 5. The exponential phase of hydrogen production occurred in the range of t = 60÷100h and the maximum production rate was found at about t = 70h when sucrose concentration was 51 g/l (fig. 4a).

The following section describes the use of kinetic results in order to evaluate retention time (HRT) in a continuous plant to reach optimal conditions as discussed above with a high initial sucrose concentration. By choosing the optimal concentration of sucrose at which the reactor should work for maximizing hydrogen productivity, for an established value of incoming sucrose concentration S_0, retention time τ could be easily evaluated by steady-state balance, assuming an ideal behaviour inside the reactor CSTR:

$$\tau = \frac{V}{Q} = \frac{S_0 - S_{SS}}{r_S} \tag{5}$$

where Q represents the flow (l/h) inside the reactor, S_0 and S_{SS} are respectively the inlet and optimal sucrose concentrations, V is the volume of the reactor and r_S is the sucrose consumption rate at S_{SS} value.

By fixing an initial sucrose concentration, retention time that maximizes hydrogen production could be easily found with equation (5). Nevertheless, in order to effectively obtain hydrogen, retention time must be compared with biomass growth time in order to avoid problems connected with the so called "wash out" phenomena. In this sense many reviews in literature report values of maximum specific growth rate μ_{max} in the range of 0.08÷0.125 h^{-1} (Chen et al., 2001; Mu et al., 2007). Fixing the initial sucrose concentration in the range of 60÷70 g/l, the dilution rate $D = \tau^{-1}$, calculated according to the eq. (5), varies in the range of 0.011÷0.025 h^{-1} which is much smaller than μ_{max}, well distant from wash out conditions.

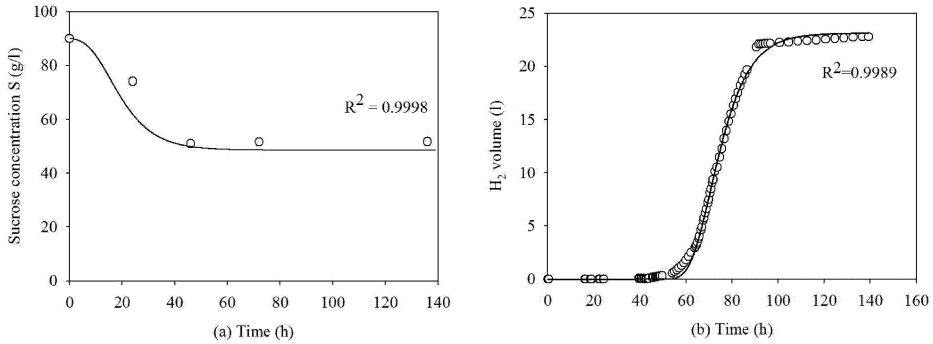

Fig. 4 – (a) Regression curves for sucrose consumption and (b) hydrogen production

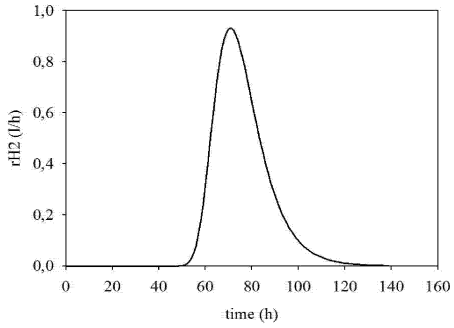

Fig. 5 – Hydrogen production rate r_{H2}

4. Discussion and conclusions

This experiment proved that it is possible to produce biohydrogen in a pilot scale reactor using digested sludge as inoculum and sucrose as a substrate, without enriching the culture with clostridial species. The experiment confirmed that acid pre-treatment is a valid method to inhibit methanogenic bioactivity, since no methane nor hydrogen sulphide was observed in gas produced.

After a lag phase of 48h, necessary for the bacteria sporulation, as suggested by Hawkes et al. (2002), hydrogen production began with a maximum rate of 0.94 l/h at t = 74h, resulting in a final volume of hydrogen produced of 23 l on a total volume (H_2 + CO_2) of 66.9 l. At the end of production, considering only the contributions of hydrogen and carbon dioxide, a concentration of 46% in H_2 was reached, equivalent to a hydrogen/carbon dioxide ratio of 0.86. Sucrose concentration reduced from 90 g/l to 51 g/l, with a final yield in hydrogen production of 0.32 mol H_2/mol sucrose. This value, obtained working at 20°C and with mixed microflora, is lower than the values that could be found by many researchers (Taguchi et al., 1995) working at higher temperatures (30÷35°C) and in some cases with pure cultures. Total Clostridium plate count showed a maximum of $1.8x10^9$ CFU/ml at t = 64h, when ATP reached its maximum of 11000 rlu; pH decreased constantly from 7.2 to 5.2, while ORP diminished showing a minimum of -440 mV at t = 72h, in correspondence of the maximum hydrogen production rate. This value indicates that a reducing atmosphere required for hydrogen producing bacteria was established, while at the same time the reduction of pH is connected with the formation of volatile fatty acids.

Fang et al., 2002, found that predominant bacteria present in a mixed culture enriched by acid pre-treatment belong to species in the genera *Clostridium*, *Enterobacter* and *Citrobacter*. Some species, i.e. *C. butyricum* and *C. tyrobutyricum*, produce butyrate and acetate as their main fermentation byproducts, whereas other species, like *C. acetobutyricum* follow the homoacetogenic pathway.

In this study the major volatile fatty acids produced are essentially acetate and butyrate, according to the following reactions

$$C_{12}H_{22}O_{11} + 5\ H_2O \rightarrow 4\ CH_3COOH + 4\ CO_2 + 8\ H_2 \quad (6)$$

$$C_{12}H_{22}O_{11} + H_2O \rightarrow 4\ CH_3CH_2CH_2COOH + 4\ CO_2 + 4\ H_2 \quad (7)$$

This suggests that mixed microflora observes a typical butyrate-type fermentation as main metabolic pathway, even though small amounts of propionic acid and acetate could be detected along the process, as a result of other types of fermentations, such as propionate-type or homoacetogenic. Observing Fig. 3 it is clear that reaction (6) and (7) are only a rough approximation of reality, so that biochemical pathways need to be analyzed in more detailed experimental tests. The study of the kinetics of hydrogen production and sucrose consumption through the modified Gompertz equations led to the definition of the optimal conditions (initial sucrose concentration S_0 and retention time τ) for working in a continuous mode. As a first consideration an optimal sucrose concentration for maximizing hydrogen productivity was found at a value of 51 g/l. Further on, a relationship between S_0 and τ was outlined, so that for initial values of

sucrose of 60÷70 g/l, a dilution rate $D = \tau^{-1}$ of 0.011÷0.025 h^{-1} is needed to obtain the maximum H_2 production rate preventing at the same time wash out. In any case all of the above considerations are valid for high sucrose concentrations experimentally tested (i.e. S > 50 g/l).

5. References

Chen, W.M., Tseng, Z.-J.,. Lee, K.-S, Chang J.-S., 2005, Fermentative hydrogen production with *Clostridium Butyricum* CGS5 isolated from anaerobic sewage sludge. International Journal of Hydrogen Energy.

Fan, Y.Z., Wang, Y.Y., Qian, P.Y., Gu, J.D., 2004, Optimization of phthalic acid batch biodegradation and the use of modified Richards model for modelling degradation. Int. Biodeter. Biodegr.

Kim, S.-H., Han S-K, Shin H-S., 2006, Effect of substrate concentration on hydrogen production and 16S rDNA-based analysis of the microbial community in a continuous fermenter. Process Biochem.

Lin, C.Y., Lay, C.H., 2004, Carbon/nitrogen-ratio effect on fermentative hydrogen production by mixed microflora. International Journal of Hydrogen Energy.

Lin, C.Y., Lay, C.H., 2005, A nutrient formulation for fermentative hydrogen production using anaerobic sewage sludge microflora. International Journal of Hydrogen Energy.

Liu, X., Zhu, Y., Yang, S.-T., 2006, Butyric acid and hydrogen production by *Clostridium tyrobutyricum* ATCC 25755 and mutants. Enzyme and Microbial Technology.

Mohan, S.V., Babu, V.L., Sarma, P.N., 2007, Effect of various pretreatment methods on anaerobic mixed microflora to enhance biohydrogen production utilizing dairy wastewater as substrate. Bioresource Technology.

Mu, Y., Yu, H.Q., Wang, G., 2006, Evaluation of three methods for enriching H2-producing cultures from anaerobic sludge. Enzyme and Microbial technology.

Taguchi F, Mikukami N, Saito-Taki T, Hasegawa K., 1995, Hydrogen production from continuous fermentation of xylose during growth of *Clostridium spp*. strain No. 2.Can JMicrobiol.

Ting. C.H., Lee, D.J., 2007, Production of hydrogen and methane from wastewater sludge using anaerobic fermentation. International Journal of Hydrogen Energy.

Zhang, Y., Shen, J., 2006, Effect of temperature and iron concentration on the growth and hydrogen production of mixed bacteria. International Journal of Hydrogen Energy

Istituto di Ricerca Sulle Acque, CNR, 2006, Metodi Analitici per i Fanghi, Quaderni, 64, Parte Seconda.

Lay, J.J., Lee, Y.J., Noike, T., 1999. Feasibility of biological hydrogen production from organic fraction of municipal solid waste. Water Res.

Chen, C-C., Lin, C-Y. Chang, J-S., 2001, Kinetics of hydrogen production with continuous anaerobic cultures utilizing sucrose as the limiting substrate. Appl Microbiol Biotechnol.

Mu, Y., Yu, H.-Q., Wang, G., 2007, A kinetic approach to anaerobic hydrogen-producing process. Water research.

CHEMICAL ENGINEERING TRANSACTIONS, Volume 14, 2008
Edited by G. Marino, E. Bardone, A. Viglia
 ISBN 978-88-95608-02-0

A Study on the Biochemical Reaction Engineering of Biodisel Production

Alberto Gallifuoco, Laura Cantarella[a], Agata Spera, Isa Venti, Maria Cantarella

Department of Chemistry, Chemical Engineering and Materials, University of L'Aquila, Monteluco di Roio, 67040, L'Aquila, Italy
[a]Department of Industrial Engineering, University of Cassino, Via Di Biasio 43, 03043 Cassino (FR), Italy
Corresponding e-mail: cantarel@ing.univaq.it

The bioesterification of ethyl alcohol with palmitic acid catalyzed by lipase from Candida rugosa was studied. This key model reaction of biodiesel production was assayed in two different organic solvents, n-hexane and iso-octane. The activity was studied with respect to the effect of enzyme loading, and linearity conditions were determined. Substrates concentrations were varied both at stoichiometric ratio (1:1) and keeping alternatively one substrate fixed at 100 mM and varying the other one. The presence of an optimal condition (50 mM, stoichiometric ratio) was detected. The system behaves differently depending on the organic solvent, and ethanol demonstrated to have a rate depressing effect at excess concentration. These findings confirm that the kinetic pattern is complex. Finally, the effect of temperature was investigated and the activation energies in the two different organic solvent media were determined, resulting 7268 and 8763 cal/mole respectively with iso-octane and n-hexane.

Introduction

Biodiesel (mono-alkyl esters of primary alcohol and long-chain fatty acids derived from vegetable oils or animal fats) is nowadays an important alternative, biodegradable renewable fuel for diesel engines. Although its use with internal combustion engines is technologically well assessed, the industrial production is not yet completely optimized. Most processes for making biodiesel are based on esterification reactions and require the use of a catalyst (strong mineral bases) to initiate the reaction, to promote the solubility of the reactants and to allow the process to proceed at a significant rate (Vicente et al, 2004). Several aspects are still under investigation aiming to improve the process efficiency, reduce the amount of by-products, and mitigate the ecological impact. The key chemical reaction involved in the process are esterifications and trans-esterifications (Fukuda et al, 2001). The primary raw materials used for making biodiesel are from agricultural sources: energy crops, such as sunflowers and rapeseed, or waste oils from the food industry. Till now methyl alcohol has been used in the esterifications, although green ethanol could represent a valid alternative owing to the lower toxicity and the higher yield on a weight basis (Masaru et al, 2001).
A totally green production of biodiesel should be performed in a bioprocess using lipases (EC 3.1.1.3) as catalyst (Shimada et al, 2002).

The present study deals with a model reaction, esterification between palmitic acid and ethyl alcohol catalyzed by lipase from *Candida rugosa*. This system is complex, ruled by a two-substrate kinetics, and possibly controlled by physical phenomena, such as interfacial tension between the liquid phase and the insoluble enzyme. Furthermore solvent polarity, and product and substrate solubility superimpose their effects
This contribution reports on the effect of substrate concentration and enzyme loading on the reaction rate, investigating in order to determine the optimal conditions which maximize the yield of esterification. The kinetic runs were performed in batch reactors using two different solvents, n-hexane and iso-octane. The driving force for the reaction to proceed is represented by the overall concentration of the two different substrates, but alcohol and acid play different roles, and these have been isolated performing runs at constant concentration of one substrate and varying the concentration of the other. An optimal ratio of substrate concentration has been detected. The effect of enzyme loading was also investigated maintaining the system at the best substrate concentration. Finally, the effect of temperature has been studied.
The body of the results so far obtained provides essential information to address further on the future research to ascertain the best reactor configuration and feeding policy in order to perform the quantitative continuous bioconversion, and to lessen the amount of solvent to be removed at the end of the reaction to produce a biodiesel suitable as commercial fuel.

Materials and methods

Lipase (triacyl glycerol lipase, EC 3.1.1.3) from *Candida rugosa* was the type VII lyophilized powder from Sigma-Aldrich (USA). The enzyme powder was directly suspended in the reaction media. Ethyl alcohol (EtOH) was from Fluka Chemika (Germany). Palmitic acid (PA), ethyl palmitate (EP), iso-octane and n-hexane were from Sigma-Aldrich (Germany). All the chemicals were laboratory grade pure reagent.
Two different stirred reactors were employed in the kinetic runs: one of 4 ml volume, thermostated in a Reacti-Therm model 18971 module (Pierce, USA) by insertion in an aluminium plate controlled for stirring speed and temperature; the second one is a water-jacketed glass reactors, 10 ml volume, designed on purpose, whose temperature and stirring control is assured by a thermostatic bath (Haake D8, Denmark) and a magnetic stirrer (Heidolph, Germany). The analytical determination of residue substrates and products was performed using a HP 5890 series II gas chromatograph equipped with a flame ionization detector, a capillary column HP-FFAP, and an autosampler HP 6890. The whole equipment was from Hewlett-Packard (USA).
Unless otherwise specified, all the kinetic runs were performed at 40 °C under 300 rpm stirring conditions and according to the following procedure. Substrates were dissolved carefully into the appropriate solvent, iso-octane or n-hexane, until a clear solution was obtained. The mixture was introduced into the reactor and allowed to equilibrate at the set temperature. The reaction was started adding the amount of enzyme powder. The reactor was then sealed to reduce losses by evaporation. At fixed time intervals, samples of negligible volume (50 μl) were withdrawn using a syringe through a Teflon cap, diluted with 150 μl of solvent to adjust the concentration range of analytes, filtered with a syringe microfilter for removing traces of enzyme powder, and injected in the column. Two different blanks were prepared for each run: just before the enzyme addition and a few seconds after. The peak areas of the two blanks resulted similar in all the

experiments and the average was taken as reference. The samples, prepared in the autosampler vials and where then analyzed.
The standard temperature program of analysis was the following. Injector: 220 °C; column: initial, 80 °C (2.5 min); up to 120 °C (2 min); hold at 120 °C (9.5 min); up to 230 °C (6 min); hold 230 °C (5 min). Carrier gas was helium at 16 ml/min. Under these conditions, total analysis time resulted 25 min and retention times were: ethanol, 2 min; ethyl palmitate, 12 min; palmitic acid 21 min. Peak resolution was fair, and the concentration of each chemical was easily estimated using as reference calibration lines performed with internal standards expressly prepared. In order to reduce the errors, all the analyses were performed at least in duplicate.

Results and discussion

In preliminary runs, the enzyme activity was assayed with both solvents with 100 mM of the two substrates at stoichiometric ratio. Enzyme loading varied from 4 to 20 mg/ml. Linearity conditions were verified with both solvents and the specific activities were 0.0056 and 0.0049 EU/mg respectively for iso-octane and n-hexane, resulting the activity 14% higher in iso-octane. This activity ratio should be considered a reference datum, since varying the concentrations of the two substrates different results could be obtained. The bioesterification was assayed in the jacketed reactor performing kinetic runs at fixed amount of enzyme (10 mg per ml of iso-octane) and different concentration of the two substrates (stoichiometric ratio [EtOH]/[PA] = 1). The reaction was followed up to 240 min withdrawing samples at regular time intervals and assaying for substrates and products. Results are reported in Figure 1 as substrate conversion *vs* process time.

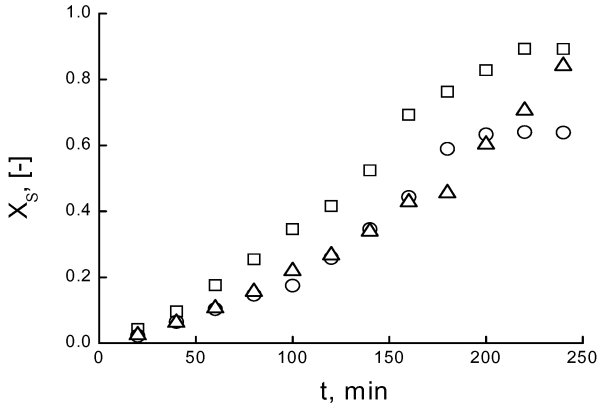

Figure 1. Substrate conversion as a function of process time. $[S]_0$ (mM): □, 20; Δ, 40; ○, *60.*

The enzyme activity increases with substrate concentration, but not linearly, as evident from the initial derivatives of the curves (respectively 0.055, 0.065, and 0.066 min^{-1}). As the reaction proceeds, substrate concentration diminishes, causing initially an acceleration then, at longer process time, the rate depletes: consequently, s-shaped

curves are generated. The higher the initial substrate concentration, the more evident this behaviour. This indicates that substrate(s) act as driving force for the reaction to proceed but that an excess could depress the kinetics. Data of Figure 1 also show that conversion as high as 90% could be attained.
In order to sustain the bioprocess, substrate concentration should be carefully maintained close to the optimal value. Experiments performed in 4 ml reactors aiming to detect this optimal substrate concentration are shown in Figure 2.

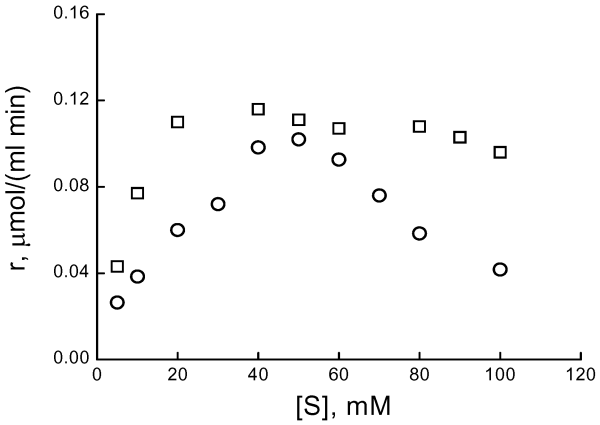

Figure 2. Reaction rate as a function of substrate concentration. Solvent: □, iso-octane; ○, n-hexane.

The amount of enzyme powder per ml of reaction medium was the same of the previous experiments while substrate concentrations varied from 5 to 100 mM, at constant ratio [EtOH]/[PA] = 1:1. The obtained data show a rather different behaviour with both the solvents. The rate depression effect is more evident using n-hexane as solvent, with the existence of a maximum at roughly 50 mM. Besides, whatever the substrate concentration, the reaction rate in the n-hexane medium is lesser than that in iso-octane. These results indicate that solvent plays an important role, presumably modifying forces acting at the enzyme/liquid interface. To reduce costs of production, the industrial bioprocess should be performed in scarcity of solvent and this should be selected considering both the enzyme activity and the easiness of separation. On the other hand, the kinetic pattern of this reaction is complex, and several equations are available in the literature for modelling the biocatalytic system. As a general rule, these equations contain too more parameters and non linear terms to be easily handled. The preliminary results here reported could help to address further on the research aiming to get a lumped kinetic equation simple but predictive with respect to the effect of operational parameters variations.
To meet this goal, further experiments were performed varying alternatively one substrate concentration from 15 to 180 mM, while keeping the other one constant at 100 mM. Results obtained with both solvents are reported in Figure 3 (constant [PA]) and Figure 4 (constant [EtOH]).

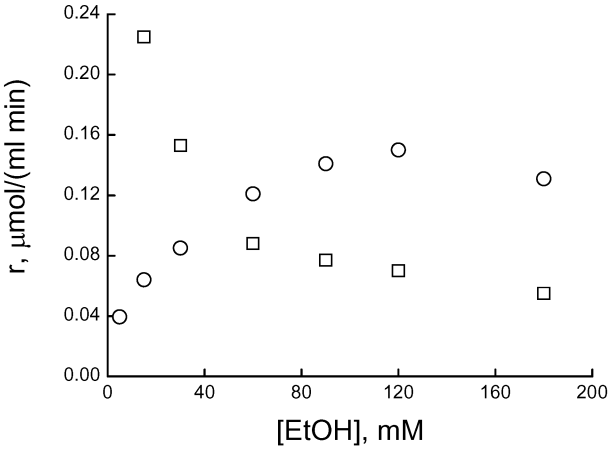

Figure 3. Reaction rate as a function of ethanol concentration. Solvent: □, iso-octane; ○, n-hexane.

Observing Figure 3, the effect of solvent is dramatically evident. In the iso-octane medium, the higher the ethanol concentration, the lower the reaction rate in the whole range explored. Using n-hexane, the reaction rate passes through a maximum. Obviously, if no ethanol was present, the esterification could not occur at all, so that also with iso-octane there should be a maximum, but this evidently occurs at a concentration below 15 mM. The other substrate, PA, acts similarly in both solvents. In fact, as PA concentration increases, the reaction accelerate and, at the experimental conditions adopted in Figure 4, the bioconversion occurs at higher rate using n-hexane.

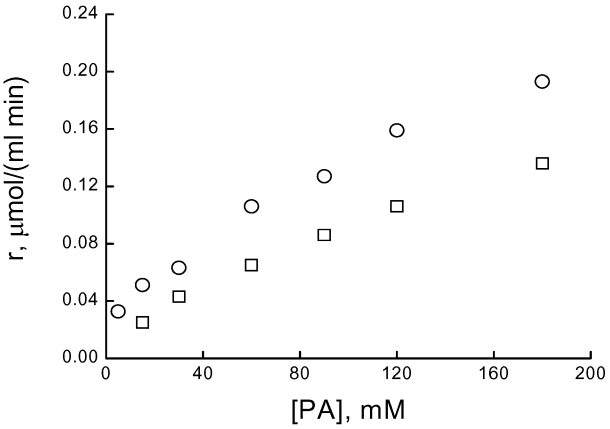

Figure 4. Reaction rate as a function of palmitic acid concentration. Solvent: □, iso-octane; ○, n-hexane.

The last part of the research was devoted to determine the effect of temperature on the bioesterification rate (see Figure 5). Experiments were performed at 100 mM stoichiometric substrate ratio and demonstrated that in both solvents the reaction follows the Arrhenius law.

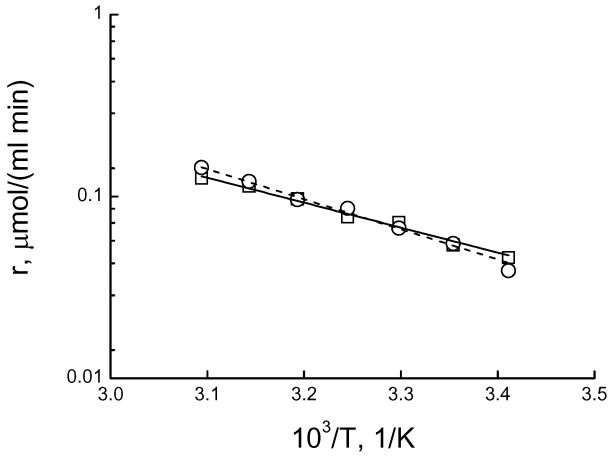

Figure 5. Arrhenius plot. Solvent: □, iso-octane; ○, n-hexane.

The activation energies detected were 7268and 8763cal/mole respectively for iso-octane (dashed line) and n-hexane (full line), thus indicating that the kinetics is not masked significantly by physical phenomena, such as mass transport or interfacial interactions. which could superimpose their effect to the biocatalytic act.

Conclusions

The body of the experimental findings here discussed constitutes a good starting point for extending the experiments on this model reaction. Useful information has been obtained for addressing further research. The main points to be studied appear to be the optimal substrate feeding policy, the strategies to get 100% bioconversion lessening the amount of organic solvent employed.

Acknowledgments

The authors would like to acknowledge the support of University of L'Aquila Research Fund, and MIUR-PRIN 2002095553_002

References

Masaru K, S. Taichi, K. Akihiko, H. Fukuda, 2001, Effect of methanol and water contents on production of biodiesel fuel from plant oil catalyzed by various lipases in a solvent-free system. J. Biosci. Bioeng., 91, 1, 12.

Fukuda H., A. Kondo, H. Noda, 2001, Biodiesel fuel production by transesterification of oils. J. Biosci. Bioeng., 92, 405.

Vicente G., M. artinez, J. Aracil, 2004, Integrated biodiesel production: a comparison of different homogeneous catalysts system. Biores. Technol., 92, 297.

Shimada Y., A. Watanabe, Y. Sugiharaand, T. Tominaga, 2002, Enzymatic alcoholysis for biodiesel fuel production and application to the reaction tomoil processing. J. Mol. Catal. B-Enzym., 17, 133.

CHEMICAL ENGINEERING TRANSACTIONS, Volume 14, 2008
Edited by G. Marino, E. Bardone, A. Viglia
 ISBN 978-88-95608-02-0

Assessment of the Kinetics of Butanol Production by *Clostridium acetobutylicum*

F. Napoli, G. Olivieri, A. Marzocchella, P. Salatino
School of Biotechnological Science
Dipartimento di Ingegneria Chimica - Università degli Studi di Napoli 'Federico II'
P.le V. Tecchio, 80 – 80125 Napoli, Italy

Preliminary results of a research activity aiming at investigating the feasibility of the acetone-butanol-ethanol (ABE) production by *Clostridium acetobutylicum* ATCC824 are reported. The contribution regards the characterization of the kinetics related to the ABE production process by free *C. acetobutylicum* ATCC824. Lactose solutions were adopted as medium with the aim of emulating cheese whey. The conversion process is characterized in terms of cells, acids, solvents, pH and total organic compounds as a function of time. Tests carried out under batch conditions show that: i) cells growth is constant for lactose concentration (C_L) smaller than 100 g/L; ii) the butanol specific production rate as a function of C_L may be represented by a Monod-like kinetics; iii) the lactose conversion - measured at the end of the solventogenesis phase - decreases with C_L; iv) the selectivity of butanol with respect to total solvents increases with C_L and stabilizes at about 72%$_W$ for C_L larger than 30 g/L.

1. Introduction

The economic scenario has revived the interest in Acetone-Butanol-Ethanol (ABE) fermentations. Recent developments in molecular techniques applied to solventogenic microrganisms in combination with recent advances in fermentation systems and downstream processing have contributed to improve ABE fermentation processes feasibility and competitiveness. The challenges raised over the last years as regards ABE production may be synthesized in: i) use of renewable resources as substrate; ii) selection of strains characterized by high ABE productivity; iii) development of new fermentation systems; iv) development of new downstream strategies for enhanced solvent recovery. The selection of unconventional substrates is favoured by the ability of clostridia strains to metabolize a wide range of carbohydrates like glucose, lactose, etc...., typically present in wastewater streams e.g. from the food industry. In particular, studies available in literature point out the potential of the ABE production process by fermentation of lactose (Welsh and Veliky, 1984) or cheese whey (Welsh and Veliky, 1986; Maddox, 1980).

Even though clostridia have been proven successful to produce ABE, information available in literature to support industrial scale-up is still lacking. The missing information regards either the kinetics of substrate conversion, cell growth and butanol production (Jones and Woods, 1986; Shinto et al., 2007) or the reactor systems.

Typically, the ABE fermentation process has been studied by means of reactor systems belonging to the batch and fed-batch typologies. Only a few attempts are reported in literature regarding continuous fermentation by means of clostridia strains confined in the reactor by immobilization (Huang et al., 2004; Qureshi et al., 2005; Ezeji et al., 2007) or cell-recycling (Tashiro et al., 2005). In a review on the state of art of the "white biotechnology", Villadsen (2007) has specifically mentioned the ABE process as an example of how and how far a more fundamental based approach makes process development more effective and successful.

The present study reports the preliminary results of a research activity aiming at investigating the feasibility of the ABE production by *Clostridium acetobutylicum* ATCC824 in a continuous biofilm reactor adopting cheese whey as feedstock. The contribution regards the characterization of the kinetics related to the ABE production process by free *C. acetobutylicum* ATCC824. Lactose solutions were adopted as medium with the aim of emulating cheese whey. The conversion process is characterized in terms of cells, acids, solvents, pH and total organic compounds as a function of time. Results are worked out to assess the kinetics of the cells growth and of the ABE production. The yields of the carbon source in cells, acids and solvents are also assessed.

2 Materials and Method

2.1 Microorganism and culture media

Clostridium acetobutylicum DSM 792 was supplied by DSMZ. Stock cultures were reactivated according to the DSMZ procedure and stored at 4°C.

Synthetic medium adopted consisted of Yeast Extract (YE) at 5 g/L and of D-Lactose, typically at 50 g/L. $CaCO_3$ was added in the stock medium at concentration of 18 g/L. The medium was sterilized in autoclave.

2.2 Apparatus

Pre-cultures were carried out in 15 mL Hungate tubes. D-lactose bioconversion by *C. acetobutylicum* was investigated batchwise in screw-cap bottles (250 mL) housed in a thermostated room at 35°C.

2.3 Operating conditions and procedures

All tests were carried out at 35°C under anaerobic conditions and no pH control was adopted.

Precolture was prepared inoculating 2 mL of the stock culture into 5 mL of synthetic medium and incubated for two days. The precoltures were inoculated into the reactors containing synthetic medium consisting of YE and lactose at pre-fixed concentration (up to 110 g/L). Typically, the initial cells concentration was fixed at 4 mg_{DM}/L. The culture was periodically sampled to measure cell and metabolites concentrations, until lactose concentration approached a stationary state. Each measurement was carried out in triplicate.

2.4 Analytical methods

pH was measured off-line on 3 mL samples by a pHmeter (Hanna Instruments). Analysis of culture samples was carried out after centrifugation at 11,000 rpm for 10 min. The solid phase was characterized for biomass concentration. Liquid phase was characterized for lactose and metabolites concentration, and total organic carbon (TOC). Cell density was determined by measuring the absorbance at 600 nm (Cary-Varian mod. 50 scan UV-VIS spectrophotometer). Calibration tests indicated that the optical density is proportional to *C. acetobutylicum* dry mass under the operating conditions tested, in particular 1 OD_{600} corresponded to 0.4 g_{DM}/L. Lactose concentration was measured by means of an enzymatic kit (Biopharm). A GC apparatus was used, equipped with a FID, and outfitted with a capillary column poraplot Q (25 m x 0.32mm). External standards were adopted to assess acids and alcohols and their concentrations. The TOC was measured with a Shimadzu TOC 5000A analyzer.

3. Results

Figure 1 reports the time resolved profiles of the concentration of *C. acetobutylicum* cells (X), of lactose (C_L) and of metabolites (acetic acid, butyric acid, ethanol, acetone and butanol) as well as of the pH, measured during a batch culture carried out at 50 g/L initial lactose concentration (C_L^0). It is possible to identify two phases: the acidogenosis and the solventogenesis phases. The onset of solvents production marks the beginning of the solventogenesis phase ($t_A \cong 22$ h). Provided an 8 hour time-lag, the acidogenesis phase is characterized by: i) the steady increase of concentration of cells and of acids; ii) a cell concentration vs time profile that mirrors the lactose consumption; iii) the decrease of pH; iv) a molar ratio between acids (butyric/acetic) constant and equal to 1.5. The solventogenesis phase is triggered by pH=4, in agreement with previous results (Jones and Woods, 1986). The solventogenesis phase is characterized by: i) the gradual decrease of the lactose concentration approaching a stationary value; ii) the acid molar ratio constant and equal to 1.5.

The culture was further characterized in terms of: i) cells specific growth rate (μ) estimated according to usual procedures for kinetic analysis from batch culture data under the assumption of first-order growth kinetics with respect to biomass concentration in the exponential phase; ii) fractional yield of lactose-to-biomass estimated with reference to the acidogenesis phase $(Y_{X/L})_{ac}$; iii) fractional yield of lactose-to-butanol $(Y_{B/L})_{sov}$ with reference to the solventogenesis phase; iv) fractional yield of lactose-to-solvents $(Y_{Sol/L})_{ov}$ and fractional yield of lactose-to-butanol $(Y_{B/L})_{ov}$ with reference to the overall conversion test; v) overall lactose conversion (ξ_L). The maximum butanol specific rate (r_B) was estimated at the threshold of the solventogenesis phase as the slope of the butanol concentration (C_B) vs time curve (see Fig. 1). With reference to the run reported in figure 1 it results: $\mu = 0.29\ h^{-1}$; $(Y_{X/L})_{ac}=0.18$; $(Y_{Sol/L})_{ov}=0.20$; $(Y_{B/L})_{ov}=0.17$; $\xi_L = 0.34$; $r_B = 80\ mg_B/g_{DM}h$.

The mass balance on carbon takes into account the carbon content of the liquid phase and *C. acetobutylicum* and that converted into CO_2, according to the Embden-Meyerhof

pathway (Jones and Woods, 1986). A compact form of the global balance, referred to the acidogenesis phase [0, t_A], reads:

$$\left(TOC_0 + X_0 \cdot \alpha_C\right) - \left(TOC_A + X_A \cdot \alpha_C\right) - 4 * \frac{MW_C}{MW_L}\left(C_L^0 - C_{L,A}\right) = 0 \quad (1)$$

where α_C is the carbon mass fraction of *C. acetobutylicum* (0.4), MW_C and MW_L the molecular masses of carbon and lactose, X_A and $C_{L,A}$ the concentration of the cells and of lactose, respectively, at $t=t_A$, TOC_0 and TOC_A the total organic carbon at the beginning of the run and at $t=t_A$. The accuracy of the carbon balance is expressed as:

$$\frac{\left(TOC_A + X_A \cdot \alpha_C\right) + 4 * \frac{MW_C}{MW_L}\left(C_L^0 - C_{L,A}\right)}{\left(TOC_0 + X_0 \cdot \alpha_C\right)} \approx \delta_{ac} \quad (2)$$

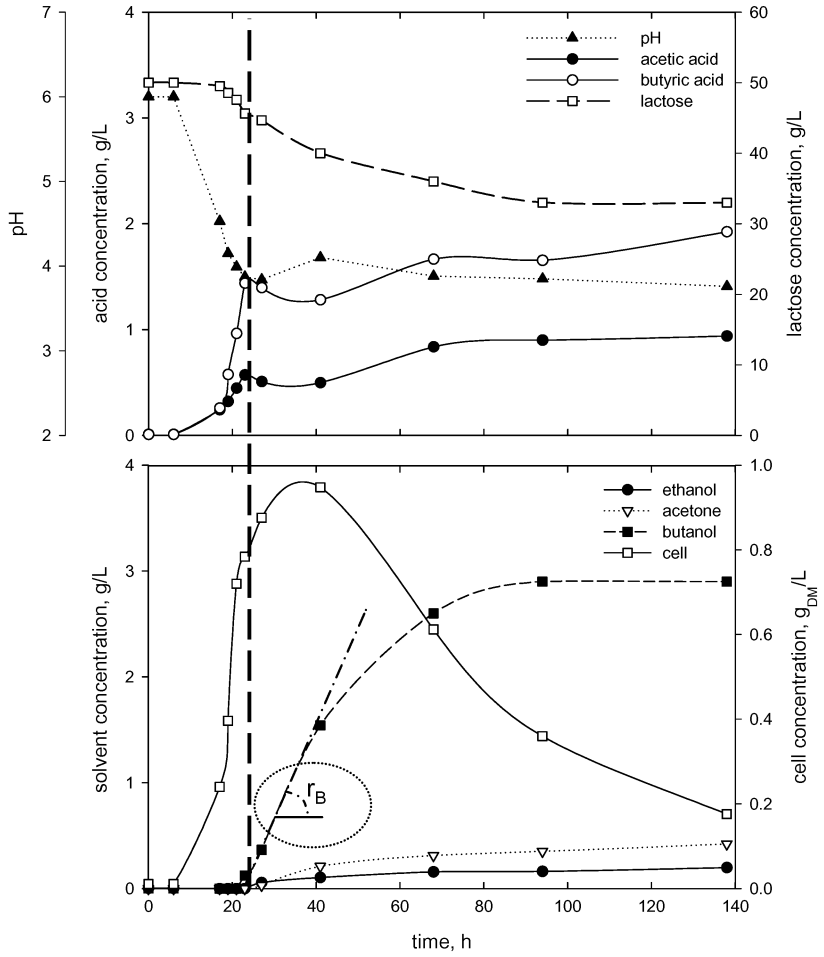

Figure 1 Data measured during a lactose conversion test: C_L^0 *=50 g/L. The vertical dashed line marks the beginning of the solventogenesis phase.*

The mass balance on carbon referred to the overall test takes into account the extra CO_2 released during acetone production (Jones and Woods, 1986). Assuming that the cell concentration decreases as a consequence of the sporulation without any cell leases, the global balance reads:

$$\left(TOC_0 + X_0 \cdot \alpha_C\right) - \left(TOC_A + X_{max} \cdot \alpha_C\right) - 4 * \frac{MW_C}{MW_L}\left(C_L^0 - C_L\right) - \frac{MW_C}{MW_{Ac}} C_{Ac} = 0 \qquad (3)$$

where X_{max} is the maximum concentration and C_L and C_{Ac} the concentration of lactose and acetone and the end of the test. The accuracy of the test assessment has been expressed by δ_{ov} estimated as in eq. (2).
Data regarding the test reported in figure 1 are characterized by δ_{ac}= 0.96 and δ_{ov}=0.90.

Figure 2 reports relevant data of lactose conversion as a function of the initial lactose concentration. The accuracy of the tests expressed in terms of δ_{ac} and δ_{ov} was always between 0.90 and 1. Main results are herein reported
Acidogenesis phase (figure 2A). Data of concentration of lactose, acetic and butyric acids measured at the end of the acidogenesis phase are reported. The process is characterized by cells specific growth rate, acid molar ratio and the $(Y_{X/L})_{ac}$ constant with C_L^0, under operating conditions tested. Except for the run carried out at C_L^0 = 2 g/L, the pH at the threshold of the solventogenesis phase does not change with C_L^0. During the run carried out at C_L^0 = 2 g/L, the pH decreases with the time and stabilizes at 4.4 when the conversion stops as a consequence of the lactose depletion. It is noteworthy that: i) the amount of lactose converted during the acidogenesis phase is about 4 g/L, if available; ii) the combination of $(Y_{X/S})_{ac}$ and of the amount of lactose converted until t_A results in a cell concentration at the threshold of the solventogenesis phase nearby constant and equal to 0.7 g_{DM}/L; cell growth is characterized by a zero-order kinetic with respect to the lactose with a specific growth rate equals to 0.29 h^{-1} under the operating conditions tested.
Solventogenesis phase. Figure 2B reports data of butanol concentration and of lactose-to-butanol fraction yield estimated at the end of the solventogenesis phase. Analysis of the figure highlights that: i) the final butanol concentration increases with C_L^0; ii) the yield of lactose in butanol is characterized by a maximum at C_L^0=50 g/L.

Results regarding the overall conversion process carried out at C_L^0 ranging between 2 and 110 g/L (figure 2C) highlight some important features. The butanol fractional yield is characterized by a maximum of about 0.2 g_B/g_L at C_L^0=50 g/L, about the half of the maximum theoretical value (0.4 g_B/g_L). The lactose conversion degree and the overall selectivity with respect to the butanol $(Y_{B/S}/Y_{Sol/S})_{ov}$ decreases with C_L^0 approaching, respectively, 0.3 and 0.65 (molar basis).

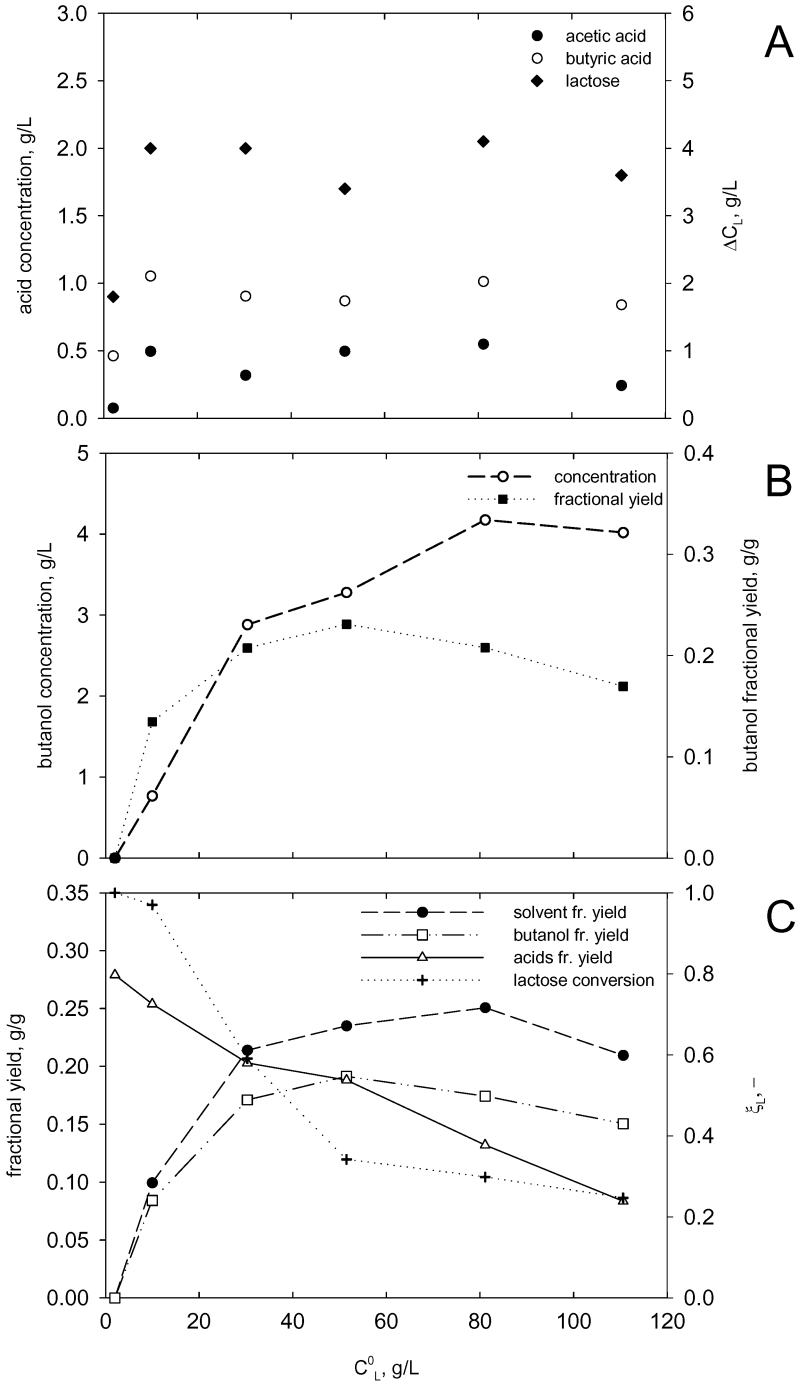

Figure 2 Relevant data assessed during lactose conversion as a function of the initial lactose concentration. A) Acidogenesis phase. B) Solventogenesis phase. C) Overall data.

The maximum butanol specific rate (r_B) as a function of the C_L measured on the verge of the solventogenesis phase is reported in Figure 3. It appears that the r_B may be described by a Monod-like model. The regression of data reported in figure 3 yields: $r_B=128C_L/(28+C_L)$ $mg_B/g_{DM}h$.

Some information about the optimal operating conditions to adopt in batch bioconversion may be drawn by working out data reported in the previous figures. The yield of butanol with respect to the initial lactose concentration (product of lactose conversion and of $Y_{B/S}$) is characterized by a maximum of about 0.10 at C_L^0=30 g/L. Altogether, the butanol productivity by fermentation increases with C_L^0 even though the pureness becomes progressively lower. Therefore, the operating conditions to adopt for the butanol production should be optimized by taking into account both the fermentation and the recovery process. It should be remarked that for batch operations a fraction of lactose available is converted for stabilize the environment appropriate for the butanol production (pH lower than 4). In a continuous operation such fraction is just consumed during the reactor start-up.

Acknowledgements

This work was supported by grants from the Ministero dell'Università e della Ricerca Scientifica (Progetti di Rilevante Interesse Nazionale, PRIN).

References

Ezeji T.C., Qureshi N., Blaschek H.P., 2007, Current Opinion in Biotechnology, 18: 220-227

Huang W.-C., Ramey D.E., Yang S.-T., 2004, Appl. Biochem Biotechnol, 113: 887-898

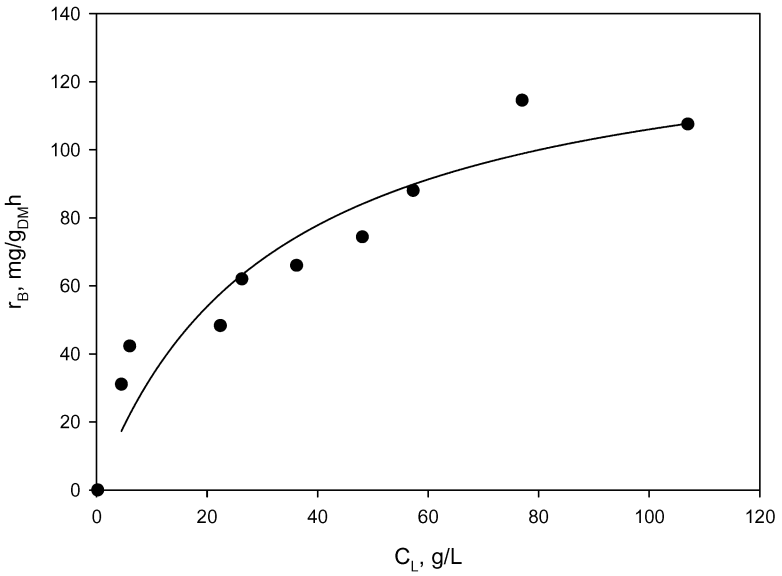

Figure 3 Specific production rate of butanol at the onset of the solventogenesis phase

Jones D.T, Woods D.R., 1986, Microb. Reviews, Dec:484-524
Maddox, I.S., 1980, Biotechnology Letters, Vol 2, 11, 61-64
Qureshi N., Blaschek H.P., 2005, Eds Shetty K., Pometto A. and Paliyath G. Boca Raton, FL: Taylor & Francis Group: 525-551
Shinto, H., Tashiro Y., Yamashita M., Kobayashi G., Sekiguchi T., Hanai T., Kuriya Y., Okamoto M., Sonomoto K. ,2007, J. of Biotechnology, 131: 45-56
Tashiro Y., Takeda G., Kobayashi G., Sonomoto K., 2005, J. of Biotechnology, 120: 197-206
Villadsen, J., 2007, Chemical Engineering Science 62, 6957-6968
Welsh, F.W., Veliky, I., 1984, Biotechnology Letters, Vol 6, 1, 61-64
Welsh, F.W., Veliky, I., 1986, Biotechnology Letters, Vol 8, 1, 43-46

CHEMICAL ENGINEERING TRANSACTIONS, Volume 14, 2008
Edited by G. Marino, E. Bardone, A. Viglia
 ISBN 978-88-95608-02-0

Production of 2,3-butanediol by *Bacillus stearothermophilus*: fermentation and metabolic pathway

Pier Paolo Giovannini, Matteo Mantovani, Alessandro Medici and Paola Pedrini
Dipartimento di Biologia ed Evoluzione, Università di Ferrara
C.so Ercole I d'Este 32, 44100 Ferrara, Italy

The fermentation of different sugars by *Bacillus stearothermophilus* ATCC 2027 to obtain 2,3-butanediol is described. Fermentation tests in shake flasks show the complete conversion of sucrose to butanediol (91% yield) and acetoin (3-hydroxy-2-butanone) using a starting sugar concentration of 30 g/L. A similar result is obtained with sugar cane molasses, whereas glucose and fructose afford lower yields. Other disaccharides and monosaccharides are also tested without appreciable results. *B. stearothermophilus* forms a mixture of 2*R*,3*R*-butanediol and the *meso* isomer derived both from reduction of *R*-acetoin and from the butanediol cycle as demonstrated by the presence of acetoin reductase and acetylacetoin synthase.

Introduction

2,3–Butanediol (BD) is a colorless and odorless liquid with a large number of industrial applications. Actually by dehydration it can be converted to methyl ethyl ketone, a fuel additive, or to 2,3-butadiene, an important monomer for the manufacture of synthetic rubber. It's a potential fuel additive too, having a heating value comparable to ethanol and methanol (Perego et al., 2003). Furthermore it can be easily converted to diacetyl, a flavouring agent used in food industry and its *levo*-form is used as antifreeze agent. Recently, interest for its microbial production is increasing. Many bacteria produce BD but among them only *Bacillus polymyxa* and *Klebsiella pneumoniae* are used for fermentation on industrial scale (Syu, 2001). BD exists in three stereoisomeric forms (i.e. (-)-(2*R*,3*R*)-BD, (+)-(2*S*,3*S*)-BD, and the *meso*-form) and microrganisms generally give a mixture of *meso*-BD and one of the two enantiomer. Acetoin (AC) is the main precursor of BD and is formed in bacteria from pyruvate by action of the two enzymes α-acetolactate synthase, that catalyzes the condensation of two pyruvate molecules with a single decarboxylation to afford α-acetolactate, and α-acetolactate decarboxylase that decarboxylates this last one to acetoin (Juni, 1952) (catabolic pathway), (Fig.1). The different isomeric forms of BD can be produced by AC-reduction with various AC-reductase with different stereospecificity (Ui et al., 1984) or by a cyclic pathway called "butanediol cycle" which existence has been reported in different bacteria (Ui et al., 1994) (Fig 1). Using *Bacillus stearothemophilus* ATCC 2027 as biocatalyst for the synthesis of optically active secondary alcohols and *vic*-diols (Bortolini et al., 1997), we found high concentration of BD and AC in the culture broth when sucrose was used as carbon source.

Figure 1. BD formation in bacteria: catabolic pathway and BD cycle.

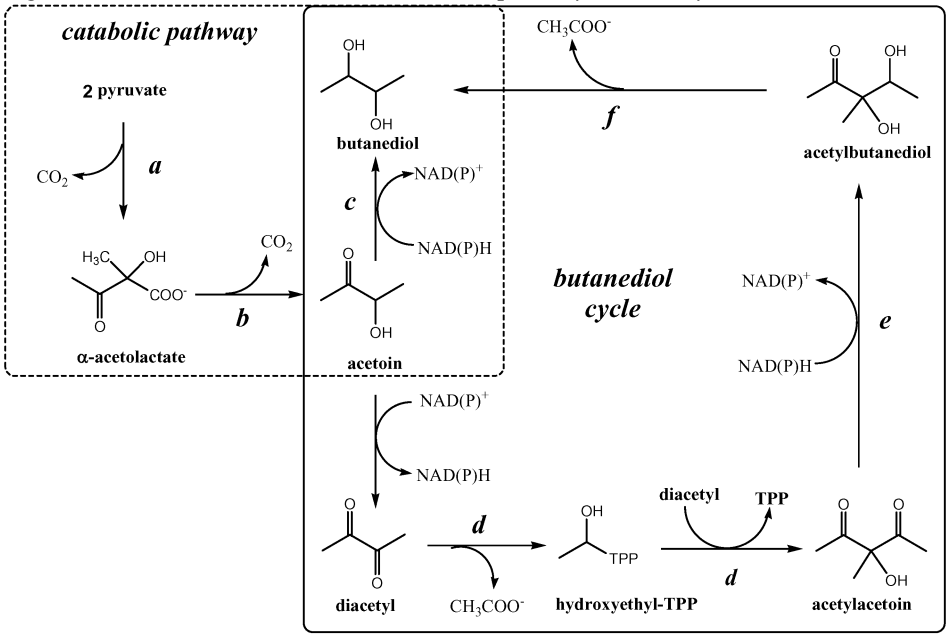

a: α-acetolactate synthase; **b**: α-acetolactate decarboxylase; **c**: AC reductase; **d**: acetylacetoin synthase; **e**: acetylacetoin reductase; **f**: acetylbutanediol hydrolase

On the basis of this observation, a preliminary study to evaluate the potential of this bacterium in bioconversion of different mono- and disaccharides to BD was performed. Since a mixture of (2*R*,3*R*)-BD and *meso*-isomer was produced in a 1:1.5 ratio, we focused our attention also in the metabolic pathway mechanisms.

Results and discussion

Fermentation of various carbohydrates

Since *B. stearothermophilus* ATCC 2027 easily grows on sucrose producing interesting amounts of BD and AC, the fermentation was carried out in order to evaluate the effect of sucrose concentration (0, 10, 20, 30 and 40 g/L, respectively) on BD production. The best result of fermentation was obtained with 30 g/L sucrose in shake flasks at 40°C (Table 1). Although the 40 g/L sucrose fermentation afforded the highest BD concentration after 32 h (18.3 g/L), at this time unutilized sucrose was about 7 g/L. On the contrary, *B. stearothermophilus* fermentation of 30 g/L sucrose gave lower amount of BD after 28 h (14.4 g/L) but practically no sucrose was detected. It can be pointed out that the BD concentration increased till the sucrose consumption was fast, subsequently, when a low amount of sucrose was present, AC concentration increased due to the oxidation of BD as demonstrated by the trend of the sum of both metabolites (Fig. 2).

Table 1. Production of BD and AC with *B. stearothermophilus* using various sugars.

Sugar (g /L)	Time H	Residual sugar g/L	2,3-BDL[a] g/L (yield)	AC[b] g/L (yield %)	2,3-BDL + AC g/L (yield%)
Sucrose (40)	32	7.0	18.3 (87%)	1.3 (6%)	19.6 (93%)
Sucrose (30)	28	0.8	14.4 (91%)	1.7 (11%)	16.1 (102%)
Glucose (30)	32	16.4	8.7 (58%)	2.6 (18%)	11.3 (72%)
Fructose (30)	36	15.4	7.1 (47%)	4.5 (31%)	11,6 (78%)
Molasses(30)[c]	40	7.8[d]	12.0 (76%)	1.5 (10%)	13.5 (86%)

[a] The data are the total of 2*R*,3*R*-BD (ee ≥95%) and *meso*-BD in ratio 1:1.5. [b] *R*-AC is obtained (ee ≥ 95%). [c] The sugar concentration is the sum of sucrose (63%) and invert sugar (37%). [d] Only invert sugar.

On the basis of these data the fermentability of other carbohydrates (30 g/L) was tested. Cellobiose, maltose and lactose were not fermented probably due to the lack of efficient glycosidases as confirmed by the high concentration of the corresponding disaccharides in the fermentation broth after 48 h. Among the tested monosaccharides (i.e. glucose, fructose, galactose and xylose) only glucose and fructose gave appreciable results even though showing lower yields in comparison with sucrose (Table 1). When the higher BD concentrations were reached (8.7 g/L with glucose and 7.1 g/L with fructose) about 16 g/L of unutilized monosaccharide were still present in the fermentation broth. Also in these cases the amount of BD decreased in favour of AC at longer time. Finally sugar cane molasses was tried too. In this case the broth was obtained simply diluting the molasses in order to have a final sugar concentration of 30 g/L (sucrose 63% and invert sugar 37%) without adding supplemental nutrient.

Figure 2. Time course of sucrose fermentation (30 g/L) by *B. stearothermphilus*

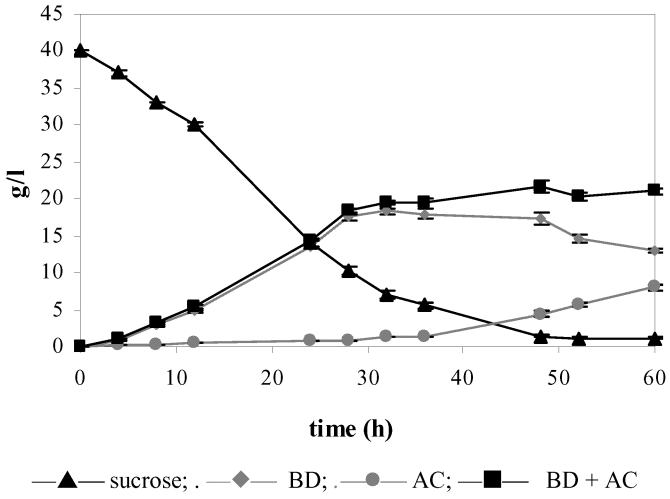

The trend of BD and AC production was similar to that reported for the 30 g/L sucrose fermentation affording, after 40 h, 12.0 g/L of BD and 1.5 g/L of AC together with 7 g/L of invert sugar. This data confirm that sucrose is the elective carbohydrate for BD production using *B. stearothermophilus* ATCC 2027 and that glucose and fructose are fermentable too but with lower efficiency.

Metabolic pathway and metabolite stereochemistry

All the main BD forming bacteria convert pyruvate to AC with *R* configuration (Ui et al., 1986) by action of the two enzymes α-acetolactate synthase and α-acetolactate decarboxylase (Figure 1. react. a and b). In order to confirm this behaviour in *B. stearothermophilus* ATCC 2027, we determined the configuration of the AC formed by adding freshly prepared cell free extract to a solution of sodium pyruvate in phosphate buffer at pH 6.0. After standing two hours at 30°C, the reaction mixture was extracted with ethyl acetate and analyzed by GC. Only one AC enantiomer was detected (e.e. >96%) and its configuration was deduced on the basis of the BD isomers formed by reduction with $NaBH_4$. This reduction afforded a mixture of 2*R*,3*R*- and *meso*-BD proving that AC produced was the *R*-enantiomer according to the other BD forming bacteria. In our previous work we described the purification and characterization of a diacetyl (acetoin) reductase from *B. stearothermophilus* (Giovannini et al., 1996). This NAD-dependent enzyme showed a *S*-enantioselectivity in the reversible reduction of AC so it could be responsible of the *meso*-BD formation from *R*-AC (Fig.1, react.c). In addition this strain has another NAD-dependent dehydrogenase able to catalyze the oxidation of 2*R*,3*R*-BD as demonstrated by formation of NADH when this substrate was added to a solution containing NAD^+ and cell free extract in phosphate buffer at pH 8.4. Unfortunately, this enzyme, until today, was not completely purified, so we can only suppose its activity in the reduction of *R*-acetoin to form 2*R*,3*R*-BD. Finally we verified the existence of BD cycle in *B. stearothermophilus* following a procedure described for *B. cereus* YUF-4 (Ui et al., 1994). After addition of diacetyl (10 g/L) to a culture grown on a medium containing AC (5 g/L) as carbon source, we observed a significant accumulation (about 2 g/L) of acetylacetoin. Its presence proves the existence of an acetoin-inducible acetylacetoin synthase (Fig 1, react. d), that has been proposed as a marker enzyme of BD-cycle (Ui et al., 2002).

Experimental

Material

All the reagents are commercially available. Sugar cane molasses was kindly furnished by prof. G. Vaccari from Ferrara University. For the GC analysis, a Carlo Erba 6000 chromatograph was used. ^{1}H-NMR spectra were acquired on a Varian Gemini 300 MHz spectrometer.

Fermentation tests

A culture of *Bacillus stearothermophilus* ATCC 2027 was grown 24 h at 38-39° C and 110 rpm in a medium containing sucrose (40 g/L), peptone (20 g/L), yeast extract 10 (g/L), $Na_2HPO_4 \cdot 6H_2O$ (6.8 g/L), K_2SO_4 (2.6 g/L), and $MgSO_4$ (0.3 g/L). Each

fermentation was started adding 5 ml of this culture to a medium (115 ml in 500 ml flask) with the same composition except for the carbon source (see Table 1). A similar inoculum was used to start fermentations with sugar cane molasses as unique medium component. The concentration and stereochemistry of BD, AC, and acetylacetoin were determined by gas chromatographic analyses. Each sample (2 mL) was centrifuged (6000 rpm, 10 min), added with NaCl (0.2 g) and extracted with ethyl-acetate (0.8 mL) containing 0.1% (v/v) of acetophenone as internal standard. Separations were performed with a fused capillary column Megadex 5 (25 m X 0.25 mm) containing dimethyl-*n*-pentyl-β-cyclodextrin on OV 1701 (from Mega snc): helium as carrier gas (68 kPa); temp. 90-200°C (2°C/min). Retention times (in min): (-)-3*R*-AC, 2.95; (+)-3*S*-AC, 3.10; (+)-2*S*,3*S*-BD, 5.90; (-)-2*R*,3*R*-BD, 6.20; *meso*-BDL, 6.60; acetophenone 11.30. Glucose, fructose, and sucrose concentrations were determined by enzymatic analysis (SIGMA kits).

Biosynthesis of AC from pyruvate

Sodium pyruvate (0.1 g, 0.9 mmol) was added to a solution containing 4.0 mL of cell free extract obtained as described (Bortolini, 1997) in phosphate buffer 50 mM, pH 6.0 (100 mL). After two hours at 30°C the reaction mixture was saturated with NaCl and extracted with ethyl-acetate (3 X 20 mL). The organic phase was dried over anhydrous sodium sulphate and analyzed by gas chromatography using the above reported conditions. A single peak at 2.95 min. was detected. Ethyl-acetate was removed under reduced pressure, and the residue was dissolved in diethyl-ether/methanol 5:1 (20 mL). The mixture was cooled (ice bath) and $NaBH_4$ (35 mg, 0.9 mmol) was added. After 30 min. the mixture was diluted with water (10 mL), the organic phase was separated, dried with anhydrous sodium sulphate and analyzed by GC. Two peaks were detected at 6.20 and 6.60 min corresponding to 2*R*,3*R*- and *meso*-BD.

Biosynthesis of acetylacetoin from diacetyl

Diacetyl (2.0 g, 23.3 mmol) was biotransformed as described by Ui et al. (1994) in a 200 mL culture of *B. stearothermophilus* grown on Bouillon medium containing AC (1.0 g, 11.4 mmol) as carbon source. Acetylacetoin (0.3 g, 10 %) was recovered and purified according to the same reference. It is a colorless oil, ^{1}H-NMR ($CDCl_3$): δ 4.70 (s, 1 H, OH); 2.25 (s, 6 H, 2 Ac); 1,60 (s, 3H, Me). Its concentration in the broth was determined by gas chromatographic analysis using acetophenone as internal standard as described for BD and AC (retention time 4.30 min).

Conclusions

B. stearothermophilus ATCC 2027 has demonstrated to convert efficiently sucrose to BD and although with lower yields, it ferment also glucose and fructose. Otherwise this bacterium can grows at temperature above 40°C, so we intend to study its potential in bioreactor to understand if it could be a candidate for industrial application. About the BD production routes, we will focus on the specificity of the AC- and acetylbutanediol reductases to make clear the influence of the catabolic pathway and BD cycle on the stereochemistry of the product.

References

Bortolini, O., G. Fantin, M. Fogagnolo, P. P. Giovannini, A. Guerrini, and A. Medici, 1997, An easy approach to the synthesis of optically active *vic*-diols: a new single-enzyme system. J. of Org. Chem. 62, 1854.

Giovannini, P. P., A. Medici, C. M. Bergamini, and M. Rippa, 1996, Properties of Diacetyl (Acetoin) Reductase from *Bacillus stearothermphilus*, Bioorg. and Med. Chem. 4, 1997.

Juni, E., 1952, Mechanisms of formation of acetoin by bacteria, J. Biol. Chem. 195, 715.

Perego P., A. Converti and M. Del Borghi, 2003, Effect of temperature, inoculum size and starch hydrolyzate concentration on butanediol production by *Bacillus licheniformis*, Bioresource Technology 89, 125.

Syu M. J., 2001, Biological production of 2,3-butanediol, Appl. Microbiol. Biotechnol. 55, 10.

Ui, S., T. Masuda, H. Masuda and H. Muraki, 1984, Mechanism for the formation of 2,3-butanediol stereoisomers in *Klebsiella pneumoniae*, J. Ferment. Technol. 62, 551.

Ui, S., K. Watanabe and T. Magaribuchi, 1994, Production of acetylacetoin by bacterial fermentation, Biosci. Biotech. Biochem. 58, 2271.

Ui, S., T. Masuda, H. Masuda, and H. Muraki, 1986, Mechanism for the formation of 2,3-butanediol stereoisomers in *Bacillus polymyxa*, J. Ferment. Technol. 64, 481.

Ui, S., T. Hosaka, K. Mizutani, T. Ohtsuki and A. Mimura, 2002, Acetylacetoin synthase as a marker Enzyme for detecting the 2,3-butanediol cycle, J. of Biosci. 93, 248.

CHEMICAL ENGINEERING TRANSACTIONS, Volume 14, 2008
Edited by G. Marino, E. Bardone, A. Viglia
 ISBN 978-88-95608-02-0

Glycerol fermentation to 1,3-propanediol by *Klebsiella oxytoca* NRRL B-199: study of the inhibition of the final products of both the oxydative and the reductive routes

Galdeano, C.[a]; Salguero G.[a]; Santos, V.E.[a]; Zazo, M [b];Garcia, J.L.[b]; Garcia-Ochoa, F.[b]
[a]Dpto. Ingenieria Quimica. Facultad CC. Quimicas. Universidad Complutense. Avda Complutense s/n, 28040. Madrid. Spain
[b]Dpto. Microbiologia Molecular. Centro Investigaciones Biologicas. CSIC. c/Ramiro de Maeztu, 9. 28040 Madrid. Spain

As an important chemical intermediate, 1,3-Propanediol (1,3-PD) is used as a monomer to produce poly(propileneterephthatlate). The microbial conversion of glycerol to 1,3-PD, has recently paid more attention because, as consequence of the growing use of biodiesel, glycerol has become a very suitable compound. In this work, the conversion of glycerol is carried out by *Klebsiella oxytoca* NRRL B-199, a non pathogenic bacteria and an excellent 1,3-PD produced. In the biological production of 1,3-PD, a number of by-products (acetic acid, ethanol, 2,3-butanediol, succinic acid and lactic acid) are simultaneously produced together with 1,3-PD. In this work, the study of product inhibition is carried out. To quantify their influences, specific growth rate, μ, yield into biomass, Y_{XG} and yield into product, Y_{PG} have been calculated. In this work, is stated that all products inhibit 1,3-PD production, being EtOH the most important inhibition agent.

1. Introduction

The recent development of a new polyester called poly(propylenterephtalate), a biodegradable polymer with unique physicochemical properties for the fibber industry has increased the attention towards the production of 1,3-propanediol (1,3-PD), a product with this and other applications in cosmetics, foods, lubricants and medicines (Deckwer, 1995).

Traditional chemical production of 1,3-PD by means of conversion of acrolein requires high temperature, high pressure and expensive catalysts. The microbial conversion of glycerol to 1,3-PD has recently received more attention because it is carried out using milder operational conditions than the chemical process and it does not generate toxic by-products (Yang et al., 2007).

Moreover, the microbial process can use glycerol as substrate; therefore, it will be a very suitable compound when the biodiesel production had increased its production as consequence of the application of the European Directive 2003/30/CE, which imposes

the growing use of biofuels. Glycerol is the main by-product obtained from biodiesel production around 10 % of biofuel

Glycerol can be naturally fermented into 1,3-PD by bacteria belonging to the genera *Klebsiella, Clostridia, Citrobacter* and *Enterobacter* under anaerobic or microaerobic conditions (Chen *et al.,* 2003). Best yields are reached with *Klebsiella genus* of *Enterobacteriaceae*, mainly with *Klebsiella pneumoniae*. *K. pneumoniae* is commonly associated with human respiratory and genitourinary infections, and also, other bacteria belonging to the genera *Klebsiella* has been implicated in urinary tract infections. The genera *Klebsiella* is more commonly regarded as an inhabitant of soil, plants, and the aquatic environment (Brown *et al*., 1973). However, *Klebsiella oxytoca*, that is closely related to *K. pneumoniae*, is a human non-pathogenic bacteria.

The fermentation of glycerol involves two parallel pathways: oxidative and reductive, as shows Figure 1. Through the oxidative pathway, glycerol is dehydrogenated to dihydroxyacetone (DHA) and then to dihydroxyacetonephosphate (DHAP). Acetic acid (HAc), succinic acid (HSucc), lactic acid (HLac), 2,3-butanediol (2,3-BD) and ethanol (EtOH) are the final products of the oxidative route. Through the reductive pathway, a glycerol dehydratase removes a water molecule from glycerol to form 3-hydroxypropionaldehyde (3-HPA) which is then reduced to 1,3-PD, that is not metabolized further, and, as a result, it is accumulated in the media (Cameron *et al*., 2002). All the final products of both routes have been observed to inhibit microbial production of 1,3-PD from glycerol in *Enterobacter agglomerans* (Barbirato et al, 1996).

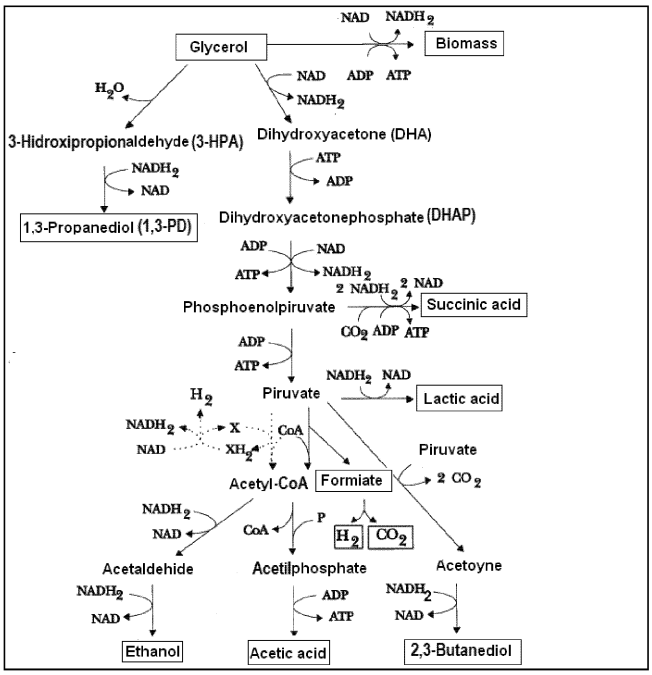

Figure 1. Routes of anaerobic glycerol metabolism in *Klebsiella sp.*

The aim of this work is to study the inhibition both in the *K oxytoca* growth and in the production of 1,3-PD by the main product of its fermentation, 1,3-PD, and also by all the by-products, using glycerol as carbon source.

2. Materials

2.1 Microorganism

The microorganism used in this work was *Klebsiella oxytoca* NRRL B-199, from the Biological Research Center (CIB, Madrid, Spain).

2.2 Medium composition

The medium composition used for the growth of *K. oxytoca* (and for the production of 1,3-PD, because it is an associated growth product) was determined and optimized by in a previous work (Galdeano *et al*, 2007). It contains (per litre): 40 g glycerol, 0.15 g yeast extract, 0.5 g NH_4NO_3, 3.5 g K_2HPO_4, 1.5 g KH_2PO_4, 0.25 g Mg SO_4 and 2 g NH_4Cl.

3. Methods

3.1 Inoculum preparation

Pre-inoculum was prepared in the culture medium in a 25-mL shake flask, containing 10 mL of culture medium which were inoculated with a loop of cells from the stock conserved in glycerol at -20ºC and incubated in orbital shaker Gallenkamp (model INR-200) at 210 rpm, 30 ºC, for 12 h, under anaerobic conditions.

3.2 Microorganism growth

Pre-inoculum was used to inoculate 10mL of culture medium in a 25mL shake flask, at an initial concentration at 0.1 g/L. Samples were withdrawn from the flasks at one hour intervals, to measure cell growth. Afterwards, cells were harvested from the sample by centrifugation at 14000×*g* for 5 min at 12ºC. The supernatant obtained after centrifugation was analyzed by HPLC.

3.3 Analytical methods

Cell growth was monitored as Optical Density at 600 nm. The concentration of glycerol, 1,3-PD and the other by-products (EtOH, HLac, HAc, HSucc, 2,3-BD) were determined by HPLC using an Aminex HPX-87H column and a refractive index detector. Operation conditions were: 0,005 M H_2SO_4 , flow rate 0,6 ml min^{-1}, column temperature 60 ºC and refractometer temperature 55ºC.

4. Results and discussion

4.1 Results

Twelve experiments have been carried out. Each experiment has been performed introducing into the growth medium one of the products of the glycerol metabolism in *Klebsiella oxytoca*, as shown in Table 1.

4.2 Discussion

To evaluate the inhibitory effect of the differents compounds, specific growth rate (μ), the yield into biomass (Y_{XG}) and into 1,3-PD (Y_{PG}) were calculated using equations (1), (2) and (3).

$$C_x = \frac{C_{Xo} \cdot \exp(\mu \cdot t)}{1 - \frac{C_{Xo}}{C_{X,m}} \cdot (1 - \exp(\mu \cdot t))} \quad (1)$$

$$Y_{XG} = \frac{C_{X,m} - C_{Xo}}{C_{Go}} \quad (2)$$

$$Y_{PG} = \frac{C_P^{max}}{C_{Go}} \quad (3)$$

Table 1. Sets of experiments, using different initial concentations of 1,3-PD, HAc, HLac, HSucc , 2,3-BD and EtOH.

Run	1,3-PD (g/L)	HAc(g/L)	HLac(g/L)	HSucc(g/L)	2,3-BD (g/L)	EtOH(g/L)
1	0	0	0	0	0	0
2	8	0	0	0	0	0
3	16	0	0	0	0	0
4	20	0	0	0	0	0
5	0	1	0	0	0	0
6	0	2	0	0	0	0
7	0	0	1	0	0	0
8	0	0	2	0	0	0
9	0	0	0	1	0	0
10	0	0	0	2	0	0
11	0	0	0	0	1	0
12	0	0	0	0	2	0

The influence of both the different products and concentrations on specific growth rate is shown in Figures 2a and 2b. It can be seen that all the studied compounds inhibit growth of *Klebsiella oxytoca*, being succinic acid the product more affecting microorganism growth. However, the different concentrations used for each product do not increase the inhibition efect in a great way.

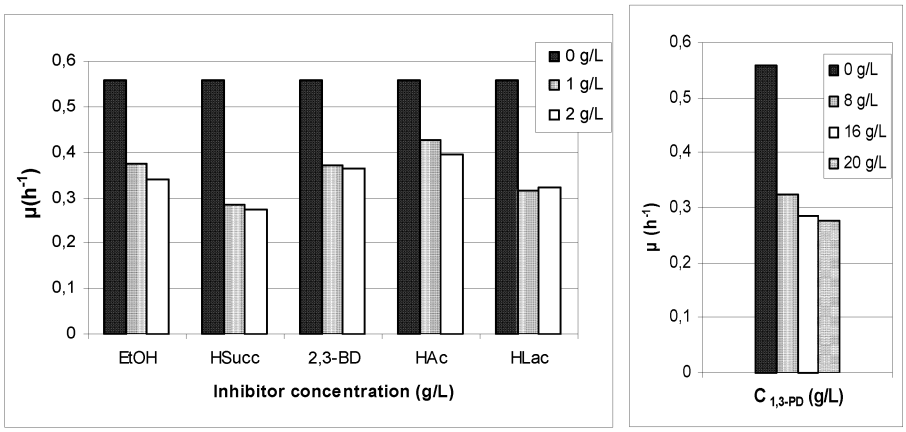

Figure 2a and 2b. Specific growth rate (μ) vs. different inhibitors.

Y_{XG} seems to decrease when the initial concentration of EtOH, HSucc, 2,3-BD, HLac and 1,3-PD is increased, as show Figures 3a and 3b. The decrease of Y_{XG} is specially significant when the EtOH is the studied inhibitor. The different concentrations of HSucc seem to affect strongly in the yield.

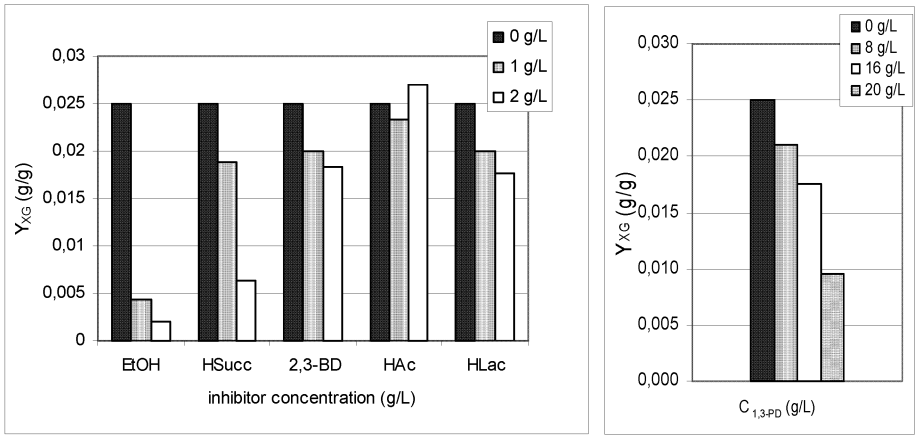

Figura 3a and 3b. Yield in biomass (Y_{XG}) vs. different inhibitors.

Figures 4a and 4b show the values of Y_{PG}. It can be seen that the higher initial concentration of the studied compound, the less Y_{PG} is obtained. Values of Y_{PG} are severely affected by the different concentrations of each product added to the medium. The highest influence in Y_{PG}, is observed when EtOH is studied as inhibition agent. Moreover, the inhibition effect is very significant when $C_{1,3\text{-}PD}$ is higher than 8g/L, reducing dramatically the value of Y_{PG}.

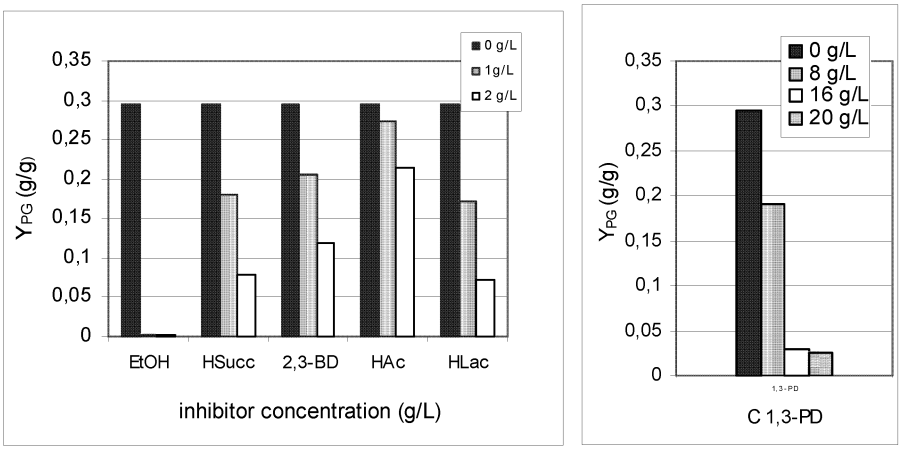

Figura 4a and 4b. Yield in 1,3-PD (Y_{PG}) vs. different inhibitors

5. Conclusion

In this work, the inhibition effect caused by all the final products of both the oxydative and the reductive routes, involve in the fermentation of glycerol, has been studied

Specific growth rate is affected by all the studied compounds, showing all of them to inhibit *K. oxytoca* growth.

Experimental results show that not only the main product, 1,3-PD, but also all the by-products, do affect to the biomass yield of *K. oxytoca.* The most important growth inhibition is observed when EtOH is studied.

Moreover, the results above showed demonstrate that exists a strong influence on the production of 1,3-PD by all the studied compounds. The different compounds and concentrations affect to values of Y_{PG}. The highest decreases of Y_{PG} have been observed when the inhibition caused by EtOH and 1,3-PD is studied.

6. Nomenclature.

1,3-PD : 1,3-Propanediol

2,3-BD: 2,3-Butanediol

Cx: Biomass concentracion (g/L)

C_{xm} : Biomass concentration reached at stacionay phase (g/L)

C_{PO}: Initial concentration of 1,3-PD (g/L)

C^{max}_{P}: maximum concentration of 1,3-PD, reached at stacionay phase (g/L)

C_{GO}: Initial concentracion of Glycerol (g/L)

C_j: Concentration of the compound j (g/L)

EtOH: Ethanol

HAc: Acetic acid

HLac: Lactic acid

HSucc: Succinic acid

Y_{PG}: Yield in 1,3-PD (g/g)

Y_{XG}: Yield in biomass (g/g)

μ: specific rate of growth (h^{-1})

7. Acknowlegments

This word was supported by the Ministerio de Educación y Ciencia (*CTQ2007-60919) and* by Ministerio de Medioambiente *(MMA-PR21/06-039/2006/3-11.2)*

8. References

Barbirato F., Grivet, J.P., Soucaille, P. and Bories, A. 1996. 3-Hydroxypropionaldehyde, an inhibitory metabolite of glycerol fermentation to 1,3-Propanediol by *Enterobacter agglomerans* species. Appl. Environ. Microbiol 62, 1448-1451

Brown, C. and Seidler, R. J. 1973. Potential pathogens in the environment: *Klebsiella pneumoniae*, a taxonomic and ecological enigma. Appl. Microbiol. 25:900–904.

Cameron D.C., Zhu Marie M., Lawman P.D. (2002) Improving 1,3-propanediol production from glycerol in a metabolically engineered *Escherichia coli* by reducing accumulation of sn-glycerol-3-phosphate. Biotechnol Prog. Jul-Aug;1 8(4):694-699.

Chen X, Long Z., Feng J., and Zhang D. (2003). Stoichiometric analysis and experimental investigation of glycerol bioconversion to 1,3-propanediol by *Klebsiella pneumoniae* under microaerobic conditions. Enzyme and Microbial Technology, 33, 386–394

Deckwer W-D. Microbial conversion of glycerol to 1,3-Propanediol. FEMS Microbiology Reviews 16, 143-149

European Directive 2003/30/CE of the European Parliament and of the Council of 8 May 2003, relating to the promotion of the use of biofuels or fuel alternatives.

Galdeano, C.; Zazo, M.; Santos, V.E.; Garcia, J.L.; Garcia-Ochoa, F. Production of 1,3-Propanediol using *Klebsiella oxytoca* NRTL B-199 growing cells: medium composition optimization using Taguchi method. ECCE-6. Accepted communication

Yang G., Tian R. and Jilun L. (2007) Fermentation of 1,3-propanediol by a lactate deficient mutant of *Klebsiella oxytoca* under microaerobic conditions. Applied Microbiology and Biotechnology, 73 (5). 1017-1024.

CHEMICAL ENGINEERING TRANSACTIONS, Volume 14, 2008
Edited by G. Marino, E. Bardone, A. Viglia
 ISBN 978-88-95608-02-0

Study on Reaction Parameters in Lipase-Catalyzed Methanolysis of Plant Oil

M. Hajar [a], F. Vahabzadeh [a,*], S. Shokrollahzadeh [b]

[a] Food Process Engineering and Biotechnology Research Center, Department of Chemical Engineering, Amirkabir University of Technology (Tehran Polytechnic) 424 Hafez Ave., Tehran 15914, Iran.
[b] Institute of Chemical Technologies, Iranian Research Organization for Science and Technology P.O.Box: 15815-3538, Tehran, Iran.

Biodiesel fuel, as fatty acid alkyl ester, which is produced by the transesterification of plant oil or animal fat sources with an alcohol, is an attractive alternative to petroleum-based fuel because it is produced from renewable resources. In this research, the enzymatic esterification of plant oil and methanol was studied. The reaction was catalyzed by commercial immobilized lipase from *candida antarctica* in solvent-free media. The influences of several reaction parameters, i.e. the amount of enzyme, molar ratio of methanol to oil and reaction temperature, on methanolysis reaction were investigated. The inhibitory effect of undissolved methanol on lipase activity was eliminated by stepwise addition to the reaction mixture. The optimum conditions for the reaction were as follows: enzyme amount 4%, molar ratio of methanol to oil 3:1, and temperature 35 °C in three-step addition of methanol. The maximum methyl ester yield of 84.4% was obtained after 72 h of reaction at optimum conditions.

1. Introduction

Biodiesel fuel, as fatty acid alkyl ester, which is produced by the transesterification of plant oil/animal fat with an alcohol, i.e. alcoholysis, is an alternative to petroleum-based fuel because it is produced from renewable resources. Moreover, biodiesel is biodegradable, non-toxic, and has a low emission profile. Enzymatic production of biodiesel from plant oils has drawn a great attention because of some advantages over conventional chemical catalysis such as having mild operating conditions, high purity of the products, and eliminated environment pollution (Fukuda et al., 2001). In number of studies, enzymatic synthesis of fatty acid esters in presence of organic solvents has been proposed (Nelson et al., 1996). However, in order to avoid solvent separation, toxicity, flammability and costs of organic solvents, a solvent-free system would be the process of choice (Selmi and Thomas, 1998). Methanol is the most commonly used alcohol as

* Corresponding author. Tel.: +98 21 64543161; fax: +98 21 66405847.
E-mail: far@aut.ac.ir (F. Vahabzadeh)

the acyl acceptor in the transesterification reaction because of its low cost and high reactivity. Lipases from various sources, such as *Candida antarctica*, *Rhizopus oryzae*, *Rhizomucor miehei* and *Pseudomonas cepacia* have been used for esterification reaction (Kaieda et al., 1999, 2001; Noureddini et al., 2005; Soumanou and Bornscheuer, 2003). Several researchers have reported that the immobilized *C. antarctica* lipase can be effectively used for the enzymatic production of biodiesel (Hernandez-Martin and Otero, 2008).

The aim of the present study was to investigate the influence of several operating conditions such as the amount of enzyme, molar ratio of methanol to oil and reaction temperature on the methyl ester synthesis. Commercial immobilized lipase from *C. antarctica*, Novozym 435, was employed as the biocatalyst to perform the methanolysis reaction of canola oil in a solvent free system.

2. Materials And Methods

2.1 Materials

Immobilized lipase from *C. antarctica*, commercially known as Novozym 435, was kindly donated by Novo Nordisk (A.S., Denmark-Tehran office). Refined canola oil was purchased from Behshahr Industrial Co. (Tehran, Iran). According to the gas chromatography analysis, the fatty acid composition was: palmitic acid 4.8%, stearic acid 2.3%, oleic acid 60.9%, linoleic acid 22.6%, arachidic acid 0.6%, linolenic acid 7.3%, gadoleic acid 1.2% and behenic acid 0.3%. From this composition, an average molecular weight of 881.6 for the canola oil was determined. All other chemicals were of analytical grade.

2.2 Methanolysis reaction

Methanolysis reaction of canola oil was performed in a 30 ml screw-capped bottle with a working volume of 10 ml. The reaction mixture consisted of canola oil, methanol and immobilized lipase at the conditions of experiment. This mixture was incubated in a shaker at 130 rpm and at specified temperature for 72 h. After the end of reaction, the lipase enzyme was removed by decantation from the reaction mixture and glycerol as the lower phase, was separated from the mixture by centrifugation at 5000 rpm for 10 min. The methanolysis yield was measured based on the amount of methyl ester present in the upper phase of the reaction mixture.

2.3 Analysis of methyl esters

The yield of methyl esters contained in the reaction mixture was determined using ^{1}H nuclear magnetic resonance (NMR) spectroscopy according to the method described by Gelbard et al. (1995). ^{1}H NMR spectra were recorded at 500 MHz on a Bruker Avance DRX-500 spectrometer using $CDCl_3$ as the solvent.

3. Results And Discussion

3.1. Stepwise addition of methanol

The stoichiometric ratio of reactants for the transesterification reaction is normally 3 mole alcohol/1 mole triglyceride. The effect of methanol-addition manner to the reaction mixture on methyl ester yield was studied. As shown in Fig. 1, stepwise addition of methanol is more effective than one-step methanolysis reaction.

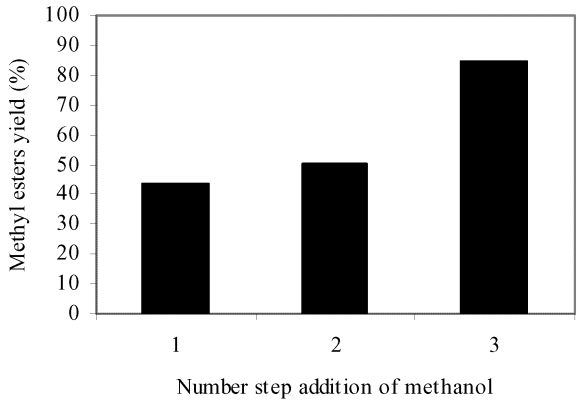

Fig. 1. Effect of number step additionof methanol on lipase-catalyzed methanolysis reaction. Reactin conditions: amount of enzyme 4%, temperature 35 °C, molar ratio of methanol to oil 3:1.

If a stoichiometric amount of methanol was added at the beginning of the reaction, a low methyl ester yield (i.e. 43.7%) was obtained. However, the yield of reaction could be significantly increased to more than 84% when the same amount of methanol was added in a three-step to the reaction mixture.

The short-chain alcohols, specially methanol may damage lipases on account of its intense polarity and the hydrophilic property. Because the immobilized lipase was irreversibly inactivated by contact with insoluble methanol which exists as drops in the oil, the enzyme activity could be significantly decreased (Shimada et al., 1999). We thus hypothesized that immobilized lipase was not inactivated at lower methanol concentrations. Therefore, subsequent experiments were thereafter carried out using a three-step addition of methanol to the reaction mixture, i.e. the first portion at the beginning of the reaction, the second and third portions after 24 and 48 h reaction time, respectively.

3.2 Enzyme quantity

To study the effect of the enzyme quantity on methyl ester formation, different quantities of immobilized lipase ranging from 1% to 6% were added to the starting reaction mixture. The obtained results are shown in Fig. 2.

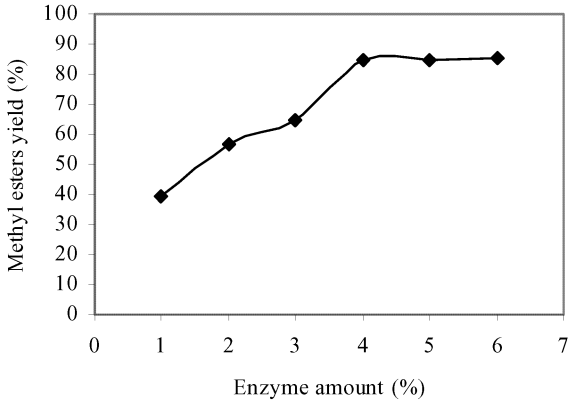

Fig.2. Effect of enzyme amount on lipase-catalyzed methanolysis reaction. Reaction conditions: temperature 35 °C, molar ratio of methanol to oil 3:1, and three-step addition of methanol.

The yield of reaction increased with increasing the lipase amount and reached to 84.4% using 4% of immobilized lipase. However, further increase in lipase amount did not show any increase in methyl ester yield. It is concluded that at low enzyme loadings, enzyme quantity would be the rate-limiting factor of methanolysis reaction. This achievement is consistent with results reported by Modi et al. (2006; 2007) that maximum conversions for esterification of vegetable oils were obtained at enzyme dosage of more than 10%.

3.3 Molar ratio of substrates

Methanolysis reaction was performed using different substrate molar ratio of methanol to oil varying in the range 3–6. The results (Fig.3) demonstrate that the yield of methanolysis reaction significantly decreases with increasing the methanol to oil molar ratio. The highest methyl ester yield of 84.4% was achieved at a methanol to oil molar ratio of 3:1, and decreased to 40.8% when the molar ratio of 6:1 was utilized.

This is in agreement with the earlier observation that excessive methanol concentration lead to lipase enzyme inactivation. The addition of methanol more than stoichiometric amounts, exerts an inhibitory effect on enzyme performance. This could be due to the fact that the immiscible methanol was accumulated around the lipase structure including its active sites, reaching a concentration level sufficient to cause a denaturation of the protein. This phenomenon might lead to enzyme inactivation.

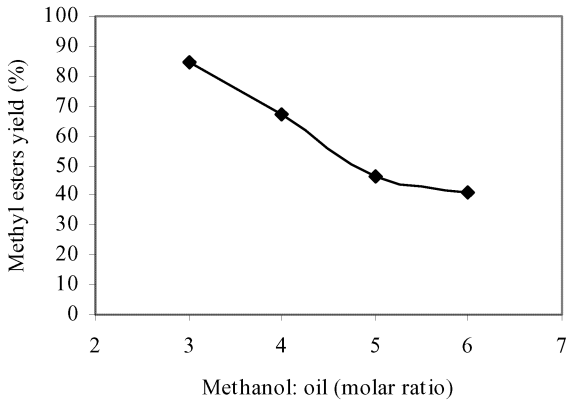

Fig. 3. Effect of methanol to oil molar ratio on lipase-catalyzed methanolysis reaction. Reactin conditions: temperature 35 °C, amount of enzyme 4%, and three-step addition of methanol.

3.4 Effect of temperature

The effect of temperature on the methanolysis reaction was determined in the range 25–55 °C. As shown in Fig. 4, the methyl esters yield initially increases with temperature from 25 to 35 °C and reaches to its maximum at 35 °C. However, a further increase in temperature leads to decrease in the reaction yield. This decrease in methyl ester yield can be explained by enzyme thermal denaturation.

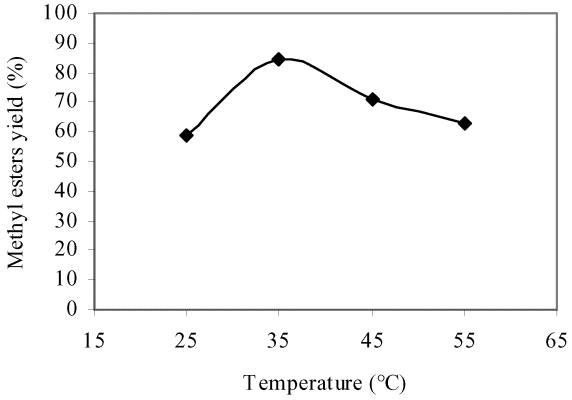

Fig. 4. Effect of temperature on lipase-catalyzed methanolysis reaction. Reaction conditions: amount of enzyme 4%, molar ratio of methanol to oil 3:1, and tree-step addition of methanol.

4. Conclusions

The enzymatic transesterification of canola oil with methanol in a solvent free media is carried out using an immobilized lipase as catalyst. The influence of several operation conditions on the reaction yield was analyzed. The inactivation of the lipase enzyme was successfully avoided by addition of methanol in step by step manner. The optimum reaction conditions was achieved by setting the experiment with the amount of enzyme at 4%, molar ratio of methanol to canola oil 3:1, and temperature 35 °C in three-step addition of methanol. The maximum methyl ester yield of 84.4% was obtained after 72 h reaction at optimum conditions.

5. References

Fukuda, H., A. Kondo, and H. Noda, 2001, J. Biosci. Bioeng. 92, 405.

Gelbard, G., O. Bres, R.M. Vargas, F.Vielfaure and U.F.Schuchardt, 1995, J. Am. Oil Chem. Soc. 72, 1239.

Hernandez-Martin, E. and C. Otero, 2008, Bioresour. Technol. 99, 277.

Kaieda, M., T. Samukawa, T. Matsumoto, K.Ban, A. Kondo, Y. Shimada, H. Noda, F. Nomoto, K. Ohtsuka, E. Izumoto and H. Fukuda, 1999, J. Biosci. Bioeng. 88, 627.

Kaieda, M., T. Samukawa, A. Kondo and H. Fukuda, 2001, J. Biosci. Bioeng. 91, 12.

Modi, M.K., J.R.C. Reddy, B.V.S.K. Rao and R.B.N. Prasad, 2006, Biotechnol. Lett. 28, 637.

Modi, M.K., J.R.C. Reddy, B.V.S.K. Rao and R.B.N. Prasad, 2007, Bioresour. Technol. 98, 1260.

Nelson, L.A., T.A. Foglia and W.N. Marmer, 1996, J. Am. Oil Chem. Soc. 73, 1191.

Noureddini, H., X. Gao and R.S. Philkana, 2005, Bioresour. Technol. 96, 769.

Selmi, B., D. Thomas, 1998, J. Am. Oil Chem. Soc. 75, 691.

Shimada, Y., Y. Watanabe, T. Samukawa, A. Sugihara, H. Noda, H. Fukuda and Y. Tominaga, 1999, J. Am. Oil Chem. Soc., 76, 789.

Soumanou, M.M. and U.T. Bornscheuer, 2003, Enzyme Microb. Technol., 33, 97.

CHEMICAL ENGINEERING TRANSACTIONS, Volume 14, 2008
Edited by G. Marino, E. Bardone, A. Viglia
 ISBN 978-88-95608-02-0

Enhancement of lycopene extraction from tomato peels by enzymatic treatment

Roberto Lavecchia and Antonio Zuorro
Department of Chemical Engineering, "Sapienza" University
Via Eudossiana, 18 – 00184 Roma (Italy)

Four food-grade enzyme preparations (Citrozym CEO and Ultra L, Peclyve EP and LI) with pectinolytic, cellulolytic and hemicellulolytic activities were investigated to assess their suitability for improving lycopene recovery from tomato peels. After a preliminary screening, the influence of solvent type and enzyme incubation time on the extraction efficiency was studied. Under the best conditions (1-h enzyme incubation followed by a 3-h solvent extraction at 40 °C) up to 440 mg of lycopene per 100 g of dry tomato peels were obtained. Experiments on the peel fraction of tomato processing waste confirmed the significant increase in yields resulting from the use of enzymes. Overall, lycopene recovery from the enzymatically treated material was between 70 and 98%, while yields from the untreated peels were in the range of 3–40%.

1. Introduction

In recent years lycopene, the major carotenoid pigment found in ripe tomato fruits and responsible for their characteristic red colour, has been the focus of considerable attention for its potential health benefits (Shi et al. 2002; Rao and Rao, 2004). Results from epidemiological and experimental studies support the view that lycopene may provide protection against cardiovascular disease and certain types of cancer (Giovannucci, 2005; Omoni and Aluko, 2005). Beneficial effects are believed to arise from its antioxidant properties which, in turn, are related to the extensive conjugation of double bonds in the molecule (Figure 1).

Because of the growing demand for natural lycopene, considerable interest has been directed to the possibility of obtaining lycopene from tomato processing waste. Tomato skins can, in fact, contain up to 5 times more lycopene than the pulp (Sharma and Le Maguer, 1996). However, the available solvent extraction technologies do not seem to allow a fast and economic recovery of the carotenoid. For example, only about 50% of total lycopene was extracted from tomato processing waste using supercritical CO_2 at 60 °C and 30 MPa (Sabio et al., 2003). Similar results were obtained by Rozzi et al. (2002) with supercritical CO_2 at 86 °C and 34.5 MPa. Low extraction efficiencies can be ascribed to the difficulty for the solvent to penetrate the compact tomato peel tissue and solubilize the pigment, which is deeply embedded within the chromoplast membrane structures (Harris and Spurr, 1969).

To overcome the above limitations, we have explored the possibility of using cell-wall degrading enzymes as a means for enhancing lycopene recovery from tomato peel tissue. With a view to industrial exploitation, commercial enzyme preparations and

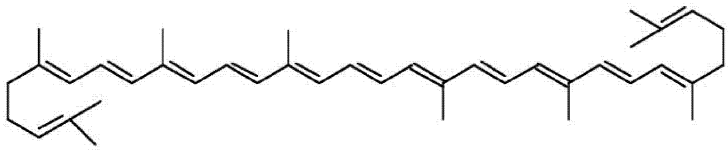

Figure 1 – Molecular structure of lycopene.

organic solvents approved for food applications were utilized. The results obtained indicate that a mild enzymatic treatment can lead to the almost complete recovery of lycopene from tomato peels or from the peel fraction of tomato processing waste.

2. Experimental

2.1 Materials

Fresh ripe tomatoes were purchased from a local market and stored at 4 °C for a maximum of 2 days before use. Tomato processing wastes were supplied by DESCO SpA (Terracina, Italy) and Az. DE LUCA (Anzio, Italy). As soon as obtained they were divided into small lots and frozen at −30 °C.

Citrozym CEO and Citrozym Ultra L were from NOVOZYMES (Denmark) and had a declared activities of 9,500 PGU/mL and 4,500 PECTU/mL, respectively. Peclyve EP and Peclyve LI were from LYVEN (France). All preparations were produced from *Aspergillus* strains and their main activities were pectinolytic.

Acetone, ethanol, ethyl acetate and hexane were obtained from CARLO ERBA (Italy). Their purities were greater than 99.7%, 99.5%, 99% and 95%, respectively.

2.2 Methods

Sample preparation and characterization

Ripe tomato fruits were immersed in boiling water for 1–2 min and, after being rapidly cooled, were hand-peeled.. The peels were partially dried in air for a few hours and stored at 4 °C. Just before use an appropriate amount of frozen tomato waste was thawed. The skins were hand-separated from the seeds and other impurities.

Each peel sample was characterized for moisture and total lycopene content. Moisture was determined by oven drying at 105 °C to constant weight. Total lycopene content was evaluated according to the procedure of Fish et al. (2002).

Lycopene assay

Lycopene concentration in the extracting solvents was determined by spectrophotometric measurement at room temperature in the wavelength range 350–600. A double-beam UV–VIS spectrophotometer (Perkin–Elmer Lambda 25) and quartz cells of 1-cm path length were used. The absorption spectra of the extract, independently of the solvent used and/or application of enzymes, displayed the three characteristic peaks of lycopene at around 445, 472 and 503 nm (Figure 2). To minimise interference from other carotenoids measurements were made at 503 nm, using a molar extinction coefficient of $1.585\ 10^5\ M^{-1}cm^{-1}$ (Merck et al., 1989).

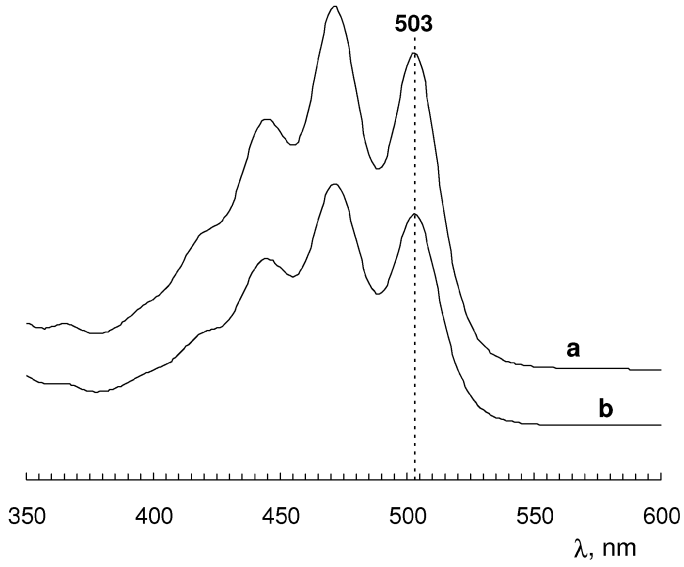

Figure 2 – VIS absorption spectra of hexane extracts from: (a) enzyme-treated and (b) untreated tomato peels.

Screening of enzyme preparations

The four enzyme preparations were screened for their ability to enhance lycopene extraction from tomato peel tissue using ripe tomato peels. 0.2 g of peels and 3.5 mL of an enzyme solution prepared by dissolving 0.1 mL of the commercial enzyme product in 3.4 mL of distilled water were initially charged into 50-mL conical flasks. The flasks were magnetically stirred and incubated at 25 °C for 4 h. 30 mL of hexane were then poured into the flasks and the system was kept under agitation, at the same temperature, for further 1 h. After this time, stirring was stopped and the aqueous and organic phases allowed to separate. A 2-mL sample of the hexane layer was taken and analysed for lycopene content.

Study of the influence of extraction conditions on yields

Peclyve LI, the preparation yielding the greatest improvement in lycopene extraction, was used to investigate the effects of solvent type and enzyme incubation time on yields. Hexane, ethyl acetate or the ternary mixture hexane/acetone/ethanol (50:25:25 v/v) were used as solvent. The latter was chosen because of its proven efficacy for the extraction of carotenoids from plant material (Olives Barba et al., 2006). The enzyme incubation time was varied between 1 and 15 h.

Lycopene extraction was carried out according to the procedure described in the previous section. The temperature and the extraction time were set at 40 °C and 3 h, respectively. These values were found to be a good compromise between the efficiency of extraction and the loss of lycopene due to oxidation.

3. Results and Discussion

Extraction yields were expressed as mg of lycopene per 100 g of dry plant material. Depending on the material considered, the moisture content was between 85 and 95 wt%, while the total lycopene content was between 280 and 540 mg/100 g dw (Table 1). Differences in the lycopene content for the two tomato processing wastes may be due to the different ripeness of the tomatoes used and/or the storage conditions of the material.

Screening of enzyme preparations

Lycopene extraction by the enzyme preparations tested gave the results shown in Table 2. As is evident, all four preparations increased the extraction yields. Peclyve EP and LI were the most efficient, with recoveries of 317.6 and 356 mg/100 g dw, respectively. These values correspond to an almost 20-fold increase with respect to the untreated peels.

The observed increase in yields can be explained by considering that pectin, cellulose and hemicellulose are the major polysaccharide components of tomato peel tissue (Gross, 1984). Accordingly, a more or less considerable fraction of these components can be expected to be degraded by the enzymes used, thus favouring solvent penetration and lycopene dissolution. The higher efficiency of Peclyve LI suggests that this preparation has the best activity profile, *i.e.*, the best combination of type and concentration of hydrolyzing enzymes for the tomato peels used. However, since the polysaccharide composition of tomato peels is dependent on fruit variety and ripening stage (Wakabayashi, 2000), a preliminary screening of enzyme preparations should always be performed on the specific material to be processed.

Table 1 – Characterization of tomato peels and tomato processing wastes.

Material source	Moisture (wt %)	Lycopene content (mg/100 g dw)
Ripe tomatoes	85.0	450 ± 21
DESCO SpA	95.0	280 ± 16
Az. DE LUCA	90.5	540 ± 30

Table 2 – Screening of enzyme preparations. Y represents lycopene recovery and Y_0 refers to control.

Enzyme preparation	Y (mg/100 g dw)	Y/Y_0 –
Citrozym CEO	95.3	5.3
Citrozym Ultra L	228.5	12.7
Peclyve EP	317.6	17.6
Peclyve LI	356.0	19.8

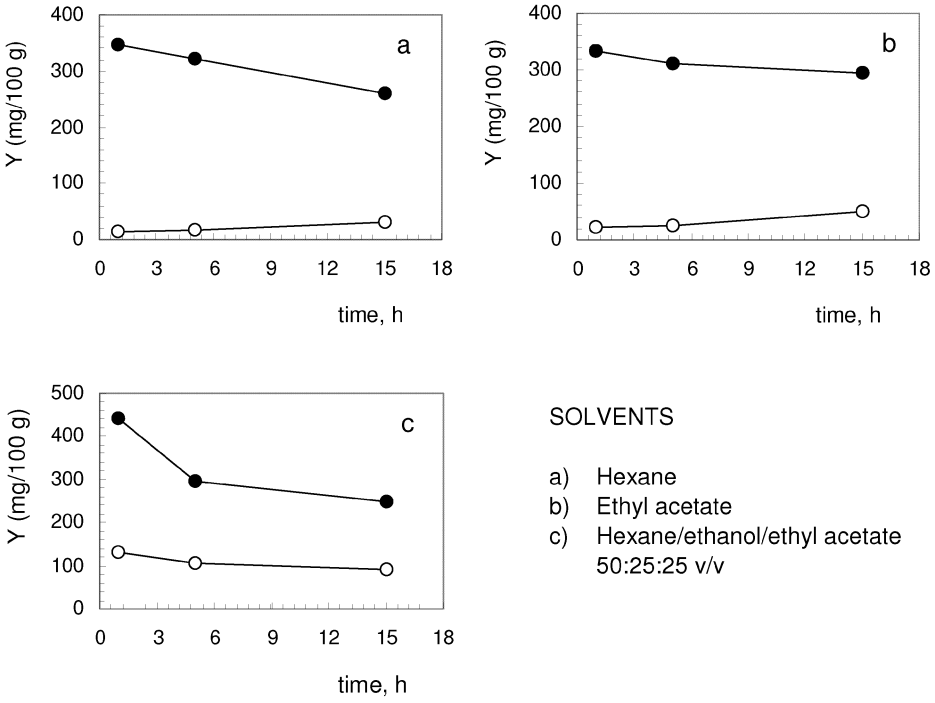

Figure 3 – Influence of enzyme incubation time on lycopene recovery (Y, mg/100 g dw) from untreated (open circles) and enzyme-treated (solid circles) tomato peels using different extraction solvents (T = 40 °C; enzyme preparation: Peclyve LI; extraction time: 3 h).

Study of the influence of extraction conditions on yields

Figure 3 shows the influence of extraction conditions on the recovery of lycopene from peels pretreated by Peclyve LI, the enzyme preparation with the best performance. As can be seen, and in line with what was found in screening tests, the enzymatic treatment increased significantly the extractability of lycopene. Overall, the extraction yields were 3- to 25-fold higher than those from the untreated material.

For all solvents, the highest recovery was achieved with an enzyme incubation time of 1 h. Under these conditions, lycopene extraction yields in hexane, ethyl acetate and the mixture hexane/acetone/ethanol 50:25:25 were 346.4, 334.3 and 440.2 mg/100 g dw, respectively. Increasing the incubation time resulted in a progressive reduction in yields. This suggests that the enzymatic degradation of cell-wall components is very fast and occurs within the first hour of incubation. Therefore, the vast majority of lycopene molecules contained in the plant tissue is likely to be rapidly released from the protective chromoplast structures and exposed to the conditions of the external environment. Because of their high reactivity, the released lycopene molecules can

undergo rapid oxidative degradation (Xianquan et al., 2005). Although the underlying mechanisms are only partially elucidated, it has been shown that lycopene oxidation leads to the formation of several cleavage products, including apo-lycopenals/ones and apo-carotendials, whose spectra are shifted to shorter wavelengths compared to that of lycopene (Caris-Veyrat et al., 2003). So, the reduction in extraction yields observed at prolonged incubation times could be a reflection of the progressive lycopene loss due to oxidation. The molecular structures of some oxidation products are depicted in Figure 4.
As regards the influence of solvent type, we note that using hexane or ethyl acetate did not produce significant differences in extraction efficiency. In contrast, the mixture hexane/acetone/ethanol 50:25:25 appeared to be much more effective, both in the presence and absence of enzymatic treatment. Since hexane is the only component of the mixture with a high affinity for lycopene, it follows that acetone and ethanol must play some auxiliary role in the overall extraction process. A possible explanation is that the two polar compounds, due to their small molar volume, high hydrogen bonding capability and large basicity, could cause the swelling of the plant tissue (Mantanis et al., 1995; Obataya and Gril, 2005), thus facilitating solvent penetration. In support of this hypothesis we note (see Figure 3) that beneficial effects associated with the ternary mixture are more evident when the structural integrity of the tomato peel tissue is preserved, *i.e.*, for untreated samples or, to a lesser extent, for short enzyme incubation times.
Considering that the tomato peels used had a lycopene content of 450 mg per 100 g dw, percentage recoveries at 1 h were of about 77%, 74% and 98% with hexane, ethyl acetate or the mixture hexane/acetone/ethanol 50:25:25 as the solvent. The corresponding values for untreated samples were 3%, 4.7% and 29%, respectively.

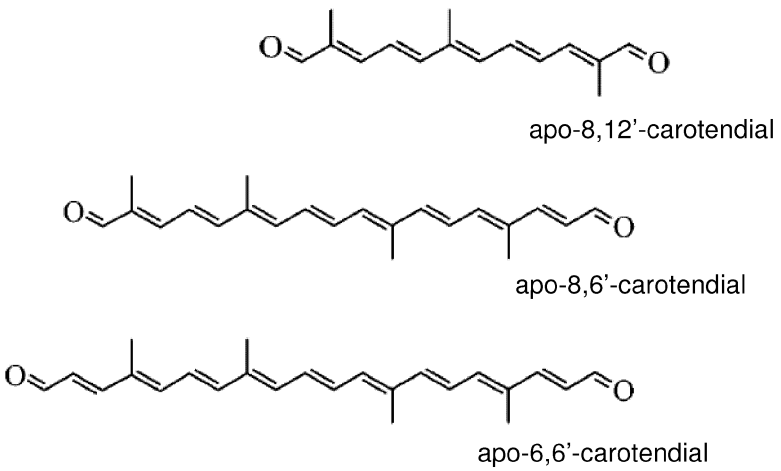

Figure 4 – Molecular structures of some apo-carotendials, cleavage products generated from lycopene oxidation (adapted from Caris-Veyrat et al., 2003).

Finally, Figure 5 shows lycopene extraction yields from the tomato processing waste supplied by Az. DE LUCA. Similar results were obtained with the waste from DESCO SpA. On the whole, recovery values were between 70 and 94% (and between 5 and 40% for the untreated material), which are very close to those for ripe tomato peels, indicating that the enzymatic procedure developed could also be applied to the peel fraction of tomato waste.

4. Conclusions

From the results of this study the following conclusions can be drawn: (1) Recovery of lycopene from tomato peels can be greatly enhanced, even at low temperatures and short incubation times, by the use of cell-wall degrading enzymes. (2) By proper selection of process conditions (*e.g.* 1 h incubation at 40 °C followed by a 3-h solvent extraction) lycopene can be almost completely extracted from the tomato peel tissue. (3) Conventional single or mixed organic solvents approved for food applications can be advantageously used.

Overall, the above points strongly support the possibility of using commercial enzyme preparations to obtain lycopene from the peel fraction of tomato processing waste. The utilization of this material as a source of lycopene could add significant value to the tomato processing chain, improving economic performance and decreasing disposal problems.

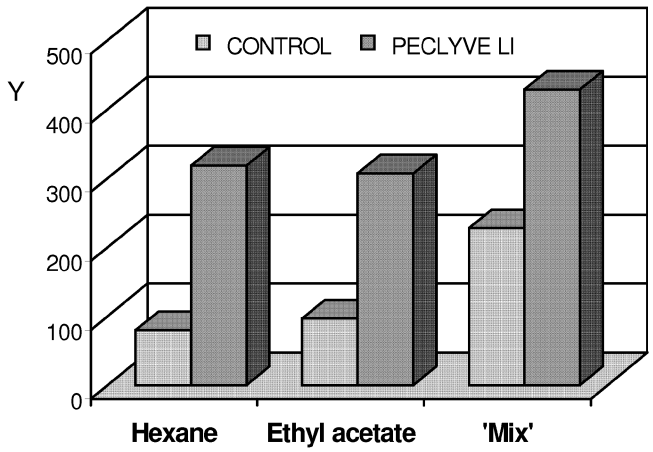

Figure 5 – Lycopene recovery (Y, mg/100 g dw) from untreated and enzyme-treated tomato processing waste after an incubation time of 1 h (T = 40 °C; enzyme preparation: Peclyve LI; extraction time: 3 h). 'Mix' denotes the mixture hexane/acetone/ethanol 50:25:25.

5. Acknowledgements

We wish to thank NOVOZYMES A/S (Bagsvaerd, Denmark) and LYVEN S.A. (Colombelles, France) for their kind gift of enzyme preparations. We also acknowledge DESCO SpA (Terracina, Italy) and Az. DE LUCA (Anzio, Italy) for providing the tomato processing waste used in this study.

6. References

Caris-Veyrat C., A. Schmid, M. Carail and V. Bohm, 2003, J. Agric. Food Chem. 51, 7318.

Fish W.W., P. Perkins-Veazie and J.K. Collins, 2002, J. Food Comp. Anal. 15, 309.

Giovannucci E., 2005, J. Nutr. 135, 2030S.

Gross K.C., 1984, Physiol. Plant. 62, 25.

Harris W.M. and A.R. Spurr, 1969, Am. J. Bot. 56, 380.

Mantanis G.I., R.A. Young and R.M. Rowell, 1995, Cellulose 2,1.

Merck & Co, 1989, The Merck Index, 11th edn. Rahway, New York, p 884.

Obataya E. and J. Gril, 2005, J. Wood Sci. 51,124.

Olives Barba A.I., M. Cámara Hurtado, M.C. Sánchez Mata, V. Fernández Ruiz and M. López Sáenz de Tejada, 2006, Food Chem. 95, 328.

Omoni A.O. and R.E. Aluko, 2005, Trends Food Sci. Technol. 16, 344.

Rao A.V. and L.G. Rao, 2004, Curr. Top. Nutrac. Res. 2, 27.

Rozzi N.L., R.K. Singh, R.A. Vierling and B.A. Watkins, 2002, J. Agric. Food Chem. 50, 2638.

Sabio E., M. Lozano V. Montero de Espinosa, R.L. Mendes, A.P. Pereira, A.F. Palavra and J.A. Coelho, 2003, Ind. Eng. Chem. Res. 42, 6641.

Sharma S.K. and M. Le Maguer, 1996, Ital. J. Food Sci. 2, 107.

Shi J., M. Le Maguer and M. Bryan, 2002, Lycopene from Tomatoes, in: Functional Foods: Biochemical and Processing Aspects, CRC Press, Boca Raton.

Wakabayashi K., 2000, J. Plant Res. 113, 231.

Xianquan S., J. Shi, Y. Kakuda and J. Yueming, 2005, J. Med. Food 8, 413.

CHEMICAL ENGINEERING TRANSACTIONS, Volume 14, 2008
Edited by G. Marino, E. Bardone, A. Viglia
 ISBN 978-88-95608-02-0

Water contact angle and FTIR study of the surface modification of PET by lipolytic enzyme

Ilaria Donelli,[1] Paola Taddei,[2] Vincent A. Nierstrasz,[3] Giuliano Freddi[1]
[1]Stazione Sperimentale per la Seta, via Giuseppe Colombo 83, 20133 Milano, Italy;
[2]Dipartimento di Biochimica 'G. Moruzzi', Sezione di Chimica e Propedeutica Biochimica, Universita di Bologna, via Belmeloro 8/2, 40126 Bologna, Italy;
[3]Department of Textiles, Ghent University, Technologiepark 907, B-9052 Gent Belgium

The goal of this study was to investigate the interaction of a lypolytic enzyme with poly-(ethylene terephthalate) (PET). Chemical, physical and structural changes induced on PET substrates with different degree of crystallinity were systematically investigated by water contact angle measurements and FTIR-ATR analyses. Treatment of PET with a commercial cutinase resulted in increased hydrophylicity and improved wettability of the PET materials. Water contact angle measurements indicate that cutinase displayed higher hydrolytic activity towards less crystalline PET. FTIR-ATR allowed to elucidate some chemical and structural features of the enzymatically-modified PET surface and provided some insight into the mechanism of the interaction of the lypolytic enzyme with PET.

1. Introduction

Polyethylene terephtalate, PET, is a polymer of major industrial importance because of its unique physico-mechanical and chemical properties. It is widely used in different commercial applications such as textile fibers and plastics. The material shows excellent strenght properties, a high hydrophobicity and resistance to chemicals. However, to improved dyeability with water-soluble dyes, an increased hydrophilicity of the surface is necessary. High temperature alkali treatment with sodium hydroxide is a conventional way of rendering PET fibres hydrophilic, but also the bulk properties of fibres are affected.

Recent studies have demonstrated that enzymes appear to be a safer and ecologically acceptable alternative to conventional chemical techniques for improvement of synthetic fibres properties in an environmentally friendly process (Alisch et al., 2004; Fischer-Colbrie G. et al., 2004; Gübitz and Cavaco Paulo, 2003; Heumann et al., 2006; Vertommen at al., 2005; Yoon et al. 2002). A highly specific and controlled enzymatic modification of synthetic fibres generates great benefits in terms of quality and performance. Enzymatic systems active on synthetic polymers are esterases, lipases and cutinases. In particular, the hydrolysis of PET by a fungal cutinase from *Fusarium solani* f. sp. *pisi*, wild-type (Alisch et al., 2006; Vertommen at al., 2005; Nimchua et al., 2006) or genetically modified near the active site (Araújo et al., 2007), and by a bacterial thermostable hydrolase from *Thermobifida fusca* has been demonstrated (Muller et al., 2005). Contrary to lipases, whose activity is greatly enhanced in the

presence of a lipid-water interface, cutinases do not display, or display little interfacial activation, being active on both soluble and emulsified substrates.
For this study, a commercial cutinase has been chosen. The activity of this enzyme increases the number of hydroxyl and carboxyl free groups on the surface, improving hydrophilicity and faciliting dyeing. The effects are clearly visible, but the parameters that regulate such activity are still poorly understood. In fact, recent studies have underlined that chemical and physical properties of PET, in particular the degree of crystallinity, affect the capability of the enzyme to hydrolize the ester bonds. The goal of this study was to investigate the interaction of the enzyme with PET, in relation to chemical and physical features of the sample.

2. Materials and Methods

2.1 Materials

2.1.1 Enzymes and chemicals

TEXAZYM EM, a commercial enzyme formulation, was obtained from inoTEX Ltd, Dvur Kralove, Czech Republic.

2.1.2 Polyester substrates

Two different poly(ethylene terephthalate) (PET) membrane substrates were used: crystalline/oriented PET, obtained from Fait Plast S.p.A. (Italy) and amorphous PET, obtained from University of Twente (The Netherlands), abbreviated as M-PET-A and M-PET-B, respectively.
The M-PET-A thickness is 70 µm, while that of M-PET-B is 200 µm. The degree of crystallinity of M-PET-A and M-PET-B is about 35% and 10%, respectively, as determined by single DSC run (Sichina, 2000).

2.2 Methods

2.2.1 Pre-Treatment of the commercial enzyme preparation

The commercial enzyme preparation TEXAZYM EM was diluted 1:1 with water and dialyzed in a cellulose tube (molecular cut-off: 12000 Da, purchased from Sigma-Aldrich, product no. D9652-100FT) against distilled water for 2 days at room temperature. After dialysis, the aqueous enzymatic solution was centrifuged at 10000 rpm for 25 minutes, freeze-dried and stored in a refrigerator prior to use. The aim was to remove the low molecular weight additives (wetting and softening agents) present in the commercial enzyme formulation in order to avoid any undesired interference during the reactions

2.2.2 Activity assay

Esterase activity (EC 3.1.1.1) was measured using 4-nitrophenyl butyrate as a substrate (Sigma-Aldrich assay). The increase of the absorbance at 405 nm was measured at room temperature using Schimadzu UV 1601 spectrophotometer. The increase of the absorbance at 405 nm indicates an increase of 4-nitrophenolate due to hydrolysis of the substrate. The activity was calculated in units, where 1 unit is the amount of enzyme required to hydrolyze 1 µmol of substrate per minute under the given assay conditions (pH 7.5 at 25°C).

2.2.3 Enzyme treatment of PET membranes

The samples were cut into pieces of 10 x 1.5 cm and washed with 1% SDS solution for 30 minutes, at 50/60°C and then thoroughly rinsed with distilled water. The reactions were done in phosphate buffer (50 mM, pH 8.0). Reaction conditions are shown in

Table 1. Control samples without enzyme were prepared as well. After incubation, the samples were washed with 1% SDS solution for 30 minutes at 50/60°C and then with distilled water until foam was removed. Samples were dried at room temperature overnight.

Table 1: Texazyme Em reaction conditions

Temperature	40°C ± 1°C
Time	120 min
Material/Liquor ratio mg/ml	1:85
Enzyme/Substrate ratio	20 U/mg
Mixing (Agitation)	40 rpm/min ± 2 in Linitest Heraeus

2.2.4 Contact angle measurements

Water contact angles were measured at room temperature using a FTA188 Contact Angle and Surface Tension Analyzer (First Ten Ångstroms). Each value reported is the average of left and right contact angle with respective standard deviation. Samples were fixed to the support with sticky tape and measurements were made each 5 mm. The aim was to reduce the superficial variability of measurements. Therefore, a profile of the superficial properties was obtained for each sample. Measurements were made on the same sample before and after enzyme treatment.

2.2.5 Infrared Spectroscopy (FTIR-ATR)

Measurements were performed on a NEXUS Thermo Nicolet FTIR spectrometer employing an Attenuated Total Reflection (ATR) accessory. All spectra were obtained with a Ge crystal cell (maximum depth 0.8 μm). Spectra were normalized to the 1410 cm^{-1} peak. Each spectrum reported is the average of three spectra.

3. Results and Discussion

To evaluate the superficial properties of the samples after enzyme treatment, water contact angle measurements were performed by sampling progressively the surface of each sample before and after treatment. The average water contact angle values of untreated membranes were 74.1°±1.3° and 75.1°±1.4° for the crystalline and amorphous sample, respectively. They decreased to 67.6°±4.1° (crystalline) and 58.3°±3.1° (amorphous) after cutinase treatment, as shown in Figure 1.

These results indicate that cutinase displayed higher hydrolytic activity towards amorphous PET, confirming the data reported in a previous work about a higher amount of soluble hydrolysis products after cutinase treatment of a less crystalline sample (Vertommen at al., 2005).

FTIR-ATR measurements of PET membranes were performed on both crystalline and amorphous samples before and after enzyme treatment. Here we report the data obtained on the amorphous membrane M-PET-B, where spectral changes were more evident. Typical FTIR-ATR spectra before and after cutinase treatment are shown in Figure 2. Several spectral changes attributable to enzymatic modification are observable in the 1800-800 cm^{-1} wavenumber range.

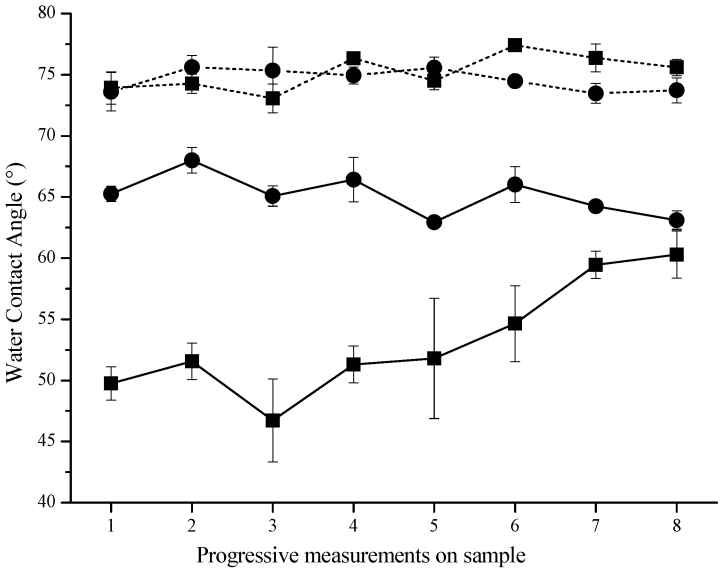

Figure 1: Average water contact angle profiles of M-PET-A (•) and M-PET-B (■) membranes. Dotted line: untreated samples; solid line: samples treated with the enzyme.

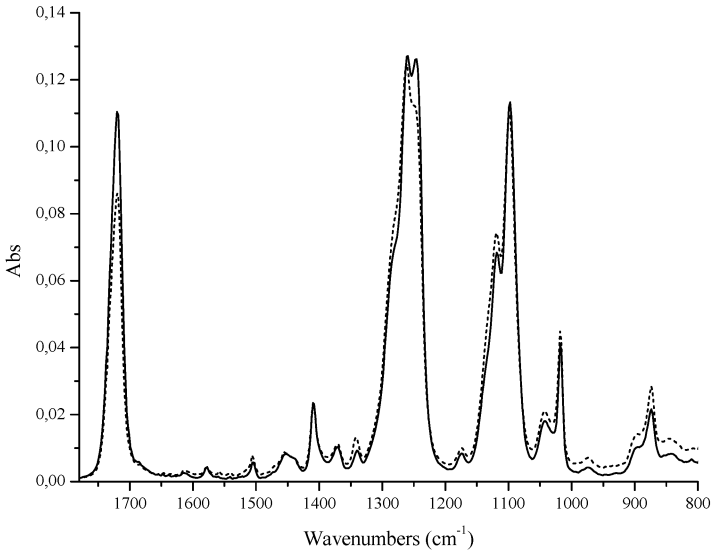

Figure 2: FTIR-ATR spectra of M-PET-B membrane untreated (solid line) and after enzyme treatment (dotted line).

One of the most important aspects of PET structure concerns the existence of *trans* and *gauche* rotational conformers for the ethylene glycol moiety. Both types of conformers are present in the amorphous phase, but only the *trans* conformer is present in the crystalline phase (Cole et al., 1994; Walls, 1991; Ward, 1977). Because of the sensitivity of molecular vibrations to bond strengths and configurations, IR spectroscopy is a sensitive method for determining conformers and potential changes induced to them from enzyme activity.

With reference to the remarkable spectral changes induced on the amorphous M-PET-B membrane by the enzymatic reaction, the absorbance of the carbonyl stretching band at 1725 cm^{-1} decreased significantly after enzyme treatment, and the strong bands near 1260 and 1100 cm^{-1}, attributed mainly to C-O stretching, also changed in shape and relative intensity of band components after reaction. These changes confirm that the ester bonds of PET were the main target of the enzyme activity.

Additionally, the peak at 1340 cm^{-1}, which arises from CH_2 wagging of *trans* conformers of the ethylene glycol unit, became much stronger than the peak at 1370 cm^{-1}, which corresponds to *gauche* conformers. It can be inferred from this result that upon enzyme treatment the *trans* conformers were enriched either by selective hydrolysis and removal of the *gauche* conformers or by *gauche* → *trans* conversion. Therefore, it is confirmed that cutinase displays significantly higher hydrolytic activity towards amorphous regions of PET. The mechanism of enzyme-PET interaction is still under investigation through quantitative analysis of the above discussed spectral changes.

4. Conclusions

In this study, the hydrolytic activity of a lypolytic enzyme, cutinase, toward PET materials was confirmed. In particular, water contact angle measurements and FTIR-ATR analysis indicated that cutinase displays higher activity toward the amorphous phase of PET.

FTIR-ATR spectra allowed to highlight some chemical and structural changes induced by the enzyme on the outermost layers of the PET substrates. These changes are worth of being further investigated in order to obtain more information on the mechanism driving the enzyme-PET interactions.

Detailed and fundamental knowledge in this field may not only contribute to the development of bio-treatment processes for polyester substrates, but also address the genetic engineering of lypolytic enzymes with enhanced hydrolysing activity with respect to the native ones.

References

Alisch-Mark M., Feuerhack A., Muller H., Mensak B., Andreaus J. and Zimmermann W., 2004, Biocatalytic modification of polyethylene terephthalate fibres by esterases from Actinomycete isolates. Biocatal Biotrans, 22, 347.

Alisch-Mark M., Herrmann A. and Zimmermann W., 2006, Increase of the hydrophilicity of polyethylene terephthalate fibres by hydrolases from Thermomonospora fusca and Fusarium solani f. sp. pisi. Biotechnol Lett, 28, 681.

Araújo R., Silva C., O'Neil A., Micaelo N., Guebitz G., Soares C.M., Casal M. And Cavaco-Paulo A, 2007, Tailoring cutinase activity towards polyethylene terephthalate and polyamide 6,6 fibers. J Biotech, 128, 849.

Cole K.C., Guevremont J., Ajji A., and Dumoulin M.M., 1994, Characterization of surface orientation in poly (ethylene terephthalate) by front-surface reflection infrared spectroscopy. Appl Spectrosc., 48, 12, 1513.

Fischer-Colbrie G., Heumann S, Liebminger S., Almansa E., Cavaco-Paulo A. and Guebitz G.M, 2004, New enzymes with potential for PET surface modification. Biocatalysis and Biotransformation, 22, 341.

Gubitz G.M. and Cavaco-Paulo A, 2003, New substrates for reliable enzymes: enzymatic modification of polymers. Curr Opin Biotech, 14, 577.

Heumann S., Eberl A., Pobeheim H., Liebminger S., Fischer-Colbrie G., Almansa E., Cavaco-Paulo A., Gübitz G.M, 2006, New model substrates for enzymes hydrolysing polyethyleneterephthalate and polyamide fibres. J Biochem Biophys Methods, 69, 89.

Muller R.J., Schrader H., Profe J., Dresler K., Deckwer W.D, 2005, Enzymatic degradation of poly(ethylene terephthalate): rapid hydrolyse using a hydrolase from T.fusca. Macromol Rapid Commun, 26, 1400.

Nimchua T., Punnapayak H. and Zimmermann W, 2006 Comparison of the hydrolysis of polyethylene terephthalate fibers by a hydrolase from Fusarium oxysporum LCH I and Fusarium solani f. sp. pisi. Biotechnol. J., 1, 1.

Sichina WJ. DSC as problem solving tool: measurement of percent cristallinity of thermoplastics. Application note. 200. Perkin Elmer TM instruments.

Vertommen MAME, Nierstrasz VA, Veer Mvd, Warmoeskerken MMCG, 2005, Enzymatic surface modification of poly(ethylene terephthalate). J Biotechnol, 120,:376.

Walls DJ, 1991, Application of ATR-IR to the analysis of surface structure and orientation in uniaxially drawn poly(ethylene terephthalate). Appl Spectr, 45, 1193.

Ward I.M. and Wilding M.A. Infra-red and Raman spectra of poly(m-methylene terephthalate) polymers. Polymer 1977. 18: 327-335.

Yoon MY, Kellis J, Poulouse AJ, 2002, Enzymatic modification of polyester. AATCC Rev, 2, 33.

CHEMICAL ENGINEERING TRANSACTIONS, Volume 14, 2008
Edited by G. Marino, E. Bardone, A. Viglia
 ISBN 978-88-95608-02-0

Laccase-catalyzed azodye synthesis

Trovaslet Marie[1], Enaud Estelle[1], Bazes Alexandra[1], Jolivalt Claude[2], Van Hove François[1,3], Vanhulle Sophie[1]

[1] Microbiology Unit, Université catholique de Louvain, Croix du Sud 3 bte 6, B-1348 Louvain-la-Neuve, Belgium

[2] Laboratoire de Synthèse Sélective Organique et Produits naturels, ENSCP, 11 rue Pierre et Marie Curie, 75231 Paris cedex 05, France

[3] Mycothèque de l'Université catholique de Louvain (BCCM™/MUCL), Croix du Sud 3 bte 6, B-1348 Louvain-la-Neuve, Belgium

There is an increasing demand of the chemical industry to develop eco-friendly processes. In numerous cases, biocatalysis represents an attractive route towards one-step safe synthesis. In this context, the finding that laccases are able to create azo bonds represents a good potential for the dye industry. This work investigates the properties and biosynthesis of an azodye named LAR1, which stands for Laccase Acid Red 1. LAR1 is made up of two anthraquinonic moieties coupled through an azo bond and demonstrated good dyeing properties on nylon, polyamide and particularly on leather. LAR1 has been shown not to be cytotoxic, mutagenic and ecotoxic. Further investigations aimed at optimizing the process of LAR1 production. Several laccases from bacterial and fungal (ascomycetes and basidiomycetes) origin proved to be useful to produce LAR1 in short reaction times. Whatever the laccase tested, optimal pH for LAR1 synthesis was 4 while the highest rates of oxidation for ABTS were obtained between pH 3 and 4. In our conditions, two isoenzymes from *Trametes versicolor* have been shown to be the most efficient to transform ABu62. It was also found that oxidation of the anthraquinonic precursor by these laccases did not follow a classical Michaelis-Menten kinetic.

1. From traditional dye industry to biosynthesis

Since the discovery of the first synthetic dye mauvein by a young English chemist William Perkin in 1856, traditional dyes from animal (*Hexaplex trunculus, Kerria lacca, Kermes vermilio* …) or plant (*Isatis indigota, Rubia cordifolia, Rhamnus lycioides*…) origin have been progressively replaced by synthetic dyes (Cardon, 2003). The colour chemical industry was an important activity in Europe until the end of 20th century. It suffers now displacement to the developing world due to the high labour costs in Europe as well as to both worker and environment non-friendly character of dyes synthesis (Integrated Project SOPHIED, 2005). Since several groups (Shaw and Freeman, 2004; Bruyneel *et al.*, 2008) described the ability and the efficiency of laccases to catalyze the formation of coloured compounds, these enzymes now represent an attractive route towards dye synthesis. Laccases (EC 1.10.3.2) are benzenediol:oxygen oxidoreductases coupling the one-electron oxidation of an organic reducing substrate (mainly a phenol or an aromatic amine) to the concomittant reduction

of dioxygen to water (Solomon *et al.*, 1996). By contrast to peroxidases which share with laccases a low specificity for the reducing substrate but require hydrogen peroxide as co-substrate, laccases have a strong preference for dioxygen. As this compound is easily renewed in the reaction medium, this represents an advantage for industrial applications.
Our group (Vanhulle 2007a; Vanhulle *et al.*, 2008) reported the production of a red azo-compound LAR1 (Laccase Acid Red 1) during fungal laccases biotransformation of an anthraquinonic acid compound (Acid Blue 62-ABu62) (Figure 1).

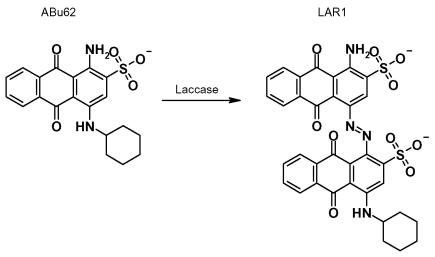

Figure 1: Laccases catalyzed the synthesis of Laccase Acid Red 1 (LAR1) from Acid Blue 62 (ABu62) (from Vanhulle et al., 2008).

LAR1 was tested for its ability to dye textile. In particular, the fastness properties of the dyeings on nylon, polyamide and leather were measured in accordance with ISO standards. All results demonstrated that the dye has a good behaviour, except for light fastness, which was only medium. Besides demonstrating good dyeing properties, LAR1 has also prove its safety through several adequate toxicity studies. Nowadays, 60% to 70% of the dyes used are azodyes and many of them have demonstrated toxicity in the past (Vanhulle *et al.*, 2007b). NRU test with Caco-2 cells was used to evaluate LAR1 cytotoxicity. Mini-Ames and Standard Ames tests allowed to assess its mutagenic potential whereas mortality studies using zebra fish egg, *Vibrio fisherii*, *Daphnia magna* and green alga *Desmodesmus subspicatus* were used to evaluate its ecotoxicity. The new azodye was neither mutagenic nor ecotoxic (Enaud *et al.*, 2008).

2. Laccases in azodye synthesis

Interest in the use of laccase-catalyzed LAR1 synthesis for a future industrial production being established, robust and efficient biocatalysts must be selected. Accordingly, the catalytic properties of several laccases from both bacterial and fungal origins were compared for ABu62 biotransformation: CotA is a recombinant enzyme from *Bacillus subtilis* (Martins *et al.*, 2002); Bioscreen, a commercial laccase from *Trametes versicolor*, purchased from BIOSCREEN, Germany and delivered under the commercial trademark Oxizym LA - batch n° LA 2000/001; PS7, a laccase from *Pycnoporus sanguineus* MUCL 41582 (Trovaslet *et al.*, 2007); PS344, a laccase from the aquatic fungus *Phoma sp.* strain UHH 5-1-03 (Junghanns and Schlosser, personal communication) and TVA and TVB are two isoenzymes purified from *Trametes versicolor* ATCC 32745 (Bertrand *et al.*, 2002a and b).

These enzymes differ for their kinetic parameters using ABTS as substrate (Table 1). In our conditions, TVA and PS344 laccases showed the highest affinities towards ABTS (K_m < 10 µM while all other K_m values were between 30 and 50 µM) and the k_{cat}/K_m ratios showed that ABTS substrate was more efficiently converted by TVA laccase (54 400 $mM.s^{-1}$) than by all other enzymes, suggesting that this enzyme could be an efficient catalyst for biotransformation applications. Very similar K_m were obtained for TVB and Bioscreen, both *Trametes versicolor* laccases, suggesting that the commercial enzyme Bioscreen could be an inducible form of laccase as TVB.
For all tested laccases, oxidation rate of ABTS decreased when increasing pH from 3-4 to 7-8 and no transformation of ABTS could be detected anymore at pH 7-8, except for PS344 and CotA laccases which retain activity until pH 8-9. Moreover, all fungal laccases displayed a maximal activity between 50 and 70°C and have close activation energy (10-15 $KJ.mol^{-1}$). The activity of the bacterial laccase CotA raised in a linear manner with temperature up to the highest temperature tested (80°C) and its activation energy was two fold higher than the one of other tested laccases.

Table 1: Kinetic characterization of laccase catalyzed ABTS biotransformation.

Laccases	k_{cat} (s^{-1}) *	K_m (µM) *	k_{cat}/K_m (x 10^3 $mM^{-1}.s^{-1}$) *	Optimum pH **	Optimum temperature ***
Cot A	17	39.5	0.4	4	> 80°C
Bioscreen [a]	ND	30.8	ND	3	55°C
PS7	21.4	47.4	0.4	3	65-70°C
PS344 [b]	24.7	9.7	2.5	4	65°C
TVA	386	7.1	54.4	ND	ND
TVB	442	30.5	14.5	ND	ND

[a]: Neither purity nor specific activity of the enzyme preparation were known.
[b]: PS344 laccase is a dimeric enzyme consisting of 75 KDa monomers (Junghanns and Schlosser, personal communication).
*: Reactions were carried out in acetate 0.1 M pH 4.5. The apparent k_{cat} and K_m values were evaluated using six ABTS concentrations and Lineweaver-Burk linearisation.
**: The optimum pH was determined by oxidation of 4 mM ABTS, over a range of pH 2 to 10 in phosphate 0.1 M adjusted to desired pH using HCl or NaOH.
***: The optimum temperature was determined by oxidation of 4 mM ABTS, between 20 and 75°C in phosphate 0.1 M pH 4 solution.
ND: not determined.

2.1. Optimum pH conditions for LAR1 production

For all laccases, the ABu62 transformation rate as a function of pH exhibited a bell-shaped activity profile with an optimum pH around 4 (Figure 2A). At pHs higher than pH 7-8, ABu62 was not transformed, excepted with CotA and PS344 laccases. As previously evidenced for phenylureas derivatives (Jolivalt *et al.*, 2006) and as suggested

from the colour changes of the reaction solution during the biotransformation course, pH influenced the nature of the ABu62 biotransformation products: indeed, a decolourisation was observed at neutral to alkaline pH while the reaction medium turned from blue, the ABu62 colour, to red in acidic conditions. At the optimal pH for ABu62 consumption, the main biotransformed product was identified as LAR1.

Laccases stability studies as a function of the pH showed that for all laccases, the stability increased with pH, up to pH 7 to 9. Acidic pH is required to produce the targeted product, LAR1, but in such conditions, laccases are likely to lose their activity, thus limiting the transformation yield. However, in the presence of ABu62, laccase stability was improved between pH 3 and 8 (Figure 2B). It is noteworthy that bacterial laccase CotA has an unusual stability behaviour, both in the presence or in the absence of ABu62 (data not shown). At pH 2, a rapid loss of activity occurred while, at other pHs, an activity increase (between 2 and 30 folds) was observed when increasing the storage duration. Contrary to fungal laccases, deactivation mechanism of this biocatalyst seems to involve intermediate(s) that has (have) more activity than the initial form of the enzyme. Work is currently under progress to better characterize this (these) intermediate(s).

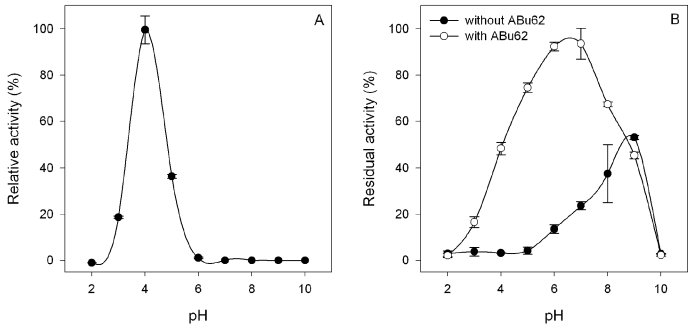

Figure 2: A. Effects of pH on Bioscreen catalyzed ABu62 biotransformation. B. Bioscreen stability, after a one week storage, as a function of pH, in the presence or in the absence of 70 µM ABu62. All reaction media contained 10 U.l^{-1} laccase and phosphate 0.1 M adjusted to desired pH using HCl or NaOH. All experiments were triplicated.

2.2. Kinetic parameter evaluation

Although not really favourable in terms of laccase stability, pH 4.5 was chosen for the kinetic studies for two reasons: (i) pH 4.5 is close to the optimum pH for ABu62 transformation; (ii) at this pH, LAR1 is the main biotransformed product.

To estimate the kinetic parameters of each laccase for ABu62, apparent K_m and k_{cat} values were first evaluated from Lineweaver-Burk linearisations, assuming a Michaelis-Menten behaviour of the enzymes (upper part of Table 2). In these conditions, k_{cat} values were in the same range of those calculated for ABTS substrate. Deducted K_m values varied from 165 µM for CotA laccase to 472 µM for PS7 enzyme, suggesting

that the affinity of the enzymes for ABu62 is significantly lower than the one observed for ABTS.

Table 2: Kinetic parameters for laccases catalyzed ABu62 biotransformation. Excepted for TVA and TVB laccases, reactions were carried out in acetate 0.1 M pH 4.5. The apparent k_{cat} and K_m values were evaluated using height substrate concentrations and Lineweaver-Burk linearisation.

Laccases	k_{cat} (s^{-1})	K_m or $S_{0.5}$ (µM)	k_{cat}/K_m (x 10^3 $mM^{-1}.s^{-1}$)	K_i (mM)	h
Cot A [1]	3.1	165	0.02	-	-
Bioscreen [a (1)]	ND	305	ND	-	-
PS7 [1]	35.7	472	0.07	-	-
PS344 [1]	34.1	194	0.17	-	-
TVA [1]	1 376	302	4.55	-	-
TVB [1]	898	204	4.41	-	-
TVA [2]	1 200	189	6.34	230	-
TVB [3]	477	63	7.57	-	1.6

[a]: Neither purity nor specific activity of the enzyme preparation were known.
[1] Apparent kinetic parameters were evaluated using the classical Michaelis-Menten equation.
[2] Reactions were carried out in 100 mM tartaric buffer pH 4.5. The ABu62 concentrations ranged from 0 to 450 µM. Apparent kinetic parameters were calculated using a modified Michaelis-Menten equation which includes an inhibition constant Ki (*Eqn. 1*).
[3] Reactions were carried out in 100 mM tartaric buffer pH 4.5. The ABu62 concentrations ranged from 0 to 450 µM. Apparent kinetic parameters were calculated using Hill equation (*Eqn. 2*).

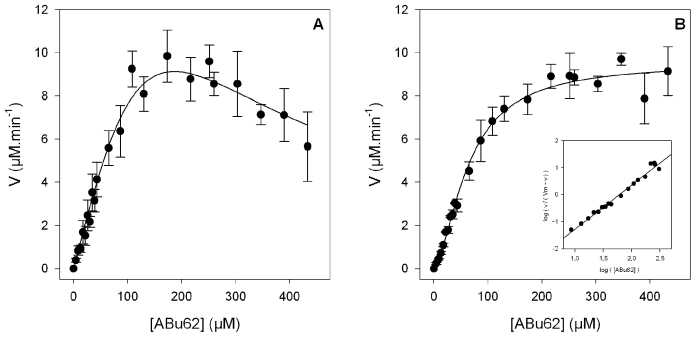

Figure 3: TVA (A) and TVB (B) laccases activity vs. ABu62 concentration. Insert: Hill plot. Reactions were carried out in 100 mM tartaric buffer pH 4.5 as previously described in Trovaslet et al. (2007).

However, observation of Figure 3 shows that the kinetic behaviour of these two enzymes differs somewhat from an ideal Michaelis-Menten mechanism. On the one hand, a substrate-inhibition phenomenon occurred at ABu62 concentrations higher than 150-200 µM for TVA laccase (Figure 3A). Therefore, apparent kinetic parameters were calculated using the modified Michaelis-Menten equation (*Eqn.* 1) which includes an inhibition constant K_i. On the other hand, a sigmoïdal curve was observed when plotting the reaction rate *vs.* substrate concentration for TVB laccase (Figure 3B). To account this behaviour, kinetic data were fitted according to a Hill equation (*Eqn.* 2) including three parameters: $S_{0.5}$, the half-saturating substrate concentration; h, the Hill coefficient and k_{cat}. Based on our results (second part of Table 2), TVB laccase presents the highest affinity for ABu62 (K_m value about 63 µM *vs.* 189 µM for TVA) whereas TVA has the highest turnover (1 200 s^{-1} *vs.* 477 s^{-1} for TVB). Overall efficiency of both laccases are therefore very similar. The kinetic behaviour of TVB suggests a positive cooperativity with respect to ABu62 substrate with a Hill coefficient of about 1.6, which is very similar to what was previously obtained for a laccase from *Pycnoporus sanguineus* (Trovaslet *et al.*, 2007).

$$v = \frac{V_m[S]}{K_m + [S] + ([S]^2 / K_i)} \quad (1)$$

$$v = \frac{V_m[S]^h}{S_{0.5}{}^h + [S]^h} \quad (2)$$

An enzymatic kinetic following a Hill equation can be the result of the presence of two different binding sites of the substrate on the enzyme. As ABu62 is substrate (it is transformed by laccase into LAR1), it obviously binds into the oxidation active site of the enzyme. It can thus be assumed that a second binding site for ABu62 exists. Crystallisation experiments of TVB in the presence of ABu62 are currently in progress to address this issue and localise the second hypothetical binding site for ABu62.

2.3. *Oxidation of ABTS in the presence of ABu62*

Based on the hypothesis of two-binding sites for ABu62, this dye may be considered as both a substrate and an activator of TVB laccase. To determine if ABu62 could also increase the transformation efficiency of laccase towards another substrate, ABTS oxidation was carried out with TVA and TVB laccases, in the presence of increasing ABu62 concentrations (Figure 4).

Transformation of ABTS was followed by measuring the absorbance changes at 414 nm. At this wavelength, concomitant oxidation of ABu62 also contributed to absorbance increase. However, it has been verified that the transformation of ABu62 accounts at most for 8% of the total absorbance changes.

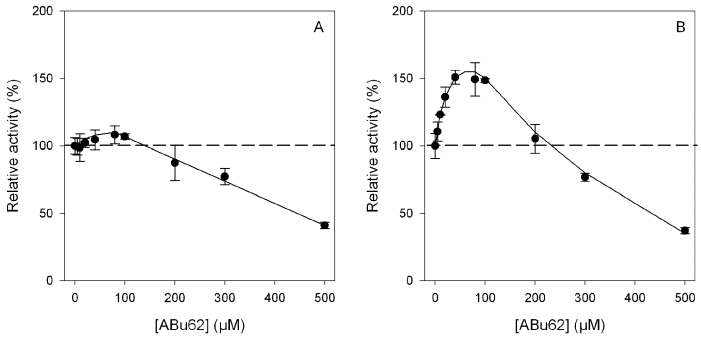

Figure 4: Biotransformation of 20 µM ABTS in the presence of increasing ABu62 concentration (between 0 and 500 µM), in tartaric buffer 100 mM pH 4.5. Activities were expressed as a percentage of activity measured without dye. Reactions were carried out with 10 U.l^{-1} TVA (A) or TVB (B) laccase activity.

From 0 to 100 µM ABu62, the transformation rate of ABTS by TVA laccase is not significantly different if compared to the transformation rate of ABTS alone (Figure 4A). For ABu62 concentrations higher than 100 µM, a decrease of the transformation rate is observed, as expected in presence of two competitive substrates. For TVB laccase (Figure 4B), the kinetic behaviour was different: for ABu62 concentration lower than 200 µM, a significant increase of the transformation rate of ABTS is observed, with a maximum for 100 µM ABu62 concentration. At this ABu62 concentration, ABTS is oxidized more than 1.5 times faster than without ABu62, suggesting an activation effect of this dye. For higher ABu62 concentrations, the transformation rate of ABTS decreased, as a consequence of the competition of both ABTS and ABu62 at the active site of laccase.

3. Conclusion

Laccases are cheap biocatalysts useful in azodye synthesis. Our study focused on the laccase biotransformation of a blue anthraquinonic dye (ABu62) oxidized into a red, non toxic and industrially interesting azodye (LAR1). Based on kinetic parameters evaluation of bacterial and fungal laccases, two enzymes from *Trametes versicolor* (TVA and TVB) have been shown to be the most efficient to transform ABu62. Furthermore, it was evidenced that one of the *Trametes versicolor* laccase (TVB) is activated by anthraquinonic substrate. Work is currently under progress to confirm the occurrence of this activation effect with other laccase substrates and different experimental conditions. These findings represent not only the synthesis of a new compound with good dyeing properties (LAR1), but also open the way to new safe and environmental friendly routes to azodye synthesis.

4. Acknowledgement

This work was supported by the Directorate for Technology, Research and Energy of the Walloon Regional Government of Belgium (LACOMAT), the European Commission, Sixth Framework Program (SOPHIED contract NMP2-CT2004-505899). F. Van Hove received financial support from the Belgian Federal Science Policy Office (contract BCCM C3/10/003). The authors kindly acknowledge F. Naveau, D. Ingels and S. Bizet for their efficient collaboration. L. Martins, C. Junghanns, D. Schlosser, G. Sannia, D. Wesemberg and S. Agathos are acknowledged for providing their laccases.

5. References

Bertrand T., C. Jolivalt, E. Caminade, N. Joly, C. Mougin and P. Briozzo, 2002a, Acta Cryst. D 58, 319.

Bertrand T., C. Jolivalt, P. Briozzo, E. Caminade, N. Joly, C. Madzak and C. Mougin, 2002b, Biochemistry 41, 7325.

Bruyneel F., E. Enaud, L. Billottet, S. Vanhulle and J. Marchand-Brynaert, 2008, Eur. J. Org. Chem. 1, 72.

Cardon D., 2003, Le monde des teintures naturelles. Belin, Paris.

Enaud E., M. Trovaslet, F. Bruyneel, L. Billottet, R. Karaaslan, P. Coppens, A. Casas, I.J. Jaeger, C. Hafner, R.C.A. Onderwater, A.M. Corbisier, J. Marchand-Brynaert and S. Vanhulle, 2008, submitted to Dyes and Pigments.

Integrated Project SOPHIED - FP6-NMP2-CT-2004-505899, 2005. 1st report on current shortcomings of the existing dyes and changes required to improve it, and create the next generation dyes (standards, market, cost).

Jolivalt C., C. Jauffret, L. Neuville, F.D. Boyer, L. Kerhoas and C. Mougin, 2006, J. Agric. Food Chem. 54, 5046.

Junghanns C. and D. Schlosser, Personal communication.

Martins L.O., C.M. Soares, M.M. Pereira, M. Teixeira, T. Costa, G. Jones and A.O. Henriques, 2002, J. Biol. Chem. 277, 18849.

Shaw S.D. and H.S. Freeman, 2004, Textile Research Journal 74(3), 215.

Solomon E.I., U.M. Sundaram and T.E. Machonkin, 1996, Chemical Review. 96(7), 2563.

Trovaslet M., E. Enaud, Y. Guiavarc'h, A.M. Corbisier and S. Vanhulle, 2007, Enzyme Microb. Technol. 41, 368.

Vanhulle S., E. Enaud, M. Trovaslet, N. Nouaimeh, C.M. Bols, T. Keshavarz, T. Tron, G. Sannia and A.M. Corbisier, 2007a, Enzyme Microb. Technol. 40, 1723.

Vanhulle S., M. Trovaslet, E. Enaud, M. Lucas, S. Taghavi, D. van der Lelie, B. van Aken, M. Foret, R.C.A. Onderwater, D. Wesenberg, S.N. Agathos, Y.J. Schneider and A.M. Corbisier, 2007b, Environ. Sci. Technol. doi : 10.1021/es071300k.

Vanhulle S., E. Enaud, M. Trovaslet, L. Billottet, L. Kneipe, J.L. Habib Jiwan, A.M. Corbisier and J. Marchand-Brynaert, 2008, Chemosphere 70(6), 1097.

CHEMICAL ENGINEERING TRANSACTIONS, Volume 14, 2008
Edited by G. Marino, E. Bardone, A. Viglia
 ISBN 978-88-95608-02-0

Nicotinic acid bioproduction in UF-membrane reactor *via* nitrile hydratase-amidase catalyzed reactions

Maria Cantarella[a], Laura Cantarella[b], Alberto Gallifuoco[a], Anna Malandra[a], Agata Spera[a], Ludmila Martínková[c]
[a]Department of Chemistry, Chemical Engineering and Materials, University of L'Aquila, Monteluco di Roio, 67040, L'Aquila, Italy, E-mail: cantarel@ing.univaq.it
[b]Department of Industrial Engineering, University of Cassino, via di Biasio 43, 03043 Cassino (FR), Italy,
[c]Laboratory of Biotransformation, Institute of Microbiology, Academy of Sciences of the Czech Republic, CZ-142 20 Prague 4, Czech Republic.

In this study *Microbacterium imperiale* CBS 498-74 resting cells are used as catalyst for the bioconversion of 3-cyanopyridine into nicotinic acid. Nitrile bioconversion into the corresponding acid is performed by this strain *via* a two step cascade reaction catalysed by nitrile hydratase and amidase with an amide as intermediate. Both enzymes that operate under mild conditions suitable for the synthesis of labile organic molecules have been characterized independently for activity and stability in a UF-membrane bioreactor. The reactor was fed with buffered solutions of appropriate substrate, either 3-cyanopyridine or nicotinamide. The effluent containing unreacted substrate, products and buffer were collected and analysed for product determination. The operational conditions (temperature, residence time) that strongly influence continuous UF-membrane bioreactor performances (conversion yield and selectivity) are presented.

1. Introduction

Nowadays there is a widespread use of nicotinic acid (niacin, a form of soluble vitamin B3) in the treatment of schizophrenia, diabetes, auto-immune diseases and cholesterol-related diseases and in cosmetic skin care. However, both nicotinamide and nicotinic acid, that are building blocks for NADH and NADPH co-enzymes, have to be supplied to the human body through food. Niacin is also exploited in animal feed supplementation, for vitamin enrichment of cereal products, as meat additive, as a biostimulator for the formation of activated sludge and as deodorant for air and waste gases in pollution control.
Recently much industrial and academic interest has been focused on the search of a bioproduction route alternative to the chemical one. The chemical production of nicotinic acid from 3-cyanopyridine or picoline is an uneconomical process (low yield and high cost) that calls for harsh conditions such as strong base, high temperature, catalyst (Anderson and Bovine, 1985). Thus, the conversion of 3-cyanopyridine using nitrile hydrolyzing enzymes is attractive owing to the mild conditions and high conversion (Nagasawa et al., 1988) due to the absolute selectivity of the bioconversion. At industrial level Nitto, BASF and Lonza companies developed a biotechnological

process to convert 3-cyanopyridine into niacinamide making use of enzymes from *Rhodococcus rhodochrous* (Chuck, 2005).

In most cases the microbial degradation of nitrile proceeds through two different pathways as shown in Figure 1: nitrile hydratase (NHase) catalyzes the hydration of a nitrile to the corresponding amide which is further converted into the acid; this second reaction being catalyzed by amidase (AMase), while in the second pathway nitrilase catalyses the direct transformation of the nitrile into the corresponding acid (Kobayashi and Shimizu, 1994; Martínková and Křen, 2002; Martínková et al., 2008; Stolz et al., 1998; Sugai et al., 1997).

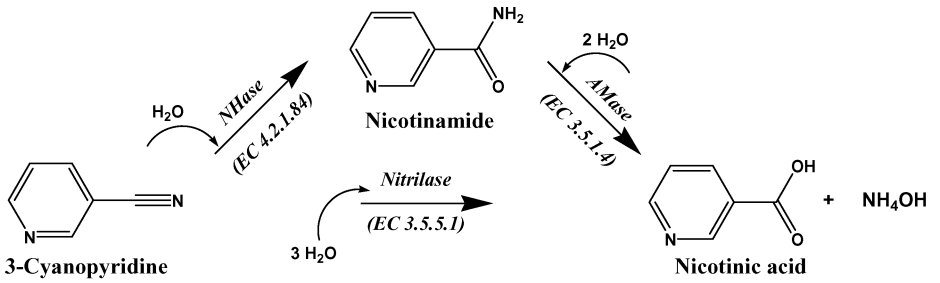

Figure 1: Alternative enzymatic pathways in microbial degradation of nitrile

This study makes use of resting cells of *Microbacterium imperiale* CBS 498-74 as catalyst for the bioconversion of 3-cyanopyridine into nicotinic acid. The strain follows the two step cascade reactions catalysed by NHase and AMase in nitrile bioconversion into the corresponding acid *via* an amide as intermediate. Both enzymes operate under mild conditions suitable for the synthesis of organic molecules (Cantarella et al., 1998; Cantarella et al., 2006). Though, the activity loss due to operational conditions strongly affects conversion yield and selectivity of the investigated process, NHase activity being rather labile (Alfani et al., 2001; Cantarella et al., 2004).

The scale up of 3-cyanopyridine bioconversion calls for the characterization of each enzyme of the cascade system. To this end, NHase and AMase have been characterized independently for activity and stability using a UF-membrane bioreactor, a useful reactor configuration (Cantarella et al., 2006, 2008a, 2008b) fed with buffered solutions of appropriate substrate, 3-cyanopyridine or nicotinamide. The effects of different operational conditions (temperature, residence time) on continuous UF-membrane bioreactor performances are discussed and a process layout with reactors in series is examined.

2. Materials and Methods

2.1 Materials

3-Cyanopyridine, nicotinamide and nicotinic acid were of analytical grade and purchased from Aldrich USA.

2.2 Methods

2.2.1Culture conditions and preparation of resting cells

The cultivation conditions for *Microbacterium imperiale CBS 498-74* for the production of nitrile hydratase were optimized previously (Cantarella et al., 2002). The subculture

was carried out in 100 mL of sterile YMP medium, prepared in 50 mM Na_2HPO_4/NaH_2PO_4 buffer, pH 7.0, consisting of (in g/L) yeast extract 3.0, malt extract 3.0, bacteriological peptone 5.0. After 24 h, 10 ml of subculture were used to inoculate 90 mL of YMPG medium (YMP added with 5g/L glucose). Both cultures were carried out at 28°C for 24 h in an orbital shaker (220 rpm). The cells obtained were washed three times with buffer, pH 7.0, centrifuged at 11,400 rpm, and then suspended in buffer. This cell suspension was kept at -18 °C till its use in the resting-cell reaction.

2.2.2 Activity assays

NHase activity (EC 4.2.1.84) was assayed for the production of nicotinamide using 50 mM 3-cyanopyridine, as substrate. AMase activity (EC 3.5.1.4) was assayed with nicotinamide (50 mM) as substrate. Each reaction was carried out, for 20 min. under stirring conditions (250 rpm) in a standard reaction mixture (2 ml) containing 50 mM Na-phosphate buffer (pH 7.0) and 1 and 2 mg_{DCW} of cell suspension. The reaction was stopped by adding 1mL of 0.5 M HCI, and centrifugating at 10,000 rpm for 10 min. One unit of NHase or of AMase activity was defined as the amount of enzyme (cells) required to release 1 μmol min^{-1} of relative product.

2.2.3 Analytical high-pressure liquid chromatography (HPLC)

The amounts of residual substrate and products in the reaction mixture were assayed by HPLC performed with a Perkin-Elmer Series 2 HPLC system (USA) equipped with a Merck (Germany) LiChro-CART 250-4 LiChrospher 100 reverse-phase-C18 column (5 μm) and a Merck (Germany) LiChro-CART 4-4 guard column. The mobile phase was: acetonitrile (12% v/v) -10 mM Na_2HPO_4-NaH_2PO_4 buffer (pH 7.0 at a flow rate of 1.0 ml/min at 30°C. The samples adequately diluted with mobile phase were placed in an LC Auto-sampler LS 3200 SGE (Australia). The absorbance of products and substrates was measured at 230 nm with a UV detector from Perkin-Elmer LC 290 (USA), associate to JASCO Borwin Chromatography software for area integration.

2.2.4 Bioconversion in continuous UF-membrane bioreactor

Amicon stirred cell (Mod 8050, Grace, USA) equipped with a fluoro-polymer membrane (DDS, Denmark) (NMWCO, 20 kDa) were used in continuous runs as fully described elsewhere (Cantarella et al., 2008).

3. Results and Discussion

3.1 Effect of temperature on NHase-AMase activities

The effect of temperature was tested on the NHase/AMase system in a UF-membrane reactor. The NHase activity was characterized feeding the reactor with 3-cyanopyridine, 10 mM as substrate; the operational conditions are those detailed in caption of Figure 2 that displays the results.

As part of the nicotinamide produced by the NHase activity is rapidly transformed by the AMase activity, as shown in the reaction scheme illustrated in Figure 1, the nicotinamide concentration, produced by NHase activity, is therefore calculated as the sum of the nicotinamide plus the nicotinic acid concentration evaluated in the sample. At 10°C the activity and stability of NHase are acceptable but the AMase activity at that temperature is almost negligible, the amount of nicotinic acid produced being rather low. Different attempts have been carried out to drive the reaction to completeness. At 30°C, all the nicotinamide produced by NHase is transformed by the successive step, catalyzed by AMase, but NHase activity drops rapidly, arresting the reaction. Higher amount of resting cells in the reactor, apparently mitigates the inactivation process, and

assures higher process time. Such limitations could be to some extent overcome with a series arranged bioreactors. To this end the dependence of AMase activity on temperature was investigated in a previous paper (Cantarella et al., 2006) where UF-membrane reactors were fed with nicotinamide as substrate. AMase displayed its activity in a larger temperature range and resulted quite stable up to 50 °C, its thermal inactivation constant, k_d, being equal to 0.0034 h^{-1} as a first-order deactivation process holds (Cantarella et al., 2008).

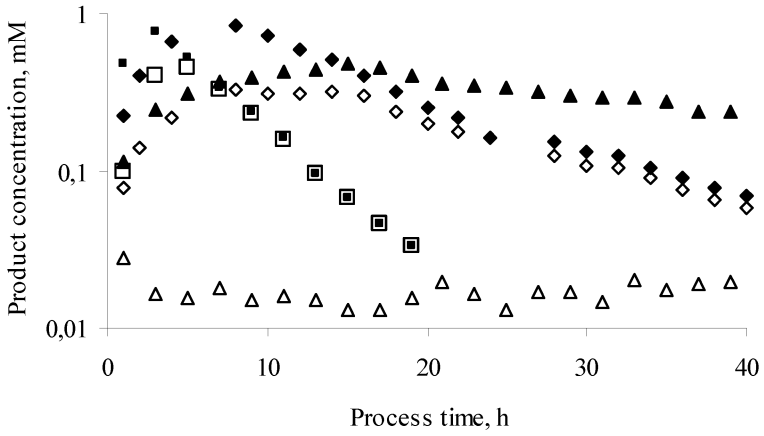

Figure 2: UF-membrane reactor operated at different temperatures, at constant flow-rate, 12,5 ml/h, loaded with 2.5 mg_{DCW} of resting cells and continuously fed with 10 mM 3-cyanopyridine buffered solution. 10°C - △, ▲; 20°C -◇ ◆; 30°C □,■. Full symbols nicotinamide produced by NHase activity; empty symbols nicotinic acid.

Several trials to reach higher yield and total conversion of substrate were made and parameters such as substrate and biocatalyst concentration, and residence time were investigated. The most satisfactory result, 80-88% conversion, was attained operating the reactor at 50°C with a mean residence time of roughly 47 h (flow-rate 1.5 ml/h) and a nicotinamide concentration of 100 mM the AMase catalyzed reaction being affected by substrate inhibition at higher concentration.

3.2 Effect of two reactors operating in series

Preliminary results of two reactors working in series are illustrated in Figure 3. The first reactor, containing 20 mg_{DCW} of resting cells, was kept at 50°C and fed at constant flow-rate of 6.5 ml/h with 100 mM nicotinamide bufferd solution. The effluent was collected in a fraction collector and, once analyzed for product determination, all the fractions were pooled together and continuously fed to the second reactor, containing the same cell concentration as the first one. Nicotinic acid concentration in the effluent of the first run was about 40 mM, while after the residence in the second reactor the concentration was roughly 68-70 mM. The reaction conversion in the first and in the second reactor being 40% and 47-50%, respectively, the overall conversion reached about 70%. These first indications appear rather encouraging and a more in-depth investigation is in

progress aiming to define the optimal temperature and flow rate conditions for each reactor.

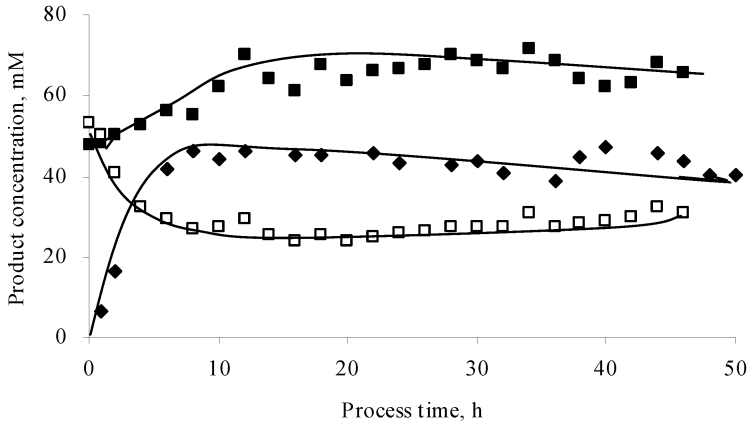

Figure 3: Two reactors operating in series at 50°C the first one was fed (flow-rate 6.5 mL/h) with buffered solution with 100 mM Nicotinamide. Once analyzed, the fractions were pooled together to feed (flow-rate 5.5 mL/h) the second reactor. ◆- nicotinic acid in the effluent of the first reactor, ■ - nicotinic acid and □ - nicotinamide in the effluent of the second reactor .

4. Conclusions

Microbacterium imperiale CBS 498-74 resting cells were used as catalyst for 3-cyanopyridine biotransformation in a continuous dead-end UF-membrane bioreactor. A two-step cascade reaction occurs: nicotinamide, produced as intermediate in the NHase catalyzed reaction, is further transformed by AMase activity. The investigation in a continuous UF-bioreactor enlighted the difficulties to drive reaction to completness also because of the thermal stability of the enzymes. Preliminary results in a series arranged UF-membrane reactors, indicate the possibility to increase reaction conversion.

Acknowledgments

The authors would like to acknowledge the support of University of L'Aquila Research Fund, ESF COST Action CM0701 "Cascade Chemoenzymatic Processes - New synergies between Chemistry and Biochemistry" and the institutional research concept AV0Z50200510 (Institute of Microbiology).

References

Alfani F., M. Cantarella, A. Spera and P. Viparelli, 2001, Operational stability of *Brevibacterium imperialis* CBS 489-74 nitrile hydratase. J. Mol. Catal. B- Enzym. 11, 687.

Anderson, A., and J. 0. Bovine, 1985, Amorphous vanadium oxide catalyst surface selective in the ammoxidation of 3-picoline. Naturwissenschaften 72, 209.

Asano Y., Y.Tani and H.Yamada, 1980, A new enzyme "Nitrile hydratase" which degrades acetonitrile in combination with amidase. Agric. Biol. Chem., 44, 2251.

Cantarella M., L. Cantarella, A. Gallifuoco, R. Frezzini, A. Spera and F. Alfani, 2004, A study in UF-membrane reactor on activity and stability of nitrile hydratase from *Microbacterium imperiale* CBS 498-74 resting cells for propioamide production. J. Mol. Catal. B-Enzym. 29/1-6, 105.

Cantarella M., L. Cantarella, A. Gallifuoco, R. Intellini, O. Kaplan, A. Spera and L. Martínková, 2008a, Amidase-catalyzed production of nicotinic acid in batch and continuous stirred membrane reactors. Enzyme Microb. Technol. 42, 222.

Cantarella M., L. Cantarella, A. Gallifuoco and A. Spera, 2006, Use of a UF-membrane reactor for controlling selectively the nitrile hydratase - amidase system in *Microbacterium imperiale* CBS 498-74 resting cells. Case study: benzonitrile conversion. Enzyme Microb. Technol. 38, 126.

Cantarella M., L.Cantarella, A. Spera and F. Alfani, 1998, Acrylamide production in an ultrafiltration-membrane bioreactor using cells of *Brevibacterium imperialis* CBS 489-74. J. Membr. Sci. 147, 279.

Cantarella M., A. Gallifuoco, A. Spera, L. Cantarella, O. Kaplan and L. Martínková, 2008b UF- Membrane bioreactors for kinetics characterization of nitrile hydratase-amidase catalyzed reactions: a short survey. Chap 12 in "Modern biocatalysis" Eds. T. Anthonsen W.-D. Fessner, Wiley-VCH in press

Cantarella M., A. Spera, P. Leonetti and F. Alfani, 2002, Influence of initial glucose concentration on nitrile hydratase production in Brevibacterium imperialis CBS 498-74. J. Mol. Catal. B- Enzym. 19-20C, 405.

Chuck R., 2005, Technology development in nicotinate production. App. Catal. A: Gen. 280, 75.

Kobayashi, M. and S. Shimizu, 1994, Versatile nitrilases: Nitrile hydrolysing enzymes. FEMS Microbiol. Lett. 120, 217.

Nagasawa T., C.D. Mathew, J. Mauge and H. Yamada, 1988, Nitrile hydratase catalyzed production of nicotinamide from 3-cyanopyridine in Rhodococcus rhodochrous J1. Appl. Environ. Microbiol. 54, 1766.

Martínková, L. and V. Křen, 2002, Nitrile- and amide-converting microbial enzymes: stereo, regio- and chemoselectivity. Biocat. Biotrans. 20, 73.

Martínková L., V. Vejivoda, O. Kaplan, V. Křen, K. Bezouška, M.Cantarella, 2008, Nitrilases from filamentous fungi. Chap 9 in "Modern biocatalysis" Eds. T. Anthonsen W.-D. Fessner, Wiley-VCH in press

Stolz A., S. Trott, M. Binder, R. Bauer, B. Hirrlinger, N. Layh and H. J. Knackmuss, 1998, Enantioselective nitrile hydratases and amidases from different bacterial isolates. J. Mol. Catal. B 5, 137.

Sugai T., T. Yamazaki, M.Yokoyama and H. Ohta, 1997, Biocatalysis in organic-synthesis the use of nitrile-hydrolyzing and amide-hydrolyzing microorganisms. Biosci. Biotechnol. Biochem. 61,1419.

CHEMICAL ENGINEERING TRANSACTIONS, Volume 14, 2008
Edited by G. Marino, E. Bardone, A. Viglia
 ISBN 978-88-95608-02-0

Immobilization-Stabilization of *Candida antarctica* Lipase B in Agarose-Glyoxyl and Agarose-Octyl: Deactivation Kinetics

C. Belver[a], J.J. Tamayo[a], L. Molinero[a], M. Ladero[a], B.C.C. Pessela[b], J.M. Guisán[c], F. Garcia-Ochoa[a].

[a]Dpt. Ingeniería Química, Facultad C.C. Químicas. Universidad Complutense de Madrid. Ciudad Universitaria 28040 Madrid. Spain.

[b]Dpt. Microbiología, Instituto de Fermentaciones Industriales, CSIC. C/ Juan de la Cierva, 3. 28006 Madrid. Spain.

[c]Dpt. Biocatálisis. Instituto de Catálisis y Petroleoquímica, CSIC. C/ Marie Curie, 2. Cantoblanco, 28049 Madrid (Spain).

Lipases are a well-known working-horse in the synthesis of several substances, mainly esters and amides. Their importance is increasing with time, with a high number of publications every year, in organic, analytical, and industrial chemistry, as well as in biochemistry and other health related sciences. CALB is the most used lipase in organic and industrial chemistry nowadays. On the other hand, glycerol is a good stabilizer for enzymes as well as a plentiful raw material whose market price is low due to the energy policy regarding biodiesel. This work is focused on the immobilization-stabilization of CAL-B for its use with glycerol, using both a mild and reversible immobilization, based on octyl-agarose, and an irreversible strong stabilizing immobilization on glyoxyl-agarose. The enzyme has been immobilized with and without a previous chemical modification based on the increase of amino groups on its surface. A kinetic study of the deactivation of the biocatalysts is presented to compare their performance in glycerol and other media, based on their activity and stability, being the octyl-agarose derivate the most promising for its use in glycerol.

1. Introduction

CALB is a well-known lipase used as a work horse in many biocatalytic applications, due to its flexibility in accepting many subtrates and to its relatively high activity, when compared to other lipases. An adequate immobilization technique is, in this situation, most convenient for getting a very stable and, sometimes, reversible biocatalyst (Mateo et al., 2007; Arroyo et al., 1999). On the other hand, glycerol seems a promising feedstock due to the biodiesel impact in the energy market.

In this work, the immobilization of CAL-B to agarose via glyoxyl (Mateo et al., 2006) and C8 groups (Fernández-Lorente et al., 2007; Torres et al., 2006), as well as the obtained thermal stability in several media, are studied. The enzyme was subjected, also, to chemical modification to increase the number of amino groups in its surface, so that more bonds can be formed and the stability increase because of the more rigid

protein-support structure created. After testing the retained activity, the thermal and chemical stability of the immobilized enzyme preparations, as well as that of the free enzyme were studied and the remaining activity data was used to select among several kinetic models by fitting them to the available experimental data using the integral kinetic methodology (Ladero el al., 2006; 2005).

2. Materials and Methods

2.1 Materials

The enzyme employed, lipase CALB-L, was kindly supplied by Novozymes (Bagsvaerd, Denmark). It is an enzymatic semi-purified solution in glycerol. Agarose was a kind gift from Hispanagar (Burgos, Spain), while octyl-agarose was purchased from Pharmacia Biotech (Uppsala, Sweden). P-nitrophenyl butirate, ethylcarbodiimide (ECI), ethylendiamine (EDA), sodium borohydride and Triton X-100 were purchased from Sigma Chem. Co. (St. Louis, USA). All other reagents and solvents were of analytical grade and provided also by Sigma Chem. Co.

2.2 Immobilization Methods

Amidation of the protein was performed after adsorption to octyl-agarose: the so immobilized protein is mixed with EDA and ECI in a relation 1 g: 10mL: 10mM. Afterwards, the enzyme is desorbed with with a 0.2% water solution of Triton X-100 and immobilized in glyoxyl-agarose at pH 9 and 10.5. Immobilization of the CALB on octyl-agarose was performed according to Torres (Torres et al., 2006). Immobilization of the enzyme on glyoxyl-agarose was carried out according as previously reported (Mateo et al., 2006). In all steps were enzyme is contacted with a support, 8 mg of enzyme were used per gram of support, being the protein always totally immobilized. Protein concentration was determined by the Bradford´s method (Torres et al., 2006). Activity was tested with p-NPB, as described in paragraph 2.4.

2.3 Deactivation assays

2 UI of enzyme (free or immobilized) were contacted with buffer phosphate 25 mM pH 7.0, dioxane, or glycerol, and incubated at 70 and 80°C when thermal deactivation were studied (buffer, glycerol) and at 25°C when the dioxane effect was studied. Several samples were withdrawn during the deactivation and activity tested as mentioned later.

2.4 Activity test

The enzyme activity test was performed by measuring the increase in the absorbance at 348 nm produced by the release of p-nitrophenol in the enzymatic hydrolysis of 0.4 mM p-NPB in 25 mM phosphate buffer at pH 7 and 25°C. One international unit (U) was defined as the amount of enzyme that is necessary to hydrolyze 1 μmol p-NPB/min under the assay conditions describe above.

2.5 Mathematical methods

Integral method was applied in order to determine the kinetic model adequate in each deactivation run, and to optimize the kinetic parameters. Data were treated using the Aspen Custom Modeler, in the Aspen Program Package 11.1.

Table 1. Kinetic models fitted to deactivation data in phosphate buffer 25 mM pH 7.0 and in glycerine

Mechanism	Kinetic model	
1) Inactivation following elemental reactions from a unique enzyme at zero time		
$E \xrightarrow{k_1} D$	$a = e^{-k_1 t}$	Model 1
$E \xrightarrow{k_1} E^*$	$a = (1-\beta^*)e^{-k_1 t} + \beta^*$	Model 2
2) Inactivation following consecutive reactions from a unique enzyme at zero time		
$E \xrightarrow{k_1} E^* \xrightarrow{k_2} D$	$a = e^{-k_1 t} + \beta^* \frac{k_1}{k_2 - k_1}\left(e^{-k_{21} t} - e^{-k_1 t}\right)$	Model 3
$E \xrightarrow{k_1} E_1^* \xrightarrow{k_2} E_2^*$	$a = \left(1 + \beta^*_1 \frac{k_1}{k_2 - k_1} - \beta^*_2 \frac{k_2}{k_2 - k_1}\right)e^{-k_1 t} - \frac{k_1}{k_2 - k_1}\left(\beta^*_1 - \beta^*_2\right)e^{-k_2 t} + \beta^*_2$	Model 4

3. Experimental results and discussion

Table 2 shows the results obtained with the different immobilization strategies, both with regard to the real final activity of the enzymatic biocatalyst refer to the free enzyme, and the stability of the biocatalysts in buffer phosphate, an aqueous solution where its stability is usually tested. It can be seen that the covalent bonding (glyoxyl-agarose) affects much more the retained activity compared to the free enzyme, as chemical bonding is much more prone to inactivate the enzyme during the immobilization process. Much milder conditions, as those used with the octyl-agarose supports, lead to an immobilized enzyme retaining much of the activity of the free enzyme (Torres et al., 2006). Consequently, the latter immobilization affects with lower intensity the structure of the enzyme, as expected with a reversible immobilization technique (Mateo et al., 2007). The lower interaction of enzyme and octyl groups leads, in this situation, to a lower stabilization when biocatalysts are subjected to high temperature in this buffer. However, dioxane does not affect neither the free enzyme nor any of the immobilized biocatalysts, so, seemingly, deactivation of the enzyme involves always polar species that solvate the outer region of the enzyme. Glyoxyl immobilization involves always a lower deactivation rate, and, in the case of not modifying the surface of the enzyme with amino groups, some activity seems to be retained even at high deactivation times. With the phosphate buffer media, deactivation always proceeds rapidly following a first-order reaction, usually towards a totally deactivated protein. In Figure 1, the fit of the selected kinetic models to experimental data is shown, being it reasonable in every case.

Table 2. Retained activity after immobilization and kinetic modelling of the thermal deactivation of free and immobilized CAL-B in buffer phosphate 25 mM pH 7.0 at 80°C

Enzymatic biocatalyst	Retained activity (%)	Model	Kinetic and statistical parameters			
			k_d	β	SQR	F
Free CAL-B	100	1	4.30± 0.87	-	0.046	399
Agarose-C8-CAL-B	58	1	5.68± 0.39	-	0.105	77
Agarose-C8-aminated CAL-B	52	1	7.50± 0.96	-	0.105	78
Agarose-glyoxyl-CAL-B	39	2	1.21± 0.29	0.30± 0.05	0.530	75
Agarose-glyoxyl-CAL-B aminated (pH 9.0)	9	1	0.98± 0.08	-	0.067	67
Agarose-glyoxyl-CAL-B aminated (pH 10.5)	16	1	0.56± 0.08	-	0.078	56

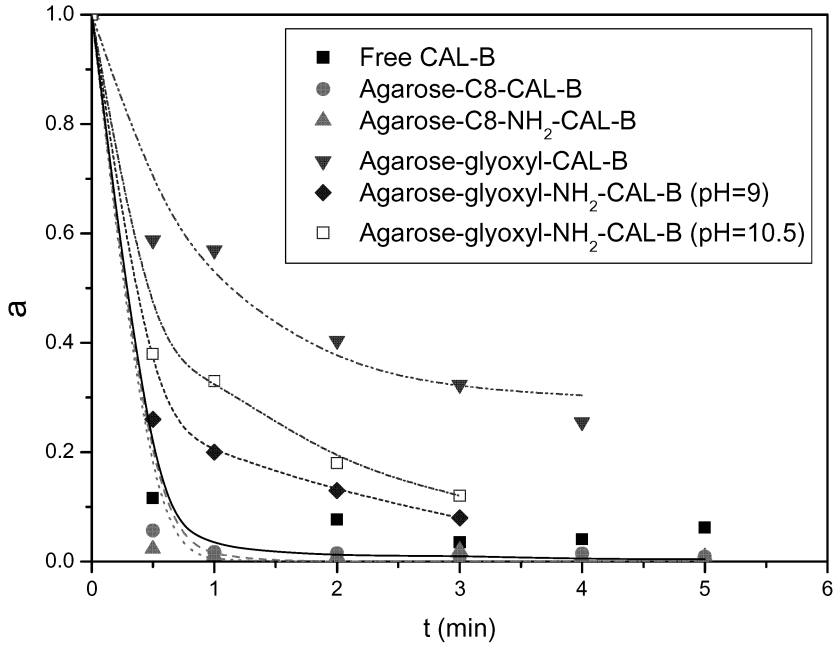

Figure 1.- Thermal deactivation at 80°C of several biocatalysts based on CAL-B on agarose in buffer phosphate 25 mM pH 7.0. The fitting of the models is shown by the lines.

When the biocatalysts are subjected to deactivation in glycerol, a promising alcohol that can act both as a substrate and a solvent (i.e. solvent-less esterifications to render monoglycerides and structured triglycerides), the stabilizing effect of this polyol is observed both in the more complex reaction scheme and in the lower values of the kinetic constants (at 80°C). The two reactions involved are first-order and are consecutive reactions. At any temperature tested, the initial lipase evolves towards a more active intermediate species. This enzymatic intermediate can be deactivated totally (at 70°) or partially (at 80°), yielding, in this latter case, an enzyme that sometimes has still a high activity, as when octyl-agarose is used with the native enzyme.

Deactivation in glycerol is always slower than in phosphate buffer and, what is more, the biocatalyst that was more stable in glycerol was that with the octyl moieties linked to the agarose chains. This can be due to the fact that glycerol can, as other higher carbohydrates, interact with both the support and the enzyme, yielding a more stable biocatalyst. Thus, though the initial linkage leading to immobilization is of an hydrophobic nature, hydrophilic interactions during deactivation or reaction can be of importance for the stability of the immobilized enzyme. Glyoxyl bonding, being much stronger, does not mean a higher interaction, in this case. Thus, it seems that stability depends much on the solvent used, polar or apolar, capable of interactions (hydrogen links or others) or not.

Surprisingly, deactivation at lower temperature, though at lower rate, proceeds towards a totally inactive protein. As enzyme deactivation involves a complex mechanism, with dissociation, coagulation, disruption of internal interactions and other phenomena involved, different temperature values can mean a different final species (Ladero 2006, 2005).

Table 3. Kinetic modelling of the thermal deactivation of free and immobilized CAL-B in glycerol at 70°C.

Enzyme biocatalyst	**Model**	**Kinetic and statistical parameters**				
		k_{d1}	k_{d2}	β	**SQR**	**F**
Free CAL-B	3	0.36± 0.08	0.020± 0.002	2.01± 0.11	0.045	738
Agarose-C8-CAL-B	3	0.01± 0.001	0.002± 0.0004	1.10± 0.15	0.034	922
Agarose-C8-aminated CAL-B	3	0.04± 0.003	0.011± 0.003	1.65± 0.15	0.112	543
Agarose-glyoxyl-CAL-B	3	0.01± 0.002	0.002± 0.0003	1.43± 0.15	0.043	846
Agarose-glyoxyl-CAL-B aminated (pH 9.0)	3	0.24± 0.014	0.015± 0.004	0.42± 0.08	0.145	436
Agarose-glyoxyl-CAL-B aminated (pH 10.5)	3	0.01± 0.002	0.002± 0.0007	1.62± 0.12	0.095	518

Table 4. Kinetic modelling of the thermal deactivation of free and immobilized CAL-B in glycerol at 80°C

Enzyme biocatalyst	Model	Kinetic and statistical parameters					
		k_{d1}	k_{d2}	β_1	β_2	SQR	F
Free CAL-B	4	0.89± 0.24	0.89± 0.09	5.95± 0.24	0.15± 0.059	0.097	352
Agarose-C8-CAL-B	4	0.78± 0.24	0.012± 0.003	1.76± 0.38	0.43± 0.059	0.048	428
Agarose-C8-aminated CAL-B	4	0.06± 0.004	0.011± 0.003	1.15± 0.13	0.79± 0.032	0.086	396
Agarose-glyoxyl-CAL-B	4	0.83± 0.34	0.22± 0.022	1.49± 0.04	0.45± 0.019	0.032	1637
Agarose-glyoxyl-CAL-B aminated (pH 9.0)	4	0.72± 0.21	0.042± 0.009	0.35± 0.13	0.05± 0.003	0.048	1134
Agarose-glyoxyl-CAL-B aminated (pH 10.5)	4	0.73± 0.36	0.014± 0.005	0.61± 0.11	0.30± 0.024	0.039	1395

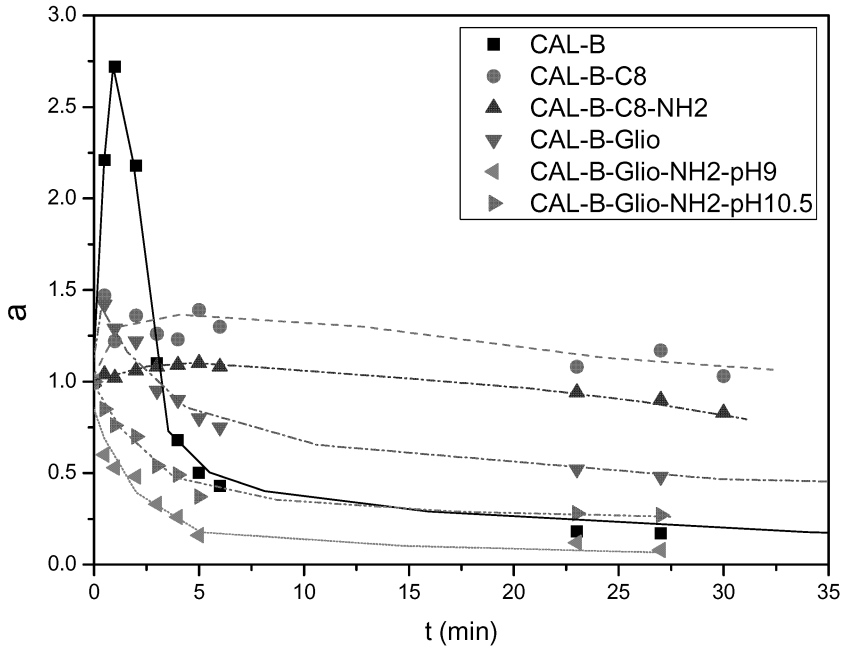

Figure 2.- Thermal deactivation at 80°C of several biocatalysts based on CAL-B on agarose in glycerol. Lines show the fitting of the selected kinetic models.

4. Conclusions

The obtained results show that the enzyme is stabilized both by the immobilizing strategy and the deactivation media, being dioxane the less harming for the enzyme. In phosphate buffer 25 mM pH 7.0, the enzyme was always scarcely stable when subjected to a high temperature, while much higher stability is observed in glycerol. In fact, the octyl derivative is much more stable in glycerol than in buffer phosphate, showing that the interaction of this substance with both the support and the enzyme is important for the stability of CAL-B. Moreover, even the stronger interaction due to chemical bonding in glyoxyl-agarose is not as strong as the myriad of little interactions in the octyl derivative when glycerol is the deactivation medium. The modification of the enzyme via amidation decreases both its activity and stability compared to the non-modified CAL-B. Thus, native CAL-B immobilized on octyl-agarose seems a promising biocatalyst to use with glycerol when this polyol is both the solvent and one of the substrates.

5. Nomenclature

a= remaining activity
D=inactive enzyme
E=active enzyme
F= Fischer's F
k_d, k_{d1}, k_{d2} = kinetic constants for deactivation
SQR = Sum of squares of the residuals
t=time (min or h)
β, β_1, β_2 = activities relative to that of the original enzyme

6. References

Arroyo, M., Sanchez-Montero, J.M., and Sinisterra, J.V. Thermal stabilization of immobilized lipase B from *Candida antarctica* on different supports: effect of water activity on enzymatic activity in organic media. Enz. Microb. Technol. 24 (1999) 3-12.

Fernandez-Lorente, G., Palomo, J.M., Cabrera, Z., Guisan, J.M., and Fernandez-Lafuente, R. Specificity enhancement towards hydrophobic substrates by immobilization of lipases by interfacial activation on hydrophobic supports. Enz. Microb. Technol. 41 (2007) 565-569.

Ladero, M., Ruiz, G., Pessela, B.C.C., Vian, A., Santos, A., and Garcia-Ochoa, F. Thermal and pH inactivation of an immobilized thermostable β-galactosidase from *Thermus* sp. strain T2: Comparison to the free enzyme. Biochem. Eng. J. 31 (2006) 14-24.

Ladero, M., Santos, A., and Garcia-Ochoa, F. Kinetic modelling of the thermal inactivation of an industrial β-galactosidase from *Kluyveromyces fragilis*. Enz. Microb. Technol. 38 (2005) 1-9.

Mateo, C., Palomo, J.M., Fernandez-Lorente, G., Guisan, J.M.,and Fernandez-Lafuente, Roberto. Improvement of enzyme activity, stability, and selectivity via immobilization techniques. Enz. Microb. Technol. 40 (2007) 1451-1463.

Mateo, C., Palomo, J.M., Fuentes, M., Betancor, L., Grazu, V., Lopez-Gallego, F., Pessela, B.C.C., Hidalgo, A., and Fernandez-Lorente, G., Fernandez-Lafuente, R., Guisan, J.M. Glyoxyl agarose: a fully inert and hydrophilic support for immobilization and high stabilization of proteins. Enz. Microb. Technol. 39 (2006) 274-280.

Torres, R., Ortiz, C., Pessela, B.C.C., Palomo, J.M., Mateo, C., Guisan, J.M., and Fernandez –Lafuente, R. Improvement of the enantioselectivity of lipase (fraction B) from *Candida antarctica* via adsorption on polyethylenimine-agarose under different experimental conditions. Enz. Microb. Technol. 39 (2006) 167-171.

CHEMICAL ENGINEERING TRANSACTIONS, Volume 14, 2008
Edited by G. Marino, E. Bardone, A. Viglia
 ISBN 978-88-95608-02-0

Evaluation of orange peel and green soybean as a substrate for the production of α-galactosidase by a soil isolated *Aspergillus oryzae* in solid state fermentation

Álvarez D. and Sánchez O.*
Department of Chemical Engineering –Product and Process Design Group
Universidad de los Andes, Carrera 1E No. 19 A 40, Bogotá, Colombia
carol-al@uniandes.edu.co, *osanchez@uniandes.edu.co

Orange peel and green soybean were used as substrate in Solid State Fermentation by a native strain of *Aspergillus oryzae* to produce α-galactosidase. During four culture days was evaluated the pH and incubation temperature effect on the enzyme production. Results displayed the green soybean like a better substrate than orange peel, but both can be used as potential substrates with considerable enzyme activity 6.48±1.24 U g^{-1} and 2.19±0.30 U g^{-1}, respectively. For both substrates the best culture condition obtained for the enzyme production was at 30ºC and pH 5.00. Use of green soybean and orange peel as a substrate could be of great commercial significance in agro-industrial countries like Colombia giving value to agriculture wastes. The process of α-galactosidase production using the isolated strain and the green soybean as substrate in laboratory scale may have the potential to scale-up.

1. Introduction

α-Galactosidase (α-D-galactopyranoside galactohydrolase EC 3.2.1.22) is widely distributed in the domain eukarya. α-galactosidase catalyzes the cleavage of terminal α-1,6 linked galactosyl residues from a wide range of organic and synthetic substrates like linear and branched oligosaccharides, polysaccharides and synthetic substrates as substituted phenyl α-D-galactosides. (Li *et al.*, 2006; Yip and Withers, 2004; Ademark *et al.*, 2001; Varbanets *et al.*, 2001; Dey and Pridham, 1972). Filamentous fungi like *Aspergillus oryzae* and *Aspergillus niger* are an attractive source for enzyme production because their hability to produce extracellular enzymes, especially those that hydrolyses a wide variety of complex polysaccharides (Kobayashi *et al.*, 2007).

α-Galactosidase has several industrial applications. In food industry can be used in the sugar beet preparation hydrolyzing rafinosse, this action avoid the inhibition of normal sucrose crystallization (Shankar and Mulimani, 2006; Li *et al.*, 2006; Ademark *et al.*, 2001; Arora, 1991). It is also used in the cleavage of galacto-oligosaccharides present in soybean milk and other food obtained from legumes, and is used to improve the gelling properties of galactomannans commonly used as food thickeners (Pandey *et al.*, 2005; Ademark *et al.*, 2001). In paper industry α-Galactosidase hydrolyze hemicelluloses main groups (galactomannanes and galactoglucomannanes) present in soft wood to obtain paper pulp (Golubev *et al.*, 2004; Shabalin *et al.*, 2002). In the pharmaceutical

industry is used to avoid the discomfort sensation of indigestibility caused by the presence of non digestible sugars like rafinosse and stachyose present in various leguminous and fruits (Donkor *et al.*, 2007; Li *et al.*, 2006). α-galactosidase is also used in the treatment of Fabry Disease, which is caused by a lysosomal enzyme deficiency of α-galactosidase, this results in the storage of globotriaosylceramide (Gb_3) in a variety of organs and cells. Also, it is used in medicine in blood group transformation (Bodary *et al.*, 2007; Khan *et al.*, 2006; Varbanets *et al.*, 2001; Maranville and Zhu, 2000).

Solid state fermentation (SSF) is a traditional way for the production of food and alcoholic beverages in oriental countries (miso and sake) (Pandey *et al.*, 2005). In SSF, microorganisms grow in a solid environment, this cause them to feel in their natural environment, and because of this can produce metabolites that can not produce in an artificial environment (Ramana *et al.*, 1993). SSF offer some advantages over the classic process. These include less waste of energy, less space per substrate unit, higher concentrations of products, simple fermentation equipment and no effluent problems. Also SSF has some disadvantages, for example the control in the system and the scale up process presents problems because of heat accumulation (Li *et al.*, 2006; Pandey *et al.*, 2005; Ramana *et al.*, 1993; Arora, 1991). SSF is a useful technique because it uses agro-industrial wastes without a pretreatment of the substrate, this make SSF a very feasible and economic operation (Yovita *et al.*, 2006). Filamentous fungi are most exploited in this technique of fermentation, due to their ability to grow on complete solid substrates, producing a wide range of extracellular enzymes (Li *et al.*, 2006; Bennett, 1992).

In the present work orange peel and green soybean were studied as a substrate for the production of *α*-galactosidase by a native strain of *Aspergillus oryzae*, and the pH and incubation temperature effect was evaluated for the enzyme production.

2. Materials and methods

2.1 Chemicals and reagents

All chemicals were analytical grade. Orange peel and green soybean were obtained in Cundinamarca and Meta (Colombia), respectively. Enzyme substrate *p*-nitrophenyl-α-D-galactopyranoside (PNPG) was purchased from Sigma chemicals (USA).

2.2 Culture medium and conditions

The native strain *Aspergillus oryzae* used in this work was isolated from soil. It was grown on malt extract agar (MEA) for 14 days at 30±1ºC. To prepare spore suspensions, spores were scrapped down from the MEA plates with a sterilized tensoactive solution (15% $^{w}/_{v}$, glycerol; 0.1% $^{w}/_{v}$, Tween 80 and acetate buffer 0.1 M (pH 6.0) q.s.f. 100 mL). Spores were counted in a Neubauern chamber. The final solution contained 1×10^6 spores ml^{-1}. The spore suspensions were kept at –20±1ºC and subcultured once a month.

2.3 Fermentation media

Ten grams of chopped dry substrate were taken into 250 mL shake flask, separately. Each flask was moistened with a mineral salt solution in a ratio of 2:1($^{w}/_{v}$) (containing in g L^{-1} K_2HPO_4 (6.3), KH_2PO_4 (1.8), $(NH_4)_2SO_4$ (1), $MgSO_4 \cdot 7H_2O$ (1), $CaCl_2 \cdot 2H_2O$ (0.1), $FeSO_4$ (0.1)). The sterilized medium was inoculated with 1.0 mL of spore suspension. To evaluate the pH and temperature effect, the inoculated mediums were incubated at 30±1ºC and 25±1ºC, for each temperature three pH values were studied (3.00, 5.00 and 8.00) for four days. pH media was adjusted using 0.1M HCl or 0.1M NaOH. Each assay was made by triplicate.

2.4 Enzyme extraction

Enzyme extraction was carried out by mixing 1 g of fermented mass with 10 mL sodium acetate buffer 0.2 M (pH 4.8) for 1 h in an orbital shaker at 150 rpm. Contents of the flask were filtered using a vacuum pump and a muslin cloth, the filtrate was centrifuged at 2100 g for 10 min. The supernatant obtained was used as a crude extract of α-galactosidase and used for enzyme assay (Shankar and Mulimani, 2007).

2.5 Assay of α-galactosidase

α-Galactosidase activity was assayed according to the method proposed by Dey and Pridham (1972). Reaction mixture contained: 0.1 mL of enzyme crude extract, 0.8 mL of 0.2 M acetate buffer (pH 4.8) and 0.1 mL of 0.2 mM PNPG. The mixture was incubated at 50±1ºC for 15 min. Reaction was stopped by adding 3 ml of 0.2 M Na_2CO_3 solution. Absorbance of the mixture was measured at 405 nm (Thermospectronic GENESYS 5) to determine the amount of *p*-nitrophenol (PNP) released in the reaction.

One unit of enzyme activity was defined as the amount of enzyme that produces 1μmole of PNP min^{-1} under assay conditions. α-Galactosidase production was expressed as U g^{-1} of dry fermented mass.

3. Results and discussion

Fermentations were carried out at different incubation temperatures 25 and 30±1ºC and different pHs (3.00, 5.00 and 8.00), using orange peel and green soybean in order to find the best conditions for α-galactosidase production.

3.1 α-galactosidase production by *A. oryzae* in orange peel

The obtained results for orange peel at the conditions mentioned above are shown in Figure 1. The results of the enzyme activity evaluation at 25±1ºC were: pH 3 (1.07±0.22 U g^{-1}), pH 5 (2.17±0.22 U g^{-1}) and at pH 8 (0.9±0.21 U g^{-1}), while in the evaluation at 30±1ºC they were: pH 3 (0.9±0.09 U g^{-1}), pH 5 (2.19±0.30 U g^{-1}) and at pH 8 (0.95±0.25 U g^{-1}).

The results show a higher activity of α-galactosidase activity (2.19±0.30 U g^{-1}) compared with the study made by Shankar and Mulimani (2007), they obtained an enzyme activity of 0.810±0.04 using the same substrate at 30±1ºC and pH 5.5, this value of pH was the optimum for α-galactosidase production by *A. oryzae* (Shankar and

Mulimani, 2007), this shows that we get an activity increase of aproximately 2.5 times the previosly reported.

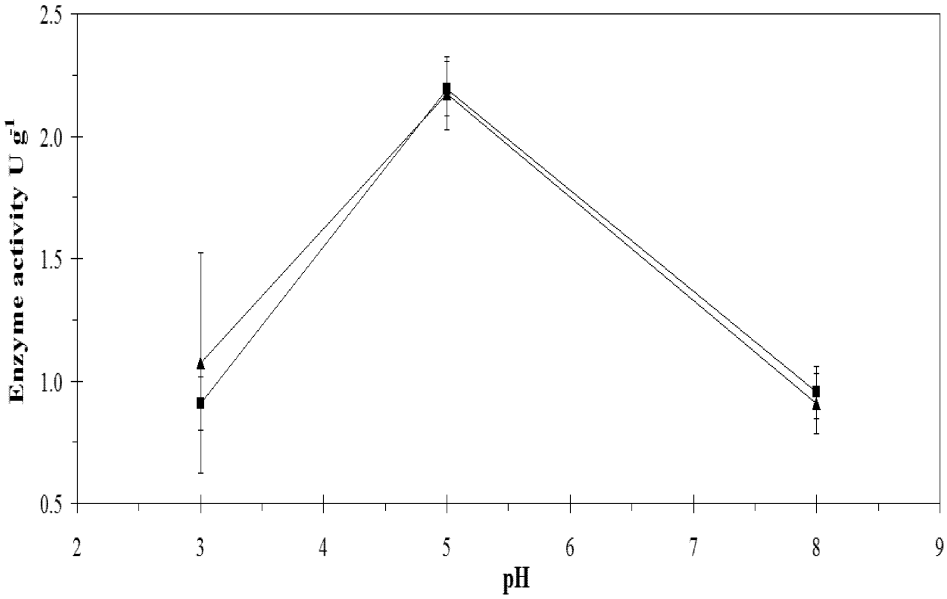

Figure 1. *pH and incubation temperature (25-▲- and* 30ºC-■*-) effect on the* α-*galactosidase activity in SSF using orange peel as substrate.*

The differences could be atributted to external conditions as the orange peels composition (carbohydrates, proteins, salts, acids and moist content) or process conditions as the particle size of the substrate and the fungal strain. Shankar and Mulimani(2007) report a particle size of 1200µm, while we did not make further transformations about this condition, however this is an important variable in SSF because it determines the mass and heat transfer regimes in the process as encountered by Annunziato *et al.* (1986), who evaluate different particle sizes as a process condition in the production of α-galactosidase by *A. oryzae.* The results obtained by Annuziato, showed a high enzyme activity when the particle size of solid substrate passed trought mesh 6 obtaining an enzyme activity of 9.32 U g^{-1}. Changing the particule size (mesh 8 and 20) resulted in a decrease of enzyme activity obtaininig 6.05 U g^{-1} and 5.54 U g^{-1} respectively. (Annunziato *et al.*, 1986)

3.2 α-galactosidase production by *A. oryzae* in green soybean

The obtained results for green soybean at the conditions mentioned above are shown in Figure 2. The results of the enzyme activity evaluation at 25±1ºC were: pH 3.00 (3.28±0,91 U g^{-1}), pH 5.00 (6.31±1.88 U g^{-1}) and at pH 8.00 (4.56±0,26 U g^{-1}), while in the evaluation at 30±1ºC they were: pH 3.00 (3.67±0,24 U g^{-1}), pH 5.00 (6.48±1.24 U g^{-1}) and at pH 8.00 (3.66±0,92 U g^{-1}).

Up to now no further studies have been published for the production of α-galactosidase in SSF using green soybean. However, there are many studies of the production of this enzyme using soy products as soybean (ground), soy flour, other studies use wheat bran enriched with soybean carbohydrate solution.

The results obtained by Annunziato *et al.* for the production of α-galactosidase in soy bean ground (8.63 U g^{-1}) and soybean flour (10.4 U g^{-1}) show higher enzyme activity, but there are significant differences between both process conditions. Cruz and Park (1892) obtained an enzyme activity of 2.58U g^{-1} using wheat bran as a substrate enriched with soybean carbohydrate solution, the soybean carbohydrate solution increases enzyme production 2,5 times the activity in wheat bran without soybean carbohydrate solution. Because of this, we can presume that the presence of soybean products in the fermentation cause a higher yield in enzyme production, making soy products specially green soybean a potential substrate in SSF for the production of α-galactosidase.

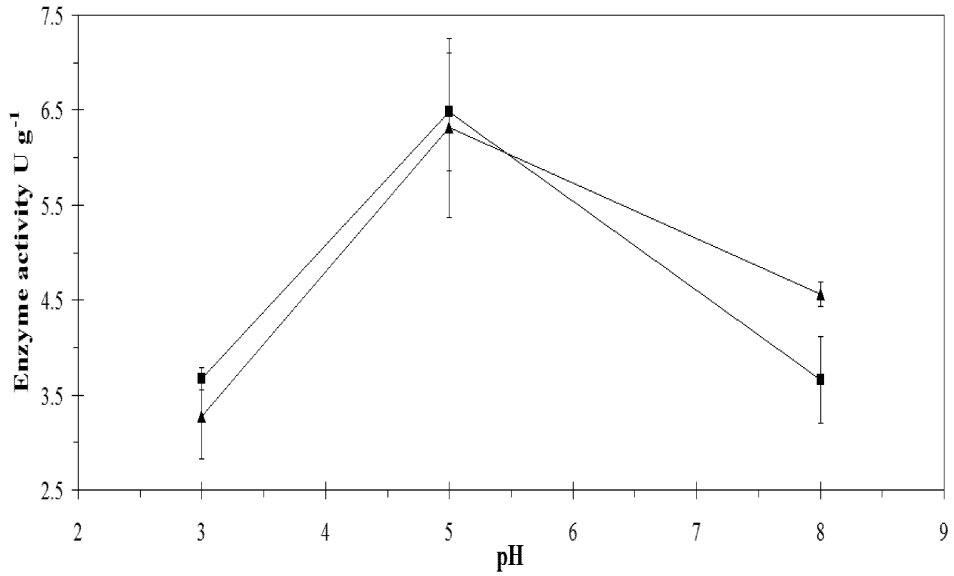

Figure 2. *pH and incubation temperature (25-▲- and* 30ºC-■*-) effect on the* α*-galactosidase activity in SSF using green soybean as substrate.*

3.3 Effect of pH and temperature in α-galactosidase production

The results obtained show that the best condition for α-galactosidase production is pH 5.00 and a culture temperature 30±1ºC when evaluated in both substrates. Likewise results reported Shankar and Mulimani (2007) who obtained an optimal pH 5.5 for the enzyme production. Changes in medium pH have important impact, at pH values of 3.00 and 8.00 enzyme activity decreases about a 50% in the evaluated substrates. This

result is valid just for SSF, for submerged cultivation, more acidic pH can be obtained as the optimal (Shankar and Mulimani, 2007).

The best culture temperature for α-galactosidase production was 30±1ºC, which is similar to reported by Shankar and Mulimrani (2007). Incubation tempeature is an important factor in SSF; due to the absence of water, heat is acumulated in the bed this affect the fungus metabolism, decreasing enzyme production (Raghavarao *et al.*, 2003). In the present study, for both substrates no significant difference (about 1%) was observed in the enzyme activity for the best pH (5.00) at 25±1ºC and 30±1ºC, because of this, fermentations could be carried at the lower temperature 25ºC, avoiding metabolic inactivation of the microorganism because of heat acumulation.

3.4 Effect of incubation time in α-galactosidase production

Figure 3 shows the fermentation profiles for the best conditions of α-galactosidase production in the evaluated substrates.

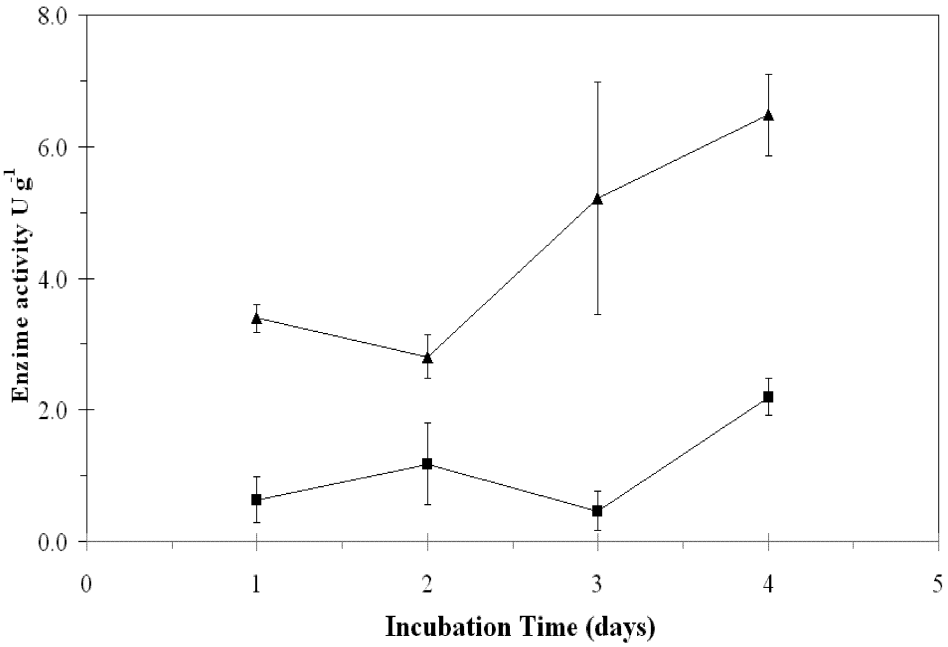

Figure 3. *Effect of incubation time in the α-galactosidase production by A. oryzae in SSF. (green soybean-▲- and orange peels-■-)*

For the fermentation in orange peels, activity didn't show considerable changes during the first 3 days, and in the fourth day activity increased about 100%, this suggest that in the first days of fermentation, the microorganism was on its lag phase, and in the last day it begins its exponential phase increasing the enzyme production, suggesting that growth of the mycelium is nedded for the production of extracellular proteins. (Ramachandran *et al.*, 2004)

For the fermentation in green soybean, the increase in enzyme activity began in the second day. This posibly is due to the composition of green soybean, which could be a better carbon source for α-galactosidase production than orange peels.

Profiles show a better enzyme activity in the last day of incubation, this suggest that fermentations could be carried out for more than 4 days obtaining a better enzyme activity, this is supported by Cruz and Park (1982) and Mulimani *et al.*(1986), who reported a fermentation time of 5 days. Further assays should be made to find the greater enzyme activity.

4. Conclusions

Orange peel and green soybean can be used as a potential substrate for α-galactosidase production under solid state fermentation by *A. oryzae,* with higher enzyme production in the fermentation using green soybean producing 6.48±1.22. The enzyme activity in orange peels is higher than the reported previously by Shankar and Mulimani (2007). The best pH and incubation temperature obtained were 5.00 and 30±1°C. The difference between evaluated temperatures at best pH is not significant, because of this, fermentations can take place at lower temperatures, which result in energy saving.

The use of green soybean as a substrate for the production of α-galactosidase under SSF could be of great commercial value, especially in agroindustrial countries like Colombia. The employed native strain is a potential source for α-galactosidase production; further assays should be made for the scale-up of the solid state fermentation process in order to increase the enzyme production.

5. References

Ademark, P., M. Larsson, F. Tjerneld, and H. Stalbrand, 2001, *Enzyme Microb. Technol.*, 44-448.

Annunziato, M., R. Mahoney, and R. Mudget, 1986, *J. Food Sci.*, 1370-1371.

Arora, D. K., 1991, Handbook of Applied Mycology (Vol. 4). New York.

Bennet, J. and M. Klich, 1992, *Aspergillus:* Biology and Industrial Applications. Boston.

Bodary, P. F., J.A. Shayman, and D.T. Eitzman, 2007, *Trends Cardiovasc. Med.,* 17:129-133.

Cruz, R., and Y.K. Park, 1982, *J. Food Sci.*, 1973-1975.

Dey, P. M., and J.B. Pridham, 1972. *Adv Enzymol. Relat. Subj. Biochem.*, 91-130.

Donkor, O. N., A. Henriksson, T. Vasiljevic and N.P. Shah, 2007, *Food Chem.*, 10-20.

Khan, M. I., D.V. Gokhale, K.B. Bastawde and J.M. Khire, 2006, *Process Biochem.*, 1311-1317.

Kobayashi, T., K. Abe, K. Asai, K. Gomi, P.R. Juvvadi and M. Tareuchi, 2007, *Biosci. Biotechnol. Biochem.*, 71(3):646-670.

Li, H., W.Q. Liang, Z.Y. Wang, N. Luo, X.Y. Wu, J.M. Ju, *et al.,* 2006, *World J. Microbiol. Biotechnol.*, 22:1-7.

Maranville, E. and A. Zhu, 2000, *Eur. J. Biochem.*, 1495-1501.

Raghavarao, K. S., V.T. Ranganathan and G.N. Karanth, 2003, *Biochem. Eng. J.*, 127-135.

Ramachandran, Sumitra., Patel, A. K., Francis, F., Nagy, V., Szakacs, G., Pandey, A., (2004). *Bioresource Technology* , 169-174.

Ramana, M., N. Murthy, K. Karanth and M. Raghava, 1993, *Adv. Appl. Microbiol.*, 99-145.

Shankar, S. and V. Mulimani, 2006, *Bioresour. Technol.*, 958-961.

Yip, V. L. and S.G. Withers, 2004, *Org. Biomol. Chem.*, 2707-2713.

CHEMICAL ENGINEERING TRANSACTIONS, Volume 14, 2008
Edited by G. Marino, E. Bardone, A. Viglia
 ISBN 978-88-95608-02-0

Evaluation of drying techniques measuring proteolytic activity of Papain obtained from unripe fruit and skin juice

Puig A., Gil I. and Sánchez O.*
Department of Chemical Engineering –Product and Process Design Group
Universidad de los Andes, Carrera 1E No. 19 A 40, Bogotá, Colombia
a-puig@uniandes.edu.co, igil@uniandes.edu.co, *osanchez@uniandes.edu.co

The papain is one of the most used enzymes in the industry. A comparative study between four drying process types: Tray drier, oven, vacuum oven and a lyophilizator at different temperatures was made with the aim of evaluating the impact of the treatment on the enzyme proteolytic activity of the crude papain. No significant statistical difference was found for the different drying process at the selected conditions. The activity measurements were realized by casein hydrolysis and molecular weight was determinated by SDS-PAGE electrophoresis finding an average weight of 22086 Da. The crude enzyme extract was purified by means of a salting out and an ionic exchange chromatography. The purification procedure enhanced up to 20-folds the specific enzyme activity (7.5×10^{-4} and 1.5×10^{-2} U mg^{-1} of protein for crude and purified enzyme, respectively). In Colombia there is not an industrial papain production; due to the large papaya crops that exist, the evaluation of these drying and purification procedures as potential alternatives for the purified and crude papain production is important for future industrial investment.

1. Introduction

The papaya is the fruit of the papaya tree (*Carica papaya*) native of Central America. The fruit ripens from 4 to 6 months depending on the climate where it is grown (Salunkhe and Kadam, 1995). The cultivation of this fruit has two main purposes: the sale of the fruit for human consumption and the extraction of enzymes that constitute 40% of the latex in 1 mM concentrations (Azarkan *et al.*, 2004). The papain is a natural proteolytic enzyme that is extracted from the latex in the leaf, the stem and the papaya's unripe fruits (Baeza *et al.*, 1989). Papain is used in a many industrial fields (like pharmaceutical, brewery, meat, dairy, textile, photographic, optical, tanning, cosmetic, detergents, food and leather industry), because a synthetic enzyme is not capable of simulating the properties of the natural enzyme, which increased its demand. The process to obtain raw papain consists of two main stages: latex extraction and drying. A third stage, purification, may be used if a purified papain is wanted. This work compares the crude enzymatic activity obtained from locally *Carica papaya* using the unripe fruit and the skin juice under different drying processes and evaluates the enzyme activity for the proposed purification procedure.

2. Materials And Methods

2.1 Materials

The papaya fruit, *C. papaya* grown locally (Cundinamarca, Colombia) was used as starting latex material. Polyacrylamide, bis-acrylamide, ammonium persulfate and casein were purchased from Sigma–Aldrich (USA). Molecular weight marker and Q-Shepadex™ were purchased to Bio-Rad (USA). Others reagents were analytical grade.

2.2 Latex extraction

The extracted latex was obtained by several longitudinal incisions with a rustless-steel blade on the unripe fruits using Nitsawang's protocol *et al.* (2006). This latex was allowed to run down the fruit and drip in plastic containers. Before being stored at -20ºC NaOH 0.3 M was added to avoid oxidation (Ortiz *et al.*, 1980). The other used latex was obtained from the unripe fruits skin, which were peeled and crushed in a food processor obtaining a humid paste. NaOH 0.3 M was added to this paste before being stored at -20ºC.

2.3 Drying process

To evaluate the different drying process, 10 g samples of each latex source were arranged in aluminum trays of 15cm^2. A tray drier with an air flow of 10 Km h^{-1}, a conventional oven (Memmert), a vacuum oven (Cole-Parmer 5053-20) and a lyophilizator (Freezone 6 plus Labconco) were used to dry the obtained latex and to establish the temperature effect on the crude enzyme activity. Table 1 presents the operational conditions for the different dryers. To each condition three different assays were made.

Table 1. Operational conditions for the different dryers used in the latex drying.

Number	Origen	Drier type	Temp (°C)	Pressure (mbar)	Time (h)
1	Latex	Oven	40	746.6	8
2	Skin	Oven	50	746.6	8
3	Latex	Oven	40	746.6	8
4	Skin	Oven	50	746.6	8
5	Latex	Tray Drier	40	746.6	2
6	Skin	Tray Drier	50	746.6	2
7	Latex	Tray Drier	40	746.6	2
8	Skin	Tray Drier	50	746.6	2
9	Latex	Vacuum Oven	40	137.06	18
10	Skin	Vacuum Oven	50	137.06	18
11	Latex	Vacuum Oven	40	137.06	18
12	Skin	Vacuum Oven	50	137.06	18
13	Latex	Lyophilizator	-30	0.1	24
14	Skin	Lyophilizator	-40	0.1	24
15	Latex	Lyophilizator	-30	0.1	24
16	Skin	Lyophilizator	-40	0.1	24

2.4 Enzymatic activity determination

Protease enzymatic activity was determinated by Sigma's SSCASE01.001 protocol (1999). This uses casein as protease substrate. Dried samples of 0.05 g were dissolved in 5 mL sodium acetate buffer 10 mM (pH 7.5) and 5 mL calcium acetate buffer 10 mM (pH 7.5). For each sample 455 µL Casein 65%($^{w}/_{v}$) were preheated in a thermal bath at 37±1ºC for 10 minutes and then 20 µL of these were added. After 10 min of reaction, the reactions were stropped by the addition of 455 µL trichloroacetic acid 110 mM. and were kept in the thermal bath for another 30 min. Each reaction has its negative control, which did not have enzyme during preincubation, but it was added after the trichloroacetic acid addition.

The two form phases were separated by centrifugation at 9000 rpm and 4ºC during 20 min (Fresco 17 Thermo) in order to discard the solid formed. The supernatant was taken for protease assays. Aliquots of 625 µL supernatant were added to 1570 µL sodium carbonate 500 mM and 250 µL of Folin – Ciocalteus reagent. The protease activity was detected spectrophotometrically since the released tyrosine developed a blue coloration. Each sample was read in a spectrophotometer (Thermospectronic Genesys 5) at 660nm and compared with a calibration curve. One protease unit was defined as the amount of casein hydrolyzed to produce color equivalent to 1.0 µmole (181 µg) of tyrosine per minute at pH 7.5 and 37°C (color by Folin and Ciocalteu's reagent) and was calculated by Eq. 1. (Sigma, 1999).

$$\frac{\text{Units}}{\text{mL Enzyme}} = \frac{(\text{mol Tyrosine})\,(V_T)}{(V_E)(t)(V_C)} \qquad (1)$$

where V_T is the total assay volume in mL, V_E is the volume of the enzyme used mL, t is the reaction time in min, and V_C is the volume used in the colorimetric reaction in mL.

The protein presented in each sample was determinated by Biuret´s method, where 5µL of sample was added to 5 µL of water and 20 µL of Biuret reagent stirring gently for 30 min. The absorbance was determinated (Nanodrop, spectrophotometer ND-1000) at 540nm and compared with a pattern curve constructed with albumin. Biuret´s test was only applied to latex sample and not to skin samples due to color interference. The specific activity was calculated as the ratio between the activity calculated by Eq. 1 and the mg of protein determinated per mL of enzyme extract.

2.5 Papain purification and molecular weight determination

Non-denaturing electrophoresis was carried out by the method of Reisfield *et al.*, 1962 for basic proteins, using 12% polyacrylamide gel, 34 mM ß-alanine buffer, pH 4.3, and a constant 4 mA current per tube. SDS-PAGE was carried out by the method of Laemmli (1970), using 12% acrylamide. The samples were prepared in Trisglicerol-b-mercaptoetanol and placed in boiling water during 60 s. Gels were stained with Coomassie-Blue R-250 and Brilliant Blue G colloidal concentrated by the method of Neuhoff (1988).

To determine the molecular weight of papain obtained by the method described in this paper. To 1 mL sample was added 65%($^{w}/_{v}$) ammonium sulphate solution until complete precipitation and centrifuged at 13000 rpm and 4ºC during 20 min. The precipitated obtained was reconstituted with sodium acetate 10mM (pH 5.0), after that was dialyzed in a sodium acetate buffer 10mM (pH 5.0) with a volumetric ratio (1:100), then the sample was lyophilized and reconstituted in 1 mL of sodium acetate buffer 10mM (pH 5.0) to be pass through a column (11x100 mm) of Q-Sephadex^{TM} fast flow previously equilibrated with a 0.1 M sodium acetate buffer (pH 5.0). The elution was made with NaCl solutions from 0.1 a 0.5 M, for the obtained fractions protease activity was evaluated. The fraction that presented activity was dialyzed in a sodium acetate buffer 10mM (pH 5.0) with a volumetric ratio (1:100) and its final activity was determinated.

3. Results And Analysis

Table 2 presents for the different drying conditions and latex source the activity obtained in units mg^{-1} of sample.

Table 1. Enzymatic activity for the different drying processes and latex source.

Activity (units mg^{-1} solid sample)							
		Latex			Skin x 10^2		
Drying	**Temp (°C)**	**Test 1**	**Test 2**	**Test 3**	**Test 1**	**Test 2**	**Test 3**
Oven	40	0.067	0.109	0.175	1.024	0.137	2.139
Oven	50	0.143	0.146	0.175	7.351	0.296	1.001
Tray Drier	40	0.143	0.144	0.197	0.228	0.501	0.273
Tray Drier	50	0.037	0.041	0.037	1.866	1.821	1.843
Vacuum Oven	40	0.158	0.102	0.173	1.547	0.273	0.660
Vacuum Oven	50	0.161	0.152	0.165	1.707	1.752	1.684
Lyophilizator	-30	0.104	0.143	0.154	1.866	1.297	1.365
Lyophilizator	-40	0.140	0.144	0.172	0.614	0.660	1.070

For the different drying process is observed that the enzymatic activity obtained for latex is major than for the skin, however by a statistical analysis. A factorial experiment design was selected for the analysis of drying temperature effect and latex source over the protease activity after latex drying in the oven, tray drier and vacuum oven, while lyophilization was analyzed separately because the temperature differences (Montgomery, 2005).

The ANOVA factorial design analyses were made by the used MINI-TAB® v.15. The ANOVA showed that the temperature factor was not significant for any design (α = 0,05), which indicated that enzymatic activity was not affected by the selected temperatures in the drying processes but the latex source did. The enzyme activities obtained according to the latex source were likewise to results reported by Baeza *et al.* (1989). The obtained ANOVA for the specific enzymatic activity analyses using all the drying process presented no significant statistic difference among them (Table 3-4).

These results differed to report by Baeza *et al.*, (1989) who found that lyophilization is the best drying procedure, nevertheless the drying conditions were different.

Table 3. Specific enzymatic activity obtained for the latex from the unripe fruits. The number process is associated with the drying process described in Table 1.

	Enzyme Activity (units ml^{-1} sample) x 10^4			Enzyme Activity (units mg^{-1} protein) x 10^4		
Number	**Test 1**	**Test 2**	**Test 3**	**Test 1**	**Test 2**	**Test 3**
1	6.8	11.0	17.5	4.0	8.1	11.3
2	14.3	14.6	17.5	9.7	9.3	10.2
5	14.3	14.5	19.7	8.5	9.3	12.7
6	3.8	4.2	3.7	2.1	2.5	2.3
9	15.9	10.3	17.4	8.8	5.6	11.5
10	16.2	15.2	16.5	8.0	5.5	8.9
13	10.4	14.3	15.4	3.8	7.9	6.0
14	14.0	14.4	17.2	7.3	6.9	8.7

Table 2. Variance analysis to establish the effect of the drying process on the specific enzyme activity.

Factor	**GL**	**Seq SS**	**Adj SS**	**F**	**P-value**
Drying Process	3	0.0000002	0.0000001	0.92	0.450
Error	20	0.0000017	0.0000001		
Total	23	0.0000020			

An electrophoresis test was made with non-denatured samples, to observe if the drying process had denatured the papain enzyme. As a result the same colored pattern was obtained to each treatment indicating that there was no denaturizing effect due to the drying process. Therefore the tyrosine measured corresponded to the one produced through the hydrolysis reaction. Figure 1 presents SDS-PAGE for latex samples dried under different conditions. The average molecular weight obtained was 22086.7 Daltons. This molecular weight is similar to reported by Daliya and Ruey-Shin (2005).

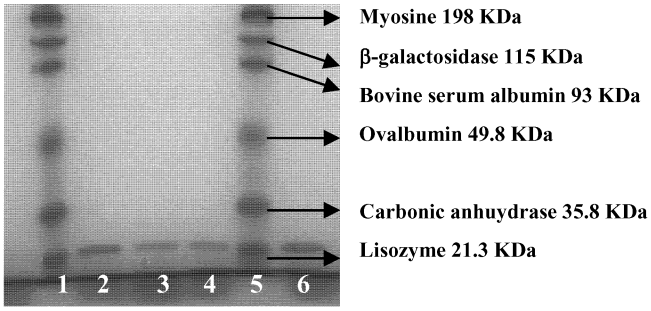

Figure 1. *SDS-PAGE electrophoresis gel. Samples 1 and 5 are molecular weight markers and 2, 3, 4 and 6 belongs to latex dried in conventional oven, tray dryer, vacuum oven and lyophilizator, respectively.*

The purification process displayed an increase in the specific enzyme activity of papain obtained from the unripe fruit. It was 20-fold higher than the obtained from the crude latex extract: 7.5×10^{-4} and 1.5×10^{-2} U mg^{-1} of protein for crude and purified enzyme, respectively.

4. Conclusions

The locally papaya fruit is a potential alternative for the papain extraction, now that the latex from these unripe fruits presented a high activity compared with the fruit skin.

Under the temperature evaluated conditions does not exist a significant statistic difference for the specific enzymatic activity for the selected drying processes. The only main difference presented was obtained according to the latex source.

The purified papain presented an average molecular weight of 22086.79 Da and specific enzymatic activity of 1.5×10^{-2} U mg^{-1} of protein 20-fold higher than the activity obtained in the crude extract 7.5×10^{-4} U mg^{-1} of protein.

5. Recommendations

It would be interesting to compare the four processes of drying using a wider range of temperatures and ratifying the independence of the proteolytic activity obtained and the process used.

6. References

Azarkan, M., A. Moussaoui, D. van Wuytswinkel, G. Dehon and Y. Looze, 2003, *J. Chromatogr. B*. 790:229-238

Baeza, G., D. Correa and C. Salas, 1989, *J. Sci. Food. Agric.*, 51:1-9.

Daliya, S.M. and J. Ruey-Shin, 2005, *Biochem. Eng. J.*, 25, 219–225.

Laemmli, U.K.C, 1970, *Nature*, 227:680-85

Montgomery, D.C., 2005, Design and analysis of experiments (6^{Th} Ed). New York, U.S.A, John Wiley & Sons.

Nitsawang, S.,Hatti-Kaul, R., Kanasawuda, 2006, *Enzyme Microb. Technol.*, 39:1103-1107

Neuhoff, V., R. Stamm, and H. Eibl, 1988, Electrophoresis, Vol. 9:255-56.

Ortiz, A., L. Madrigal, R. Fernández and R. Cooke, 1980, *J. Sci. Food Agric*., 31:510-514

Salunkhe, D.K. & Kadam, S.S. (1995) Handbook of Fruit Science and Technology: Production, Composition, Storage and Processing. U.S.A., Taylor & Francis Ltd.

Sigma Quality Control Test SSCASE01.001, 1999, Enzymatic Assay of Protease.

CHEMICAL ENGINEERING TRANSACTIONS, Volume 14, 2008
Edited by G. Marino, E. Bardone, A. Viglia
 ISBN 978-88-95608-02-0

Bio-extraction of olive oil: improvement of quality and extraction outputs

Aliakbarian B.,[a] De Faveri D.,[a] Casazza A.A.,[a] Oliveira R.P.S.,[b] Oliveira M.N., [b] Converti A[a]. and Perego P.[a]
[a]Department of Chemical and Process Engineering "G.B. Bonino", Genoa University, Via Opera Pia 15, 16145 Genoa, Italy
[b]Department of Biochemical and Pharmaceutical Technology, University of São Paulo, Av. Prof. Lineu Prestes 580, Bloco 16, 05508-900 São Paulo, Brazil

This work focuses on the development of a bio-extraction process by means of enzyme formulations, added at the beginning of the malaxation step, aiming at producing olive oils of *Coratina* cultivar with increased quality characteristics and extraction outputs. In particular, a combination of a 3^2 full factorial design with response surface methodology was used to investigate the combined effects of the malaxation time (t) and the concentration of the enzyme formulation (X). The concentrations of total polyphenols (TP) and *o*-diphenols (OD), antiradical power (ARP) and the oil extraction yield (Y) were selected as response variables. The optimum operating conditions predicted by the model (t = 92.00 min and X = 24.68 mL/kg$_{paste}$) assured the following responses: TP = 855.60 μg$_{CAE}$/g$_{oil}$, OD = 128.40 μg$_{CAE}$/g$_{oil}$, ARP = 25.28 μg$_{DPPH}$/μL$_{extract}$ and Y = 15.45 g$_{oil}$/100g$_{paste}$.

1. Introduction

The beneficial health effects of olive oil are due to both its high content of monounsaturated fatty acids and its high content of antioxidative substances (Visioli & Galli, 1998). The olive oil industry is very important in Mediterranean countries, both in terms of wealth and tradition. In particular, during extraction, the content of some components is significantly modified, depending on technique employed (Morales & Aparicio, 1999; Amirante et al., 2001), and also new components can be formed as a result of chemical and/or enzymatic pathways (Ranalli et al., 1999a). Many factors, such as malaxation temperature, time of exposure of olive paste to air contact (Servilli et al., 2003), use of microorganisms (Kachouri & Hamdi, 2004, 2006) or enzymes (Vierhuis et al., 2001), among others, may significantly influence the extraction efficacy.
Several authors reported that the addition of commercial enzyme preparations during malaxation degrade the walls of the oil bearing cells which retain the oil droplets and can also reduce the complexation of hydrophilic phenols with polysaccharides, increasing the concentration of free phenols in the olive paste and their consequent release into the oil and waste waters during processing (Ranalli & De Mattia, 1997; Vierhuis et al., 2001; De Faveri et al., under revision).
In order to face the increased competition of foreign products as well as to avoid the risk of marginalization and the loss of home and foreign market shares, the Italian olive oil sector has to concentrate on quality. So, with the aim of contributing to the increase in

the competitiveness of Italian olive oils, the present work focuses on the development of new technologies for its production studying the effect of an enzymatic treatment during olive paste malaxation on the phenolics content in olive oil of the *Coratina* cultivar using three different enzyme formulations at three different concentrations as well as their binary and ternary mixtures at a constant level and finally, to identify the most suitable operating conditions for the process, different tests were performed according to a 3^2 full factorial design, selecting the time of the malaxation process (t) and the concentration of the homogeneous ternary mixture of the enzyme formulations (X) as independent variables and total polyphenols concentration (*TP*), *o*-diphenols concentration (*OD*), antiradical power (*ARP*) and the oil extraction yield (Y) as response variables, and the collected results were worked out by RSM.

2. Materials and method

2.1 Enzyme preparation and experimental process

For the experimental extraction tests stoned olive paste of *Coratina* variety was used. Olive oil bio-extractions were carried out according to the procedure described by De Faveri et al. (under revision). The enzyme formulations (A, B and C) were added to the paste at the beginning of the malaxation step using three different levels (5, 10 and 15 mL/kg_{paste}) and their synergistic effects were also assessed by using their binary (A:B, A:C and B:C, 50:50%, v/v) and ternary (A:B:C, 33.3:33.3:33.3%, v/v/v) mixtures at a constant level (10 mL/kg_{paste}). Afterwards, the ternary mixture at three different levels and different malaxation times, according to the experimental design (see later), was used. In particular, A, B and C are complex formulations essentially containing pectinase plus cellulase and hemicellulase, pectinase and hemicellulase, and pectinase plus some minor activities, respectively.

2.2 Oil samples analyses

Phenolics were extracted from the oils according to the procedure described by Aliakbarian et al. (under revision). Total ploypheno1s (*TP*) and *o*-diphenols (*OD*) analyses, both expressed as $\mu g_{CAE}/g_{oil}$, were determined with Folin-Ciocalteau reagent and molybdate, respectively, according to Gutfinger (1981). Antiradical power were estimated using the DPPH assay in accordance with Brand-Williams et al. (1995) and was expressed as $\mu g_{DPPH}/mL$.

2.3 Experimental design

A 3^2 full-factorial experimental design was used to point out the relationship existing between the response functions and process variables as well as to determine those conditions able to optimise the extraction process. The two independent variables were coded according to the following equation:

$$x_i = \frac{\left(X_i - X_0\right)}{\Delta X_i} \qquad i = 1, 2 \qquad (1)$$

where x_i and X_i are the dimensionless and the actual values of the independent variable i, X_0 the actual value of the independent variable i at the central point, and ΔX_i the step

change of X_i corresponding to a unit variation of the dimensionless value. In order to simultaneously optimise the oil extraction process, the malaxation time (t, i = 1) in the range 60-120 min and the concentration of the ternary mixture (X, i = 2) in the range 5-25 mL/kg_{paste} were selected as the independent variables and *TP*, *OD*, *ARP* and *Y* ($g_{oil}/100g_{paste}$), were chosen as responses.
The behavior of the system can be described by the following second-order polynomial equation:

$$Y = \beta_0 + \sum \beta_i x_i + \sum \beta_{ii} x_i^2 + \sum \beta_{ij} x_i x_j \qquad (2)$$

where Y is the predicted response, β_0 is the interception coefficient, β_i are the linear terms, β_{ii} are the quadratic terms, β_{ij} are the interaction terms, and x_i and x_j represent the coded levels of the independent variables. The Student's t-test permitted us to check the statistical significance of the regression coefficients. The Fisher's test for analysis of variance (ANOVA) was performed on experimental data to evaluate the statistical significance of the model. The ''Statistica'' software (version 6.0, StatSoft, Tulsa, OK) and the ''Design Expert'' software (trial version 6.0.10, Stat-Ease, Minneapolis, MN) were employed for the regression analysis and the graphical optimization, respectively.

3. Results and discussion

3.1. Influence of malaxation temperature

Results illustrated in Fig. 1 demonstrate that a raise of malaxation temperature from 20 to 30°C resulted in an increased phenolics content, probably due to an enhanced release of oil constituents from vegetable tissue (Ranalli et al., 2001). A malaxation temperature higher than 30°C led to a decrease of these components in olive oil. Such a behaviour is in good agreement with a previous work which ascribed the increasing oxidation of phenolic contents of olive oil to the polyphenol oxidase and proxidase activities as a negative effect of high temperature (Servilli et al., 2003). Thus, malaxation temperature of 30°C was selected as the optimal temperature and the successive tests were performed at this temperature.

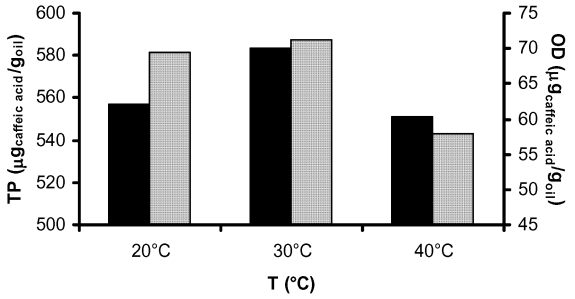

Fig.1 Effect of different malaxation temperatures on TP (■) and OD (▒) contents in olive oils obtained from stoned olive paste of Coratina variety.

3.2. Effect of single, binary and ternary mixtures of enzyme formulations and levels

As illustrated in Fig. 2a and Fig. 2b, increasing the enzyme level from 5 up to 15 mL/kg_{paste} and working with formulation A, followed by formulations B and C, gave rise to greater amounts of both *TP* and *OD*. These results confirm the more marked effect of the enzymes when pectolytic was used in combination with both cellulase and hemicellulase activities (formulation A), followed by the combined effect of pectinase and hemicellulase activities (formulation B), which resulted in significantly increased phenolics contents in the oils if compared with control tests (without using enzyme formulations).

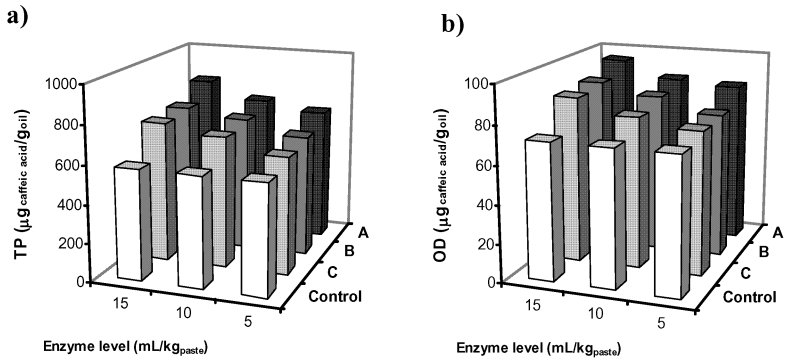

Fig.2 Effect of different enzyme formulations (A, B and C) and levels on TP (a) and OD (b) contents in olive oils obtained from stoned olive paste of Coratina variety.

In addition, four additional tests were performed using both binary and ternary mixtures of the three enzyme formulations. Table 1 lists *TP* and *OD* contents in olive oils treated with these formulations (A, B and C) at 10 mL/kg_{paste} or with binary and ternary mixtures at the same level.

Table 1
Effect of single, binary and ternary mixtures of enzyme formulations on *TP* and *OD* contents in olive oils obtained from stoned olive paste of *Coratina* variety compared with control test.

Enzyme formulation	*TP* ($\mu g_{CAE}/g_{oil}$)	*TP* increase (%)	*OD* ($\mu g_{CAE}/g_{oil}$)	*OD* increase (%)
A:B:C	804.3	40	97.69	37
A:B	786.3	37	87.77	23
A:C	723.3	26	83.15	17
B:C	690.9	20	82.20	15
A	740.6	29	86.17	21
B	705.6	23	82.75	16
C	686.4	19	78.77	10
Control	575.1	-	71.31	-

As expected, the effect of the ternary system (A:B:C) was more marked, followed by A:B, A:C and B:C, which put in evidence the importance of cellulase activity which was only contained in formulation A. Besides, results confirm the usefulness of pectinase, which are claimed to break down complex polysaccharides of plant tissue and are used in various biotechnological applications (Kashyap et al., 2001). For instance, similar commercial enzyme preparations, such as Olivex (Vierhuis et al., 2001) and Cytolase 0 (Ranalli et al., 1999b), were successfully used to enhance the release of phenolics in olive oil.

Our results point out the synergistic effect of different enzymatic activities in the extraction of phenolic compounds. Finally, since the best results were obtained when using the ternary mixture, such an enzymatic complex was selected to investigate the effect of enzyme processing aids as a function of malaxation time.

3.3. Statistics

3.3.1 Statistical modeling of TP, OD, ARP and Y according to the 3^2 full-factorial design

In order to optimise the oil extraction process, tests were carried out varying the malaxation time (t) in the range 60-120 min and the concentration of the ternary mixture (X) in the range 5-25 mL/kg_{paste} and *TP*, *OD*, *ARP* and *Y* were chosen as responses. Each test was performed in duplicate, while the central points were tested three times. The predicted models developed for *TP* (Y_1), *OD* (Y_2), *ARP* (Y_3), and *Y* (Y_4) are reported in Table 2.

Table 2
Response Surface Equations of *TP* (a), *OD* (b), *ARP* (c) and *Y* (d)

	Response function	Coefficient of Determination (R^2)
a)	$Y_1 = 717.30 - 12.05x_1 + 143.90x_2 - 43.82x_1^2$	0.968
b)	$Y_2 = 85.36 + 16.58x_1 + 28.37x_2 + 15.40x_2^2$	0.954
c)	$Y_3 = 23.80 - 0.79x_1 + 1.59x_2 - 2.26x_1^2$	0.789
d)	$Y_4 = 14.19 + 1.17x_1 + 1.21x_2$	0.760

Fig. 3 shows the three dimensional graphs obtained from the model calculated for the four responses. Both the best *TP* (Fig. 3a) and *ARP* (Fig. 3c) results were obtained at the highest X value (25 mL/kg_{paste}) and an intermediate t value (90 min), while a further increase in *OD* was found in the range 90-120 min malaxation time, irrespective of enzyme concentration (Fig. 3b). Finally, the response surface of the oil extraction yield (Fig. 3d) is represented by a plane, showing the maximum values at the highest level of both the independent variables.

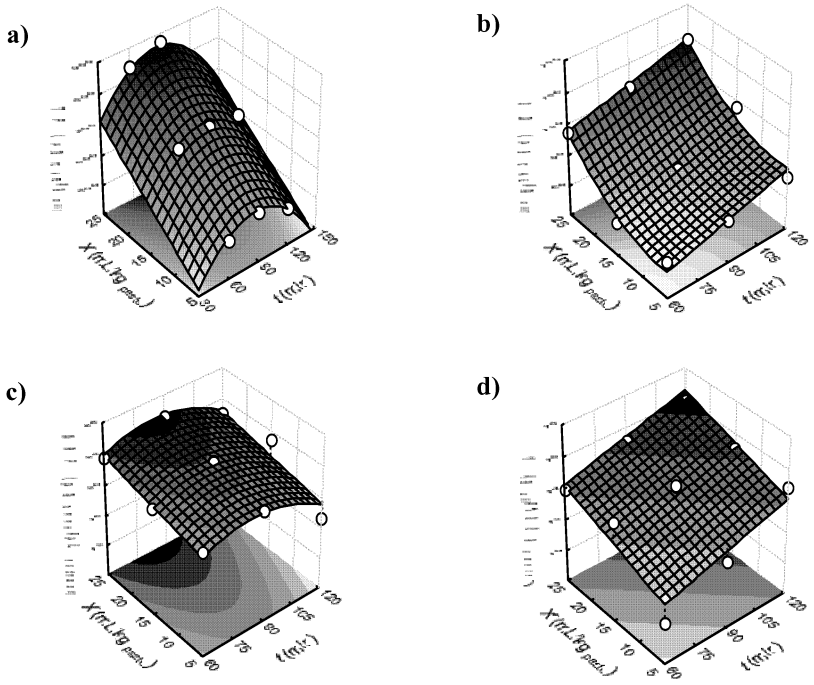

Fig.3 Response surfaces of TP (a), OD (b), ARP (c), and Y (d), as simultaneous function of (t) and (X) according to the 3^2 full-factorial design.

The regression analysis points out the significance of the linear *X* term (x_2) on each of the responses under investigation, while the quadratic term (x_2^2)of this independent variable was statistically significant only for Y_2. The linear term of *t* (x_1) was statistically significant for both Y_2 and Y_4, while it was kept in the other models (Y_1 and Y_3) to respect the hierarchical property. Moreover, no statistically significant interaction between the two independent variables ($x_1 \cdot x_2$) took place for all the four models under investigation.

3.3.2 Graphical optimisation

With the aim of definitely pointing out the optimal conditions of olive oil extraction by means of the proposed enzymatic treatment, a graphical optimisation was conducted using the "Design expert" software. Such a methodology essentially consists of overlaying the curves of the four models, obtained from the 3^2 full-factorial design, according to the specific criteria imposed.

The optimal working conditions were defined so as to get a high-quality olive oil with an increased phenolics level, in terms of both *TP* and *OD*, with a high *ARP*, and simultaneously maximizing the *Y*, to meet industrial economic requirements. Thus, the following constraints were imposed: $TP > 800$ $\mu g_{CAE}/g_{oil}$, $OD > 100$ $\mu g_{CAE}/g_{oil}$, $ARP > 24$ $\mu g_{DPPH}/\mu L_{extract}$ and $Y > 15$ $g_{oil}/100g_{paste}$.

Fig. 4 shows the overlay plot in which the white area represents the *t*-*X* dominion satisfying the imposed criteria. The point identified by the flag was chosen in the graph as representative of the optimised area corresponding to a malaxation time of 92.00 min and an enzyme concentration of 24.68 mL/kg_{paste}. Under these conditions the model predicted *TP* = 855.60 $\mu g_{CAE}/g_{oil}$, *OD* = 128.40 $\mu g_{CAE}/g_{oil}$, *ARP* = 25.28 $\mu g_{DPPH}/\mu L_{extract}$ and *Y* = 15.45 $g_{oil}/100g_{paste}$.

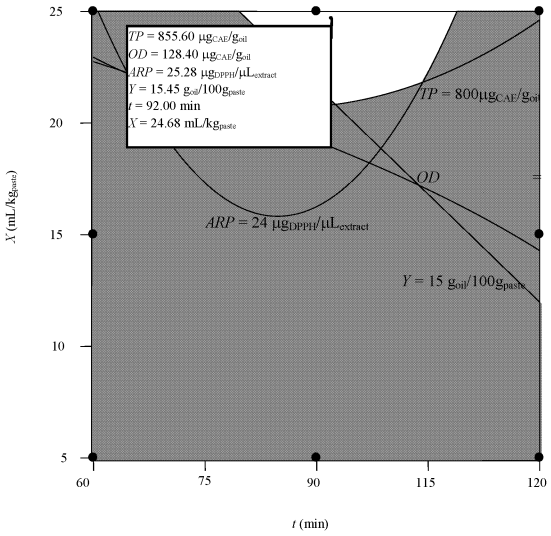

Fig. 4 Graphical optimisation identified by overlying plots of the four responses, TP, OD, ARP, and Y, as simultaneous functions of (t) and (X) according to the 3^2 full-factorial design.

4. Conclusion

A synergistic effect between the different enzymatic activities was observed and the ternary mixture was selected as the most efficient enzymatic system. The combined effects of malaxation time and the concentration of the selected enzyme formulation on the oil extraction process from olive fruits of the Italian cultivar *Coratina* were then studied. The highest levels of *TP* (874 $\mu g_{CAE}/g_{oil}$) and *ARP* (25.1 $\mu g_{DPPH}/\mu L_{extract}$) were reached at an intermediate malaxation time (*t* = 90 min) and the highest enzyme concentration (*X* = 25 mL/kg_{paste}), while the highest *OD* (147 $\mu g_{CAE}/g_{oil}$) was achieved at a malaxation time of 120 min and the same enzyme concentration. Moreover, the highest *Y* (16.0 $g_{oil}/100g_{paste}$) was reached at the highest malaxation time (t = 120 min), always at the highest enzyme concentration. The statistical model allowed identifying the optimum operating conditions (*t* = 92.00 min and *X* = 24.68 mL/kg_{paste}) able to simultaneously maximize *TP* (855.60 $\mu g_{CAE}/g_{oil}$), *OD* (128.40 $\mu g_{CAE}/g_{oil}$), *ARP* (25.28 $\mu g_{DPPH}/\mu L_{extract}$) and *Y* (15.45 $g_{oil}/100g_{paste}$).

5. References

Aliakbarian, B., D. De Faveri, A. Converti and P. Perego, Optimization of Olive Oil Extraction by means of Enzyme Processing Aids using Response Surface Methodology, Biochem. Eng. J. , under revision

Amirante, R., E. Cini, G.L. Montel and A. Pasqualone, 2001, Influence of mixing and extraction parameters on virgin olive oil quality. Grasas Aceites, 52 (3-4), 198–201

Brand-Williams, W., M.E. Cuvelier and C. Berset, 1995, Use of free radical method to evaluate antioxidant activity. LWT-Food Sci. Technol., 28 (1), 25-30

De Faveri, D., B. Aliakbarian, M. Avogadro, P. Perego and A. Converti, Improvement of olive oil phenolics content by means of enzyme formulations: effect of different enzymatic activities and concentrations, Biochem. Eng. J., under revision

Gutfinger, T., 1981, Polyphenols in olive oil. J. Am. Oil Chem. Soc., 58, 966-968

Kachouri, F. And M. Hamdi, 2004, Enhancement of polyphenols in olive oil by contact with fermented olive mill wastewater by *Lactobacillus plantarum*. Process Biochem., 39 (7), 841-845

Kachouri, F. And M. Hamdi, 2006, Use *Lactobacillus plantarum* in olive oil process and improvement of phenolic compounds content. J. Food Eng., 77 (3), 746-752

Kashyap, D.R., P.K. Vohra, S. Chopra and R. Tewari, 2001, Applications of pectinases in the commercial sector: a review. Bioresource Technology, 77(3), 215-227

Morales, M.T. and R. Aparicio, 1999, Effect of extraction conditions on sensory quality of virgin olive oil. J. Am. Oil Chem. Soc., 76 (3), 295-300

Ranalli, A. and G. De Mattia, 1997, Characterisation of olive oil produced with a new enzyme processing aid. J. Am. Oil Chem. Soc., 74 (9), 1105-1113

Ranalli, A., M.L. Ferrante, G. De Mattia and N. Costantini, 1999a, Analytical evaluation of virgin olive oil of first and second extraction. J. Agric. Food Chem., 47 (2), 417-424

Ranalli, A., A. Sgaramella and G. Surricchio, 1999b, The new "Cytolase 0" enzyme processing aid improves quality and yields of virgin olive oil. Food Chem., 66 (4), 443-454

Ranalli, A., S. Contento, C. Schiavone and N. Simone, 2001, Malaxation temperature affects volatile and phenol composition as well as other analytical features of virgin olive oil. Eur. J. Lipid Sci. Technol., 103 (4), 228-238

Servilli, M., R. Selvaggini, A. Taticchi, S. Esposto and G.F. Montedoro, 2003, Volatile compounds and phenolic composition of virgin olive oil: optimization of temperature and time of exposure of olive paste to air contact during the mechanical extraction. J. Agric. Food Chem., 51 (27), 7980-7988

Vierhuis E., M. Servili, M. Baldioli, H.A. Schols, A.G.J. Voragen and G.F. Montedoro, 2001, Effect of enzyme treatment during mechanical extraction of olive oil on phenolic compounds and polysaccharides. J. Agric. Food Chem., 49 (3), 1218-1223

Visioli, F. and C. Galli, 1998, Olive oil phenols and their potential effects on human health. J. Agric. Food Chem., 46 (10), 4292-4296

CHEMICAL ENGINEERING TRANSACTIONS, Volume 14, 2008
Edited by G. Marino, E. Bardone, A. Viglia
 ISBN 978-88-95608-02-0

Chiral Aromatic Alcohols Production by Thermophilic NADH-dependent Carbonyl Reductase

Angela Pennacchio [1], Biagio Pucci [1], Francesco Secundo [2], Francesco La Cara [1], Mosè Rossi[1], and Carlo A. Raia [1]

Istituto di Biochimica delle Proteine, Consiglio Nazionale delle Ricerche, Via P. Castellino 111, I-80131 Napoli, Italy [1]
Istituto di Chimica e del Riconoscimento Molecolare, Consiglio Nazionale delle Ricerche, Via M. Bianco 9, I-20131 Milano, Italy [2]

Dehydrogenases/reductases (ADHs) are nowadays among the most requested enzymes used for the preparation of optically active compounds, for the inherent advantages over chemocatalysts in terms of their high chemo-, enantio-, and regioselectivity as well as to be environmentally friendly. Our aim was to identify and characterize novel ADHs for the selective bioreduction of sterically demanding ketones or alcohols, preferably NAD(H)-dependent and endowed with good operational stability. The gene encoding a novel dehydrogenases/reductase that belongs to the short-chain dehydrogenases/reductases (SDRs) superfamily has been identified in the genoma of *Thermus thermophilus* HB27. The *ttadh* gene has been heterologously overexpressed in *E. coli* and the protein, named TtADH, has been purified to homogeneity and characterized. The enzyme was found to be a thermophilic and thermostable NAD(H)-dependent SDR, active on both aromatic alcohols as well as a discrete spectrum of carbonyl compounds, including substituted benzaldehydes, aromatic ketones, and α-ketoesters. TtADH shows a good tolerance towards common organic solvents such as methanol, acetonitrile, ethyl acetate, and 2-propanol used at 2–10% concentration and at a temperature range from 25° to 60°C. The preparative applicability of TtADH was investigated by way of an efficient *in situ* NADH-recycling system involving 2-propanol and a second NAD(H)-dependent ADH. TtADH enzyme catalyses the reduction of acetophenone, 2,2,2-trifluoroacetophenone, methyl and ethyl benzoylformate with high yields and excellent enantiomeric excess.

1. Introduction

Biocatalysis is increasingly being used in synthetic routes for the preparation of enantiomerically pure compounds due to their importance in the pharmaceutical, agricultural, fragrance and flavour industries (Kroutil et al., 2004, and refs. therein). This is reflected in the fact that the sales of single-enantiomer small-molecule drugs has reached about US $10 billion in 2002 and the percent of chiral compounds as pharmaceutical intermediates is expected to grow to 70% by 2010. Moreover, the FDA has become increasingly reluctant to permit the introduction of additional racemic drugs, as these therapies are by definition saddled with 50% of chemical ballast (Rouhi, 2003).

Among many kinds of biocatalysts, dehydrogenases/reductases from various microorganisms have been used to prepare optically pure alcohols from carbonyl compounds. Furthermore, NAD(H) dependence and preference for bulky side-chained ketones/alcohols are two features that make a dehydrogenase/reductase more attractive from an application perspective; however, there is still a striking lack of sturdy ADHs with these characteristics that are even stable and active in organic solvents and in a broad range of temperature (Kroutil et al., 2004). Therefore, our aim was to search for novel activities, following the criterion to identify one or more gene(s) in the genome sequence of thermophilic microorganisms present in the database with the highest amino acid sequence identity with respect to that of *Lactobacillus brevis* ADH, a very well-known enantioselective NADPH-dependent SDR, active mainly on various aromatic ketones (Schlieben et al., 2005).

2. Materials and Methods

2.1 Chemicals. $NAD(P)^+$ and NAD(P)H were obtained from AppliChem (Darmstadt, Germany). Alcohols, aldehydes, ketones and ketoesters were obtained from Sigma-Aldrich. Other chemicals were A grade substances from Applichem. Recombinant *Bacillus stearothermophilus* ADH (BsADH) was prepared and assayed as previously described (Fiorentino et al., 1998).

2.2 Purification and characterization. The cloning and expression of the *ttadh* gene, and the purification of recombinant enzyme were performed according to Pennacchio et al., (2008).

2.3 Enzyme assay. TtADH was assayed spectrophotometrically at 65°C by measuring the change in absorbance of NADH at 340 nm using a Cary 1E spectrophotometer equipped with a Peltier effect-controlled temperature cuvette holder. The standard assay for the reduction reaction was performed by adding 5–25 μg of the enzyme to 1 ml of preheated assay mixture containing 20 mM methyl benzoylformate and 0.3 mM NADH in 50 mM potassium phosphate, pH 6.0. The standard assay for the oxidation reaction was performed using a mixture containing 20 mM (*S*)-(−)-1-phenylethanol and 3 mM NAD^+ in 100 mM glycine-NaOH, pH 10.5. 1 unit of TtADH and BsADH represented 1 μmol of NADH produced or utilized per min at 65° and 60°C, respectively on the basis of an absorption coefficient of 6.22 mM^{-1} for NADH at 340 nm.

2.4 Enantioselective biosynthesis. The enantioselectivity of TtADH was determined by reduction of aryl ketones and α-ketoesters using an NADH-regeneration system consisting of BsADH and 2-propanol. The reaction mixture contained 1 mM NAD^+, 20 mM carbonyl compound (3 mg), 11 U of BsADH , 260 mM 2-propanol, and 7 U TtADH in 1 ml of 100 mM MES, pH 6.0, 5 mM 2-mercaptoethanol and 100 mM KCl. The reactions were carried out at 50° and 60°C at different times in a temperature controlled water bath. Upon termination, the reaction mixture was extracted twice with ethyl acetate. The enantiomeric excess of the product (ee) and conversion were determined by GLC (Agilent 6850) equipped with a dimethylpentyl, β-cyclodextrin 25 m, 0.25 mm ID,

MEGA column (Legnano, Italy). Conditions for 1-phenyl-ethanol and α-(trifluoromethyl)benzyl alcohol were: oven temperature from 90°C (initial time 10 min) to 110°C (final time 5 min), with a heating rate of 2.5°C/min. Conditions for ethyl and methyl mandelate were: oven temperature from 100°C (initial time 5 min) to 130°C (final time 5 min), with a heating rate of 2.5°C/min. The conversion yield was determined on the basis of the peak areas of carbonyl substrate and alcohol products on GC chromatograms.

3. Results and Discussion

3.1 Enzyme properties. Gel filtration chromatography, SDS-PAGE and kinetic studies assessed that TtADH is a homotetrameric SDR (MW =108 kDa), markedly thermophilic (optimal temperature ≈ 80°C) and thermostable ($T_{1/2,\ 30\ min}$ ≈ 90°C). The optimal pH for the reduction and oxidation reaction catalysed by TtADH resulted around 6 and 10, respectively (Pennacchio et al., 2008).

3.2 Coenzyme and substrate specificity. The enzyme showed no activity with NADP(H) and full activity with NAD(H). Moreover, the following compounds resulted substrates of TtADH (reported in decreasing order of relative %). Alcohols: (*S*)-(−)-1-phenylethanol (100), 4-methoxybenzyl alcohol (99), (±)-1-phenyl-1-propanol (59), 1-(4-fluorophenyl)ethanol (45), 1-(4-chlorophenyl)ethanol (26), *trans*-cinnamyl alcohol (25), 2-methoxybenzyl alcohol (25), 1-phenyl-2-propanol (16), (*R*)-1-phenyl-2-propen-1-ol (14) and 3-methoxybenzyl alcohol. Carbonyl compounds: 1-phenyl-1,2-propanedione (146), 2,2,2-trifluoroacetophenone (100), 2,2-dichloroacetophenone (32), benzaldehyde (14), 2-, 3-, and 4-methoxybenzaldehyde (13, 14, 13). α-Ketoesters: ethyl benzoylformate (100) and methyl benzoylformate (57). Kinetic constants analysis indicated that the enzyme is *S* stereospecific and that the physiological direction of the catalytic reaction is reduction rather than oxidation (data not shown).

3.3 Stability in organic solvents. The effect of common organic solvents such as methanol, 2-propanol, acetonitrile, dioxane and ethyl acetate was studied by assaying TtADH activity in their presence at two different times and temperatures. Table 1 shows that the enzyme activity increases significantly in aqueous buffer, as well as in the presence of all the solvents tested. Moreover, the activity measured after 65 h incubation at 25°C in TtADH samples containing 10% methanol, 2-propanol, acetonitrile, dioxane, ethyl acetate, 1-propanol, and *n*-hexane resulted increased by 172, 110, 167, 160, 115, 173 and 182%, respectively, whereas that of the control remained unchanged. Furthermore, standard assays performed in the presence of 0.01 to 0.5% 2-propanol resulted in no change in activity, suggesting that the activity enhancement is not due to an immediate effect of solvent on the protein structure. A considerable body of literature exists which describes the activation of thermophilic enzymes by loosening of their rigid structure in the presence of protein perturbants (Fontana et al., 1998). To account for the observed enhancements of TtADH activity, the organic solvent is proposed to induce a

Table 1. Effect of organic solvents on *T. thermophilus* ADH.

Solvent	Activity[a] (%)[b] 50°C		Activity[a] (%)[b] 60°C	
	5 h	24 h	5 h	24 h
None	131	142	129	134
5% Methanol	138	137	185	185
2% 2-Propanol	165	151	193	168
10% 2-Propanol	174	180	211	174
5% Acetonitrile	131	158	167	177
5% 1,4-Dioxane	152	180	177	161
5% Ethyl acetate	151	183	176	145

[a] Activity assays were performed as described in M. M. using ethyl benzoylformate as the substrate. [b] The percent of activity was calculated with respect to the value measured before the addition of solvent.

conformational change in the protein molecule to a more relaxed and flexible conformation into one which is optimal for activity.

3.4 Enantioselective biosynthesis. The enantioselectivity of TtADH was tested using acetophenone, 2,2,2-trifluoroacetophenone, methyl and ethyl benzoylformate as substrates, and an efficient NADH-regeneration system (Figure 1) consisting of Zn-containing, homotetrameric ADH from the moderate thermophilic bacterium *Bacillus stearothermophilus LLD-R strain* (BsADH) (Fiorentino et al., 1998). This NAD(H)-dependent ADH is mainly active on aliphatic and aromatic primary and secondary alcohols and aldehydes, but not on aliphatic and aromatic ketones, nor on the carbonyl substrates of TtADH and corresponding alcohols (data not shown). Since 2-propanol is not a substrate of TtADH, it may be a suitable substrate for BsADH in NADH recycling, as well as being used as a co-solvent. Experimental conditions including buffer, pH,

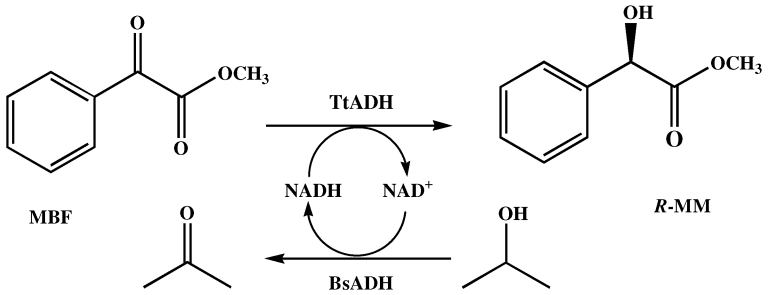

Figure 1. Coenzyme recycling in the production of (*R*)-methyl mandelate with *T. thermophilus* ADH (TtADH) utilizing *B. stearothermophilus* ADH (BsADH) and 2-propanol. MBF, methyl benzoylformate; *R*-MM, methyl (*R*)-(–)-mandelate.

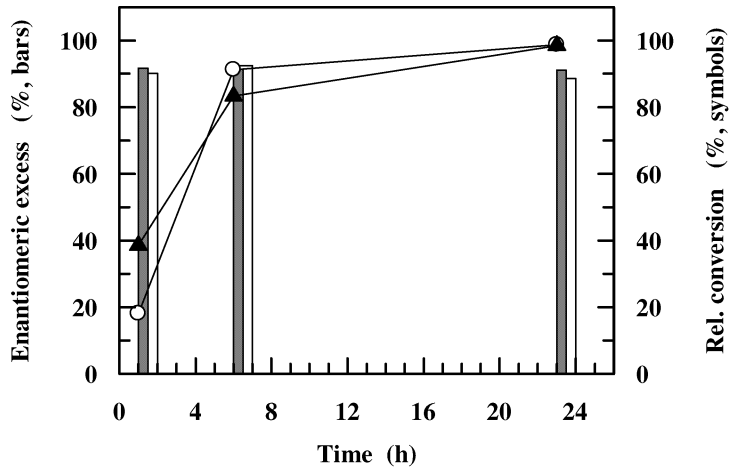

Figure 2. Conversion and enantiomeric excess of methyl benzoylformate by *T. thermophilus* ADH at different reaction times. Biotransformations were carried out at 50°C (white bars and circles) and 60°C (grey bars and triangles) as described in M. M. The reactions were stopped by addition of ethyl acetate at the times indicated. The dried extracts were analysed by chiral GC and the relative conversion calculated as the area of alcohol products divided by the total area.

temperature and reaction time were chosen to optimise productivity. The k_{cat}/pH profiles indicated that MES buffer, pH 6.0 and 60°C were the optimal pH and temperature conditions for catalysis by the two enzymes. Conversion experiments were carried out at 50° and 60°C, and the reactions allowed to proceed for 1, 6 and 24 h. Figure 2 shows that methyl benzoylformate was reduced by TtADH to methyl (*R*)-(−)-mandelate with 18, 91, and 99% conversion at 50°C and 38, 83, and 98% conversion at 60°C following 1, 6, and 24 h, respectively. The higher ee value (92%) was achieved after 6 h reaction at 50°C, whereas it was 91% at 60°C after 6 h, and 89 and 91%, at 50 and 60°C, respectively after 24 h reaction. However, the reaction with larger amounts of substrate and enzyme (100 mg, 92 and 62 U of BsADH and TtADH, respectively, in 30 ml) resulted in 93.5% ee and 90% conversion after 24 h reaction at 50°C.

The reaction with ethyl benzoylformate performed for 6 h at 50°C yielded ethyl (*R*)-(−)-mandelate with a conversion of 90% and 95% ee. Acetophenone was reduced to (*S*)-(−)-1-phenylethanol following a 6 h reaction at 50°C, with a conversion of 70% and 99% ee. The conversion of 2,2,2-trifluoroacetophenone was 20 and 40% in 1 h at 50° and 60°C respectively, approximating 100% in 6 h at both the temperatures. TtADH preferably reduced this arylketone to (*R*)-α-(trifluoromethyl)benzyl alcohol with an ee of 90 and 93% at 60° and 50°C respectively, after 3 h of reaction. However, reaction times extended to 24 h did not improve the yield or ee of the biotransformation (data not shown).

On the whole, enantioselectivity data indicate that the hydride ion of NADH is transferred to the *re* face of the carbonyl of acetophenone, 2,2,2-trifluoroacetophenone,

as well as that of methyl and ethyl benzoylformate, suggesting that TtADH exhibits Prelog specificity (Prelog, 1964). Noteworthy, the optically active alcohols produced are used as chiral building blocks in organic synthesis. *O*-protected methyl (*R*)-(−)-mandelate is used as an intermediate for the synthesis of pharmaceuticals (Kobayashi et al., 1990), and optically pure trifluoromethyl-substituted benzyl alcohols are important precursors for specialty chemicals used in electro-optical devices such as LCDs (Fujisawa et al., 1993).

4. Acknowledgements

This work was funded by FIRB (Fondo per gli Investimenti della Ricerca di Base) RBNE034XSW, and by the ASI project MoMa n. 1/014/06/0.

5. References

Fiorentino G., R. Cannio, M. Rossi and S. Bartolucci, 1998, Decreasing the stability and changing the substrate specificity of the *Bacillus stearothermophilus* alcohol dehydrogenase by single amino acid replacements. Protein Eng. 11, 925.

Fontana A., V. De Filippis, P. Polverino de Laureto, E. Scaramella and M. Zambonin, 1998, Rigidity of thermophilic enzymes, p. 277–294. *In* Ballestreros A., F. J. Plou, J. L. Iborra and P. J Halling (ed.), Stability and Stabilization in Biocatalysis, vol. 15. Elsevier Sciences, Amsterdam.

Fujisawa T., K. Ichikawa and M. Shimizu, 1993, Stereocontrolled Synthesis of *p*-Substituted Trifluoromethylbenzylic Alcohol Derivatives of High Optical Purity by the Baker's Yeast Reduction. Tetrahedron: Asymmetry 4, 1237.

Kobayashi Y., Y. Takemoto, Y. Ito and S. Terashima, 1990, A novel synthesis of the (2R,3S)- and (2S,3R)-3-amino-2-hydroxycarboxylic acid derivatives, the key components of a renin inhibitor and bestatin, from methyl (*R*)- and (*S*)-mandelate. Tetrahedron Letters 31, 3031.

Kroutil W., H. Mang, K. Edegger and K. Faber, 2004, Recent advances in the biocatalytic reduction of ketones and oxidation of *sec*-alcohols. Curr. Opin. Chem. Biol. 8, 120.

Pennacchio A., B. Pucci, F. Secundo, F. La Cara, M. Rossi and C. A. Raia, 2008, A Novel Short-Chain, Highly Enantioselective, NAD(H)-dependent Alcohol Dehydrogenase from *Thermus thermophilus*. Characterization of the Recombinant Enzyme. (Submitted).

Prelog V., 1964, Specification of the stereospecificity of some oxido-reductase by diamond lattice sections. Pure Appl. Chem. 9, 119.

Rouhi A. M., 2003, Chiral business. Chem. Eng. News 8, 45.

Schlieben N. H., K. Niefind, J. Muller, B. Riebel, W. Hummel and D. Schomburg, 2005, Atomic resolution structures of R-specific alcohol dehydrogenase from *Lactobacillus brevis* provide the structural bases of its substrate and cosubstrate specificity. J. Mol. Biol. 349, 801.

CHEMICAL ENGINEERING TRANSACTIONS, Volume 14, 2008
Edited by G. Marino, E. Bardone, A. Viglia
 ISBN 978-88-95608-02-0

Albumin-Bound Toxin Removal in Liver Support Devices: Case Study of Tryptophan Adsorption and Dialysis

M. Cristina Annesini, Vincenzo Piemonte, Luca Turchetti
Department of Chemical Engineering, University of Rome "La Sapienza"
via Eudossiana 18, 00184 Roma (Italy)

Dialysis and adsorption processes are commonly implemented in liver support devices for the removal of albumin-bound toxins such as tryptophan. In this work, dialysis and adsorption of tryptophan from albumin-containing solutions were investigated; in particular, the effect of albumin concentration on both processes was analysed. Theoretical models accounting for albumin-tryptophan binding were proposed and fitted to the experimental data in order to obtain equilibrium and kinetic parameters.
The results allowed to perform a simulation of an albumin-dialysis liver support device session and compare the performance of different dialysate recirculation/regeneration policies.

1. Introduction

Acute and acute-on-chronic liver failure are associated with high plasmatic levels of toxins that are responsible for secondary life-threatening multi-organ pathologies. In such clinical conditions, liver support devices aimed at removing toxins from blood offer a temporary solution, helping to keep patients alive in wait of a recovery of liver functionality or an organ transplantation (Stange et al., 2002).
Toxins not cleared by the failing liver include both small water-soluble molecules and hydrophobic molecules that are tightly bound to plasma proteins. While a conventional dialysis treatment can remove selectively the former class of toxins, more complex processes are required to remove molecules of the latter type. At present, the most widely used artificial liver devices are the Single Pass Albumin Dialysis (SPAD) (Sauer et al., 2004), MARS (Mitzner et al., 2001) and Prometheus (Rifai et al., 2003) systems. Schemes of these devices are reported in figure 1. Although several clinical studies on the performance of these apparatus are available, until now only few works have been devoted to the analysis of the fundamental phenomena involved in the detoxification processes, while this information could help in designing and optimizing these systems. In spite of the differences between clinically used liver support devices, all of them are based on membrane separation and adsorption processes. Modelling of these operations is a well consolidated knowledge of chemical engineering and the evaluation of the performance of these apparatus can be confidently carried out once equilibrium conditions and transport phenomena kinetics are known.
In order to obtain such information, in this work tryptophan removal from albumin-containing solutions is investigated. Tryptophan is an aromatic amino acid relevant for the onset of hepatic coma; it can form complexes with albumin, even if the binding

constant (10^4-10^5 M^{-1}, as reported by McMenamy et al., 1958, and Sun et al., 1993) is largely lower than that of other hepatic toxins such as bilirubin.
In the first part of this work, dialysis and adsorption process are considered separately: as for dialysis, the effect of albumin as tryptophan binder in the dialysate is investigated; as for adsorption, equilibrium conditions and fixed-bed adsorption kinetics on two different adsorbents (activated carbon and polymeric non-ionic resin) are reported. In the second part, theoretical models of the dialysis and adsorption units are used to simulate a complete liver support device session.

2. Experimental

Materials and Methods
Bovine serum albumin (Cohn fraction V, MW=66000) and L-Tryptophan (MW=204) were purchased from Sigma-Aldrich (St.Louis, MO, USA); activated carbon for gas chromatography 05112 (Fluka Chemie GmbH, Buchs, Switzerland) and polymeric resin Lewatit VP OC 1064 (Bayer AG, Leverkusen, Germany) were used as adsorbents. All the solutions were prepared in phosphate buffer 0.15 M at pH 7.4.
Analysis of tryptophan solutions was carried out by an UV-VIS spectrophotometer (Perkin Elmer Lambda 25) at 279 nm or, in presence of albumin, by HPLC with a Spherisorb ODS2 (Agilent Technologies, Santa Clara, CA, USA) column and an UV detector set at 279 nm (Annesini et al., 2005, 2007).

Dialysis
Dialysis experiments were carried out in a two compartment closed loop system, using a hollow fibre membrane module (Fresenius F40): 300 ml of an albumin-tryptophan solution (hitherto referred to as "feed") was recirculated at constant flow rate (150 ml/min) in the fibre-side of the dialysis module; 300 ml of dialysis solution (buffer solution or albumin-containing solution, hitherto referred to as "dialysate") was recirculated at the same flow rate in countercurrent in the shell-side of the membrane

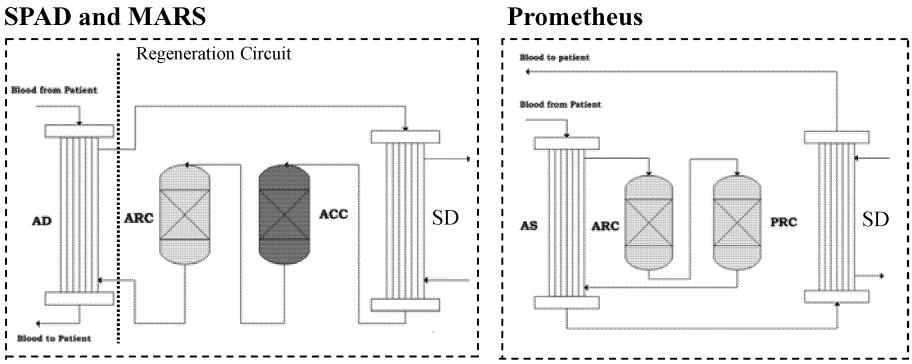

Figure 1: Artificial liver systems (*AD: albumin dialyser; KD: secondary dialyser; ARC: anionic resin column, ACC: activated carbon column; PRC: polymeric non-ionic resin column; AS: plasma fractionator). In SPAD, the albumin dialysis solution is discarded, while in MARS it is continuously regenerated and recycled to the membrane module; in Prometheus adsorption is performed directly after filtration of the albumin fraction on a polysulphone membrane.*

module. Samples were collected at the fibre and shell outlet and analysed at different times, to determine tryptophan and albumin concentrations. The transmembrane pressure was controlled in order to have a null net water flow across the membrane. In all the experiments, absence of albumin transfer across the membrane and tryptophan adsorption on the membrane was checked by a mass balance.

Adsorption

Adsorption equilibrium experiments were carried out contacting 40 ml of albumin-tryptophan solution with different amounts of adsorbent in stirred flasks for 16 hours; then the suspension was settled and the supernatant filtered and analysed. Preliminary experiments showed that no significant changes in the liquid concentration occur after this contact time.

Kinetic experiments were carried out in a fixed bed column (10 mm ID, 60 mm bed length) at 25±0.5°C, with a constant flow-rate tryptophan-albumin feed. Samples were collected at regular time intervals at the column outlet and analysed.

3. Dialysis process

The influence of albumin concentration both in feed (fibre-side) and dialysate (shell-side) on the membrane module clearance was investigated. Figure 2a reports the decrease in tryptophan concentration in the albumin-containing feed, obtained with a traditional dialysis process (albumin-free dialysate); it is evident that the higher the albumin concentration the lower the tryptophan clearance. This result is easily explained by tryptophan-albumin binding considerations: albumin in feed reduces the free tryptophan concentration gradient across the membrane, that is the true driving force of the dialysis process, since only free tryptophan can cross the membrane.

Addition of albumin to the dialysis solution (albumin dialysis process) results in a significant increase in tryptophan clearance, as shown in Figure 2b. Clearly, in this case, the higher the albumin concentration in the dialysis solution, the lower the free tryptophan concentration in the dialysate and the higher the dialysis driving force. This result agrees with similar findings reported in the literature, referring both to *in vivo* and *in vitro* experimental evidence (Stange et al., 1993), confirming that the presence of albumin in the dialysate enhances albumin-bound toxin transfer across the membrane. Therefore, albumin dialysis is indeed a more efficient process for albumin-bound toxin removal that traditional dialysis.

A simple model of the albumin dialysis process has been previously proposed by Patzer (2006), accounting for albumin-toxin equilibrium in the liquid phases and free-toxin diffusion across the membrane. According to this model, the solute mass balances in the feed-side and in the shell-side solutions are given by

$$\frac{\partial c_{t,f}}{\partial t}\left(1+\frac{k_{eq}c_{alb,f}}{\left(1+k_{eq}c_{t,f}\right)^2}\right)=-v_f\frac{\partial c_{t,f}}{\partial z}\left(1+\frac{k_{eq}c_{alb,f}}{\left(1+k_{eq}c_{t,f}\right)^2}\right)-a_fK_c\left(c_{t,f}-c_{t,s}\right) \quad (1)$$

$$\frac{\partial c_{t,s}}{\partial t}\left(1+\frac{k_{eq}c_{alb,s}}{\left(1+k_{eq}c_{t,s}\right)^2}\right)=-v_s\frac{\partial c_{t,s}}{\partial z}\left(1+\frac{k_{eq}c_{alb,s}}{\left(1+k_{eq}c_{t,s}\right)^2}\right)-a_sK_c\left(c_{t,f}-c_{t,s}\right) \quad (2)$$

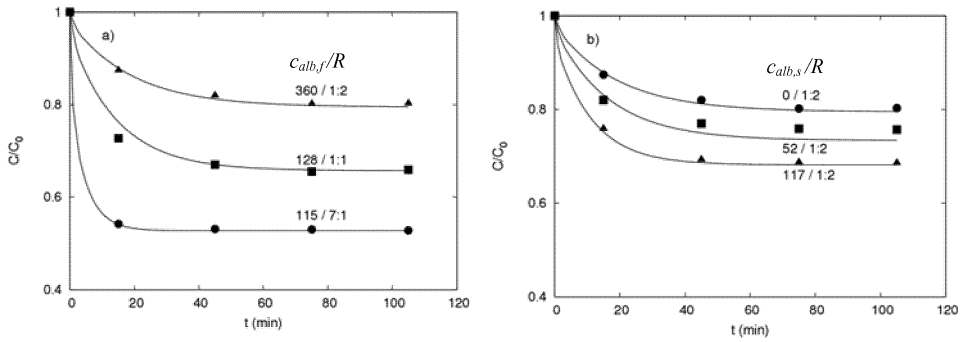

Figure 2 *Tryptophan concentration decrease during traditional (a) and albumin (b) dialysis processes. C/ C_0 : fraction of initial tryptophan concentration in feed.*
(a) Data sets refer to different albumin concentrations ($c_{alb,f}$) and different initial tryptophan-to-albumin molar ratios (R) in the feed.
(b) Data sets refer to different albumin concentrations in the dialysate ($c_{alb,s}$) and different tryptophan-to-albumin molar ratios in the feed. Albumin concentration in feed $c_{alb,f}$ =360 μM

Equations (1) and (2) can be integrated with the following initial and boundary conditions:

$$t = 0 \qquad 0 \le z \le L \qquad c_{t,f} = c_{t,f}^{0} \;\; ; \;\; c_{t,s} = 0 \tag{3}$$

$$t > 0 \qquad z = 0 \qquad c_{t,f} = c_{t,f}^{in} \;\; ; \;\; z = L \qquad c_{t,s} = c_{t,s}^{in} \tag{4}$$

In the above equations, c_t and c_{alb} are the free tryptophan and total albumin concentrations, respectively, k_{eq} the albumin-tryptophan binding constant, K_c is the overall mass transfer coefficient, a is the membrane specific surface and v the fluid velocity. Additional subscripts *f* and *s* refer to fiber-side and shell-side solutions, respectively. This model of the dialysis module was solved together with mass balances in the feed and dialysate reservoirs, which were considered perfectly mixed.
In the analysis of the experimental data, the albumin-tryptophan binding constant was set to 10^{-4} M^{-1}, according to the order of magnitude reported in the literature; this value was also confirmed by the experimental measurements of tryptophan concentrations (fibre and shell side) at long dialysis time (approaching equilibrium conditions).
The overall mass transfer coefficient K_c was obtained by fitting of the experimental data; both traditional and albumin dialysis data can be described with the same K_c value ($K_c = 7.5 \cdot 10^{-9}$ cm/s); figures 2a and 2b show a good agreement between the experimental data and the calculated curves and confirm the validity of the model.

3. Adsorption process

The design of an adsorption process to remove tryptophan requires information both on equilibrium and kinetics. As for tryptophan adsorption equilibrium in albumin-containing solutions, a simple model has been previously proposed (Annesini et al. 2005 and 2008). This model relies on the assumptions that 1) only 1:1 toxin-albumin complexes are formed, with an equilibrium constant K_{eq}; 2) only free toxin is adsorbed.

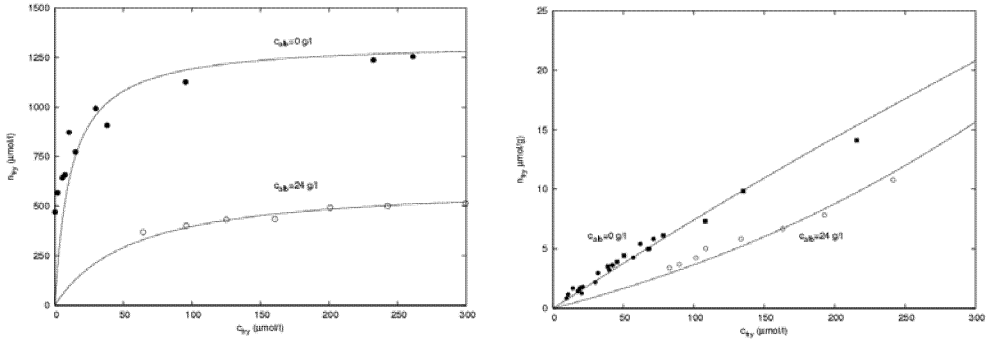

Figure 3 *Typical tryptophan adsorption isotherms on (a) activated carbon (data from Annesini et al., 2008) and (b) polymeric resin. c_{alb}: albumin concentration in the solution; lines: model fitting; circles: experimental data.*

Under these hypotheses, the amount of adsorbed tryptophan per unit adsorbent mass, n_t, is related to the total (albumin-bound and free) toxin concentration, c_{try}, by:

$$n_t = n_{\max} \frac{\alpha c_{try}}{k_{try} + \alpha c_{try}} \tag{5}$$

or , for $\alpha c_{try} << k_{try}$

$$n_t = \frac{n_{\max}}{k_{try}} \alpha c_{try} \tag{6}$$

where the free tryptophan fraction $\alpha = c_t / c_{try}$ depends on K_{eq}, c_{try} and c_{alb}. If albumin interaction with tryptophan adsorption is limited to tryptophan binding in solution, parameters $n_{\max}$ and k_{try} should coincide with the Langmuir parameters of the free tryptophan adsorption isotherm; however, effects such as competitive adsorption or steric hindrance could be significant and, in order to fit the experimental data, it could be necessary to consider a dependence of $n_{\max}$ on albumin concentration.

In figure 3 tryptophan adsorption equilibrium on polymeric resin and activated carbon are compared. As for adsorption onto the resin in albumin-free solutions, the adsorption isotherm is fairly linear ($n_{\max}$ / k_{try} =0.077 l/g); when albumin is added to the solution, it is sufficient to consider only the effect of albumin-toxin binding in the liquid phase, in order to predict the reduction of tryptophan uptake.

As for tryptophan adsorption onto activated carbon in albumin-free solutions, Langmuir parameters $n_{\max}$=1330 µmol/g and k_{try}=11.6 µmol/l are obtained; in this case, when albumin is added to the solution, both binding effects and a reduction of maximum tryptophan uptake must be considered in order to predict the reduction in tryptophan adsorbed amount (Annesini et al., 2008).

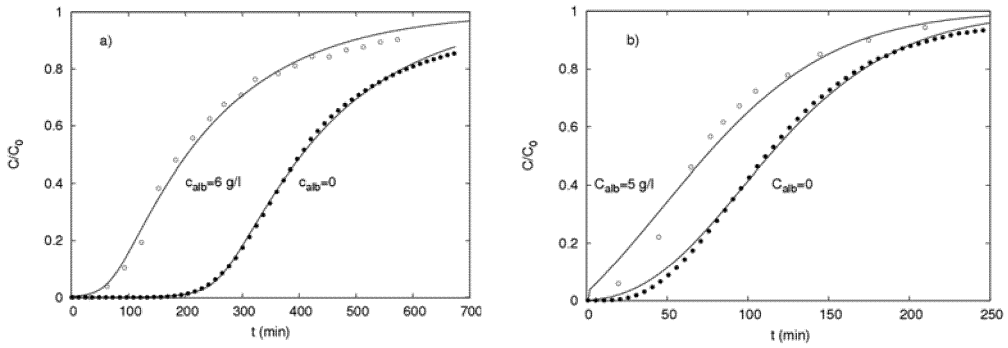

Figure 4 *Typical tryptophan breakthrough curves on activated carbon (a) and polymeric non-ionic resin (b). Line: model fitting; circles: experimental data.*
(a) Activated Carbon: Q=6 ml/min ; M=2 g ; C_{alb}=800 µmol/l ; K_c=1.4 10^{-6} cm/s
(b) Polymeric Resin: Q=1.3 ml/min ; M=2.4 g ; C_{alb}=400 µmol/l ; K_c=1.3 10^{-7} cm/s

The equilibrium experiments show that both the polymeric resin and the activated carbon tested can be considered as tryptophan adsorbents, even if the adsorption capacity of the activated carbon is much higher than that of the resin.
As for fixed-bed adsorption kinetics, figure 4 reports typical breakthrough curves for tryptophan on activated carbon (a) and polymeric resin (b). In both cases, tryptophan breakthrough curves from albumin-free and albumin-containing solutions are compared. Albumin presence causes a "back translation" of tryptophan breakthrough curves, as a consequence of the reduction of efficiency of the adsorption process.
Tryptophan adsorption from albumin-free solutions in fixed bed column was described assuming linear driving force (LDF) mass transfer kinetics. Under this hypothesis, tryptophan mass balances in the liquid and solid phases can be written as follows:

$$\varepsilon \frac{\partial c_{tox}}{\partial t} + (1-\varepsilon)\frac{\partial q_{tox}}{\partial t} = D\frac{\partial^2 c_{tox}}{\partial z^2} - v\frac{\partial c_{tox}}{\partial z} \tag{7}$$

$$\frac{\partial q_{tox}}{\partial t} = \frac{3}{R}K_c(q^*_{tox} - q_{tox}) \tag{8}$$

Equations (7) and (8) were integrated with the following initial and boundary conditions

$$t = 0 \qquad 0 \le z \le 1 \qquad c_{tox} = 0 \qquad q_{tox} = 0 \tag{9}$$

$$t > 0 \qquad z = H \qquad \frac{\partial c_{tox}}{\partial z} = 0; \qquad t > 0 \qquad z = 0 \qquad vc^{in}_{tox} = -D\frac{\partial c_{tox}}{\partial z} + vc_{tox} \tag{10}$$

In the above equations, q_{tox} is the specific toxin adsorbed amount per unit volume of adsorbent, q^*_{tox} the specific toxin adsorbed amount in equilibrium with the toxin concentration in the liquid phase and K_c is the LDF mass transfer coefficient;

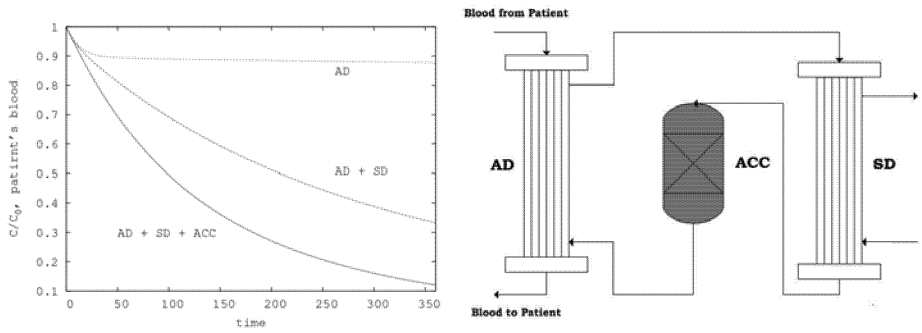

Figure 4 *Example of patient-artificial liver device simulation (flow rate: blood 230 ml/min, dialysate 150ml/min; albumin concentration: blood 600 μmol/l, dialysate from 300 to 3000 μmol/l; initial tryptophan concentration 471 μmol/l; mass of activated carbon 200 g; mass of polymeric resin 100 g; for the albumin dialyser and secondary dialysis module data are taken from specification sheet (Fresenius F40).*

furthermore, ε is the bed porosity, v the interstitial fluid velocity, D the toxin dispersion coefficient, calculated by the model proposed by Chung et al. (1968) and R the radius of adsorbent particles. This model was fitted to the experimental breakthrough curves obtained with albumin-free solutions, using K_c as adjustable parameter (see figure 4).

The same model proved to predict adequately the breakthrough curves obtained with albumin-containing solutions, accounting only for changes in equilibrium conditions caused by the presence of albumin in the liquid phase: figure 4 shows an example of prediction obtained assuming that the same K_c value applies to same flow-rate experiments, regardless of albumin concentration in the feed solution.

Finally, is worth noting that the overall mass transfer coefficient for activated carbon is one order of magnitude higher than that of the polymeric resin, confirming the better performance of activated carbon as tryptophan sorbent. Nevertheless, a polymeric resin can be chosen when an higher biocompatibility of the adsorbent is required, as in the Prometheus system, in which plasma comes into direct contact with adsorbents.

4. Simulation of a liver support device session

The theoretical models presented in the previous sections were used to model an albumin dialysis liver support device, including recirculation and regeneration of the dialysate solution (see scheme in figure 5). A single compartment model was used for the patient, neglecting endogenous tryptophan production.

Different recirculation/regeneration policies were compared in the simulations: recirculation without regeneration (AD), regeneration with a standard dialysis module (AD+SD) and regeneration with a standard dialysis module and an activate carbon adsorption column (AD+SD+ACC). Respect to tryptophan removal, the latter regeneration policy is equivalent to a MARS treatment; actually the, MARS device include also an anionic resin column in the regeneration circuit, but, as shown by (Look et al. 2002), this unit has a considerably minor adsorption capacity for tryptophan and its contribution to tryptophan removal from dialysate is negligible.

Some simulation outputs are reported in figure 5, where the performance of different dialysate regeneration policies are compared. It is evident that without dialysate regeneration, the detoxification process becomes rapidly ineffective, due to the build-up of tryptophan concentration in the dialysate. A traditional dialysis module in the regeneration circuit improves the effectiveness of the process, providing a continuous removal of tryptophan. An even better result is obtained if an activated carbon adsorption column is added to the regeneration circuit, at least until column saturation is reached. It is worth considering that an high albumin concentration in the dialysate improves the performance of the albumin dialysis module, but reduces the efficiency of both the standard dialysis module and adsorption column in the regeneration line. Further investigation of these processes could allow to evaluate a trade-off between these two aspects and help in designing albumin dialysis liver support devices.

Acknowledgments

The Authors thank prof. Luigi Marrelli and ing. Gaja Croci for their useful contribution.

References

Annesini, M.C., Di Paola L., Marrelli L., Piemonte V., Turchetti L., 2005, The International journal of artificial Organs, 7, 28.

Annesini, M.C. Di Carlo C., Piemonte V., Turchetti L., 2008, Biochemical Engineering Journal (in press).

Patzer, J., 2006, Therapeutic Apheresis and Dialysis, 10, 2.

Stange, J., Hassanein I.T., Mehta R., Mitzner S.R., Barlett R.H., 2002, artificial Organs, 26, 2.

Sauer I.M., Goetz M., Steffen I., Walter G., Kehr D.C., Schwartlander R., Hwong Y.J., Neuhaus P., 2004, Hepatology 39,5.

Rifai K., Ernst T., Kretshmer U., Bahr M.J., Schneider A., Hafer C., Haller H., Fliser D., 2003, Journal of Hepatology, 39.

Mitzner, S.R., Stange, J., Klammt, S., Peszynski, P., Schmidt, R., Nöldge-Schomburg, G., 2001, Journal of the American Society of Nephrology, 12S.

Stange, J., Ramlow, W., Mitzner, S., Schmidt, R., Klinkmann, H., 1993, Artificial Organs, 17.

McMenamy R.H., Onkley J.L., 1958, Juornal of Biological Chemistry, 233.

Sun S.F., Hsiao C.L., 1993, Journal of Chromatography, 648, 2.

Chung S.F., Wen S., 1968, AIChE Journal, 14.

Look J., Mitzner S.R., Peters E., Schmidt R., Stange J., 2002, Liver, 22, 35.

CHEMICAL ENGINEERING TRANSACTIONS, Volume 14, 2008
Edited by G. Marino, E. Bardone, A. Viglia
 ISBN 978-88-95608-02-0

Optimisation studies on multiple elicitor addition in microbial systems: *P. chrysogenum* and *B. licheniformis*

R. Nair[1], T. Murphy[1], I. Roy[1], A. Harrop[2], K. Dixon[2], T. Keshavarz[1].
[1]Applied Biotechnology Research Group, Department of Molecular & Applied Biosciences, University of Westminster, London, United Kingdom
[2]Bioprocess Development Group, Pfizer limited, Sandwich, United Kingdom

Addition of oligosaccharide elicitors results in a series of coordinated events in microbial cells leading to changes in morphological and/or physiological responses in the microbial cultures. To expand the potential of elicitation in microbial systems from laboratory to industrial scale it is essential to establish the potential generic nature of the elicitors' effects and provide concrete reasons for the changes observed. Mannan oligosaccharides derived from locust bean gum, oligomannuronate and oligoguluronate from sodium alginate were used in this study. The effect of multiple addition of the same elicitor was investigated with a prospect that repeated addition would re-trigger the stimulation resulting in either maintenance of the antibiotic at high levels or enhancement of the production rate. Repeated addition of the same elicitor did not show any significant increase in the antibiotic concentrations compared to single elicitor additions. However, optimisation studies based on multiple additions of different elicitor types at different time and concentration showed increases of 74% and 34% in the penicillin G and 108% and 61% in the bacitracin A production compared to the control and single elicitor-supplemented cultures, respectively.

Introduction

Improvement of strains and cultivation procedures to obtain high yields has been one of the main objectives in industrial research. Strain improvement has been achieved by repeated rounds of random mutation and subsequent selective screening (Díez *et al.*, 1996). This classical approach is very powerful but has limited mutagenic potential and lacks specificity. The world demand for antibiotic production is ever increasing and one of the ways to supply this demand is to look for novel approaches to increase antibiotic production. One of the possible methods by which secondary metabolite production can be increased is through elicitation. An elicitor can be defined as a substance which, when introduced in trace amounts to a living cell system as a non-nutrient additive, can trigger certain morphological and/or physiological changes in the system. This phenomenon is termed as elicitation. Elicitors are classified as physical or chemical, biotic or abiotic and complex or defined depending on their origin and molecular structure (Radman *et al.*, 2003).

From early studies carbohydrates have been implicated in the overproduction of secondary metabolites in plant cell cultures. Elicitation studies in microbial cultures have focused mainly on the use of carbohydrates as elicitors. Carbohydrates are the building blocks of many of the structural polymers that give form to living cells and organisms, and they play important roles in the interactions of cells with one another as well as with their environment (Albersheim *et al.*, 1992). The extensive stereochemistry, multiple hydroxyl groups, oxygen atoms and accessible hydrophobic regions characteristic of glycosyl residues make oligosaccharides ideal ligands for precise interactions with recognition sites. However, only few oligosaccharides and polysaccharides have been screened for their elicitation effects. A fast screening method for characterization of a range of carbohydrates is needed for use in microbial cultures as effective and efficient elicitors. The use of oligosaccharides and polysaccharides as elicitors to enhance production of plant metabolites has been extended recently to different microbial cultures for overproduction of commercially useful by-products such as pigments (Nair *et al.*, 2005), antimicrobials (Ariyo *et al.*, 1997; Murphy *et al.*, 2007) and enzymes (Petruciolli *et al.*, 1999). Most of the commercially important secondary metabolites are produced by microbial cultures. The increased production through elicitation of the secondary metabolites from microbial cultures has opened up a new area of research which might have important economical benefits for the bio-pharmaceutical industry. It is clearly of practical as well as theoretical interest to seek the evidence of enhancement of secondary metabolites in microbial cultures.

In this work we have optimised the addition of multiple elicitors and studied the subsequent effect of addition at different times and concentrations on the antibiotic production in *P. chrysogenum* and *B. licheniformis* cultures.

Materials And Method

Microorganisms

Penicillium chrysogenum ATCC 48271 from American Type Culture Collection, Rockville, Maryland, USA and *Bacillus licheniformis* NCIMB 8874 from Natural Collection of Industrial and Marine Bacteria, UK, were used in this study.

Elicitor preparation

Three oligosaccharide elicitors were prepared. Mannan oligosaccharides (MO) were prepared from locust bean gum by enzymatic hydrolysis (Ariyo *et al.*, 1998). Oligomannuronate (OM) and oligoguluronate (OG) was prepared from sodium alginate by partial acid hydrolysis (Ariyo *et al.*, 1997).

Addition of elicitors

Oligosaccharide elicitors were dissolved in distilled water at the required concentrations and sterilised at 115°C for 15 min. No elicitor was added to the control culture. Experimental setup for the optimisation of the multiple elicitor addition studies in *P. chrysogenum* and *B. licheniformis* are presented in Table 1 and 2.

Table 1. Experimental setup for the optimisation of multiple elicitor addition for the enhancement of penicillin G in the cultures of *P. chrysogenum*

Flask Set	Elicitor I	Concentration (mg L^{-1})	Addition time (h)	Elicitor II	Concentration (mg L^{-1})	Addition time (h)
1 (Control)	-	-	-	-	-	-
2	MO	150	48	-	-	-
3	MO	150	48	MO	75	72
4	MO	150	48	MO	75	96
5	MO	150	48	MO	150	72
6	MO	150	48	MO	150	96
7	MO	150	48	OM	75	72
8	MO	150	48	OM	75	96
9	MO	150	48	OM	150	72
10	MO	150	48	OM	150	96

Table 2. Experimental setup for the optimisation of multiple elicitor addition for the enhancement of bacitracin A in the cultures of *B. licheniformis*

Flask Set	Elicitor I	Concentration (mg L^{-1})	Addition time (h)	Elicitor II	Concentration (mg L^{-1})	Addition time (h)
1 (Control)	-	-	-	-	-	-
2	OG	200	24	-	-	-
3	MO	100	0	OG	200	24
4	MO	150	0	OG	150	24
5	MO	200	0	OG	100	24
6	MO	150	0	MO	150	24
7	OG	100	0	MO	200	24
8	OG	150	0	MO	150	24
9	OG	200	0	MO	100	24
10	OG	150	0	OG	150	24

Culture conditions

P. chrysogenum: Two culture media were used: *Penicillium* Growth Medium and Penicillin Production Medium (Nair *et al*., 2005). Both media were adjusted to pH 6.5 with 2 M KOH before sterilization. Calcium carbonate was added as a buffering agent to a final concentration of 10 g L^{-1}. The growth medium was inoculated with spores at a final concentration of 10^6 spores mL^{-1}. The flasks were maintained at 26°C in a rotary shaking incubator at 200 rpm with a 2 cm throw for 48 h. For penicillin G production, 10% of the seed culture was added to the production medium and maintained at the same conditions as for growth. Phenylacetic acid was added to 24 h old cultures as a precursor for penicillin G synthesis and maintained at 1-1.5 g L^{-1}. Experiments were carried out in triplicate.

B. licheniformis: Chemical defined media was used for growth and bacitracin A production by *B. licheniformis* as decribed by Murphy *et al*. (2007). Growth Medium was inoculated with 1 mL of spore suspension (10^7 spores mL^{-1}) and incubated at 37ºC on a rotary shaker at 200 rpm for 16 h. For bacitracin A production, 10% of seed culture was used to inoculate the production medium, fermentation conditions were kept as described for the growth. Experiments were carried out in triplicate.

Assay

Penicillin G assay: Penicillin G and phenylacetic acid concentration in the culture broth were analysed by a gradient HPLC method (Adlard *et al.,* 1991) using a Phenomenex C8 (5 µm) column where the flow rate was set to 1.0 mL min^{-1} and the data measured at 220 nm. Standard calibration curve was constructed using sodium salts of penicillin G as standard.

Bacitracin A assay: Bacitracin A production was quantified by a gradient HPLC method (Pavli and Kmetec, 2001) using a Kromasyl Phenomenex C8 (5µm) column maintained at 40ºC. The flow rate was set to 1.4 mL min^{-1} and measurements were obtained at 254 nm. Standard calibration curve was constructed using zinc bacitracin as standard.

Biomass assay: Biomass production by *P. chrysogenum* was measured as cell dry weight per litre of culture broth. For determination of biomass in *B. licheniformis* cultures, optical density at 650 nm was used. Biomass assay was carried out in triplicate.

Results And Discussion

In this study repeated addition of the same elicitor from a single source was designed along with addition of different oligosaccharide elicitor derived from another source. The aim of this study was to investigate if repeated contact of the cells with the same or different elicitor would show an increase in the concentration or sustain the antibiotic production, compared to single addition and control cultures. The elicitors chosen, for the studies with *P. chrysogenum* were MO and OM. OG was not selected because it chelates with the calcium carbonate in the medium forming precipitates/complexes. Besides, previous studies have demonstrated that, MO at 150 mg L^{-1} had the highest increase in penicillin G production followed by OM and then OG; the latter two coming from the same source (Radman *et al.,* 2003). Following the experimental setup as shown in Table 1, multiple addition of the same elicitor (MO) derived from locust bean gum failed to show any significant increase in the penicillin G production compared to single addition and control cultures ($p>0.05$) (Figure 1). However multiple addition of the elicitor (OM) derived from sodium alginate, along with MO as the first elicitor showed significant increase in the penicillin G concentration ($p<0.01$). Maximum penicillin G concentration achieved at 144 h (1.7 g L^{-1}) was observed with OM at 75 mg L^{-1} added at 96 h as shown in Figure 2. As shown in Table 3, the percentage increase in penicillin G production in single elicitor added culture was 34% at 120 h compared to the control. This increase in production decreased gradually as the fermentation progressed. Whereas in Flask 8, after multiple elicitor addition, the percentage increase in penicillin G concentration compared to control was 58% at 120 h and continued increasing for another 24 h.

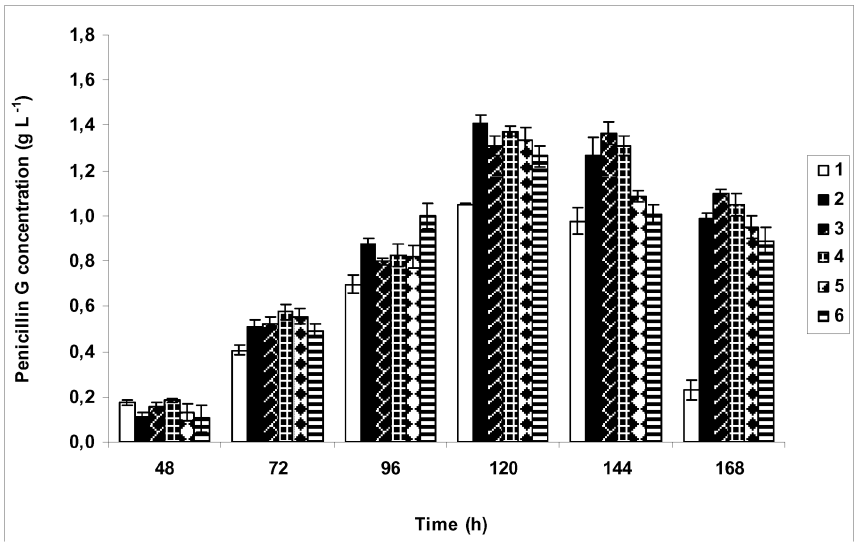

Figure 1. Effect of multiple elicitor addition (MO, MO) on penicillin G production. Flasks: 1 (no elicitors added), 2 (MO: 150 mg L^{-1}, 48 h), 3 (MO: 150 mg L^{-1}, 48 h; MO: 75 mg L^{-1}, 72 h), 4 (MO: 150 mg L^{-1}, 48 h; MO: 75 mg L^{-1}, 96 h), 5 (MO: 150 mg L^{-1}, 48 h; MO: 150 mg L^{-1}, 72 h), 6 (MO: 150 mg L^{-1}, 48 h; MO: 150 mg L^{-1}, 96 h).

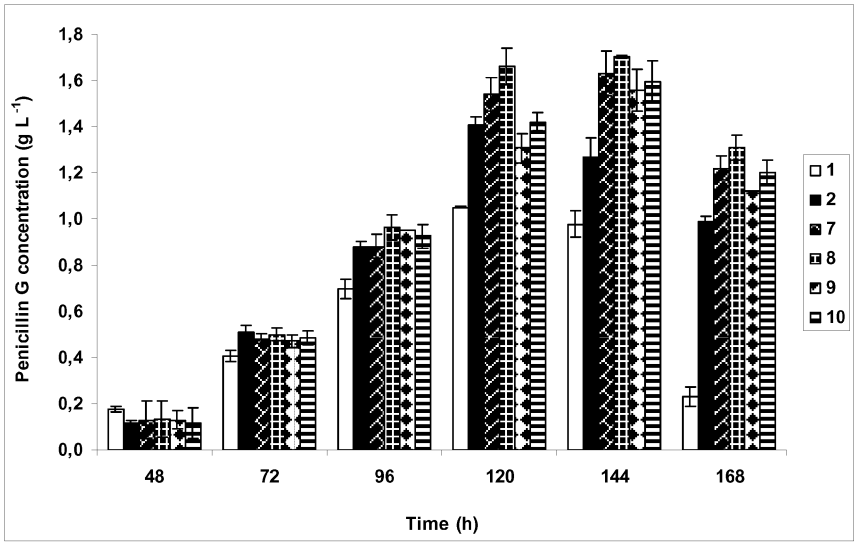

Figure 2. Effect of multiple elicitor addition (MO, OM) on penicillin G production. Flasks: 1 (no elicitors added), 2 (MO: 150 mg L^{-1}, 48 h), 7 (MO: 150 mg L^{-1}, 48 h; OM: 75 mg L^{-1}, 72 h), 8 (MO: 150 mg L^{-1}, 48 h; OM: 75 mg L^{-1}, 96 h), 5 (MO: 150 mg L^{-1}, 48 h; OM: 150 mg L^{-1}, 72 h), 6 (MO: 150 mg L^{-1}, 48 h; OM: 150 mg L^{-1}, 96 h).

In the case of bacitracin A, earlier optimisation studies investigating the best elicitation conditions for the enhancement of this antibiotic revealed that 24 h and 0 h were the addition times which resulted in the increase of bacitracin A production. It was also found that OG and MO were the most suitable elicitors under the conditions of this study (Murphy *et al*. 2007). For the reasons mentioned above, only 0 h, 24 h (addition time) and OG, MO elicitors were chosen as parameters for this study.

Maximum bacitracin A production was observed at 60 h for Flasks 1, 2, 3, 4, 5, 8 and 10 (Figure 3, Figure 4). Although multiple elicitor supplementation with the same elicitor (OG, Flask 6) increased the bacitracin A production after its addition, the maximum titre obtained at 60 h was not significantly different ($p>0.05$) compared to the control. In contrast, as observed in Figure 4, when elicitors OG followed by MO were added to the culture, the antibiotic production was not only significantly ($p<0.01$) enhanced reaching concentrations of 0.9 g L^{-1} and 0.8 g L^{-1} for Flask 7 and 8, respectively, but also the maximum bacitracin A concentration was reached 12 h earlier than in control cultures (Flask 1: 0.4 g L^{-1} at 52 h).

There was no significant difference ($p>0.05$) observed in the biomass between the control and elicited cultures in both microbial cultures tested.

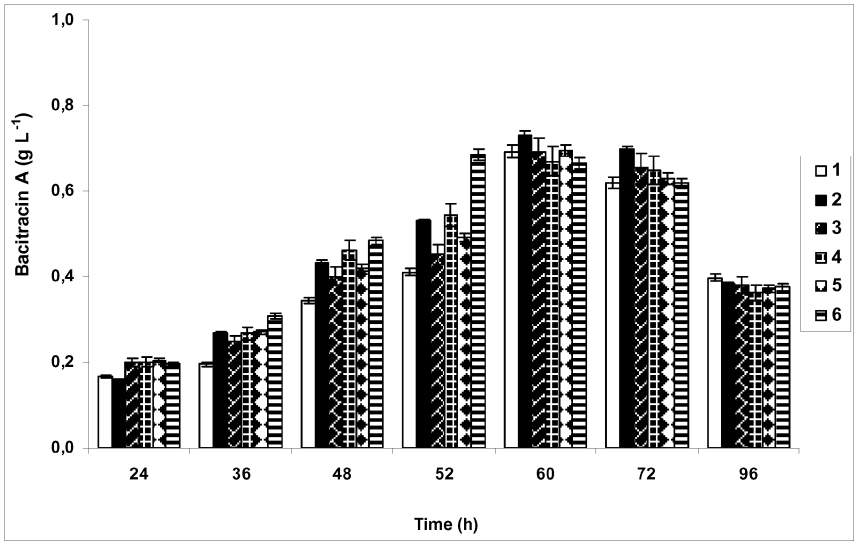

Figure 3. Effect of multiple elicitor addition (MO, OG) on bacitracin A production. Flasks: 1 (no elicitors added), 2 (OG: 200 mg L^{-1}, 24 h), 3 (MO: 100 mg L^{-1},0 h; OG: 200 mg L^{-1}, 24 h), 4 (MO: 150 mg L^{-1}, 0 h; OG: 150 mg L^{-1}, 24 h), 5 (MO: 200 mg L^{-1},0 h; OG: 100 mg L^{-1}, 24 h), 6 (OG: 100 mg L^{-1}, 0 h; MO: 200 mg L^{-1}, 24 h).

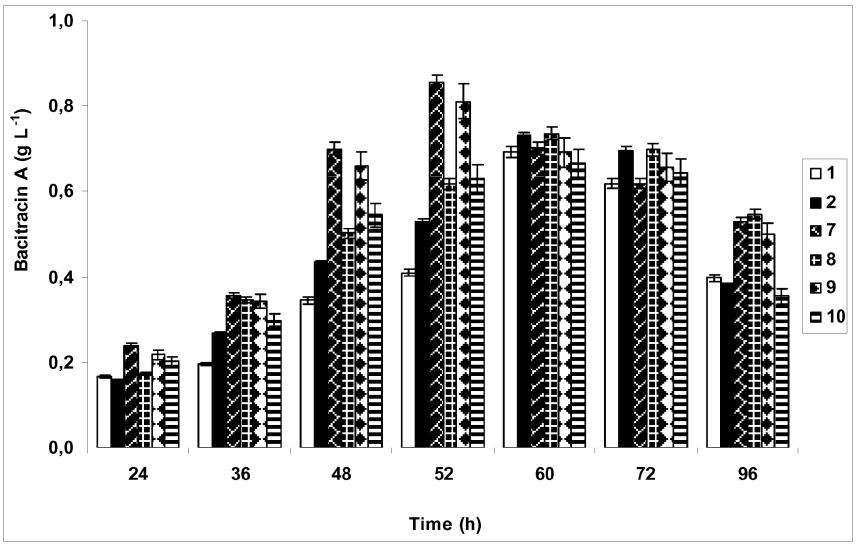

Figure 4. Effect of multiple elicitor addition (OG, MO) on bacitracin A production. Flasks: 1 (no elicitors added), 2 (OG: 200 mg L^{-1}, 24 h), 7 (OG: 100 mg L^{-1}, 0 h; MO: 200 mg L^{-1}, 24 h), 8 (OG: 150 mg L^{-1},0 h; MO: 150 mg L^{-1}, 24 h), 9 (OG: 200 mg L^{-1}, 0 h; MO: 100 mg L^{-1}, 24 h), 10 (OG: 150 mg L^{-1}, 0 h; OG: 150 mg L^{-1}, 24 h).

Antibiotic enhancement was achieved by both cultures (*P. chrysogenum* and *B. licheniformis*) upon addition of oligosaccharide-based elicitors. Increases on penicillin G and bacitracin A using the optimal single elicitor addition condition over the control were 33.9% and 29.5%, respectively. However, as shown in Table 3, higher enhancement of both studied antibiotics was achieved when two different elicitors were added at different time points.

Table 3. Percentage increases in antibiotic production during multiple elicitation addition fermentations.

	Percentage Increase (%)			
	Penicillin G		Bacitracin A	
Flask Set	120 h	144 h	52 h	60 h
2	33.9	29.9	29.5	5.6
7	--	--	108.7	1.2
8	58.3	74.2	--	--

These results relate with the hypothesis put forward for plant cells where cells respond to stimulation by elicitors, but behave refractory to second treatment with the same stimulus (Felix *et al.,* 1998). Investigation of this phenomenon in plant cell culture has established that repeated addition of elicitor causes desensitization of cells in a time and concentration-dependent manner.

This desensitization was not associated with increased inactivation of the stimulus or with the disappearance of high-affinity binding sites from the cell surface and thus appears to be caused by an intermediate step in signal transduction. In another experiment, cells did not respond when treated with a second dose of chitin fragments, although they still reacted to xylanase or ergosterol (Granado *et al.,* 1995). Reciprocally, when cells were treated with ergosterol, they were refractory to further stimulation with ergosterol but still responded to chitin fragments and xylanase (Granado *et al.,* 1995). These observations suggest a complex responsiveness of the system, thereby, indicating that the different chemoperception systems are desensitized in an independent manner.

In our study with microbial cells, it was observed that both cultures show similar behaviour to repeated and mixed elicitor addition. From the optimisation studies, MO (150 mg L^{-1}) added at 48 h followed by OM (75 mg L^{-1}) added at 96 h was the optimised condition for the enhancement of penicillin G production. While OG (100 mg L^{-1}) added at 0 h followed by MO (200 mg L^{-1}) added at 24 h was chosen for the enhancement of bacitracin A. The optimisation of multiple elicitor addition in microbial cultures leading to significant enhancement of a secondary metabolite production is reported for the first time. The work carried out so far suggests that application of elicitation can greatly contribute to future improvement in secondary metabolite production, which is crucial, given the economic benefits. This work can have an impact for larger scale production and the selection of this model system was used as a control for future application in different microbial systems.

Acknowledgement

The authors would like to thank Pfizer Ltd. for its partial support of this project.

References

1. Adlard M.W., B.M. Gordon, T. Keshavarz, C. Bucke, M.D. Lilly, A.T. Bull and G. Holt, 1991, Biotechnol. Tech. 5, 121.
2. Albersheim, P., A. Darvill, C. Augur, J-J. Cheong, S. Eberhard, M.G. Hahn, V. Marfa, D. Mohnen, M.A. O'Neil, M.D. Spiro and W.S. York, 1992, *Acc. Chem. Res*. 25, 77.
3. Ariyo, T.B., C. Bucke and T. Keshavarz, 1997, Biotechnol. Bioeng. 53, 17.
4. Ariyo, T.B., C. Bucke and T. Keshavarz, 1998, FEMS Microbiol. Letters. 166, 165.
5. Díez, B., E. Mellado, M. Rodríguez, M. Fouces and J.L. Barredo, 1996, *Biotechnol. Bioeng.* 55, 216
6. Felix, G., M. Regenass and T. Boller, 1993, Plant J. 4, 307.
7. Felix, G., K. Baureithel and T. Boller, 1998, Plant Physiol. 117, 643.
8. Granado, J., G. Felix and T. Boller, 1995, Plant Physiol. 107, 486.
9. Murphy, T., R. Parra, R. Radman, I. Roy, A. Harrop, K. Dixon and T. Keshavarz, 2007, Enzyme Microb. Technol. 40, 1518.
10. Nair, R., R. Radman, I. Roy, C. Bucke and T. Keshavarz, 2005, AIDIC. 7, 239.
11. Pavli, V and V. Kmetec, 2001, J. Pharm. Biomed. Anal. 24, 977.
12. Petruccioli, M., F. Federici, C. Bucke and T. Keshavarz, 1999, Enzyme Microb. Technol. 24, 397.
13. Radman, R.,T. Saez, C. Bucke and T. Keshavarz, 2003, Biotechnol. Appl. Biochem. 37, 91.

CHEMICAL ENGINEERING TRANSACTIONS, Volume 14, 2008
Edited by G. Marino, E. Bardone, A. Viglia
 ISBN 978-88-95608-02-0

Optimization Of Capsaicin Acylase Production From *Streptomyces Mobaraensis* In Bench-Top Reactor

Crognale S., Barghini P., Di Matteo P., Federici F., Ruzzi M.
Department of Agrobiology and Agrochemistry, University of Tuscia
Via C. de Lellis, snc – 01100 Viterbo (Italy)
crognale@unitus.it; ruzzi@unitus.it

Capsaicin, the major pungent principle in hot pepper fruit, can be hydrolyzed enzymatically to vanillylamine (a natural precursor of vanillin) using a specific acylase from *Streptomyces mobaraensis*. Production of this enzyme using strain DSM40847 was studied under batch fermentation conditions in stirred tank (STR) and airlift (AR) bioreactors. The process performance in both fermentation devices was different with respect to biomass, enzyme concentration and specific yield (enzyme activity/biomass content); in particular the specific yield was lower in the AR (5.7 mU/g of biomass) than in the STR (6.25 mU/g of biomass). Experiments carried out in STR bioreactors at controlled (DO = 20% of saturation) and uncontrolled dissolved oxygen concentration, and at constant stirrer speeds (300, 450 and 600 rpm) demonstrated that the DO level has no remarkable effect on the production of the capsaicin-hydrolyzing enzyme, which is mainly produced in a cell-associated form.

1. Introduction

Vanillin (4-hydroxy-3-methoxybenzaldehyde) is the major component of natural vanilla, which is one of the most widely used and important flavouring ingredient worldwide. Since current production of natural vanilla is not sufficient to meet the increasing demand for this flavour compound, vanillin has been a target for biotechnological production by several approaches: use of enzymes to release or generate vanillin from *Vanilla* and other plant material, development of tissue cultures, genetic modification and, finally, use of microbial cultures (Priefert *et al*., 2001; Walton *et al*., 2003). Capsaicin (8-methyl-N-vanillyl-6-nonenamide), the major pungent principle in hot pepper fruit (*Capsicum annuum L.*), is a potentially attractive and cheap feedstock for the production of vanillin. Capsaicin can be hydrolyzed enzymatically to vanillylamine (4-hydroxy-3-methoxybenzylamine), a natural precursor of vanillin, by either specific bacterial acylases (Koreishi et al, 2006; Flagan and Leadbetter, 2006) or mammalian carboxylesterases (Oi et al., 1992). So far, the only one bacterial acylase, which efficiently hydrolyzes capsaicin and has been characterized, is the capsaicin acylase from *Streptomyces mobaraensis*. This enzyme is an heterodimeric protein that consists of two dissimilar subunits (61 and 19 KDa) and has a specific activity toward capsaicin 100-10000 times higher than that of capsaicin-hydrolyzing enzymes found in mammalian (Koreishi *et al.*, 2006). The vanillin production from capsaicin as natural source using a bi-enzymatic process (with mammalian and bacterial enzymes) has been

previously described (van den Heuvel *et al*., 2001), but it was never translated into a commercial process because the mammalian enzyme used to obtain vanillylamine was too expensive. The discovery of microbial acylases that efficiently hydrolyze capsaicin provides a valuable opportunity to develop a cost-effective process for enzymatic synthesis of vanillin. We are examining different strategies for enhancing fermentative production of capsaicin acylase from *S. mobaraensis* strain DSM40847 in the effort to reduce the cost of acylase enzymes suitable for vanillin production.

2. Materials and Methods

2.1 Chemicals

All chemicals and HPLC solvents were of the highest purity commercially available and were purchased from Fluka (Buchs, Switzerland) and Carlo Erba (Milan, Italy).

2.2 Microorganism cultivation

S. mobaraensis DSM40847 was used in this work. Batch fermentation were carried out in duplicate in Erlenmeyer flasks on an orbital shaker at 180 rpm or in stirrer tank reactors Applikon (Schiedam, The Netherlands) and in air lift reactors, unless indicate otherwise, under the following conditions: incubation temperature 30°C, aeration rate, 1vol/vol min^{-1}; stirrer speed, 450 rpm; silicone antifoam 1ml/L.

2.3 Culture media

The following media were used in the present work:
Pre-inoculum medium: glucose (10.0 g/L), dextrin (10.0 g/L), N-z amine (5.0 g/L), yeast extract (5.0 g/L), $CaCO_3$ (1.0 g/L).
Medium A: soluble starch (40.0 g/L), polypeptone (20.0 g/L), beef extract (40.0 g/L), $MgSO_4$ (20.0 g/L), K_2HPO_4 (2.0 g/L).
Medium C: glucose (20.0 g/L), yeast extract (5.0 g/L), asparagine (1.5 g/L), $CaCO_3$ (5.0 g/L), NaCl (1.0 g/L), $MgSO_4 \times 7\ H_2O$ (0.5 g/L), $CaCl_2 \times 2H_2O$ (0.1 g/L), 1 ml of mineral solution (boric acid 0.5 g/L; $CuSO_4 \times 5\ H_2O$ 0.04 g/L; KI 0.1 g/L; $FeCl_3 \times 6\ H_2O$ 0.2 g/L; $MnSO_4 \times H_2O$ 0.4 g/L; $FeSO_4 \times 7\ H_2O$ 0.4 g/L; ammonium molybdate 0.2 g/L).
Medium S/BIS: glucose (10.0 g/L), peptone (4.0 g/L), yeast extract (4.0 g/L), $MgSO_4 \times 7\ H_2O$ (0.5 g/L), K_2HPO_4 (4.0 g/L).
Medium M8: meat extract (2.0 $g \cdot l^{-1}$), yeast extract (2.0 $g \cdot l^{-1}$), casein hydrolysate (4.0 g/L), glucose (10.0 g/L), soluble starch (20.0 g/L), $CaCO_3$ (3.0 g/L).
AF/Ms: glucose (20.0 g/L), soybean meal (8.0 g/L),yeast extract (2.0 g/L), NaCl (1.0 g/L).
AUR/M: maltose (20.0 g/L), dextrin (10.0 g/L), yeast extract (2.0 g/L), meat extract (4.0 g/L), peptone (4.0 g/L), soybean meal (15.0 g/L),$CaCO_3$ (2.0 g/L).
Medium T: glucose (5.0 g/L), meat extract (4.0 g/L),yeast extract (1.0 g/L), peptone (4.0 g/L), soybean meal (10.0 g/L), $CaCO_3$ (1.0 g/L), NaCl (2.5 g/L).

2.4 Analytical assays

Biomass concentration was determined as dry weight; broth samples were recovered by filtration on pre-weighed Whatman GF/A discs, the filters were dried at 105°C for 24 h, cooled in desiccator and weighed. Acylase activity was determined by a

spectrophotometric method using a double enzymatic reaction with DAO and POD. Total protein content was measured using the Bradford method.

3. Results and Discussion

3.1 Effect of media composition on acylase production

Fermentations in a number of different liquid media were carried out using shaken flasks to find a medium that promoted production of capsaicin hydrolytic enzymes. Selected media investigated are shown in Table 1. Medium A, which contains soluble starch, polypeptone and beef extract, produced the highest titres of biomass and capsaicin acylase and was chosen for future investigations.

Table 1: Effect of medium composition on biomass and acylase production by *S. mobaraensis* DSM40847 in shaken cultures after 144 hours of growth.

	Biomass (g/L)	**Acylase (U/ml)**
Medium A	32 ± 0.9	0.02
Medium C	9.29 ± 0.2	0.00053
***Medium S/BIS*:**	8.4 ± 0.3	0.003
Medium M8	12.9 ± 0.7	0.0081
AF/Ms	8.12 ± 0.5	0
AUR/M:	9.94 ± 0.2	0.008
Medium T	4.93 ± 0.06	0.015

3.2 Effect of agitation speed

Since there was no literature on the effect of agitation speed on the production of capsaicin acylase by *S. mobaraensis* in a stirred tank reactor (STR), the fermentations were carried out at the constant temperature of 30°C and aeration rate of 1.0 vvm, but with different agitation speeds of 300, 450 and 600 rpm, respectively. The maximum level of acylase activity was achieved at 450 rpm after 168 hours of fermentation (Fig.1). When the agitation speed was higher or lower than 450 rpm, we observed a reduction in the bacterial growth that was attributed to the effect of shear stress at the higher agitation speed (600 rpm) and of oxygen limitation at the lower speed (300 rpm). Time profiles of biomass dry weight, secreted proteins and enzyme production at 450 rpm are shown in Figure 1. Biomass concentration increased rapidly (up to 7.3 g [dry weight]/L) during the first 24 hours of fermentation and continued to increase, albeit at a lower rate, until the end of the experiment. Dissolved oxygen concentration rapidly dropped at values near zero during the first 24 hours, remained unaltered for the next 120 hours and then increased till the end of the fermentation. Surprisingly, production of acylase activity rapidly increased between 144-168 hours of fermentation, when an increase in dissolved oxygen levels was measured, and reached a maximum level (0.17 U/ml) at the end of the fermentation. Under optimal culture conditions in STR the production of acylase could be increased 8-fold when compared with shake flask.

3.3 Effect of dissolved oxygen tension

The influence of different percent of air saturation on cell growth and acylase production was investigated by controlling DO at constant concentration of 20%. The effects of DO on the fermentation are shown in Figure 2. At 20% of air saturation, we could not observe a significant increase of dry cell weight which indicated that the availability of molecular oxygen in the growth medium is not a limiting factor. The highest acylase yield was obtained in the experiments at uncontrolled dissolved oxygen concentration. In both case the maximal acylase production was obtained at the end of fermentation when the DO levels raised up.

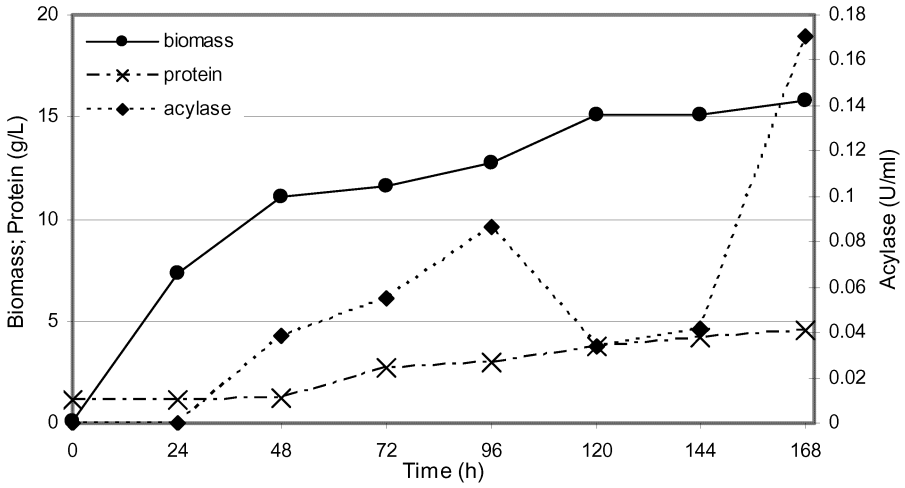

Figure 1. Time courses of biomass, proteins and acylase production during STR (450 rpm) fermentation of *S. mobaraensis* DSM40847.

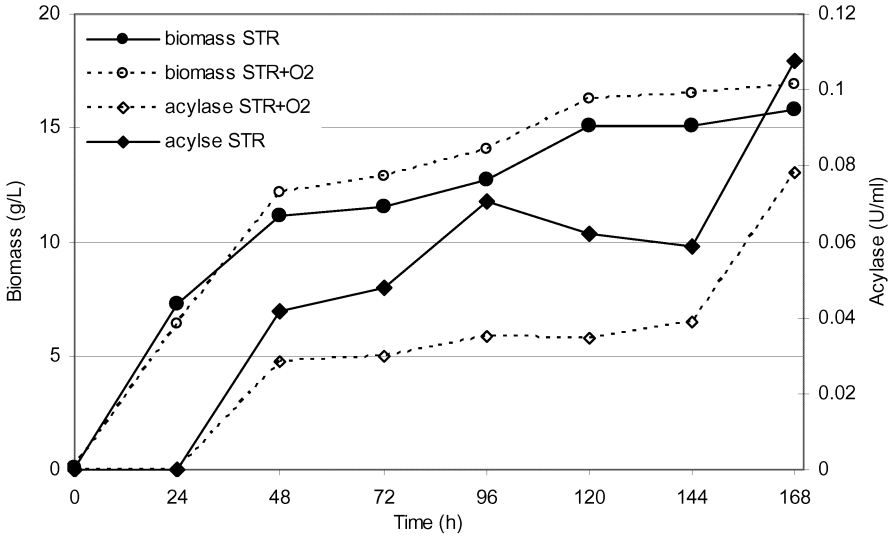

Figure 2. Time profiles of cell growth and acylase production of batch cultures of *S. mobaraensis* DSM40847 maintained at controlled (STR+O_2; DO=20% of saturation) and uncontrolled (STR) dissolved oxygen concentration.

3.4 Comparison of different bioreactor systems

Since the shear force arising in STR bioreactors caused undesired effects on the growth of *S. mobaraensis*, the possibility to cultivate the microorganism in air lift (AR) reactors was also evaluated. Biomass and acylase production in the AR were higher than that achieved in the STR (Table 2). However, the increase in acylase levels was not proportional to changes in biomass concentration and consequently the specific yield (enzyme activity/biomass content) in the AR (5.7 mU/g of biomass) was lower than that achieved in the STR (6.25 mU/g of biomass).

Table 2: Maximal acylase and biomass production obtained in STR and AIR LIFT (AR) reactors.

	Acylase (U/ml)	**Biomass (g/L)**
STR	*0.10*	*16*
AR	*0.16*	*28*

3.5 Acylase localization

Analysis of acylase activities associated with *S. mobaraensis* DSM40847 showed the presence of a cell associated enzyme active against capsaicin. At the end of the fermentation, capsaicin-hydrolytic activity of DSM40847 cells cultured in STR reactors was about 6-7 U/g of biomass. Approximately 90% of this enzymatic activity could be extracted with phosphate buffer containing 0.8 M KCl, suggesting that the enzyme is

probably associated with cell walls of *S. mobaraensis*, primarily by ionic-type interactions.

5. Conclusion

Production of acylases with capsaicin hydrolytic activity is possible by batch fermentation of *S. mobaraensis* using different reactor systems (STR and AR). Strain DSM40847 was able to produce a cell-associated enzyme active on capsaicin. The optimization of culture conditions permitted to obtain a total (extracellular plus cell-associated) acylase activity of 7 U/g of biomass.

This research was supported by the MIUR through the PRIN 2006.

6. References

Flagan, S.F., Leadbetter, J.R., 2006, Utilization of capsaicin and vanillylamine as growth substrates by *Capsicum* (hot pepper)-associated bacteria. Environ Microbiol. 8: 560-565.

Koreishi, M., Zhang, D., Imanaka, H., Imamura, K., Adachi, S., Matsuno R., Nakanishi, K., 2006, A novel acylase from *Streptomyces mobaraensis* that efficiently catalyzes hydrolysis/synthesis of capsaicins as well as N-Acyl-L-amino acids and N- Acyl-peptides. J. Agric. Food. Chem. 54: 72-78.

Priefert, H., Rabenhorst, J., Steinbüchel, A., 2001, Biotechnological production of vanillin. Appl. Microbiol. Biotechnol. 56: 296–314.

Prince, R.C., Gunson, D.E., 1994, Just plain vanilla? Trends Biochem. Sci. December: 521.

Oi, Y., Kawada, T., Watanabe, T., Iwai, K., 1992, Induction of capsaicin-hydrolyzing enzyme activity in rat liver by continuous oral administration of capsaicin. J Agric Food Chem. 40: 467-470.

Van den Heuvel,H., R., Fraaje M.W., Laane, C., van Berkel W.J. 2001 Enzymatic synthesis of vanillin. J. Agric. Food. Chem. 49: 2954-2958.

Walton, N.J., Mayer, M.J., Narbad, A., 2003, Vanillin. Phytochemistry. 63: 505-515.

CHEMICAL ENGINEERING TRANSACTIONS, Volume 14, 2008
Edited by G. Marino, E. Bardone, A. Viglia
 ISBN 978-88-95608-02-0

The *mini* BioArtificiaLiver: a cellular biosensor in the drug development process

B.Andria[1], A. Bracco[1], E.Alimenti[1], C.Attanasio[1], A.Tammaro[1], S.Scala[1], RAFM Chamuleau[3], F.Calise[1&2]

[1]Center of Biotechnologies, [2] Liver Transplant Unit, Antonio Cardarelli Hospital

[3] Academic Medical Center, Amsterdam

Address: 9, Antonio Cardarelli Street – 80131 – Naples – Italy

Tel & Fax: 0039 081 747 34 33; e-mail: biotecnologie@ospedalecardarelli.it

Aims

Every year a great amount of financial resources is spent by pharmaceutical companies on unsuccessful Clinical Trials because of poor activity/toxicity ratio, pharmacokinetics and pharmacodinamics accidents including poor Absorption-Distribution-Metabolism-Excretion/Toxicology profiles.
Considering the key role accomplished by the liver in toxicology and metabolism of drugs there is a great need for screening tools using human cells. Furthermore the set up of bio-systems using human cells and able to test candidate drugs could be helpful in reducing the use of animals in the experimental testing as well as lowering costs concerning the drug development process.

Methods

In the Center of Biotechnologies of Cardarelli Hospital, in Naples, in collaboration with the Academic Medical Center of Amsterdam University, we assembled a *mini Bioartificial Liver (mini BAL)* able to host approximately 300,000 millions of viable human hepatocytes. The mini BAL is a three-dimensional system which resembles the best conditions for hepatocyte culturing and, differently from other monolayer approaches, shows a system-integrated oxygenation addressed to metabolism and respiratory functions optimization. Human hepatocytes are obtained by livers discarded from transplantation as well as surgical liver resections. Considering the low availability of human liver cells and in view of our experience, we used porcine hepatocytes in order to standardize the overall process.
Previously we were able to successfully investigate in the mini BALs the effects of different doses of amphetamine, a well-known hepatotoxic drug, for 7 days.
In this experiment we assessed the function of n° 3 minibal charged with 300,000 million viable human hepatocytes (viability$\geq$ 80%) evaluating the specific cell functions through urea production, ammonia clearance, albumin synthesis.
We observed a sharp, dose-dependent, decrease in hepatocytes functionality (urea production) with a restoration of the functionality in the following days.

Results

In the Center of Biotechnologies (Cardarelli Hospital, Naples) we have assembled, in cooperation with Amsterdam University, a *mini Bioartificial Liver (mini BAL)* able to host approximately 300,000 millions of viable human hepatocytes.
In the present study we propose to evaluate the hepatotoxicity of candidate drugs in the miniBAL environment closely resembling an *in vivo* system by utilizing a primary cell culture system in a three dimension oxygenated structure.
The miniBAL is a three-dimensional system which designs the better conditions for hepatocyte culturing and, differently from other monolayer approaches, shows a system-integrated oxygenation addressed to metabolism and respiratory functions optimization.

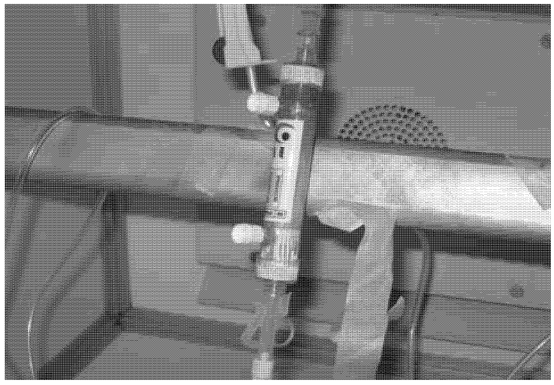

Figure 1: the miniBAL

Human hepatocytes are obtained by surgical resections (under informed consent signed by patients) or livers discarded from organ transplantation. Considering the low availability of human liver cells and in view of our experience, we firstly used porcine hepatocytes in order to standardize the overall procedure.
Our proposal is to use the miniBAL as a system able to detect CYP450-dependent biotransformation reactions of drugs and metabolites as well as for the evaluation of liver specific toxicity when exposed to different molecules. *In other words, this device can be characterized as a human cellular biosensor to evaluate the potential toxicological effects of known and unknown compounds*.
The development of this miniBAL charged with human hepatocytes, as well as the advantages in the standardization procedures of this system, could represent a very important tool to test drugs for potential use in man and to further evaluate, in a simultaneous sequence, more molecules to be assessed for potential hepato-toxic or hepato-trophic effect [(10)].
In particular we are going to investigate how much the variation in conventional biomarkers of hepatic functions (urea synthesis, ammonia clearance, cell viability, etc) is altered by hepatotoxicity-inducing compounds in the miniBAL as an in vitro cell culture system.
We have already successfully investigated the effects of administration of a well-known hepatotoxic drug, amphetamine, in the miniBAL circuit over a 5 days observation. In this experiment we assessed the function of n° 3 minibal charged with 300,000 million viable human hepatocytes (viability≥ 80%) evaluating the specific cell functions through urea production, ammonia clearance, albumin synthesis.

We observed a sharp, dose-dependent, decrease in hepatocytes functionality (urea production) with a restoration of the functionality in the following days.

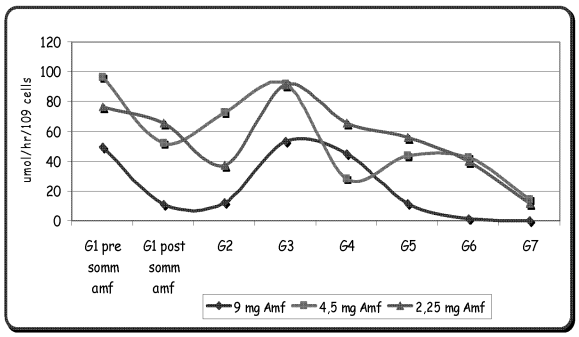

Figure 2: results about urea production

In *vitro* models of liver using isolated primary hepatocytes have been used as screening systems for metabolism evaluation, hepatocyte proliferation studies, and as bioartificial liver support .
The development of tissue and in vitro models based on human cells provides a potential bridge to the gap between animal models and human studies screening the efficacy and safety of new drugs before clinical trials.
We propose the use of the mini BAL system as a method between *in vitro* testing and clinical studies of promising compounds for human healthcare. Our purpose is to use the mini BAL as a system able to detect hepatocellular biotransformation reactions CYP450-dependent and to evaluate the hepatotoxicity of molecules developed for clinical application.
Moreover our report has a paramount significance related to the ethical aspects of preclinical studies. The mini BAL may allow a sensible reduction of the number of animals used in drug testing and a reliable tool for toxicological and pharmacological studies.
We are currently investigating the possibility of performing multiple toxicological profiles with hepatocytes coming from the same source targetet to reproducible and translational data , in order to use a system between *in vitro* testing and clinical studies
Additionally this system will provide long-lasting, data in a early stage ,improving the drug development process as well as the financial and human resources.
The mini bioartificial liver may allow a sensible reduction of use of animals in and can be considered as a "biological hybrid", and a powerful, and reliable tool for toxicological and pharmacological studies

Concluding:
- we have previously investigated the large size BAL as a hepatic system used in a Clinical Trial to metabolically support liver failure bridging 14 acute patients to orthotopic liver transplantation [1, 2, 3, 8,9,11,12,13,14,15].
- now we have set up the miniBAL as a substitute replacing the use of animals and representing a reproducible and reliable tool for toxicological and pharmacological studies of classic molecules and biotechnological drugs.

Conclusions

We propose the use of the mini BAL system as an ”hybrid” in the biological scale, between *in vitro* testing and clinical studies of promising compounds for human healthcare. Our proposal is to use our mini BAL as a system able to detect hepatocellular biotransformation reactions CYP450-dependent.

Finally our report has a paramount significance related to the ethical aspects of preclinical studies. The mini BAL may allow a sensible reduction of the number of animals used in drug testing and a reliable tool for toxicological and pharmacological studies.

Drug-induced liver toxicity is worldwide the leading cause of acute liver failure and post-market drug withdrawals. Every year a great amount of financial resources is spent by pharmaceutical companies on unsuccessful Clinical Trials because of poor activity/toxicity ratio, pharmacokinetics and pharmacodinamics accidents (including poor *Absorption-Distribution-Metabolism-Excretion*-ADME/toxicology profiles) as well as serious adverse effects occurring in the post-marketing *surveillance* phase.
In addition, many candidate compounds have been compelled to cease further development as possible new drugs because they lack of an exhaustive safety evaluation in the early stage of drug discovery.
The liver plays a crucial role in drug metabolism and toxicology, accomplishing many physiological functions (such as synthesis, storage, metabolism, secretion of biogenic components in the living body) as well as in cellular homeostasis. Since these functions are dependent on human parenchymal liver cells, primary cultures of these cells are suitable to be used for toxicological evaluation, such as related to hepatocytes necrosis, etc.
Many human diseases and drug toxicities are very complicated events that can be represented only in animal models, but unfortunately these models lack in human physiology. At this regard preclinical animal studies are often inadequate to evaluate toxicity because of species-specific variation between animal and human hepatocellular functions, necessitating supplementation of animal data with assays to assess human responses.
The evolution from monolayer to collagen sandwich cultures up to three-dimensional systems, able to maintain higher differentiation over a longer term, has led to the development of more suitable and reliable systems for toxicity assessment. The introduction of a compound-specific in vitro cell culture system has numerous advantages, but of most importance, the generation of sufficient results for a toxicology screening and safety evaluation at a low cost, high speed and less animal use can be expected.
More recently the need for screening tools for microscale toxicology assays is becoming greater and more pressing [4,5,6,7]. There is a real need for more predictive systems able to test candidate drugs; moreover these systems could be aimed to lower the costs of drug development process as well as to play a significant role in the 3Rs – the reduction, refinement and replacement of the use of animals in preclinical drug development research.
Pharmaceutical companies have started a toxicity evaluation of candidate drugs at a very early stage in the discovery process in order to reduce the chances of late-stage failure. . Such early-stage toxicity informations require the development of accurate, practical and reproducible in vitro assays reliable for human toxicity prediction .

References

1. Calise F, Mancini A, Amoroso P, Belli A, Bracco A, Ceriello A et al. Functional evaluation of the AMC-BAL to be employed in a multicentric clinical trial for acute liver failure. Transplant Proc 2001;33(1-2):647-9. Chamuleau RAFM, Deurholt T, Hoekstra R. Which are the right cells to be used in a bioartificial liver? Metab Brain Dis 2005;20(4):327-35
2. Chamuleau RAFM, Poyck PP, Van de Kerkove MP. Bioartificial liver: its pros and cons. Ther Apher Dial 2006;10(2):168-74
3. Di Nicuolo G, van de Kerkhove MP, Hoekstra R, Beld MG, Amoroso P, Battisti S et al. No evidence of in vitro and in vivo porcine endogenous retrovirus infection after plasmapheresis through the AMC-bioartificial liver. Xenotransplantation 2005 Jul;12(4):286-92.
4. Gebhardt R, Hengstler JG, Muller D, Glockner R, Buenning P, Laube B et al. New hepatocyte in vitro systems for drug metabolism: metabolic capacity and recommendations for application in basic research and drug development, standard operation procedures. Drug Met Reviews 2003; 35(2&3): 145-213
5. Khetani SR, Bhatia SN. Microscale culture of human liver cells for drug development. Nature Biotechnology 2008 Jan; 26(1): 120-26
6. Kola I, Landis J. Can the pharmaceutical industry reduce attrition rates? Nat Rev Drug Discov 2004 Aug; 3(8):711-5
7. Lee M-Y, Kumar RA, Sukumaran SM, Hogg MG, Clark DS, Dordick JS. Three-dimensional cellular microarray for high-throughput toxicology assays. PNAS 2008; 105(1):59-63
8. Navarro VJ, Senior JR. Drug-related hepatotoxicity. N Engl J Med 2006;354(7):731-9
9. Poyck PP, Hoekstra R, van Wijk AC, Attanasio C, Calise F, Chamuleau RA et al. Functional and morphological comparison of three primary liver cell types cultured in the AMC bioartificial liver. Liver Transpl 2007;13(4):589-98.
10. Poyck PP, Hoekstra R, Chhatta A, Bloemendaal LT, van Wijk AC, Galavotti D et al. Time-related analysis of metabolic liver functions, cellular morphology, and gene expression of hepatocytes cultured in the bioartificial liver of the Academic Medical Center in Amsterdam (AMC-BAL). Tissue Eng 2007 Jun;13(6):1235-46.
11. Schmitmeier S, Langsch A, Jasmund I, Bader A. Development and characterization of a small-scale bioreactor based on a bioartificial hepatic culture model for predictive pharmacological in vitro screenings. Biotech and Bioengineering 2006; 95(6): 1198-1206
12. Van de Kerkove MP, Poyck PP, Van Wijk ACWA, Galavotti D, Hoekstra R, Van Gulik TM et al. Assessment and improvement of liver specific function of the AMC-bioartificial liver. Int J Artif Organs 2005 Jun;28(6):617-30.
13. Van de Kerkove MP, Di Florio E, Scuderi V, Mancini A, Belli A, Bracco A et al. Phase I Clinical Trial with the AMC-bioartificial liver. J Artif Organs 2002 Oct;25(10):950-9.
14. Van de Kerkove MP, Di Florio E, Scuderi V, Mancini A, Belli A, Bracco A et al. Bridging a patient with acute liver failure to liver transplantation by the AMC-bioartificial liver. Cell Transplant 2003;12(6):563-8.
15. Van de Kerkove MP, Poyck PP, Deurholt T, Hoekstra R, Chamuleau RAFM, van Gulik TM. Liver support therapy: an overview of the AMC-Bioartificial Liver research. Dig Surg 2005;22:254-64

CHEMICAL ENGINEERING TRANSACTIONS, Volume 14, 2008
Edited by G. Marino, E. Bardone, A. Viglia
 ISBN 978-88-95608-02-0

Further Studies On Nucleopeptides With DABA-based Backbone

Roviello G. N.[1]*, Musumeci D.[2]*, Bucci E. M.[3], Castiglione M.[1], Pedone C.[1], Benedetti E.[4], Sapio R.[3] and Valente M.[3]
[1] Ist. di Biostrutture e Bioimmagini-CNR, via Mezzocannone 16, I-80134 Napoli;
[2] Bionucleon srl, via D. Montesano 49, I-80131 Napoli;
[3] Bionucleon srl, via Ribes 5, Colleretto Giacosa, I-10010 (TO);
[4] Dip. Scienze Biologiche, Università Federico II, via Mezzocannone 16, I-80134 Napoli.

*these authors contributed equally to this work
correspondence to dmusumeci@bionucleon.com

In continuing our studies on new ODN-like molecules suitable for a wide variety of biomedical and bioengineering applications, here we report further studies relative to a chiral nucleopeptide with a diaminobutyric acid (DABA) backbone. In particular, in this work we describe the synthesis of the nucleoaminoacid monomer with the D stereochemistry, performed in analogy to our previous reports on the L-DABA derivative, and the oligomerization using both enantiomers to form an alternate D,L-nucleopeptide. This oligomer was studied for its ability to bind complementary DNA by CD and UV spectroscopies. Furthermore, the new nucleopeptide showed binding evidence with a free nucleobase probably forming a three-dimensional network based on hydrogen bonding. This kind of structures is of particular interest for the development of new nanomaterials with many desirable properties as well as of new ODN-analogues for biotechnological applications.

In memory of Dr Silvano Fumero, an eminent scientist.

1. Introduction

Polymer gels, typically formed by molecular or macromolecular species cross-linked into network structures, have been intensively studied due to their interesting properties suitable for a wide variety of biomedical and bioengineering applications, including selective drug/gene delivery or sensing devices. Of particular interest are gels stabilized by noncovalent and relatively weak linkages allowing the cross-links to form in reversible fashion (Shay *et al.* 2001) and that respond to changes in the environment, such as temperature, pH or other external stimuli (Sato *et al.* 2001).
By taking advantage of the base recognition in nucleic acids, based on Watson-Crick (W-C)

hydrogen bonding, many researchers investigated gel systems based on DNA (Li *et al.* 2004) able to form extended oligonucleotide structures with well-defined sizes, shapes, branching density and surface functionality (Shchepinov *et al.* 1999) in order to develop new drug delivery systems (Luo *et al.* 2006) or new nanomaterials (Luo 2003) with many desirable properties.

Despite the remarkable advantages of DNA utilization in many research fields, some drawbacks, including a low cellular uptake, as well as enzimatic degradation or acidic depurination susceptivity, limit DNA use in biomedical or bioengineering applications (Uhlmann and Peyman 1990). Therefore, many efforts have been made to introduce new DNA-like molecules more resistant to enzymatic or chemical degradations but still able to form hydrogen bonding with complementary molecules (Matsukura *et al.* 1987, Nielsen *et al.* 1991, Kurreck *et al.* 2002).

In this context, recently we designed, synthesised and characterized a new ODN analogue containing a chiral γ-peptide backbone, based on the diaminobutyric acid (DABA), on which the nucleobase is anchored through a methylene carbonyl linker (Roviello *et al.* 2006 and 2007). Our interest for this non protein diamino carboxylic acid resides on the fact that DABA was found in many natural sources (Foster *et al.* 1987), was produced in simulated stellar conditions (Wolman *et al.* 1972) and also recovered in extraterrestrial meteoritic soil (Meierhenrich *et al.* 2004). Therefore, DABA-based molecules could be developed not only for biotechnological applications, as in the case of polyDABA for gene delivery systems (Iwashita *et al.* 2005), but also to throw light on their possible prebiotic role as nucleopeptides (Nielsen 1993, Meierhenrich *et al.* 2004, Strasdeit 2005). In our research the homothymine oligomer synthesized, containing a backbone entirely formed by L-DABA moieties, didn't show significant ability to bind complementary DNA (Roviello *et al.* 2006 and 2007).

Here we report the synthesis of the homothymine oligomer containing an alternate D,L-DABA-based backbone. This oligomer was studied for its ability to bind complementary DNA or a free nucleobase in order to form a supramolecular structure based on hydrogen bonding and controlled in a thermoreversible fashion. This kind of structures is of particular interest for the development of new nanomaterials with many desirable properties or of new ODN-analogues in biotechnological applications.

2. Results And Discussion

The synthesis of the new D-DABA-based thymine monomer (**2**), suitably protected for peptide solid phase synthesis based on Fmoc chemistry, is reported in Scheme 1 and is analogous to that recently reported in our previous works for the synthesis of the L-DABA monomer (Roviello *et al.* 2006 and 2007), but starting from the commercial Boc-(D)-DAB(Fmoc)-OH (**1**).

The DABA-based hexathymine with alternating chirality [$(t_{D\text{-}dab}t_{L\text{-}dab})_3$, **3**] was synthesized in solid phase by using $t_{D\text{-}dab}$ monomer **2** and its L-enantiomer, with a protocol which minimizes racemization during the coupling steps (Sforza *et al.* 2002, Roviello *et al.* 2006

and 2007). Oligomer **3** was cleaved from the solid support by acidic treatment (TFA/m-cresol, 4:1, v/v) and purified by RP-HPLC on a C-18 column with a linear gradient of CH_3CN (0.1% TFA) in H_2O (0.1% TFA) over 25 min. LC-ESI-MS characterization confirmed the identity of **3**: *m/z* 900.30 (found), 900.8 (expected for $[H\text{-}G\text{-}(t_{L\text{-}dab}\text{-}t_{D\text{-}dab})_3K\text{-}NH_2+2H]^{2+}$).

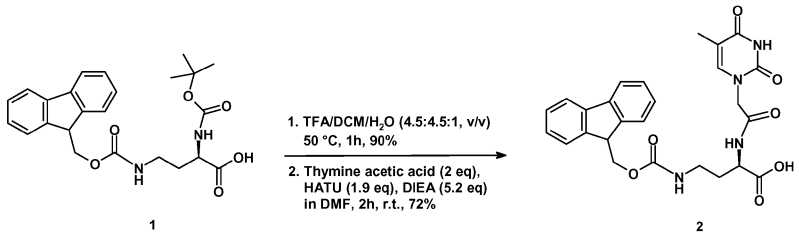

Scheme 1: Synthesis of the Fmoc-protected thymine D-DABA monomer.

CD binding experiments of the homothymine oligomer **3** with the complementary DNA (dA_6) were performed using a Tandem cell. This cuvette is constituted from two separated reservoir communicating just by the upper part of the cell in which two solutions, initially separated, come in contact only after mixing by turning upside down the cell. Initially, a solution of dA_6 in phosphate buffer was kept in one of the Tandem cell reservoirs (1 mL), while oligomer **3**, in the same buffer conditions, was in the other one. CD spectrum from 200 to 320 nm, corresponding to the sum spectrum of the separated strands, was recorded. Successively, the cell was turned upside down to allow the mixing of the two samples and again a CD spectrum was registered. Differences between sum and mix spectra are indicative of binding. In our case, $(t_{D\text{-}dab}t_{L\text{-}dab})_3$ didn't show evidence of binding with complementary DNA (Figure 1). No significant differences between the sum and mix spectra, and therefore no binding evidence, were revealed recording CD spectra of the "mix" sample at different times, performing a kinetic experiment. Furthermore, the binding was not detected even adding one more equivalent of oligomers **3**, in a 2:1 ratio of $(t_{dab})_6/dA_6$, in order to verify the possibility to form a triple helix complex.

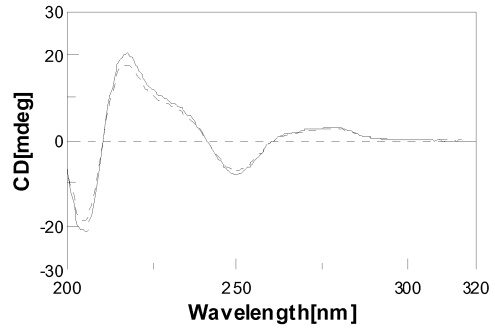

Figure 1: Sum (dashed line) and Mix (solid line) CD spectra of $(t_{D,L\text{-}dab})_6$ ***3*** *and DNA, 4μM in H_2O.*

Successively, the ability of the hexamer **3** to form molecular networks cross-linked with free adenine base was investigated.

Firstly, the CD profile of the hexathymine single strand in water (pH 7) was analysed. A weak CD signal was detected for our chiral oligomer and more exactly a maximum centred at 272 nm was observed (Figure 2, dashed line). This suggests a structural preorganization for our chiral nucleopeptide in aqueous medium that should be confirmed by NMR and RX studies.

On the other hand, as expected, no CD signal was detected for solutions at different concentration of free adenine in water, as reported in Figure 2 for the 0.1 mM case (solid line).

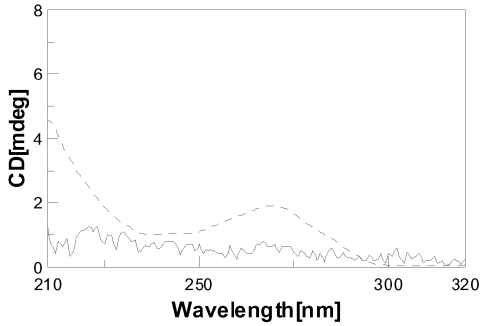

Figure 2: CD spectra of 15 μM $(t_{D\text{-}dab}t_{L\text{-}dab})_3$ ***3*** *(dashed line) and 0.1 mM adenine in* H_2O *(solid line, noise).*

CD titration of the $(t_{D\text{-}dab}t_{L\text{-}dab})_3$ oligomer with increasing amounts of adenine furnished many interesting evidences of interaction that could be at the basis of extensive molecular network formation.

Increasing amounts (30 nmol each) of a concentrated solution of adenine in water were added to 2 mL of 15 μM oligomer **3** solution (180 nmol in thymine). The CD band centred at 272 nm underwent an increase in intensity and a shift of the maximum to lower wavelengths, as adenine was added. Since adenine solutions don't give rise to CD signal, the differences revealed between the CD spectrum of **3** alone and of a mixture of **3**/adenine, is a clear evidence of interaction, as reported in Figure 3 for the case of **3**/adenine in a 2/1 ratio in bases (solid line).

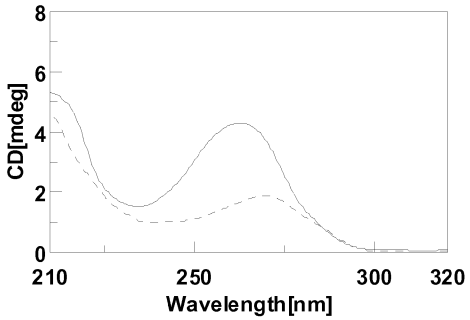

Figure 3. CD spectra of 15 μM $(t_{D\text{-}dab}t_{L\text{-}dab})_3$ ***3*** *(dashed line) and a 2:1 ratio in bases of* ***3*** *and adenine in* H_2O *(solid line).*

In our opinion, when thymines in **3** are in excess respect to the adenines, it could be hypothized the formation of a three-dimensional network in which DABA-based hexathymine strands are crosslinked by adenine molecules, by means of both W-C and Hoogsteen hydrogen bonds. In analogy to the polyT_2/polyA triplexes, our system could be schematically represented as in Figure 4. Obviously, adenines, not anchored to sugar moieties, have two more sites for hydrogen bonding formation (indicated in Figure 4 by the arrows) that are other probable cross-linking points.

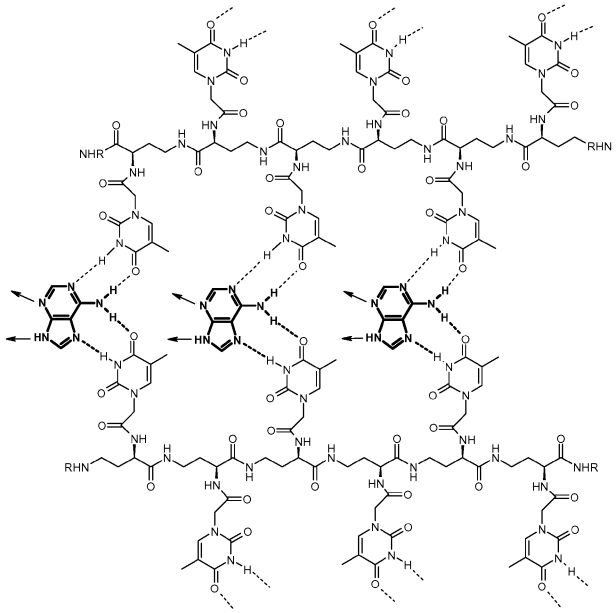

Figure 4: Schematic representation (for simplicity in 2D) of a T_2*/A nucleopetide/adenine network.*

Nevertheless, the comparison of literature CD data and the completely different CD profile obtained in our case, suggests a substantial structural difference between our chiral system, involving free adenine molecules, and the classical polyT_2 /polyA one, in which adenine moieties are anchored to the sugar-phosphate backbone.

Continuing the CD titration of **3**, further adding of adenine beyond the 2:1 T/A ratio caused an increase in the signal intensity and a substantial change in the CD spectrum shape. At 1:1 A/T ratio, the CD spectrum appeared as reported in Figure 5a (solid line). In this case we observed the formation of complexes that are probably based mainly on W-C hydrogen bonding.

The effect of further adding of adenine was the increase of the CD signals and the appearance of three bands centred at about 215, 247 and 269 nm (Figure 5b). It's very interesting to note that when adenine amounts exceeded the 1:1 ratio in A/T bases we didn't observe the stabilization of the CD spectrum, but a continuing increase of the band intensities was revealed, even though adenine alone, also in high concentrations, does not show any CD signal (Figure 2, solid line).

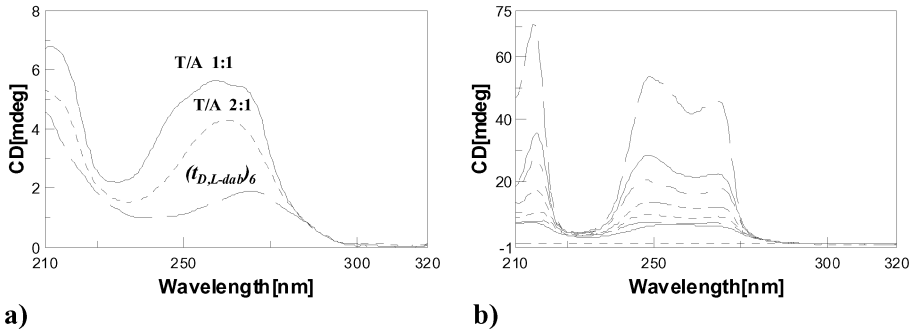

*Figure 5 a) comparison between the CD spectra of $(t_{D,L\text{-}dab})_6$ **3** and of the complex **3**/adenine (2:1 and 1:1 ratio in bases); b) CD spectra recorded after adenine adding to the solution containing 30 nmol of **3**: from 180 to 480 nmol adenine, corresponding, respectively, to 1:1 and 2.7:1 ratio in T/A bases.*

Indeed, when the chiral solution of **3**, also in traces, was added to the adenine solution (1 mM), achiral and lacking of CD signal, we observed a strong CD signal (Figure 6) not justifiable by the presence of so little amounts of the chiral compound **3**, but explainable by admitting the induction of a chiral molecular disposition of adenines in solution.

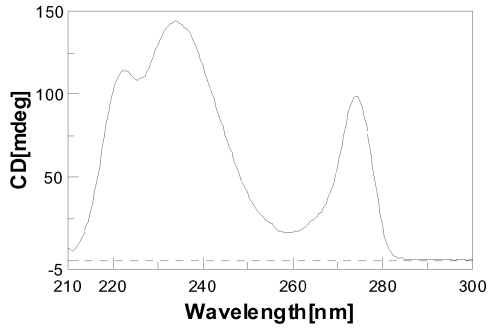

*Figure 6: CD spectrum of 1 mM adenine solution in presence of oligomer **3** (traces).*

The stability of the system composed of $(t_{D\text{-}dab}t_{L\text{-}dab})_3$ **3** and free adenine in water was studied by UV denaturation experiment. The solution of 1:18 ratio **3**/adenine (1:3 in bases) afforded a melting temperature (T_m) of 37 °C, as reported in Figure 7.

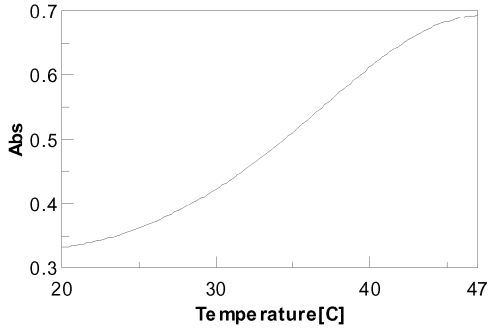

*Figure 7: UV melting of the complex **3**/adenine (1:18 ratio) in H_2O, pH 6.5*

3. Conclusions

In conclusion, our experiments showed that chiral nucleopeptides like our hexathymine oligomer with alternating D,L-chirality, are able to interact with adenine molecules in aqueous solution as clearly evidenced by CD spectroscopy. This finding also supports the use of chiral nucleopeptide systems for the realization of molecular networks, like hydrogels, to be used in drug delivery applications that we are going to study as a prosecution of the present research. Indeed, gelation and microrheology experiments on complexes $(t_{D,L\text{-}dab})_6$/adenine are in progress in various conditions of concentration, temperature and pH.

Another interesting point resides in the influence of DABA-based nucleopeptide chirality on the formation of a chiral environment in optically inactive solutions of adenine. Our results, together with the isolation of D,L-DABA and nucleobases in the extraterrestrial soil of the Murchison meteorite, reinforce the hypothesis that chiral nucleopeptides constituted a

primordial genetic material that introduced chirality in the actual nucleic acids/proteins world.

4. References

Foster J.G., W.D. Cress, S.F. Wright, J.L. Hess, 1987, Plant Physiol. 83(4), 900-904.
Iwashita Y., S. Goto, M. Tominaga, A. Sasaki, N. Ohmori, T. Goto, S. Sato, M. Ohta, S. Kitano, 2005, Cancer Sci. 96, 303-307.
Kurreck J., E. Wyszko, C. Gillen, V.A. Erdmann, 2002, Nucleic acid Res. 30, 1911-1918.
Li Y., Y.D. Tseng, S.Y. Kwon, L. D'Espaux, J.S. Bunch, P.L. Mceuen, D. Luo, 2004, Nat. Mater. 3, 38-42.
Luo D., 2003, Materials today 6 (11), 38-43.
Luo D., Y. Li, S. Ho Um, Y. Cu, 2006, Methods Mol Med. 127, 115-26.
Matsukura M., K. Shinozuka, G. Zon, H. Mitsuya, M. Reitz, J.S. Cohen, S. Broder, 1987, Proc. Natl Acad Sci. 84, 7706-7719.
Meierhenrich U.J., G.M. Muñoz Caro, J.H. Bredehöft, E.K. Jessberger, W.H.P. Thiemann, 2004, Proc. Natl. Acad. Sci. 101(25), 9182-9186.
Nielsen P.E, M. Egholm, R.H. Berg, O. Buchardt, 1991, Science 254, 1497-1500.
Nielsen P. E., 1993 Origins Life Evol. Biosphere 23, 323-327.
Roviello G.N., M. Moccia, R. Sapio, M. Valente, E.M. Bucci, M. Castiglione, C. Pedone, G. Perretta, E. Benedetti and D. Musumeci, 2006, J. Pept. Sci. 12, 829-835.
Roviello G.N., D. Musumeci, M. Moccia, M. Castiglione, R. Sapio, M. Valente, E.M. Bucci, G. Perretta, C. Pedone, 2007, Nucleos. Nucleot. Nucleic Acids 26, 1307-1310.
Sato Y., A. Hashidzume, Y. Morishima, 2001, Macromolecules 34, 6121-6130.
Sforza S., G. Galaverna, A. Dossena, R. Corradini, R. Marchelli, 2002, Chirality 14, 591-8.
Shay J.S., S.R. Raghavan, S.A. Khan, 2001, J. Rheol. 45, 913-927.
Shchepinov M.S., K.U. Mir, J.K. Elder, M. D. Frank-Kamenetskii, E.M. Southern, 1999, Nucleic Acids Res. 27(15), 3035–3041.
Strasdeit H., 2005, *ChemBioChem.* 6 (5), 801-3.
Uhlmann E., A. Peyman, 1990, Chem. Rev. 90, 543-584.
Wolman Y., W.J. Haverland, S.L. Miller, 1972, Proc. Nat. Acad. Sci. 69(4), 809-811.

Acknowledgments: *We gratefully thank Dr. Giuseppe Perretta for his invaluable technical assistance.*

CHEMICAL ENGINEERING TRANSACTIONS, Volume 14, 2008
Edited by G. Marino, E. Bardone, A. Viglia
 ISBN 978-88-95608-02-0

Experimental models in large size animals for devices in vascular pathologies

Pantaleo A.[1], Di Tommaso L.[1], Monaco M.[1], Castaldo S.[2], Di Napoli D.[2], Corona M.[2], De Martinis C.[2], De Marinis P.[3], Cozzolino S.[2], Iannelli G.[1]

[1]Department of Cardiosurgery , University of Naples "Federico II"
[2]Center of Biotechnologies, Antonio Cardarelli Hospital
[3]Functional Neurosurgery , Antonio Cardarelli Hospital

Background

Biotechnology Center A.O.R.N. "A. Cardarelli" in Naples is equipped with experimental animal laboratories for research, and training in surgery and microsurgery, through ministerial authorization.

These laboratories developed and tested large animal models for bio-medical and pre-clinical studies. Pre-clinical experiments with animal models that closely match human morphology, physiology and genetic variability provide data that can easily be transferred to humans. On anatomical-functional grounds, there are many analogies between swine and humans.

These reasons have driven many investigators to seek these animals for different fields of preclinical research. The circulatory system is particularly similar to man and therefore readily adaptable to experimentation in the field of cardio-vascular surgery.

The experience gained by the staff at the Biotechnology Center has been significantly important in laying the scientific and cultural foundation for fruitful collaboration with researchers and scientific companies. This is seen with the development of four different models: 1) atrial-aortic cannulus for surgery on aortic valves in a beating heart; 2) prostheses for aortic arch aneurisms; 3) The use of devices for carotid aneurisms by digital angiogram 4) The use of devices to resolve carotid thromboses.

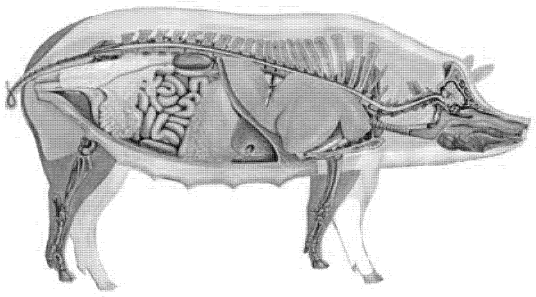

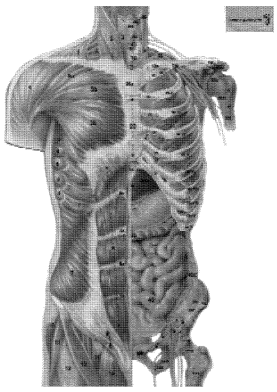

Materials and Methods

1) The experiment was performed on pig models in a pre-clinical study of cannulus use for surgery on the aortic valve and ascending aorta. This cannulus allows oxygenated blood within the left atrium to arrive in the ascending aorta without passing through the left ventricle. This allows the surgeon to operate on the ascending aorta while the heart is beating, thus avoiding extra corporeal circulation. The aim of the project is to increase the aortic valve surgery in patients in advanced age, so to prolong their life prospect.

Swine aortic ostium and semilunar valve

2) Aiming to resolve the problems linked to extra corporeal circulation in conventional surgery and to the hybrid two-phase treatment (consisting in a preventive revascularization of epiaortic or visceral vessels, followed by endovascular treatment) a new prosthesis has been designed that may allow us to:
- Treat aortic arch or thoracic abdominal aneurisms with one operation, by conventional surgery (sternotomy or thoracic-phreno-laparotomy);
- Avoid aortic clamp, extra corporeal circulation, deep hypothermia and the need for selective cerebral or vascular perfusion;
- Resection the aneurism wall, with intraoperative monitoring of bleeding and the perfect adhesion of the prosthesis.

3) An experimental human carotid aneurism model was made by creating a closed-lateral anastomosis. This procedure foresaw the use of a graft of the external jugular vein. This section divided into two parts, each of desired length is clamped at one end and anastomosed to the common carotid at the other end. The differet elastic component of the giugular, in comparison to carotid artery, allow the vein graft to puff up and simulate an artificial aneurism. This kind of tecnique permitt to realize different kind of aneurismes by size and conformation. Later an experimental device was inserted into the femoral artery, in which previously was created an access, to reach and to set right the aneurism. The entire experiment was performed by using an angiograph. This model is reliable and repeatable. It provides endovascular and embolus skills using of state-of-the-art materials. In addition, this experimental model will be able to be used to develop new patented devices.

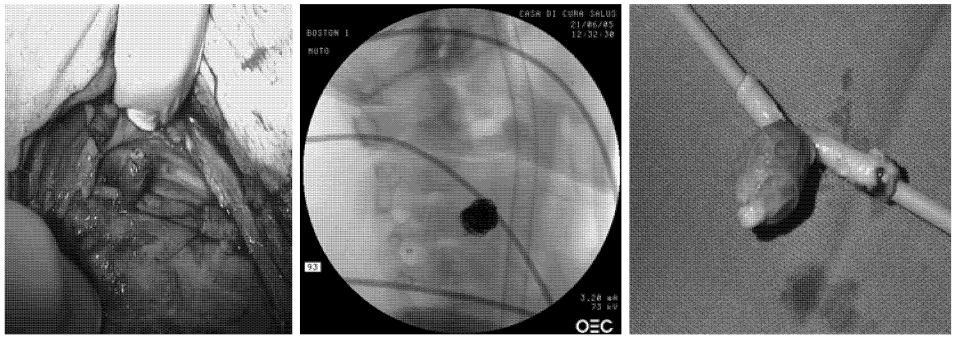

Artificial carotid aneurism in three steps of the experiment

4) An experimental model was made for a new arterial device to resolve thromboses in the medial cerebral artery. In the animal model used a surgical incision was made for femoral artery access. Later was performed two techniques to simulate a thrombus: first we made an *in-vivo* thrombus doing an injection of bovine thrombin and barium sulphate directly on internal carotid which was pre-clamped, after 2 hours the thrombus was ready to get operate. In second approach an *in-vitro* thrombus was created using homologous blood with added bovine thrombin and barium sulphate. This was inoculated into the femoral artery until reaching the common carotid artery where the thrombus was positioned. The entire experiment was followed by angiography. Once reaching the zone with the device, using the femoral access, the thrombus was

penetrated. Dilation of the device crushed the thrombus against the walls of the vessel allowing blood to pass through the artery once again and restoring the flow.

Conclusions

The swine results to be an animal model realy reliable for the testing of new devices and for training new techniques. Overcoming the difficulties encountered with these devices, in the study they have been achievable in an anatomically complex animal, with optimism we look forward to their use in a simpler vascular structure such as in man.

Bibliography

1. Kazui T,Yamashita K, Washiyama N, Terada H, Bashar AH, Suzuki K, Suzuki T.: Aortic arch replacement using selective cerebral perfusion. Ann Thorac Surg. 2007 ;83(2):S796-8.

2. Black JH III, and Cambria RP. Current results of open surgical repair of descending thoracic aortic aneurysms. J Vasc Surg 2006; 43 (A): 6-11.

3. Saito N, Kimura T, Odashiro K, Toma M, Nobuyoshi M, Ueno K, Kita T, and Inoue K. Feasibility of the Inoue single-branched stent-graft implantation for thoracic aortic aneurysm or dissection involving the left subclavian artery: Short- to medium-term results in 17 patients. J Vasc Surg 2005;41:206-12.

4. Greenberg RK, West K, Pfaff K, Foster J, Skender D, Haulon S, Sereika J, Geiger L, Lyden SP, Clair D, Svensson L, Lytle B. Beyond the aortic bifurcation: branched endovascular grafts for thoracoabdominal and aortoiliac aneurysms. J Vasc Surg. 2006; 43(5): 879-86; discussion 886-7.

5. Saleh HM, and Inglese L. Combined surgical and endovascular treatment of aortic arch aneurysms. J Vasc Surg 2006;44:460-6.

6. Alexander KP, Anstrom KJ, Muhlbaier LH, Grosswald RD, Smith PK, Jones RH. Et al. Outcome of cardiac surgery in patient > or = 80 years: results from the National Cardiovascular Network. J Am Coll Cardiol. 2000 Mar 1; 35(3):731-8

7. Sundt TM, Bailey MS, Moon MR, Mendeloff EN, Hudleston CB, Pasque MK, et al. Quality of life after aortic valve replacemenet at age of >80 years. Circulation 2000; 102[supp1 III]:III-70-III-74

8. Akins CW, Dagget WM, Vlahakes GJ, Hilgenberg AD, Torchiana DF, Madsen JG, et al. Cardiac operations in patients 80 years old and older. Ann Thorac Surg 1997;64:606-15

9. Fruitman DS, MacDougall CE and Ross DB. Cardiac surgery in octogenarians: can elderly patient benefit. Quality of life after cardiac surgery. Ann Thorac Surg 1999;68:2129-35

10. Ascione R, Lloyd CT, Underwood MJ, Lotto AA, Pitsis AA, Angelini GD. Inflammatory response after coronary revascularization with or without cardiopulmonary bypass. Ann Thorac Surg 2000;69:1198-1204.
11. Benetti FJ, Naselli G, Wood M, et al. Direct myocardial revascularization without extracorporeal circulation. Experience in 700 patients. Chest 1991;100:312-6.

CHEMICAL ENGINEERING TRANSACTIONS, Volume 14, 2008
Edited by G. Marino, E. Bardone, A. Viglia
 ISBN 978-88-95608-02-0

Model Investigation of Fungal Activity on a Synthetic Biorecalcitrant Wastewater

Alessio D'Urso[1,a], Daniel Gapes[2,b] and Marco Bravi[1,c]

[1] Dipartimento Ingegneria Chimica Materiali Ambiente, Sapienza – Università di Roma. Via Eudossiana 18, 00184 – Rome (Italy).
[2] Scion Research Institute – 49 Sala Street, P.B. 3020, Rotorua (New Zealand)

[a] alessio.durso@uniroma1.it; [b] daniel.gapes@scionresearch.com
[c] m.bravi@ingchim.ing.uniroma1.it

The remediation of those effluents containing pollutants which are hard to be metabolized (biorecalcitrant) is becoming an increasingly important enviromental problem, due to the complex nature of many wastewaters. An example is the class of polyphenols. In this work, the capability of the fungus *Trihcoderma viride* to act as bioremediation agent for the treatment of a synthetic wastewater containing glucose, acetic acid and gallic acid (chosen as phenolic model pollutant) was characterized. The investigation was carried out in a Sequencing Batch Reactor (SBR) with a Hydraulic Retention Time of 5 d. No settling phase was operated as this work is intended to be only a model study focused on the metabolic biomass performance (i.e., the removal of pollutant from the liquor). After few days, the organic load was completely removed, including the depletion of gallic acid from the medium. Furthermore, a 0.57 yield (C-mmol based) was achieved, thus indicating the absence of inhibition phenomena.

1. Introduction

One of the most important resources of humanity is fresh water. In fact, although water is very abundant on the Earth, only a small amount is easily accessible and can be used for antropic purposes, such as domestic (drinking and washing) utilization, irrigation and industrial applications.
After being used in both domestic and agro-industrial cases, the outcoming water contains an excess of organic matter that has to be removed prior to be discharged in order to avoid polluting effect on the receiving water bodies and to preserve the integrity of the existing micro- and macro- acquatic systems.
To remove part of the organic load, activated sludge processes are usually deployed. In these processes, the removal of pollutants is due to a bacterial biomass suspension which is confined into a biological reactor. The main reactions which take place are the mineralization (conversion into CO_2 and H_2O) and the conversion of the organic soluble matter into new biomass (which is solid and then gravimetrically separable through a settling phase). Whenever it is possible, biological processes are used as they are more economic than chemical processes. In some cases, however, due to the high organic load, toxicity or presence of biorecalcitrant compounds, biological processes could not be used, since no chemical oxygen demand (COD) removal is achieved biologically.

Thus, being a biological treatment infeasible, a chemical pre-treatment can represent an adequate way to reduce the COD prior to biological treatment, as for example the advanced oxidation process (San Sebastian Martínez et al., 2003).
A typical example of great concern in industrialized countries is the treatment of the class of polyphenols, which are both bio-recalcitrant and inhibitory (Paixao et al., 1999). They arise from petroleum refining, coking and coal conversion, chemical plants, pulp and paper plant and agro-industrial processes, like olive oil extraction (Borja et al., 2006) and cork manufacturing (Mendonça et al., 2007).
The removal of this class of pullotants enjoys a lot of attention from researchers because it usually represents a significant fraction of many wastewaters coming from diffusely formed European (Table 1) wastewaters. In Europe, the main responsible for the emissions of phenols is the metallurgic industry, which in 2004 released about 240 tons as direct emission and 637 tons of phenols as indirects emissions (2004 EPER data).

Table 1 - Emission of Phenols from agro-industrial activities in Europe (EPER, 2004)

ActivityDescription	**Emission in water (tons/year)**	
	Direct	**Indirect***
Basic inorganic chemicals or fertilisers	39.51	0.652
Basic organic chemicals	135.22	510.02
Biocides and explosives	0.366	7.55
Coke ovens	5.17	823.00
Combustion installations > 50 MW	9.62	0.642
Industrial plants for pulp from timber or other fibrous materials and paper or board production	13.30	0.879
Installations for surface treatment or products using organic solvents	0.1218	0.7445
Installations for the disposal of nonhazardous waste and landfills	2.62	7.22
Installations for the disposal or recovery of hazardous waste or municipal waste	2.22	9.18
Installations for the production of carbon or graphite	0.5099	-
Installations for the production of cement klinker, lime, glass, mineral substances or ceramic products	0.1151	2.68
Metal industry and metal ore roasting or sintering installations, Installations for the production of ferrous and non-ferrous metals	239.84	637.61
Mineral oil and gas refineries	45.99	85.45
Pharmaceutical products	4.17	83.15
Plants for tanning of hides and skins	-	2.71
Plants for the pre-treatment of fibres or textiles	0.03	1.95
Slaughterhouses, plants for the production of milk, other animal raw materials or vegetable raw materials	0.6347	3.34

(*) transfer to an off-site waste water treatment

A recent development in wastewater technology consists in the enhancement of the fungal fraction of microbial consortia owing to their interesting characteristics.
For example, they are usually more resistant to low pH, they are able to degrade substrates which are commonly considered as recalcitrant or inhibitory and they have the ability to form pellets (in the appropriate process conditions). Furthermore, previous investigations have been carried out by these authors as batch studies with a particular kind of fungal biomass, *Trichoderma viride* (D'Urso et al, 2007), on the capability to degrade polyphenols in a binary (the carbon sources were glucose and gallic acid) synthetic wastewater. Thus, an investigation of the bio-remediation ability of such a fungus (strain 8/90) in a continuos reactor fed with a more complex model phenol-containing wastewater was performed.
Activated Sludge Models (ASMs) are the most widely used model systems for simulating the biological processes occurring in activated sludge plants (Henze et al., 2000). In (ASMs), the soluble organic matter is divided in three fractions:

- Readily biodegradable material (RBM);
- Fermentation products (FPs).
- Slowly biodegradable (i.e. inert and recalcitrant) material (SBM);

On this basis, a synthetic mixture was formulated. RBM was modelled by glucose, while FPs, as customary, by acetate.
Gallic acid was adopted to represent SBM,. In this way, the presence effect of one compound of the class of phenols in high concentration (3 g/l) on the removal process performance was investigated. Besides, macro- (N and P) and micronutrients (trace elements) were dosed in excess. Particulate matter was not included in the model substrate formulation. Only the growth which takes place by degradation of soluble substrates based on the consumption of oxygen was considered, where ammonia nitrogen is incorporated into cell mass.
Autotrophic nitrogen removal, storage phenomena and hydrolysis of particulate matter were not targeted by this work.

2. Materials and Methods

2.1 Biomass

For this work, *Trichoderma viride* Pers:Fr. Isolate 8/90 has been used. It was kept on Petri dishes as a pure culture and stored at 26° C.

2.2 Analytical Methods

Glucose analysis was performed through the Somogyi-Nelson (Somogyi, 1926) method while gallic acid was analysed by the Folin-Ciocalteau (Singleton and Rossi, 1965) one. Acetic acid was analysed by gas chromatography (see Table 2). The dissolved carbon content was determined using an Elemental HiTOC (Germany) analyser and auto-injector: a filtered (0.45μm) sample was injected into a catalyst furnace where all carbon was oxidised to carbon dioxide.
Another sample was injected into a reactor containing dilute acid, where the inorganic component, assumed to be carbonate, was converted into carbon dioxide. The carbon dioxide was removed from each reaction in two carrier gas streams to separate infra red detectors. The output of the detectors was integrated and expressed as elemental carbon.

Organic carbon was calculated as the difference between the total and inorganic carbon readings.
Standard solid content analyses for wastewater treatment systems (TSS, VSS and SVI as reported by APAT and IRSA-CNR, 2004) were also performed.

Table 2 - Gas Chromatograph Conditions for acetic acid analysis

Injector temperature	170°C
Liner	Gooseneck with glass wool
Injection technique	Purge splitless
Purge on time	0.5 minutes
Oven temperature profile	Initial temperature 30°C (2 min) Ramp 10°C/min to 110°C (10 min) Ramp 10°C/min to 150°C (5 min)
Run length	31min (45min total - includes cooling to 30°C)
Detector	FID (190°C)
Headpressure	50kPa
Carrier gas (Helium)	20 mL/min over a 0.5% formic acid reservoir
Hydrogen	18 mL/min
Oxygen	32 mL/min
Nitrogen	40 mL/min

2.3 Reactor Management

The study was performed as a continuous treatment in a Sequencing Batch Reactor (SBR) system (volume = 2 l).
The SBR was fed with a solution containing glucose (10 g/l), gallic acid (3 g/l) and acetic acid (2 g/l) and the required nutrients.
A Hydraulic Retention Time (HRT) and Solid Retention Time (SRT; no settling phase) of 5 days was adopted for modelling purposes. The pH and temperature set points were fixed, respectively, at 3.5 (aim of this investigation was also identifying the biomass behaviour in extremely acidic conditions) and 25°C.
The reactor was managed as a batch one during the first three days, to allow for *Trichoderma viride* biomass growth: a diluted (1:4) substrate mixture was introduced as growth medium. After three days, the above mentioned medium was continuously fed to the system.
The phases of the reactor were the following:

- Load phase: 5 min
- Reaction phase: 340 min
- Discharge phase: 15 min

The feeding consisted on a synthetic solution with the following composition (g/L): glucose (10), gallic acid (3), acetic acid (2), KH_2PO_4 (1), $(NH_4)_2SO_4$ (5), $MgSO_4 \cdot 7H_2O$ (1.23), $FeSO_4 \cdot 7H_2O$ (0.00271), $MnSO_4 \cdot H_2O$ (0.0016), $ZnSO_4 \cdot H_2O$ (0.0014), $CoCl_2 \cdot 6H_2O$ (0.0036), $CaCl_2 \cdot 2H_2O$ (0.8). The organic load rate was equal to 3240 mgCOD/d (or 1260 mg/l in term of Dissolved Organic Carbon, DOC).

3. Results and discussions

The feeding described in Section 2.3 was initially diluted (1:4) and used as growth medium for the *T. viride* biomass. Such a phase lasted three days during which the reactor was managed in batch mode. Afterwards, feeding was continuosly provided to reactor.

Glucose and acetic acid were immediately utilized by the biomass, while gallic acid was not metabolised (see Figure 1). After 24 h from the start-up (time d = 1) it is possible to observe an increase in the substrates' concentration due to water loss in the outflowing gas. Subsequently, the reactor volume was adjusted daily with the addition of some distilled water.

During reactor feeding, both glucose and acetic acid were depleted (see Figure 2). Interestengly, gallic acid didn't provide any inhibition to the growth of the fungal biomass as usually can be expected in the case of bacterial biomass (Caffaz et al., 2007). However, an increase of gallic acid concentration was recorded till t = 10 d. Thereafter gallic acid concetration decreased and from t = 16 d gallic acid was completely removed from the biomass.

A possible explanation for this behavior could be the following: the biomass was able to remove the above mentioned compound but with a slower specific removal rate with respect to glucose and acetic acid thus leading to its accumulation in the liquor. With the biomass concentration becoming higher and higher, the overall removal rate became sufficient to provide a depletion of gallic acid from the medium.

This explanation can be confirmed looking at the profiles in Figure 3. The actual gallic acid concentration profile was lower than that calculated with the hypotesis of no removal, thus indicating a partial gallic acid utilization. As the biomass concentration become higher enough, a decrease in gallic acid concentration in the outflowing effluent and, later on, a complete removal were observed.

Furthermore, Dissolved Organic Carbon (DOC) content was measured as well. this quantity exibited a profile similar to the gallic acid one, . i.e. it raised while gallic acid removal was not complete and then decreased to a constant but lower value when gallic acid was almost depleted.

After t = 16 d, all the substrates were completely removed. However, even though there was a 96% removal, on DOC basis, a stable DOC value was always recorded, likely because of the formation of by-products.

In the end, it must be observed that the low pH conditions didn't affect the biomass growth.

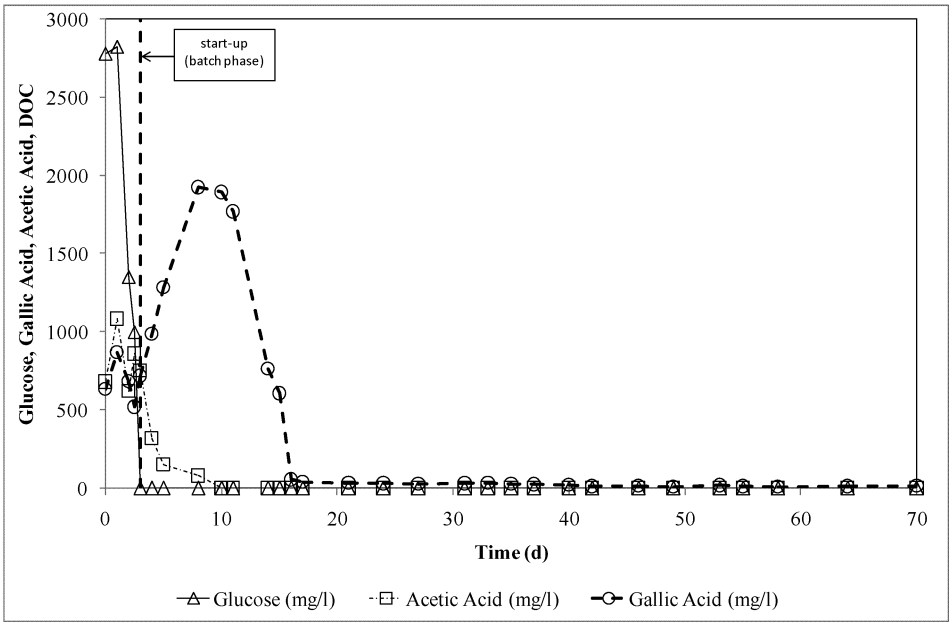

Figure 1 – Substrates' profiles in the reactor effluent.

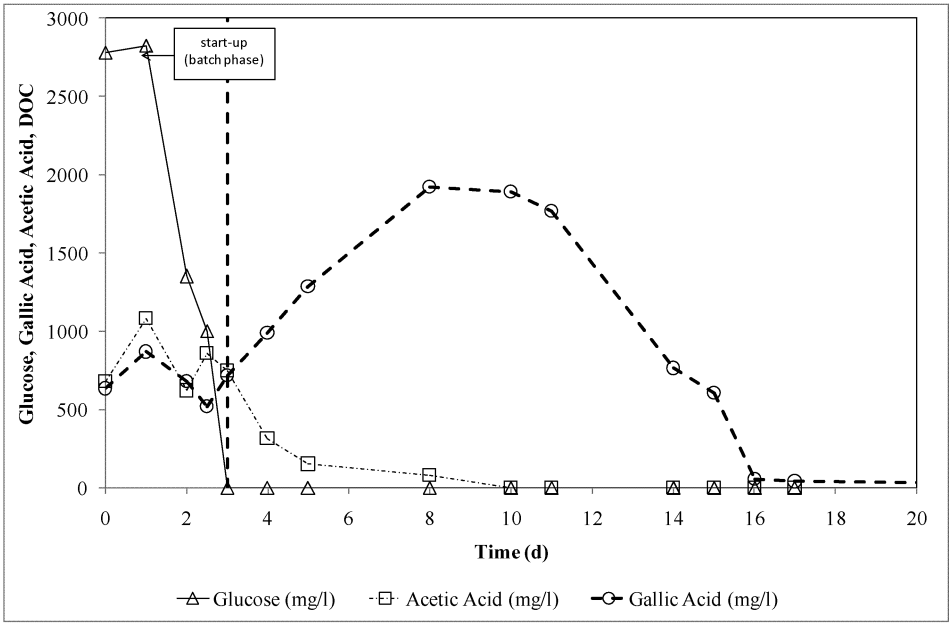

Figure 2 – Substrates' profile in the reactor effluent (detail on the first 20 days).

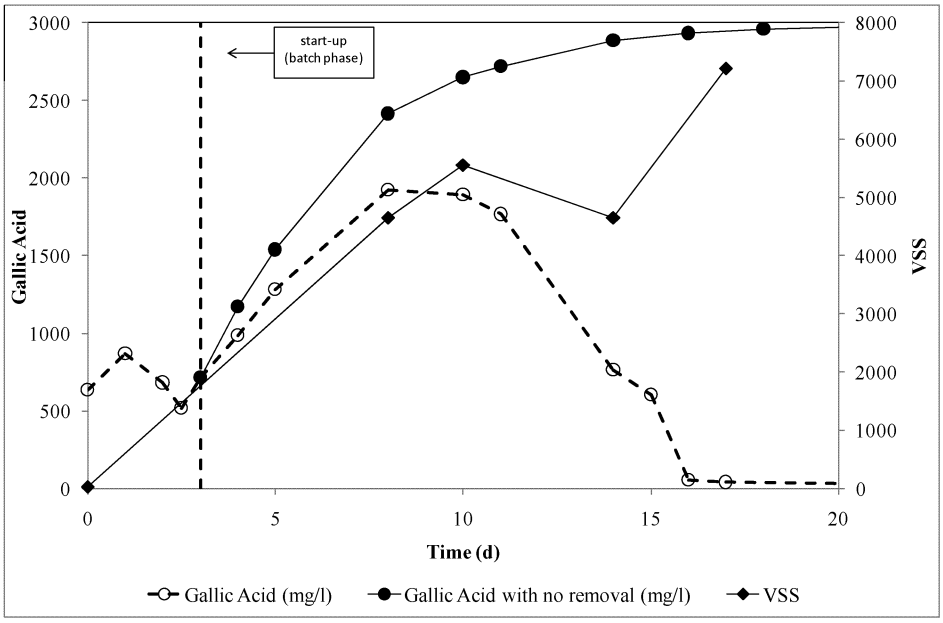

Figure 3 – Comparison bewteen gallic acid concentration in the outcoming effluent and the calculated concentration under the hypotesis of no removal (accumulation) during the first 20 days.

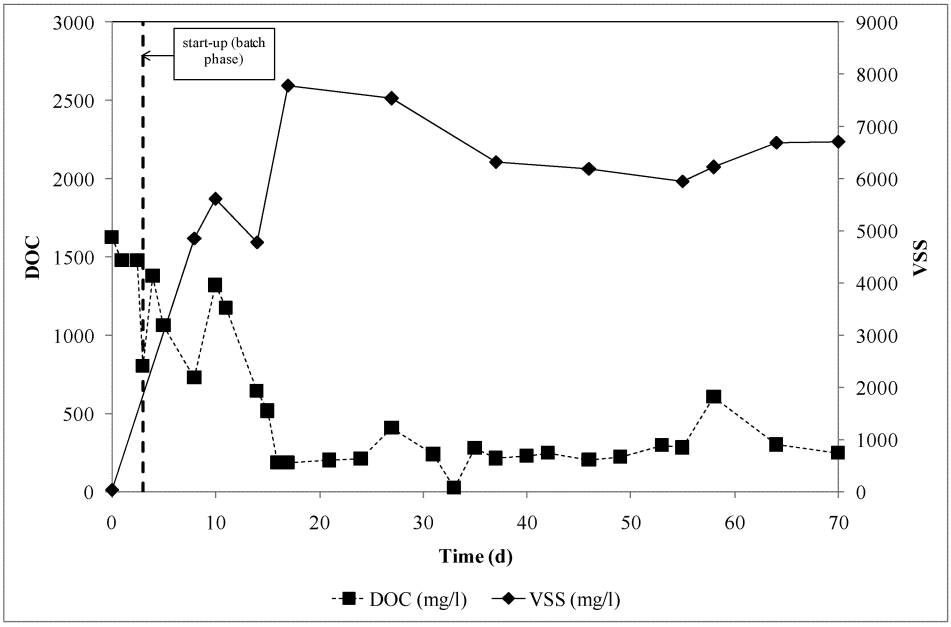

Figure 4 – Dissolved Organic Carbon (DOC) and biomass content (as Volatile Suspended Solids, VSS) content.

4. Conclusions

The treatment of wastewaters containing phenols-like compounds usually represents a problem because of the inhibitory effects exibited on microorganisms. Instead, fungi can withstand high concentrations of these compounds and even remove them. In this work, unacclimatised *T. viride* was challenged in a slightly modified continuous biological treatment model treatment; the biomass showed the ability to completely and simultaneously remove the RBM, FB and SBM components of a low (3.5) pH substrate fed to the reactor (being the 24.6% made up of gallic acid on DOC basis) from the very beginning.

These results suggest that the ability of fungi to contribute essential steps of the carbon cycle occurring in nature can also be exploited in biological treatments of biorecalcitrant wastewaters, where their resistance to high concentrations of SBM provide tolerance to concentration fluctuations of this latter and therefore reduce the requirements on the equalisation basin.

5. References

APAT and IRSA-CNR, 2004, Metodi Analitici per le Acque (in Italian).

Borja, R. and B. Rincon and F. Raposo, 2006, Anaerobic biodegradation of two-phase olive mill solid wastes and liquid effluents: kinetic studies and process performance, Journal of Chemical Technology and Biotechnology 8, 1450-1462.

D'Urso, A., M. Galimberti and M. Bravi, 2007, Fungal biomass-based processing of phenolics-rich wastewaters. In Proceedings of ICHEAP8 Congress, Ischia, Naples.

Caffaz , S., C. Caretti , M. Morelli, C. Lubello and E. Azzari, 2007, Olive mill wastewater biological treatment by fungi biomass, Water Science & Technology 55 (10), 89-97.

Henze, M., W. Gujer, T. Mino and M. C. M. van Loosdrecht, 2000, Activated Sludge Models ASM1, ASM2, ASM2d and ASM3. Scientific and Technical Report No. 9, IWA Publishing, London.

Mendonça, E. A., L. Picado, L. Silva and A.M. Anselmo, 2007, Ecotoxicological evaluation of cork-boiling wastewaters, Ecotoxicology and Environmental Safety 66, 384–390.

Paixao, S. M., E. Mendonca, A. Picado and A. M. Anselmo, 1999, Acute toxicity evaluation of olive oil mill wastewaters: a comparative study of Three aquatic organisms, Environmental Toxicology 14(2), 263-269.

San Sebastián Martínez, N., J. Fíguls Fernández, X. Font Segura and A. Sánchez Ferrer, 2003, Pre-oxidation of an extremely polluted industrial wastewater by the Fenton's reagent, Journal of Hazardous Materials 101(3), 315-322.

Singleton, V. L. and J. A. J. Rossi, 1965, Colorimetry of total phenolics with phosphomolybdicphoshotungstic reagents. American Journal of Enology and Viticolture 16, 144-158.

Somogyi, M., 1926, Notes on sugar determination. The Journal of Biological Chemistry 70(3), 599-61.

Wilderer, P.A., R. L. Irvine and M. C. Goronszy, 2001, Sequencing Batch Reactor Technology. Scientific and Technical Report N.10, IWA Publishing, London.

CHEMICAL ENGINEERING TRANSACTIONS, Volume 14, 2008
Edited by G. Marino, E. Bardone, A. Viglia
 ISBN 978-88-95608-02-0

Study on laboratory reactors for biodegradation of textile dyes by immobilized white-rot fungi mycelium

Pocedič J.[1)], Hasal P.[1)], Novotný Č.[2)]

[1)]Department of Chemical Engineering, Institute of Chemical Technology, Prague, Technická 5, 166 28 Praha 6, Czech Republic, e-mail: Pavel.Hasal@vscht.cz; [2)]Institute of Microbiology, Academy of Sciences of the Czech Republic, Vídeňská 1083, 142 20 Praha 4 – Krč, Czech Republic

A laboratory scale trickle-bed reactor (length of 20 cm, 7 cm i.d., bed volume of 385 cm^3) was constructed for the biodegradation of the Remazol Briliant Blue R and Reactive Orange 16 dyes by immobilized *Irpex lacteus* mycelium. Three carriers (Filtren TM30 polyether foam, polyamide kitchen scourers and lufa sponge slices) were chosen for the mycelium immobilization. Each carrier bed was characterized by the liquid hold-up value and the mean retention time at four volumetric flow rates of the liquid phase. Distributions of the retention times were also measured for each mycelium carrier at various liquid media flow rates. The lowest liquid hold-up value was achieved in the reactor packed with the plastic kitchen scourers, the largest value was observed in the reactor filled with the lufa sponge. The longest mean retention time, 430 s, was achieved in the reactor with the lufa carrier at liquid flow rate of 6.81 cm^3min^{-1}, the shortest mean retention time was achieved in the reactor filled with the plastic kitchen scourers.

Using various Filtren TM carriers any dependence of the activity of the enzymes laccase, lignin peroxidase and mangan peroxidase secreted by the mycelium of the fungus *Irpex lacteus* on the porosity of the carrier was not observed. The ability of *Irpex lacteus* to secrete laccase and mangan peroxidase enzymes in the bioreactor with all kinds of carriers was proved.

The ability of *Irpex lacteus* to biodegrade the dyes Remazol Brilliant Blue R and Reactive Orange 16 was verified experimentally. The degree of decolorization of 80% was achieved within 2 days in all reactors. In the experiments with the reactor packed with the plastic kitchen scourers and the lufa sponge slices the decolorization degree equaled 90% within 2 days.

1. Introduction

Long lasting focus on degradation of toxic substances in waste waters from the textile industry was even increased in recent years due to steadily growing environmental pollution. The pollutants from the textile industry are, in general, only hardly removable by traditional chemical and microbiological technologies devised for the municipal wastewater treatment. Due to their enzymatic systems, white-rot fungi mycelia immobilized on solid carriers are capable to biodegrade these residues (Cripps et al., 1990; Forgacs et al., 2004; Swamy and Ramsay, 1999; Ruiz-Aguilar et al., 2002; Novotný et al., 2001; Tavčar et al., 2006; Wang and Yu, 1998). *Irpex lacteus, Phanerochaete chrysosporium, Trametes versicolor* and *Pleurotus ostreatus* belong to the most often used fungi in the waste water treatment (Novotný et al., 2001; Tien and Kirk, 1984; Wesenberg et al., 2003). Most of the published literature concerning the

bioremediation of dyes focus on biological and biochemical aspects of the biodegradation phenomena, but only quite a few papers concern the construction of reactors (bio-filters) suitable for an application of the white-rot fungi mycelium. Stirred batch reactors or shaken flasks (see, e.g., Cripps et al., 1990; Novotný et al., 2001; Ruiz-Aguilar et al., 2002; Valentín et al., 2007), trickle bed reactors (Chang and Lu, 2004; Lu and Gang, 2004; Mielgo et al., 2001; Pielech-Przybylska et al., 2006) and rotating biological contactors (RBC reactor, see, e.g., Zheng and Obbard, 2002) represent the most frequently used reactor setups for the biodegradation processes performed by the white-rot fungi. Simple construction, an absence of moving parts and easy operation are the main reasons why the trickle bed reactor with the white-rot fungi immobilized on a suitable solid carrier is very often used in environmental applications (Chang and Lu, 2004; Lu and Chang, 2004; Mielgo et al., 2001; Pielech-Przbylska et al., 2006). Wood chips, polymer foams, ceramics particles, fibrous structures and special plastics biomass supporting particles can be used as the mycelium carriers. The most serious problem when these carriers and their beds are used represents their susceptibility to clogging by the growing mycelium.

The biodegradation of remazol brilliant blue R and reactive orange 16 dyes by the white-rot fungus *Irpex lacteus* immobilized on polyurethane foam in a small laboratory trickle bed reactors and in a rotating-disc reactor was studied recently by Tavčar et al., 2006 who confirmed applicability of the fungus for the wastewater treatment. The

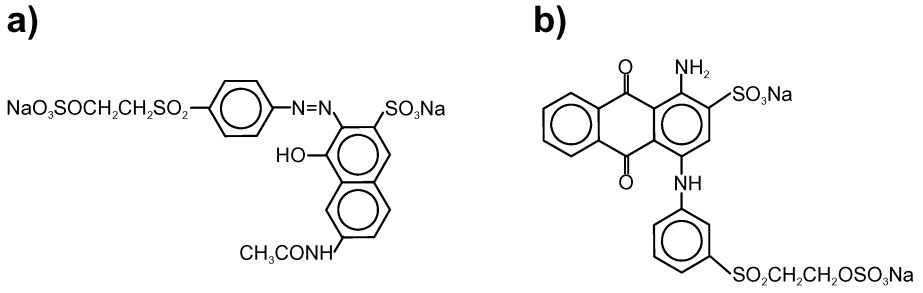

Figure 1: Structures of: a) *Remazol Brilliant Blue R* (*RBBR*), *and* b) *Reactive Orange 16* (*RO16*) *dyes*.

authors considered disc reactors as more suitable for the long term operation, in spite of the fact that their efficiency is slightly lower, as they prevent clogging by the mycelium biomas. The biodegradation of remazol brilliant blue R and reactive orange 16 dyes by the white-rot fungi *Irpex lacteus* immobilized on three macroporous carriers in a small laboratory trickle bed reactor was recently studied also by Pocedič, 2007 who proved practical applicability of all carriers used in his experiments.

Contrary to the biochemical and biological aspects of the bioremediation processes relatively low attention is devoted to studies on their engineering aspects, e.g., structure of the beds, the liquid phase hold-up, the wetting efficiency, residence time distributions, the axial dispersion etc. An attempt to fill some gaps in the knowledge of engineering parameters of the bioremediation processes and their relation to the biological efficiency of pollutants removal is done in this paper.

2. Materials and methods

2.1 Organism

The fungus *Irpex lacteus*, strain Fr. 238 617/93 (isolated from woods of the Czech Republic) was obtained from the Culture Collection of Basidiomycetes (CCBAS) of the Academy of Sciences of the Czech Republic, Prague.

2.2 Chemicals

The chemical structures of dyes used in decolorization experiments, namely remazol brilliant blue R (RBBR) and reactive orange 16 (RO16), are shown in Fig. 1 and were purchased from Sigma-Aldrich. All other chemicals used in experiments were of analytical grade and were purchased from local sources.

2.3 Bioreactor and mycelium carriers

The bioreactor was constructed of glass tube (20 cm long, 7 cm i. d., total bed volume 385 cm^3) sealed with two stoppers fabricated from the polydimethylsiloxane elastomer (Sylgard, DuPont, USA). The stoppers were equipped with tubular ports for the liquid and air inlets and outlets. A simple liquid distributor formed of a bunch of 5 curved Teflon capillaries was fitted to the upper stopper of the reactor. The distributor provided fairly even liquid distribution across the carrier beds at the liquid volumetric flow rates ranging from 5 to 25 cm^3min^{-1}. The overall bioreactor configuration is depicted in Fig. 2.

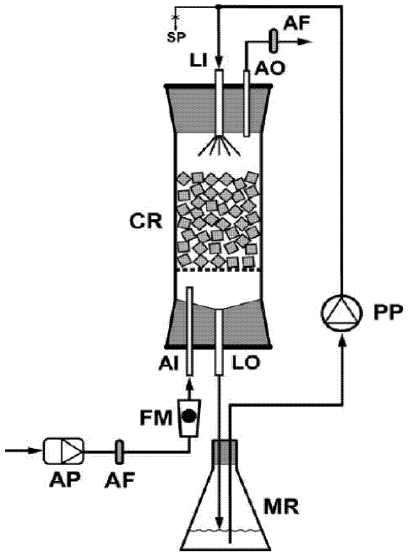

Figure 2: Schematics of the bioreactor and experimental set-up used for biodegradation experiments with immobilized mycelium of I. lacteus. CR… reactor tube; LI, LO … liquid inlet and outlet; AI, AO ... air inlet and outlet; FM … flow-meter; AF ... air filters; AP … air pump; MR … medium reservoir; PP … peristaltic pump; SP … sampling port.

Three kinds of mycelium carriers were used to evaluate their effects on the biodegradation of the RBBR and RO16 dyes: i) polyether macroreticulate foam Filtren® TM30 (Eurofoam, Brno, CZ) with inner porosity about 0.91, ii) the slices (thickness: 15 mm, diameter: 70 mm) of the cosmetic lufa sponge (dried pulp of *Luffa acutangula* fruits), and iii) polyamide kitchen scourers (height: 30 mm, diameter: 70 mm). Each carrier was three times washed in boiling distilled water prior its use. Configurations of carrier beds in the bioreactor are shown in Fig. 3.

2.4 Analytical methods

Decolorization

The degree of decolorization of liquid media was evaluated by the absorbance measurements at 592 nm for RBBR and at 490 nm for RO16.

Adsorption of the dyes to carriers used for immobilization
30 cm^3 of the aqueous dye solution (concentration: 150 mg dm^{-3}) was added to 1 g of dry carrier material cut to small pieces and the mixture was intensively shaken. The absorbance of the supernatants was measured at appropriate time intervals.

Liquid hold-up
The liquid medium was pumped to the reactor packed with the dry carrier bed at a constant volumetric flow rate. Amounts of the medium at both the inlet and the outlet of the reactor were recorded till steady values were reached. By material balancing the liquid hold-up in the carrier bed was evaluated.

Residence time distribution (*RTD*)
RTD of the liquid phase in the bioreactor was measured by standard stimulus–response method at four volumetric flow rates (6.8, 13.2, 19.6 and 25.2 cm^3min^{-1}). Copper(II) phthalocyanine-tetrasulfonic acid tetrasodium salt was used as the tracer and its concentration at the bioreactor outlet was measured at 694 nm by the spectrophotometer.

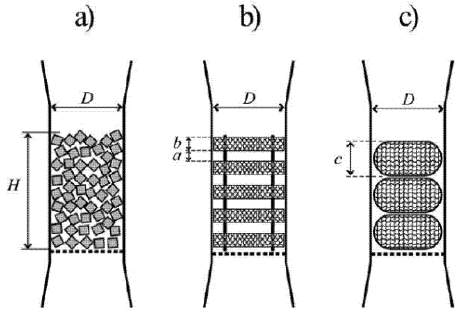

Figure 3: Configurations of mycelium carriers in the bioreactor. a) Filtren TM cubes (cube size 1×1×1 cm); b) lufa sponge slices; c) plastic kitchen scourers. Dimensions: D = 70 mm, H = 100 mm, a = 10 mm, b = 15 mm, c = 30 mm; total bed volume in bioreactor: approx. 385 cm^3.

2.5 Biodegradation experiments
The microorganism was first pre-cultivated on the agar plates (5 g dm^{-3} yeast extract, 10 g dm^{-3} nutrient agar, 10 g dm^{-3} glucose). The Erlenmeyer's flasks with 30 cm^3 of the Kirk's medium (Pocedič, 2007) were inoculated with the mycelium scraped from the agar plates after one week of the pre-cultivation. The *Irpex lacteus* mycelium was cultivated in the stationary flasks for one week at 28°C. Then the culture was homogenized by the Ultra-Turrax T25 homogenizator and the homogenate was used for the inoculation of the carriers. Each carrier together with the Kirk's medium was sterilized (121°C, 20 min) before addition of the homogenate. The Filtren TM30 carrier was inoculated in Erlenmeyer's flasks (total volume of 500 cm^3) filled with 30 cm^3 of fresh Kirk's medium to what 5 cm^3 of the mycelium homogenate was added. Plastics scourers were inoculated in separate bottles with 50 cm^3 of the Kirk's medium. 3 cm^3 of the homogenate was added to each piece of the scourers. Each lufa sponge slice was inoculated in the glass Petri dish with 30 cm^3 of the Kirk's media and 2 cm^3 of the homogenate was used per each slice. Inoculated carriers were then transferred to the bioreactor under sterile conditions and the decolorization experiments were started by pumping the medium. The volumetric flow rate of the medium was set to 20 cm^3min^{-1}.

The temperature was kept at 28°C during all decolorization experiments. The growth of the mycelium on the carriers was observed visually and the concentrations of the dyes in the liquid medium were measured at appropriate time intervals.

3. Results and Discussion

3.1 Liquid hold-up in carrier beds

Values of the liquid phase hold-up (expressed as the volumetric fraction of the liquid in the bed, ε_L) are listed in Table 1. The lowest values of the hold-up were obtained with the plastic kitchen scourers as the scourers material (a polyamide) exhibits very poor surface wettability and is totally non-porous. This material would thus be, in principle, unsuitable as the carrier in the bio-filters. The Filtren TM30 polyether foam with the cellular structure is very suitable for mycelium immobilization and the liquid phase hold-up values in this carrier were quite high. The highest hold-up values were obtained with the lufa sponge carrier due to its highly porous structure and high surface wettability. The lufa sponge, however, exhibited large volumetric instability of the bed. The liquid hold-up values in all studied beds exhibit rather irregular dependence on the liquid phase volumetric flow rate, probably due to experimental errors.

Table 1: Liquid hold-up in the carrier beds

Liquid flow rate [cm^3min^{-1}]	**Filtren TM30** ε_L [%]	**Plastic scourers** ε_L [%]	**Lufa sponge** ε_L [%]
6.81	1.99	0.29	1.93
13.23	1.48	0.93	3.93
19.59	1.84	1.39	3.43
25.18	1.62	0.79	2.77

3.2 Dyes adsorption to carriers

Results for both dyes and for all support media are summarized in Table 2. It is obvious that both tested dyes exhibited no adsorption to either of the tested carriers. Therefore the rate of dyes biodegradation is not influenced by the adsorption processes.

3.3 RTD of liquid phase

The experimentally determined residence time distribution (RTD) functions in the biorector packed with all three carriers at fixed liquid volumetric flow rate value of 6.81 cm^3min^{-1} are shown in Fig. 4. The RTDs for the bioreactor packed with the Filtren TM30 cubes and with the plastic kitchen scourers share common features: The residence times are relatively short as the liquid hold-up within the bed is low. The liquid phase flow in the bioreactor can be described by a model of the axial dispersion combined with the dead zones within the bed resulting to apparent skewness of the RTDs towards the longer residence times. The residence times in the bioreactor packed with the lufa sponge slices are significantly longer due to the diffusion of the tracer dye into the lufa sponge material (the Filtren foam and the scourers materials are impermeable for the tracer).

3.4 Biodegradation experiments

Two parallel biodegradation experiments with the column bioreactor for each of both dyes were performed – see Fig. 5. In the case of the RBBR dye 90% degree of

Table 2: Adsorption of dyes RBBR and RO16 on mycelium carriers

RBBR[1)]	**lufa sponge slices**	**plastic kitchen scourers**	**Filtren TM30 foam**
time [minutes]	average absorbance	average absorbance	average absorbance
0	0.669	0.669	0.657
10	0.673	0.665	0.664
30	0.659	0.672	0.664
120	0.671	0.676	0.666
1440	0.694	0.689	0.665
R016[2)]	**lufa sponge slices**	**plastic kitchen scourers**	**Filtren TM30 foam**
time	average absorbance	average absorbance	average absorbance
0	0.749	0.756	0.759
10	0.760	0.755	0.783
30	0.753	0.793	0.766
120	0.743	0.749	0.757
1440	0.738	0.770	0.740

[1)] 0.5021 g in 25 cm^3; [2)] 0.5223 g in 25 cm^3

decolorization was achieved in two days. The same rates of the biodegradation were observed for the lufa sponge and the plastic scourers carriers, the lower rate was observed with the Filtren TM30 carrier, probably due to limitation of the mycelium growth within the foam pores, where the oxygen and the substrate transport rates can be strongly limited. Some clogging problems due to the growing mycelium occurred in the Filtren cubes beds (Pocedič, 2007). The clogging does not pose a serious problem with the lufa sponge and the plastic scourers carriers. The biodegradation of the RO16 dye in the bioreactor proceeded in a quite similar way – cf. Fig. 5. The rate of the decrease of the RO16 concentration was, however, especially at the beginning stage of the experiment, notably lower and only 85% degree of the decolorization was observed after 4 days.

4. Conclusions

The decolorization experiments performed in a small scale laboratory trickle-bed bioreactor with three different kinds of solid carriers with the immobilized mycelium of *Irpex lacteus* Fr. 238 617/93 proved its ability to decolorize the dyes RBBR and RO16. The decolorization was achieved within 2–4 days). All carriers tested proved to be almost identically efficient in the decolorization experiments despite huge differences in their hydrodynamical properties. Fundamental process parameters characterizing the bioreactor were determined over a range of operating conditions of the bioreactor. The knowledge gained will be used in design of a larger scale bioreactor.

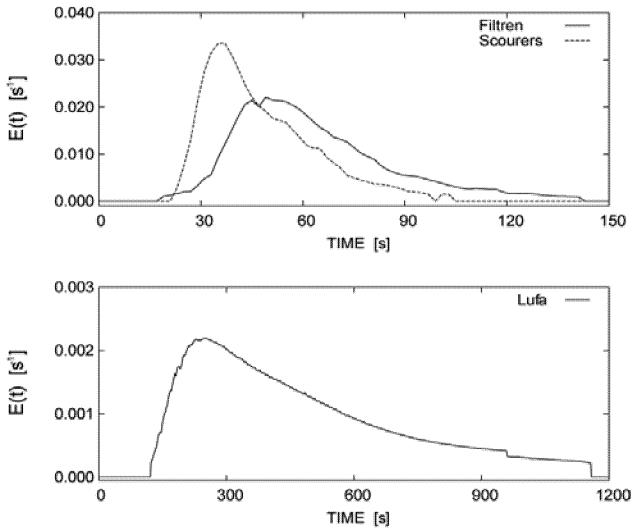

Figure 4: RTD of liquid phase in bioreactor packed with different carriers.

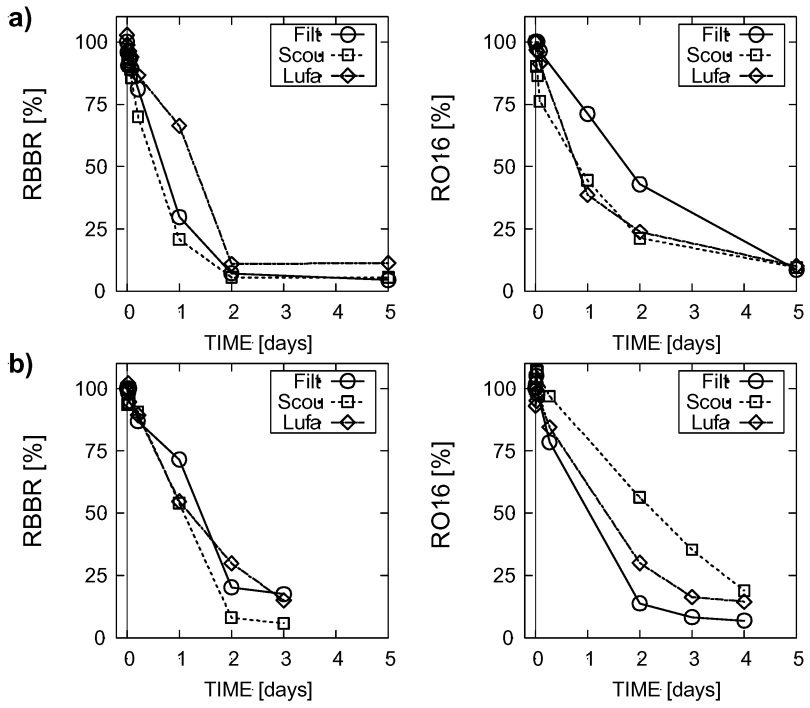

Figure 5: Time course of decolorizations of RBBR and RO16 dyes in two experiments (a, b). Concentrations of dyes are related to their initial values. Filt …Filtren TM30 carrier, Scou … plastic scourer carrier, Lufa …lufa sponge

Acknowledgements: The financial support by the Ministry of Education of the Czech Republic (Grant: MSM 6046137306) and by the Czech Science Foundation (Grant No. 104/08/H055) is gratefully acknowledged.

References

Cripps C., Bumpus J.A., Aust S.D.: Biodegradation of azo and heterocyclic dyes by *Phanerochaete chrysosporium*. Appl. Environ. Microbiol. 56, 1114–1118 (1990).

Forgacs E., Cserháti T., Oros G.: Removal of synthetic dyes from wastewaters: a review. Environment International 30, 953– 971 (2004).

Chang K., Lu Ch.: Biofiltration of isopropyl alcohol and acetone mixtures by a trickle-bed air biofilter. Proc. Biochem. 39, 415–423 (2003).

Lu C., Chang K., Hsu S., Lin J.: Biofiltration of butyl acetate by a trickle-bed air biofilter. Chem. Eng. Sci. 59, 99–108 (2004).

Mielgo I., Moreira M.T., Feijoo G., Lema J.M.: A packed-bed fungal bioreactor for continuous decolourisation of azo dyes (Orange II). J. Biotechnol. 89, 99–106 (2001).

Novotný Č., Rawal B., Bhatt M., Patel M., Šašek V., Molitoris H.P.: Capacity of *Irpex lacteus* and *Pleurotus ostreatus* for decolorization of chemically different dyes. J. Biotechnol. 89, 113–122 (2001).

Pielech-Przybylska K.,Ziemiński K.,Szopa J.St.: Acetone biodegradation in a trickle-bed biofilter. International Biodeterioration & Biodegradation 57, 200–206 (2006).

Pocedič J.: Study of biofilters for removal of toxic substances from waste waters. MSc. Thesis, Institute of Chemical Technology, Prague 2007 (in Czech).

Ruiz-Aguilar G.M.L., Fernández-Sánchez J.M., Rodríguez-Vázquez R., Poggi-Varaldo H.: Degradation by white-rot fungi of high concentrations of PCB extracted from a contaminated soil. Adv. Environ. Res. 6, 559–568 (2002).

Swamy J. Ramsay J.A.: The evaluation of white rot fungi in the decoloration of textile dyes. Enzyme Microb. Technol. 24, 130–137 (1999).

Tavčar M., Svobodová K., Kuplenk J., Novotný Č., Pavko A.: Biodegradation of Azo Dye RO16 in Different Reactors by Immobilized *Irpex lacteus*. Acta Chim. Slov. 53, 338–343 (2006).

Tien M., Kirk T.K.: Lignin-degrading enzyme from *Phanerochaete chrysosporium*: purification, characterization and catalytic properities of unique H_2O_2 requiring oxygenase. Proc. Natl .Acad. Sci. USA 81, 2280–2284 (1984).

Valentín L., Lu-Chau T.A., López C., Feijoo G., Moreira M.T., Lema J.M.: Biodegradation of dibenzothiophene, fluoranthene, pyrene and chrysene in a soil slurry reactor by the white-rot fungus *Bjerkandera sp.* BOS55. Proc. Biochem. 42, 641–648 (2007).

Wang Y., Yu J.: Adsorption and degradation of synthetic dyes on the mycelium of *Trametes versicolor*. Water Sci. Technol. 38, 233–238 (1998).

Wesenberg D., Kyriakides I., Agathos S.N.: White-rot fungi and their enzymes for the treatment of industrial dye effluents. Biotechnol. Adv. 22, 161–187 (2003).

Zheng Z., Obbard J.P.: Removal of surfactant solubilized polycyclic aromatic hydrocarbons by *Phanerochaete chrysosporium* in a rotating biological contactor reactor. J. Biotechnol. 96, 241–249 (2002).

CHEMICAL ENGINEERING TRANSACTIONS, Volume 14, 2008
Edited by G. Marino, E. Bardone, A. Viglia
 ISBN 978-88-95608-02-0

Use of Enzymes in the Pre-Treatment of Cotton

Klaus Opwis, Dierk Knittel, Eckhard Schollmeyer
Deutsches Textilforschungszentrum Nord-West e.V.
Adlerstr. 1, D-47798 Krefeld, Germany

Due to the ever-growing costs for water and energy worldwide investigations are carried out to substitute conventional chemical textile processes by environment-friendly and economically attractive bioprocesses using enzymes. Here, a successful strategy for the combined use of α-amylase, hemicellulase and pectinase in the pre-treatment of cotton is described. After hot bleaching enzymatically pre-treated cotton exhibits similar or even better properties compared to conventionally desized, alkaline scoured and bleached cotton. The combined use of the enzymes allows to omit the alkaline scouring without a loss of quality in the finishing result. The described enzymatic procedure is accompanied by a significant lower demand of energy, water, chemicals, time and therefore costs. So it has advantages as well in terms of ecology as in economy. Another field of investigations targets the subsequent bleaching process. The authors developed a new concept combining the use of two oxidoreductases in bleaching processes. Starting with glucose as substrate for glucose oxidase (GOD) hydrogen peroxide is generated in situ. The freshly built substrate H_2O_2 is used immediately by peroxidases (POD) to oxidize colored impurities on cotton yielding a higher degree of whiteness.

1. Introduction

The potential of the so-called “white biotechnology” as an ecological advantageous and moreover economical beneficial technology is beyond all question. Caused of the ever-growing costs for energy and polluted waste water, enzymatic technologies will stay in the focus of science and technique, and their relevance will increase significantly in the future. Enzymes, biological catalysts with high selectivities, have been used in the food industry for hundreds of years, and play an important role in many other industries (washing agents, textile manufacturing, pharmaceuticals, pulp and paper). Currently, enzymes are becoming increasingly important in sustainable technology and green chemistry. In the opinion of many experts and based on different studies, by 2010, 20 % of all chemical products in a dimension of 300 billion US dollar will be produced using biotechnology. This would represent a tenfold increase compared to 2001 [1-3].

Especially in textile manufacturing the use of enzymes has a long tradition. The enzymatic desizing of cotton with α-amylases is state-of-the-art since many decades [4]. Moreover, cellulases, pectinases, hemicellulases, lipases and catalases are used in different cotton pre-treatment and finishing processes [5]. Other natural fibers are also treated with enzymes. Examples are the enzymatic degumming of silk with sericinases [6], the felt-free-finishing of wool with proteases [7] or the softening of jute with cellulases and xylanases [8]. In future, also synthetic fibers such as polyester [9] or

polyacrylonitrile [10] will be modified by an enzymatic treatment. The application of enzymes has many advantages compared to conventional, non-enzymatic processes. Enzymes can be used in catalytic concentrations at low temperatures and at pH-values near to neutral. Their high substrate selectivity allows a very gentle treatment of the goods. Moreover, enzymes are biologically degradable and can be handled without risk [11,12].

Besides cellulose cotton contains in the so-called primary wall natural compounds such as pectins, hemicelluloses, proteins, waxes and lignin, which can impair the finishing results. In conventional pre-treatment these substances are removed by a strong alkaline treatment at high temperatures after the enzymatic desizing of raw cotton fabrics with α-amylases. This inspecific alkaline scouring process has a high energy, water and alkali consumption and can also cause a damage of the cellulosic material [13].

The aim of this work is the development of a comprehensive concept for the enzymatic pre-treatment of cotton to replace the alkaline scouring (**Figure 1**). The material should be desized and prepared for following bleaching and dyeing in a single step using α-amylases and further enzymes such as pectinases and hemicellulases. The renouncement of the alkaline scouring process leads to ecological and economic advantages for industrial users.

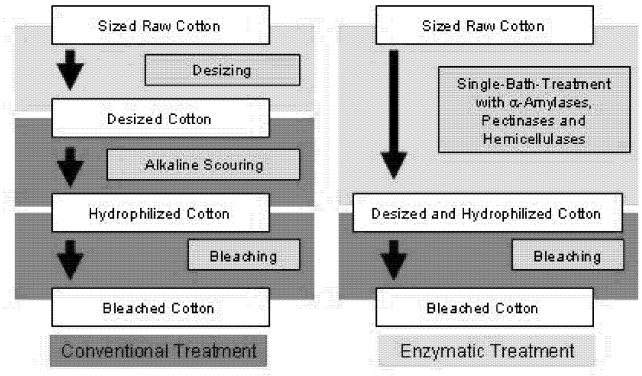

Figure 1: Processing steps for the conventional and enzymatic pre-treatment of cotton.

Moreover, investigations were carried out to substitute the subsequent hot and alkaline bleaching step by the use of oxidoreductases under moderate conditions. Former investigations were focussed on the enzymatic generation of hydrogen peroxide as bleaching agent with glucose oxidases (GOD) using sugar from desizing liquors [14-16]. This process failed in technical applications because of its general problems. At first, the used glucose oxidase has to be free of catalase, which is often found as a by-product in technical GOD preparations. This enzyme destroys any generated hydrogen peroxide immediately. Moreover, in bleaching processes the decomposition of hydrogen peroxide into radicals needs alkaline conditions at high pH-values and high temperatures - so the process has only a small benefit in terms of economy and ecology.

Another approach was to use peroxidases (POD), which are successfully applied in the decoloration of dyeing baths [17,18], for cotton bleaching [14]. While decoloration of dissolved dyestuffs works fast, in the two-phase system POD-solution/cotton the enzymatic oxidation of cotton impurities is significantly slower. During the process POD is attacked by hydrogen peroxide resulting in a high loss in activity.

Therefore, a new concept for a simultaneous application of glucose oxidase and peroxidase was developed as illustrated in **Figure 2**. Starting with glucose as substrate for the GOD hydrogen peroxide is generated in situ, which is immediately used by the POD to oxidize colored compounds in dyeing baths. In this way the stationary peroxide concentration is nearly zero during the whole process and the enzymes are not degraded by the oxidizing agent. Moreover, experiments are carried out to check if this two-compound-system is suitable for textile bleaching of natural cotton fibers.

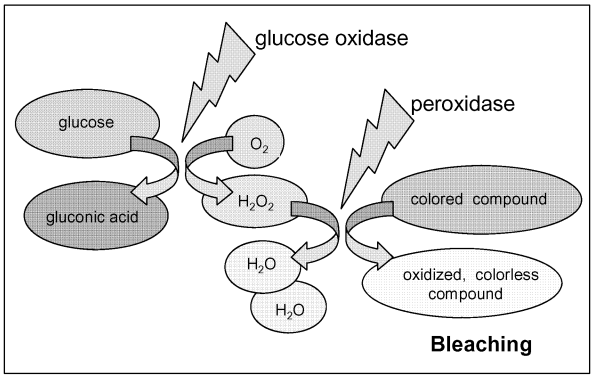

Figure 2: Use of oxidoreductases in bleaching processes.

2. Experimental

2.1 Combination of Desizing and BioScouring

A common industrial, sized cotton fabric with a starch layer of 8 wt.-% is used (187 g/m^2, width 160 cm). As Enzymes the α-amylase Beisol T 2090® (CHT, Tübingen, Germany) and the mixed hemicellulase/pectinase product Beisol DHP® (CHT) are used. All enzymes are industrial products. As auxiliaries the non-ionic surfactant Felosan Jet® (CHT), the biological degradable complexing agent Beixon NE® (CHT) and the buffer Neutracid NVM 200® (CHT) are used. After optimizing the process on lab scale industrial experiments are carried out at the "Textilveredlung an der Wiese" at Lörrach (Germany). Raw cotton is treated with enzymes via a cold pad-batch procedure. The conventional treatment (desizing with α-amylases) is followed by a common alkaline scoring (experiment C). The enzymatic treatment (experiment E) is done with a mixture of Beisol T 2090® and Beisol DHP® without following alkaline scouring. Finally the cotton is dried in a stenter frame. The differently treated materials are subsequently stitched together and bleached hot. All procedures correspond to conventional industrial practise.

2.2 Enzymatic Bleaching

The bleaching was done with a commercial desized and alkaline scoured cotton fabric. A nearly catalase-free GOD was delivered from Erbslöh (Geisenheim, Germany). Glucose was purchased from Fluka. POD is a commercial Baylase®RP system from Lanxess (Germany). The incubation investigations of the POD were done in combination with Baylase®Assist RP, which contains the hydrogen peroxide. Moreover, decoloration and bleaching experiments were done using a new chloro-peroxidase (CPO) from ASA-Spezialenzyme (Wolfenbüttel, Germany).

Decoloration of dyestuff with GOD, glucose and POD

20 mg Sirius Supra Blue®FGG 200 %, 1 mg GOD and 0.5 ml Baylase®RP respectively 0.5 ml CPO were added to 50 ml buffer pH 7 (T = 37 °C). The reaction was started by adding 125 mg glucose. After different times (range 0 min to 75 min) the absorption of the solutions was measured with an UV-Vis-spectrometer (Cary 5E).

Bleaching of cotton with GOD, glucose and POD

1 g cotton was stirred in 50 ml buffer with 50 mg GOD and 0.5 ml Baylase®RP respectively 0.5 ml CPO at 37 °C. The bleaching process was started by adding 600 mg glucose. After 90 min the cotton was removed and washed with distilled water.

3. Results

3.1 Combination of Desizing and BioScouring

It had to be examined, whether the alkaline scouring can be substituted by an alternative one-step enzymatically catalyzed process. After detailed preparatory work on lab scale industrial experiments are realized on sized raw cotton. The fabrics are wetted with an enzyme containing liquor (α-amylases, pectinases and hemicellulases, experiment E) with no subsequent alkaline scouring. PH-value is 5 due to the pH-optima of the enzymes. For comparison a classical desizing followed by a conventional alkaline scouring is carried out (experiment C). Both experiments are completed by a subsequent hot bleaching step, which is necessary to remove the coloured compounds of cotton (chromophores, pigments) and to fulfil a degree of whiteness of at least 90 (Stensby).

Table 1 shows the most important parameters of textile interest for the cotton fabrics after the bleaching process. All samples reach an excellent degree of whiteness of more than 90. The enzymatic treatment E gives the highest levels. Moreover the materials show no visible residues of seeds capsules. In both cases the degree of desizing is excellent The level of 8 of the enzymatic treatment using α-amylase and hemicellulase/pectinase (E) is only insignificantly lower than the level of the conventional treatment C. Moreover hot bleaching shows a particularly dramatic effect in terms of the wettability. The enzymatic decomposition of pectins and hemicelluloses improves the accessibility of the fiber for the bleaching chemicals, which remove remaining hydrophobic residues completely. So the wettability of the enzymatically treated material is excellent and as good as the conventional treated fabric. Pre-treatment - especially inspecific alkaline scouring - has a direct influence on the weight and the mechanical properties of cotton. Weight loss is mainly caused by desizing and

removal of undesired cotton components. But moreover the alkaline treatment causes a partial hydrolysis of the cellulosic material, which might damage the fiber material. As expected the conventionally treated material shows the highest weight loss. The mass per unit area decreases from 187 g/m^2 to 166 g/m^2 (- 11.2 %). Compared to this the enzymatic procedure using the hemicellulase/pectinase formulation reduces the weight only by 8.0 %. The different damage of cotton fabric is shown best regarding the tensile strength, the elongation and the average degree of polymerisation. The enzymatic procedure E delivers the best mechanical properties.

Table 1: Parameters of different treated cotton after hot bleaching.

Parameter	C	E
Degree of desizing	8 - 9	8
Drop penetration time [s]	3	1
Mass per unit area [g/m^2]	166	172
rel. Weight loss to raw material [%]	- 11.2	- 8.0
Degree of whiteness (Stensby)	90.2	90.5
Seeds capsules	none	none
Tensile strength [daN]	61.6	63.0
Elongation at F_{max} [%]	24.4	24.7
Degree of polymerisation DP	1590	1694

Table 2: Saving potential of combined use of Beisol T 2090 and Beisol DHP compared to conventional cotton pre-treatment related to one metric ton cotton (*calculated for an average German middle-class textile finishing company)

Water demand	6,000 l
Energy	2.21 GJ or 615 kWh
CO_2	115 - 250 kg
NaOH	75 kg
Costs*	226.-- €

With regard to all producing parameters such as e.g. water consumption, energy input, productivity, working staff **Table 2** summarizes the economic and ecological advantages of the combined enzymatic pre-treatment using α-amylase, hemicellulase and pectinase (E) compared to the conventional procedure including alkaline scouring (C). In both cases the quality of the treated goods after a bleaching step is equivalent. All items are related to one metric ton cotton and can be easily transferred to each manufacturing amount to find the specific potential saving of a cotton pre-treating company.

3.2 Enzymatic Bleaching

As described in the introduction peroxidases (POD) are used in textile decoloration processes, but their activity is limited by the hydrogen peroxide concentration, which

attack the POD during the reactions. To maintain the activity of the POD over a long time period the new combined system of GOD and glucose as the hydrogen peroxide source and additional the POD as an oxidation catalyst was used exemplarily for the slow decoloration of Sirius Supra Blue®FGG 200 %.

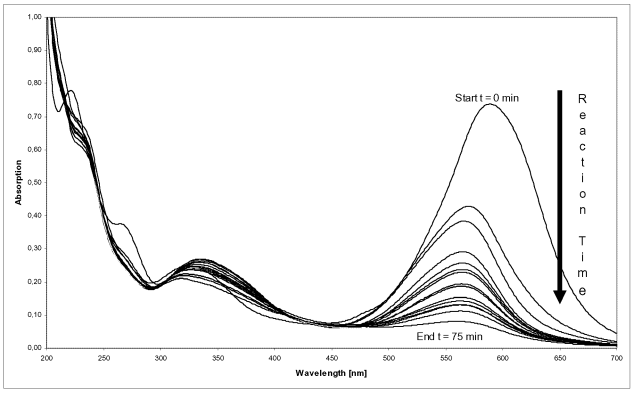

Figure 3: Decoloration of Sirius Supra Blue®FGG 200 % with glucose oxidase, glucose and peroxidase (Baylase®RP).

Figure 3 shows UV-Vis-spectra of the Sirius Supra Blue®FGG 200 % solutions after different reaction times. The dyestuff has an absorption maximum at approximately 600 nm and the intensity decreased during the reaction time. The GOD oxidizes glucose to gluconic acid and generates hydrogen peroxide, which can be used by the POD for the oxidation of the dyestuff over a long period without inactivating the enzymes. After 75 min the decoloration has finished. Similar results can be achieved using the new chloro-peroxidase from ASA-Spezialenzyme. In this case the oxidation of the dyestuff is finished already after 60 minutes.

After showing that the suggested combined use of both oxidoreductases works in principle for decoloration processes investigations were carried out to use this enzyme cascade for textile bleaching processes. In **Figure 4** the results of different bleaching procedures of cotton are summarized. The starting material has a degree of whiteness (according to Berger) of 55. Bleaching of cotton with POD (Baylase®RP) in the presence of hydrogen peroxide fails, the degree of whiteness remains at 55, because the POD is inactivated by H_2O_2 after a short time. Using the combined system with GOD, glucose and POD (Baylase®RP) the degree of whiteness increases up to 64. Applying GOD and the new chlor-peroxidase from ASA-Spezialenzyme simultaneously in the presence of glucose a degree of whiteness of 66 can be reached. Compared to a conventional non-enzymatic bleaching process using only hydrogen peroxide at high pH-value and high temperature the bleaching result is not satisfactory but the investigations show that this environment-friendly enzymatic bleaching procedure at low temperature and a pH-value near to neutral basically works.

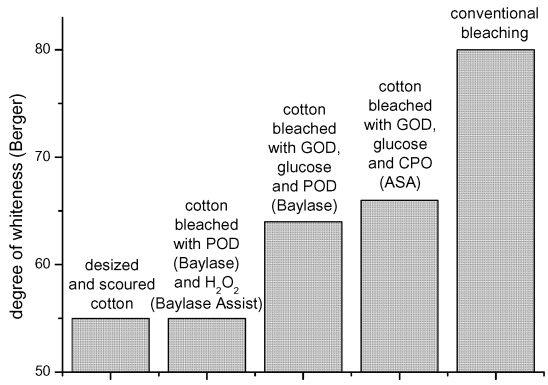

Figure 4: Bleaching of cotton with glucose oxidase, glucose and different peroxidases.

4. Conclusions

Due to the ever-growing costs for water and energy worldwide investigations were carried out to substitute conventional chemical textile processes by environment-friendly and even economic attractive bioprocesses using enzymes.

Here, a successful strategy for the combined use of α-amylase and hemicellulase/pectinase in the pre-treatment of cotton is developed. The pectin and hemicellulose degrading enzymes are given to the desizing liquor. Besides the desizing the removal of undesired substances can be fulfilled in one step. In the sunsequent bleaching step residual hydrophobic components such as fats and waxes can be mobilised and removed. It can be shown that the enzymatic pre-treated cotton has similar or even better properties after a hot bleaching than the conventional desized and alkaline scoured material. So the combined use of the α-amylase Beisol T 2090 and the hemicellulase/pectinase Beisol DHP in the pre-treatment of cotton allows to renounce the alkaline scouring without a loss of quality in the finishing result. Neither the wettability nor the degree of whiteness or the dyeability of the bleached material are worse than for the conventional treated cotton; moreover the material is treated more gently and shows better mechanical properties. The new enzymatic procedure is corresponding with a significant lower demand of energy, water, chemicals, time and therefore costs. So it has advantages as well in terms of ecology as in economy.

An enzymatic cotton bleaching process is not realized up to now because of different problems such as the use of catalase contaminated GODs or the inactivation of PODs by hydrogen peroxide. Therefore a new concept was developed combining the use of two oxidoreductases, GOD and POD, in textile decoloration and bleaching processes. Under gentle conditions in terms of temperature, pH-value and even the peroxide concentration different peroxidases (commercial POD from Lanxess and a new chloro-peroxidase from ASA-Spezialenzyme) are stable over a long period of time, what offers the

possibility to use this enzyme cascade also in heterogeneous systems such as the bleaching of cotton fabrics. First results are of great promise. Up to now, indeed this concept is not able to compete with conventional bleaching, but the authors show that the combined use of oxidoreductases works in principle in decoloration and bleaching processes. In future further investigations have to be carried out to open this environment-friendly concept for an even economic attractive application in large-scale industrial manufacturing.

5. Acknowledgement

The authors wish to thank the Deutsche Bundesstiftung Umwelt for the financial support of the project DBU AZ 13058 and the Arbeitsgemeinschaft Industrieller Forschungsvereinigungen “Otto-von-Guericke” e.V. for the financial support of the project KF 0112601MD5 (Pro Inno II).

6. References

[1] Thomas, M.J. and R. Raja, 2005, Annu. Rev. Mater. Res. 35, 315.
[2] Bachmann, R., 2003, Industrial Biotech - New Value-Creation Opportunities, Presentation at the Bio-Conference, New York .
[3] Festel, G., J. Knöll, H. Götz and H. Zinke, 2004, Chemie Ingenieur Technik 76, 307.
[4] Marcher, D., H.A. Hagen and S. Castelli, 1993, ITB Veredlung 39, 20.
[5] Meyer-Stork, L.S., 2002, Maschen-Industrie 52, 32.
[6] Gulrajani, M.L., 1992, Rev. Prog. Coloration 22, 79.
[7] Fornelli, S., 1994, Melliand Textilber. 75, 120.
[8] Kundu, A.B., B.S. Ghosh, S.K. Chakrabarti and B.L. Ghosh, 1991, Textile Res. J. 61, 720.
[9] Yoon, M.-Y., J. Kellis and A.J. Poulose, 2002, AATCC Review 2, 33.
[10] Tauber, M., G. Gübitz and A. Cavaco-Paulo, 2001, AATCC Review 1, 17.
[11] Uhlig, H., 1991, Enzyme arbeiten für uns, C. Hanser Verlag, München.
[12] Ruttloff, H., 1994, Industrielle Enzyme, Behr´s Verlag, Hamburg.
[13] N. N., 2002, Reference Document on Best Available Techniques for the Textiles Industry, European Integrated Pollution Prevention and Control (IPPC) Bureau, European Commission.
[14] Schacht, H., W. Kesting, E. Schollmeyer, 1995, Textilveredlung 30, 237.
[15] Opwis, K., A. Kele, D. Knittel, E. Schollmeyer, 1999, Starch 51, 348.
[16] Buschle-Diller, G. and X.D. Yang, 2001, Textile Res. J. 71, 388.
[17] Abadulla, E., L. Silva, K.H. Robra, A. Cavaco-Paulo and G.M. Gübitz, 2000, Text. Res. J. 70, 409.
[18] López, C., M. T. Moreira, G. Feijoo and J. M. Lema, 2004, Biotechnol. Prog. 20, 74.

CHEMICAL ENGINEERING TRANSACTIONS, Volume 14, 2008
Edited by G. Marino, E. Bardone, A. Viglia
 ISBN 978-88-95608-02-0

Pseudomonas aeruginosa Growth in Microwave Irradiated Environment

Renzo Carta and Francesco Desogus
Dipartimento di Ingegneria Chimica e Materiali
Università degli Studi di Cagliari
Tel.: +39 070 675 5068 – Fax: +39 070 675 5067 – e-mail: carta@dicm.unica.it

In this work we present the variation of the growth rate constant, of the microorganism *Pseudomonas aeruginosa* (PA) (a not spore forming and gram negative species), in microwave irradiated fields with respect to that obtained in the same experimental conditions but in absence of radiation. The microwaves, produced by a solid state oscillator, were used to irradiate a reacting suspension in a plug flow reactor positioned into a WR430 waveguide. The radiation powers used were 0, 100, 200, 300 and 400 mW. Also the frequency was varied (2.20, 2.30, 2.40 and 2.50 GHz). The reacting mixtures were obtained by adding 1 cc of a suspension containing 10^6 cells/cc of PA to a sterilized nutrient solution; the nutrient solutions were made by dissolving, in 200 cc of distilled water, 4.4 g of lyophilized Müller Hinton® broth. The growth kinetic constants were derived from optical density (OD) experimental determinations of the reacting mixtures. The measured OD values in the exponential growth region were processed by linear regression. To confirm the results, the growth rate values were also derived by the traditional method of the bacterial count (CFU/cc vs. t data). No effects of the microwave radiation were observed in the field of power 0÷300 mW. Low, but greater then experimental errors, reductions in the growth rate constant were observed with a radiation of 400 mW of power and in the range 2.3÷2.4 GHz of frequency.

1. Introduction

The aim of this work was to see if it is possible to reduce the growth rate of a bacterial population in an aqueous solution of a nutrient medium by radiating the reactor with low power microwaves at frequencies from 2.20 GHz to 2.50 GHz and at the controlled temperature of 37°C. The reduction of the bacterial growth rate by using low power microwave radiation could be an important fact because it would show the possible presence of non-thermal effects of this kind of radiation on biological systems; furthermore, it could address to the possibility of using that radiation in the food materials processing, so increasing the shelf life of the final products besides the preservation of their nutritional and organoleptic properties.
So our objective is to study the possibility of obtaining the reduction of the growth rate of bacteria using low power microwave (MW) radiation and working at temperatures lower than 37°C; in fact at these temperatures we are confident that all nutritional and organoleptic properties of interest for human being are saved.
The electromagnetic radiation of frequencies ν in the range between 2.20 and 2.50 GHz, notwithstanding it has not a photon energy ($E=h\cdot\nu$) high enough to modify the atomic

structure of the components in the radiated environment, can however interact with the super-molecular structures (like the cells), changing their characteristics; in the same way it can interact with the bacterial populations (Webb and Dodds, 1968; Webb and Dodds, 1969). Moreover, the accepted idea that interactions between the MW radiation and the human body (Hardell et al., 2006; Uloziene et al., 2005) can exist brings to the conclusion that if microwaves produce interferences with fully-developed and rich of natural protections organisms they can produce effects on the microorganisms populations that have less natural protections.

2. Experimental

2.1 Apparatus

The experimental procedure started with the inoculation of about 1 cc of seed to 200 cc of a sterile nutrient solution containing 4.4 g of lyophilized Müller Hinton (MH) nutrient. So the population of *Pseudomonas aeruginosa* could develop, and the growth process happened either in irradiated or in non-irradiated fields; to avoid any contamination all the process must run in a system that is completely isolated from the environment. Also the analysis of the bacterial concentration in the reacting suspension (after the growth starting the original nutrient solution becomes an heterogeneous mixture) leaving the reactor was made continuously without any drawing that could be a vehicle of contaminations. In Figure 1 the experimental structure is shown. The pirex bottle (5), filled with the MH nutrient solution, was hermetically sealed (4) with a cap and connected to the circuit, that could be sterilized as whole. The reacting fluid was

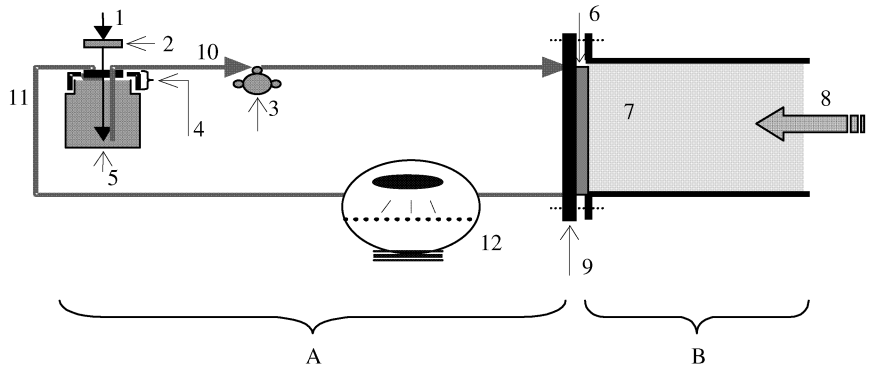

Figure 1. Sketch of the proposed experimental apparatus (1: external air; 2: ceramic filter of the external air 20 μm; 3: peristaltic pump; 4: cap that can be sterilized; 5: bottle containing the suspension to be irradiated; 6: PFR where the bacterial suspension is irradiated; 7: waveguide; 8: incident microwave radiation; 9: plate containing the PFR and closing the waveguide; 10: withdrawal of the bacterial suspension from the bottle; 11: recycle of the bacterial suspension to the bottle; 12: spectrophotometric analysis system).

pumped by a peristaltic pump (3) with a flow rate of 40 cc/min. The circuit was made of silicon tubes (ID 2 mm; OD 4 mm) and, if necessary, tubes of stainless steel (ID 2 mm). The reactor, from a fluidodynamic point of view, can be thought as a plug flow reactor (PFR); it was made with a silicon tube (ID 4 mm; OD 6 mm) and it was placed on the irradiated part of the stainless steel plate (9); the residence time of the suspension in the reactor was 24 s. The stainless steel plate was also used to close the waveguide (7). The silicon tubes were chosen because of their flexibility and their transparency to microwave radiation (Von Hippel, 1954, p. 361). Junctions were made using Swagelok® products, that made a full insulation from the external environment and safe connections possible. Then the 200 cc of MH nutrient solution were put into the container that was sealed and the entire part A of the circuit was sterilized. The sterilization was made by putting the complete block in an autoclave for 20 minutes at 121°C.

2.2 Generation and transport of the microwave radiation

The microwave radiation was generated by a YIG oscillator (1 in Figure 2) at the frequencies of 2.20, 2.30, 2,40 and 2.50 GHz; so the power of radiation was increased in an amplifier (4 in Figure 2) and then sent through a waveguide-cable converter to a WR430 waveguide where the PFR was lodged in the final part and the reacting mixture was irradiated.

3. Discussion

Starting from the Monod equation, if the growth of a bacterial species happens in a large excess of substrate environment, it is possible to write:

$$\mathrm{Ln}\,(C_C/C_{0C})=kt \qquad (1)$$

In Eq. (1) C_{0C} is the concentration of microorganisms at the time t=0. The analysis of the reacting mixture was performed by reading the optical density (OD) by a spectrophotometer (Varian Cary 50®); if the zero point of the spectrophotometer is made using the mixture of the MH nutrient and the inoculum (at t=0), a relation

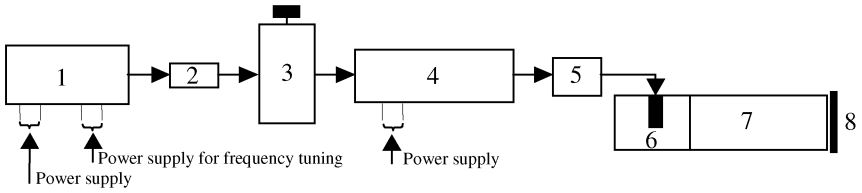

Figure 2. Sketch of the microwave generating apparatus (1: oscillator; 2: fixed attenuator; 3: rotating attenuator; 4: amplifier; 5: insulator; 6: cable–waveguide converter; 7: WR430 waveguide; 8: final plate with the reactor). Connection made with RG316 cables.

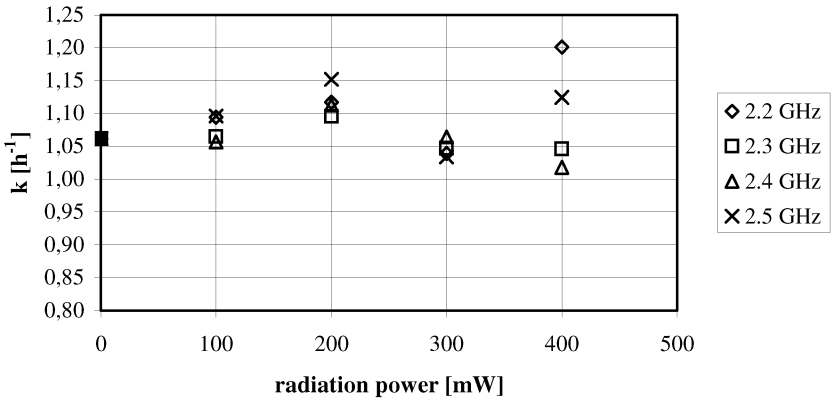

Figure 3. Experimental growth rate constant as a function of the radiation power and frequency.

between the optical density and the biomass concentration can be written as:

$$C_C=\alpha OD \quad (2)$$

Eq. (2) is valid only for low OD values (Ageno, 1992, pp. 44-49); if this condition is respected, Eq. (1) can be rewritten in the form:

$$\text{Ln}\,(OD_t/OD_0)=kt \quad (3)$$

where OD_t is the optical density of the reacting solution read at the time "t", and OD_0 that read at the beginning of the experimental run (t=0).
The experimental OD vs. t curves were obtained by using radiation powers of 0, 100, 200, 300 and 400 mW and frequencies of 2.20, 2.30, 2.40 and 2.50 GHz. The kinetic constant k was derived from Eq. 3 by a linear regression of the experimental data points in the form Ln (OD_t) vs. t. In Figure 3 the values obtained for k in the different experimental conditions are reported; each data point is the medium value of nine different experimental data. To confirm the validity of the obtained values for the kinetic constant, derived from the OD experimental measurements collected in the exponential growth zone, at the exit of the PFR some samples were withdrawn and analysed to obtain the concentration of the living microorganisms with the traditional methods of the bacterial count, then the kinetic constants derived from the OD measurements were compared to those derived from the determination of the real number of living bacteria. The comparison between the two measuring procedures highlighted the substantial methodological correctness of the k values derived from the OD measurements; in Figure 4 a typical experimental points series regression curve

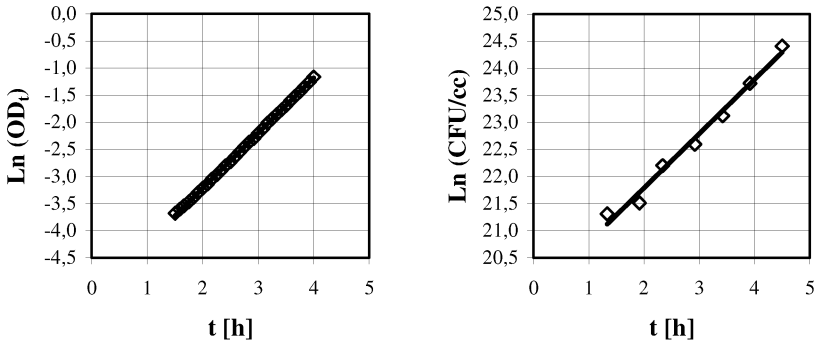

Figure 4. Regression curves of experimental Ln (OD_t) vs. t (part a) and Ln (CFU/cc) vs. t (part b). Part a: slope=1.0148, R^2=0.9997; part b: slope=1.0017, R^2=0.9852.

from OD vs. t measurements and the corresponding regression curve of Ln (CFU/cc) vs. t data are shown; the linear regression results in both cases confirms (as can be seen with very different R^2 values) the goodness of the obtained results, so the not invasive method that did not require any withdrawn from the reacting material was employed rest upon the correctness of the obtained results.

4. Conclusions

The obtained results bring to three main conclusions:

1) about the microorganism *Pseudomonas aeruginosa* we did not see any effect of the MW radiation power in the field 0÷300 mW; in fact the values of the kinetic constant show variations into the field of error connected with the experimental determinations. The value of the kinetic constant obtained at powers 100, 200 and 300 mW are about equal to that obtained for non irradiated mixtures;
2) the effect of frequency, as shown in Figure 3, can be seen only at 400 mW; at this power we noted, for frequencies in the field 2.30 – 2.40 GHz, a low, but greater than the experimental errors, reduction of the growth rate constant with respect to those obtained at powers lower than 400 mW,
3) at frequencies out of the range specified in the previous point the experimental values of k are very different from those obtained at 2.30 and 2.40 GHz. This can be a poor but important rally of a possible specific effect of the radiation at frequencies in the field 2.30 – 2.40 GHz on the growth rate of the bacillus *Pseudomonas aeruginosa*.

In future we plan to extend our experimental work in the field of frequencies 2.30 – 2.40 GHz and for power greater than 400 mW to highlight, if exist, a possible MW effect.

5. References

Ageno, M., 1992, La Macchina Batterica, Lombardo Editore, Rome (in Italian).
Hardell, L., K. Hanson Mild, M. Carlberg and F. Soderqvist, 2006, J. of Surg. Oncol. 11, 4.
Uloziene, I., V. Uloza, E. Gradauskiene and V. Saferis, 2005, BMC Public Health 19, 5.
Von Hippel, A., 1954, Dielectric Materials and Applications, Technology Press of MIT, Cambridge.
Webb, S. J. and D. E. Dodds, 1968, Nature 218, 374.
Webb, S. J. and D. E. Dodds, 1969, Nature 222, 1199.

CHEMICAL ENGINEERING TRANSACTIONS, Volume 14, 2008
Edited by G. Marino, E. Bardone, A. Viglia
 ISBN 978-88-95608-02-0

Membrane filtration of surface water for the removal of humic substances

Marina Prisciandaro, Annarita Salladini and Diego Barba
Dipartimento di Chimica, Ingegneria Chimica e Materiali, Università dell'Aquila, Monteluco di Roio, 67040 L'Aquila, Italy

In this study the removal of humic substances from synthetic water through ultrafiltration (10, 100 kDa) and microfiltration membranes (0.2 μm) has been investigated. Two membrane configurations (flat sheet and tubular) have been used, and their performances compared. Permeate and retentate samples were analyzed by UV254 nm absorbance to evaluate humic acid removal while permeability and flux decay test were performed to estimate biofouling caused by organic material. Filtration tests with a model solution have shown that the studied UF membranes are effective, with a removal efficiency of UF membrane of 85-90% at humic acid concentration over 7.5 mg/L, while MF membrane are very efficient only if used in tubular configuration, reaching organic matter removal of 90%.

1. Introduction

Membrane processes have increased rapidly over the past decade in potable water production offering several advantages over conventional treatment such as compact module, lower energy consumption, environmental friendliness and high quality product independently on fluctuations in feed quality. MF and UF processes have been increasingly used in drinking water treatment as an alternative technology to conventional filtration and clarification, in order to remove particles, turbidity, microorganisms and natural organic matter (NOM). The latter can be considered a mixture of organic compounds whose major fraction is the one relative to the humic substances (Yuan and Zyney, 1999). Humic substances are complex, acidic organic molecules formed by the decomposition of plants, animals and microbial material. They first came to prominence in agriculture, because of their positive influence on the structure, water retention properties, and nutrient status of soils but they pose problems to the water supply industry. Removal of NOM is extremely important and it has became a challenging research in current development of water purification technologies, not only because it affects the odour, colour and taste of water but mainly because it is considered as a precursor of disinfection by-products (DBPs). The most dangerous DBPs, recently recognised to be human carcinogens are halogenated organic compound such as trihalomethanes (THMs) and haloacetic acids (HAAs), derived from reaction of organic material with free chlorine used as a disinfectant in conventional treatment. DBPs control can be done by minimizing natural organic matter (precursors) in the raw water, by reducing disinfectant doses, by removing DBPs after they form or by using alternative disinfectants. Katsoufidou et al. (2005) studied humic acid rejection on polyethersulfone hollow fiber membrane (whose Molecular Weight Cut-Off –

MWCO – was 150 kDa) obtaining rejections close to 20% in the absence of calcium and up to 75% with 2 mM Ca^{2+}. Mozia and Tomaszewska (2004) studied a hybrid process (powdered activated carbon PAC/UF) with membranes prepared from polyacrylonitrile (MWCO 110 kDa); filtration test on natural waters showed that a PAC dosage of 100 mg/L enhanced organics removal from 44% to 64% and reduced membrane fouling by preventing organics from adsorption onto the membrane surface. Other researchers (Lin et al., 1999) found that the use of PAC either as a pretreatment agent or as an additive in the integrated PAC-UF system exhibits an increased membrane fouling. Aoustin et al. (2001) studied the influence of calcium concentration on humic acid rejection through membrane of MWCO 10 and 100 kDa. They obtained rejections of 84-92% at $CaCl_2$ concentration in the range of 0.5-4 mM. Domany et al. (2002) tested four polyether-sulfon membrane of MWCO 5, 6, 15, 100 kDa obtaining a satisfactory removal efficiency of 85-90% for model solution and 62-69% for natural well-water.

In this study the removal of humic substances from model-solution through ultrafiltration (10, 100 kDa – flat sheet configuration) and microfiltration membranes (0.2 μm - flat sheet and tubular configuration) has been investigated. Permeate and retentate samples were analyzed by UV254nm absorbance to evaluate humic acid removal while permeability and flux decay test were performed to estimate biofouling caused by organic material.

2. Materials and Methods

2.1 Experimental apparatus

Experimental studies have been carried out in a tangential flow laboratory pilot plant Minitan S, (Millipore) equipped with a single flat sheet polyvinylfluoride membrane and a tangential flow laboratory pilot plant Membralox® XLAB 3 (EXEKIA, Bazet–France) with a single tube ceramic ultrafiltration membrane Membralox® Tl-70. Figure 1 shows the two pilot plants used for the present study. Temperature is controlled by the tank jacket, which is connected to a thermostat CRIOTERM 10–80. Three flat sheet membranes were tested with a MWCO of 10, 100 kDa and 0.2 μm, while the tubular membrane used has a MWCO of 0.2 μm.

2.2 Feed water characteristics

A model solution was created to supply constant quality of water sample by simulating real surface water: it contained $CaCl_2$ as a representative of naturally occurring multivalent cations, $NaHCO_3$ as a natural buffer system, kaolinite and α-alumina as natural turbidity and humic acid as natural organic matter. A commercial humic acid (Aldrich) was employed in the present experiments. Humic acid stock solution was prepared by dissolving 100 mg Aldrich Humic Acid (AHA) in 1 L distilled water, the pH of the solution was set to 10 by using NaOH to assure complete dissolving of humic acid since the latter is insoluble at low pH; solution was then filtered through 0.2 μm membrane filter. Background solution was prepared by dissolving 2.5 mg/l α-alumina and 2.5 mg/l kaolinite in deionized water (Milli-Q) in ultrasound bath for 20 min. Solution was then supplemented with $NaHCO_3$ and $CaCl_2$ and the desired humic acid concentration was adjusted using humic acid stock solution (100 mg/L AHA). After all the components were added, the solution was mixed rapidly for an hour with magnetic stirrer.

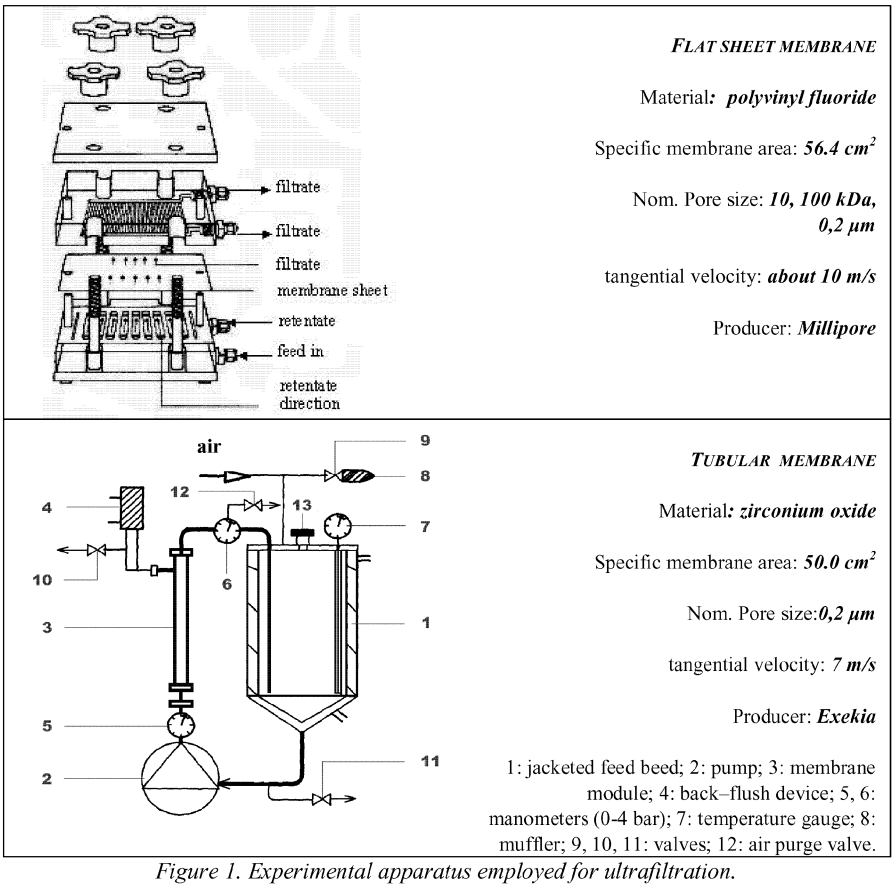

Figure 1. Experimental apparatus employed for ultrafiltration.

The average characteristics of synthetic water are presented in Table 1.

Table 1. Synthetic water characteristics.

NOM	
(Aldrich Humic Acid)	2.5-5.0-7.5-10 mg/L
Inorganic particles	
Kaolinite	2.5 mg/L
α-Alumina	2.5 mg/L
Salts	
$NaHCO_3$	0.5 mM
$CaCl_2$	0.5 mM

2.3 Testing procedure

The effect of membrane cut-off and AHA concentration on membrane performance was studied. Permeability, flux decay and concentration tests were executed for different AHA concentrations for each membrane. During the flux decay tests, the transmembrane pressure (TMP) was adjusted to 1 bar and temperature was controlled by the water jacket and kept constant to the value T = 20°C. Permeate flux was measured for 3 h manually and the samples were collected from retentate and permeate and analyzed for the parameters such as humic acid concentration, pH, turbidity.

AHA concentrations were determined by UV absorbance measurements in a spectrophotometer (Lambda 2S PerkinElmer) at the wavelength 254 nm; AHA concentration was correlated linearly with UV 254nm (R^2= 0.9994). After each test, the equipment and membrane were washed with an alkaline solution (NaOH) and rinsed with distilled water until pH returned to the value of about 7.

2. Results

In this study UF an MF filtration test with three flat sheet membranes and a tubular membrane were carried out to evaluate the effects of membrane cut-off (10, 100 kDa and 0.2 µm), membrane configuration (flat sheet and tubular) and feed composition on membrane performance regarding AHA rejections and fouling.

3.1 Permeability and flux decay tests

Permeability tests were performed to evaluate membrane resistance to mass transfer at different AHA concentration; they were carried out by measuring the permeate flowrates with varying transmembrane pressure. In each run the operating parameters (temperature, cross flow velocity and feed concentrations) were constant (steady-state conditions). Figures 2 and 3 show the influence of TMP on permeate flowrates at different AHA concentrations, for flat sheet membranes of 10 and 100 kDa MWCO, respectively. Figure 4 and 5 show instead the effect of TMP for MF membranes (0.2 µm), for flat sheet (Fig. 4) and tubular (Fig. 5) configurations.

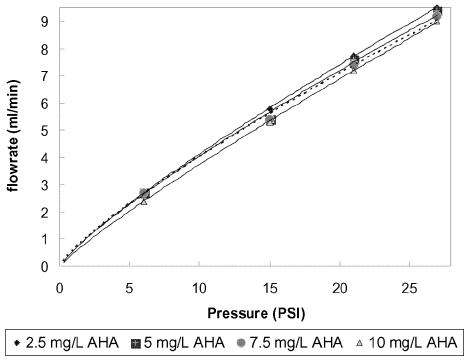

Figure 2. Influence of TMP and AHA on permeate flow rates for 10 kDa membrane.

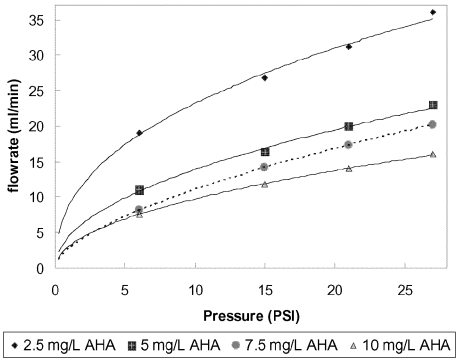

Figure 3. Influence of TMP and AHA on permeate flow rates for 100 kDa membrane.

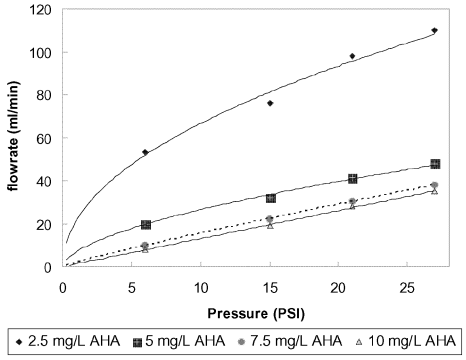

Figure 4. Influence of TMP and AHA on permeate flow rates for 0.2 µm flat sheet membrane.

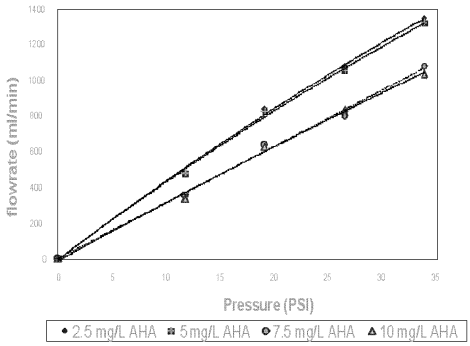

Figure 5. Influence of TMP and AHA on permeate flow rates for 0.2 µm tubular membrane.

The analysis of Figs 2-5 shows that permeate flowrates increase at higher transmembrane pressures and at higher AHA concentrations for both UF and MF membranes. As can be seen, all tested membranes present no significant flux decline over the running time; this has been addressed to a minimal concentration polarisation.

3.1 Rejection tests

Figure 6 shows the results of rejection experiments towards three parameters, *i.e.* AHA, turbidity and conductivity, representative of organic material, dissolved solids and dissolved salts present in surface water, respectively. As for AHA retention, the examined UF membranes (10, 100 kDa) are both suitable for the humic acid removal; rejections of AHA is higher than 90% at 7.5 mg/L AHA for both MWCO. As a consequence of the higher pore size, flat sheet MF membrane (0.2 μm), with respect to UF membranes, shows very lower rejections ranging from 15-20%, thus confirming a previous experimentation (Salladini et al., 2007), in which the removal efficiency of MF flat sheet membranes was improved by adding divalent cations ($CaCl_2$) enhancing AHA removal. On the contrary, tubular membrane having the same cut-off (0.2 μm) exhibits average rejections of more than 90%, even higher than those of UF membranes. This excellent behaviour has been attributed to the different configuration used (tubular instead than flat) but can be also due to the different membrane material (ceramic instead than polymeric); as a matter of fact, it is recognized that ceramic membranes are rarely used in the treatment of water due to their low mechanical resistance. As for turbidity and conductivity, 10 kDa UF membrane is still effective, reaching rejection of about 60% and 50%, respectively, while 100 kDa UF membrane is less effective with rejections ranging from 10 to 25%; on the contrary, both MF membranes are effective towards turbidity, reaching very high rejection coefficients independently from their configuration, while both of them are low efficient towards conductivity; as a matter of fact a reduction of conductivity can be reached by using membranes with lower cut-off, able to retain also dissolved salts in solution (nanofiltration and reverse osmosis). Figs 7-8 show AHA rejections as a function of TMP for MF membranes, showing that the above reported rejections are quite independent on the applied pressure. Only flat sheet MF membrane shows a higher rejection coefficient for high AHA levels (7.5 – 10 mg/L) at low TMP (6 PSI), but it seems of low significance.

4. Conclusions

Filtration test with a model solution have shown that the studied UF flat sheet membranes are effective in the removal of humic acid. Permeate flow rates and AHA rejections were found to be quite stable during filtration time, suggesting that no cake development on the membrane surface occurred. Removal efficiency of UF membrane is high enough (85-90%) at AHA concentration over 7.5 mg/L.

As a consequence of larger pore diameter, flat sheet MF membrane resulted ineffective in AHA removal with rejection ranging from 15-20%, while tubular MF membrane showed removal efficiency of 90%, attributed to the different membrane configuration. Further studies may clarify if this effect should be attributed to the different membrane material (ceramic instead than polymeric), by using MF tubular polymeric membrane.

5. Acknowledgements

Authors are very grateful to Ms. Lia Mosca for her precious collaboration in the experimental work.

6. References

Aoustin E., A.I. Schaefer, A.G. Fane and T.D. Waite. 2001. Ultrafiltration of natural organic matter . Sep. Purif. Technol. 22–23, 63–78.

Domany Z., Galambos I., Vatai G., Bekassy-Molnar E. 2002. Humic substances removal from drinking water by membrane filtration. Desalination, 145, 333-337.

Katsoufidou K., Yiantsios S.G., Karabelas A.J. 2005. A study of ultrafiltration membrane fouling by humic acids and flux recovery by backwashing: Experiments and modelling . Journal of Membrane Science, 266, 40-50.

Lin C.F., Lin T.Y., Hao O.J. 1999. Effect of humic substance characteristics on UF performance. Water Research, 34, 1097-1106

Mozia S. and Tomaszewska M. 2004. Treatment of surface water using hybrid processes-adsorption on PAC and ultrafiltration . Desalination, 162, 23-31.

Salladini A., L. Mosca, M. Prisciandaro, D. Barba. 2007. Humic substances removal from surface water by membrane filtration. Varirei 2007, L'Aquila (Italy).

Yuan W. and Zydney A.L. 1999. Effect of solution environment on humic acid fouling during microfiltration. Desalination, 122, 63-76.

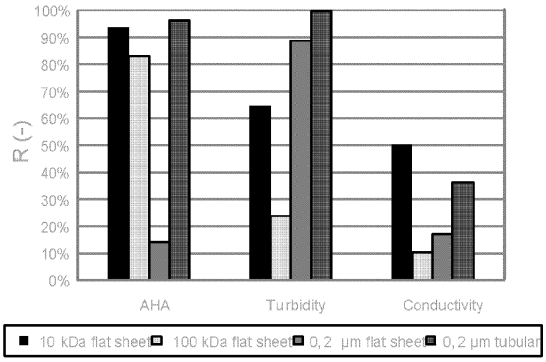

Figure 6. Rejection coefficient during filtration through 10 kDa,100 kDa, 0.2 µm flat sheet membrane and 0.2 µm tubular membrane at pH=7, TMP=18.9 PSI, T=20°C, AHA 7.5 mg/L.

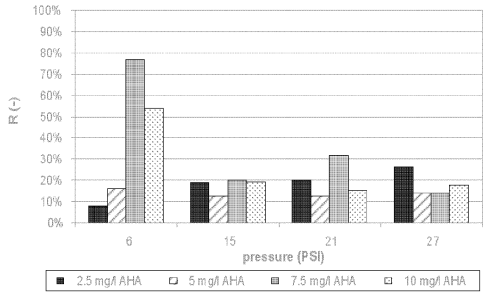

Figure 7. Influence of TMP on AHA rejection for 0.2 µm flat sheet membrane.

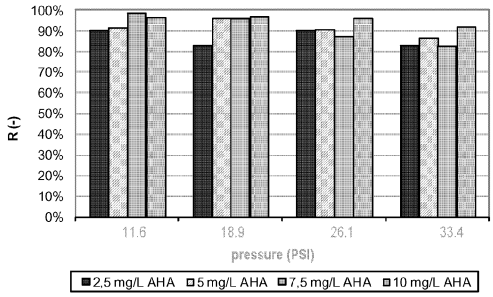

Figure 8. Influence of TMP on AHA rejection for 0.2 µm tubular membrane.

CHEMICAL ENGINEERING TRANSACTIONS, Volume 14, 2008
Edited by G. Marino, E. Bardone, A. Viglia
 ISBN 978-88-95608-02-0

Biofiltration of TCE vapours in a mixed compost-inert carrier trickle bed

Luca Della Vedova, Iginio Colussi, Angelo Cortesi, Vittorino Gallo
DICAMP, Department of Chemical, Environmental and Raw Materials Engineering,
University of Trieste
Piazzale Europa, 1 – 34127 Trieste, ITALY

Trichloroethylene (TCE) is a common air pollutant particularly stiff to be biodegraded. TCE removal has been here exploited using a pilot-scale biotrickling filter in counter-current conditions filled with a mixed compost-inert carrier bed. Bioreactor operated for about five months obtaining a maximum elimination capacity of about 5.6 g/(m^3h) and a removal efficiency between 50 and 85%. Pressure drop and pH inside the bed remained constant and did not affect bioreactor performance during the whole experiment. Using both organic and inert carrier likely reduced the compaction of the bed and limited the pH drop inside the reactor. Data of elimination capacity were fitted using an original Ottengraf-modified model for steady state conditions.

1. Introduction

Biotechniques for air pollution control have excited an increasing interest in the last years. The reason can be found in the fact that biotreatments have shown many advantages comparing with other control techniques: they operate at room temperature, are safe and effective, do not generate hazardous by-products, they require low investment and running costs. Many different air pollutants have been treated in bioreactors, including *Volatile Organic Compounds* (VOCs), NH_3 and H_2S. Trichloroethylene (TCE) is a very common and hazardous VOC, which is particularly stiff to be biodegraded. Besides being slowly soluble in water, its degradation pathway requires a cometabolite and it generates both toxic and acidifying compounds (Wilson and Wilson, 1984, Cox et al., 1998, Devinny et al., 1999). Conventional biofilters (BFs) and biotrickling filters (BTFs) are very common bioreactors for air pollution control which have been widely used for the removal of TCE as well (Sun and Wood, 1997, Lackey et al., 2002, Den et al., 2004, Iranpour et al., 2005). In both designs, degradation occurs by means of the passage of the contaminated gas throughout a packed bed covered with an active biofilm. Differences basically concern the system to supply water for maintaining biomass activity: while in BTFs a mobile liquid phase trickles throughout the bed and it is normally recirculated at the top of the bioreactor, in BFs design the right moisture level is mostly assured by a pre-humidification system. Trickling liquid is a good mean to supply alkali for pH control, or additional nutrients for biomass activity. Since the mobile liquid phase allows the control of the process, BTFs are often preferred. Organic packages are widely used in conventional biofilters, because of their high specific surface area, their good buffer properties, and because they already hold a well-developed biomass; on the contrary, organic packages are normally avoided in biotrickling filters, since the risk of bed compaction is much

higher. Inert carrier has conversely good mechanical properties but low buffer and retention capacity, and a biomass inoculum is required. Biotrickling filters can operate both in co-current and in counter-current mode, and no experimental evidence has demonstrated which is the optimal design configuration (Kennes and Veiga, 2001). Counter-current operation is normally avoided, because process performance could be affected by the great amount of pollutant sorbed and recirculated with the leachate at the top of the reactor.
In this study, the performance of a biotrickling filter treating TCE was evaluated. BTF design was preferred because of the possibility to remove toxics from inside the bed, to control the pH of the leachate and to add the required primary substrate for the cometabolic degradation. Packed bed was constituted by a mixture of organic and inert carrier, in order to have good mechanical properties and high buffer and retentive capacities as well. BTF operated in counter-current mode to promote mass transfer. Before being recirculated, the leachate was treated in an additional trickle bed unit set below the gas inlet, in order to reduce the content of pollutant into the liquid phase: with this design, the limits of counter-current application were overcome.
Experimental data of elimination capacity and mass loading rate were fitted using a new mathematical model, whose theoretical bases were drawn from Ottengraf's study (Ottengraf and van den Oever, 1983). The model here proposed is based on one equation only and it can simultaneously take into account effects of reaction and diffusion limitations on the overall process rate.

2. Materials and methods

2.1 Pilot-plant

The BTF under investigation was configured as a two glass cylinders unit (see figure (1)). Each cylinder was 1 meter high, with an internal diameter of 9.5 cm and it was filled with a packed bed of 6 l volume. Counter-current mode was achieved in each cylinder using an upward gas flow. Gas stream was generated by a membrane pump and it was divided into three streams. The main stream had an average flow rate of 210 l/h: it passed throughout two gas bubbling bottles for pollutant addition and it was subsequently fed at the bottom of the upper cylinder. A lower gas stream flew throughout the lower cylinder for maintaining biomass activity. Outlet gas stream had a gas flow rate of 280 ± 5 l/h. Third stream served as split-flow, to avoid stress on the air pump. A peristaltic pump recirculated the trickling liquid and the nutrients solution at the top of the bioreactor. Trickling liquid flow rate was maintained constant at 4.50 ± 0.2 ml/min.

2.2 Packing

Packing was constituted by a mixture of compost and little glass hollow cylinders with a organic/inert volume ratio of 1:5. Compost came from a composting plant treating municipal solid wastes: it had an overall density of 510 kg/m^3 and a humidity of 30%. Glass cylinders were 1 cm height with an external diameter of 1 cm, 2000 kg/m^3 of bulk density and a specific surface area of about 250 m^2/m^3.

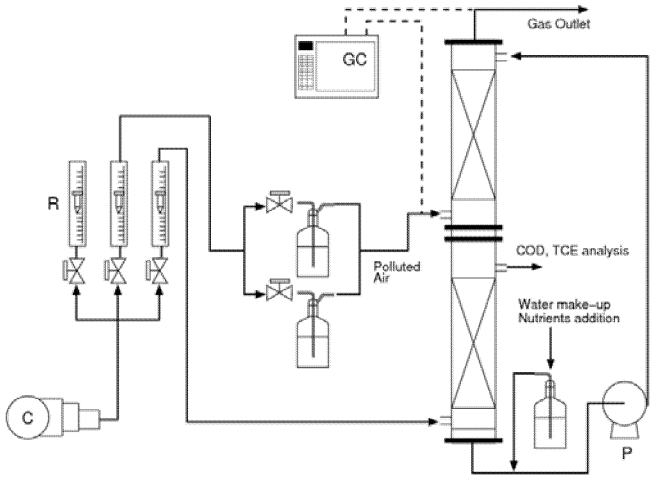

Figure 1. Scheme of the pilot-scale BTF under investigation. C: air pump, P: recirculating pump, R: rotameters.

2.3 Analysis

TCE concentrations in the gas and in the trickling liquid were measured by means of a Gas Chromatograph (DANI GC1000 DPC) equipped with an *Electron Capture Detector* (ECD). Gaseous samples were collected and automatically injected by an autosampler provided with a sampling loop of 250 µl. According with the standard methods for solvent determination in aqueous samples, *static head space* method was employed to measure TCE concentration in the leachate. The pH of the liquid phase was measured using a HANNA HI98150 portable pH-meter. The pressure drop along the whole bioreactor was also considered and it was measured by means of an U-shaped manometer. The measurement of the gas flow rate was achieved by some rotameters and by a volumetric flowmeter (SIM Brunt).

2.4 Nutrients solution

A simple nutrients solution was prepared with Sodium Acetate (20 g/l) and Sodium Nitrate (10 g/l). Nutrients addition was set in order to obtain a recirculated liquid with 120 mgCOD/l and 11 mgN-NO_3/l. Further nutrients were supposed to be provided by the compost itself.

2.5 Biotrickling-filter piloting

The study was carried out for about 5 months. First month was necessary to assess the fluidodynamic stability of the bioreactor in absence of pollutants. Afterwards, a very diluted waste gas containing TCE was fed to the system during a period of about 2 months, for biomass acclimatization. The first day of TCE addition was set as "day zero". After that, TCE concentration in the inlet gas flow was increased until a maximum value of 0.192 g/m^3, in order to determine the maximum degradation capability of the pilot-plant.

3. Theoretical model

The model here proposed is a mathematical modification of the Ottengraf and van den Oever model (Ottengraf and van den Oever, 1983). The original model is based on

some simple assumptions: stationary state, zero-order kinetics for biological degradation, Henry's law for fluid interface equilibrium, two phases (gas and water/biofilm), one pollutant only, and plug flow conditions. Depending on the profile of pollutant concentration into the water/biofilm phase, two different regimes could be identified. When inlet gas stream is highly contaminated, pollutant can be easily absorbed into the water/biomass film and it diffuses completely throughout it. In such condition, biomass could not be able to degrade all the amount of pollutant sorbed, and biological reaction is the rate determining step of the process. Conversely, with a diluted gas flow, mass transfer is moderate and it determines the rate of the process. By the mass balances for the gas phase and the water/biofilm phase, two equations can be written for the reaction limitation region (1) and for the diffusion limitation region (2) respectively:

$$\frac{C_{go}}{C_{gi}} = 1 - \frac{A_s k_0 \delta H}{C_{gi} U_g} \tag{1}$$

$$\frac{C_{go}}{C_{gi}} = \left(1 - \frac{A_s H}{U_g} \sqrt{\frac{k_0 D}{2 C_{gi} m}} \right)^2 \tag{2}$$

where C_{go} and C_{gi} are the pollutant concentration in the outlet and in the inlet gas stream respectively [g/m^3], A_s is the specific surface area [m^2/m^3], k_0 is the zero-order kinetic constant [g/(m^{3}h)], δ is the biofilm thickness [m], D is the diffusivity in water [m^2/h], m is the air/water partition coefficient [g/g], H is the bed height [m], and U_g the superficial gas velocity [m/h]. By using the definition of elimination capacity (EC, [g/(m^{3}h)]) and mass loading rate (L, [g/(m^{3}h)]), equation (1) and (2) can be rewritten in terms of these new process parameters (Delhomènie et al., 2002):

$$EC_{rl} = A_s k_0 \delta \; ; \tag{3}$$

$$EC_{dl} = L \left(1 - \left(1 - A_s \sqrt{\frac{k_0 D}{2m}} \sqrt{\frac{V}{QL}} \right)^2 \right) \tag{4}$$

with V the bed volume [m^3] and Q the volumetric gas flow rate [m^3/h]; the subscript rl stands for reaction limitation and the subscript dl stands for diffusion limitation. A simple equation can be used to pass continuously from equation (3) to equation (4). This equation should consider that, as the inlet concentration increases, the contribution of mass transfer limitation will reduce, while the contribution of the biological reaction will become greater. The following equation can accomplish these conditions:

$$EC = EC_{rl} + \frac{EC_{dl} - EC_{rl}}{1 + \left(L / L_{cr} \right)^p} \tag{5}$$

where L_{cr} is the mass loading rate at which transition between reaction and diffusion limitation area occurs [g/(m^{3}h)] and p is a dimensionless parameter of the model. Using the critical Thiele number as proposed by Ottengraf, L_{cr} can be calculated as follows:

$$L_{cr} = \frac{\delta^2 k_0 m Q}{2DV} \quad (6)$$

Equation (5) was used to fit the data of elimination capacity and mass loading rate obtained by the experiments.

4. Results and Discussion

TCE concentrations in the inlet and in the outlet gas flows are reported in figure (2) with the corresponding removal efficiency. It can be observed that the total TCE removal was not achieved even at very low inlet concentrations: this fact was likely due to some mass transfer limitations or to an incomplete biomass acclimatization. From day 30 to day 90, the removal efficiency remained mainly constant, with values included between 70% and 80%. In the following days, the progressive increase in TCE concentration reduced the process efficiency to a minimum value of about 50%. At the maximum inlet concentration of 0.192 g/m^3, a removal efficiency of 63.4 % was obtained. Considering the TCE emissions limit of 0.02 g/m^3, as established by the Italian legislation (D. Lgs 152/2006), outlet stream exceeded this limit for inlet concentrations higher than 0.07 g/m^3.

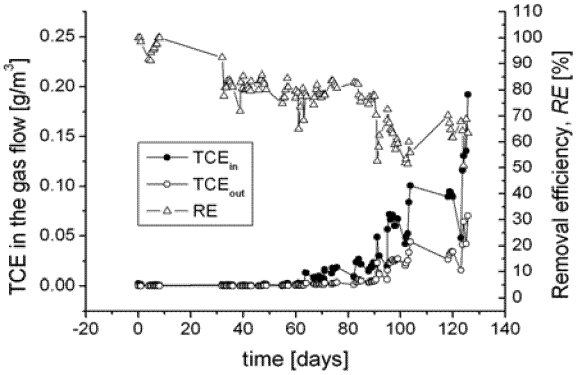

Figure 2. TCE concentration in the inflow and in the outflow and the corresponding removal efficiency during the whole experiment along.

Figure (3) reports data of TCE concentration into the leachate sampled at the top and at the bottom of the lower unit. Obviously, TCE_{top} increased as the pollutant concentration in the gas inflow increased. The removal efficiency related to the leachate (RE_L) was higher than 95% during the whole experiment. Stripping effects and biological activity could both contribute to this high removal. Thanks to the lower unit, the amount of TCE recirculated at the top of the BTF was therefore strongly reduced, limiting the problems related to counter-current operations. However, since the ratio between gas and liquid flow rates was very low, the favourable contribute of the leachate treatment to the overall removal efficiency was almost negligible. Lower unit can play a more important role when operating with low gas and high trickling liquid flow rates or with more soluble pollutants.

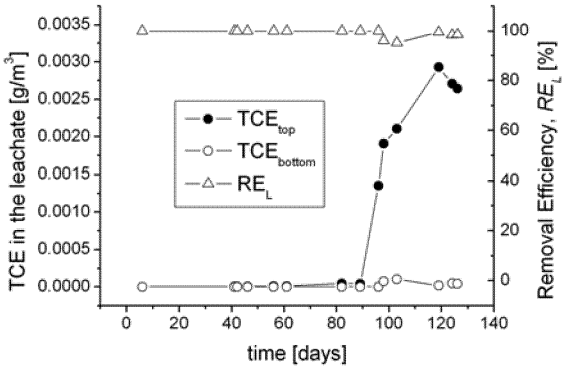

Figure 3. TCE concentration in the leachate at the top and at the bottom of the lower unit and the corresponding removal efficiency.

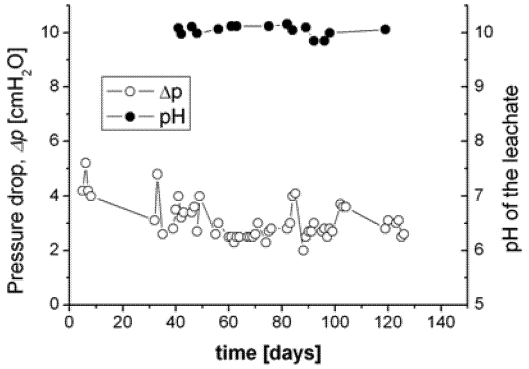

Figure 4. Pressure drop along the whole bioreactor and pH of the leachate during the whole experiment.

As it can be observed in figure (4), pressure drop and pH of the leachate remained mainly constant during the experiment. This fact can be attributable to the employment of a mixture organic/inert carrier as packed bed. An average pressure drop of 3.1 cmH_2O was obtained and the moderate fluctuations in its values were essentially due to tube fouling rather than to an effective pressure drop inside the bioreactor. Leachate had a constant pH with an average value of 10.02. Alkaline conditions are not common in biofiltration processes (Kennes and Veiga, 2001), since it has been reported that biomass activity is promoted at pH values close to 7, for TCE removal as well (Misra and Gupta, 2001). Buffer capacity of compost reduced the acidifying effect of some by-products of TCE biodegradation. Since its alkaline properties, sodium acetate could also have given its contribution to pH control.

Figure (5) reports data of elimination capacity (*EC*) vs. mass loading rate (*L*). An *EC* maximum value of 5.61 $g/(m^3h)$ was obtained for L = 8.86 $g/(m^3h)$. This value was much higher than that reported by other studies concerning TCE removal in conventional biofilters and biotrickling filters (Sun and Wood, 1997, Lackey et al., 2002, Den et al., 2004, Jung and Park, 2005). This fact confirms the goodness of the process for the removal of this target pollutant. By the same graph, it can be observed

that the condition of reaction limitation area was not achieved along the whole experimental range. Indeed, when this condition occurs, elimination capacity is constant and it does not depend on the mass loading rate. Thus, it can be stated that mass transfer had limited the process rate during the whole experiment.
Figure (5) reports also the curve obtained by data fitting using the Ottengraf's modified model. Parameters used in the model are reported in table (1). Data fitting was carried out using the Levenberg-Marquardt algorithm, obtaining a coefficient of determination R^2 of 0.921. Considering the theoretical basis of the new Ottengraf's modified model, data from both reaction and diffusion limitation area should be available to improve the goodness of the model itself. In this case, the lack of experimental data for the reaction limitation condition had a particular effect on the determination of the biofilm thickness, which appears in the definition of EC_{rl} only. Indeed, the value of this parameter obtained by data fitting was extremely high (about 1.6 cm), with no physical meaning, considering the experimental set-up. In spite of this, the model could be an useful mean for a first evaluation of the process and for the determination of a good initial set of parameters for a further numerical implementation.

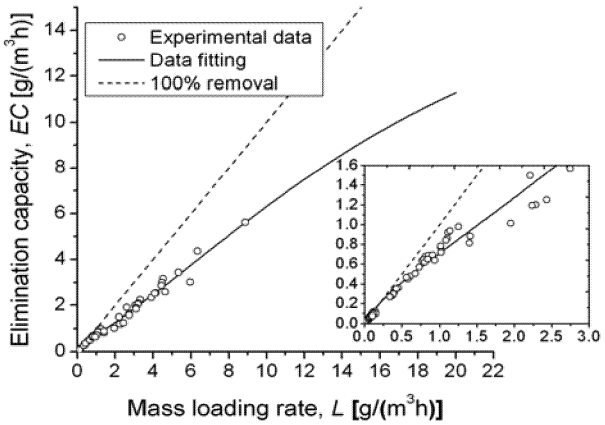

Figure 5. EC vs. L plot and curve obtained bt data fitting, using the Ottengraf's modified model

Table 1. List of fixed and fitted parameters used in the Ottengraf's modified model. References: (a) Folsom et al., 1990, (b) Chiao et al., 1994

Fixed parameters	Values	Fitted parameters	Initial Set	Final Set
Average gas flow rate Q [m^3/h]	0.2816	Specific surface area A_s [m^2/m^3]	1000	999.496
Bed volume V [m^3]	0.006	Biofilm thickness δ [m]	0.001	0.01614
Air/water partition coefficient m [g/g]	0.4 (a)	Zero-order kinetic constant k_0 [g/(m^3h)]	10	1.21367
Diffusivity in water D [m^2/h]	3.75×10^{-3} (b)	Critical mass loading rate L_{cr} [g/(m^3h)]	25.03	19.9813
		Exponent, p	1	1.64868

5. Conclusions

The effectiveness of a bioreactor, characterized by a mix organic/inert trickle bed was here demonstrated for the treatment of TCE vapours. The choice of this specific packing allowed to carry out long-term operation: indeed, the typical malfunctioning of this kind of process (high pressure drop and bed acidification) had not been observed during the whole experiment. The biotrickling filter under investigation had shown good efficiency and high elimination capacity. However, its effectiveness could be strongly enhanced, reducing limitations due to mass transfer, which had been demonstrated to be the rate determining step of the process. The lower trickle-bed unit could remove almost completely the pollutant content of the leachate. Anyway, its contribution to the overall removal efficiency can be enhanced if operating with higher trickling liquid flow rates. This oppurtunity is currently under investigation and it is one of the most promising features for this bioreactor design. A new simple model was proposed and validated. The model shows the advantage of having one equation only which can be applied for the entire range of mass loading rate.

6. References

Chiao, F.F., R.C. Currie, and T.E. McKone, 1994, Intermedia Transfer Factors for Contaminants Found at Hazardous Waste Sites - Trichloroethylene, Final Draft Report

Cox, C.D., H.Woo, and K.G. Robinson, 1998, Water Science Technology, 37, 8

Delhoménie, M., L. Bibeau, N. Bredin, S. Roy, S. Brossau, R. Brzezinsky, J.L. Kugelmass, and M. Heitz, 2002, Advances in Environmental Research, 6

Den, W., C. Huang, and C.Li, 2004, Chemosphere, 57

Devinny, J.S., M.A. Deshusses, and T.S. Webster, 1999, Biofiltration for Air Pollution Control, Eds. CRC/Lewis Publisher

Folsom, B.R., P.J. Chapman, and P.H. Pritchard, 1990, Applied and Environmental Microbiology, 56, 5

Iranpour, R., H.H.J. Cox, M.A. Deshusses, and E.D. Schroeder, 2005, Environmental Progress, 24, 6

Jung, I. And O. Park, 2005, Journal of Bioscience and Bioengineering, 2005

Kennes C. and M.C. Veiga, 2001, Bioreactors for Waste Gas Treatment, Eds. Klewer Academic Publishers

Lackey, L.W., J.R. Gamble, J.J. Boles, 2002, Advances in Environmental Research, 7

Misra, C. and S.K. Gupta, 2001, Water Research, 35,1

Ottengraf, S.P.P., A.H.C. van den Oever, 1983, Biotechnology and Bioengineering, 25

Sun, A.K. and T.K. Wood, 1997, Biotechnology and Bioengineering, 55

Wilson, J.T. and B.H. Wilson, 1984, Applied and Environmental Microbiology, 49, 1

CHEMICAL ENGINEERING TRANSACTIONS, Volume 14, 2008
Edited by G. Marino, E. Bardone, A. Viglia
 ISBN 978-88-95608-02-0

High-rate anaerobic-aerobic biological treatment of a wastewater from a Fischer-Tropsch process

M. Beccari*, M. Majone*, D. Dionisi*, A. Donadio*, E. N. D'Addario**, and R. Sbardellati**

* Sapienza University of Rome, Dept of Chemistry, P.le A. Moro 5, 00185 Rome, Italy
** Eni S.p.A, Refining and Marketing Division, via E. Ramarini 32, 00016 Monterotondo, Italy

This study investigates the anaerobic-aerobic treatment of an industrial wastewater from a Fischer-Tropsch process. The considered synthetic wastewater has an overall concentration of 28 gCOD/L, mainly due to alcohols. The continuous anaerobic process was studied in a fixed-bed reactor under mesophilic conditions (35°C). Gradual start-up, starting from 3.4 gCOD/L/day, was used in order to overcome potential inhibition from long-chain alcohols (>C6). Then, the process was operated successfully by feeding with the wastewater, with neither pretreatment nor dilution, up to an organic load rate of 20 gCOD/L/day (hydraulic retention time 1.4 days). 96% COD removal and full conversion of removed COD into methane was obtained (about one third coming from hydrogenophilic methanogenesis). By considering a potential of 200 tCOD/day to be treated, that would also correspond to a net production of electric energy of about $8*10^7$ kWh/year. The effluent of the anaerobic reactor contained only acetic and propionic acids, that were easily removed under aerobic conditions.

1. Introduction

This paper is aimed to study the anaerobic continuous treatment of a high-strength industrial wastewater from hydrocarbon liquefaction by Fischer-Tropsch process. The considered wastewater is characterised by a high COD content (28 gCOD/L) and by a high organic load (200 tCOD/day). Anaerobic treatment is therefore the desired treatment option for the considered wastewater.

However, most of the wastewater COD (85%) is due to alcohols with different chain length (from methanol to decanol) and literature data on anaerobic treatability of alcohol-containing wastewaters are scarce. Moreover, most of these studies only consider short-chain alcohols. Han et al. (2005) studied the UASB treatment of a wastewater mainly composed of volatile fatty acids and ethanol, obtaining high conversion into methane up to organic loading of 13 gCOD/L/day; with similar substrates, O'Flaherty et al. (1998) also obtained almost complete COD removal; C3 and C4 alcohols were successfully treated in an hybrid (fixed bed-suspended biomass) reactor (Henry et al., 1996). On the other hand, long-chain alcohols are much less studied and there are some evidences that they can inhibit bacterial activity (Carlsen et al., 1991).

A previous study by this research group (Dionisi et al., 2007) has investigated the anaerobic treatment of the considered wastewater by batch tests. It has been shown that the long-chain alcohols (from 6 to 10 C atoms) strongly inhibit the anaerobic

metabolism, both of acetogenic and methanogenic microorganisms. However, biomass activity resumed after long adaptation (about 20 days).
On the basis of the previous investigation, the present study was aimed to investigate the performance of a continuous packed-bed anaerobic bioreactor fed with the considered wastewater. In order to overcome inhibition from long chain alcohols, appropriate start up was performed starting from low organic load and by using modified feed (diluted with no or less long-chain alcohols). Then, the organic load and long-chain alcohol concentration were progressively increased, while monitoring reactor performance in terms of COD removal, methane production, and effluent concentration of the main substances. The maximum methanogenic activity of the microorganisms grown in the reactor was also measured through batch tests.

2. Materials and methods

2.1 Wastewater

Based on typical composition of aqueous waste streams generated from the liquefaction of hydrocarbons with the Fischer-Tropsch process, a synthetic wastewater was prepared. Main components of the wastewater were alcohols (84.8% as COD). Other components of the wastewater include acids (10.7% as COD) and hydrocarbons (4.5% as COD). The complete wastewater composition has been previously reported (Dionisi et al., 2007).

2.2 Reactor

The anaerobic reactor was a fixed-bed biofilm reactor, with a working volume of 1 L. The biomass was grown on Anox-Kaldnes KMT-k1supports. Above the packed bed, space was left for effluent clarification and gas separation. The liquid effluent was recirculated through an internal heat exchanger, in order to maintain the desired temperature (35 °C) and a high degree of axial mixing. The reactor was inoculated with sludge from the anaerobic digester of a municipal wastewater treatment plant and maintained under batch conditions until biofilm developed. Then, a continuous organic load of 3.4 gCOD/L/day was applied, by using a diluted modified wastewater without long-chain alcohols in the feed. Then, the influent flow-rate was gradually increased and the long-chain alcohols were gradually added to the feed, first at 1:8 dilution (organic load rates 6 and 12 gCOD/L/day), then without any dilution (organic load rates 13.5 and 20 gCOD/L/day). The reactor was regularly sampled for effluent and gas-phase composition. During the run at 13.5 gCOD/L/day, batch tests were carried out by switching the feed off and spiking the desired susbstrate (acetic acid, propionic acid, methanol or hydrogen). Time profiles of the added substrate and of the produced methane were then collected.

2.3 Analytical methods

Gas-chromatography was used for methane determination (stationary phase 1% SP1000 on 60/80 Carbopack B, FID, column temperature 80°C) as well as for alcohols (stationary phase 4% Carbowax 20M on Carbopack B-DA, FID, column temperature: 80°C 4 min, from 80 to 220°C at 12°C/min, 220°C 10 min). Hydrogen was analysed through gas chromatography (molecular sieve column 2 m x 2 mm at 105 °C, reduction

gas detector, RGD). Acids were analysed through HPLC (column SupelcoGel C-610H, photodiode array detector).

3. Results and discussion

3.1 Performance of the anaerobic reactor

The time evolution of the performance of the reactor during the run (approximately 1 year) is presented in Figure 1, while average values of the measured parameters are shown in Table 1.

After the adaptation period at the lowest organic load (3.4 gCOD/L/day) with no long chain alcohols, the organic load was increased to 6 and 12 gCOD/L/day by using modified wastewater (long chain alcohols diluted 1:8). Reactor performance was characterised by a progressive increase of residual acetic and propionic acids in the effluent (other compounds were never detected). However, methane was the main product at both organic load rates, corresponding to an average of 61% and 74% of influent COD, respectively. Then, the unmodified wastewater was used and the organic load rate slightly increased (from 12 to 13.5 gCOD/L/day, due to the increased concentration of long chain alcohols). Two distinct phases could be observed 13.5 gCOD/L/day. In the first phase (days 140-225), the performance of the reactor closely matches that of the previous runs (6 and 12 gCOD/L/d), characterised by increasing effluent COD values at increasing organic load rates. Overall effluent concentrations of acetic plus propionic acid were approximately 6.5 gCOD/L, corresponding to a 77% COD removal. The removed COD was all converted to methane. At day 225 the feed to the reactor was switched off, in order to carry out batch tests (next paragraph). After the feed was switched on again, the performance of the reactor was significantly improved: indeed, the liquid-phase effluent COD was quite lower (at 0.63 g/L as average value) and virtually all the influent COD was converted into to methane. The improved performance of the reactor can likely be explained with an increased adaptation of the biomass to the inhibiting substances, i.e. the long-chain alcohols. Because long-chain alcohols were never detected in the effluent, it is likely that they were initially adsorbed in the biofilm within the reactor, because of an organic load higher than removal rate from the slowly acclimating biomass; during the no-feed phase the biomass removed the residual long-chain alcohols, thus removing any inhibition, while also becoming able to remove them at higher rates. Hydrogen concentration in the reactor basically followed acetic and propionic acids in the effluent, so showing similar effects of organic load rate and long chain alcohols on activity of acetoclastic and hydrogenophilic methanogens. However, hydrogen was always very low (below $2*10^{-4}$ mg/L), that indicates a high activity of the hydrogenophilic methanogens.

At the final tested operating conditions, 20 gCOD/L/day, the complete removal of the influent COD was confirmed, with complete conversion to methane.

With regard to final treatment of the residual COD from the anaerobic reactor, batch tests (data not reported) have confirmed that it is readily biodegradable under aerobic conditions, with high removal rates and with no inhibiting effect on biomass metabolism.

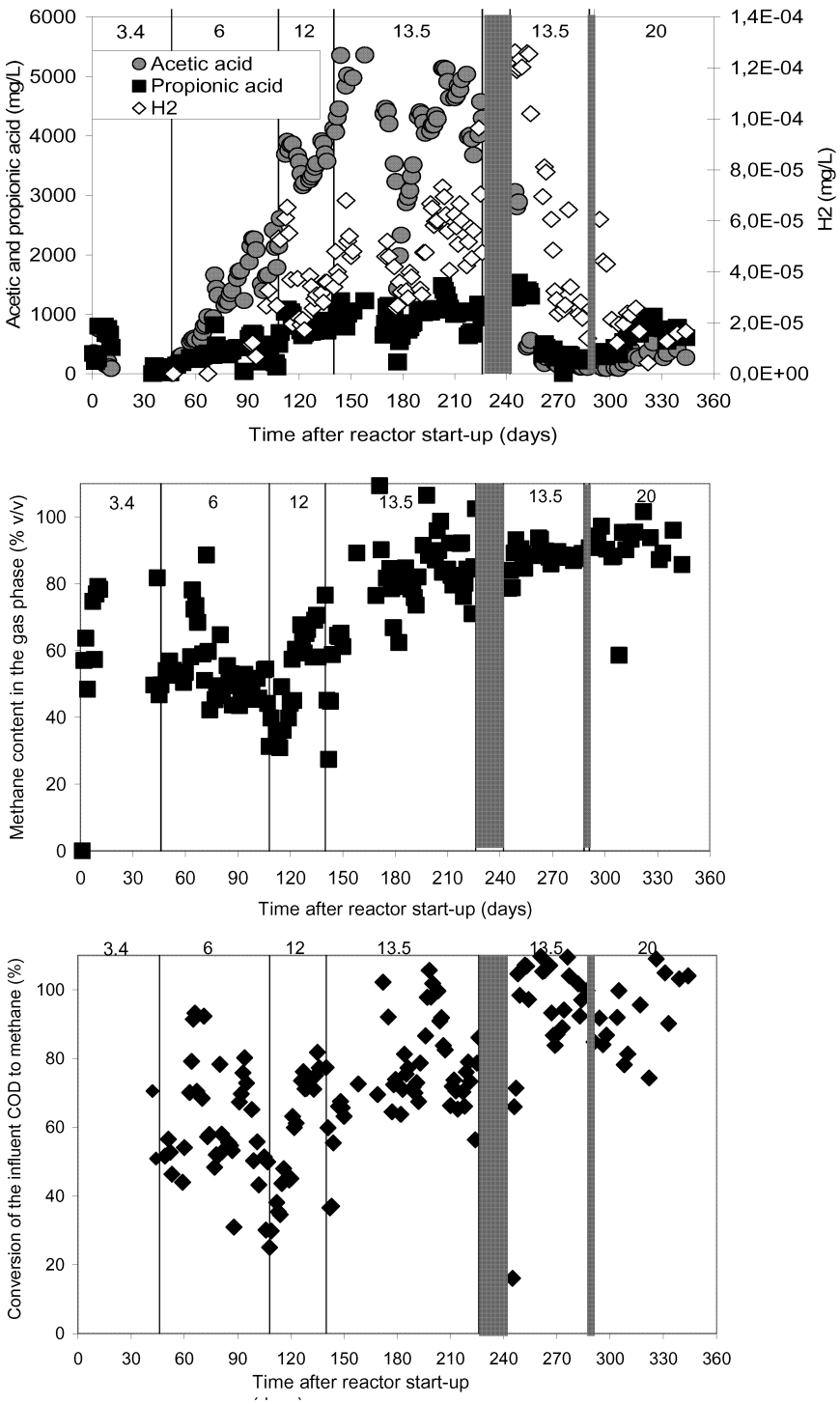

Figure 1. Time profiles of the main measured parameters during reactor operation (grey columns indicate that usual feed was interrupted and batch tests performed)

Table 1. Summary of the average performance of the anaerobic reactor at steady-state

	Organic load rate (gCOD/L/day)				
	6	12	13.5 (first phase)	13.5 (second phase)	20
Gas Phase					
Overall gas production (L/d)	2.51	4.89	4.28	5.20	7.80
Methane content (%, v/v)	52	63	88	89	89
Methane production (L/d)	1.28	3.14	3.76	4.62	7.00
Conversion of influent COD to methane (%)	61	74	78	98	98
Liquid phase (g/L)					
Acetic acid	1.67	3.61	4.46	0.17	0.25
Propionic acid	0.4	0.83	1.04	0.29	0.61
Butanoic acid	0	0	0.042	0	0
Pentanoic acid	0	0	0	0	0
Hexanoic acid	0	0	0	0	0
Methanol	0	0	0.045	0	0
Ethanol	0	0	0	0	0
Propanol	0	0	0	0	0
Butanol	0	0	0	0	0
Pentanol	0	0	0	0	0
Hexanol	0	0	0	0	0
Hepthanol	0	0	0	0	0
Overall solubile COD in the liquid effluent (gCOD/L)	2.39	5.11	6.54	0.63	1.2
Overall COD removal (%)	89	78	75	97	96

3.2 Batch tests and mass balance

Batch tests were carried out with acetate, propionate, methanol and hydrogen in the reactor, in order to calculate their maximal removal rates during the run at 13.5 gCOD/L/day (at the end of each of the two phases),. As a typical example, Figure 2 shows the test with methanol, carried out during the first phase of the run. It is evident that methanol is completely and directly converted to methane at high rate (about 3.5 gCOD/L/day). This finding is also relevant because it shows that other possible methanol metabolisms, such as the conversion to acetic acid (Batstone et al., 2002), were not important for the biomass grown in the reactor.

With regard to acetic acid removal rate (data not shown), batch tests confirmed that its removal rate was much higher in the second phase of the run (approximately 15 gCOD/L/day), than in the first phase (approx. 3 gCOD/L/day). The test with hydrogen (data not shown) also confirmed the quite high activity of hydrogenophilic

methanogens (about 5.6 gCOD/L/day). Maximal conversion rates of selected compounds under batch conditions can be compared with the actual conversion rates in the reactor under usual conditions (Table 2). The latter have been estimated from mass balance in the reactor, by assuming a set of conversion reactions for all compounds in the feed, as reported in Table 3 (Dionisi et al. 2001).

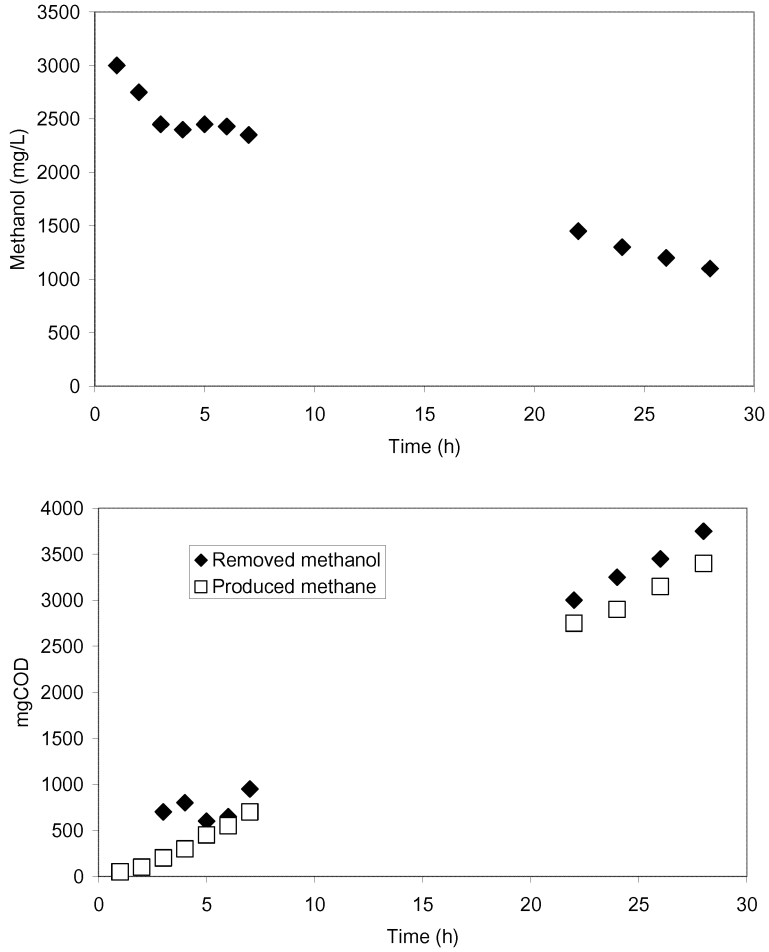

Figure 2. Batch test with methanol (organic load rate 13.5 gCOD/L/day, first phase)

Table 2 shows the good agreement between the actual rates as estimated from Table 3 and reactor mass balance with the maximal rates as determined from batch tests. Indeed, at 13.5 gCOD/L/day, maximal rates were always quite higher than estimated from mass balance in the mixed reactor (where kinetics was limited by the low substrate concentration). The only exception was acetic acid which batch removal rate during the I phase was slightly lower than estimated from mass balance. Such discrepancy confirms the fluctuating profile of acetic acid and its tendency to increase in the effluent. On the other hand, during the second phase the batch removal rate is quite higher than required from mass balance, in agreement with the observed better

performance of the reactor. By combining batch tests results during the run at 13.5 gCOD/L/day and mass balance, it was anticipated that the reactor could be operated up to 20 gCOD/L/day with no loss of performance. This was indeed confirmed during the last reactor run. Finally, it is noteworthy the important role of hydrogenophilic methanogens to the overall methane production (about one third at both 13.5, II phase, and 20 gCOD/L/day)

Table 2. Comparison of maximal rates from batch tests and estimated actual rates from reactor mass balance (all the rates are in gCOD/L/day); n.a. data not available.

	Maximal rates from batch tests		Estimated rates from mass balance in the continuous reactor		
	run at 13.5 gCOD/L/day		run at 13.5 gCOD/L/day		run at 20 gCOD/L/day
Compound	I phase	II phase	I phase	II phase	
Acetic acid	3.15	15.9	4.03	6.53	9.40
Methanol	3.54	n.a.	1.71	1.71	2.54
Hydrogen	5.64	n.a.	4.02	4.24	6.10
Overall COD	12.3	25.0	9.76	12.48	18.0

Table 3. Scheme of the possible anaerobic reactions of the main wastewater components. 1) Thauer et al., 1977; 2) Eichler and Schink, 1985; 3) Batstone et al., 2001

Substrate	**Reaction**
Methanol[1]	$4CH_3OH \rightarrow 3CH_4 + CO_2 + 2H_2O$
Ethanol[2]	$CH_3CH_2OH + H_2O \rightarrow CH_3COOH + 2H_2$
Propanol[2]	$CH_3CH_2CH_2OH + H_2O \rightarrow CH_3CH_2COOH + 2H_2$
Butanol[2]	$CH_3CH_2CH_2CH_2OH + H_2O \rightarrow CH_3CH_2CH_2COOH + 2H_2$
Pentanol[2]	$CH_3CH_2CH_2CH_2CH_2OH + H_2O \rightarrow CH_3CH_2CH_2CH_2COOH + 2H_2$
Propionic acid[3]	$CH_3CH_2COOH + 2H_2O \rightarrow CH_3COOH + 3H_2 + CO_2$
Butanoic acid[3]	$CH_3CH_2CH_2COOH + 2H_2O \rightarrow 2CH_3COOH + 2H_2$
Pentanoic acid[3]	$CH_3CH_2CH_2CH_2COOH + 2H_2O \rightarrow 2CH_3COOH + 3H_2 + CO_2$
Acetic acid[3]	$CH_3COOH \rightarrow CH_4 + CO_2$
Hydrogen[3]	$4H_2 + CO_2 \rightarrow CH_4 + 2H_2O$

4. Conclusions

The present study showed that the considered wastewater, characterised by a high organic load and by high concentrations of potentially inhibiting substances (long-chain alcohols), could be successfully treated under anaerobic conditions in a high rate packed bed biofilm. In particular, after appropriate start up, the reactor was operated up to 20 gCOD/L/day organic load rate, by removing most of the COD (96%) and transforming it into methane. This applied organic load rate is among the highest reported in the literature for fixed-bed biofilm reactors.

Under the estimated overall load of 200 tCOD/day, methane produced in the anaerobic reactor could provide, through typical cogeneration, a net electric power of 9 MW (or $8*10^7$ kWh/year), in addition to the power required by the anaerobic reactor. Moreover,

based on mass balance and batch tests it was estimated that about one third of overall methane production was due to hydrogen production from alcohols and propionic acid fermentation and to simultaneous hydrogenophilic methanogenesis. Thus, as a perspective, the process could be also interesting for hydrogen production, provided that methanogenesis is appropriately inhibited.
The residual effluent COD from the anaerobic reactor was composed only of acetic and propionic acids, and was readily biodegradable under aerobic conditions. Thus, this study showed that a combined anaerobic-aerobic process, with both stages operated at high organic load rates, is suitable for the treatment of the considered wastewater.

3. Acknowledgments

This research was carried out under the contract 122/2006 between the Department of Chemistry and Enitecnologie S.p.A (now Eni S.p.A). The kind assistance of ACEA-ATO2 staff at the “Roma Nord” WWTP is gratefully acknowledged.

4. References

Batstone D.J., Keller J., Angelidaki I., Kalyuzhnyi S.V., Pavlostathis S.G., Rozzi A., Sanders W.T., Siegrist H. and Vavilin V.A. (2002). Anaerobic Digestion Model No. 1. *Wat. Sci. Tech.*, **45**(10), 65-73.

Carlsen H.N., Degn H. and Lloyd D. (1991). Effects of alcohols on the respiration and fermentation of aerated suspensions of baker's yeast. *J. Gen. Microbiol.*, **137**, 2879-2883.

Dionisi D., Beccari M., D’Addario E.N., Donadio A., Majone M., Sbardellati R. (2007). Anaerobic biotreatability of an industrial wastewater containing alcohols at different chain length. AD11, 11th World Congress on Anaerobic Digestion, Brisbane, Queensland, Australia.

Eichler B. and Schink B. (1985). Fermentation of primary alcohols and diols and pure culture of syntrophically alcohol-oxidizing anaerobes. *Arch. Microbiol.*, **143**, 60-66.

Han S.K., Kim S.H and Shin H.S. (2005). UASB treatment of wastewater with VFA and alcohol generated during hydrogen fermentation of food waste. *Proc. Biochem.*, **40**(8), 2897-2905.

Henry M.P., Donlon B.A., Lens P.N., Colleran E.M. (1996). Use of anaerobic hybrid reactors for treatment of synthetic pharmaceutical wastewaters containing organic solvents. *J. Chem Technol. Biotechnol.*, **66**, 251-264.

O’Flaherty V., Colohan S., Mulkerrins D. and Colleran E. (1999). Effect of sulphate addition on volatile fatty acid and ethanol degradation in an anaerobic hybrid reactor. I: Process disturbance and remediation. *Biores. Technol.*, **68**, 101-107.

Thauer R.K., Jungermann K. and Decker K. (1977). Energy conservation in chemotrophic anaerobic bacteria. *Bacteriol. Rev*., **41**, 100-180.

CHEMICAL ENGINEERING TRANSACTIONS, Volume 14, 2008
Edited by G. Marino, E. Bardone, A. Viglia
 ISBN 978-88-95608-02-0

Optimization of a Desulfurizating Biocatalyst by Combining Cells of Different Cell Age of *Pseudomonas putida* CECT 5279

Calzada, J.[1]; Heras, S.[1]; Carbajo, J.[1]; Alcon, A.[1]; Santos, V.E.[1]; García, J.L.[2] and García-Ochoa, F.[1]
[1]Dpto. Ingeniería Química. Facultad de Ciencias Químicas.
Universidad Complutense de Madrid. Avda. Complutense s/n 28040 Madrid
[2]Dpto. Microbiología Molecular. Centro de Investigaciones Biológicas.
Consejo Superior de Investigaciones Científicas. 28040 Madrid

Biodesulfurization is proposed as an alternative technology able to reduce sulfur content in fossil fuels, in order to aminish sulfur oxide emissions to the atmosphere. In this work, a genetically modified microorganism, *Pseudomonas putida* CECT5279, is employed as a desulfurizing biocatalyst. The combination of two cell age biomass can be used in order to optimize an effective biodesulfuring catalyst. Hereby, 5 hours and 23 hours were the selected growth times when cells were collected, combined in different biomass concentrations and tested by carrying out resting cells assays. In these experiments dibenzothiophene (DBT) was used as sulfur model compound. Biodesulfurization percentage, X_{BDS}, initial DBT elimination rate, $R_{DBT}{}^{0}$, employed biomass, C_x, and time for desulfurization, t_{BDS}, were the chosen parameters in order to search for the best biocatalyst. After this study, the mixture of 0,7 and 1,4 gDCW/L biomass concentration were selected for 5 hours and 23 hours growth time cells respectively, because of the best effectiveness achieved with formulation for a biodesulfurizing catalyst.

1. Introduction

World energy expense overcame 7900 Mtoe in 2005 and it is showing an annual increase of 2.2% (International Energy Agency, 2007). Population consumption of fossil fuels causes an important emission of sulfur oxides to the atmosphere. These compounds are recognized to be involved in many environmental, health and material stability problems. Therefore, more and more restrictive legal limitations about sulfur content in fossil fuels have been imposed in order to control emissions in combustion processes. For instance, European Union has fixed maximum sulfur content at 10 ppm for 2009 in diesel fuel (European Directive, 2003). Many technologies have been proposed to achieve these low limits (Babich and Moulijn, 2003). Among them, hydrodesulfurization (HDS) has been the most extensively employed. However, the severe conditions of pressure and temperature needed to be employed in deep HDS cause alterations in fuel final characteristics (Babich and Moulijn, 2003).

As a proposed technique, biodesulfurization (BDS), joined to a previous HDS process, could succeed in obtaining high quality fuels, and respecting in force regulations, as well. This technique, consisting on employing microorganisms (both wild and genetically modified) as catalysts, allows degrading sulfur aromatic molecules using mild conditions of temperature and pressure, avoiding C-C bond breakdown, and maintaining fuel properties. The main model compound employed in BDS studies is dibenzothiophene (DBT), which is transformed through 4S metabolic route (Oldfield et al., 1997) into 2-hydroxybiphenyl (HBP), removing the molecular sulfur while maintaining hydrocarbon skeleton.

In this work, the combination of cells from a GMO, *Pseudomonas putida* CECT 5279, is proposed for the formulation of a biocatalyst in a BDS process. The aim of this work is the optimization of an effective biocatalyst. The experimental variables considered in this study were biomass concentration and cell age.

2. Materials and Methods

2.1 Microorganism

The bacterial strain employed, *Pseudomonas putida* CECT5279 (Galán, 2001), have been supplied by Dr. José Luis García (Biological Research Center, CIB-CSIC, Spain). Cultures were maintained on frozen concentrated stock with glycerol in serum solution.

2.2 Biocatalyst production

Cells employed as biodesulfurizing catalyst were obtained in a 2L stirred tank bioreactor using a BSM medium (Martin et al., 2004), at 30ºC, 1 L/L/min of air flow rate and 200 rpm of stirrer speed, following an standard method in order to obtain comparative and reproducible experimental results (Martin et al., 2005). Two growth time cells were collected in order to carry out BDS resting cells assays: 5 and 23 hours, because of their maximum abilities to produce HBP or to remove DBT, respectively, as previously observed (Calzada et al., 2007).

2.3 BDS assays

BDS resting cells experiments were conducted in an orbital shaker at 30ºC and 210 rpm, using 100 mL Erlenmeyer flasks containing 16 mL HEPES medium with 25 μM DBT as sulfur substrate. 5 and 23 hours growth time cells were added in different proportions and biomass concentrations, as shown in Table 1.

2.4 Analytical methods

Biomass evolution was monitored by measuring absorbance at 600 nm (with a UV 1630 SHIMADZU spectrometer). Samples collected during BDS assays were centrifugated and acidified with HCl. HPLC-UV-diode Array (with a C-18 Komasil, 5μm, 150 x 4.6 mm column) was employed to analyze the evolution of DBT and HBP. Both mobile phase concentration (acetonitrile:water from 30 to 70%) and flow (from 1 to 2 ml/min) gradients were used in order to achieve 4S compounds separation.

Run	Y^{23}	C^{5}_{x} (gDCW/L)	C^{23}_{x} (gDCW/L)	C_x (gDCW/L)
U11	0,00	0,7	0,0	0,7
U12	1,00	0,0	0,4	0,7
U21	0,00	1,4	0,0	1,4
M22	0,50	0,7	0,7	1,4
U23	1,00	0,0	1,4	1,4
U31	0,00	2,1	0,0	2,1
M32	0,33	0,7	1,4	2,1
M33	0,67	1,4	0,7	2,1
U34	1,00	0,0	2,1	2,1

Table 1. Experimental design.

2.5 Mathematical methods

Differential method was applied in order to estimate DBT elimination rate at zero time, for each BDS assay. Experimental data were treated by using OriginPro ® 7.5 software so that fit calculations for initial rates were carried out.

3. Experimental results and discussion

3.1. Experimental results

An experimental design combining the two cell age biomass concentration was proposed in order to find out the best biocatalyst formulation, as shown in Table 1. That means maximizing DBT transformation while minimizing biomass waste and time of BDS. Total dry weight cell concentrations from 0,7 to 2,1 g/L were employed to carry out biodesulfurization assays.

As an example, evolution of DBT and HBP along BDS time for one of these assays is shown in Figure 1. In this case, 100% percentage of BDS is reached so that 25 mM initial DBT concentration is completely transformed into HBP.

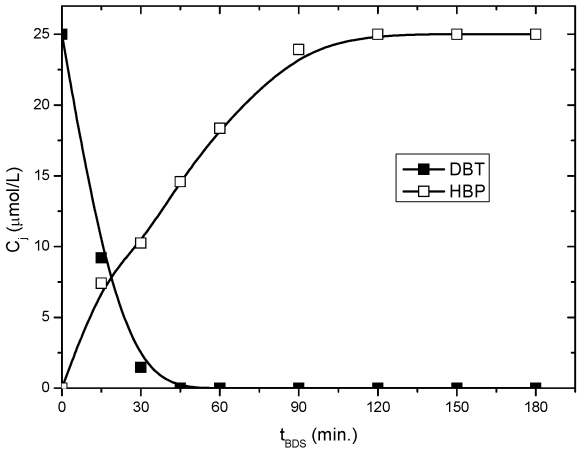

Figure 1. DBT and HBP evolution obtained from a BDS assay.

3.2. Discussion

Evolution of both DBT and HBP concentration were analyzed and studied in each assay by using the following parameters.

Maximum biodesulfurization percentage

$$X^{\max}{}_{BDS} = \frac{C^{\max}{}_{HBP}}{C^{0}{}_{DBT}} \cdot 100 \quad (1)$$

Initial DBT elimination rate

Differential method was employed so that initial DBT elimination ($R_{DBT}{}^{0}$) rate is estimated as follows:

$$R_{DBT}{}^{0} = -\frac{dC_{DBT}}{dt}\bigg|_{t=0} \quad (2)$$

Concentration of biomass

Total biomass concentration was expressed in dry cell weight as the contribution of both kind of cell concentration.

$$C_x = C_x{}^{5} + C_x{}^{23} \quad (3)$$

Specific desulfurization grade

E represents the goodness of each tested cell combination. It relates $X^{max}{}_{BDS}$, C_X and $t_{BDS}^{X_{BDS}^{\max}}$.

$$E = \frac{\left[X_{BDS}^{\max} \Big/ t_{BDS}^{x_{BDS}^{\max}} \right]}{C_x} \quad (4)$$

23 hours growth time mass fraction of cells, Y^{23}

Y^{23} shows the mass fraction that 23 hours growth time cells represent in the biocatalyst formulation.

$$Y^{23} = \frac{C_X^{23}}{C_X^{5} + C_X^{23}} \quad (5)$$

Values of parameters X^{max}_{BDS}, $R_{DBT}{}^{0}$ and E were represented versus Y^{23}, as shown in Figures 2 to 4, in order to compare the different cell mixtures and their abilities to become a good BDS biocatalyst.

BDS percentage is increased when higher biomass concentrations is used for biocatalyst formulation, as it can be seen in Figure 2. However, 23 hours growth time cell contribution is always higher than 5 hours growth time ones, because of their bigger ability to remove DBT (Calzada et al., 2007).

As shown in Figure 3, total biomass concentration has a similar influence on initial DBT elimination rate. Using only one cell age used in biocatalyst formulation does not obtain the highest values for $R_{DBT}{}^{0}$. Instead, certain combinations of 5 and 23 hours growth times achieve higher initial DBT elimination rates.

Finally, specific desulfurization grade is represented in figure 4. For 0,7 and 1,4 gDCW total biomass, the higher the value of Y^{23} is, the biggest the E factor becomes. However, when 2,1 gDCW/L is employed, a maximum is observed by using a Y^{23} of 0,67.

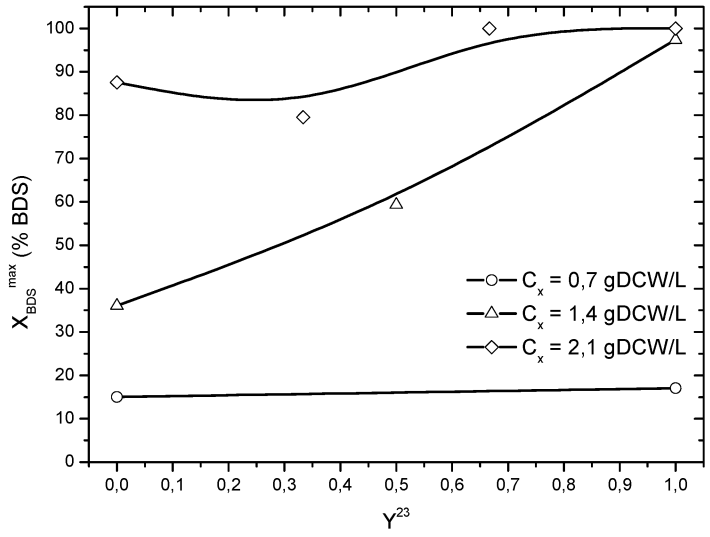

Figure 2. X^{max}_{BDS} versus 23 growth time mass factor of cells for different total biomass concentration.

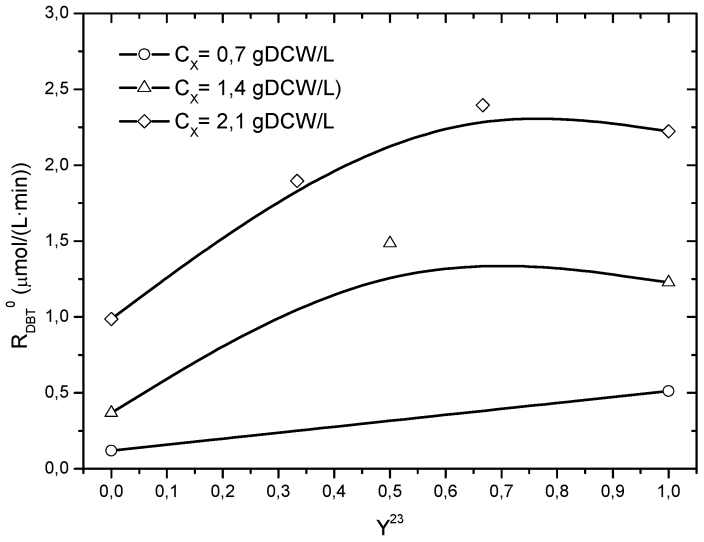

Figure 3. Initial DBT elimination rate versus 23 growth time mass factor of cells for different total biomass concentration.

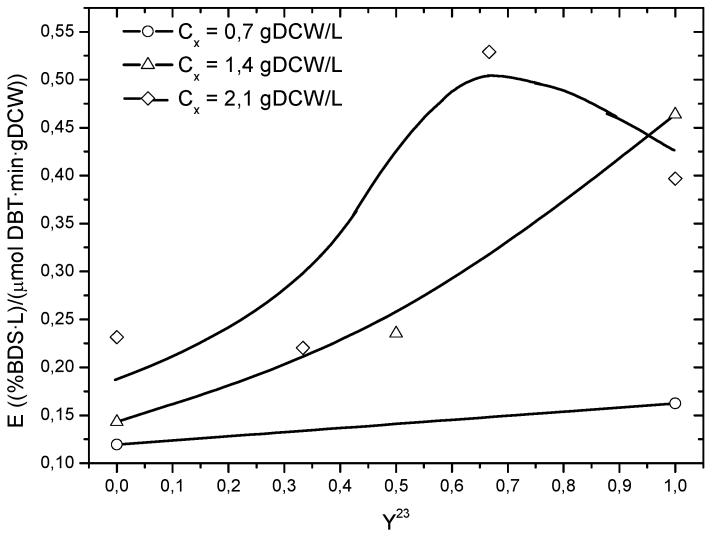

Figure 4. Biocatalyst effectiveness factor versus 23 growth time mass factor of cells for different total biomass concentration.

4. Conclusions

Experimental results show the possibility of optimizing a biocatalyst by mixing two age cells of *Pseudomonas putida* CECT5279. Complete transformation of DBT in a minimized reaction time is achieved by mixing different biomass concentration of both higher DBT removal activity cells and higher HBP production activity ones.

Combining 5 and 23 hours growth time cells, in 0,7 and 1,4 gDCW/L respectively, is found to be the best combination. This biocatalyt formulation gets 100% DBT conversion, while reducing BDS time. In addition, this cell combination achieves higher initial BDS elimination rate than 23 hours cells used alone. This combination have been selected because of the *E* maximun shown among the tested combinations.

5. Nomenclature

BDS = biodesulfurization
C^{i}_{x} = concentration of biomass (gDCW/L), total or at *i* growth time
C_j = concentration of compound *j* (µmol/L)
DBT = dibezothiophene
E = specific desulfurization grade ((%BDS·L)/(·min·gDCW))
HBP = 2-hydroxybiphenyl
HDS = hydrodesulfurization
R_{DBT}^{0} = initial DBT removal rate (µmol/(L·min))
R_{HBP}^{0} = initial HBP production rate (µmol/(L·min))
t^{k}_{BDS} = biodesulfurization time (min), at any or *k* condition
X^{max}_{BDS} = maximum percentage of biodesulfurization (%BDS) given by equation (3)
Y^{23} = 23 hours growth time mass fraction of cells, which can be defined as:

Subindexes
BDS = biodesulfurization
DBT = refers to dibezothiophene
HBPS = refers to 2-(2-hydroxybiphenyl)-benzenesulfinate (sulfinate)
HBP = refers to 2-hydroxybiphenyl

Superindexes
0 = refers to initial time
5 = refers to 5 hours growth cell time
23 = refers to 23 hours growth cell time
X^{max}_{BDS} = refers to maximum percentage of biodesulfurization

6. Acknowledgements

This work has been supported by the Ministerio de Educación y Ciencia under Contract CTQ2007-60919. The grant awarded to one of the authors (J. Calzada) is gratefully recognized.

7. References

Babich, I.V. and J.A. Moulijn, 2003, Science and technology of novel processes for deep desulfurizationof oil refinery streams: a review, Fuel 82, 607

Calzada, J., Zamarro, M.T., Alcon, A., Santos, V.E., Garcia, J.L. and F. Garcia-Ochoa, 2007, Intracellular activity of the enzymes involved in 4S route biodesulphurization of DBT by *Pseudomonas putida* CECET 5279 as function of cell age, Journal of Biotechnology 131 (2S), S84

European Directive 2003/17/EC of the European Parliament and of the Concil of 3 March 2003 amending Directive 98/70/EC relating to the quality of petrol and diesel fuels. OJ L76, 22.3.2003, p. 10.

Galán, B., (2001), Un procedimiento para desulfurar dibenzotiofeno utilizando como biocatalizador una cepa de *Pseudomonas putida* recombinante, W0170996, Spain, PCT/ES01/00112/2001

International Energy Agency, 2007, Key World Energy Statistics 2007 [on line], [consultation date: January 29th 2008] OECD/IEA 2007, <http://www.iea.org/textbase/nppdf/free/2007/key_stats_2007.pdf>

Martin, A.B., Alcon, A, Santos, V.E. and F. García-Ochoa, 2004, Production of a biocatalyst of *Pseudomonas putida* CECT5279 for dibenzothiophene (DBT) biodesulfurization for different media composition, Energy & Fuels 18, 851

Martin, A.B., Alcon, A, Santos, V.E. and F. García-Ochoa, 2005, Production of a biocatalyst of *Pseudomonas putida* CECT5279 for dibenzothiophene (DBT): influence of the operational conditions, Energy & Fuels 19, 775

Olfield, C.; Pogrebinsky, O.; Simmonds, J.; Olson, E. S. and C.F. Kulpa, 1997, Elucidation of the metabolic pathway for dibenzothiophene desulfurization by *Rhodococcus* sp. strain IGTS8 (ATCC 53968), Microbiology 143, 2961

CHEMICAL ENGINEERING TRANSACTIONS, Volume 14, 2008
Edited by G. Marino, E. Bardone, A. Viglia
 ISBN 978-88-95608-02-0

Reductive dechlorination of weathered PCBs in the marine sediments of Brentella canal of Venice Lagoon

G. Zanaroli[1], A. Negroni[1], A. Balloi[2], D. Daffonchio[2], F. Fava[1]
[1]DICASM, Faculty of Engineering, University of Bologna
Viale Risorgimento 2, 40136 Bologna, Italy
[2]DISTAM, University of Milano
Via Celoria 2, 20133 Milano, Italy

The occurrence microbial-mediated reductive dechlorination processes towards polychlorinated biphenyls (PCBs) has been documented in several subsurface sediments of contaminated freshwater and, less frequently, marine systems, spiked with exogenous PCBs and suspended in synthetic media. This work was aimed at detecting and characterizing the occurrence of reductive dechlorination processes towards weathered PCBs in contaminated marine sediments of Porto Marghera area (Venice lagoon, Italy) within slurry microcosms of sediments suspended in the water coming from the same contaminated site. Reductive dechlorination of weathered PCBs occurred in both sediments. The detected processes exhibited *meta*- and *para*-specificity and were not significantly "primed" after spiking with exogenous PCBs, that were rapidly and extensively dechlorinated. PCB dechlorination seemed to be mediated by sulfate-reducing bacteria, that probably started to use PCBs as electron acceptors during the sulfate reduction but in particular when their native electron acceptor was completely depleted. Such activities were detected under geochemical conditions that closely mimic those occurring in situ, and this allows to speculate that similar processes might also be in progress in situ.

1. Introduction

PCBs are poorly biodegradable and highly toxic contaminants. Due to their high hydrophobicity, PCBs released into aquatic systems tend to strongly accumulate in anoxic freshwater, estuarine and marine sub-surface sediments, where they can persist for several months up to many years, and through which they enter the food chain (Brown and Wagner 1990; Bedard and Quensen, 1995; Wiegel and Wu, 2000).
Several studies have documented that highly chlorinated PCBs occurring in anaerobic sediments can undergo a progressive reductive dechlorination mainly directed to the *meta* and *para* position of the biphenyl ring through which they are bio-converted into low-chlorinated, mainly *ortho*-substituted congeners, generally less toxic and prone to bioaccumulate than parent compounds (Bedard and Quensen, 1995; Wiegel and Wu, 2000). The process has been often ascribed to methanogenic bacteria and less frequently to $SO_4^=$-reducing bacteria, even though recent studies on highly enriched cultures ascribed PCB dechlorination to members of the phylum *Chloroflexi*, able to use organic acids and/or H_2 as electron donors and PCBs as electron acceptors (Haggblom and

Bossert, 2003; Bedard et al., 2006; Bedard et al., 2007; Fagervoldet al., 2005; Fagervold et al., 2007; Yan et al., 2006a; Yan et al., 2006b).
On the contrary, a little is known about the occurrence of PCB reductive dehalogenation processes and of PCB dehalogenating microbial populations in marine sediments (Alder et al., 1993; Berkaw et al., 1996; Lake et al., 1992; Øfjord et al., 1994; Palekar et al., 2003), where in general sulfidogenic conditions prevail on methanogenesis (Ward and Wrinfey, 1985; Kafkewitz and Togna, 1998). Thus, more information on the potential fate of aged PCBs in marine contaminated sediments are required. In particular, evidences for these processes under geochemical conditions that closely mimic those occurring in situ are highly required, as these might provide information on the occurrence of the same processes in situ (Bedard and Quensen, 1995; Wiegel and Wu, 2000; Apitz et al., 2004).
Therefore, a long term study was undertaken to detect and characterize the microbial reductive dechlorination processes *vs.* weathered PCBs in sediments of the Brentella Canal of the Porto Marghera area (Venice lagoon, Italy) suspended in water coming from the same site, i.e. under geobiochemical conditions close to those of the site, to determine the potential of the site to undergo in situ microbial decontamination.

2. Experimental Approach

Two sets of 30 ml slurry-phase anaerobic microcosms consisting of sediment suspended at 25% (v/v) in its own site water were developed with two PCB contaminated sediments (referred to as sediment 1 and sediment 2, respectively) collected from different locations in the Brentella canal, Porto Marghera (Venice lagoon, Italy).
The first set, developed with sediment 1, consisted of untreated microcosms as well as of pasteurized microcosms (15 minutes treatment at 90°C), molybdate-amended (20 mM) and 2-bromoethanesulfonate (BES)-amended (30 mM) microcosms, in order to select for spore-forming bacteria, to inhibit sulfate-reducing bacteria and to inhibit methanogenic bacteria, respectively. In addition, sterile microcosms were set up under each condition. A parallel group of identical microcosms was also spiked with 2,3,4,5,6-pentachlorobiphenyl (20 mg/kg dry wt sediment) in order to study the possibility of "priming" (i.e. stimulating) the dechlorination of the sediment aged PCBs and the mechanism through which they were dechlorinated under each of the experimental conditions.
The second set of microcosms, developed with sediment 2, consisted of 4 untreated microcosms (2 biologically active and 2 autoclave-sterilized) and 4 microcosms (2 biologically active and 2 autoclave-sterilized) spiked with 3,3',4,4'-tetrachlorobiphenyl, 3,3',4,4',5-pentachlorobiphenyl, 2,3',4,4',5-pentachlorobiphenyl, 3,3',4,4',5,5'-hexachlorobiphenyl and 2,3,3',4,4',5-hexachlorobiphenyl at 100 mg/kg of dry sediment each, in order to investigate: a) the possibility of "priming" the dechlorination of PCBs pre-existing in the sediment, and b) the potential biological fate of target co-planar dioxin-like PCBs under the geochemical conditions created in the microcosms.
Sterile microcosms were prepared through autoclave-sterilization performed at 121°C for 1 h in three consecutive days; in the case of spiked control microcosms, exogenous PCBs were added after autoclave sterilization. All the developed microcosms were then incubated stationary at 25 ± 1°C in the dark and periodically sampled and analyzed to

determine the volume and composition of the head-space gas as well as the concentration of PCBs and inorganic anions ($SO_4^{=}$ and Br^-)(Fava et al., 2003a,b; Zanaroli et al., 2006).

3. Results

A total PCB concentration of 0.784 ± 0.351 μmol (kg dry wt sediment)$^{-1}$ was detected in the biologically-active and sterile microcosms of sediment 1 at the 7th day of incubation. Significant changes of the initial PCB distribution profile were unequivocally observed in the untreated microcosms at the 20th week, where an extensive depletion of highly chlorinated biphenyls together with a stoichiometric accumulation of tri- and di-chlorinated, *ortho*-substituted biphenyls were observed (Figure 1A).
A less extensive but significant transformation of endogenous PCBs was also observed in the pasteurized microcosms, where the accumulation of 2-chlorobiphenyl was also observed (Figure 1B), whereas only a poor PCB transformation was detected in the microcosms supplemented with BES or molybdate (Figures 1, C and D, respectively).

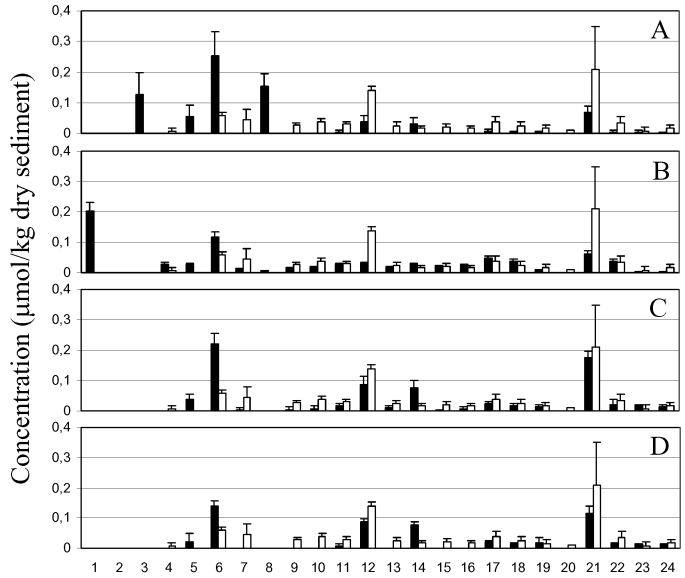

Figure 1. Bioconversion of sediment-carried PCBs after 20 weeks of incubation. White bar: sterile microcosms; Black bar: biologically active microcosms. A: sediment and water; B: pasteurized microcosms; C: BES; D: Molybdate (After Fava et al. 2003b).
(1):2-CB; (2):4-CB; (3):2,6-/2,2'-CB; (4):2,4-/2,5-CB; (5):2,4'-/2,3-CB; (6):2,4,6-CB; (7):2,2',5-/2,2',4-/4,4'-CB; (8):2,3,6-/2,3',6-CB; (9):2,3,3'-/2',3,4-/2,2',5,6'-CB; (10):2,2',4,6'-/2,3,4'-CB; (11):2,2',5,5'-CB; (12):3,3',4-CB; (13):2,2',3,5-CB; (14):3,4,4'-/2,3,3',6-/2,2',3,4'-CB; (15):2,2',3,4-/2,3,4',6-CB; (16):2,3',4',5-CB; (17):2,3',4,4'-/2,2',3,5',6-CB; (18):2,2',3,4',5-/2,2',4,5,5'-CB; (19):2',3,4,4',5-/2,2',3,4',5',6-/2,3',4,4',5-CB; (20):2,2',3,4',5,5'-CB; (21):2,2',3,3',4,6'-/2,2',4,4',5,5'-/2,3,3',4,4'-CB; (22):2,3,3',4,5,6-/2,2',3,4,4',5-/2,3,3',4,4',6-CB; (23):2,2',3,3',4,5,6-/2,3,3',4,4',5'-/2,2',3,3',4,5',6,6'-CB; (24):2,2',3,4,4',5,5'-CB.

Table 1. Microbial activities detected in the microcosms after 20 weeks of incubation.

Microcosms	Sulfate depletion (%)	Produced Gas (ml)	Produced CH_4 (ml)	Released Br^- (mg/l)
S + W	29.9 ± 7.8	1.25 ± 0.21	0	0
Pasteurized	41.2 ± 14.2	0.65 ± 0.21	0	0
with molybdate	-12.4 ± 2.7	2.40 ± 1.00	0.17 ± 0.01	0
with BES	47.3 ± 35.0	1.55 ± 0.64	0	6.01 ± 0.88

Comparable changes in the endogenous PCBs distribution profiles were observed in the 2,3,4,5,6-pentachlorobiphenyl-spiked microcosms (Fava et al. 2003b).

A detectable production of gas was observed in all the biologically active microcosms during the 20 weeks of incubation (Table 1). In the molybdate-amended microcosms a significant methane production and no consumption of the initial 2.1±0.1 g l^{-1} of $SO_4^=$ were observed (Table 1). On the contrary, a consumption of about 30-50 % of the initial $SO_4^=$ was observed in the untreated, pasteurized, and BES-amended microcosms, where no methane production was detected. In addition, in the BES-amended microcosms a release of about 6 mg l^{-1} of Br^- was measured (Table 1). The same changes were observed in the PCB-spiked set of microcosms, except for sulfate consumption in the untreated microcosms, where it was slightly faster and more extensive than in the corresponding non-spiked microcosms (data not shown) (Fava et al. 2003b).

Taken together, these results indicate that indigenous sulfate-reducing bacteria were responsible for the detected PCB-reductive dechlorination. A low dechlorination activity was detected in the microcosms supplemented with BES, where a marked consumption of $SO_4^=$ was observed. A significant release of Br^- was also observed in these microcosms; this suggests that BES acted as the preferential electron acceptor for the dehalogenating bacteria, thus inhibiting PCB dechlorination. The detection of both reductive dechlorination activity and sulfidogenic activity in the pasteurized microcosms, indicates that spore-forming, sulfate-reducing bacteria were involved in the process. The exogenous 2,3,4,5,6-pentachlorobiphenyl was markedly bioconverted into its tetra-, tri- and di- *ortho*-chlorinated daughter products in the spiked untreated and pasteurized microcosms, showing that the process had a higher selectivity towards *meta*- and *para*- positions. Finally, the dechlorination of the spiked PCB did not significantly affect the onset of the pre-existing PCB dechlorination, probably because of the low concentration (≈ 1 mg/kg) of the weathered PCBs in the sediment and/or the inhibition by high concentrations of $SO_4^=$ and salt occurring in these microcosms.

A total amount of sediment carried PCBs corresponding to 1.60 ± 0.13 mg/kg of dry sediment was found to occur in the non-spiked sterile and biologically active microcosms of sediment 2 after 7 days of microcosm incubation. The total amount of pre-existing PCBs in the spiked microcosms was expected to be the same; however, we could not determine it, as the added PCBs interfered with GC-ECD congeners estimation.

No transformation of sediment-carried PCBs was detected in the sterile microcosms until the end of the experiment. On the contrary, a significant change in PCB profile was found to occur in the corresponding non-spiked biologically active microcosms, as compared to the sterile ones, starting from the 5th month of incubation. At the end of the experiment (after 16 months), several hexa-, penta- and tetra-chlorinated congeners were found to be bioconverted on a molar basis into less chlorinated PCBs, such as 2,2',5/2,2',4/4,4'-chlorobiphenyl and 2,4/2,5-chlorobiphenyl (Figure 3). 4-monochlorobiphenyl also accumulated in the biologically active microcosms at the end of the experiment, whereas 2-monochlorobiphenyl was depleted.

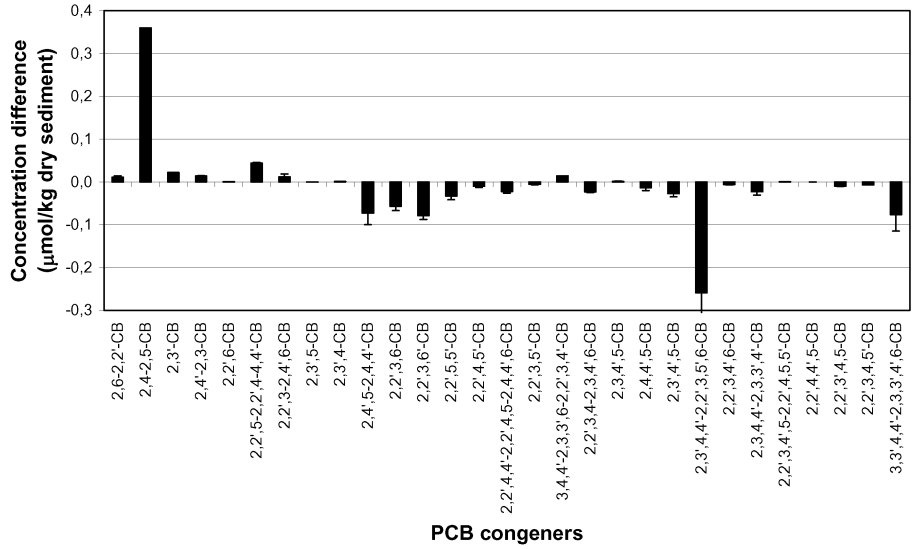

Figure 3. Difference in the concentration of each sediment-carried PCB congener in the non spiked biologically active microcosms as compared to the corresponding sterile ones after 16 months of incubation.

A little sulfate consumption was observed in the active microcosms since the first month of incubation. Sulfate was then quickly depleted, becoming 8.4% of the initial concentration (1.95± 0.03 g/l) after 2 months of incubation and undetectable at the end of the 3rd month of experiment (Table 2). No significant biogas production was observed in the active microcosms until sulfate was not completely depleted. A large amount of biogas (27.5 ± 16.5 ml) consisting of more than 47% of methane was detected in the same microcosms between the 3rd and the 5th month of incubation, i.e. immediately after complete sulfate depletion and before PCB dechlorination started. Methane production was detected at a lower rate all over the experiment (up to the 16th month) (Table 2).

Table 2. Overall sulfate consumption, gas and methane production (± standard deviation) in the biologically active microcosms after 16 months of incubation. Initial sulfate concentration in all microcosms was 1.95± 0.03 g/l.

	Non spiked microcosms	Spiked microcosms
$SO_4^=$ consumption (%)	100	100
Biogas production (ml)	34.7 ± 20.4	20.4 ± 4.9
CH_4 production (ml)	15.0 ± 8.5	8.6 ± 2.9

Very similar trends, both in terms of sulfate consumption and methane production, were observed in the parallel biologically active spiked microcosms, where the overall amount of produced methane was about 60% of that detected in the non spiked ones (Table 2). The biotransformation of several sediment-carried PCBs could not be quantified in the spiked microcosms, as some of them were produced from the spiked congeners dechlorination. However, the fate of about 30% of the GC-ECD peaks ascribed to pre-existing PCBs could be monitored and compared with that observed in the non spiked microcosms (data not shown). A significant transformation of such pre-existing PCBs and of the exogenous PCBs was detected starting from the 5th month of incubation. However, the dechlorination of the exogenous PCBs only slightly influenced the bioconversion extent and pattern of pre-existing PCBs), suggesting that the dechlorination of the latter was not significantly primed by the addition of the 5 exogenous coplanar congeners.

The exogenous PCBs were markedly bioconverted into less chlorinated congeners, such as 3,3',5,5'-/2,3',4,4'-, 2,3',4',5- and 2,4,4',5-tetrachlorobiphenyl, 2,4,4'-, 2,3',4- and 2,3'5-trichlorobiphenyl and 3,4- and 3,4'-dichlorobiphenyl between the 5th and the 8th month of incubation, and were found to be depleted by more than 80% at the end of the experiment (data not shown). This finding is of great relevance, as indicates that indigenous microbial consortia selected in the spiked primary microcosms were able to rapidly and extensively dechlorinate some dioxin-like coplanar PCBs that are regarded as some of the most toxic PCBs reported in the literature (Kimbrough 1995). The extensive dechlorination of the spiked PCBs only slightly intensify rate and extent of the dechlorination of the PCBs pre-existing in the sediment.

4. Conclusions

The occurrence of microbial-mediated, reductive dechlorination processes towards weathered PCBs and spiked high chlorinated and co-planar PCBs has been demonstrated in 2 contaminated sediment of the Brentelle Canal of the Porto Marghera area (Venice lagoon, Italy). The detected processes exhibited *meta*- and *para*-specificity (apparently they proceed through dechlorination pattern H' and M) and were not significantly "primed" by the dechlorination of exogenous PCBs, that were rapidly and extensively dechlorinated. PCB dechlorination seemed to be mediated by sulfate-reducing bacteria, that probably started to use PCBs as electron acceptors during the sulfate reduction but in particular when their native electron acceptor was completely depleted.

Such activities were detected under geochemical conditions that closely mimic those occurring *in situ*, and this allows to speculate that similar processes are also in progress *in situ*. However, the detected PCB dechlorination processes were slow and partial. In general microbial processes occurring *in situ* are very constrained temporally and spatially. Further, natural sediment systems are complex, heterogeneous, and subjected to (bio)turbation phenomena and low and variable temperatures. Thus, the findings described above do not necessarily prove that biodegradation will provide sufficient natural *in situ* decontamination of the site but for sure, if properly combined with other lines of microbial and biogeochemical evidence coming from the same site (Apitz et al., 2004), a strong indication of biodegradation *in situ*, and justify further investigations.

5. References

Alder, A.C., M.M. Häggblom, S. Oppenheimer, and L.Y. Young, 1993, Environ. Sci. Technol. 27, 530.

Apitz, S.E., B.P. Ayers and V.J. Kirtay, 2004, Use of data on contaminant/sediment interactions to streamline sediment assessment and management, http://www.spawar.navy.mil/sti/publications/pubs/tr/1918/tr1918cond.pdf.

Bedard, D.L. and J.F. Quensen III, 1995, Microbial reductive dechlorination of polychlorinated biphenyls, in Microbial Transformation and Degradation of Toxic Organic Chemicals, Eds. L.Y. Young and C.E. Cerniglia, 127.

Bedard D.L., J.J. Bailey, B.L. Reiss and G. Van Slyke Jerzak, 2006, Appl. Env. Microbiol. 72, 2460.

Bedard D.L., K.M. Ritalahti and L.E. Löffler, 2007, Appl. Env. Microbiol. 73, 2513.

Berkaw M., K.R. Sowers and H.D. May, 1996, Appl. Environ. Microbiol. 62, 2534.

Brown J.F. Jr. and R.E. Wagner, 1990, Environ. Toxicol. Chem. 9, 1215.

Fagervold S.K., J.E.M. Watts, H.D. May and K.R. Sowers, 2005, Appl. Environ. Microbiol. 71, 8085.

Fagervold S.K., H.D. May and K.R. Sowers, 2007, Appl. Environ. Microbiol. 73, 3009.

Fava F., S. Gentilucci and G. Zanaroli, 2003a, Chemosphere 53, 101.

Fava F., G. Zanaroli and L.Y. Young, 2003b, FEMS Microbiol. Ecol. 44, 309.

Haggblom M.M. and I.D. Bossert, Eds., 2003, Dehalogenation: microbial processes & environmental applications. Kluwer Press, The Netherlands.

Kafkewitz D. and M.T. Togna, 1998, Microbes in the muck: a look into the anaerobic world, in Biological treatment of hazardous wastes, Eds. G.A. Lewandowski and L.J. DeFilippi, John Wiley & Sons, Inc, USA.

Kimbrough R.D., 1995, Crit. Rev. Toxicol. 25, 133.

Lake J.L., R.J. Pruell and F.A. Osterman, 1992, Mar. Environ. Res. 33, 31.

Øfjord G.D., J.A. Puhakka and J.F. Ferguson, 1994, Environ. Sci. Technol. 28, 2286.

Palekar L.D., K.A. Maruya, J.E. Kostka and J. Wiegel, 2003, Chemosphere 53, 593.

Ward D.M. and M.R. Wrinfey, 1985, Adv. Microbiol. Ecol. 3, 141.

Wiegel J. and Q. Wu, 2000, FEMS Microbiol. Ecol., 32, 1.

Yan T., T.M. LaPara and P.J. Novak, 2006a, FEMS Microbiol. Ecol. 55, 248.

Yan T., T.M. LaPara and P.J. Novak, 2006b, Environ. Microbiol. 8, 1288.

Zwiernik M.J., J.F. III Quensen and S.A. Boyd, 1998, Environ. Sci. Technol. 32, 3360.

Zanaroli G., J.R. Pérez-Jiménez, L.Y. Young, L. Marchetti and F. Fava, 2006, Biodegradation 17, 19.

CHEMICAL ENGINEERING TRANSACTIONS, Volume 14, 2008
Edited by G. Marino, E. Bardone, A. Viglia
 ISBN 978-88-95608-02-0

Biosorption of aqueous chromium (VI) by living mycelium of phanerochaete chrysosporium

Nikazar, M.*, Davarpanah, L., Vahabzadeh, F. *

Professor of Department of Chemical Engineering, Amirkabir University of Technology (Center of Excellency for Petrochemical Engineering), No. 424, Hafez Ave., Tehran, Iran
E-mail address: * nikazar @aut.ac.ir,

In this study the biosorption of Cr(VI) from artificial wastewater onto the living mycelium pellets of white-rot fungi, *Phanerochaete chrysosporium*, was investigated in the batch mode with respect to the contact time and initial metal concentration. Biosorption equilibrium was established after about 120 min.The fungus biomass exhibited the highest sorption capacity of 48.6 mg/g and the removal efficiency was found to be higher at lower initial concentration of the Cr(VI) ion. The adsorption of Cr(VI) followed the Longmuir isotherm over the whole range of initial metal concentration tested (20-500mg/l) and kinetic was found to be best-fit pseudo-second order equation.

Key words: Biosorption, Heavy metal, Chromium, Isotherm, Kinetic, Phanerochaete chrysosporium

1. Introduction

Human activities, such as mining operations and the discharge of industrial wastes, have resulted in the accumulation of metals in the environment.
Many industries such as tannery, coating, car aeronautic and steel industries generate great quantities of wastewater containing various concentrations of Cr .The potential use of microorganisms in the treatment of heavy metal contaminated wastewater and in the recovery of metals in mining wastes or in metallurgical effluents is of special importance.
Conventional methods of treating solutions which contain heavy metals include: precipitation, ionic exchange, reduction process, coagulation, membrane technologies and adsorption in activated coal .These methods are associated with either a high cost or a low efficiency, not guaranteeing the limits of metal concentration demanded by legal standards.
The search for alternative and innovative treatment techniques has focused attention on the use of biological materials such as algae, fungi, yeast and bacteria for the removal and recovery technologies and has gained importance during recent years because of the better performance and low-cost of these biological materials.

So far some studies have been conducted on the biosorption of zinc, cadmium, copper, lead and mercury by P.chrysosporium (Arica, M., Y., Bayramoglu, G (2005) and Park, D., and et al (2005) and Han, X.and et al (2007)), but none of them investigated the biosorption of Cr(VI), the soluble and highly toxic anion [4], from aqueous solutions. The present study aims to confirm the potentialities of this fungal biomass as a cost-effective metal biosorbent for Cr(VI) removal and also explain the adsorption equilibrium by isotherm models.

2. Materials and methods

2.1 Biomass preparation

The white rot basidiomyycete, P.chrysosporium ATCC 24725 was obtained from microbial collection of Iranian Research Organization of Science and Technology. The fungal strain was maintained by subculturing on a 2% YMG agar medium (yeast extract 4g, malt extract 10 g, glucose 6g per liter of distilled water, pH=6.0).The fungus was grown on YMG agar for 5 days at 27°C and a small portion (0.5cm×1cm) of the agar medium covered with the fungus was cut into 0.2cm × 0.2cm pieces. For the preparation of an aqueous fungal suspension, the small pieces were transferred to 150 ml of YMG broth in a 500 ml Erlenmeyer flask and incubated at 27°C on a shaker incubator (Kuhner ISF-W) at 150 rpm and 27°C. After 5 days 3-5 fungal pellets were formed. Mycelium pellets were harvested from the medium, washed twice with distilled water and stored at 4°C until metal adsorption.

2.2 Metal solution

Standard stock solutions of Cr(VI) was prepared with $K_2Cr_2O_7$ salt from Merck and was used to make the required concentrations metal ion.

2.3 Biosorption tests

The biosorption capacity of biosorbent was determined by contacting a known amount of metal solution (100mg/l) in 250 ml flasks and incubating with biosorbent on an orbital shaker at 100 rpm and room temperature. Biomass was then removed from metal solution by centrifugation at 5000 rpm for 5 min.

Residual metal concentration in the metal supernatant solutions were determined spectrophotometrically (540 nm) after complexation with 1, 5 diphenyl carbazide. The amount of absorbed metal ions per g biomass was obtained by using the following expression.

$$Q= [(Co-C).V] /M$$

Where Q is the amount of metal ions adsorbed on the biomass (mg/g dry weight of fungal pellets).Co and C are the concentrations of the metal ions in the solution (mg/l) initially and after biosorption.V is the volume of the medium (ml) and M is the dry weight of fungal biomass.

3. Results and Discussion

3.1 Effect of contact time on biosorption

Fig. 1 shows the effect of reaction time on the biosorption of Cu(II) and Cr(VI) by biosorbent from aqueous solutions. The rate of metal biosorption by the living biomass was rapid in the first 30 min of contact, accounting about 80.4% and 77.3% of sorption for Cu(II) and Cr(VI), respectively. Time required for attaining equilibrium for both metal ions was about 120 min.

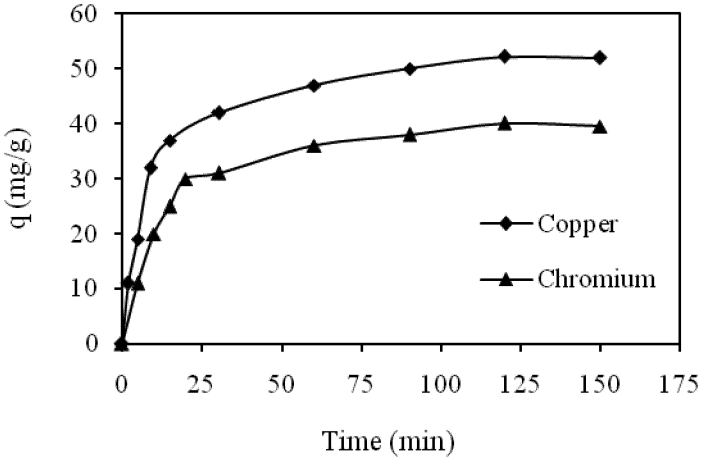

Fig. 1. Time-course profiles for Cu(II) and Cr(VI) biosorption by fungal pellets.

3.2 Effect of initial metal ion concentration on biosorption

Heavy metal ion biosorption capacities of fungal biomass are presented as a function of the initial concentration of Cu(II) and Cr(VI) ions within the aqueous solution in Fig. 5. These experiments were performed using single solutions (20-500 mg l^{-1}) of the metal ions at optimum pH. The amount of metal ions adsorbed per unit mass of biosorbent increases with an increase in initial metal ion concentration. This could be due to an increase in electrostatic interactions (relative to covalent interactions), involving sites of progressively lower affinity(Iqbal, M., Edyvean, R.G.J.(2004)). Moreover, higher initial concentration provides increased driving force to overcome all mass transfer resistance of metal ions between the aqueous and solid phases resulting in higher probability of collision between Cu(II) and Cr(VI) ions and sorbents. This also results in higher metal uptake.

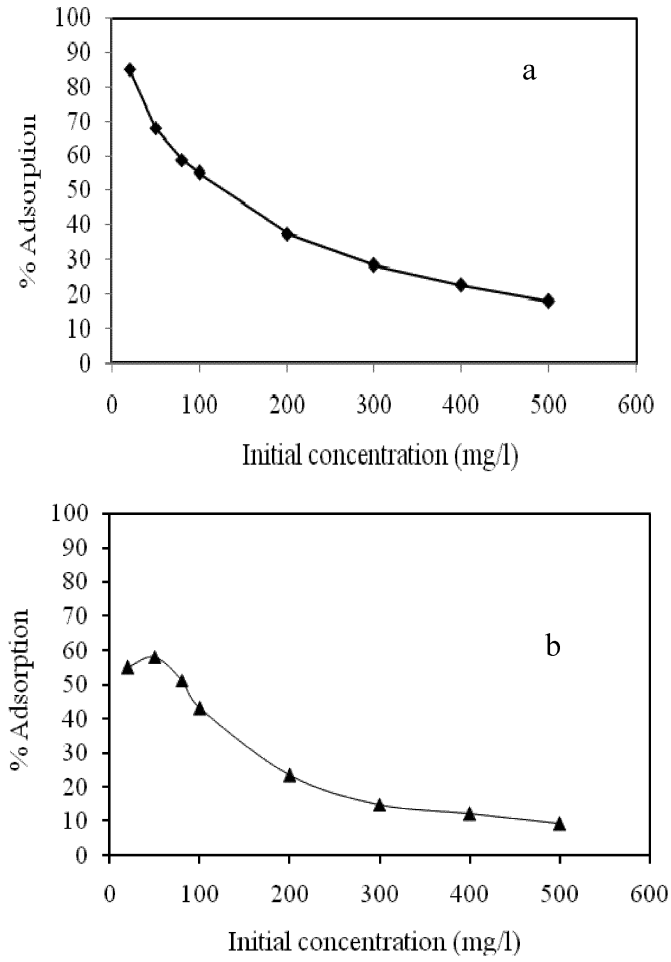

Fig. 2. Effect of initial metal on concentration on percentage adsorption of (a) Cu (II) and (b) Cr (VI).

3.3 SEM studies results

SEM micrographs of the hyphae of fresh pellets and Cu (II) and Cr(VI) loaded pellets are compared in Fig. 3. The fresh pellets had a highly porous mycelium matrix and their large surface areas were clean for metal uptake.

In living cells the sorption mechanisms include both metabolism dependent and independent processes. Metabolism independent uptake process essentially involves cell surface binding through ionic and chemical interaction, while dependent process deals with the binding of both the surfaces followed by intracellular accumulation.

The appearance of the hyphae loaded with chromium is completely different from that of copper implying different biosorption mechanism such as complexation and precipitation in addition to ion exchange.

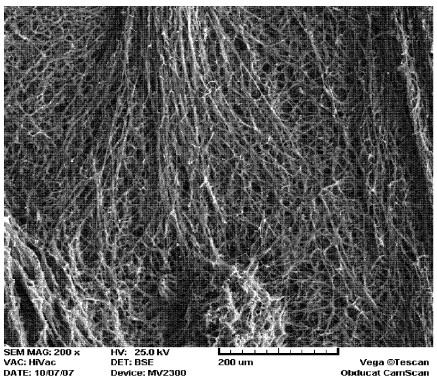

(a)

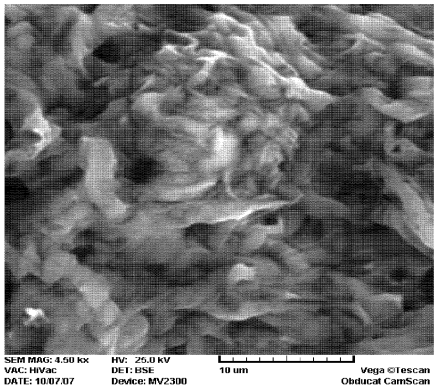

(b)

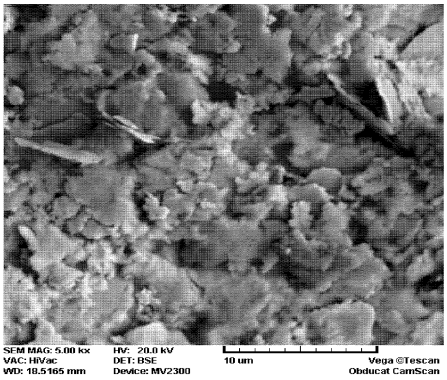

(c)

Fig. 3. Scanning electrn micrographs of fungal hyphae; (a) fresh pellets, (b) copper loaded pellets, (c) chromium loaded pellets.

4. Conclusions

The experiments conducted with the biosorption showed that *Phanerochaete chrysosporium* can remove Cu (II) and Cr (VI) by biosorption. Living mycelium of white-rot fungus exhibited the highest copper and chromium adsorption capacity of 90.6 and 48.6 mg/g. The sorption capacity was found to increase with increase of solute concentration. The biosorbent has the potential to be used in industrial wastewater treatments, since the fouling and structure damage are not problems of the living fungal mycelium (Sing, C., Yu, J (1998)).

5. References

Arica, M., Y., Bayramoglu, G., "Cr(VI) biosorption from aqueous solutions using free and immobilized biomass of Lentinus sajor-caju: preparation and kinetic characterization", J. Colloids. Surf., A: Physicochem. Eng. Asp., 253(2005), PP 203-211.

Han, X., Wong, Y., S., Wong, M., H., Tam, N., F., Y., "Biosorption and bioreduction of Cr(VI) by a microalgal isolate, Chlorella miniata", J. Hazard. Mat., 146(2007), PP 65-72.

Iqbal, M., Edyvean, R.G.J., "Biosorption of lead, copper and zinc on loofa sponge immobilized biomass of Phanerochete chrysosporium", J. Min. Eng., 17(2004), PP 217-223.

Park, D., Yun, Y., S., Jo, J., H., Park, J., M., "Mechanism of hexavalent chromium removal by dead fungal biomass of Aspergillus niger", Water Res., 39(2005), PP 533-540.

Sing, C., Yu, J., "Copper adsorption and removal from water by living mycelium of white-rot fungus Phanerohaete chrysosporium", J. Wat. Res., 32(1998), PP 2746-2752.

CHEMICAL ENGINEERING TRANSACTIONS, Volume 14, 2008
Edited by G. Marino, E. Bardone, A. Viglia
 ISBN 978-88-95608-02-0

Bioremediation of Olive Oil Mill Wastewaters by Fungal (*Trichoderma viride*, strain 8/90) Sequencing batch reactor

Alessio D'Urso[1,a], Daniel Gapes[2,b] and Marco Bravi[1,c]

[1] Dipartimento Ingegneria Chimica Materiali Ambiente, Sapienza – Università di Roma. Via Eudossiana 18, 00184 – Rome (Italy).
[2] Scion Research Institute – 49 Sala Street, P.B. 3020, Rotorua (New Zealand)

[a] alessio.durso@uniroma1.it; [b] daniel.gapes@scionresearch.com;
[c] m.bravi@ingchim.ing.uniroma1.it

Olive oil mill wastewaters (OOMWs) still represent an important environmental problem due to the several difficulties which has to be faced for their disposal.The performance of a lab-scale Sequencing Batch Reactor (SBR) for olive oil mill wastewater (OOMW) treatment was investigated. The reactor, preliminarily filled with suspended solids free OOWM was inoculated with *Trichoderma viride* (strain 8/90) fungal biomass. Influent and effluent dissolved organic carbon (DOC), total suspended solids (TSS) and polyphenols concentrations were monitored. The obtained results showed that the steady state removal of the organic carbon was about 66%, whereas phenolic compounds were reduced by about 50%.

1. Introduction

Olive oil is one of the most used food products in the world. Nevertheless oil is a typical product of the so called Mediterranean Region, which comprises Southern European (Spain, Italy, Greece), Northern African (Algeria, Morocco, Tunisia) and some Middle East (Turkey, Syria) countries, the olive oil market is very significant in all over the world, as reported in Figure 1. In 2005 the estimated world oil production (and consumption) was about $2.5 \cdot 10^6$ tonnes (http://www.unctad.org/).
The New Zealand olive oil industry, even still small (2005 production was estimated to be about 112 tonnes, http://www.olivesnz.org.nz), is promisingly growing. An interesting factor for New Zealand new season's olive oils is that they are available on the market when the Northern hemisphere oils are already six months old. Even though New Zealand had no indigenous olive trees, a suitable cultivar of this species was introduced in the country with olives brought in during the nineteenth century.
Oil industry, however, raises concerns wherever it develops. The wastewater co-generated during the productive process – commonly named as Olive Oil Mill Wastewater, (OOMW) – is very polluting (Borja et al., 2006): it is characterized by a very high COD content, a low pH, a suspended solids fraction and features the presence of biorecalcitrant and inhibiting compounds – mainly polyphenols – which make traditional biological treatment processes scarcely effective. A typical OOMW characterization in reported in Table 1.

Table 1 – Typical OOMW (from Proietti and Nasini, 2006) and utilized wastewaters compositions.

Parameter (unit)	Typical OOMW Range	Utilized OOMW (soluble fraction)
pH	4.3 ÷ 5.8	5.08
COD (g/l)	15 ÷ 390	136 (78)
Organic Carbon	n/a	54 (34)
Organic Matter (g/l)	35 ÷ 150	45
Sugars (g/l)	5 ÷ 80	12*
Nitrogen Compounds (g/l)	5 ÷ 24	1.1
Polyphenols (g/l)	3 ÷ 24	4.7*
Lipids (g/l)	1 ÷ 15	n/a
P (mg/l)	20 ÷ 1100	1740

(*) expressed as glucose equivalents
(**) espressed as gallic acid equivalents

So far, the disposal of OOMW is not a stringent environmental problem in New Zealand (contrary to the situation of the main producing countries, like Italy and Spain); however, as the New Zealand oil industry is promisingly growing, a preventive investigation for the set-up of a treatment technology may play an important role in the future. In this work, the results of a continuous OOMW-treating reactor are shown. The key point is that a selected fungal biomass (*Trichoderma viride*) has been deployed to inoculate the reactor; indeed, this fungal species has been demonstrated to be able to withstand critical conditions (low pH, high polyphenols concentration, high COD content) and to successfully operate the treatment process in both model (D'Urso et al., 2007a) and semi-model (D'Urso et al., 2007b) applications. Furthermore, other authors obtained interesting results utilizing OOMW spontaneous fungal flora for the treatment (Caffaz et al., 2007). Last, but not least, New Zealand has a remarkable track of smart uses of *Trichoderma* spp. biomass, such as crops biocontrol (Agrimm Technologies Limited, www.tricho.com).

2. Materials and Methods

2.1 Biomass

For this work, Trichoderma viride Pers:Fr. Isolate 8/90 has been used. It was kept as pure culture on Petri dishes and stored at 26° C.

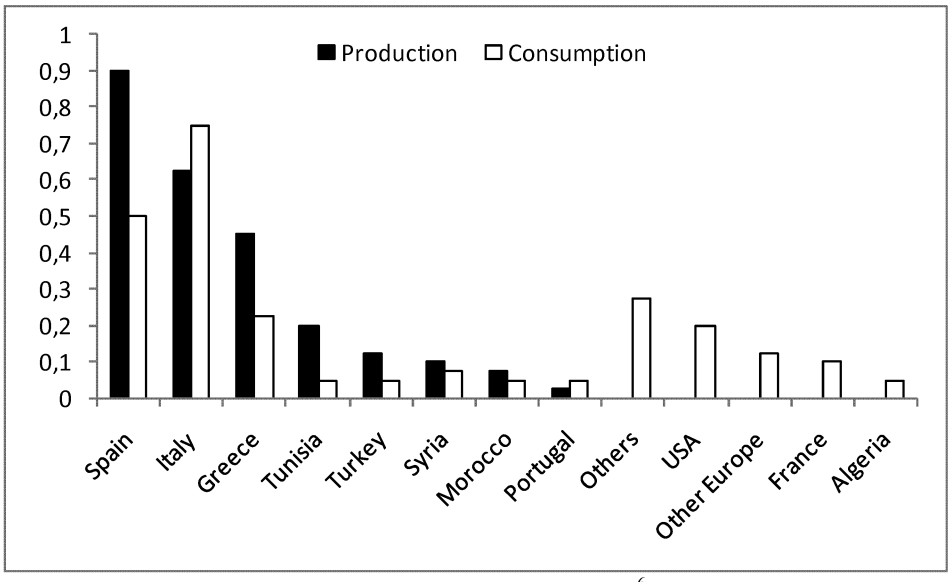

Figure 1 – Olive oil world production and consumption (10^6 tonnes), from http://www.unctad.org.

2.2 Wastewater

The OOMW was collected from "The Village Press" mill, located in Hawkes Bay, which is one of the most important regions for the production of extra virgin olive oil in New Zealand. After reception in the laboratory it was characterized, then stored at 4° C until use.

2.3 Reactor Management

The study was performed as a continuous treatment in a Sequencing Batch Reactor (SBR) system (volume = 2 l).

The SBR was fed with pre-treated OOMWs. They were centrifuged at 4000 rpm for 30 minutes and then filtered (75 micron); thus, a removal of about the 50% of the initial TOC level was achieved. This solid material has been shown from other authors to be elegible for an energy recovery by thermal conversion (Caffaz et al., 2007).

A biological treatment policy featuring equal Hydraulic Retention and Solid Retention times (HRT and SRT) of 5 days that is, without settling phase, was adopted for modelling purposes. The pH and temperature set points were fixed, respectively, at 3.5 (aim of this investigation was also identifying the biomass behaviour in extremely acidic conditions) and 25°C. The air flow rate was 3 vvm.

The reactor was managed as a batch one during the first three days, to allow for *T. viride* biomass growth: diluted (1:4) OOMW was introduced as growth medium. After 8 days, the centrifuged OOMW was continuously fed to the system.

The reactor was operated according to the following schedule:

- Load phase: 5 min;
- Reaction phase: 340 min;
- Discharge phase: 15 min.

3. Results and discussions

DOC, polyphenols concentration and suspended solids content, together with biomass concentration (VSS) and COD removal (these latter representing the quantities most descriptive of the quality of the devised treatment), were monitored during the whole duration of the experiment. The results of the performed treatment are reported in Figure 2.

During the start-up phase about 1300 mg_{DOC}/l (i.e. 108 C-mmol) were removed and the biomass concentration rose to 950 mg_{VSS}/l. Considering the general raw formula of microbial biomass ($C_5H_7O_2N$), it means that 42 C-mmol of biomass were produced. Thus leading to an observed biomass yield of 0.39 (on a C-mmol base).

On the other hand, a polyphenols analysis showed that these compounds were not removed from the medium, likely because the biomass was not acclimatized and ready to use them for growth yet.

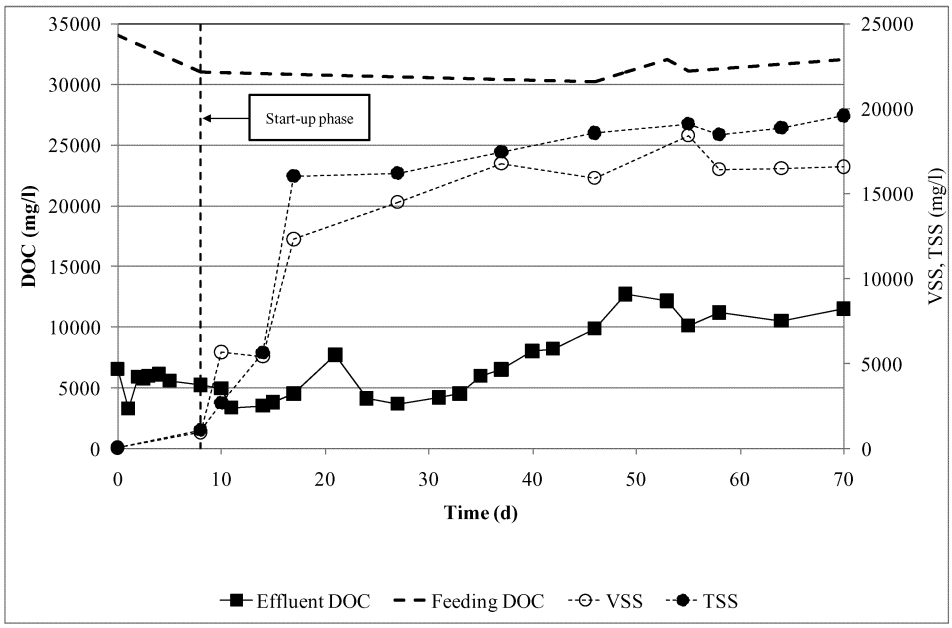

Figure 2 – Biomass profile and COD concentration in the outcoming effluent.

From t = 9d onwards, OOMWs were continuously fed to the reactor. Interestingly, DOC and polyphenols concentration followed two different behaviours.

DOC profile revealed that the biomass was immediately able to remove part of the fed soluble organic matter using it as a substrate for its growth. After about 45 days, the reactor reached a steady state, in term of DOC removal percentage and biomass concentration as well. Considering the average concentration of the feed equal to 30000mg_{DOC}/l and the (almost stationary) concentration in the outflow of about 11350 mg_{DOC}/l, a 62% treatment efficiency can be calculated. At the steady state biomass concentration of 17000 mg_{VSS}/l, this evaluates to an observed yield of 0.48 (on a C-mmol base), which is just a little bit higher with respect to that relevant to the start-up phase. The polyphenols profile, instead, revealed that these compounds were not

removed in both the batch start-up phase and in the first period of the experimentation, as can be depicted in Figure 3. However, from t = 17 d onwards, the polyphenols level in the reactor effluent started to progressively decrease according to a linear profile.
A comparison between the actual time profile of the effluent polyphenol concentration and that calculated on the basis of their measured concentration in the feed, under the hypotesis of null removal efficiency (see Figure 3), highlighted that in the first 35 days no removal were occuring. Thereafter, the difference between the calculated values and the experimental ones became significant, thus indicating that the biomass had activated/adapted its metabolic machinery to degrade polyphenols as well.
Comparing these results with those in D'Urso et al. (2008), it is readily apparent that the development of the capability of degrading phenolics takes longer on OOWM than on a

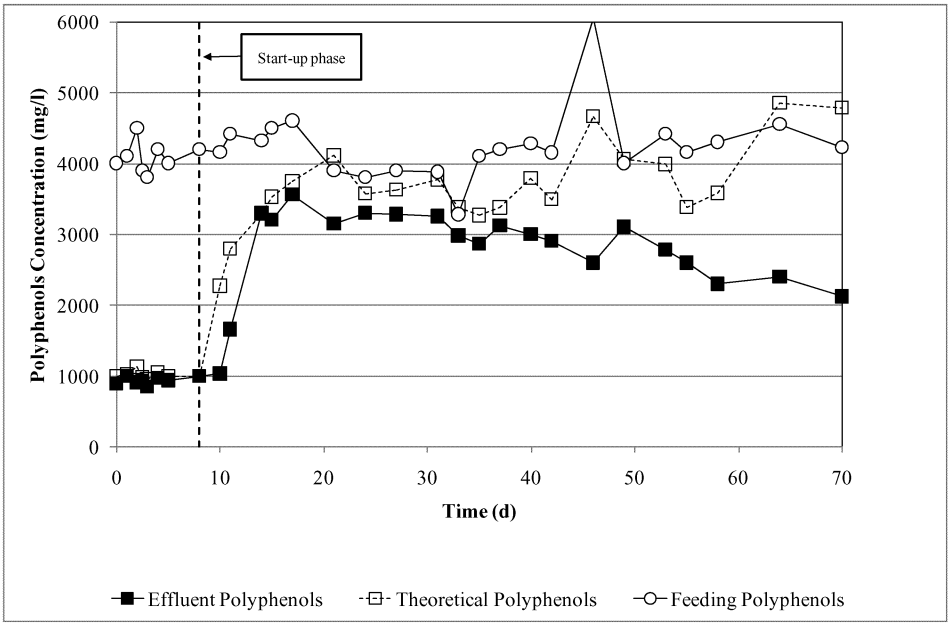

Figure 3 – Polyphenols concentration profiles. The theoretical values are calculated on the basis of the feeding concentration and considering an accumulation in the reactor (i.e., no removal).

synthetic medium including gallic acid. Most likely, this is due to the presence of complex structure phenolic compounds which take longer to degrade (or may never be degraded). Indeed, we showed earlier (D'Urso et al., 2007) that, while gallic acid is almost immediately metabolised, tannic acid was never removed from the broth.

4. Conclusions

T. viride biomass showed the capability to grow on OOMW. DOC content removal reached a steady state and in the effluent a concentration of one third with respect to the influent level was found. Polyphenols removal, instead, was showing an increasing performance as the effluent concentration was going down with a linear-shape behavior.

A resonable C-mol yield showed that the biomass was able to grow on the wastewater with no significant inhibition.

Although further studies should be done in order to transfer this technology to full-scale application (e.g. oxygen supply optimization) two practical conclusions can be immediately drawn: i. compounds of increased complexity might require time for the biomass to become able to treat them, during which the treated wastewater cannot be expected to meet the design specifications and ii. the biomass is able to grow in the medium with no inhibition at any time and therefore requires no particular care during the reactor start-up phase..

5. References

APAT and IRSA-CNR, 2004, Metodi Analitici per le Acque (in Italian).

Borja, R. and B. Rincon and F. Raposo, 2006, Anaerobic biodegradation of two-phase olive mill solid wastes and liquid effluents: kinetic studies and process performance, Journal of Chemical Technology and Biotechnology 8, 1450-1462.

D'Urso, A., M. Galimberti and M. Bravi, 2007, Fungal biomass-based processing of phenolics-rich wastewaters. In Proceedings of ICHEAP8 Congress, Ischia, Naples.

D'Urso, A., M. Russo and M. Bravi, 2007b, Phenolic fraction removal by *Trichoderma viride*: an investigation on olive oil mill, distillery and cork processing wastewater treatment, In Proceedings of 3rd CIGR Sec. VI-Food and Agricultural Products: Processing and Innovations Congress, Ischia, Naples.

Caffaz , S., C. Caretti , M. Morelli, C. Lubello and E. Azzari, 2007, Olive mill wastewater biological treatment by fungi biomass, Water Science & Technology 55 (10), 89-97.

D'Urso, A., D. Gapes and M. Bravi, 2008, Model Investigation of fungal activity on a synthetic biorecalcitrant wastewater. In Proceedings of IBIC2008 Congress.

Paixao, S. M., E. Mendonca, A. Picado and A. M. Anselmo, 1999, Acute toxicity evaluation of olive oil mill wastewaters: a comparative study of Three aquatic organisms, Environmental Toxicology 14(2), 263-269.

Proietti, P. and L. Nasini, 2006, L'Utilizzo dei Reflui Oleari nel Nuovo Panorama Normativo (in Italian).

Singleton, V. L. and J. A. J. Rossi, 1965, Colorimetry of total phenolics with phosphomolybdicphoshotungstic reagents. American Journal of Enology and Viticolture 16, 144-158.

Somogyi, M., 1926, Notes on sugar determination. The Journal of Biological Chemistry 70(3), 599-61.

Wilderer, P.A., R. L. Irvine and M. C. Goronszy, 2001, Sequencing Batch Reactor Technology. Scientific and Technical Report N.10, IWA Publishing, London.

CHEMICAL ENGINEERING TRANSACTIONS, Volume 14, 2008
Edited by G. Marino, E. Bardone, A. Viglia
 ISBN 978-88-95608-02-0

Kinetic Modeling of Biosorption of Heavy Metals by Loofa-sponge Immobilized Phanerochaete chrysosporium From Aqueous Solution

M. Nikazar, P. Namiranian, F. Vahabzadeh
Chemical Engineering Faculty of Amirkabir University of Tehran, Iran
Center of Excellency for Petrochemical Engineering
E-mail address : nikazar@ aut.ac.ir

Mat of mycelia of Phanerochaete chrysosporium were immobilized on loofa-sponge discs, as an inert support, to obtain a suitable biosorbent .Mean amount of immobilized P.chrysosporium on loofa-sponge was 376 mgg^{-1} of dry loofa-sponge. In this study immobilized P.chrysosporium and naked loofa-sponge discs were used as biosorbent to remove Pb (II) and Cd (II) from aqueous solution .At kinetic study residual concentration of metal ions was determined after contacting for up to 120 min. Equilibrium was established in about 60 min for both metals. The maximum uptake of Pb and Cd was 88.9 mgg^{-1} and 63.1mgg^{-1} for immobilized P.chrysosporium and 21.6mgg^{-1} and 16.5 $mgg^{-1}$for naked loofa-sponge, respectively. In order to examine the controlling mechanism of biosorption process, kinetic models were used to test the experimental data and kinetics was found to be best-fit pseudo-second-order equation.

Key words: Cadmium; Lead; Phanerochaete chrysosporium; Wastewater; Biosorption;

1. Introduction

The increase in usage of heavy metals in industrial activities has caused the existence of them in waste water. For example lead and cadmium which the wastewater of industries such as electroplating , plastic and paint manufacturing , mining , metallurgical process , petrochemical process , batteries , paper and pulp contains them (Iqbal and Edvean,2004, Iqbal and Edvean,2005).

According to the toxicity of these metals and their dangerous effects on the environment and human health, many attemptions have been done to remove them from waste water and environment.

Conventional chemical and physical methods such as chemical precipitation, chemical oxidation and reduction, ion exchange, filtration, reverse osmosis, membrane technology and evaporation, exit to remove heavy metals from wastewater (Iqbal and Edvean,2004, Ahluwalia and Goyal,2007).
But, these technologies are often expensive, generating toxic and non eco-friendly sludge or are ineffective when the metals concentration are low (range 1-100ppm)

(Iqbal and Edvean,2004, Ahluwalia and Goyal,2007). So that, considerable attention has been given to biological technologies, such as biosorption, which is the ability of microorganisms such as algae, fungi, bacteria and yeasts to bind heavy metals non-metabolically (Iqbal and Edvean,2004, Iqbal and Edvean,2005, Ahluwalia and Goyal,2007).But commercial application of biomass is reduced by problems associated with their physical characteristics such as low rigidity, low density, low mechanical strength, small particle size and difficulty in separation of biomass from liquid-phase. Due to these problems considerable attention has been given to immobilization of biomass (Iqbal and Edvean, 2004, Iqbal and Edvean, 2005).

Several immobilization media have been used. According to above problems a suitable matrix for immobilization which has low cost, high porosity and easy usage seems necessary.

In this study mat of mycelium of a known basidiomycete fungus, Phanerochaete chrysosporium was used to immobilized on loofa-sponge due to its low cost, physical strength, rigidity and high porosity .(Iqbal and Edvean,2004, Iqbal and Edvean,2005,Ahmadi et al, 2006)
This study looks at single removal of lead and cadmium from aqueous solution in batch system. Biosorption efficiency of immobilized fungi compared with naked loofa sponge is reported for removal of Pb (II) and Cd (II) in single biosorption.

2. Materials and Methods

2.1. Microorganism and culture medium

The white-rot fungus, P.chrysosporium (ATCC 24725) was maintained by sub culturing on 1/5% YMG agar slants (yeast extract 4 gr, malt extract 10 gr, and D-glucose 6 gr per liter of distilled water). The growth medium consisted of (gr per liter of distilled water); D-glucose, 10.0; KH2PO4, 2.0; MgSO4.7H2O, 0.5; NH4Cl, 0.1; CaCl2 .H2O, 0.1; thiamine, 0.001; yeast extract, 0.1gr;

2.2. Immobilization

The loofa sponge was obtained on removing hard pericarp tissue of the ripened dried fruit of Luffa cylindrica. The fibrous sponge was cut into discs of approximately 2.5 cm diameter, 2-4 mm thick, soaked in boiling water for 30 min, washed under tap water, and left for 24 hr in distilled water, changed 3 - 4 times. The sponge discs were oven dried at 70 ^{0}c.

Preparation of the inoculum was as follows: The fungus was grown on YMG agar for 5 days at 27^{0}c and for preparation of an aqueous fungal suspension the spores were transferred to 150 ml of YMG broth in a 500 ml Erlenmeyer flask (Yeong et al,1998) and incubated at 27^{0}c on a shaker incubator at 150 rpm for 5 days. Then the YMG medium was drained and the mycelium was blended for 15s at low level with blender. This blended culture was used as inoculum. For immobilization of P.chrysosporium with in loofa discs, mat of mycelia with inoculum size of 7 %(v/v) were added to four

pre-weighted loofa-sponge discs, as an immobilized matrix, in 250 Erlenmeyer flasks. After 2 days of incubating at 35^0c and 100 rpm, the growth media was drained and loofa sponge- immobilized biomass of P.chrysosporium (LIBPC) was washed with distilled water.

Dry weight of biomass was determined by weighting dried (70^0c, 24 hr) discs before and after fungal growth.

2.3. Metal solutions

Standard stock solutions of Pb (II) and Cd (II) (1000 ±2 mg l^{-1} Pb $(NO_3)_2$ and Cd $(Cl)_2$ salts from Merck Ltd.,) were used to prepare the appropriate required concentrations of each metal for biosorption studies.

2.4. Biosorption studies

Biosorption of Cd (II) and Pb (II) was carried out in batch experiments. The biosorption capacity of biosorbent was determined by shaking 100 ml solution of known concentration (100mgrl^{-1}) with 105 mgr of immobilized P.chrysosporium (LIBPC) and 286 mgr naked loofa-sponge as control in 250 ml flasks on a shaker incubator at 35^0c, 100 rpm. For determination the rate of biosorption and the biosorption equilibrium time the residual metal ions concentration in the solution was determined by allowing biosorbent - metal contact for different periods between 5 and 120 min and pH was adjusted to 6, using NaOH 0.1 N, HCl 0.1 N. Residual concentration of metal ions in single solution was determined using an atomic absorption spectrophotometer (AA-670/G V-7) .

2.4. Data analysis

The concentration of metal ions adsorbed per unit immobilized fungal biomass (mg metal g^{-1} dry biosorbent) was determined using the following expression:

$$q = V(C_i - C_{eq})/M \qquad (1)$$

Where q is the metal uptake (mg metal ions g^{-1} dry weight of fungal biomass entrapped within sponge discs), V is the volume of metal solution (ml), C_i is the initial concentration of metal ions in the solution (mg l^{-1}), C_{eq} is the final concentration of metal ions in the solution, and M is the dry weight of fungal biomass.

3. Results

3.1. Growth of Phanerochaete chrysosporium on loofa-sponge

Growth and immobilization was rapid in the first day and complete coverage of discs occurred at the end of the first day. The biomass of P.chrysosporium immobilized on loofa-sponge reached at stationary phase at day 2.

The mean amount of immobilized fungal biomass was 376 mgg^{-1} of dry loofa-sponge (Fig.1). This is about threefold higher than for the same fungi immobilized within

Ca-alginate beads (Kacar et al, 2002) and indicates the superiority of the open structured loofa sponge over the polymeric matrices previously used for immobilization.

Fig. 1: loofa sponge- immobilized biomass of P.chrysosporium (LIBPC)

The results show that LIBPC can simply be made by inoculating sponge discs with mat of mycelia in a suitable growth medium. In contrast, production of polymeric bead immobilized fungi is expensive, laborious and requires sophisticated equipment.

3.2. Effect of contact time on biosorption of Cd (II) and Pb (II) by loofa-sponge and immobilized P.chrysosporium

Immobilized P.chrysosporium has been successfully used as biosorbing agent for removal of Cd (II) and Pb (II). The kinetic profile of Pb (II) and Cd (II) biosorption by LIBPC and loofa sponge are shown in Fig.2. Metals' accumulation is rapid for LIBPC, reaching about 82% and 75% of sorption for Pb (II) and Cd (II) in the first 25 min. It is also relevant to point out that since active sorption sites in a system is a fixed number and each active site can adsorbed only one ion in a monolayer, the metal uptake by the sorbent surface will be rapid initially, slowing down as the competition for decreasing availability of active sites intensifies by the metal ions remaining in solution. (Saeed et al, 2005) Equilibrium was reached at 60 min for both metal ions. The maximum uptake obtained by naked loofa was 21.6mgg^{-1} for Pb (II) and 16.5mgg^{-1} for Cd (II). The maximum uptake of 88.9mgg^{-1} for Pb (II) and 63.1mgg^{-1} for Cd (II) by LIBPC was obtained .

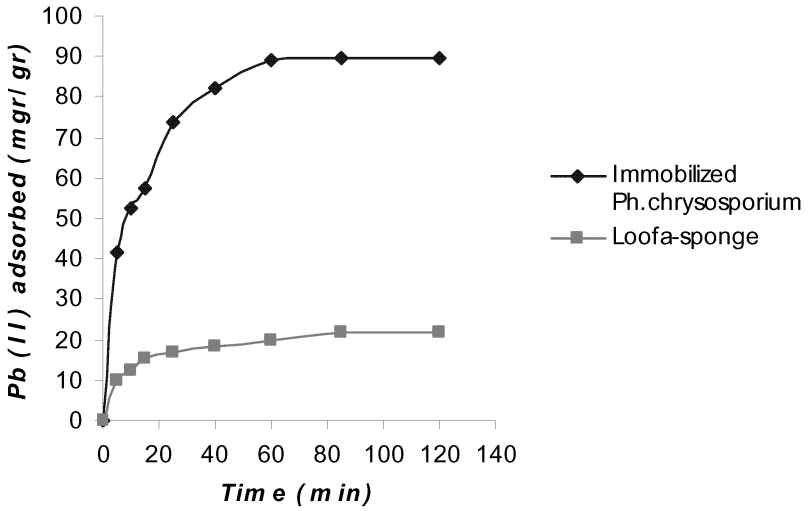

Fig. 2 (a): kinetic profile for Pb (II) biosorption

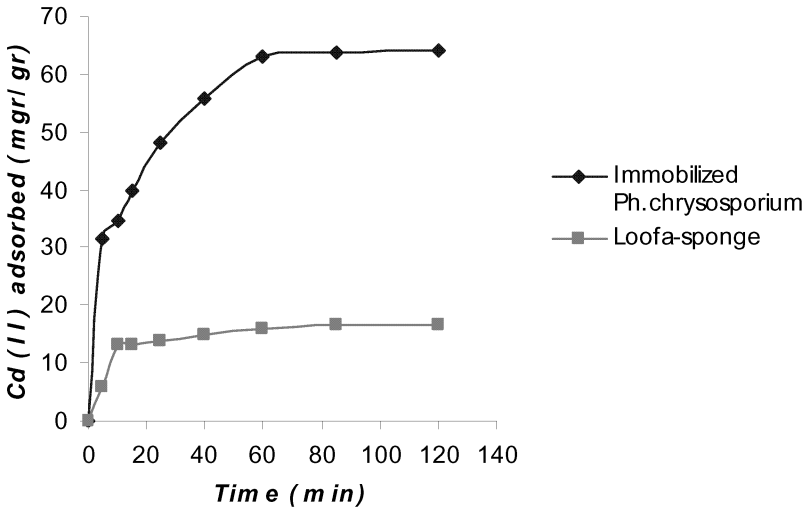

Fig. 2 (b): kinetic profile for Cd (II) biosorption

Loofa sponge discs with out fungal biomass adsorbed metals fourfold less than LIBPC, indicating little effect of the immobilized matrix on metals uptake.

This difference in the maximum level of uptake of these two metal ions has been explained in terms of difference in the ionic size of metals, the nature and distribution of active groups on the biosorbent, and the mode of interaction between the metal ions and the biosorbent .(Iqbal and Edvean,2004)

The biosorption kinetics were analyzed by applying the pseudo-first order (Lagergren equation) and pseudo-second order (Ho equation). Because LIBPC is our favorite biosorbent all the modelings are done for its data.

3.2.1. Pseudo-first order Lagergren model

The pseudo-first order model is generally express as follows:

$$\frac{dq_t}{dt} = K_l\left(q_e - q_t\right) \quad (1)$$

Where q_e and q_t have their usual meanings, and k_1 is the rate constant of first-order biosorption (min^{-1}). The integrated form of Eq. (1) is: (Wu and Yu, 2007)

$$Ln(q_e - q_t) = Ln\ q_e - t(K_l) \quad (2)$$

The first order rate constant k_1 and q_e values were determined from the slope and intercepts of the plot, presented in table 1.

Table 1. First order constants

Metal ion	First order model		
	r^2	$K_l(min^{-1})$	$q_e(mg/g)$
Pb (II)	0.9863	0.0574	67.08
Cd (II)	0.978	0.0414	39.4

3.2.2. Pseudo-second order Ho model

The pseudo-second order model is generally express as follows:

$$\frac{dq_t}{dt} = K_2\left(q_e - q_t\right)^2 \quad (3)$$

Where k_2 is the rate constant of second-order biosorption [g/(mg min)]. After integrating, the following equation is obtained: (Wu and Yu, 2007)

$$\frac{t}{q_t} = \frac{1}{K_2 q_e^2} + \frac{1}{q_e}t \quad (4)$$

The second order rate constant k_2 and q_e values were determined from the slope and intercepts of the plot, presented in table 2.

Table 2. Second order constants

Metal ion	Second order model		
	r^2	$K_2(mg/g\ min)*10^3$	$q_e(mg/g)$
Pb (II)	0.9987	1.352	96.15
Cd (II)	0.9967	1.48	69.9

The correlation regression coefficients indicate that the biosorption kinetic fits second order model better than lagergren model. Theoretical q_e values obtained from second order model were closer to the experimental q_e values than q_e values obtained from first order equation for both metal ions.

4. Conclusions

Loofa sponge is a suitable natural matrix for immobilization of P.chrysosporium. Immobilized P.chrysosporium has been successfully used as biosorbing agent for removal of Cd (II) and Pb (II). Biosorption was rapid and the equilibrium was obtained at 60 min for both metal ions and kinetics fitted second order model well.

5. Acknowledgement

The authors express their thanks to National Iranian Oil Refinery and Distribution Company for the financial support.

References

Ahluwalia, S.S., and D. Goyal, 2007, Microbial and plant derived biomass for removal of heavy metals from wastewater, Bioresource Technology, 98(12), 2243.

Ahmadi, M., F. Vahabzadeh, B. Bonakdarpour, and M. Mehranian, 2006,Empirical modeling of olive oil mill wastewater treatment using loofa-immobilized Phanerochaete chrysosporium, Process Biochemistry, 41,148.

Iqbal, M.,and R.G.J. Edyvean, 2004, Biosorption of lead, copper and zinc ions on loofa sponge immobilized biomass of Phanerochaete chrysosporium, Minerals Engineering, 17, 217.

Iqbal, M., and R.G.J. Edyvean, 2005, Loofa sponge immobilized fungal biosorbent: A robust system for cadmium and other dissolved metal removal from aqueous solution, Chemosphere, 61, 510.

Kacar, Y., C. Arpa , S. Tan , A. Denizli , O. Genc , and M.Y . Arıca, 2002, Biosorption of Hg(II) and Cd(II) from aqueous solutions: comparison of biosorptive capacity of alginate and immobilized live and heat inactivated Phanerochaete chrysosporium , Process Biochemistry ,37,601.

Saeed, A., M. Iqbal, M.,W. Akhtar, 2005.Removal and Recovery of Lead(II) from Single and Multimetal (Cd,Cu,Ni,Zn) Solutions by Crop Milling Waste(Black Grum Husk), J. of Hazardous Materials, B117,65.

Yeong, Y. , K. K., and S. Oh, 1998, Degradation of gaseous BTX by biofiltration with P.chrysosporium, Journal of microbiology, 36, 34.

Wu, J., and H.Q. Yu, 2007, Biosorption of 2, 4-dichlorophenol from aqueous solution by Phanerochaete chrysosporium biomass: Isotherms, kinetics and thermodynamics, J. of Hazardous Materials, 93, 253.

CHEMICAL ENGINEERING TRANSACTIONS, Volume 14, 2008
Edited by G. Marino, E. Bardone, A. Viglia
 ISBN 978-88-95608-02-0

Sustainable decontamination of an actual site aged PCB polluted soil by a biosurfactant-based washing followed by a photocatalytic treatment

Daniela Todaro[1,3], Fabio Occulti[1,3], Giovanni Camera Roda[2,3], Fabio Fava[1,3]
[1] DICASM, Faculty of Engineering, University of Bologna, Italy
[2] DICMA, Faculty of Engineering, University of Bologna, Italy
[3]LITCAR, Emilia Romagna Region Integrated Laboratory, Rimini, Italy

A two phases processing consisting of a Soya lecithin (SL)-based soil washing process followed by the photocatalityc treatment of resulting effluents was developed and applied at the laboratory scale in the remediation of an actual-site soil historically contaminated by 0.65 g/kg of polychlorinated biphenyls (PCBs). Triton X-100 (TX) was employed in the same process as a control surfactant. SL and TX displayed a comparable ability to remove PCBs from the soil. However, SL solution displayed a lower ecotoxicity, a lower ability to mobilize soil constituents and a higher soil detoxification capacity with respect to the TX one. The photocatalytic treatment resulted in marked depletions (from 50 to 70%) of total organic carbon (TOC) and PCBs initially occurring in the SL and TX contaminated effluents. Higher PCB depletion and dechlorination yields along with lower increases of ecotoxicity were observed in SL-containing effluents with respect to the TX ones at the end of 15 days of treatment. The two phases process developed and tested for the first time in this study seems to have the required features to become a challenging procedure for sustainable remediation of PCB-contaminated soils.

1. Introduction

Polychlorinated biphenyls (PCBs) are toxic xenobiotics widely distributed in the environment, mainly in soils and sediments. PCBs occurring in soils can be partially biodegraded by aerobic consortia of PCB-cometabolizing and chlorobenzoic acid (CBA)-mineralizing bacteria. However, the bioremediation of aged PCB-contaminated soils is very often adversely affected by the low bioavailability of PCBs, which are hydrophobic and tend to adsorb strongly onto soil organic matter, thus becoming poorly available in the soil water phase, where the PCB- and CBA-degrading microorganisms are mainly located (Fava et al., 2003a). Poorly biotreatable aged contaminated soils might be remediated through a surfactant-aided ex-situ soil-washing treatment (Chu et al., 2003). Satisfactory decontamination yields have been obtained with this technique on a variety of hydrocarbons polluted soils, but the generally used synthetic chemical surfactants were found to persist and exert toxic effects both in the soil resulting from washing and in the resulting aqueous effluents (Berselli et al., 2004). This limitation of conventional soil washing procedure can be mitigated by replacing synthetic surfactants with biogenic

pollutant mobilizing agents able to provide marked pollutant mobilization activity along with complete biodegradability and none toxicity (Berselli et al., 2006). Some commercial phytogenic surfactants, like Soya Lecithin (SL), have been found to be very effective hydrophobic pollutants-mobilizing agents in the semisolid bioremediation of PCBs contaminated soils (Fava et al., 2001). Anyway, little is generally known about the efficiency of soil washing procedures in the clean-up of actual site contaminated soils, and in particular of those polluted with PCBs. Further, the conventional soil washing procedure is also inhered by generation of large volumes of contaminated aqueous streams, which are generally not easily detoxified through conventional or advanced biological treatments. These effluents might be decontaminated through photocatalytic treatments based on the use of dispersed or fixed-bed TiO_2 catalysts (Camera Roda et al., 2005).

2. Materials and methods

2.1 Soil characteristics and soil washing

The aged contaminated soil employed, supplied by Area SpA (Ravenna, Italy), was homogenised, air-dried, sieved through a 0.2 cm sieve and analysed for its contents of organic pollutants.

Soil washing experiments were performed as described by Berselli et al. (2004). 150.0 g of air-dried soil were suspended in 1.0 L of distilled water, or a water solution of SL or TX at 2.25 g/L, in identical 3L-baffled flasks placed on a rotary shaker (120 rpm; 20 ± 2 ºC) for 72 h. Each washing agent was tested in two parallel identical reactors. At the end of the washing operations, the reactors were removed from the shaker and their content was allowed to settle down for 3 h. Then, the soil and the water phases were separated. Soil phases were air-dried for 2 days and then subjected to accelerated solvent extraction (ASE) followed by GC analysis of the resulting organic extract, and ecotoxicity analysis with the *Lepidium sativum* test organism. The water phases were subjected to batch solvent extraction, TOC and ecotoxicity analysis with *Vibrio fisheri* organism.

2.2 Photocatalytic treatment

TiO_2 powder was added to the effluents (0.5 g/L) in a 1L hermetically closed reservoir equipped with a magnetic stirring device. Then, the TiO_2 slurries were sent to the annular photocatalytic reactor. The light source was a linear fluorescent lamp (UVA in the 330-400 nm wavelength interval). The reactor (0.2 L) worked under batch mode conditions at 20 ± 2 ºC. TiO_2 slurry was continuously circulated through the reactor by means of a membrane pump. 50 mL samples were withdrawn from the medium mixing tank at the beginning and after 1, 7, 12, 15 days of photocatalytic treatment. 10 mL of each sample were subjected to batch solvent extractions to recover organic pollutants and the extracts were analyzed by GC-ECD. Polar (chloro)aromatic compounds were batch extracted from 10 mL of collected samples by diethyl-ether. The remaining water phase was centrifuged at 5,000 rpm for 10 min and the supernatant obtained was subjected to TOC and chloride ions analysis. The ecotoxicity of aqueous phase resulting after 15 days of

photocatalytic treatment was performed by applying the *Vibrio fischeri* test on 10 mL of sample.

2.3 Pollutant extraction and other procedures

PCBs and related compounds of the soil were extracted from the original soil samples resulting from washing through an ASE system operating at 140 atm and 100 ºC with a mixture of hexane-acetone (1:1). PCBs and related pollutants occurring in the washing effluents and in the aqueous phases subjected to photocatalytic treatment were recovered through two successive batch extractions with a mixture hexane-acetone according to Fava and Di Gioia (2001). The qualitative and quantitative analysis of PCBs occurring in the organic extracts obtained were performed through a gas chromatograph equipped with a capillary column (30m x 0.25mm) and an electron capture detector (ECD). Qualitative analysis of PCBs was performed by comparing the retention time (relative to Octafluoronaphtalene added as an hexane solution) of each of the GC peaks obtained with those of pure congeners and PCBs of standard Aroclor 1242 and Aroclor1260 (2003b). The TOC of the washing solution, as well as of the soil washing effluents before, during and at the end of the photocatalytic treatment, was determined by using a Shimadzu TOC-500 analyser as reported by Camera Roda et al. (2005). The ecotoxicity of the original soil and of the soil samples resulting from the washing experiment was measured by using the *Lepidium sativum* root and shoot elongation inhibition test as reported by Fava and Bertin (1999). Ecotoxicity of the solutions applied in the washing operations and that of effluents obtained before and after their photocatalytic treatment was determined as reported by Bolelli et al. (2006) employing the *Vibio fisheri* organism and the procedure recommended by the European standard EN ISO 11348.

3. Results

3.1 Soil decontamination through washing

The air-dried soil employed was found to contain about 650 mg per kg of dried soil of total PCBs ascribed to Aroclor 1242 and Aroclor 1260.

An extensive removal of PCBs was achieved through the washing operations. The two surfactants mediated a comparable overall PCB removal yields (~60%) which were not significantly influenced by the chlorination degree and pattern of eluted molecules (Table I).

		Average PCBs removal percentages in the soil after washing with	
	Initial concentration (mg/kg dry soil)	**SL**	**TX-100**
Overall PCBs concentration	640.11 ± 0.21	257.90 ± 4.68	242.15 ± 3.07
Average PCBs removal %		59.71 ± 2.03	62.17 ± 1.48

Table I. Initial PCBs concentration and average removal % after washing in the presence of SL and TX (± standard deviation).

Washing operations resulted in small changes of TOC of the washing solutions applied; TX mobilized larger extents of soil constituents than SL did (Table II).

Agent	Washing solutions TOC (mg/L)	Effluents TOC (mg/L)	TOC changes %
SL	1177.0 ± 1.7	1026.1 ± 18.1	-14.7
TX-100	1711.0 ± 78.5	1857.0 ± 53.0	+7.8

Table II. TOC of SL- and TX-amended washing solutions before and after their use in the washing operations (± standard deviation).

A remarkable depletion of original soil ecotoxicity was obtained with washing operations, in particular when SL was employed. However, the soil detoxification observed in the SL-washed soil was higher than that obtained with the TX-amended washing solution. The ecotoxicity of TX washing solution increased markedly with the washing operation (data not shown).

3.2 Photocatalytic treatment of the soil washing effluents

Comparable concentrations and composition of PCBs were observed in the two washing effluents sent to photocatalytic treatment. Marked depletions of such PCBs were generally observed at the end of effluent irradiation. Significantly higher PCB removal yields were observed in SL amended effluents with respect to the TX ones (76% vs 58%) (Table III).

	SL		TX	
	Initial concentration (mg/L)	**Removal %**	**Initial concentration (mg/L)**	**Removal %**
Initial concentration (mg/L) and average pollutants removal %	52.65	76.38	56.50	58.69

Table III. PCBs initially detected in the SL or TX effluents (average concentration ± standard deviation) and their average removal % attained at the end of photocatalytic treatment.

TOC was removed more extensively and rapidly in the SL amended effluents than in the TX ones. In particular, in the SL effluents, TOC decreased faster than total PCBs concentration during the first 7 days of irradiation, while the degradation rate of pollutants was higher than that of TOC during the remaining 8 days of treatment. In the TX effluents, instead, the degradation rate of PCBs and that TOC were comparable (Figure 1).

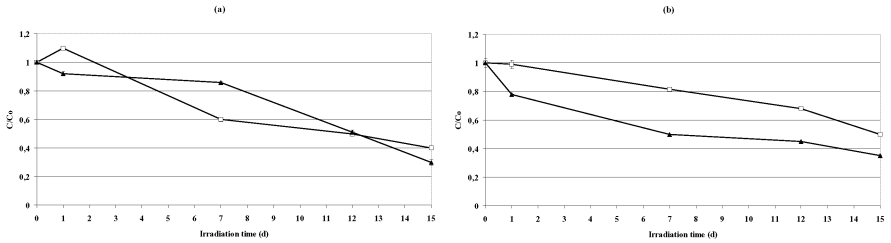

Figure 1. Fate of overall PCBs (▲) and TOC (□) in SL affluents (a) and in the TX ones (b) throughout the photocatalytic treatment as a functionof irradiation time. [C=concentration (mg/L) of total PCB ot TOC at each time, C_0 =initial concentration (mg/L) of total PCB or TOC].

A marked release of chlorine ions was observed in SL and TX effluents throughout the 15 days of treatment (Figure 2). However only about 50% of organic chlorine holds by depleted PCBs was detected as chloride ions in both types of effluents at the end of the treatment.
The photocatalytic treatment also resulted in marked increases of effluents ecotoxicity, in particular in the case of the TX amended ones (data not shown).

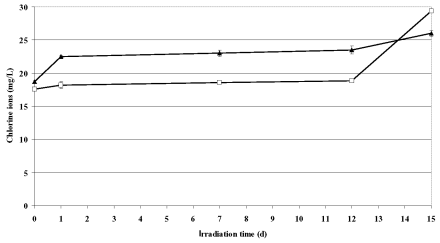

Figure 2. Change in chlorine concentration (mg/L) in the SL (▲) and TX (□) effluents throughout the whole photocatalytic treatment (error bars represent standard deviation).

4. Conclusion

In the present study, a two-phases process consisting of a biogenic surfactant assisted soil washing procedure followed by a TiO_2-photocatalytic treatment of resulting streams was developed.
SL based washing procedure provided very promising results. Indeed, SL was found to be an effective PCB mobilizing agent, by mediating, comparably to TX, the removal of about 60% of total PCBs originally occourring in the soil (Table I). Further, SL mobilized lower amounts of soil organic constituents with respect to TX (Table II) by also mediating, with respect to TX, a higher depletion of the soil initial ecotoxicity. These findings indicate that SL is a very promising soil washing

assisting agent as it as not costly biogenic agent capable of combining high and selective PCBs mobilizing activity with high biocompatibility and soil detoxification potential.

The photocatalytic treatment of effluents generally resulted in an extensive degradation of soil eluted PCBs (76% and 58% in SL and TX effluents respectively). However, PCBs disappeared through different rates and extents in the SL and TX effluents, and it suggests that surfactants affected the production of free radicals in the reactor (Table III).

The depletion of TOC was generally lower and slower than that of total PCBs (Figure 1). This finding along with the evidence that only 50% of organic chlorine was detected in the effluents at the end of the treatment (Figure 2) suggest that remarkable amounts of chlorinated intermediates of PCBs accumulated in the reactor troughout the treatment. However, none known intermediates were detected (trough CG and HPLC procedures) in the effluents.

In conclusion, the two phases process developed in this study seems to have all featurs required for being an effective new treatment for the clean-up of actual site PCBs-contaminated soils.

References

Berselli S., G. Milone, P. Canepa, D. Di Gioia, F. Fava (2004). Biotechnol Bioeng 88: 111-120.

Berselli S., E. Benitez, S. Fedi, D. Zannoni, A. Medici, L. Marchetti, F. Fava (2006). Biotechnol. Bioeng. 93: 761-770.

Bolelli L., Z. Bobrovov, E. Ferri, F. Fini, S. Menotta, S. Scandura, G. Fedrizzi, S. Girotti (2006). Pharmaceut Biomed Anal 42: 88-93.

Camera Roda G., F. Santarelli, C.A. Martin (2005). Solar Energy 79: 343-352.

Chu W., K.H. Chan (2003). Sci Total Environ 307: 83-92.

Fava F., L. Bertin (1999). Biotechnol Bioeng 64: 240-249.

Fava F., D. Di Gioia (2001). Biotechnol Bioeng 72: 177-184.

Fava F., G. Zanaroli, L.Y. Young (2003b). FEMS Microbiol Ecol 44: 309-318.

CHEMICAL ENGINEERING TRANSACTIONS, Volume 14, 2008
Edited by G. Marino, E. Bardone, A. Viglia
 ISBN 978-88-95608-02-0

Potential Of Microbial Species In Biodegradation Of Volatile Organic Compounds From Waters

Luiza Jecu[1], Amalia Gheorghe[1], Florina Popea[1], Andreea Rosu[1], Anicuta Stoica[2], Marta Stroescu[2]

[1] - National Research and Development Institute for Chemistry and Petrochemistry – ICECHIM, Spl. Independentei 202, Bucharest, Romania; 004-021.316.30.63, ljecu@icf.ro; amalia_ghe@yahoo.com
[2] - University Politehnica of Bucharest, Faculty of Applied Chemistry and Material Science, Str. Polizu nr. 1, Bucharest, Romania; 004-021.402.38.70, a_stoica@yahoo.com. marta_stroescu_yahoo.com

Keywords: bioremediation, volatile organic compounds,

Environmental contamination by volatile organic compounds (VOCs) from petrochemical and energy-producing industries is continually increasing. Among VOCs, aromatic compounds such as benzene, toluene and xylenes are the most severe contaminants because of their increasing use as gasoline, aircraft fuel and solvent. Due to their low water solubility, acute toxicity and genotoxicity, these compounds are classified as priority pollutants by European Environment Agency. Bioremediation exploits the ability of microorganisms to reduce the concentration and/or toxicity of a large number of pollutants. It is an economical, versatile, environment-friendly efficient treatment, which has a greater public acceptance and support. In this study we investigated growth patterns of microbial strains during volatile organic compounds degradation in order to select organisms for most efficient biodegradation. The aerobic batch tests were performed with *Pseudomonas putida, Candida membranes* and *Penicillium sp*, strains screened previously from various microbial species. A minimal liquid medium containing volatile organic compounds as carbon source, single substrate or in binary and tertiary mixtures was used to evaluate degradation activity of microbial strains. The content of organic compounds was analyzed with gas chromatograph coupled with mass spectrometry. As summarized, the selected strains were able of growing and transforming the volatile organic compounds tested. It was shown that benzene is the most resistant towards microbial degradation, the substitution of aromatic ring in toluene and xylene have facilitated the microbial attack.

Introduction

The environment is continuously polluted by a large array of hazardous chemicals with different structures and different toxicity levels that are released from several sources; the main sources of pollution can be identified as industrial activities, munitions waste and agricultural practice. The explosive development of chemical industries has produced a large variety of chemical compounds that include pesticides, fuels, alkanes, polycyclic aromatic compounds, dyes and more. Although these compounds have contributed to modernize lifestyle, several of them may accumulate in soil, water and air. Among volatile organic compounds resulted from petrochemical and energy-producing industries, aromatic compounds such as benzene, toluene and xylenes are severe contaminants. Due to their low water solubility, acute toxicity and genotoxicity, these compounds are classified as priority pollutants by European Environment Agency.

Bioremediation, technique that utilize the microbial ability to degrade and/or detoxify chemical substance, is relatively low cost, with low-technology level, and a high public acceptance. Much work has been done on the degradation of single pollutants (Machnicka and Suschka, 2001; Jn-Gyung J. and P. Chang-Ho, 2004).

Microbial growth on pollutant mixtures is an important aspect of bioremediation and wastewaters treatment (Burbak and Perry, 1993; Deeb and Alvarez-Cohen, 1999; Lee *et al.,* 2002; Attaway *et al*., 2001; Reardon *et al*., 2002). Recent studies have reported that the presence of benzene inhibited toluene and xylene degradation, irrespective of whether the microorganism grew in two or three components mixtures (Otenio *et al,* 2005).

Our previous studies have shown that among our microbial collection there are microorganisms able to grow and transform volatile organic compounds. Screening activities performed have allowed the selection of three microbial strains, such as *Pseudomonas putida, Candida membranes* and *Penicillium sp* (Jecu *et al*., 2007). In present paper, the above mentioned strains were cultivated in medium containing as carbon source, individual, bi- and tertiary mixtures of volatile organic compounds. In order to evaluate the microbial degradability of organic compounds containing aromatic ring and substituted benzene derivates, the experiments were performed with benzene, toluene and o-xylene.

Materials and Methods

Organism. The microorganisms applied under aerobic conditions were *Pseudomonas putida, Candida membranes, Penicillium sp.* Fungal strains and yeasts were maintained on dextrose/glucose/agar medium; the bacteria strains were maintained on gelose.
*Culture conditions.*The experiments performed in batch cultures used 150 ml glass vials sealed with teflon-coated rubber septa and aluminum caps. Vilas were rotary shaken (28^{o}C, 200 rpm). pH media was set at 7.0 and during experiments no significant modifications were observed. The inoculum was represented by microbial biomass obtained from cultures

grown on peptonate water and Czapek-Dox medium. The culture medium contained mineral salts (per liter of distilled water): a) bacteria - NH_4NO_3 (1.0); K_2HPO_4 (1.0); KH_2PO_4 (1.0); $MgSO_4$. $7H_2O$ (0.2); b) fungi and yeasts: $NaNO_3$ (2.0); KCl (0,5); K_2HPO_4 (1.0). The organic compounds were added after autoclaving to minimize losses from volatilization. The concentration of organic contaminant, the sole carbon and energy source was finally 0.1 % (v/v). For binary systems, the individual component concentrations were equal, the total being 0.1 % (v/v). In tertiary mixtures, the individual concentrations were 0.035 % (v/v). The samples performed in duplicate on rotary shaker to avoid volatilization losses, were taken at time intervals and analyzed for organic compound level, after adequate solvent extraction.

Analytic methods. The content of organic compounds was analyzed with gas chromatograph coupled with mass spectrometry. GC/MS analysis was accomplished with FOCUS GC DSQIL produced by THERMO ELECTRON CORPORATION, equipped with capillary column TR 5MS (5% phenyl methyl siloxane). The oven temperature was isothermal at 60° C for 2 minute, programmed to 300 ° C at 10o C/min and kept at 300° C for 10 min. Injector temperature was 250° C. Each measurement was done in triplicate. Aqueous samples were extracted with chloroform, metylene cloride or carbon tetrachloride. Samples were stored at 4° C in screw cap vials with teflon-lined rubber septa, until analysis.

Results and Discussion

The yield of organic compound extraction from aqueous culture media depends on the solvent used; i.e. for carbon tetrachloride extraction yield was 89%, for methylene chloride 72-74 %, and tetrachloride 75-79 %. It should be noted that all the efforts were done to minimize the losses due to volatilization of organic compounds.

The present work was focused to evaluate the ability of microbial strains to grow on volatile organic compounds, therefore the level of contaminant was kept constant, at 0.1 % (v/v), for all experiments on single or mixture substrates.

The first step was to cultivate microbial strains on a medium containing single volatile organic compound. The better results were obtained in cultures with *Candida membranes* (Table 1.), despite our expectations as regarding *Pseudomonas putida*, known to be the most versatile in metabolizing aromatic substrates.

The cultures showed that benzene was the most resistant to microbial degradation, while o-xylene and toluene presented differences, with preference for o- xylene. After 21 days of culture, the xylene degradation yields were 10% for *Pseudomonas*, 23% for *Candida* and 14% for *Penicillium*; the yield values for toluene degradation were 28.4%, 34,4% and 15 %, respectively. Similar results were presented by Jn-Gyung J. and P. Chang-Ho (2004).

Table 1. Microbial degradation of individual volatile organic compounds (initial concentration 0.1 % v/v)

Strain		Concentration x 10^{-3} (%, v/v)			
		Time (days)			
		3	9	15	21
Pseudomonas putida	B	54.3	13.0	10.14	0.8
	T	9.8	4.34	0.85	0.284
	o-X	12.4	2.3	0.94	0.105
Candida membranes	B	12.43	5.49	1.92	0.87
	T	18.3	6.2	0.55	0.344
	o-X	22.0	4.1	0.49	0.23
Penicillium sp.	B	88.70	85.51	79.51	0.249
	T	10.12	5.6	0.32	0.15
	o-X	14.0	6.1	0.47	0.138

Figure 1 presents the typical degradation curves of different binary mixtures, combination of benzene, o-xylene and toluene.

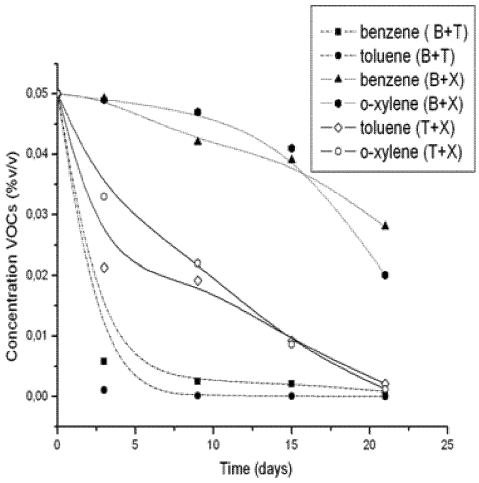

a) *Candida membranes*

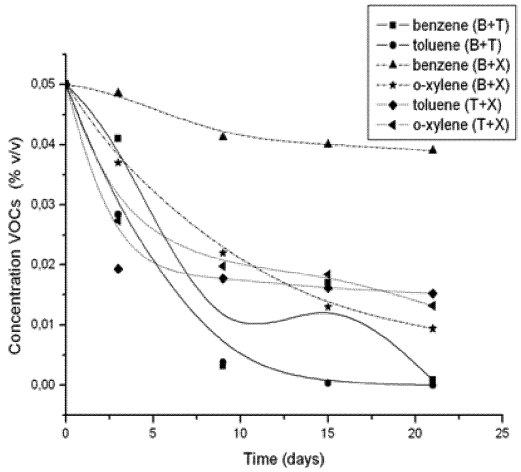

b) *Penicillium sp.*

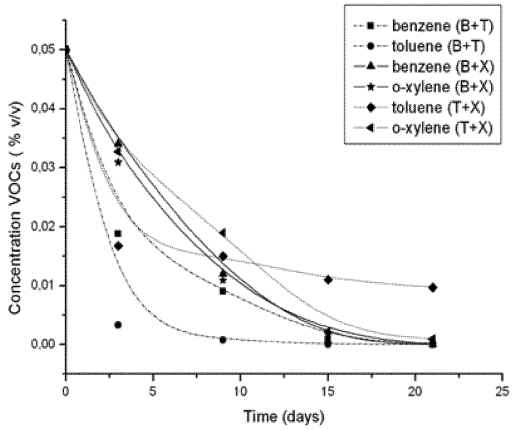

c) *Pseudomonas putida*

Figure 1. Cultivation of microbial strains on binary mixtures of VOCs. (a) *Candida membranes*; b) *Penicillium sp.; c) Pseudomonas putida*

In binary mixtures of benzene and toluene, *Candida* and *Pseudomonas* have presented the same curves shape, a rapid decrease of contaminant concentration after 5 days of cultivation, while *Penicillium sp* needed more time, about 7 days. The more resistant mixtures were, more or less, benzene with o-xylene, microbial strains presenting a different behavior. After 21 days, *Pseudomonas* have reached the total transformation of contaminants, while *Candida* and *Penicillium* have degraded about 40 % (benzene), 50 % toluene), and 15 % (benzene) 80 % (toluene), respectively.

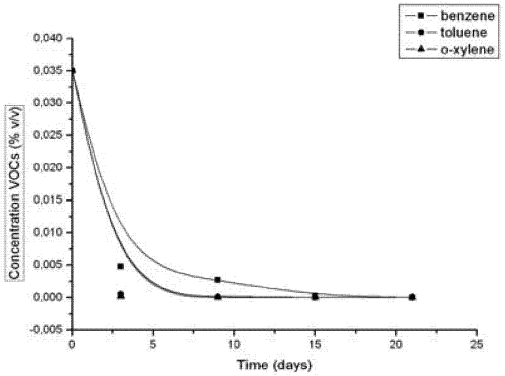

Candida membranes

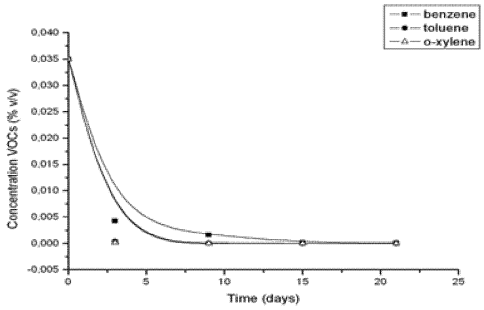

Penicillium sp.

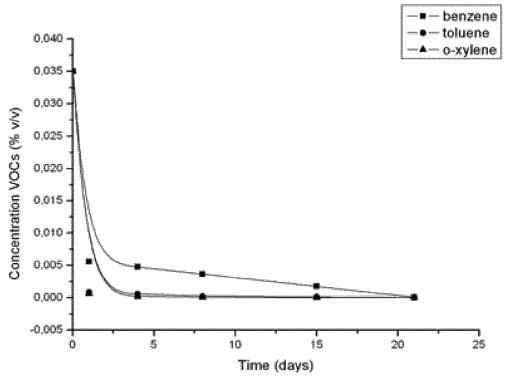

Pseudomonas putida

Figure 2. Cultivation of microbial strains on tertiary mixtures of VOCs

As regarding the tertiary mixture, the *Candida membranes* was the best microbial agent for organic pollutant degradation. The curves shape for all strains tested were very similar, benzene being most resistant to microbial degradation. But, it should be noticed that, the presence of the other compound have stimulated the benzene degradation, whose concentration decreasing to 0.

The initial concentrations of organic volatile compounds, individual and in mixtures, were different, only the total concentration being constant, therefore it is difficult to evaluate the interactions between compounds. Further researches will be directed towards substrate competitions and inhibitions during microbial degradation of organic compounds.
.

Acknowledgments

The authors gratefully acknowledge financial support from CNMP-Romania through CEEX project No. 127/2006.

References

Attaway, H., C. H. Gooding and M. G. Schmidt, 2001, Biodegradation of BTEX vapors in a silicone membrane bioreactor system, J. Inds. Microbiol. Biotechnol. 26, 316.

Burbak, B. L. and J. J. Perry, 1993, Biodegradation and biotransformation of groundwater pollutant mixtures by *Mycobacterium vaccae,* Appl. Environ. Microbial. 509, 1025.

Deeb, R. A and L. Alvarez-Cohen, 1999, Temperature effects and substrate interactions during the aerobic biotransformation of BTEX mixtures by toluene-enriched consortia and *Rhodoccocus rhodochorus,* Biotechnol. Bioeng. 62, 526.

Goudar, C. T. and K. A. Strevett, 1998, Comparison of relative rates of BTEX biodegradation using respirometry, J. Inds. Microbiol. Biotechnol. 21, 11.

Jecu, L., A. Gheorghe, G, Epure, F. Popea, A. Rosu and A. Roseanu, 2007, A biological treatment for the purification of wastewaters containing volatile organic compounds, Proceedings of Romanian International Conference on Chemistry and Chemical Engineering RICCCE ^{15th}, Sinaia (Romania), Sept 20-22, 2007.

Jn-Gyung J. and P. Chang-Ho, 2004, Characteristics of *Rhodoccocus pyridinovorans* PYJ-1 for the biodegradation of benzene, toluene, m-xylene (BTEX), and their mixtures, J. Biosci. Bioeng. 97, 429.

Lee, E. Y., Y. S. Jun, K. S. Cho and H. W. Ryu, 2002, Degradation characteristics of toluene, benzene, ethylbenzene and xylene by *Stenotrophomonas maltophila*, J. Air Waste Manag. Assoc. 52, 400.

Machnicka A. and J. Suschka, 2001, Activity of selected microorganisms and mixtures in BTX biodegradation, Polish J. Environ. Studies 10, 341.

Reardon, K. F., D. C. Mosteller, J. B. Rogers, N. M. DuTeau and K. H. Kim, 2002, Biodegradation kinetics of aromatic hydrocarbon mixtures by pure and mixed bacterial cultures, Environ. Health Pers. 110, 1005.

CHEMICAL ENGINEERING TRANSACTIONS, Volume 14, 2008
Edited by G. Marino, E. Bardone, A. Viglia
 ISBN 978-88-95608-02-0

Biological Control Of Phytopathogen Microorganisms With Antagonist Bacteria

Amalia Gheorghe[1], Luiza Jecu[1], Anca Voicu[2], Florina Popea[1],
Andreea Rosu[1], Anca Roseanu[3]

[1] National Research and Development Institute for Chemistry and Petrochemistry-ICECHIM, Spl. Independentei 202, Bucharest, Romania, tel/fax 004-021.316.30.63, amalia_ghe@yahoo.com.
[2] Institute of Biology - Romanian Academy, Spl. Independentei 296, Bucharest, Romania, tel/fax: 004-021.221.92.02/004-021.221.90.71, anca.voicu@ibiol.ro.
[3] Institute of Biochemistry - Romanian Academy, Spl. Independentei 296, Bucharest, Romania, tel/fax: 004-021.223.90.69/004-021.223.90.68roseanu@biochim.ro.

Keywords: biological control, antagonist bacteria, fungi

The use of biocontrol agents is becoming an increasingly important alternative to chemicals crop protection against weeds, insects, and diseases in both agriculture and forestry. The success of biocontrol and yield increase depends on the nature of the antagonistic properties and on the mechanisms of action of the organism. Both fungi and bacteria are able to synthesis a wide range of metabolites with fungicidal and bacterial capabilities. In this study, the antagonism between several microbial strains used as biocontrol agents and phytopathogen microorganisms was investigated. The screening of potential antagonists strains was made by the agar diffusion technique. The used pathogens were fungal strains, such as *Aspergillus sp., Penicillium sp.* and *Fusarium sp.* The biocontrol agents of plant diseases were *Bacillus* and *Pseudomonas sp,* isolated and selected from natural habitat. The evolution of dual cultures depends on strain type and antifungal secreted compounds. The results showed a direct inhibition of the pathogenic strains manifested by *Bacillus sp.*

Introduction

Fungi may produce several mycotoxins which can cause economic losses and may affect human health. Mycotoxins are toxic secondary metabolites produced under appropriate environmental conditions by filamentous fungi, mainly *Aspergillus* spp., *Penicillium* spp. and *Fusarium* spp. (Bennett and Klich, 2003).

For control fungal contamination there are two possibilities, heat treatment or chemical treatment, but it is necessary to replace chemical pesticides or fungicides to avoid soil pollution and health problems. Alternatively, antifungal agents produced by microorganisms may be used as biocontrol agent (Chitarra et al., 2003). Biological control offers an important alternative to synthetic chemicals. The use of bacteria like *Pseudomonas sp.*, *Bacillus sp.*, have been investigated because theirs properties to produce antifungal metabolites and protect plants from fungal infection (Radheshyam et al., 1990; Moita et al., 2005; Siddiqui et al., 2005; Nourozian et al., 2006). The materials based on microorganisms have following properties: high specificity against target plant pathogens; easy degradability; and low mass production cost. *Bacillus sp*. have the characteristics of, being widely distributed in soils, having high thermal tolerance, showing rapid growth in liquid culture, and readily form resistant spores. It is considered safe biological agents and their potential as biocontrol agents is considered to be high (Kim et al., 2003). Extracellular antifungal metabolites produced by *Bacillus pumilus* inhibited mycelial growth of many species of *Aspergillus, Penicillium* and *Fusarium* .(Munimbazi and Bullerman, 1998*).*

The aim of this research was to evaluate the potential of different species of *Bacillus* and *Pseudomonas* as biocontrol agents with antagonist properties by the disc diffusion method.

Materials and Methods

Microorganisms

The strains selected as potential biocontrol agents were: *Bacillus subtilis*, *Bacillus licheniformis, Bacillus amylolichefaciens* and *Pseudomonas putida*. The fungal strains target were *Aspergillus niger, Aspergillus oryzae, Aspergillus flavus, Penicillium sp., Fusarium sp.* All the organisms belong to Microbial Collection of ICECHIM. Bacteria were grown in agar nutrients slants tubes at 28^0C, for 48 hours. 2 ml aliquot was inoculated in 300ml Erlenmayer flasks with 48 ml peptonated water, and incubated at 28^0C, at 200 rpm for 24h. Fungi were grown in PDA tubes at 28^0C for 5 days. Then, they were inoculated in Czapek-Dox for 5 days, at 28^0C, 200 rpm.

Antimicrobial activity

Antimicrobial activity was determinate by agar diffusion technique. Several plant pathogens have been tested: *Aspergillus niger strain 38* and *strain 105 , Aspergillus oryzae strain 107* and *strain 100, Aspergillus flavus strain 111, Penicillium sp. strain 41, Fusarium sp. strain 73.* For testing antimicrobial activity, dextrose-potato-agar (DPA) medium was used. After solidification, agar surface was inoculated with 0.5ml suspension of antagonist bacteria. Agar diffusion method used 0.5 mm paper disks inoculated with 0.2µl phytopathogen fungal suspension. The cultures were examinated for the presence of a clear inhibition zone around the discs.

Mycotoxins production

The fungal strains with potential mycotoxins producing were cultivated in Erlenmayer flasks on Czapek-Dox medium for 5 days, at 28^0C, at 200 rpm. After 3 days of incubation, the liquid cultures were centrifuged and supernatants were checked for mycotoxins production.

Determination of mycotoxins

The mycotoxins content was determined using ELISA method (enzyme linked immunosorbent assay) and RIDA SCREEN kits (r-Biopharm, Darmstadt, Germany) for ochratoxin A, afltoxin B1, citrinin and fumonisin.

Results and Discussion

Fungi used in the study such as *Aspergillus, Fusarium* and *Penicillium* species were chosen according to their potential of toxins producing. Therefore, *Aspergillus* are common contaminants in agriculture, being ochratoxin and aflatoxin-producing species. Citrinin is isolated from several *Penicillium* and *Aspergillus* species, and fumonisin is produced notably by *Fusarium* sp. (Etzel, 2002; Moss, 1996)

Although the aim of current research did not comprise the mycotoxins evaluation, it is important to take into account the quantitative determination of mycotoxins. The capacity of selected microbial strains to produce fumonisin, aflatoxin B1, citrinin and ochratoxin was tested with ELISA method, in accordance with their biosynthetic origin (Table 1.)

The experimental results show that *A. niger* 38 and *A. niger* 105 are good producers of ochratoxin. Of the *Aspergillus* toxins, only ochratoxin is potentially as important as the aflatoxins. Also, *A. niger* 38 has produced the highest quantity of citrinin, 1650.2 ppb as compared with 9.14, 12.54, 3.21 for *Penicillium* 41, A. *oryzae* 100, and *Trichoderma* 103, respectively. The production of fumonisin at *Fusariumr* 37 and *Trichoderma* 103 was very small, bellow to method detection limit. A possible explanation is that *Fusarium* cultures need another conditions to enhance the fumosin biosynthesis..

The antagonism between microbial strains can be expressed in a number of ways: the most common are production of metabolites, competition and direct parasitism, but other mechanisms are involved, for example induced resistance sometimes associated with reduction of pathogen enzyme activity.

Table 1. Mycotoxins production by several fungal strains

Fungal strain	Mycotoxin						
	Fumonisin (ppm)	Ochratoxin (ppt)			Aflatoxin B1 (ppb)		Citrinin (ppb)
	nd*	nd*	1/10	1/20	nd*	conc x 5	nd*
A. niger 38			441.72	373.58	0	6.5	1650.2
Penicillium sp. 41							9.14
Fusarium sp. 73	<0.025						
A. oryzae 100							12.54
Trichoderma sp. 103	<0.025	0			0	0	3.21
A. niger 105			0	883.45	0	1	
A. oryzae 107							0
A. flavus 111					0	0	

nd-undiluted sample;fumonisin standard = 0.025-2 ppm; ochratoxin standard = 50-180 ppt; aflatoxin B1 standard =1-50 ppb; citrinin standard = 15-405 ppb.*

The antifungal effect of bacterial cultures was tested against the above mentioned pathogen microbial strains. The dual solid cultures have indicated the existence of an antagonism between several microbial strains. Different sensitivities of the fungi to the various bacteria may indicate the production of different metabolites or antifungal products.
The performed experiments based on agar diffusion technique showed that some fungi are very resistant to biocontrol agent, while others are very sensible to inhibition (Table 1.). The evaluation of the antagonism was based on visual observation of solid dual cultures.

Table 1. Antagonism between fungal pathogen and bacterial biocontrol agent (+++ very good inhibition; + + good inhibition; + poor inhibition; - no inhibition)

Pathogen fungal strain	Biocontrol agent	Time cultivation hours		
		24	48	120
A. niger strain 38	*P. putida* 1001	-	+	++

	B. licheniformis 1002	+	+	++
	B. licheniformis 1003	+	+	++
	B. subtilis 1004	-	-	-
	B. licheniformis 1005	-	-	-
	B. amylolichefaciens 1014	+	+	++
Penicillium sp. 41	*P. putida* 1001	+	+	-
	B. licheniformis 1002	+	++	++
	B. licheniformis 1003	+	++	++
	B. subtilis 1004	+	++	++
	B. licheniformis 1005	+	-	-
	B. amylolichefaciens 1014	+	++	+++
Fusarium sp. 73	*P. putida* 1001	+	++	+++
	B. licheniformis 1002	+	++	+++
	B. licheniformis 1003	+	++	+++
	B. subtilis 1004	+	++	+++
	B. licheniformis 1005	-	-	-
	B. amylolichefaciens 1014	+	++	+++
A. oryzae 100	*P. putida* 1001	+	++	+++
	B. licheniformis 1002	+	++	+++
	B. licheniformis 1003	+	++	+++
	B. subtilis 1004	+	++	+++
	B. licheniformis 1005	-	++	++
	B. amylolichefaciens 1014	+	++	+++
A. niger 105	*P. putida* 1001	-	-	-
	B. licheniformis 1002	-	-	-
	B. licheniformis 1003	-	-	-
	B. subtilis 1004	-	-	-
	B. licheniformis 1005	-	-	-
	B. amylolichefaciens 1014	-	+	++
A. oryzae 107	*P. putida* 1001	-	+	++
	B. licheniformis 1002	+	+	++
	B. licheniformis 1003	-	+	++
	B. subtilis 1004	+	+	++
	B. licheniformis 1005	-	+	++
	B. amylolichefaciens 1014	+	+	++
A. flavus 111	*P. putida* 1001	-	-	-
	B. licheniformis 1002	-	-	-
	B. licheniformis 1003	-	-	-
	B. subtilis 1004	-	-	-
	B. licheniformis 1005	-	-	-
	B. amylolichefaciens 1014	+	+	++

Our results can be considered positive for the cases where the fungal strains were inhibited, or where the inhibition zones have appeared. The evolution of dual cultures depends on

strain type and antifungal secreted compounds. Therefore, at 24 hours, 23 variants from 42 tested presented a poor inhibition of pathogen, visualized as a halo of variable diameter. We have recorded an improvement of the fungal inhibition, at 48 h of incubation, 14 variants being characterized by a good inhibition, and at 120 hours, 13 variants with very good inhibition.

Bacillus amylolichefaciens 1014 was the most active in controlling several phytopathogen microbial strains. After 120 h of incubation, the bacterial strain has totally inhibited the growth of *Penicillium sp.* 41, *Fusarium sp.* 73 and *A. oryzae* 100. Otherwise, the mycotoxins level of these strains was very low, that why the fungal growth was easily inhibited.

In the case of strains with a higher mycotoxins level, such as *A. niger* 38, and *A. niger* 105, the behavior was different. Thus *A. niger* 38 was inhibited by three bacterial cultures, while *A. niger* 105 was resistant to biocontrol, with the notable exception of *B. amylolichefaciens* 1014, which have exercised a strong inhibition. The experiments allowed the antagonism evidence between fungal

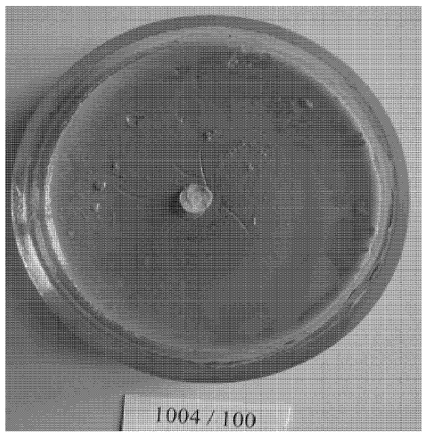

a) Total inhibition of *A. oryzae* 100 growth by *Bacillus subtilis* 1004

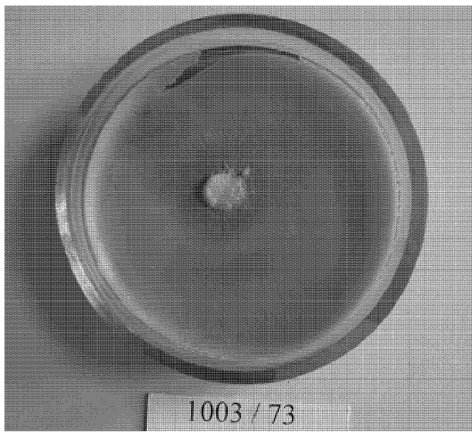

b) Total inhibition of *Fusarium sp.* 100 growth by *Bacillus licheniformis* 1003

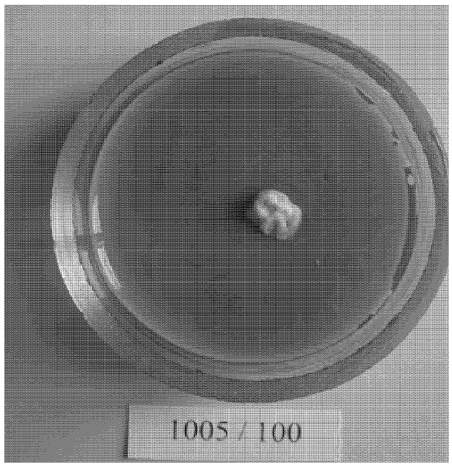

c) Partial inhibition of *A. oryzae* 100 growth by *Bacillus licheniformis* 1005

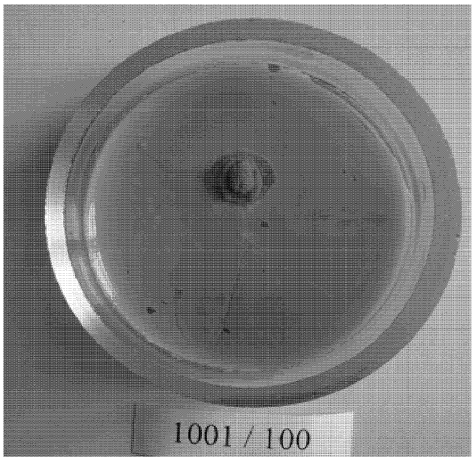

d) Partial inhibition of *A. oryzae* 100 growth by *P. putida* 1001

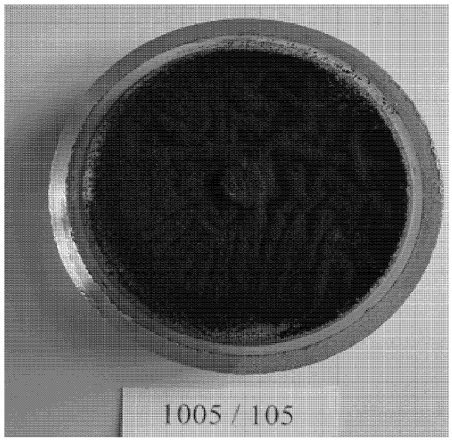

e) No inhibition of *A. niger* 105 growth by *B. licheniformis* 1005

Figure 1. Petri plates assay for antifungal activity of bacterial strains as biocontrol agent

In Figure 1 presents the degree of fungal growth inhibition, from total inhibition of fungal strains (a and b), where the bacteria covered the whole plate, through partial inhibition (c) and d), to (e) where the fungal strain was to strong to be inhibited.

These preliminary experiments indicate that several bacterial strains are able to control the fungal diseases in agriculture. *B. amylolichefaciens* 1014 is a promising agent in the inhibition of phytopathogen fungal growth.

Acknowledgments

The authors gratefully acknowledge financial support from CNMP-Romania through Project No. 61-045/2007.

References

Alippi A. and C. Mónaco, Antagonismo in vitro de especies de *Bacillu*s contra *Sclerotium rolfsii y Fusarium solani*. Revista de la Facultad de Agronomía, La Plata, 1994, vol. 70, p. 91-95.

Bennett J. W. and M. Klich, 2003, Mycotoxins, Clinical Microbiol. Rev., 16, 497.

Chitarra G. S., P. Breeuwer, M. J. R. Nout, A. C. Van Aelst, F. M. Rombouts and T. Abee, 2003, An antifungal compound produced by *Bacillus subtilis YM*10-20 inhibits germination of *Penicillium roqueforti* conidiospores, J. Appl. Microbiol., 94, 159.

Etzel R. A., 2002, Mycotoxins, J. Am. Med. Assoc., 287, 425.

Kim H-S., J. Park, S-W. Choi, K-H. Choi, G. L. Lee, S. J. Ban, C. H. Lee and C. S. Kim, 2003, Isolation and characterization of *Bacillus* strains for biological control, J. Microbiol., 41(3), 196.

Moita C., S. S. Feio, L. Nunes, M. J. M. Curto, J. C. Roseiro., 2005, Optimization of physical factors on the production of active metabolites by *Bacillus subtilis* 355 against wood surface contaminant fungi, International Biodeterioration & Biodegradation, 55, 261.

Moss M. O., 1996, Mycotoxins, Mycol. Rev., 100, 513.

Munimbazi C. and L. B. Bullerman, 1998, Isolation and partial characterization on antifungal metabolites of *Bacillus pumilus*, J. Appl. Microbiol., 84, 959.

Nourozian J., H. R. Etebarian and G. Khodakaramian, 2006, Biological control of *Fusarium graminearum* on wheat by antagonistic bacteria, Nutraceutical and Functional Food, 28, 29.

Radheshyam K., M. A. Jayaswal, Fernandez and R. G. Schroeder III, 1990, Isolation an characterization of a Pseudomonas strain that restrict growth of various phytopathogenic fungi, Appl. Environ. Microbiol., 56(4), 1053.

Siddiqui S., Z. A. Siddiqui and I. Ahmad, 2005, Evaluation of fluorescent *Pseudomonas* and *Bacillus* isolates for the biocontrol of a wilt complex of pigeonpea, World J. Microbiol. & Biotechnol., 21, 729.

CHEMICAL ENGINEERING TRANSACTIONS, Volume 14, 2008
Edited by G. Marino, E. Bardone, A. Viglia
 ISBN 978-88-95608-02-0

Evaluation of m-Nitrophenol and p-Nitrophenol degradation with biological activated carbon by immobilization of *Pseudomona putida* ATCC 700447

Escobar. E. [1], Moreno-Piraján J.C.[2], Pérez. M. [1], Sánchez O.[1*]
[1] Department of Chemical Engineering – Product and Process Design Group
[2] Department of Chemistry – Porous Solids and Calorimetric Group
Universidad de Los Andes, Carrera 1E No. 19 A 40, Bogotá, Colombia
el-escob@uniandes.edu.co, jumoreno@uniandes.edu.co , mar-pere@uniandes.edu.co
*osanchez@uniandes.edu.co

The degradation of m-nitrophenol (MNP) and p-nitrophenol (PNP) with biologically activated carbon (BAC) by the immobilization of *Pseudomonas putida* ATCC 700447 was studied. pH and nitrophenol concentration effect was evaluated on activated carbon adsorption over activated carbon (AC) and biodegradation by *Pseudomonas putida* ATCC 700447, separately. At the best conditions the Langmuir constant for each one was 100 mg g^{-1} for MNP (at pH 9.34 and 150 rpm) and 101 mg g^{-1} for PNP (at pH 8.00 and 150 rpm). The obtained biodegradation rates were 5.192 and 18.284 ppm h^{-1} for 50 and 100 ppm of MNP (at pH 9.34) with a degradation of 79 and 36% within 71 and 6 h, respectively; while, PNP was 100% degraded within 24 and 48h with degradation rates of 5.251 and 2.549 ppm h^{-1} for 50 and 100 ppm (at pH 6.00), respectively. The fixed BACs allowed to get a completely disappearance of both nitrophenolic compounds in the bulk fluid within 16 h, a higher time than the alone adsorption but lower than biodegradation process. In conclusion, BACs by *P. putida* ATCC 700447 offer advantages like greater microorganism resistance to MNP toxicity and capability of their own regeneration due to the microorganisms break out the nitrophenol molecules continuously as they are adsorpted enlarging the carbon adsorption ability.

1. Introduction

On a worldwide basis, textile and pesticide industry generate large quantities of contaminated effluents with nitro-phenols like m-nitrophenol (MNP) and p-nitrophenol (PNP). Due to the toxic character of these substances, the quantity that can be poured is found regulated. According to the Environmental Protection Agency (EPA), the water quality criterion for the aquatic life conservation and protection establishes that the limit of MNP is 200 mg L^{-1} and the level of PNP should not exceed 100 mg L^{-1}, since their easy adsorption by respiratory tract, digestive and cutaneous way (EPA, 1998; Gemini *et al.,* 2006; Kalme *et al.*, 2007).

Biological growth on activated carbon in water and wastewater treatment applications is an expected consequence of the favorable environment provided by this material. Activated carbon surfaces are excellent for colonization by microorganisms and its adsorptive properties serve to enrich substrate and oxygen concentrations, the craggy surface provides recesses that are sheltered from fluid shear forces, and the variety of

functional groups on the surface can enhance attachment of microorganisms. The principle advantage of BAC systems is increased effluent throughput until breakthrough resulting in less frequent regeneration time (Weber *et al.,* 1978).

Working with *Pseudomonas putida* in BAC facilitates the degradation of nitrophenols in contaminated effluents and at the same time offers advantages as the regeneration of these, due to the biological activity of the microorganisms that degrade continuously the compounds involved, enlarging the adsorption of the carbon toward these compounds, given that upon degrading, free spaces of adsorption on the material are liberated (Zeyer and Kearney, 1984).

The development of an efficient method in which adsorption and degradation of nitrophenol compounds are involved is of great interest for the Colombian industry. By this reason, in this work was evaluated MNP and PNP degradation through a BAC by the use of *Pseudomonas putida* ATCC 700447.

2. Materials And Methods

2.1. Chemicals

MNP and PNP were 99.9% of purity obtained from Merck. All the other reagents used were analytical grade. The activated carbon was a bituminous coal from Cesar (Colombia), which surface area and pore volume were determinated by adsorption-desorption of N_2 at 77 K (Quantachrome Sorptometer ACE-3) using BET (Bruner Emmett Teller), acid and basic groups were determinated by Boehm titrations (Titrometer TA 20 Bonus) (Barkauskas and Cannon, 2003), point of zero charge (p.z.c) and immersion enthalpy were determinated according to Bansal and Goyal (2005).

2.2 Microorganism

Pseudomonas putida ATCC 700447 which degrades PNP was obtained from culture collection (ATCC, USA). The organism was activated in a standard nutrient broth (Tryptic Soy Broth (TSB) composition per liter: Soya peptone, 3 g; dextrose, 2.5; casein peptone, 17 g; K_2HPO_4, 2.5 g; NaCl 5 g) and growth in cetrimide agar selective for *Pseudomonas.* Submerged culture in Luria-Bertani (LB) medium (LB composition per liter: Triptona, 10 g; yeast extract, 5g; NaCl, 0.5 g; Glycerin 1 mL) were made to produce the biomass used in the biodegradation assays. The minimum salt medium (MSM) used in this work for the nitrophenol compounds degradation was: K_2HPO_4, 0.75 g; KH_2PO_4, 0.2 g; $MgSO_4{\cdot}7H_2O$, 0.09 g; $FeSO_4{\cdot}7H_2O$, 0.06 g; glucose, 0.4 and enriched with the corresponding MNP or PNP (Kulkarni and Chaudhari, 2006).

2.3 Batch equilibrium studies

Equilibrium adsorption isotherms were determined from batch studies done in 250 mL shake flask containing 100 mL of the above MSM with 0.5 g AC and varying amount of initial MNP or PNP concentrations (10, 50 and 140 ppm MNP and 25, 100 and 150 ppm PNP) at different pHs (7.34, 8.34(~pKa) and 9.34±0.01 for MNP and 6.00, 7.00 (~pKa) and 8.00±0.01 for PNP) with constant agitation (0 or 150 rpm in a Branstead labline max 97000 shaker), and temperature (25°C). Samples of 2 ml were taken to measure the

MNP and PNP concentration during the different assays. Adsorption isotherms were analyzed using the Langmuir model (Ec. 1), (Annadurai *et al*., 2000).

$$q = \frac{KaC_e}{1 + aC_e} \quad (1)$$

where q is the quantity of nitrophenol adsorpted in the time (mg g^{-1}), K is the constant related to the adsorption capacity (mg g^{-1}), a is the Langmuir constant (L mg^{-1}) and C_e is the equilibrium concentration of the solute in liquid phase (mg L^{-1}).

2.4 Biodegradation of MNP and PNP

Biodegradation of MNP and PNP was determined separately from batch studies done in 250 mL shake flask containing 100 mL of the above MSM supplemented with 10 ppm of each nitrophenol at the selected pH, and inoculated with 1.7 mg of biomass in dry weight mL^{-1} obtained from LB medium. Once decoloration was achieved 1 mL of each assay was taken to inoculate the respective 50 ppm MNP or PNP solution at the selected pH. After bleaching these solutions, 1 mL was taken to inoculate 100 ppm MNP or PNP solution at respective pH. Samples from the different solutions were taken to determinate optical density (at λ:600 nm) and to monitor MNP or PNP concentration (spectrophotometrical quantification was carried out at the obtained wave length for each pH).

2.5 BAC production and degradation of mononitrophenols

The BAC was produced following the procedure: in 250 mL shake flasks containing 100 mL of MSM adjusted at the selected pH (7.34, 8.34 and 9.34±0.01 for MNP and 6.00, 7.00 and 8.00±0.01 for PNP) were added 0.5 g of autoclaved AC and subsequently were inoculated with 1.0 mL of *Pseudomonas putida* ATCC 700447 adapted previously at 50 ppm MNP or 100 ppm PNP. The growth of the microorganism was permitted for 96 hours at 25ºC and 150 rpm. After culturing, was added the respective nitrophenol to reach concentrations of 50, 100 or 150 ppm in MNP or PNP. The effect of biomass concentration on BAC activity was determinated for PNP degradation; the above procedure was carried out for PNP varying the inoculum to 0.5 mL of the adapted *P. putida* ATCC 700447.

During the decolorization samples of supernatant and few pellets of carbon were taken out to monitor spectrophotometrically the nitrophenol concentration and the microorganism immobilization by scanning electromagnetic microscopy (SEM) and surface area determination.

2.6 MNP and PNP quantification

MNP and PNP were determined spectrophotometrically (Thermospectronic GENESYS 5) at the maximum wave length obtained for MNP and PNP at different pHs according to standard methods of analysis (Shamsipur *et al*., 2005). For MNP λ_{max}:300 nm at pH

7.34 and λ_{max}:310 nm at pH 8.34 and 9.34, for PNP λ_{max}:370 nm at pH 6.00, λ_{max}:436 nm at pH 7.00 and λ_{max}:450 nm at pH 8.00.

3. Results And Discussion

3.1 Physicochemical characterization of the activated carbon

The bituminous activated carbon used was defined as a mesopore solid, with a type II isotherm according to IUPAC classification (Bansal and Goyal, 2005), with a mean pore volume of 0.438 cc g^{-1} and a surface area of 830 m^2 g^{-1}. The activated carbon displayed a basic character (acid groups 0,095 and basic groups 0,115 mmol g^{-1} of carbon), that is in agreement with the point of zero charge obtained (p.z.c: 11), similar results were reported by Navarrete *et al*. (2007). The obtained immersion enthalpy in benzene was Δ_{C6H6} 118,7 J g^{-1}, value that is in the range reported by López-Ramón *et al.* (1999) for activated carbon characterized in benzene (Δ_{C6H6} from 109,7 to 146,0 J g^{-1}).

3.2 Adsorption onto activated carbon

The single-solute adsorption of MNP and PNP at three different pHs and two agitation rates (0 and 150 rpm) were perform using a bituminous activated carbon. Langmuir isotherms of each nitrophenol compound were obtained at different conditions. Table 1 summarizes the Langmuir adsorption constants K and a gotten after the linearization of the isotherms. Adsorption affinity of the two nitrophenolic compounds to the activated carbon was found to be higher when the molecules are ionized (pH > pKa). At the best adsorption conditions for the nitrophenol compounds (150 rpm and pH 9.34 and 8.00 for the MNP and PNP, respectively) a 100% of sorption was obtain within 4.5 h. The basic pH underneath of the activated carbon point of zero charge (p.z.c 11) increases the adsorption due to the affinity between the dissociated molecule and the surface carbon charge (Bansal and Goyal, 2005). The difference in adsorption affinity can be explained mainly by the steric hindrance due to the size and shape of the solute molecules and the reduction of intermolecular hydrogen bonds in aqueous solution by the formation of intramolecular hydrogen bonds between hydroxyl group and the substituent, when nitro substituent is as much as close to hydroxyl group (Pura and Atun, 2005).

Table 1. Langmuir parameters of each nitrophenolic compound on activate carbon

	0 r.p.m		150 r.p.m.	
	K (mg g^{-1})	*a*(L mg^{-1})	*K* (mg g^{-1})	*a* (L mg^{-1})
MNP (pKa 8.34, water solubility 12.4 g L^{-1})				
pH 7.34	9.09	0.410	18.5	0.039
pH 8.34	40.0	0.011	76.9	0.009
pH 9.34	62.5	0.006	100	0.006
PNP (pKa 7.08, water solubility 13.5 g L^{-1})				
pH 6.00	28.6	0.005	29.4	0.196
pH 7.00	35.7	0.002	61.34	0.086
pH 8.00	100	0.001	101	0.028

3.3 MNP and PNP biodegradation

The single-solute biodegradation of MNP and PNP at three different pHs and constant agitation (150 rpm) were perform using *Pseudomonas putida* ATCC 700447. The initial biodegradation rate was determinated at the tested conditions (Table 2). For both concentrations 50 and 100 ppm PNP a 100% degradation was obtained at about 24 and 48h, respectively, without significant differences among the pHs; while for MNP the greatest degradation was obtained during the first 6h (79% of a 100 ppm solution) and 71h (36% of a 50 ppm solution) at pH 9.34 (Fig. 1).

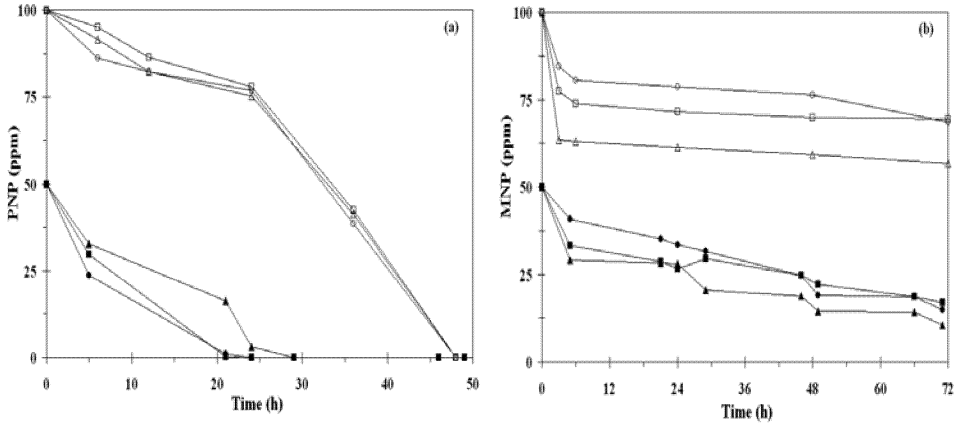

Figure 1. pH and initial concentration effect on PNP (a) and MNP (b) degradation by Pseudomona putida ATCC 700447. Full signs are for 50 ppm initial nitrophenol concentration and empty sign for 100 ppm. pH for PNP degradation were 6.00 (o), 7.00(□) and 8.00 (Δ) and for MNP were 7.34 (o), 8.34(□) and 9.34 (Δ).

Table 2. pH effect on degradation of 50 and 100 ppm MNP and PNP by *P. putida* ATCC 700447

MNP			PNP		
	50 ppm	100 ppm		50 ppm	100 ppm
pH	**Initial degradation rate (ppm h^{-1})**		**pH**	**Initial degradation rate (ppm h^{-1})**	
7.34	2.174	7.0440	6.00	5.251	2.549
8.34	4.087	10.682	7.00	4.074	0.816
9.34	5.192	18.284	8.00	3.463	1.413

The results display for both concentrations a higher MNP biodegradation at pH 9.34, although a MNP concentration increment increase the initial degradation rate, possibly by the previous adaptation of the microrganims, the MNP degraded decrease with higher concentrations. Zeyer and Kearney (1984) reported the MNP biodegradation by strain of *P. putida* at pH 6.5 and that toxicity is increased at acidic pH (< pKa), on the contrary alkaline pH (> pKa) reduced it and hence accelerates its metabolism. On the other hand, the greatest PNP biodegradation rate was presented at pH 6.00 but contrary to MNP at 100 ppm this decreased. The completed PNP degradation was obtained at the different pH. Nevertheless, Kulkarni and Chaudhari (2006), reported that PNP

degradation by a native *P. putida* was inhibited in acidic range (pH 4.0 – 6.5), and within 16.5h was degraded 300 ppm PNP at pH 7.5 – 9.5. The pK, of PNP and MNP is 7.03 and 8.34, respectively. At the pHs where a great metabolism occurred, PNP was mainly not charged whereas MNP was dissociated. Hence, metabolism does not seem to be a function of the charge, these results are similar to reported by Zeyer and Kearney (1984) for o-nitrophenol and m-nitrophenol biodegradation by a *P. putida* strain.

3.4 BAC production and degradation of mononitrophenols

The single-solute adsorption and degradation on BAC at the studied pHs and concentrations displayed higher decoloration times than the adsorption process but lower than biodegradation. The time was increased in up to 12h in front of adsorption. This possibly occurred by the biofilm formed on the carbon surface during the microorganism growth, which increase the adsorption resistance and decrease the free sorption area. The decrease in the surface area was evidenced by the SEM micrographs obtained during the culture and the drop in the sorption surface area (Fig. 2). A 100 ppm MNP solution was decolorated in at least a 90% within 16h with no significant difference for the three pHs (Fig 3b). Now that with the suspended microorganism at these conditions was obtained a 36% MNP degraded and a pH effect was observed, this perform of the BAC correlates with literature work that the cells immobilized on the activated carbon can protect the microorganisms from the toxicity of pollutants. Moreover, the suspended-cell systems are more sensitive to the change of pH (Annadurai *et al.,* 2002).

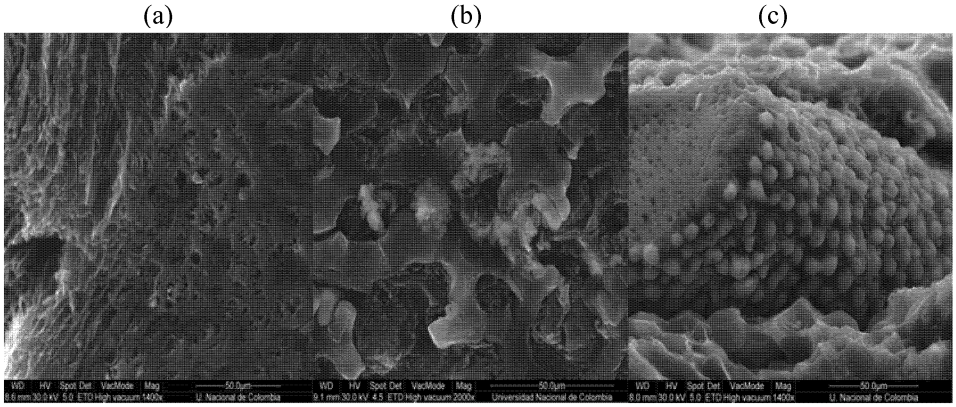

Figure 2. SEM images for (a) original activated carbon and (b-c) immobilized activated carbon.

The inoculum volume effect over the BAC production was evaluated over 150 ppm PNP solutions. The concentration profiles displayed an expected performance; while for a 1.0 mL inoculum the decoloration time was 6.5h, for the 0.5 mL inoculum was 16h (Fig. 3a). Due to the difference in cell concentration was expected a less free adsorption surface area with the 1.0 mL inoculum but a higher biodegradation rate, contrary to the 0.5 mL inoculum. The BAC performance is similar to reported by Li *et al.* (1998) who obtained a completed degradation of 50 ppm PNP within 24h by *P. putida strain* JS444, and Abu-Salah *et al.* (1996), that reported a total time of loss of color of 24 h in a rank

from 100 to 160 ppm using pulverized activated coal as backup of immobilization and a mixture of stumps where the predominant one was a remote native of *Pseudomonas sp.*. As for MNP at the end of the 16 h no significant effect of the pH is observed.

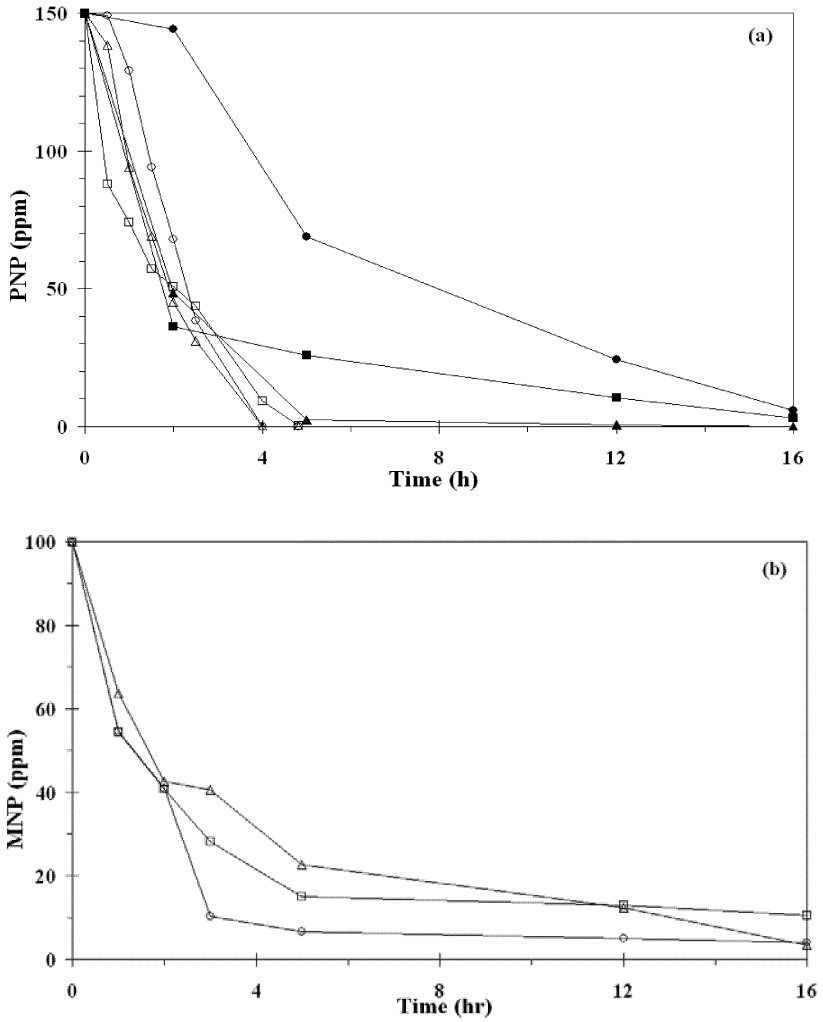

Figure 3. Inoculum volume effect on 150 ppm PNP degradation (a) and 100 ppm MNP (b) degradation by activated carbon with Pseudomona putida ATCC 700447. Full signs are for 0.5 mL inoculum and empty sign for 1.0 mL of inoculum. pH for PNP were 6.00 (o), 7.00(□) and 8.00 (Δ) and for MNP were 7.34 (o), 8.34(□) and 9.34 (Δ).

4. Conclusions

The activated carbon that was a mesopore solid displayed a good capacity of retention of the PNP and MNP, getting a complete adsorption within 4.5 h at 150 rpm for concentrations of about 150 ppm.

Pseudomonas putida ATCC 70047 degrade PNP (in a 100%) and has the capacity of degrade MNP (in up to 79%), nevertheless the degradation rate depends of the solution pH because of the dissociated state of the molecule.

The adsorption and degradation of MNP and PNP in BAC was achieved at the evaluated concentrations 100 and 150 ppm, respectively, with no significant difference among the decoloration time at the evaluated pHs. A main effect caused by the biomass concentration used in the immovilization on the activated carbon was observed on the PNP decoloration rate, possibly because of the increase in the mass transfer resistance by the formed biofilm.

5. References

Abu-Salah, K., G. Shelef, D. Levanoxf, R. Armonb and C.G. Dosoretza, 1996, *J. Biotechnol.*, 51:265-272.

Annadurai, G., R–S. Juang and D–J. Lee, 2002, *J. Environ. Sci. Health.*, A37(6):1133-1146

Annadurai, G., B.S. Rajesh, K.P.O. Mahesh and T. Murugesant, 2000, Bioprocess Eng., 22(6),493-501

Bansal, R.C. and M. Goyal, 2005, Actived Carbon Adsoption. First Edition, Taylor & Francis Group., Florida, EE.UU

Barkauskas, J. and F. S. Cannon, 2003, Potentiometric titrations: Characterize functional groups and adsorbed species on activated carbon, paper presented at Carbon 2003 - An International Conference on Carbon, Oviedo, Spain, July 6 - 10.

EPA., United States Environmental Protection Agency, 1998, Prevention, pesticides and toxic substances. EPA-738-F-97-016. December 2007. http:// www.epa.gov/REDs>.

Gemini, V.L., A. Gallego, C.E. Gómez, E.I. Planes and S.E. Korol, 2006, Biologic processes for p-nitrophenol detoxification, Higiene y Sanidad Ambiental, 6:145-149 (in Spanish)

Kalme, S.D., G.K. Parshetti, S.U. Jadhav and S.P. Govindwar, 2007, *Bioresour. Technol.*, 98(7):1405-1410.

Kulkarni, M. and A.Chaudhari, 2006, Bioresour. Technol., 97(8):982-988

Li, P.H.Y., F.A. Roddick and M.D. Hobday, 1998, *J. Chem. Technol. Biotechnol.*, 73:405–413

Navarrete L., J.C. Moreno-Piraján, L. Giraldo and V. García, 2007, Phenol 3-chlorophenol adsorption on activated carbon by immertion heat, Información tecnologica, 18(3):71-80 (in Spanish)

Pura, S. and G. Atun, 2005, *Colloids and Surfaces A: Physicochem. Eng. Aspects.* 253:137-144

Shamsipur, M., G. Raoof, H. Sharghi and B. Hemmateenejad, 2005, Ann Chim., 95(1-2):63-76

Weber, W.J., M. Pirbazari and G.L. Melson, 1978, *Env. Sci. Tech*. 127:817-819

Zeyer, J. and P.C. Kearney, 1984, *J. Agric. Food. Chem.*, 32:238-242